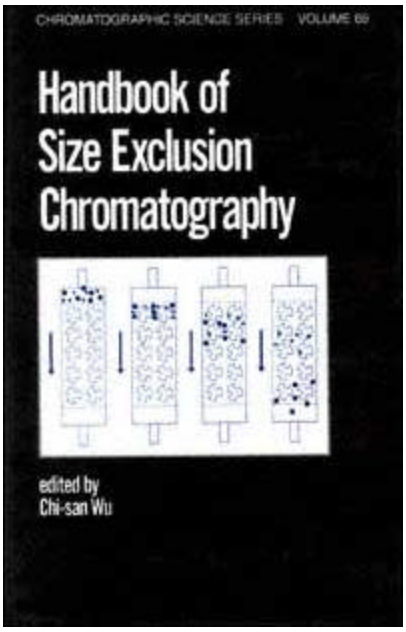

Handbook of Size Exclusion Chromatography

CHROMATOGRAPHIC SCIENCE SERIES

A Series of Monographs
Editor: JACK CAZES
Cherry Hill, New Jersey

1. Dynamics of Chromatography, *J. Calvin Giddings*

2. Gas Chromatographic Analysis of Drugs and Pesticides, *Benjamin J. Gudzinowicz*

3. Principles of Adsorption Chromatography: The Separation of Nonionic Organic Compounds, *Lloyd R. Snyder*

4. Multicomponent Chromatography: Theory of Interference, *Friedrich Helfferich and Gerhard Klein*

5. Quantitative Analysis by Gas Chromatography, *Josef Novák*

6. High-Speed Liquid Chromatography, *Peter M. Rajcsanyi and Elisabeth Rajcsanyi*

7. Fundamentals of Integrated GC-MS (in three parts), *Benjamin J. Gudzinowicz, Michael J. Gudzinowicz, and Horace F. Martin*

8. Liquid Chromatography of Polymers and Related Materials, *Jack Cazes*

9. GLC and HPLC Determination of Therapeutic Agents (in three parts), *Part 1 edited by Kiyoshi Tsuji and Walter Morozowich, Parts 2 and 3 edited by Kiyoshi Tsuji*

10. Biological/Biomedical Applications of Liquid Chromatography, *edited by Gerald L. Hawk*

11. Chromatography in Petroleum Analysis, *edited by Klaus H. Altgelt and T. H. Gouw*

12. Biological/Biomedical Applications of Liquid Chromatography II, *edited by Gerald L. Hawk*

13. Liquid Chromatography of Polymers and Related Materials II, *edited by Jack Cazes and Xavier Delamare*

14. Introduction to Analytical Gas Chromatography: History, Principles, and Practice, *John A. Perry*

15. Applications of Glass Capillary Gas Chromatography, *edited by Walter G. Jennings*

16. Steroid Analysis by HPLC: Recent Applications, *edited by Marie P. Kautsky*

17. Thin-Layer Chromatography: Techniques and Applications, *Bernard Fried and Joseph Sherma*

18. Biological/Biomedical Applications of Liquid Chromatography III, *edited by Gerald L. Hawk*

19. Liquid Chromatography of Polymers and Related Materials III, *edited by Jack Cazes*

20. Biological/Biomedical Applications of Liquid Chromatography, *edited by Gerald L. Hawk*

21. Chromatographic Separation and Extraction with Foamed Plastics and Rubbers, *G. J. Moody and J. D. R. Thomas*

22. Analytical Pyrolysis: A Comprehensive Guide, *William J. Irwin*

23. Liquid Chromatography Detectors, *edited by Thomas M. Vickrey*

24. High-Performance Liquid Chromatography in Forensic Chemistry, *edited by Ira S. Lurie and John D. Wittwer, Jr.*

25. Steric Exclusion Liquid Chromatography of Polymers, *edited by Josef Janca* *

26. HPLC Analysis of Biological Compounds: A Laboratory Guide, *William S. Hancock and James T. Sparrow*

27. Affinity Chromatography: Template Chromatography of Nucleic Acids and Proteins, *Herbert Schott*

28. HPLC in Nucleic Acid Research: Methods and Applications, *edited by Phyllis R. Brown*

29. Pyrolysis and GC in Polymer Analysis, *edited by S. A. Liebman and E. J. Levy*

30. Modern Chromatographic Analysis of the Vitamins, *edited by André P. De Leenheer, Willy E. Lambert, and Marcel G. M. De Ruyter*

31. Ion-Pair Chromatography, *edited by Milton T. W. Hearn*

32. Therapeutic Drug Monitoring and Toxicology by Liquid Chromatography, *edited by Steven H. Y. Wong*

33. Affinity Chromatography: Practical and Theoretical Aspects, *Peter Mohr and Klaus Pommerening*

34. Reaction Detection in Liquid Chromatography, *edited by Ira S. Krull*

35. Thin-Layer Chromatography: Techniques and Applications. Second Edition, Revised and Expanded, *Bernard Fried and Joseph Sherma*

36. Quantitative Thin-Layer Chromatography and Its Industrial Applications, *edited by Laszlo R. Treiber*

37. Ion Chromatography, *edited by James G. Tarter*

38. Chromatographic Theory and Basic Principles, *edited by Jan Åke Jönsson*

39. Field-Flow Fractionation: Analysis of Macromolecules and Particles, *Josef Janca*

40. Chromatographic Chiral Separations, *edited by Morris Zief and Laura J. Crane*

41. Quantitative Analysis by Gas Chromatography, Second Edition, Revised and Expanded, *Joseph Novák*

42. Flow Perturbation Gas Chromatography, *N. A. Katsanos*

43. Ion-Exchange Chromatography of Proteins, *Shuichi Yamamoto, Kazuhiro Nakanishi, and Ryuichi Matsuno*

44. Countercurrent Chromatography: Theory and Practice, *edited by N. Bhushan Mandava and Yoichiro Ito*

45. Microbore Column Chromatography: A Unified Approach to Chromatography, *edited by Frank J. Yang*

46. Preparative-Scale Chromatography, *edited by Eli Grushka*

47. Packings and Stationary Phases in Chromatographic Techniques, *edited by Klaus K. Unger*

48. Detection-Oriented Derivatization Techniques in Liquid Chromatography, *edited by Henk Lingeman and Willy J. M. Underberg*

49. Chromatographic Analysis of Pharmaceuticals, *edited by John A. Adamovics*

50. Multidimensional Chromatography: Techniques and Applications, *edited by Hernan Cortes*

51. HPLC of Biological Macromolecules: Methods and Applications, *edited by Karen M. Gooding and Fred E. Regnier*

52. Modern Thin-Layer Chromatography, *edited by Nelu Grinberg*

53. Chromatographic Analysis of Alkaloids, *Milan Popl, Jan Fähnrich, and Vlastimil Tatar*

54. HPLC in Clinical Chemistry, *I. N. Papadoyannis*

55. Handbook of Thin-Layer Chromatography, *edited by Joseph Sherma and Bernard Fried*

56. Gas-Liquid-Solid Chromatography, *V. G. Berezkin*

57. Complexation Chromatography, *edited by D. Cagniant*

58. Liquid Chromatography-Mass Spectrometry, *W. M. A. Niessen and Jan van der Greef*

59. Trace Analysis with Microcolumn Liquid Chromatography, *Milos Krejci* *

60. Modern Chromatographic Analysis of Vitamins: Second Edition, *edited by André P. De Leenheer, Willy E. Lambert, and Hans J. Nelis*

61. Preparative and Production Scale Chromatography, *edited by G. Ganetsos and P. E. Barker*

62. Diode Array Detection in HPLC, *edited by Ludwig Huber and Stephan A. George*

63. Handbook of Affinity Chromatography, *edited by Toni Kline*

64. Capillary Electrophoresis Technology, *edited by Norberto A. Guzman*

65. Lipid Chromatographic Analysis, *edited by Takayuki Shibamoto*

66. Thin-Layer Chromatography: Techniques and Applications, Third Edition, Revised and Expanded, *Bernard Fried and Joseph Sherma*

67. Liquid Chromatography for the Analyst, *Raymond P. W. Scott*

68. Centrifugal Partition Chromatography, *edited by Alain P. Foucault*

69. Handbook of Size Exclusion Chromatography, *edited by Chi-san Wu*

ADDITIONAL VOLUMES IN PREPARATION

Handbook of Size Exclusion Chromatography

edited by
Chi-san Wu
International Specialty Products
Wayne, New Jersey

Marcel Dekker, Inc.
New York•Basel•Hong Kong

Library of Congress Cataloging-in-Publication Data

Handbook of size exclusion chromatography / edited by Chi-san Wu.
p. cm -- (Chromatographic science series ; v 69)
Includes bibliographical references and index.
ISBN 0-8247-9288-2 (acid-free)
1. Gel permeation chromatography. I. Wu, Chi-san
II. Series: Chromatographic science ; v. 69.
QD272.C444H35 1995 94-42773
547.7046--dc20 CIP

The publisher offers discounts on this book when ordered in bulk quantities. For more information, write to Special Sales/Professional Marketing at the address below.

This book is printed on acid-free paper.

MARCEL DEKKER, INC.
270 Madison Avenue, New York, New York 10016

Current printing (last digit):
10 9 8 7 6 5 4 3 2 1

PRINTED IN THE UNITED STATES OF AMERICA

Preface

Molecular weight and molecular weight distribution are well known to affect the properties of polymeric materials. Even though for decades viscosity has been an integral part of product specifications used to characterize molecular weight of polymeric materials in industry, the need to define the molecular weight distribution of a product has attracted little attention. However, in recent years producers and users of polymeric materials have become ever more interested in value-added polymers with not only specific molecular weights but also optimal molecular weight distribution to offer unique performance advantages to products.

In fact, molecular weight distribution has become an important marketing feature for polymeric products in the 1990s. It is very common these days to see new grades of polymeric materials introduced to the marketplace that are specially designed to have either narrow or bimodal molecular weight distribution. In the case of a copolymer, the stress is on the uniformity in composition distribution throughout the entire molecular weight distribution. Therefore, the need to improve the analytical capability in R&D to characterize molecular weight distribution by size exclusion chromatography or gel permeation chromatography has become increasingly urgent in recent years.

Determination of molecular weight distribution of a polymer is very often not a simple task. This is one of the reasons it is still not commonly used as a final product specification. Many books have been published on size exclusion chromatography. However, there has still been a need for a book that stresses practical applications of size exclusion chromatography to the important polymeric materials in industry. Hopefully the valuable experiences of the authors in this book

Contents

1
Introduction to Size Exclusion Chromatography

Edward G. Malawer International Specialty Products, Wayne, New Jersey

Introduction

The technique that is the subject of this monograph, size exclusion chromatography (SEC), is the generic name given to the liquid chromatographic separation of macromolecules by molecular size. It has been taken to be generally synonymous with such other names as gel permeation chromatography (GPC), gel filtration chromatography (GFC), gel chromatography, steric exclusion chromatography, and exclusion chromatography. The “gel” term generally connotes the use of a nonrigid or semirigid organic gel stationary phase, whereas SEC can pertain to either an organic gel or a rigid inorganic support. Despite this, the term GPC is commonly used interchangeably with SEC. In this chapter we focus on high-performance (or high-pressure) SEC, which requires the use of rigid or semirigid supports to effect rapid separations (typically 20 minutes to 1 h).

The primary purpose and use of the SEC technique is to provide molecular weight distribution (MWD) information about a particular polymeric material. The graphical data display typically depicts a linear detector response on the ordinate versus either chromatographic elution volume or, if processed, the logarithm of molecular weight on the abscissa. One may ask, if SEC relates explicitly to molecular *size*, how can it directly provide molecular *weight* information? This is because of the relationship between linear dimension and molecular weight in a freely jointed polymeric chain (random coil): either the root-mean-square end-to-end distance or the radius of gyration is proportional

to the square root of the molecular weight (1). It follows that the log of either distance is proportional to (one-half) the log of the molecular weight.

SEC Experiment and Related Thermodynamics

A stylized separation of an ideal mixture of two sizes of macromolecules is presented in Figure 1. In the first frame, the sample is shown immediately after injection on the head of the column. A liquid mobile phase is passed through the column at a fixed flow rate, setting up a pressure gradient across its length. In the next frame the sample polymer molecules pass into the column as a result of this pressure gradient. The particles of the stationary phase (packing material) are porous, with controlled pore size. The smaller macromolecules are able to penetrate these pores as they pass through the column, but the larger ones are too large to be accommodated and remain in the interstitial space, as shown in the third frame. The smaller molecules are only temporarily retained and flow down the column until they encounter other particle pores to enter. The larger molecules flow more rapidly down the length of the column because they cannot reside inside the pores for any period of time. Finally, the two molecular sizes are separated into two distinct chromatographic bands, as shown in the fourth frame. A mass detector situated at the end of the column responds to their elution

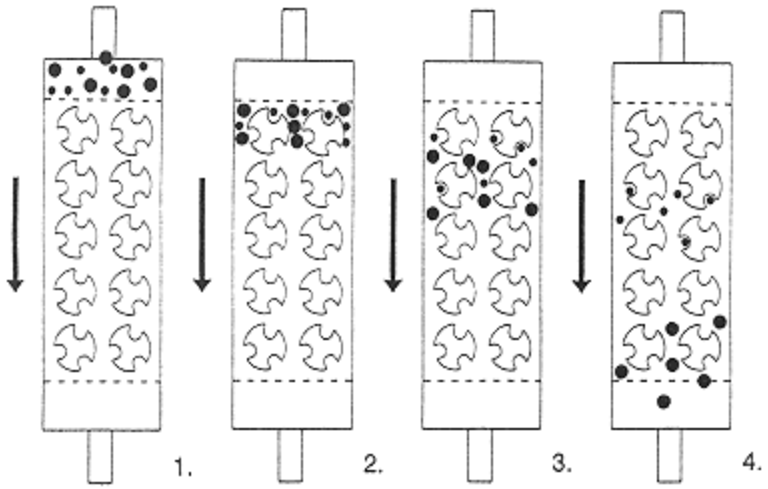

Figure 1.
SEC separation of two macromolecular sizes: (1) sample mixture before entering the column packing; (2) sample mixture upon the head of the column; (3) size separation begins; (4) complete resolution.

by generating a signal (peak) for each band as it passes through whose size is proportional to the concentration. A real SEC sample chromatogram typically shows a continuum of molecular weight components contained unresolved within a single peak.

If a series of different molecular weight polymers is injected onto such a column they elute in reverse size order. It is instructive to consider the calibration curve that results from such a series of molecular weights, depicted in Figure 2. Here we plot the molecular weight on the ordinate and the retention volume V_r on the abscissa. The left-hand edge of the chart represents the point of injection. The retention volume V_0 is the void volume or total exclusion volume. It is the total interstitial volume in the chromatographic system and the point in the chromatogram before which no polymer molecule can elute. V_t is the total permeation volume and represents the sum of the interstitial volume and the total pore volume. It is the point at which the smallest molecules in the sample mixture elute. All SEC separation takes place between V_0 and V_t. This retention volume domain is the selective permeation range. In Figure 2, the largest and the smallest molecular weight species are too large and small, re-

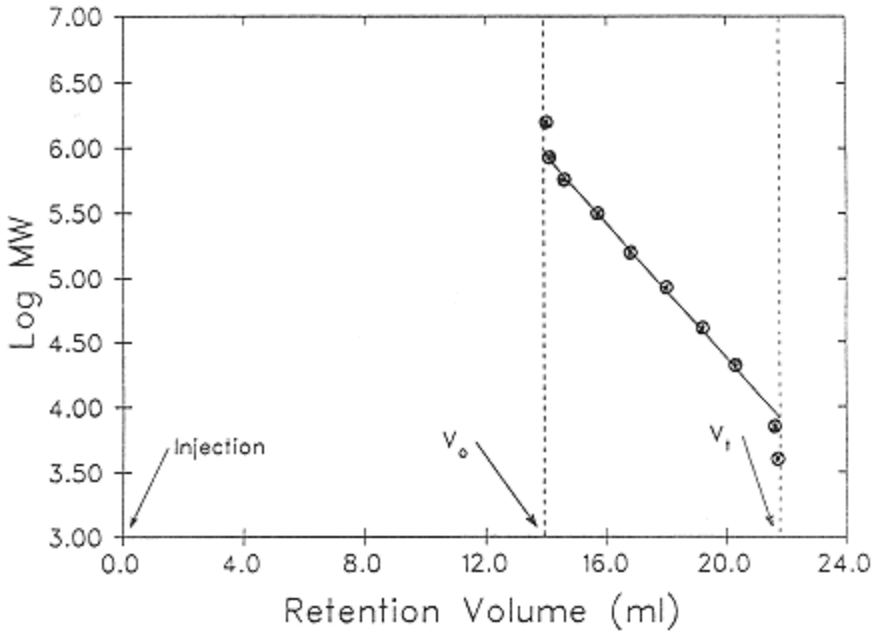

Figure 2.
Typical SEC calibration curve: logarithm of molecular weight versus retention volume.

spectively, to be discriminated by this column and thus appear at the two extremes of the selective permeation range.

The capacity factor k' is an index used in chromatography to define the elution position of a particular chromatographic component with respect to the solvent front, which in SEC occurs at V_t. Because all macromolecular separation in SEC occurs before V_t, k' is negative. In all other forms of liquid chromatography k' is positive. A further consequence of this difference is that separation in SEC occurs over one column set volume (in the selective permeation range), whereas in other forms of high-performance liquid chromatography (HPLC) separation may occur over many column volumes. Thus components in a mixture analyzed by other HPLC forms are commonly baseline resolved but SEC separations of macromolecules tend to be broad envelopes. Note that it is not necessary to separate polymer molecules by the number of repeat units to determine the molecular weight distribution. (It is possible to resolve very low molecular weight components if a sufficient number of small pore size columns are utilized.) To understand how these differences come about, one must consider the thermodynamics of chromatographic processes.

For any form of (gas or liquid) chromatography, one can define the distribution of solute between the stationary and mobile phases by an equilibrium (2). At equilibrium the chemical potentials of each solute component in the two phases must be equal. The driving force for solute migration from one phase to the other is the instantaneous concentration gradient between the two phases. Despite the movement of the mobile phase in the system, the equilibrium exists because the solute diffusion into and out of the stationary phase is fast compared with the flow rate. Under dilute solution conditions, the equilibrium constant (the ratio of solute concentrations in the stationary to the mobile phases) can be related to the standard Gibbs free-energy difference between the phases at constant temperature and pressure:

$$\Delta G^\circ = -RT \ln K \quad (1)$$

and

$$\Delta G^\circ = \Delta H^\circ - T\,\Delta S^\circ \quad (2)$$

where ΔH° and ΔS° are the standard enthalpy and entropy differences between the phases, respectively. R is the gas constant and T is the absolute temperature.

In other modes of liquid chromatography the basis of separation involves such phenomena as partitioning, adsorption, and ion exchange, all of which are energetic in nature because they involve intermolecular forces between the solute and stationary phase. In such cases the free energy can be approximated by the enthalpy term alone: the entropy term is negligible, and the equilibrium constant is given by

$$K_{LC} \simeq e^{-\Delta H^\circ/RT} \quad (3)$$

The typical exothermic interaction between the solute and stationary phase leads to a negative enthalpy difference and hence a positive value for the exponent in Equation (3). This in turn leads to an equilibrium constant greater than 1 and causes solute peaks to elute later than the solvent front.

In SEC the solute distribution between the two phases is controlled by entropy alone; that is, the enthalpy term is here taken to be negligible. In SEC the equilibrium constant becomes

$$K_{SEC} \simeq e^{\Delta S^\circ/R} \quad (4)$$

The entropy S is a measure of the degree of disorder and can be expressed as (3)

$$S = k \ln \Omega \quad (5)$$

where k is the Boltzmann constant and Ω is the number of equally probable micromolecular states. The relative ability of a small and a larger macromolecule to access an individual pore greater in size than the larger molecule is depicted in Figure 3. The number of ways in which the individual molecules can occupy space within the pore is given by the number of grid positions (representing individual states) allowed to them. The smaller molecule is retained longer within the pore than the larger because its number of equally probable states is greater (and hence it possesses a larger entropy). Yet, because the number of equally probable states is much smaller inside the pore than in the interstitial space for an individual molecule, solute permeation in SEC results in a *decrease* in entropy. This results in a negative exponent in Equation (4). K_{SEC} is less than 1 and solutes elute before the solvent front. SEC is also inherently temperature independent as opposed to the other liquid chromatographic separation phenom-

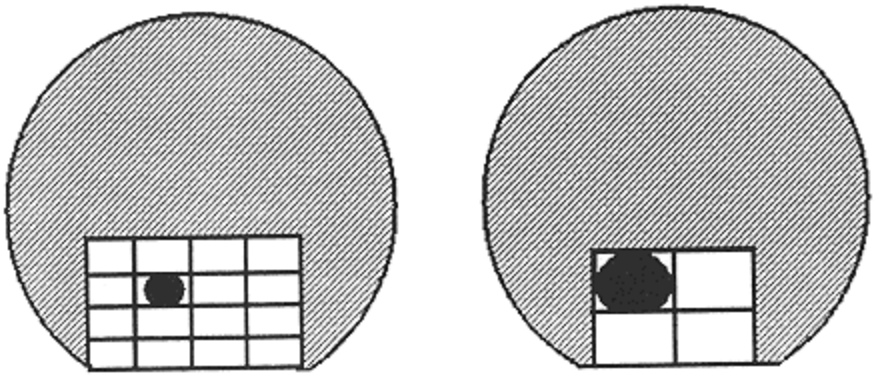

Figure 3.
Entropy of macromolecular retention in a pore: the smaller molecule at left has four times as many possibilities for retention as the molecule at right.

ena, as can be seen by comparing Equations (3) and (4). (Temperature has an indirect effect on SEC separations through its influence on the viscosity of polymeric solutions. The viscosity determines the mass-transfer rate of polymer molecules into and out of the pores of the packing material—hence the elution of the sample.)

Experimental Conditions for SEC

System Overview

A typical SEC system is essentially a specialized isocratic high-performance liquid chromatograph. A schematic is presented in Figure 4. First a solvent reservoir, typically 1–4 liters in size, is filled with the SEC mobile phase. It is commonly sparged with helium to degas it and prevent air bubbles from entering the detector downstream. A high-pressure pump capable of operating pressures up to 6000 psi forces the mobile phase through line filters and pulse dampeners to the sample injector, where an aliquot of dilute polymer solution (prepared using the same mobile-phase batch as contained in the reservoir) is introduced.

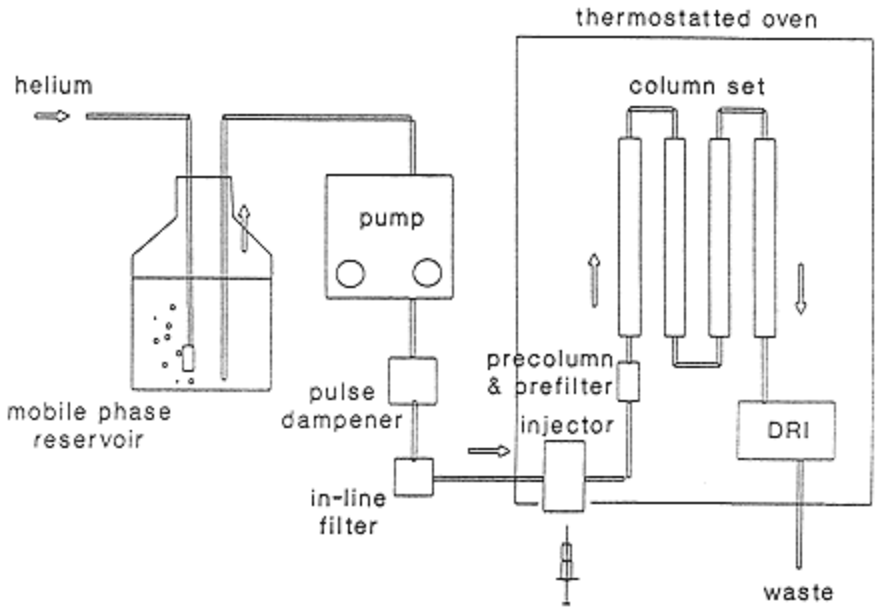

Figure 4.
A generic size exclusion chromatograph.

The sample, which initially exists as a narrow band in the system, is then carried through the precolumn and the analytical column set, where molecular size discrimination occurs. The discriminated sample elutes from the column set and passes through a universal detector, which generates an electrical (millivolt) signal proportional to the instantaneous sample concentration. The sample and mobile phase then exit the detector and are carried to a waste container; the electrical signal is transmitted to an integrator, recorder, or computer for display and/or further processing.

Universal (Concentration) Detectors

The most common type of universal detector by far is the differential refractive index (DRI) detector. (Here, the word "universal" denotes the ability to respond to all chemical functionalities.) It senses differences in refractive index between a moving (sample containing) stream and a static reference of mobile phase using a split optical cell. It responds well (at a moderate concentration level) to most polymeric samples, provided that they are different in refractive index from the mobile phase in which they are dissolved. Despite the temperature independence of the SEC separation phenomenon, the DRI is highly temperature sensitive as a result of the strong temperature dependence of refractive index. Thus one normally thermostats the DRI in a constant temperature oven along with the columns and injector (as in Figure 4). The temperature chosen is at least 5–10°C above ambient.

It is generally assumed that the response of the DRI is equally proportional to polymer concentration in all molecular weight regimes. Unfortunately, this assumption breaks down at low molecular weights (less than several thousand atomic mass units, AMU) at which the polymer end groups represent a non-negligible portion of the molecular mass and change the refractive index. The DRI is also very sensitive to backpressure fluctuations as a result of variations in flow rate caused by the pump. This effect (especially of reciprocating piston pumps) is compensated for by the use of pulse dampeners, as shown in Figure 4.

Other common types of concentration detectors are the ultraviolet (UV) and infrared (IR) detectors. Neither are truly universal detectors, but they are able to respond to a variety of individual chemical functional groups (chromophores) provided that these functional groups are not contained in the mobile phase. The IR detector is slightly more sensitive than the DRI detector; the UV detector is several orders of magnitude more sensitive. The last is most commonly employed for polymers containing aromatic rings or regular backbone unsaturation, and the IR detector has been used largely to characterize polyolefins. Other less commonly utilized concentration detectors include the fluorescence, dielectric constant, flame ionization, and evaporative light-scattering detectors (the latter produced by Varex Corp.).

Mobile Phase and Temperature

The mobile phase should be chosen carefully to fit certain criteria: it must completely dissolve the polymer sample in a continuous solution phase (non-θ condition), it must be low enough in viscosity for the SEC system to operate in a normal pressure range, and it must effectively prevent the polymer molecules from interacting energetically with the stationary phase (e.g., adsorption). Failure to achieve even one of these criteria results in the inability of the system to characterize the sample properly. Temperature is a useful parameter to adjust when one or more of these conditions has not been met but when one is constrained to use a particular mobile phase. Certain polymers (e.g., polyesters and polyolefins) may achieve dissolution only at elevated temperatures. The viscosity of inherently viscous mobile phases may also be lowered by raising the temperature.

The analysis of polymers containing one or more formal, like charges in every repeat unit (i.e., polyelectrolytes) incurs one additional requirement of the mobile phase. When solubilized in water, the repulsion of like charges along the polyelectrolyte chain causes it to take on an extended conformation (4). For normal SEC to be performed on a polyelectrolyte in an aqueous medium, its conformation must be made to reflect that of a random coil (Gaussian chain). This counteracting of the "polyelectrolyte effect" is generally accomplished by sufficiently raising the ionic strength with the use of simple salts and sometimes with concomitant pH adjustment. The former provides counterions to screen the like polymeric charges from one another and permits the extended chain to relax. The latter is used to neutralize all residual acid or basic groups. (When fully charged, these groups are no longer available to participate in hydrogen bonding interactions with the stationary phase.)

For example, it has been demonstrated that normal SEC behavior can be obtained for polymethyl vinyl ether-comaleic acid using a mobile phase consisting a of pH 9 buffer system [prepared from tris(hydroxymethyl) aminomethane and nitric acid] modified with 0.2 M $LiNO_3$ (5). Halide salts should be completely avoided: they tend to corrode the stainless steel inner surfaces of the SEC system, which in turn causes injector fouling and column contamination.

Stationary Phases

When selecting an optimum stationary phase, there are additional criteria to be met: the packing material should not interact chemically with the solute (i.e., sample), it must be rendered completely wet by the mobile phase but should not suffer adverse swelling effects, it must be stable at the required operating temperature, and it must have sufficient pore volume and an adequate range of pore sizes to resolve the sample's molecular weight distribution. For high-

performance SEC, either semirigid polymeric gels or modified, rigid silica particles are typically used.

Columns are available, from a number of vendors, packed with monodisperse or mixed-bed pore size particles. The latter are useful for building a column set that discriminates (usually on a log-linear basis) at least four molecular weight decades (i.e., several hundred to several million AMU). For rigid particles it is also possible to design a column set consisting of individual columns of different, single pore sizes yielding a calibration curve log-linear in molecular weight if the pore size and total pore volume of each column type are known (6). Typical available pore sizes range from 60 to 4000 Å. High-performance packing materials generally have particle sizes in the range of 5–10 μm with efficiencies of several thousand theoretical plates per 15 cm column.

For organic mobile phases, the most common column packings are cross-linked (with divinylbenzene) polystyrene gels or trimethylsilane-derivatized silica. For aqueous mobile phases the most common are cross-linked hydroxylated polymethacrylate or polypropylene oxide gels (7) or glyceryl-derivatized (diol) silica (8). In general, rigid packings have several advantages over semirigid gel packings: they are tolerant of a greater variety of mobile phases, they equilibrate rapidly on changing solvents, they are stable at the elevated temperatures required to characterize certain polymers, and the pore sizes are more easily defined, which facilitates column set design. Silica-based rigid packings are prone to adsorptive effects, however, and must be carefully derivatized to react away or screen labile silanol groups. An overview of typical column packing-mobile phase combinations was recently published by Yau et al (9). The reader is referred to comprehensive discussions of SEC stationary phases covered in Chapter 2 (semirigid polymeric gels) and Chapter 3 (modified, rigid silica) of this monograph.

Sample Size and Mobile-Phase Flow Rate

Sample size is defined by both the volume of the aliquot injected as well as by the concentration of the sample solution. Use of excessively large sample volumes can lead to significant band broadening, resulting in loss of resolution and errors in molecular weight measurement. As a rule of thumb, sample volumes should be limited to one-third or less of the baseline volume of a monomer or solvent peak measured with a small sample (10). The optimum injection volume is a function of the size and number of the columns employed but generally ranges between 25 and 200 μl.

Sample concentration should be minimized consistently with the sensitivity of the concentration detector employed. The use of high sample concentrations can result in peak shifts to lower retention volumes and band broadening caused by “viscous fingering” or spurious shoulders appearing on the tail of the peak.

These phenomena are likely related to a combination of causes, including chain entanglements and an inability to maintain the equilibrium between solute concentrations inside the pores and in the interstitial space. These effects are particularly problematical for high-molecular-weight polymers (of the order of 1 million AMU). Optimum sample concentrations may range from 0.1% for high-molecular-weight samples to greater than 1.0% for low-molecular-weight samples.

Another unwanted viscosity effect, the shear degradation of high-molecular-weight polymers at high flow rates that results in erroneous (larger) retention volumes and (lower) molecular weights, is avoided by minimizing the flow rate. In addition, the use of high flow rates can result in considerable loss of column efficiency because, under such conditions, mass transfer or diffusion in and out of the pores is not fast enough vis-à-vis the solute migration rate along the length of the column. Thus, flow rates in the general vicinity of 1 ml/minute are most commonly employed and represent a good compromise between analysis time and resolution. The reader is referred to Chapter 5 (aqueous SEC) and Chapter 6 (nonaqueous SEC) for comprehensive discussions of sample size and flow rate optimizations.

Calibration Methodology and Data Analysis in SEC

In modern high-performance SEC only four calibration methods are commonly employed. Three of these can be utilized in conjunction with a single (i.e., concentration) detector SEC system: direct (narrow) standard calibration, polydisperse or broad standard calibration, and universal calibration. The fourth type of SEC calibration requires the use of a second, molecular weight-sensitive detector connected in series with the concentration detector (and in front of it when employing a DRI). The purpose of calibration in SEC is to define the relationship between molecular weight (or typically its logarithm) and retention volume in the selective permeation range of the column set used and to calculate the molecular weight averages of the sample under investigation.

Direct Standard Calibration

In the direct standard calibration method, narrowly distributed standards of the same polymer being analyzed are used. The retention volume at the peak maximum of each standard is equated with its stated molecular weight. This is the simplest method, but it is generally restricted in its utility owing to the lack of availability of many different polymer standard types. It also requires a sufficient number of standards of different molecular weights to cover completely the entire dynamic range of the column set or, at least, the range of molecular

weights spanned by the sample molecular weight distributions. Polystyrene (used for nonaqueous SEC) and polyethylene oxide or polyethylene glycol standards (used in aqueous SEC) are the only narrow standards commonly available. It is instructive to study the mechanism of narrow standard calibration because all the other methods are based upon it. A thorough review of this subject has been provided by Cazes (11).

In this approach, the raw chromatogram obtained as output from the concentration detector is divided into a number of time slices of equal width, as depicted in Figure 5. For a polydisperse sample the number of time slices must be greater than 25 for the computed molecular weight averages to be unaffected by the number of time slices used. (Most commonly available SEC data programs utilize a minimum of several hundred time slices routinely for each analysis.) An average molecular weight is assigned to each time slice based upon the calibration curve, and it is further assumed for computational purposes that each time slice is monodisperse in molecular weight. A table is constructed with one row assigned to each time slice. The following columns are created for this table: retention volume, area A_i, cumulative area, cumulative area percentage, molecular weight M_i, A_i divided by M_i, and A_i times M_i. The area column and the last two are also summed for the entire table.

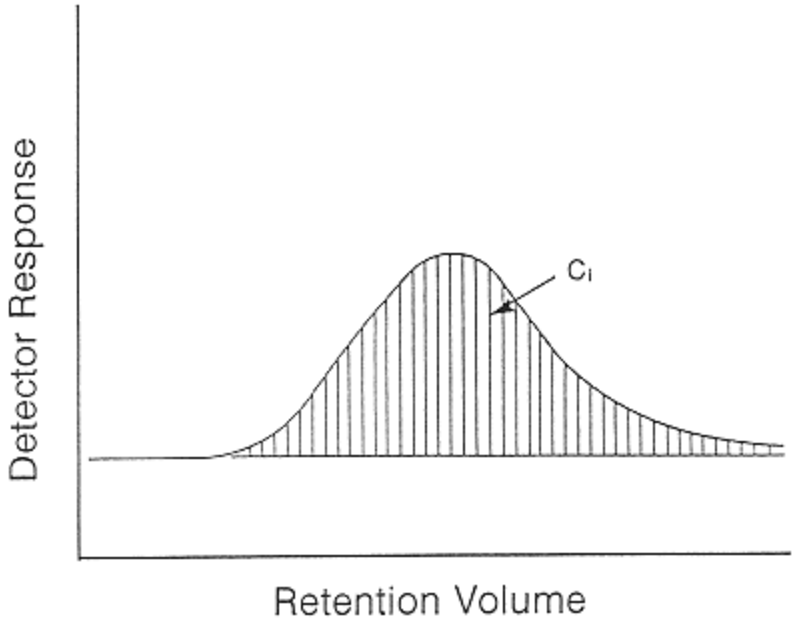

Figure 5.
Time-sliced peak output from a concentration detector (DRI).

Once this data table has been completed, it is possible to compute the molecular weight averages or moments of the distribution. The most common averages defined in terms of the molecular weight at each time slice and either the number of molecules n_i or the area of each time slice are

$$\overline{M}_N = \frac{\sum_i n_i M_i}{\sum_i n_i} = \frac{\sum_i A_i}{\sum_i A_i/M_i} \qquad \text{number average} \tag{6}$$

$$\overline{M}_V = \left(\frac{\sum_i n_i M_i^{1+a}}{\sum_i n_i M_i}\right)^{1/a} = \left(\frac{\sum_i A_i M_i^a}{\sum_i A_i}\right)^{1/a} \qquad \text{viscosity average} \tag{7}$$

where a is the Mark-Houwink exponent.

$$\overline{M}_W = \frac{\sum_i n_i M_i^2}{\sum_i n_i M_i} = \frac{\sum_i A_i M_i}{\sum_i A_i} \qquad \text{weight average} \tag{8}$$

$$\overline{M}_Z = \frac{\sum_i n_i M_i^3}{\sum_i n_i M_i^2} = \frac{\sum_i A_i M_i^2}{\sum_i A_i M_i} \qquad Z \text{ average} \tag{9}$$

The dispersity or polydispersity D is given by the ratio of the weight to the number-average molecular weight and is a measure of the breadth of the molecular weight distribution. The SEC number, viscosity, weight, and Z averages correspond to those obtained classically by osmometry, capillary viscometry (intrinsic viscosity), light-scattering photometry, and sedimentation equilibrium methods, respectively. The viscosity-average molecular weight approaches the weight average as the Mark-Houwink exponent a approaches 1. (See the subsequent discussion concerning universal calibration.) The Z and weight-average molecular weights are most influenced by the high-molecular-weight portion of the distribution, whereas the number average is influenced almost exclusively by the low-molecular-weight portion. Narrow standards employed in this calibration method are ideally monodisperse but practically must have dispersities less than 1.1.

Band-Broadening Measurement and Correction

It is important to review the molecular weight distribution generated for symmetrical and unsymmetrical band broadening that results in non-negligible errors in computed molecular weight averages. An American Society for Testing and

Materials (ASTM) method describes a procedure to calculate the magnitude of these effects and to correct the molecular weight averages (12). It is necessary to know both $\overline{M}_W$ and $\overline{M}_N$ for each of the entire series of narrow standards used. The symmetrical band-broadening factor Λ is calculated for each standard according to

$$\Lambda = \frac{1}{2}\left(\frac{\overline{M}_N(t)}{\overline{M}_N(u)} + \frac{\overline{M}_w(u)}{\overline{M}_w(t)}\right) \quad (10)$$

The skewing or unsymmetrical factor sk is calculated according to

$$\mathrm{sk} = \frac{\Phi - 1}{\Phi + 1} \quad (11)$$

where

$$\Phi = \frac{\overline{M}_N(t)\overline{M}_w(t)}{\overline{M}_N(u)\overline{M}_w(u)} \quad (12)$$

and *t* and *u* refer to the true and uncorrected moments. Under ideal conditions, $\Lambda = 1$ and sk = 0 and no corrections are necessary. Practically this is never the case, but if these values are 1.05 and 0.05 or less, respectively, then the resulting corrections are small and can be ignored. If, on the other hand, they are larger than these values, the sample's distribution moments may be corrected according to

$$\overline{M}_N(t) = \overline{M}_N(u)\ (1 + \mathrm{sk})\Lambda \quad (13)$$

and

$$\overline{M}_w(t) = \frac{\overline{M}_w(u)}{(1 - \mathrm{sk})\Lambda} \quad (14)$$

A description of the correction for band broadening of the entire molecular weight distribution is beyond the scope of this introduction to SEC, but the interested reader is referred to the technique described by Tung with Runyan (13,14). A better approach is to employ sufficiently good experimental practices to obviate the need for band-spreading corrections altogether. This has been demonstrated when sufficiently long column lengths and low flow rates are used (15).

Polydisperse or Broad Standard Calibration

In the polydisperse standard method, one employs a broadly distributed polymer standard of the same chemical type as the sample. The sample and the standard are frequently the same material. The main requirements of this technique are

that the MWD of the standard must span most if not all of the sample's dynamic range and that two moments of the standard's distribution, $\overline{M}_N$ and either $\overline{M}_W$ or $\overline{M}_V$, must be accurately known as a result of ancillary measurements. This method is particularly useful when narrow MWD standards and molecular weight-sensitive detectors are unavailable and universal calibration is impractical because of the lack of information regarding appropriate Mark-Houwink coefficients and/or the inability to perform intrinsic viscosity measurements.

Balke, Hamielec et al. described a computer method to determine a calibration curve, expressed by

$$V_e = C_1 - C_2 \log M \quad (15)$$

where V_e is the elution (or retention) volume and M is the molecular weight (16). Their original method involved a cumbersome, simultaneous search for the constants C_1 and C_2, which was prone to false convergence. Revised methods featured a sequential, single-parameter search (17,18). These methods rely on the fact that the dispersity D is a function of the slope C_2 alone. Arbitrary values are first assigned to the two constants. The resulting calibration equation is iteratively applied to the time slice data and the slope value is optimized to minimize the difference between the true and computed dispersities. Once the slope has been determined it is fixed, and the intercept C_1 is optimized to minimize the difference between the true and computed moments (either individually or their sum).

Universal Calibration

Benoit and coworkers demonstrated that it is possible to use a set of narrow polymer standards of one chemical type to provide absolute molecular weight calibration to a sample of a different chemical type (19,20). To understand how this is possible, one must first consider the relationship between molecular weight, intrinsic viscosity, and hydrodynamic volume, the volume of a random, freely jointed polymer chain in solution. This relationship has been described by both the Einstein-Simha viscosity law for spherical particles in suspension,

$$[\eta] = C \frac{V_h}{M} \quad (16)$$

and the Flory-Fox equation for linear polymers in solution,

$$[\eta] = \Phi \frac{\langle s^2 \rangle^{3/2}}{M} \quad (17)$$

where $[\eta]$ is the intrinsic viscosity, V_h is the hydrodynamic volume, $\langle s^2 \rangle^{1/2}$ is the root-mean-square radius of gyration of the polymer chain, and C and Φ are constants (21). If either equation is multiplied by M, the molecular weight, the

resulting product $[\eta]M$ is seen as proportional to hydrodynamic volume. (Note that the cube of the root-mean-square radius of gyration is also proportional to volume.) Benoit and coworkers plotted this product versus elution volume for a number of chemically different polymers investigated under identical SEC conditions and found that all points lay on the same calibration curve (19,20). This calibration behavior was said to be "universal" for all the polymer types studied.

In actual practice, one establishes the relationship

$$[\eta]_1 M_1 = [\eta]_2 M_2 \quad (18)$$

where the subscripts 1 and 2 refer to the standard and sample polymers, respectively. Even if the intrinsic viscosities are known or can be measured for each standard, it is unlikely that the value of intrinsic viscosity would be known for each time slice in the molecular weight distribution of the sample polymer. Thus, Equation (18) must be further modified to make it more useful. This can be accomplished with the use of the Mark-Houwink equation

$$[\eta] = KM^a \quad (19)$$

where the coefficient K and exponent a are known as the Mark-Houwink constants. These constants are a function of both the polymer and its solvent environment (including temperature). If the constants are available from the literature or can be determined for the sample polymer using narrow fractions in the SEC mobile phase, then one can substitute the Mark-Houwink term for $[\eta]$ into Equation (18) to yield

$$\log M_2 = \frac{1}{1 + a_2} \log \frac{K_1}{K_2} + \frac{1 + a_1}{1 + a_2} \log M_1 \quad (20)$$

which is an expression for the sample molecular weight in terms of the standard molecular weight and both sets of Mark-Houwink constants.

Molecular Weight-Sensitive Detectors

It is possible to add a second, molecular weight-sensitive detector to an SEC system to provide a direct means of absolute molecular weight calibration without the need to resort to external standards. These detectors represent refinements in classic techniques, such as light-scattering photometry, capillary viscometry (for intrinsic viscosity), and membrane osmometry for on-line molecular weight determination. Yau recently published a review of this subject with comparisons of the properties and benefits of the principal detectors currently in use (22). The present discussion is restricted to light-scattering and viscometry detectors because Yau's osmometry detector is not yet commercially available. The reader is referred to Chapter 4 for a comprehensive discussion of molecular weight-sensitive detectors.

Low-Angle Laser Light-Scattering Detection

The low-angle laser light-scattering detector (LALLS) was originally developed by Kaye with Havelik (23,24) and is now marketed by LDC Analytical. Two models, the KMX-6 and the CMX-100, are available from this company. Although the former is said to be capable of a small scattering angle variation, both units are essentially fixed, low-angle photometers. Overviews of the basic operating principles were provided by McConnell (25) and Jordan (26). [The other current LALLS vendors are Tosoh Corp. of Tokyo, Japan (Model LS-8) and Polymer Laboratories, Ltd. of Shropshire, England (Model PL-LALS). The latter is based upon the design of the Tosoh instrument but contains an integrated refractive index detector.]

The working equation for the determination of the weight-average molecular weight by light scattering (using vertically polarized light), due to Debye, is

$$\frac{Kc}{\Delta R_\theta} = \frac{1}{\overline{M}_w P(\theta)} + 2A_2 c \qquad (21)$$

where the constant K is given by

$$K = \frac{2\pi^2 n^2}{N_0 \lambda^4}\left(\frac{dn}{dc}\right)^2 \qquad (22)$$

and N_0 is Avogadro's number, n is the refractive index of the solution at the incident wavelength λ, and A_2 is the second virial coefficient, a measure of the compatibility between the polymer solute and the solvent. The term dn/dc is known as the specific refractive index increment and reflects the change in solution refractive index with change in solute concentration. The term ΔR_θ is the excess Rayleigh ratio and represents the solution ratio of scattered to incident radiation minus that of the solvent alone. The particle scattering function $P(\theta)$, which is the angular dependence of the excess Rayleigh ratio, is defined by

$$\frac{1}{P(\theta)} = 1 + \frac{16\pi^2}{3\lambda^2}\langle s^2\rangle \sin^2\left(\frac{\theta}{2}\right) \qquad (23)$$

where $\langle s^2\rangle$ is the mean square radius of gyration of the polymer chain. The Debye equation [Equation (21)] is actually a virial equation that includes higher power concentration terms; these higher terms can be neglected if the concentrations employed are small.

In the classic light-scattering experiment one solves the Debye equation over a wide range of angles and concentrations for unfractionated polymer samples. The data are plotted in a rectilinear grid known as a Zimm plot in which the ordinate and abscissa are $Kc/\Delta R_\theta$ and $\sin^2 \theta/2 + kc$, respectively, where k is an arbitrary constant used to adjust the spacing of the data points (27). The Zimm plot yields parallel lines of either equal concentration or angle. The slope

of the $\theta = 0$ line yields $\langle s^2 \rangle$ while that of the $c = 0$ line yields A_2. The intercept of either of these lines is $\overline{M}_w$. One of the major problems associated with classic light-scattering experiments relates to the effect of dust: if the entire solution contained in the large cell volume typically used is not kept scrupulously free of dust, large scattering errors can result.

The LALLS device developed by Kaye provides three significant changes that make it amenable as an SEC molecular weight detector: an intense, monochromatic light source (a HeNe laser, $\lambda = 632.8$ nm) is used, the cell volume is reduced to 10 μl and the scattering volume to 0.1 μl (26), and the single scattering angle employed is in the range of 2–7°. The net result is that the device is extremely sensitive: it can readily distinguish scattering as a result of an individual dust particle flowing through the cell from that caused by the sample, and the angular dependence is removed from the Debye equation. The latter follows from the fact that the value of $\sin^2(\theta/2)$ for a small angle is essentially zero. Under this condition, the Debye equation becomes

$$\frac{Kc}{\Delta R_\theta} = \frac{1}{\overline{M}_w} + 2A_2c \quad (24)$$

or

$$\overline{M}_w = \frac{1}{Kc/\Delta R_\theta - 2A_2c} \quad (25)$$

and $\overline{M}_w$ can be obtained at a single finite concentration provided that A_2 is known from the literature or is determined from the slope of Equation (24) using a series of concentrations. However, the removal of the angular variability from the LALLS detector means that it cannot be used to determine molecular size, that is, $\langle s^2 \rangle$.

The SEC/LALLS experiment is then conducted as follows. The LALLS and concentration detectors are connected in series after the SEC column set and interfaced with the computing system. Time slice data from both detectors is acquired, as shown in Figure 6, to have corresponding time slices in each distribution. To accomplish this, the time delay between the detectors must be accurately known. The instantaneous concentration c_i in either detector may be computed using

$$c_i = \frac{mA_i}{V\sum_i A_i} \quad (26)$$

where m is the sample mass injected, V is the effluent volume passing through the cell in the time of a single time slice, and A_i is the area of a concentration detector time slice. If one assumes that each time slice is sufficiently narrow to

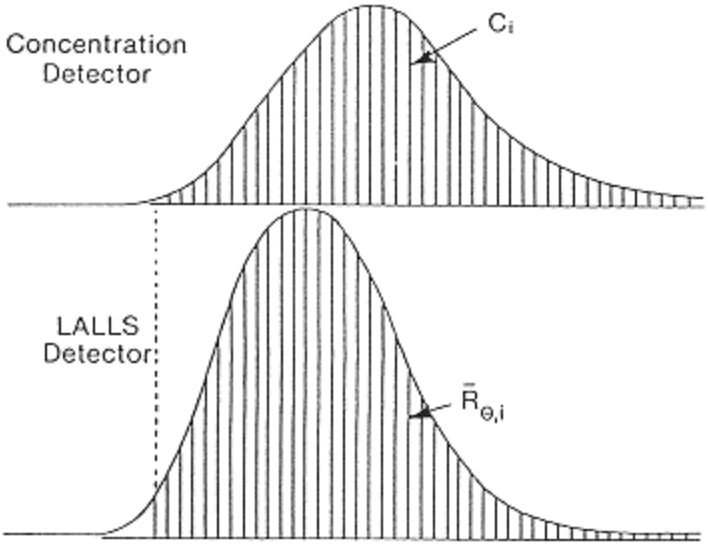

Figure 6.
Overlay of time-sliced peak output from a dual (DRI/LALLS) detector system.

be monodisperse, then the instantaneous molecular weight is determined using Equation (25). This data collectively constitute the absolute molecular weight distribution calibration.

It it generally acknowledged that LALLS used either as a stand-alone light-scattering photometer or as an SEC detector provides accurate values for $\overline{M}_w$. Yet in 1987, a number of independent workers reported that the ability of SEC/LALLS to determine $\overline{M}_N$ accurately was dependent on the polydispersity of the sample: the greater the polydispersity, the poorer the estimate of $\overline{M}_N$ (28–30). In performing SEC/LALLS on high-molecular-weight polyvinyl pyrrolidone, Senak et al. (28) demonstrated that this phenomenon is caused by the lack of sensitivity of the LALLS detector toward the low-molecular-weight portion of a broad distribution *(D* = 6.0). As shown in Figure 7, the DRI detector is still responding (the shaded area) in a region where the LALLS detector is not. As discussed by Hamielec et al., an electronic switching device and a technique for optimizing the signal-to-noise ratio of the LALLS detector throughout the LALLS chromatogram are needed to improve its utility (31).

The LALLS detector coupled to an SEC was also reported to be useful in measuring the relative amount of branching of a branched relative to a linear polymer of the same chemical type (32–34). The parameter of interest is g_M,

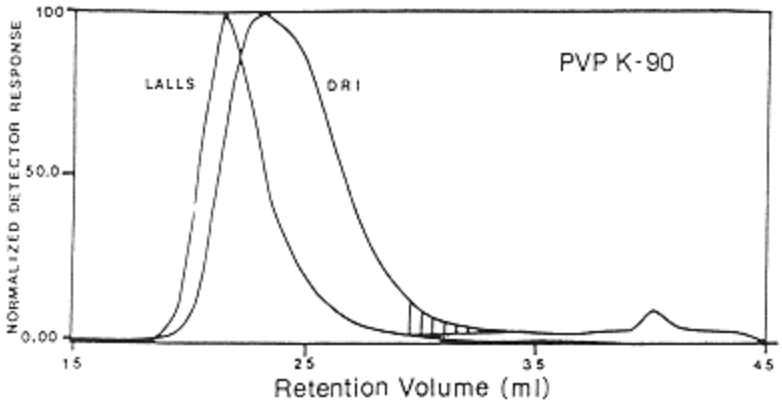

Figure 7.
Relative sensitivity of a LALLS versus a DRI detector for a broadly dispersed sample of polyvinyl pyrrolidone.

defined by Zimm and Stockmayer as

$$g_M = \left(\frac{\langle s^2\rangle_b}{\langle s^2\rangle_l}\right)_M = \left(\frac{[\eta]_b}{[\eta]_l}\right)_M \quad (27)$$

or the ratio of the mean square radii of gyration of a branched to a linear polymer at a constant molecular weight and, through the Flory-Fox equation [Equation (17)], the ratio of their intrinsic viscosities (35). The measured quantity in the SEC/LALLS experiment, however, is g_V, the branching index at constant elution volume: the ratio of molecular weights of branched to linear polymers. It has been shown that the Mark-Houwink equation [Equation (19)] can be used to convert g_V to g_M to give

$$g_M = g_V^{a+1} = \left(\frac{M_l}{M_b}\right)_V^{a+1} \quad (28)$$

where a is the Mark-Houwink exponent of the linear polymer (32,33). In principle, the variation in the branching index can be determined as a function of molecular weight provided that the exponent a is known. Complications may arise if there is significant band broadening in the SEC system and/or if the samples are highly polydisperse, as previously discussed. It must be emphasized that the ability of the SEC/LALLS to produce branching information is strictly a result of the discrimination of molecular size by the SEC column set because LALLS has no molecular size capability itself.

Multiangle Laser Light-Scattering Detection

The multiangle laser light-scattering detectors (MALLS) developed and produced by Wyatt Technology Corp. (Models DAWN B and DAWN F), unlike LALLS, have the ability to measure scattered light at either 15 (23–128°) or 18 (5–175°) different angles, depending upon the model selected (36,37). In addition, these data can be obtained simultaneously using an array of detectors. The mathematics employed is essentially based upon Equations (21) through (23). One of the claimed capabilities of this instrument is the determination of polymer radius of gyration distribution when used as an on-line SEC detector. The ability of MALLS to make this measurement accurately for very large and very small polymer molecules has recently been in dispute (38,39).

Right-Angle Laser Light-Scattering Detection

At the 1991 International GPC Symposium (San Francisco), M. Haney of Viscotek Corp. introduced a new laser light-scattering detector (RALLS) that operates at a fixed angle of 90° (40). Because the particle-scattering function $P(\theta)$ cannot be neglected at this angle (for large molecules), this device must be used in conjunction with another molecular weight-sensitive detector (i.e., a viscosity detector) to yield absolute molecular weight information. An iterative calculation is performed on each chromatogram time slice using a simplified form of the Debye Equation (Eq. 21), the Flory-Fox Equation (Eq. 17), and the particle-scattering function Equation (Eq. 23). The convergence condition is no further change in either molecular weight, radius of gyration, or $P(\theta)$. Viscotek claims an inherently better signal-to-noise ratio (because of lower noise) for the RALLS detector versus either LALLS or MALLS operating at close to 0°. This appears to be particularly significant for lower molecular weight species. At the time of this writing, no peer review references exist concerning the RALLS detector.

Viscometric Detection

An alternative molecular weight-sensitive detector is the on-line viscometer. All current instrument designs depend upon the relationship between pressure drop across a capillary through which the polymer sample solution must flow and the viscosity of the solution. This relationship is based upon Poiseuille's law for laminar flow of incompressible fluids through capillaries:

$$\eta = \frac{\pi \, \Delta P \, r^4 t}{8 V l} \quad (29)$$

where η is the absolute viscosity, ΔP is the observed pressure drop, t is the efflux time, and r, l, and V are the radius, length, and volume of the capillary, respectively. In a capillary viscometer operating at ambient pressure, one can

define the relative viscosity η_r as the ratio of the absolute viscosities of solution to solvent, which is equal to the ratio of their efflux times at low concentrations. Yet when such a capillary is used as an SEC detector, the flow time is constant the relative viscosity becomes

$$\eta_r = \frac{\eta}{\eta_0} = \frac{\Delta P}{\Delta P_0} \quad (30)$$

the ratio of the solution to solvent pressure drops. Because the intrinsic viscosity $[\eta]$ is defined as

$$[\eta] = \lim_{c \to 0} \frac{\ln \eta_r}{c} \quad (31)$$

one can combine Equations (30) and (31) to give

$$[\eta] = \frac{\ln \Delta P/\Delta P_0}{c} \quad (32)$$

provided that c is very small (generally less than 0.01 g/dl under SEC conditions).

Thus an on-line viscosity detector is capable of providing intrinsic viscosity distribution information directly using time slicing analogous to laser light-scattering detection. To act as a molecular weight detector, however, one must either obtain the Mark-Houwink constants to use the Mark-Houwink equation or possess a set of molecular weight standards that obey the universal calibration behavior. If both intrinsic viscosity and absolute molecular weight information are available for each time slice, the Flory-Fox equation may be employed to generate a similar distribution for the mean square radius of gyration (22).

A single capillary detector developed by Ouano (41) and further advanced by Lesec et al. (42–44) and Kuo et al. (45) has been internally incorporated into the Millipore/Waters Model 150 CV SEC system. Chamberlin and Tuinstra developed a single-capillary detector that was directly incorporated within a conventional DRI detector (46,47). Haney developed a four-capillary detector with a Wheatstone bridge arrangement that was commercialized by Viscotek Corp. (48,49) and further evaluated by other workers (50,51). A dual, consecutive capillary detector developed by Yau (22) (and also commercialized by Viscotek Corp.) was said to be superior to the other designs because it was better able to compensate for flow rate fluctuations: its series arrangement would cause the two capillaries to be simultaneously and equally affected, thus exactly offsetting any disturbance.

General References

The interested reader is referred to several additional general references for supplemental information on the principles of SEC separations and selected applications. The first four (52–55) are compilations of papers presented by leading authorities at various International GPC Symposia sponsored by Waters Associates (a division of Millipore Corp.). The next two volumes (56,57) are introductory books published by two other HPLC/SEC vendors. Finally, an early monograph edited by Kirkland (58) contains an excellent introductory chapter on GPC (SEC). Although all these books are relatively old, they nevertheless contain valuable information that is still applicable and useful today.

Acknowledgments

The author is grateful to C. S. Wu for his encouragement and for useful discussions, to J. F. Tancredi for his support, to M. Krass and J. Bager for help in creating several figures, to LDC Analytical for permission to reprint the work of several other researchers, and to International Specialty Products for permission to publish this review.

References

1. F.W. Billmeyer, *Textbook of Polymer Science*, 2nd ed., Wiley-Interscience, New York, 1971, p. 28.

2. W.W. Yau, J.J. Kirkland, and D.D. Bly, *Modern Size Exclusion Chromatography*, Wiley-Interscience, New York, 1979, p. 27 ff.

3. G.S. Rushbrooke, Introduction to Statistical Mechanics, Oxford University Press, London, 1949, p. 11.

4. B. Vollmert, *Polymer Chemistry*, Springer-Verlag, New York, 1973, p. 537 ff.

5. C.S. Wu, L. Senak, and E.G. Malawer, *J. Liq. Chromatogr., 12*(15), 2901–2918 (1989).

6. E.G. Malawer, J.K. DeVasto, S.P. Frankoski, and A.J. Montana, *J. Liq. Chromatogr., 7*(3), 441–461 (1984).

7. T. Hashimoto, H. Sasaki, M. Airua, and Y. Kato, J. Polym. Sci., *Polym. Phys. Ed., 16,* 1789 (1978).

8. L.R. Snyder and J.J. Kirkland, *Introduction to Modern Liquid Chromatography,* 2nd ed., Wiley-Interscience, New York, 1979, p. 489.

9. W.W. Yau, J.J. Kirkland, and D.D. Bly, Size exclusion chromatography, Chapter 6, in *Chemical Analysis: High Performance Liquid Chromatography,* Vol. 98, P.R. Brown and R.A. Hartwick, eds., Wiley-Interscience, New York, 1989, pp. 293–295.

10. W.W. Yau, J.J. Kirkland, and D.D. Bly, *Modern Size Exclusion Chromatography,* Wiley-Interscience, New York, 1979, p. 240.

11. J. Cazes, *J. Chem. Ed., 43*(7,8) (1966).

12. ASTM Method D 3593-77, Standard Test Method for Molecular Weight Averages and Molecular Weight Distribution of Certain Polymers by Liquid Exclusion Chromatography (Gel Permeation Chromatography-GPC) Using Universal Calibration,

13. L.H. Tung, *J. Appl. Polym. Sci., 13,* 775 (1969).

14. L.H. Tung and J.R. Runyan, *J. Appl. Polym. Sci., 13,* 2397 (1969).

15. M.R. Ambler, L.J. Fetters, and Y. Kesten, *J. Appl. Polym. Sci., 21,* 2439–2451 (1977).

16. S.T. Balke, A.E. Hamielec, B.P. LeClair, and S.L. Pearce, *Ind. Eng. Chem., Prod. Res. Dev. 8,* 54 (1969).

17. M.J. Pollock, J.F. MacGregor, and A.E. Hamielec, *J. Liq. Chromatogr. 2,* 895 (1979).

18. E.G. Malawer and A.J. Montana, *J. Polym. Sci., Polym. Phys. Ed., 18,* 2303–2305 (1980).

19. H. Benoit, Z. Grubisic, P. Rempp, D, Decker, and J.G. Zilliox, *J. Chim. Phys., 63,* 1507 (1966).

20. Z. Grubisic, H. Benoit, and P. Rempp, *J. Polym. Sci.,* Polym. Lett., *B5,* 753–579 (1967).

21. C. Tanford, Physical Chemistry of Macromolecules, John Wiley & Sons, New York, 1961, p. 333 ff., p. 390 ff.

22. W.W. Yau, *Chemtracts: Makromol. Chem., 1*(1), 1–36 (1990).

23. W. Kaye, *Anal. Chem., 45*(2), 221A (1973).

24. W. Kaye and A.J. Havlik, *Appl. Opt., 12,* 541 (1973).

25. M.L. McConnell, *Am. Lab., 10*(5), 63 (1978).

26. R.C. Jordan, *J. Liq. Chromatogr., 3*(3), 439–463 (1980).

27. N.C. Billingham, *Molar Mass Measurements in Polymer Science,* John Wiley/Halsted, New York, 1977, p. 128 ff.

28. L. Senak, C.S. Wu, and E.G. Malawer, *J. Liq. Chromatogr., 10*(6), 1127–1150 (1987).

29. P. Froment and A. Revillon, *J. Liq. Chromatogr., 10*(7), 1383–1397 (1987).

30. O. Prochazka and P. Kratochvil, *J. Appl. Polym. Sci., 34,* 2325–2336 (1987).

31. A.E. Hamielec, A.C. Ouano, and L.L. Nebenzahl, J. Liq. Chromatogr., *1*(4), 527–554 (1978).

32. R.C. Jordan and M.L. McConnell, Characterization of branched polymers by size exclusion chromatography with light scattering detection, Chapter 6, in Size Exclusion Chromatography (GPC), ACS Symposium Series, No. 138, T. Provder, ed., ACS, 1980, pp. 107–129.

33. L.P. Yu and J.E. Rollings, *J. Appl. Polym. Sci., 33,* 1909–1921 (1987).

34. H.H. Stuting, I.S. Krull, R. Mhatre, S.C. Krzysko, and H.G. Barth, *LC-GC, 7*(5), 402–417 (1989).

35. B.H. Zimm and W.H. Stockmayer, *J. Chem. Phys., 17,* 1301 (1949).

36. P.J. Wyatt, C. Jackson, and G.K. Wyatt, *Am. Lab., 20*(5), 86 (1988).

37. P.J. Wyatt, C. Jackson, and G.K. Wyatt, *Am. Lab., 20*(6), 108 (1988).

38. W.W. Yau and S.W. Rementer, *J. Liq. Chromatogr., 13,* 627 (1990).

39. P.J. Wyatt, *J. Liq. Chromatogr., 14*(12), 2351–2372 (1991).

40. M.A. Haney, C. Jackson, and W.W. Yau, Proceedings of the 1991 International GPC Symposium, 1991, pp. 49–63.

41. A.C. Ouano, *J. Polym. Sci.* Symp. No. 43, 299–310 (1973).

42. L. Letot, J. Lesec, and C. Quivoron, *J. Liq. Chromatogr. 3*(3), 427–438 (1980).

43. J. Lesec, D. Lecacheux, and G. Marot, *J. Liq. Chromatogr., 11*(12), 2571–2591 (1988).

44. J. Lesec and G. Volet, *J. Liq. Chromatogr. 13*(5), 831–849 (1990).

45. C.Y. Kuo, T. Provder, and M.E. Koehler, *J. Liq. Chromatogr. 13*(16), 3177–3199 (1990).

46. T.A. Chamberlin and H.E. Tuinstra. U.S. Patent 4,775,943, October 4, 1988.

47. T.A. Chamberlin and H.E. Tuinstra, *J. Appl. Polym. Sci., 35*, 1667–1682 (1988).

48. M.A. Haney, *J. Appl. Polym. Sci., 30*, 3037–3049 (1985).

49. M.A. Haney, Am. Lab., *17*(4), 116–126 (1985).

50. P.J. Wang and B.S. Glasbrenner, *J. Liq. Chromatogr., 11*(16), 3321–3333 (1988).

51. D.J. Nagy and D.A. Terwilliger, *J. Liq. Chromatogr. 12*(8), 1431–1449 (1989).

52. J. Cazes, ed., *Liquid Chromatography of Polymers and Related Materials,* Chromatographic Science Series, Vol. 8, Marcel Dekker, New York, 1977.

53. J. Cazes and X. Delamare, eds., *Liquid Chromatography of Polymers and Related Materials II,* Chromatographic Science Series, Vol. 13, Marcel Dekker, New York, 1980.

54. J. Cazes, ed., *Liquid Chromatography of Polymers and Related Materials III,* Chromatographic Science Series, Vol. 19, Marcel Dekker, New York, 1981.

55. J. Janca, ed., *Steric Exclusion Liquid Chromatography of Polymers,* Chromatographic Science Series, Vol. 25, Marcel Dekker, New York, 1984.

56. R.W. Yost, L.S. Ettre, and R.D. Conlon, *Practical Liquid Chromatography, an Introduction,* Perkin-Elmer, 1980.

57. N. Hadden, F. Baumann, et al., *Basic Liquid Chromatography,* Varian Aerograph, 1971.

58. K.J. Bombaugh, The practice of gel permeation chromatography, Chapter 7, in *Modern Practice of Liquid Chromatography,* J.J. Kirkland, ed., John Wiley & Sons, New York, 1971, pp. 237–285.

2
Semirigid Polymer Gels for Size Exclusion Chromatography

Elizabeth Meehan Polymer Laboratories Ltd., Church Stretton, Shropshire, United Kingdom

Introduction

The earliest developments in polymeric packings for size exclusion chromatography (SEC) involved the use of soft gels with aqueous-based eluants for the analysis of natural water-soluble polymers (1). Although work continued to optimize such systems, attention was directed to organic-based packings for the analysis of synthetic polymers. In 1964, Moore (2) introduced a range of rigid macroporous cross-linked polystyrene resins that proved to be successful in the analysis of a wide range of synthetic organic-soluble polymers. Since then, the technology of organic SEC has progressed steadily as successive advances in polystyrene-based packings have been made. Over recent years more attention has been directed back toward aqueous systems in an attempt to bring the technology of aqueous SEC packings to the level of the organic media. A variety of high-performance porous packing materials are available for SEC, including both silica- and polymer-based gels. This chapter discusses in detail the technology of polymer-based packings for SEC using both organic and aqueous eluants.

Column Packing and Performance

Columns of semirigid polymer gels are generally packed using a balanced density slurry packing technique at pressures in the range 2000–4000 psi (3). Column internal diameters of 6–8 mm and lengths of 20–60 cm are commonplace because these dimensions represent a good compromise between resolution and

analysis time using flow rates and operating pressures available with high-performance liquid chromatography equipment.

Column performance is often assessed by performing a plate count measurement using a relatively low viscosity eluant and a totally permeating test probe, such as toluene in tetrahydrofuran for organic SEC or glycerol in water for aqueous SEC (4,5). Figure 1 illustrates the methods for calculating plate count and asymmetry commonly supplied by column manufacturers. This type of column test is useful because it provides reference performance data for future comparison during the lifetime of the column. It is important to remember that such comparisons should always be made under consistent conditions of flow rate, eluant, solute, temperature, and apparatus.

Organic SEC

By far the most widely used organic SEC packings are based on porous polystyrene/divinylbenzene (PS/DVB) particles. This is primarily because of their

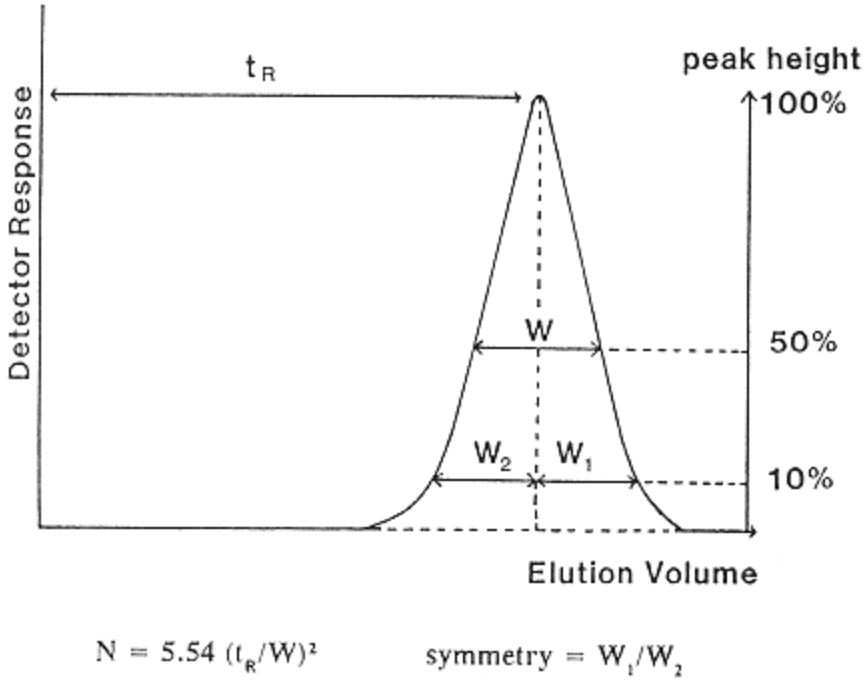

Figure 1.
Calculation of plate count, N, and symmetry factor.

availability in a wide range of pore sizes and their lack of adsorptive characteristics of commercial polymers in good solvents (6). Tables 1 and 2 outline the properties of some commercially available packings of this type.

Manufacture

PS/DVB materials are prepared by suspension polymerization using a two-phase organic/aqueous system (7). The cross-linking polymerization is performed in the presence of inert diluents that are miscible with the starting monomers but must not dissolve in the aqueous phase. Submicrometer particles (microbeads) form as the styrene/divinylbenzene polymerizes and precipitates out of solution, and these microbeads fuse together to form macroporous particles. Initially a network of microporosity may be present in the microbeads, and polymerization conditions must be controlled to minimize this type of porosity because it results in a less effective packing for the reasons outlined in Table 3. After forming the cross-linked PS/DVB porous particles, any residual reactants, diluents, and surfactants must be removed by thorough washing.

Particle Size

A range of particle sizes can be produced from the reaction just described. For packing materials to be as homogeneous as possible, with uniform flow channels, particles of equal size are most suitable. Narrow particle size distributions and regular, spherical particles are therefore desirable (8). If the particle size distribution is too broad, the permeability of the column decreases. Refinement of particle size distribution by some form of particle classification is used to produce narrow distributions for optimum performance.

Information regarding the particle shape and size can be readily obtained by microscopic methods. However, particle sizing equipment is vital for the accurate determination of particle size distribution. For SEC packings, particle diameters in the range 3–70 μm are commercially available. Smaller particles offer improved resolution but result in higher operating pressures and can prove more difficult to pack. The Van Deemter equation (9) predicts that *H,* the theoretical plate height, is proportional to the square of the particle diameter. Originally, packing materials were manufactured as 37–70 μm particles and typical column sets consisted of four 4 foot columns, resulting in analysis times of 3–4 h (10). Over the last 10 years, the gradual reduction in the particle size of analytical packings has resulted in much higher efficiency columns and a corresponding reduction in analysis time to typically 10–30 minutes (11).

Porosity

The pore size of PS/DVB particles when swollen in solvent is difficult to measure and for convenience is usually assessed by testing the packing material with

Table 1 Commercial PS/DVB Packings for Organic SEC: Individual Pore Size Packings

Type	Pore size designation	Resolving range (Polystyrene MW)	Particle size	Supplier
PLgel	50Å	100-2,000	All pore sizes available in 5µm 10µm 20µm	1
	100Å	100-4,000		
	500Å	100-30,000		
	10E3Å	200-60,000		
	10E4Å	1,000-600,000		
	10E5Å	60,000-2,000,000		
	10E6Å	100,000-20,000,000		
Shodex K series *	801	1,500	Nominally 7µm but particle size varies within family	2
	802	5,000		
	802.5	20,000		
	803	70,000		
	804	400,000		
	805	4,000,000		
	806	40,000,000		
	807	200,000,000 **		
TSK-GEL HXL *	G1000	1,000	5µm	3
	G2000	10,000	5µm	
	G2500	20,000	5µm	
	G3000	60,000	6µm	
	G4000	400,000	6µm	
	G5000	4,000,000	9µm	
	G6000	40,000,000	9µm	
	G7000	400,000,000 **	9µm	
Styragel HR	HR 0.5	0-1,000	5µm	4
	HR 1	100-5,000		
	HR 2	500-20,000		
	HR 3	500-30,000		
	HR 4	5,000-600,000		
Styragel HT	HT 3	500-30,000	10µm	4
	HT 4	5,000-600,000		
	HT 5	50,000-4,000,000		
	HT 6	200,000-10,000,000		
Styragel HMW	HMW 7	500,000-100,000,000	20µm	4

Suppliers

1. Polymer Laboratories Ltd, Shropshire UK
2. Showa Denko, Tokyo, Japan
3. Toya Soda, Tokyo, Japan
4. Waters, Milford, Mass., USA

* Supplier quotes exclusion limit only

** estimate

molecular probes (12,13). These are most commonly polymer calibrants of known molecular weight (MW) and very narrow polydispersity. This produces a SEC calibration for the packing in which log (molecular weight) versus elution time or volume is plotted. From this plot the exclusion and total permeation limits can be determined, as well as the region of shallowest slope, which es-

Table 2 Commercial PS/DVB Packings for Organic SEC: Mixed Pore Size Packings

Type	Pore Size designation	Resolving range (Polystyrene MW)	Particle size	Supplier
PLgel	MIXED-A	1,000-40,000,000	20µm	1
	MIXED-B	500-10,000,000	10µm	
	MIXED-C	200-2,000,000	5µm	
	MIXED-D	200-400,000	5µm	
	MIXED-E	< 30,000	3µm	
Shodex K series *	803L	70,000	6µm	2
	804L	400,000	6µm	
	805L	4,000,000	10µm	
	806L	20,000,000	10µm	
	807L	200,000,000 **	17µm	
TSK-GEL HXL *	GMHXL	400,000,000 **	9µm	3
	GMHXL-HT	400,000,000 **	13µm	
	GMHXL-L	400,000,000 **	6µm	
Styragel HR	HR 4E	50-100,000	5µm	4
	HR 5E	2,000-4,000,000	5µm	
Styragel HT	HT 6E	5,000-10,000,000	10µm	4
Styragel HMW	HMW 6E	5,000-10,000,000	20µm	4

Suppliers

1. Polymer Laboratories Ltd, Shropshire UK
2. Showa Denko, Tokyo, Japan
3. Toya Soda, Tokyo, Japan
4. Waters, Milford, Mass., USA

* Supplier quotes exclusion limit only

** estimate

sentially define the operating range and pore volume of the packing. For organic SEC packings pore sizes are commonly expressed in angstrom units (Å). This is not the actual pore size, however, but is related to the extended molecular chain length of a polystyrene molecule that is just excluded from the pores. Various manufacturers' Å sizes are based on different molecular models for polystyrene and are therefore not necessarily comparable. For this reason, comparisons of packing materials are best made based on the exclusion limit and pore volume calculated from the SEC calibration curves supplied by the manufacturer. A typical range of calibration curves are shown in Figure 2 for PLgel individual pore size gels.

Individual pore size packings for SEC have a finite overall separation capacity concentrated in a limited molecular weight range. Although the resolution of such columns is high, the relatively narrow range of molecular weight limits their use to SEC analyses of narrow molecular weight distribution polymers or samples. In practice, SEC columns of different pore sizes are connected in series to provide a wider molecular weight separation range (14). Most SEC users prefer convenient systems that provide a wide molecular weight separation range to analyze polymers of different molecular weight and distribution without having to change and recalibrate columns.

Table 3 Comparison of Macroporous and Microporous Polymeric Packings

Property	MACROPOROUS	MICROPOROUS
Structure		
Crosslink density	High >20%	Low 2 -12%
Swell	Low	High
Pore Size	Independent of eluent	Determined by eluent
Mechanical Strength	Good <6000psi	Poor <2000psi
Operating Conditions	High pressure, high flow rate	Low pressure, low flow rate
Examples	PS/DVB, Poly vinyl alcohol	4-8% PS/DVB, Agarose, Polyacrylamides

In combining individual pore size columns for this purpose, it is important to consider the pore size distributions of each column type. The dimensions of all the columns remain constant, but pore volume may vary from one gel to another. This has the effect of giving variable degrees of resolution over specific regions of molecular weight. Columns with widely overlapping molecular weight resolving ranges were often used in series, such as 10^6, 10^5, 10^4, 10^3, and 500 Å. However, with smaller particles and higher efficiencies, the number of columns and, therefore, analysis times were excessive (15).

Yau et al. (16) described a quantitative theory of producing individual columns in which the pore size distribution, and hence molecular weight resolving range, was broadened by blending together two or more gels. It was shown that the use of a single packing material greatly simplified the column inventory and allowed the use of reduced numbers of columns while maintaining the high chromatographic resolution and accurate molecular weight measurements associated with high-performance SEC. The application of this theory to mixed gel packings based on PS/DVB gels has been shown to yield similar improvements (17).

Mixed gel or linear SEC packings can be produced by blending together selected pore size gels and packing them as a homogeneous mixture to produce

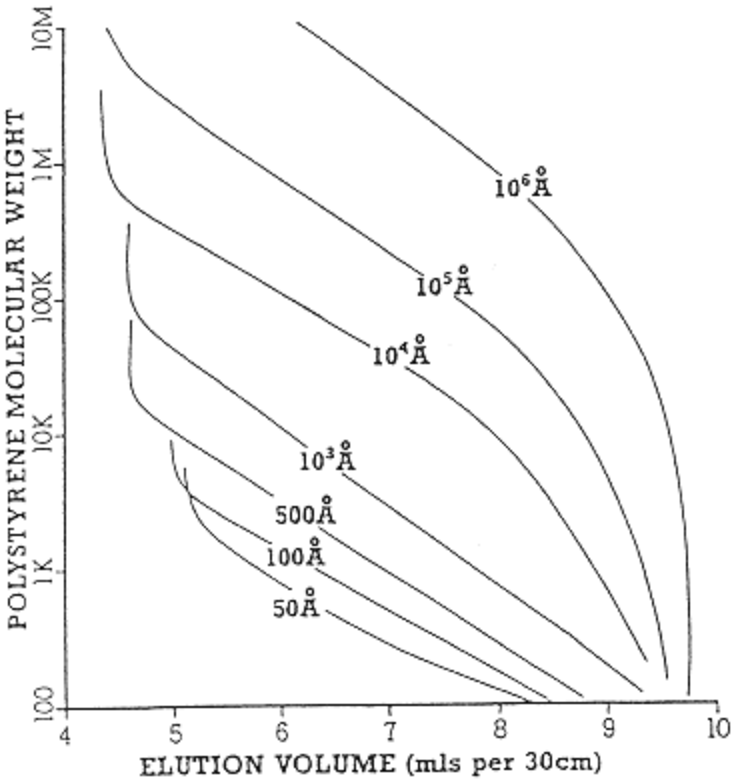

Figure 2.
SEC calibration curves for PLgel individual pore size gels, column dimensions 300 × 7.5 mm, eluant tetrahydrofuran, flow rate 1 ml/minute, calibrants narrow polydispersity polystyrene, detector ultraviolet (UV) 254 nm.

a column that exhibits a linear calibration. The highest pore size gel in the blend determines the final exclusion limit of the packing, and the blended packing material may consist of up to five or more individual pore size gels. The linear calibration plot, as shown in figure 3 for a range of PLgel MIXED gels, results in equal resolution per decade of molecular weight over the full operating range of each packing.

Mechanical and Chemical Stability

All packing materials are subject to the development of backpressure under flow conditions. The mechanical stability of the gel determines its maximum allowable flow rate in operation. The pressure and flow characteristics, as illustrated

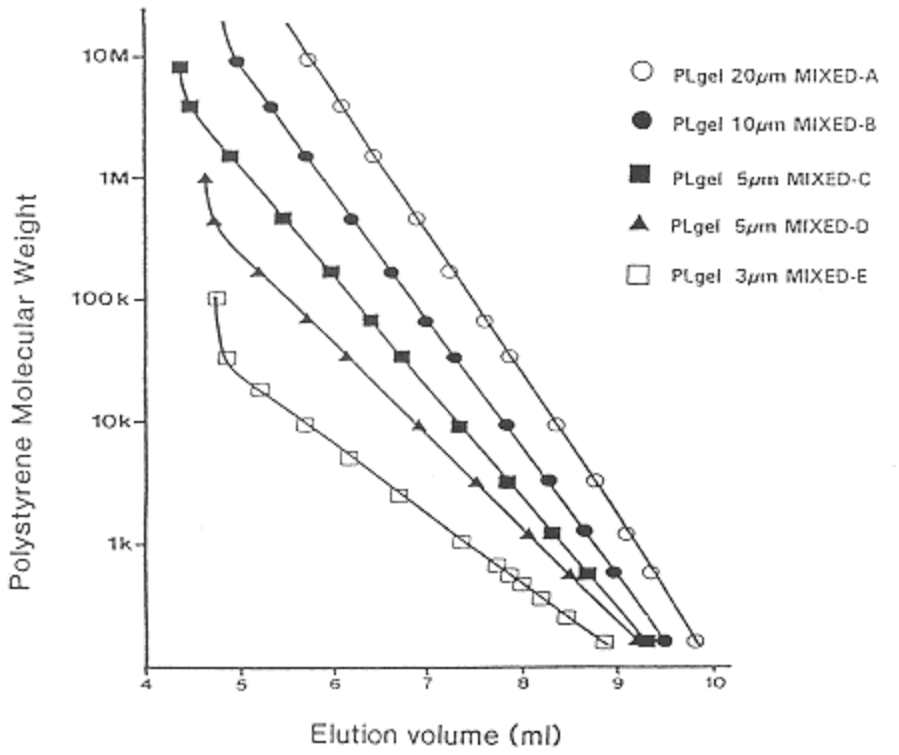

Figure 3.
SEC calibration curves for PLgel MIXED gels, column dimensions 300 × 7.5 mm, eluant tetrahydrofuran, flow rate 1 ml/minute, calibrants narrow polydispersity polystyrene, detector UV 254 nm.

in Figure 4, reveal both the permeability of the packing, from the initial linear portion of the graph, and the point at which the gel compresses and deforms. The maximum operating pressure of the packing should fall well below the compression point to avoid permanent damage and effective repacking of the column.

The chemical stability of the gel is usually most relevant to solvent compatibility. Solvents of varying solubility parameter cause a polymeric gel to swell to differing degrees. The extent of swell in different solvents depends on the degree of cross-linking, and for this reason highly cross-linked gels perform best across the widest range of solvent polarity (18). Generally, modern SEC packings can be used with a wide range of organic solvents, although because manufacturing processes may vary, the solvent compatibility of a packing material depends on the chemistry and packing techniques employed. Therefore, it is

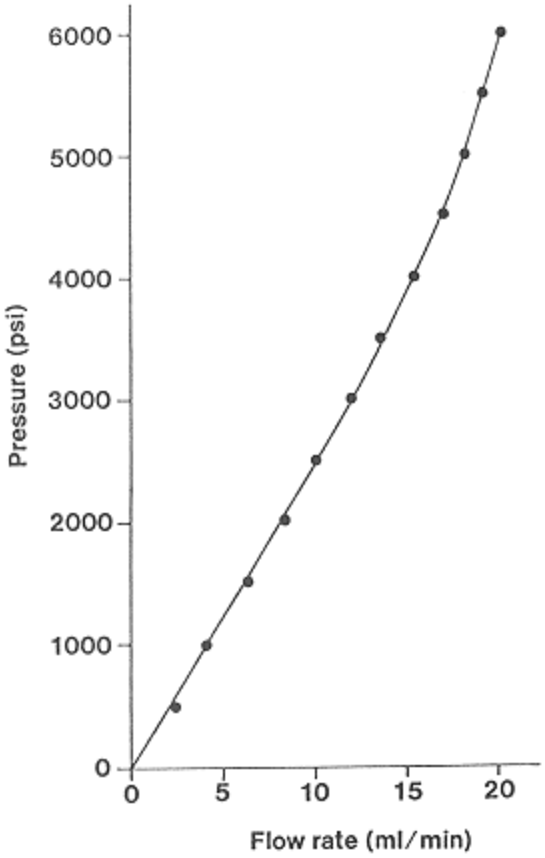

Figure 4.
Flow rate versus column pressure measured for a PLgel 5 μm 100 Å 300 × 7.5 mm column, eluant acetone.

always recommended that the manufacturers' guidelines for solvent compatibility be consulted. When transferring columns from one solvent to another, it is important to check the miscibility of the two solvents and the solubility of any additives or stabilizers present. Column blockage could occur if either of these two considerations is overlooked.

Some solvents may exhibit high viscosity at room temperature, and elevated temperature (50–120°C) can be used to reduce the viscosity, thus improving mass transfer, reducing operating pressure, and prolonging column lifetime. High-temperature SEC (130–160°C) is also required for the analysis of polymers that dissolve only at higher temperatures and readily crystallize out of solution

on cooling, classically polyolefins (19). In such cases there may be a general reduction in the lifetime of the packing brought about by two mechanisms:

1. Thermal or oxidative degradation of the gel alters the swell characteristics and changes the pore size distribution, eventually breaking down the particle. Although ultimately some degradation can be expected under such aggressive conditions, this can be substantially reduced by the addition of antioxidants to the mobile phase.

2. The production of “solvent tracks” through the gel bed is brought about by heating and cooling cycles. This phenomenon occurs when

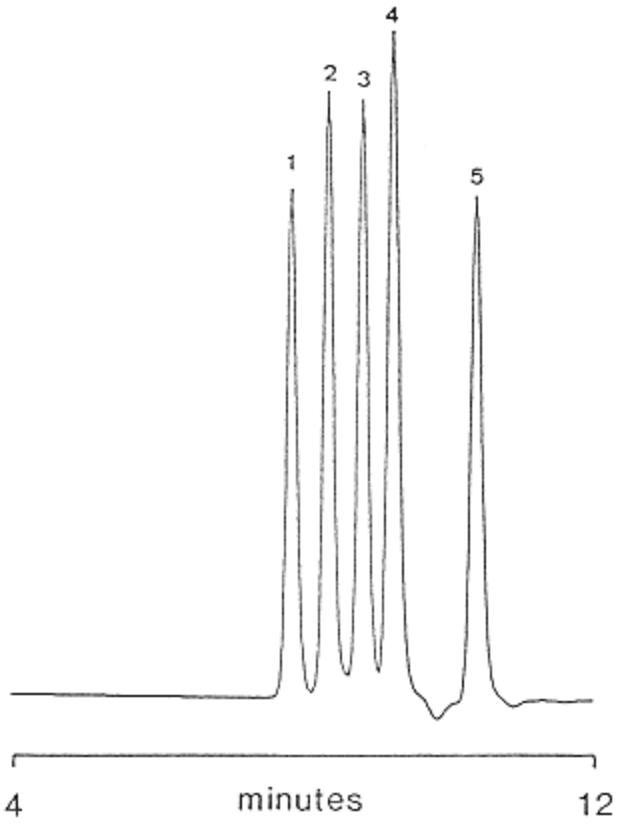

Figure 5.
Separation of dialkyl phthalates, column PLgel 5 µm 50 Å 300 × 7.5 mm, eluant tetrahydrofuran, flow rate 1 ml/minute, detector refractive index (RI); (1) dioctyl phthalate; (2) di-n-butyl phthalate; (3) diethyl phthalate; (4) dimethyl phthalate; (5) toluene.

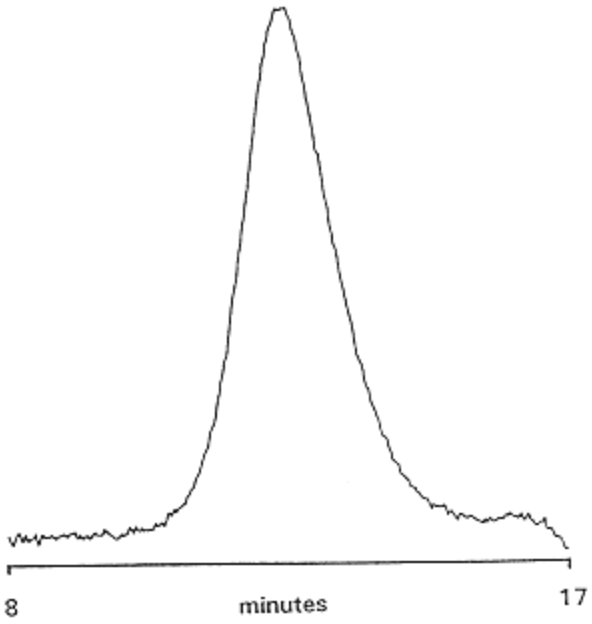

Figure 6.
Analysis of polyethylene NBS 1475, two columns PLgel 10 µm MIXED-B 300 × 7.5 mm, eluant trichlorobenzene, flow rate 1 ml/minute, temperature 140°C, detector infrared.

damage to the column packing results in regions of different packed bed density, giving rise to varying flow paths through the column. The effects can easily be observed as broad peaks or split peaks in the chromatogram. The lifetime of the gel is significantly improved by minimizing thermal shock to the columns, which means maintaining low flow rate through the column while changing the temperature at rates of around 1°C/minute or less, depending on the manufacturer.

Column Selection and Applications

The first criterion for column selection is the molecular weight of the sample to be analyzed. For some applications in which resolution is required over a relatively narrow molecular weight range, individual pore size packings are suitable. This is particularly the case for small-molecule separations, as shown in Figure 5. For polymer analyses in which resolution is required to cover several decades of molecular weight, mixed gel or linear columns are widely applicable.

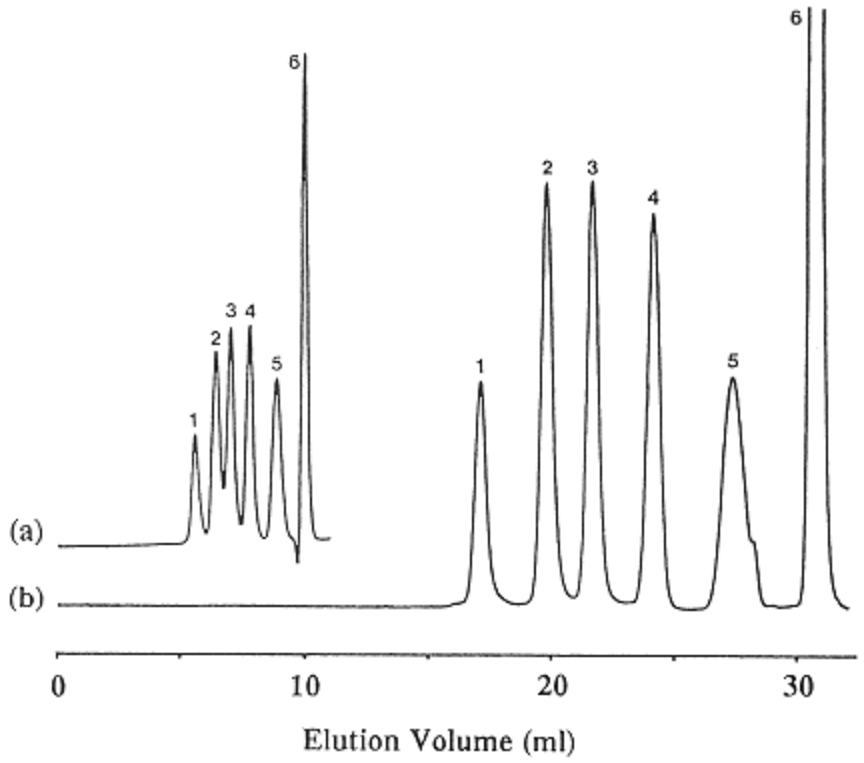

Figure 7.
Effect of column length on separation using PLgel 10 µm MIXED-B columns, eluant tetrahydrofuran (THF), flow rate 1 ml/minute, detector RI, (a) one 300 × 7.5 mm, (b) three 300 × 7.5 mm, PL EasiCal polystyrene standards; (1) M_p = 3,040,000; (2) M_p = 330,000; (3) M_p = 66,000; (4) M_p = 9,200; (5) M_p = 580; (6) toluene.

Figure 6 illustrates the application of mixed gels columns to the analysis of polyethylene, which typically has a high polydispersity.

Resolution in SEC is dependent on the slope of the calibration plot $d \log M/dv$ and efficiency, and these two parameters should be manipulated to optimize resolution (20). Calibration slope can be decreased by the addition of more columns in series, and the effect on resolution is illustrated in Figure 7. Efficiency is dependent on particle size, and smaller particle size, higher efficiency columns are generally preferred. The effect of particle size on the separation of polystyrene oligomers is shown in Figure 8. Column sets should comprise packing materials of the same particle size because the full potential efficiency of

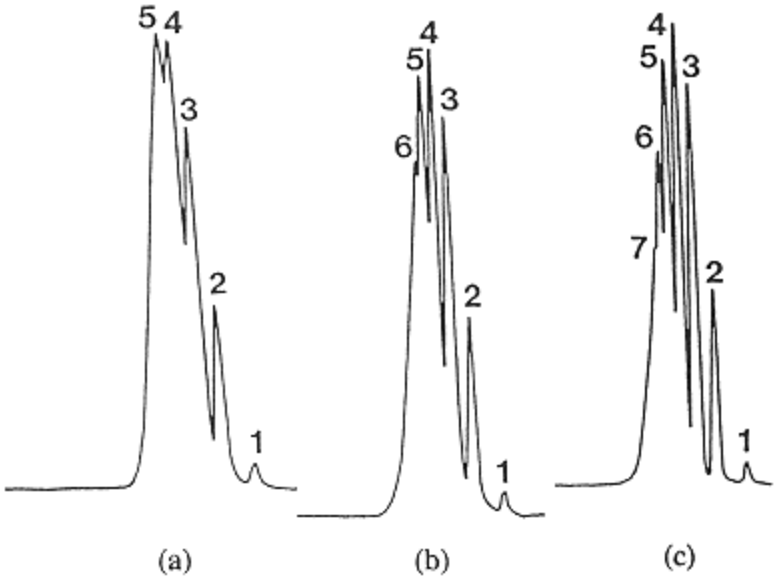

Figure 8.
Effect of particle size on separation using PLgel 100 Å column: (a) 10 µm, (b) 5 µm, (c) 3 µm; eluant THF, flow rate 1 ml/minute, detector UV 254 nm, polystyrene oligomers. (1) MW 162; (2) MW 266; (3) MW 370; (4) MW 474; (5) MW 578; (6) MW 682; (7) MW 786.

the system is never achieved if large and small particle size columns are combined.

In a chromatographic bed, the largest tangential shear stresses in the moving eluant stream are expected in the most open areas subject to the highest flows, that is, in the spaces between the particles. It has been estimated (21) that these "capillaries" may have effective diameters of 0.4 times the particle diameter. It can therefore be predicted that higher shear rates associated with small particle size packings would prove to be more likely to incur polymer shear degradation in SEC (22). This phenomenon is most relevant to the analysis of high-molecular-weight polymers, which exhibit high intrinsic viscosity in solution because shear stress $t = \cap\Gamma$, where $\cap$ is the viscosity of the polymer solution and Γ is the shear rate. To minimize the effects of shear degradation in SEC, it is therefore necessary to use larger particle size packings to lower Γ and lower sample concentrations to lower $\cap$. In addition, the porous frits at the inlet and outlet of SEC columns present a further potential source of shear because they are comprised of narrow channels, which can also be considered capillaries. The

frit porosity should be selected in accordance with the particle size of the packing to contain the packing material but not induce polymer shear degradation.

Molecular shear phenomena are evidenced by peak splitting or lower than expected calculated molecular weight values (23). Experimental data (24) have shown that when using 5 μm particle size packings errors of 15–30% in molecular weight can be observed for narrow distribution polystyrene standards greater than 4,000,000 g/mol. In these applications larger particle size (10–20 μm) columns are most suitable, and compensation for their lower efficiency is made by the addition of more columns in series.

Aqueous SEC

The first polymeric packings were developed primarily for the analysis of natural polymers and were based on cross-linked polymer networks that produced soft gel packings (8). These soft gels, based on dextran or agarose, develop porosity between the polymer chains or between clusters of polymer chains in the swollen state. They were found to be much less susceptible to secondary interaction effects than silica-based packings, so that separations dominated by size exclusion were readily achieved. However, the disadvantage was that the highly swollen, microporous networks had poor mechanical strength and were therefore not really suitable for high-performance SEC performed with relatively short, low-capacity columns at high eluant flow rates.

Packings for high-performance aqueous SEC have therefore been developed (25,26) that are rigid, have functionalities similar to those of the soft gels, and can tolerate a wide range of pH. Table 4 shows the properties of some commercial high-performance aqueous SEC packings.

Many of the comments referred to earlier apply equally to aqueous SEC. The remainder of this section discusses other important parameters specific to semirigid polymeric packings for aqueous SEC.

Porosity

Pore size distribution is expressed in the form of an SEC calibration plot, log *M* versus elution volume, but whereas for organic SEC polystyrene standards are used almost exclusively, for aqueous SEC packings resolving ranges are commonly quoted in terms of polyethylene oxide/glycol (PEO/PEG), polysaccharides, or globular proteins. A comparison of PEO/PEG and Pullulan polysaccharide calibrations is shown in Figure 9. These molecular probes vary considerably in hydrodynamic volume and can therefore be expected to yield quite different calibration curves (25). It is therefore important to base column selection on a calibration that is relevant to the application.

Table 4 High-Performance Polymeric Packings for Aqueous SEC

Type	Pore size designation	Exclusion Limit (Polyethylene oxide)	Gel Chemistry	Supplier
PL aquagel-OH	40 50 60	100,000 1,000,000 20,000,000	Macroporous matrix with OH functionality	1
Shodex OH pak *	KB-802 KB-802.5 KB-803 KB-804 KB-805 KB-806 KB-80M	4,000 10,000 100,000 400,000 4,000,000 20,000,000 20,000,000	Hydroxylated PMMA	2
TSK-GEL PW	G1000 G2000 G2500 G3000 G4000 G5000 G6000 GM	1,000 2,000 3,000 50,000 300,000 1,000,000 8,000,000 8,000,000	Hydroxylated PMMA	3
Ultrahydrogel	120Å 250Å 500Å 1000Å 2000Å	5,000 80,000 400,000 1,000,000 7,000,000	Hydroxylated PMMA	4
Asahipak *	GS-220 GS-320 GS-520 GS-620 GS-710 GFA-30 GFA-50 GFA-7M	3,000 40,000 300,000 2,000,000 10,000,000 40,000 300,000 10,000,000	PVA Copolymer	5

Suppliers

1. Polymer Laboratories Ltd, Shropshire UK
2. Showa Denko, Tokyo, Japan
3. Toya Soda, Tokyo, Japan
4. Waters, Milford, Mass., USA
5. Asahi Chemical, Kawasaki, Japan

* Supplier quotes exclusion limit for polysaccharides only

Surface Chemistry

Ideally, a packing material for aqueous SEC should be highly hydrophilic and should not possess any charge. These requirements arise from the nature of the polymers to be analyzed. Both natural and synthetic water-soluble polymers can be either nonionic (neutral) or ionic (polyelectrolyte) and in turn either hydrophilic or hydrophobic. A polymeric packing material that is not highly hydrophilic may result in hydrophobic sample-column interactions. In addition,

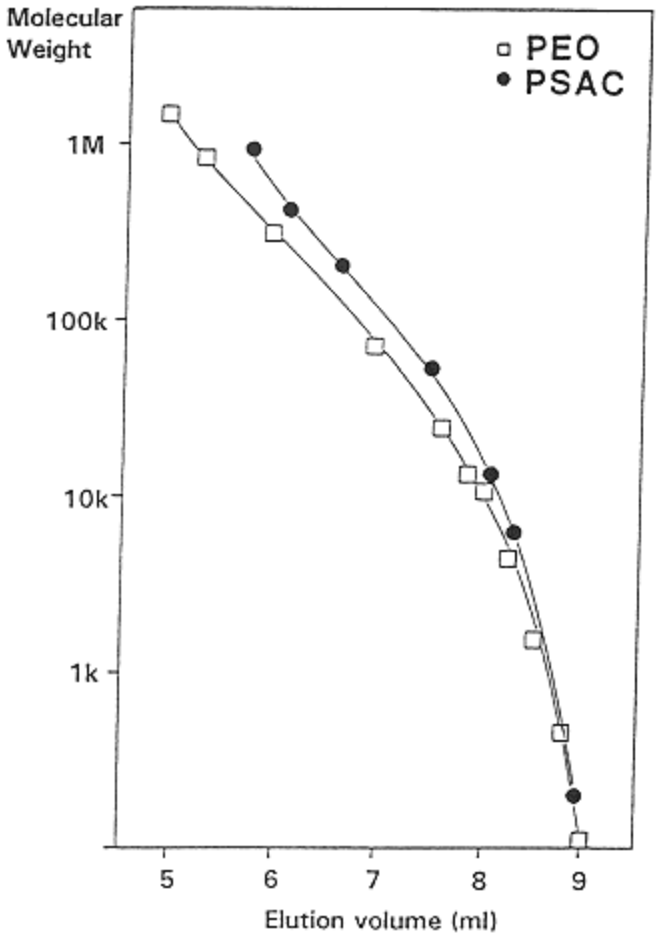

Figure 9.
SEC calibration using polyethylene oxide (PEO) and polysaccharide (PSAC) standards, column PL aquagel-OH 50 300 × 7.5 mm, eluant water, flow rate 1 m1/minute, detector RI.

charged sites on a packing material can give rise to ionic interactions with polyelectrolyte polymers (27).

In practice, most high-performance aqueous SEC packings exhibit some degree of hydrophobicity and ionic charge as a result of the chemistries involved in their manufacture. Because a variety of chemistries are available commercially (see Table 4), the ionic and hydrophobic characteristics of packing ma-

terials may differ. Often the chemistry applied is necessary to obtain a compromise between the chemical and physical properties of the final packing material. Both ionic and hydrophobic characteristics are undesirable because they result in non-size exclusion phenomena, and although manufacturers of packing materials aim to minimize such interactions, eluant modification to suppress them is routine. This normally involves the use of salt/buffer solutions (ionic interaction) and/or the addition of organic modifiers (hydrophobic interaction) to the eluant. An advantage of using such eluant systems is that the presence of salts effectively reduces polyelectrolyte viscosity, which can otherwise be excessive owing to intramolecular electrostatic attractions within the polymer chains, giving rise to viscous fingering effects in SEC (28).

Depending on the chemistry adopted by the column manufacturer, eluant selection may be limited with respect to pH and type and level of organic solvent that can be tolerated. For example, the choice and level of cross-linking agent in polyvinyl alcohol (PVA)-based packings (e.g., Asahipak) influences both the pH stability and the organic solvent compatibility. In all cases the manufacturer's literature should specify eluant compatibility.

Eluant Selection

The selection of the eluant in aqueous SEC is critical: it is often the only means of controlling secondary interactions between the sample and the column. Specific interactions can be exploited if the separation of discrete components in a sample is to be achieved, for example in the purification of biological compounds. If SEC is to be used to derive a polymer molecular weight distribution, however, then non-size exclusion behavior is undesirable (29). Although it is sometimes difficult to eliminate interactions completely, they can often be suppressed by selection of an appropriate eluant. The selection of eluant is dependent on the type of sample and the surface chemistry of the packing material. Although it cannot be assumed that an eluant used for a separation on one manufacturer's columns is suitable for a separation using a different type of column, certain general rules apply, as outlined in Table 5.

Adsorption effects can be identified by such phenomena as a sharp leading edge followed by tailing of the peak, small peak area, retardation of elution, and poor reproducibility. Ion exclusion effects can be seen by early elution close to or even slightly before the void volume. When optimizing eluant composition, the reproducibility of chromatograms resulting from systematic changes in composition can be used as an indicator to determine the best set of conditions.

For nonionic polymers pure water can often be used as eluant, although a low ionic strength is a good safety measure and adds a degree of reproducibility to the system. Polyethylene oxide and polyethylene glycol are characteristic of this sample category.

Table 5 Typical Eluant Systems for Synthetic Water-Soluble Polymers

Type of polymer	Typical sample	Suitable eluent
Nonionic, hydrophilic	polyethylene oxide polyethylene glycol	pure water pure water
	polyvinyl aclohol, hydroxyethyl cellulose, polyacrylamide	0.1-0.2M salt/buffer, pH7
Nonionic, hydrophobic	polyvinylpyrrolidone	0.1-0.2M salt/buffer with 20% organic solvent
Anionic, hydrophilic	sodium polyacrylate, sodium hyaluronate, carboxymethyl cellulose	0.1-0.3M salt/buffer, pH7-9
Anionic, hydrophobic	sodium polystyrene sulphonate	0.1-0.3M salt/buffer, pH7-9 with 20% organic solvent
Cationic, hydrophilic & hydrophobic	chitosan, poly-2-vinyl pyridine	0.3-1.0M salt/buffer, pH 2-7 with addition od organic solvent for more hydrophobic polymers

For ionic samples it is recommended that salt/buffer systems be used as eluants. The salts most commonly used are sodium sulfate, sodium nitrate, and sodium acetate because these cause little corrosion to stainless steel column hardware even at low pH. Ionic strength is varied according to sample type but generally does not exceed 1.0 M because increasing salt concentration promotes hydrophobic interaction. Often a buffer is used to allow pH to be controlled.

Anionic polymers may be eluted using 0.1–0.3 M salt/buffer at pH 7–9. Figure 10 shows the analysis of polyacrylic acid (sodium salt), which is a typical example. Polystyrene sulfonate (sodium salt) is also an anionic polymer but often does not elute under such conditions because it is relatively hydrophobic. Although the salt/buffer system is sufficient to suppress the ionic interaction, adsorption caused by hydrophobic interaction occurs, and this must be overcome by introducing some organic modifier to the mobile phase, as shown in Figure 11. With PL aquagel-OH, methanol is recommended as an organic modifier, although with other packings different solvents may be used (e.g., acetonitrile with TSK PW columns). The manufacturer's recommendations on the use of organic solvents with aqueous packings should always be followed carefully because the wrong choice of solvent may irreversibly damage the column.

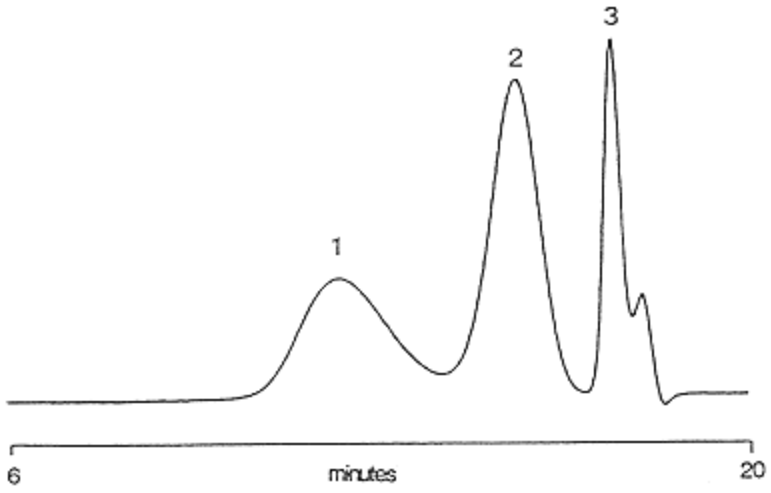

Figure 10.
Analysis of polyacrylic acid standards: two columns PL aquagel-OH 50 300 × 7.5 mm, eluant 0.25 M $NaNO_3$ and 0.01 M NaH_2PO_4, pH 7, flow rate 1 ml/ minute, detector RI. (1) M_p = 272,900; (2) M_p = 16,000; (3) salt peak.

Cationic polymers may be eluted using rather higher salt concentrations, 0.3–1.0 M, and pH in the range 2–7. A typical analysis of poly-2-vinyl pyridine is shown in Figure 12. As with the anionic samples, if there is a high degree of hydrophobicity in the sample it may be necessary to add organic modifier to the mobile phase.

Even if the ionic sample solutions are prepared from the eluant, when the mobile phase consists of a salt solution there is often a peak near total permeation caused by the salt. This is believed to be a result of ion inclusion (30), in which the porous packing acts as a semipermeable membrane and an equilibrium is established such that the ion of the same charge as the excluded sample is forced into the pores, giving rise to a permeated peak. This can be problematical: it may interfere with sample components, and in this case column selection may have to be adjusted to give more resolution for very small molecules.

Conclusion

A wide variety of commercial semirigid polymer gels exist for both organic and aqueous SEC. Following the introduction of smaller particle size packings,

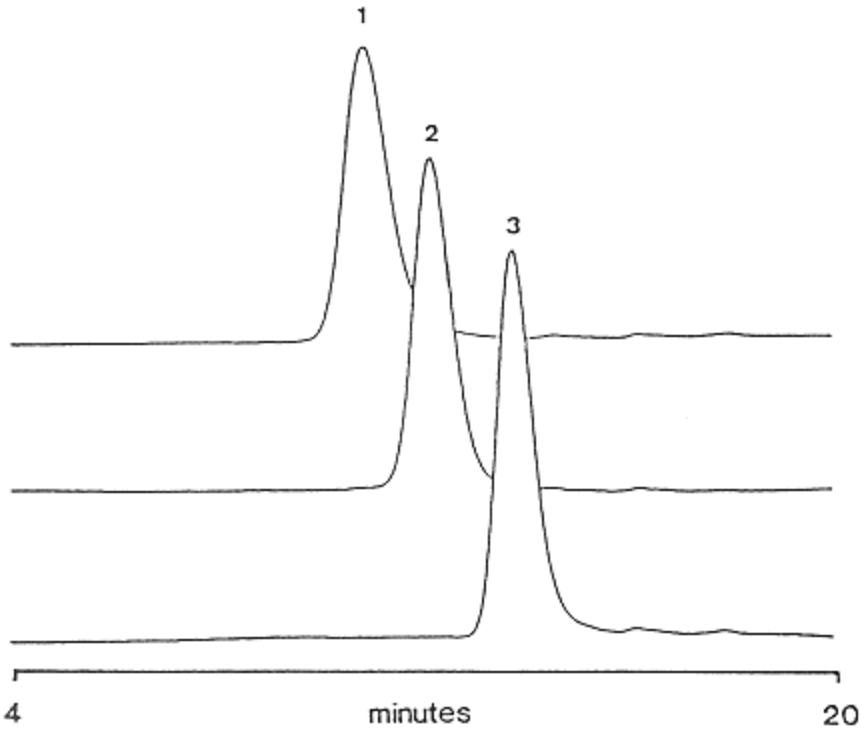

Figure 11.
Analysis of polystyrene sulfonate (sodium salt) standards: two columns PL aquagel-OH 40 300 × 7.5 mm, eluant 80% vol/vol 0.3 M $NaNO_3$ and 0.01 NaH_2PO_4, pH 9, + 20% vol/vol methanol, flow rate 1 ml/minute, detector RI. (1) M_p = 100,000; (2) M_p = 35,000; (3) M_p = 4600.

high-performance columns are available that can provide rapid analysis of compounds covering an extensive range of chemical composition and molecular weight. Mixed gel or linear columns are becoming increasingly popular for the analysis of polymers. They permit accurate molecular weight determinations using a reduced number of columns. The chemical and thermal stability of organic SEC columns may become more important in the characterization of new polymers as more exotic solvents and higher temperatures are required. Environmental considerations may increase the usage of high-performance aqueous SEC columns in the future as more water-based polymer systems are developed.

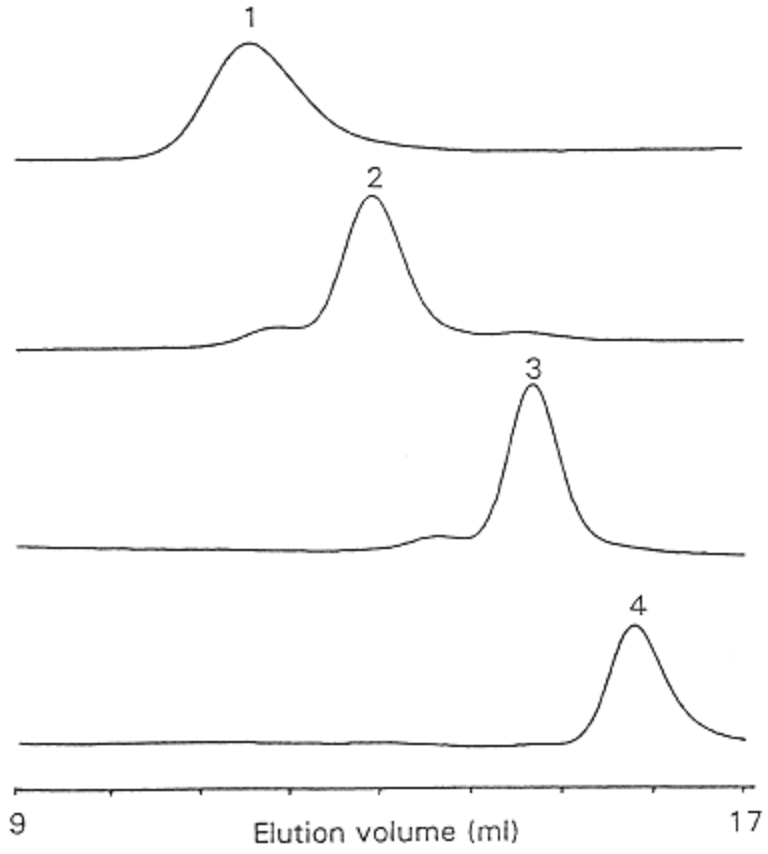

Figure 12.
Analysis of poly-2-vinyl pyridine standards: two columns PL aquagel-OH 50 300 × 7.5 mm, eluant 0.25 M $NaNO_3$ and 0.01 M NaH_2PO_4, pH 3, flow rate 1 ml/minute, detector RI. (1) M_p = 600,000; (2) M_p = 200,000; (3) M_p = 50,000; (4) M_p = 20,000.

References

1. J. Porath, P. Flodin, *Nature*, *183*, 1657 (1959).

2. J.C. Moore, *Journal of Polymer Science, Part A* 2, 835 (1964).

3. B. Ravindranath, *Principles and Practice of Chromatography,* Ellis Horwood Ltd., UK, 1989, p. 317.

4. P.A. Bristow, *Liquid Chromatography in Practise,* hept, UK, 1976, p. 16.

5. A.B. Littlewood, *Gas Chromatography,* Academic Press, New York, 1970.

6. I.C. Poinescu, C. Beldie, C. Vlad, *Journal of Applied Polymer Science, 29*, 23–34 (1984).

7. J. Seidl, J. Malinsky, K. Dusek, W. Heitz, *Advances in Polymer Science, 5,* 113 (1967).

8. G. Glockner, *Polymer Characterisation by Liquid Chromatography,* Journal of Chromatography Library, Vol. 34, Elsevier, Amsterdam, 1987, p. 170.

9. W.W. Yau, J.J. Kirkland, D.D. Bly, *Modern Size-Exclusion Liquid Chromatography,* John Wiley & Sons, New York, 1979, p. 63.

10. J.M. Evans, *RAPRA Members Journal,* August 1973.

11. E. Meehan, J.A. McConville, F.P. Warner, *Polymer International, 26,* 23–38 (1991).

12. F.V. Warren, B.A. Bidlingmeyer, *Analytical Chemistry, 56,* No. 6 (1984).

13. A.A. Gorbunov, L.Y. Solovyova, V.A. Pasechnik, *Journal of Chromatography, 448,* 307–332 (1988).

14. W.W. Yau, J.J. Kirkland, D.D. Bly, *Modern Size-Exclusion Liquid Chromatography,* John Wiley & Sons, New York, 1979, p. 267.

15. F.P. Warner, Z. Dryzek, L.L. Lloyd, New criteria influencing the selection of high performance GPC columns for polymer analysis, presented at Antec, Boston, 1986.

16. W.W. Yau, C.R. Ginnard, J.J. Kirkland, *Journal of Chromatography, 149,* 465–487 (1978).

17. E. Meehan, J.A. McConville, S. Oakley, F.P. Warner, Performance criteria for mixed gel GPC columns, presented at the International GPC Symposium, San Francisco, 1991.

18. W.G. Lloyd, T. Alfrey, *Journal of Polymer Science, 62,* 301–316 (1962).

19. M.R. Haddon, J.N. Hay, in *Size Exclusion Chromatography* (ed. B.J. Hunt and S.R. Holding), Blackie & Son, 1989, p. 57.

20. W.W. Yau, J.J. Kirkland, D.D. Bly, H.J. Stoklosa, *Journal of Chromatography, 125,* 219 (1976).

21. J.C. Giddings, *Adv. Chromatogr., 20,* 217 (1982).

22. H.G. Barth, F.J. Carlin, *Journal of Liquid Chromatography, 7(9),* 1717–1738 (1984).

23. J.G. Rooney, G. ver Strate, in *Liquid Chromatography of Polymer and Related Materials III* (ed. J. Cazes), Marcel Dekker, New York, 1981, p. 207.

24. E. Meehan, S. O'Donohue, The role of column and media design in the SEC characterisation of high molecular weight polymers, presented at ISPAC 5, Inuyama, Japan, 1992.

25. E. Meehan, L.L. Lloyd, J.A. McConville, F.P. Warner, N.P. Gabbott, J.V. Dawkins, *Journal of Applied Polymer Science: Applied Polymer Symposium, 48,* 3–17 (1991).

26. Y. Kato, T. Matsuda, T. Hashimoto, *Journal of Chromatography, 332* (1985) 39–46.

27. H.G. Barth, *Journal of Chromatographic Science, 18,* 1980.

28. C. Abad, L. Braco, V. Soria, R. Garcia, A. Campos, *British Polymer Journal, 19,* 489–508 (1987).

29. D.J. Nagy, D.A. Terwilliger, B.D. Lawrey, W.F. Tiedge, Characterisation of cationic polymers by aqueous SEC/differential viscometry, presented at the International GPC Symposium, Newton, 1989.

30. P.L. Dubin, I.J. Levy, *Journal of Chromatography, 235,* 377–387 (1982).

3
Modified Silica-Based Packing Materials for Size Exclusion Chromatography

Roy Eksteen and Kelli J. Pardue Supelco, Inc., Bellefonte, Pennsylvania

Introduction

Size exclusion chromatography (SEC), gel filtration chromatography (GFC) and gel permeation chromatography (GPC) are chromatographic techniques based on discrimination by differences in the size of the analytes. GFC uses an aqueous mobile phase and GPC an organic mobile phase. The general term SEC covers both uses. GFC was first applied in 1959 at the University of Uppsala by Porath and Flodin (1), who showed that proteins were separated as a function of their molecular weight on porous dextran beads because of their (partial) exclusion by the pores. Similarly, GPC was first employed in 1964 by Moore at Dow Chemical Company, who demonstrated the separation of organic soluble polymers on a column packed with a cross-linked polystyrene gel using an organic solvent as the mobile phase (2). Following their discoveries, GFC and GPC developed quickly into accepted laboratory techniques through the availability of commercial supplies of agarose- and polystyrene-based packing materials.

During the initial stages of development, the particle size of SEC packings did not decrease as rapidly as that of silica-based packings employed in high-performance liquid chromatography (HPLC) techniques. According to theory, the performance of HPLC columns improves in direct proportion to a decrease in particle size (3). This prediction was proven correct during the latter part of the 1960s. It was not until the late 1970s, however, that this concept led to the use of small silica-based particles for size exclusion chromatography sup-

ports. The 5 μm silica gel particles were first shown to be an efficient substitute for traditional resin-based particles in GPC (4). Later, the potential of silica and porous glass for use in GFC was demonstrated, following their chemical bonding with hydrophilic ligands to prevent adsorption of proteins and nucleic acids (5).

Since their introduction in 1978, high-performance silica-based SEC packings have made a great impact in the analysis and purification of biopolymers. Columns filled with 10 μm spherical particles and nominal pore sizes of 125, 250, and 500 Å (10 Å = 1 nm) became the state of the art for protein separations during the 1980s (6). Further improvements in speed and resolution were obtained by reducing the size of the particles from 10 to 5 μm (7). Columns filled with these high-performance particles are now manufactured and distributed by several companies. Although this chapter discusses several aspects of the use of silica-based packings for biopolymer analysis, consult Chapters 16 and 17 for details on the application of SEC for the separation of proteins and nucleic acids, respectively.

For the analysis of organic-soluble and water-soluble synthetic polymers, silica-based packing materials have not become as widely used as was originally envisioned (8). Major improvements in the properties of polymer-based supports have contributed to their increased use in GPC. Columns packed with polystyrene divinylbenzene particles are now as efficient as those filled with silica particles of the same size. Because polymer-based packings can be synthesized with very small (<60 Å) and very large (>4000 Å) pores, they provide better selectivity than silica columns for the separation of monomers, as well as for very high molecular weight (5–20 million dalton) polymers.

The use of (modified) silica gels for size exclusion chromatography has been the topic of many recent reviews and books. The 1979 book from Yau et al., enriched by the authors' contribution to the development of high-performance silica-based SEC packings, is still an often used reference for new and experienced workers alike (8). The application of silica-based packing materials for biopolymer separations is discussed in detail in References 9–14. References 15–17 focus mainly on gels (organic nonrigid packing materials), which are exclusively discussed in References 18 and 19. Refer to the comprehensive review from Barth and Boyes (20) for recent references for the analysis of organic- and water-soluble industrial polymers. References describing the use of controlled pore glass in chromatography have been compiled in a commercial bibliography (21).

This chapter first discusses the characteristics of silica as it pertains to size exclusion chromatography. Next, several methods for molecular weight calibration in SEC are examined and the effects of secondary retention discussed. The chapter concludes with an overview of practical aspects associated with the application of size exclusion chromatography.

Properties of Silica

Silicon dioxide (SiO_2), silica gel, or silica is the most abundant compound in the earth's crust. Many industries depend on it being readily and abundantly available in relatively pure form. Traditionally, silica has been an important natural resource for the glass industry. More recently, ultrapure silica particles have become the raw material for manufacturing computer chips. Other common applications of silica include its widespread use as a drying agent, food ingredient, and its incorporation in floor waxes to impart nonskid properties (22). The properties of porous silica and its use as a support in column liquid chromatography (LC) were described in a book by Unger (23). The chemistry of silica is the topic of a comprehensive book by Iler (24). Silica as a backbone of LC column packings was recently reviewed by Berthod (25). Henry discussed the design requirements of silica-based matrices for biopolymer chromatography, including their use in SEC (26).

Structure, Synthesis, and Purity

Silica gel has an amorphous structure, is highly porous, and exhibits a very large surface area, most of which is located in the pores. It consists of a three-dimensional network of SiO_2 repeating units with siloxane and silanol terminal units on the surface. Silica gel can be synthesized into particles ranging in diameter from millimeters to micrometers; the particle size of silica sols (colloids consisting of discrete silica particles—nonporous, spherical, and amorphous) is in the nanometer range. Refer to References 22–24 for thorough treatments of the synthesis of silica gel particles for use in chromatography.

The purity of silica has been a topic of debate among those studying inter-active modes of liquid chromatography. The effect of metal ion impurities on the retention of basic solutes and chelating compounds was first addressed by Verzele et al. (27). Depending on the manufacturing process, chromatographic silica gels contain impurities in concentrations ranging from low to high parts per million. Although to the knowledge of the authors this issue has not yet been discussed in the context of silica-based size exclusion chromatography, it is expected that the use of high-purity silica gels can lead to further improvements in obtaining true SEC retention behavior, as well as improved recovery of mass and biological activity, for metal binding proteins. Table 1 shows that the concentrations of sodium, calcium, iron, and aluminum vary greatly in commercial silicas. Note that the metal ion levels when measured by spectroscopic techniques represent bulk properties, not the levels present at the accessible silica surface. Deactivation procedures, such as the treatment of silica with strong acids or bases (28) or chelating agents (29), effectively remove metal ion impurities from the silica surface. The effect of surface treatments on the concentration of

Table 1 Trace Metal Impurities in Commercial Silica Gels (ppm)

Element	Na	K	Mg	CA	BA	Ti	Zr	Cr	Fe	Cu	Al
Periodic table group	Ia	Ia	IIa	IIa	IIa	IVb	IVb	VIb	VIII	Ib	IIIa
Capcell SG120	NO[a]	NO	NO	NO		7	3		1		6
Hypersil	3360								260		300
Hypersil Lot 180	4176		61	48					192		344
Hypersil Lot 180	3945		60	43					230		340
Hypersil Lot 195	3818		58	48					187		345
Kromasil	10								40		20
LiChrospher 60 RP Select B	190	<10				26	10		<5		7
LiChrospher Si-100	172		10	<5					48		150
LiChrospher Si-100	130								420		300
LiChrospher Si-200	2900			NO	81	235	NO	NO	445	NO	1100
Matrex	500								110		350
Nova Pak C18	380	18				47	160		57		25
Nucleosil 100-5	56			130	6	57	NO	NO	76	9	NO
Nucleosil 100-10	50								50		<10
Nucleosil 100-10	6	3	78	123	1	61	10	1	12		100
Nucleosil 100-30	250								110		30
Nucleosil C18	240	12				52	<5		9		10
Nyacol 2040	4404		3	2					69		107

(table continued on next page)

(table continued from previous page)

Element	Na	K	Mg	CA	BA	Ti	Zr	Cr	Fe	Cu	Al
Periodic table group	Ia	Ia	IIa	IIa	IIa	IVb	IVb	VIb	VIII	Ib	IIIa
Partisil	15								75		60
Partisil ODS-1	23	7	79	216	2	246	4	2	8		
Sephasil 120				NO	NO	30	20	10	40	1	30
Spherisorb	5600								420		300
Spherisorb S5W	4220		22	40					303		128
Supelcosil LC-18-DB	1050	65				48	58		94		120
Supelcosil LC-Si	2012		64	15					128		128
Suplex pKb-100	1050	38				47	54		100		120
TSKgel ODS-80Ts	290	<10				<5	<5		8		<5
Vydac TP	4		63	444					<1		<1
Vydac TPB-2030	30								45		10
YMC 120A-S5	4		9	<2					4		6
Zorbax BP-SIL	20								80		60
Zorbax BP-SIL	37		4	<5					24		20
Zorbax PSM-60	105			NO	NO	41	<25	115	68	245	NO
Zorbax PSM-60, EDTA	NO			NO	NO	NO	NO	NO	NO	NO	NO
Zorbax Rx-C18	48	<10				<5	<5		13		<5

[a]Not observed.

[b]AAS = Atomic absorption spectrometry; AES = atomic emission spectroscopy; ICP = inductively coupled plasma

metal ion impurities is shown for Supelcosil LC-18-DB in comparison with that of untreated Supelcosil LC-Si. Metal ions present in Zorbax PSM-60 were removed by EDTA treatment (29). The reproducibility for the measurement of metal ions in silica by ICP-AES is excellent as demonstrated by the data from duplicate blind measurements for Lot 180 of 5 μm 120 Å Hypersil silica. The reproducibility of the manufacturing process is given for two lots of Hypersil (Lot 180 and Lot 195). Of course, the level of metal ions in a silica depends on that of the raw materials. For example, Table 1 also contains data for Nyacol 2040, a commercial silica sol of 20 nm nominal particle size, used in the manufacturing of HPLC-grade silicas.

Chromatographic Characteristics

The attributes of a SEC column packing material are listed in Table 2. As indicated, the support must be optimized with respect to specific resolution, efficiency, column pressure, and mechanical, chemical, and thermal stability. Recovery of mass and activity is particularly important in the analysis and purification of biopolymers. It also plays a role in the analysis of nonbiochemical synthetic polymers on silica-based SEC columns. In addition to recovery losses by adsorption, the recovery for both groups of polymers can also be reduced by polymer degradation as a result of, for instance, mechanical shear.

As explained elsewhere in this book, resolution in SEC can be expressed in terms of the peak standard deviation and the slope of the calibration curve. As in other HPLC modes, the efficiency of SEC columns can be improved by decreasing particle size. The relationship between column efficiency (or plate number *N)* and velocity can be expressed i dimensionless (reduced) parameters. The reduced plate height h is equal to the ratio of the height of a theoretical plate and the particle size as shown in Equation (1). The reduced velocity v is equal to the product of the linear velocity $\langle v \rangle$ and particle size d_p divided by the solute diffusion coefficient D_m, as shown in Equation (2).

$$h = \frac{H}{d_p} \quad (1)$$

$$v = \frac{\langle v \rangle d_p}{D_m} \quad (2)$$

Experimental efficiency versus velocity data can be fit to any of a number of *h-v* equations, of which the Knox equation (35) is the most widely used.

$$h = \frac{B}{v} + Av^{0.33} + Cv \quad (3)$$

Table 2 Characteristics of SEC Packing Materials

Attribute	Variable	Relationship
Specific resolution	Particle size	$1/\sigma$
	Pore size/pore volume	$1/D_2$
Efficiency, HETP	Particle size	$\sim dp^2$
	Linear velocity	$\sim\langle v\rangle$
Column pressure	Particle size	Constant/dp_2
	Particle shape	Form factor Θ
Mechanical stability	Support type	Inorganic supports are in general more rigid; for all suppo pore volume), the weaker the particle; at constant pore siz strength decreases with size.
Chemical stability	Support/bonded phase	Silica slowly dissolves above pH 7; enhanced stability po bonding reaction(s); most polymer-based matrices are stal high-pH column regeneration in biopurification and wide chaotropic salts.
Thermal stability	Support/bonded phase	Silica columns have few temperature limitations; when us do not cool to ambient between high-temperature analyses bed; most modern SEC packings can be sterilized.
Recovery	Mass	Water-soluble biopolymers, synthetic polymers, and poly polymer- and silica-based columns depending on mobile-
	Activity	Maintenance of biological activity (and mass recovery) fc phase conditions, column type, and contact time.

[a]According to $R_{sp} = 0.58/\sigma D_2$, specific resolution is inversely proportional to the product of the peak standard deviation σ and D_2. See page 103 of Reference 8 for details.

[b]Pore size of commercial materials varies from very small to very large, depending on the application. For each pore size, the volume is balanced against the need for a pressure-stable particle. In a study of commercial silica-based SEC packings, the p particle varied from 55 to 80% (34).

The *A*, *B*, and *C* terms of Equation (3) symbolize contributions to sample dispersion from the interparticle flow structure *A*, axial diffusion *B*, and finite rate of equilibration of the solute between mobile and stationary phases *C*. The values of the coefficients *A*, *B*, and *C* are obtained from curve fitting of experimental data to Equation (3) for a sufficiently wide velocity range. For very good columns, $A = 0.5$, $B = 2$, and $C \simeq 0.005$ (36). Independent of particle size and solute molecular weight, *h* reaches an optimal value of 2–3 for a "well-packed" column, when *v* is in the range of 3–5. For a given solute, the linear velocity at this optimum increases with decreasing particle size. For example, for a solute with a molecular weight of 200 $(D_m \simeq 1 \times 10^{-5}\ \text{cm}^2/\text{s})$, a column filled with 5 μm particles provides the best efficiency when operated at a linear velocity of 0.6–1.0 mm/s.

The definition of linear velocity is based on the retention time for the first eluting component. In interactive modes of chromatography, linear velocity is calculated by dividing the length of the column by the retention time of an unretained (small) molecule that can freely access the total available pore structure. In SEC, linear velocity is based on the retention time of a totally excluded solute. Because the interparticle volume is about as large as the pore volume, the linear velocity in SEC $\langle v \rangle_{SEC}$ is roughly twice that in interactive modes when operating the column at the same flow rate. In other words, as in the preceding example, an SEC column filled with 5 μm particles provides the best efficiency for a 200 dalton molecular weight solute when $\langle v \rangle_{SEC}$ is 1.2–2.0 mm/s. Similarly, for a protein with a molecular weight of 100,000 dalton and a diffusion coefficient of 3×10^{-7} cm^2/s, the column efficiency is optimal when $\langle v \rangle_{SEC}$ is in the range 0.036–0.060 mm/s. In the remainder of this chapter $\langle v \rangle$ represents $\langle v \rangle_{SEC}$.

The analysis time in size exclusion chromatography is given by the retention time for an unretained small molecular weight solute. Thus, the optimal analysis time for analyzing *small* molecular weight solutes on a well-packed 30 cm (5 μm) column is 5–8 minutes. For proteins, the optimal analysis time is 3–5 h, which necessitates the use of very low flow rates. These approximations are in agreement with the calculations of Guiochon and Martin (37), who predicted an optimum analysis time of 1.6 h at a reduced velocity of 10. Sjodahl first put this principle into practice for SEC of proteins by operating a 30 cm × 7.5 mm inner diameter (ID), 10 μm, TSKgel G3000SW column at a flow rate of 50 μl/minute, as shown in Figure 1 (38). Although excellent resolution is obtained during the 12 h analysis time, most users prefer to work at linear velocities of 0.4–1.0 mm/s to keep the analysis time below 30 minutes.

In terms of efficiency, an optimal packing material should exhibit high performance as well as the appropriate specific resolution, and the column back-pressure should be low. The properties of silica gel that are important for its application as a SEC packing material are listed in Table 3. Also listed are the

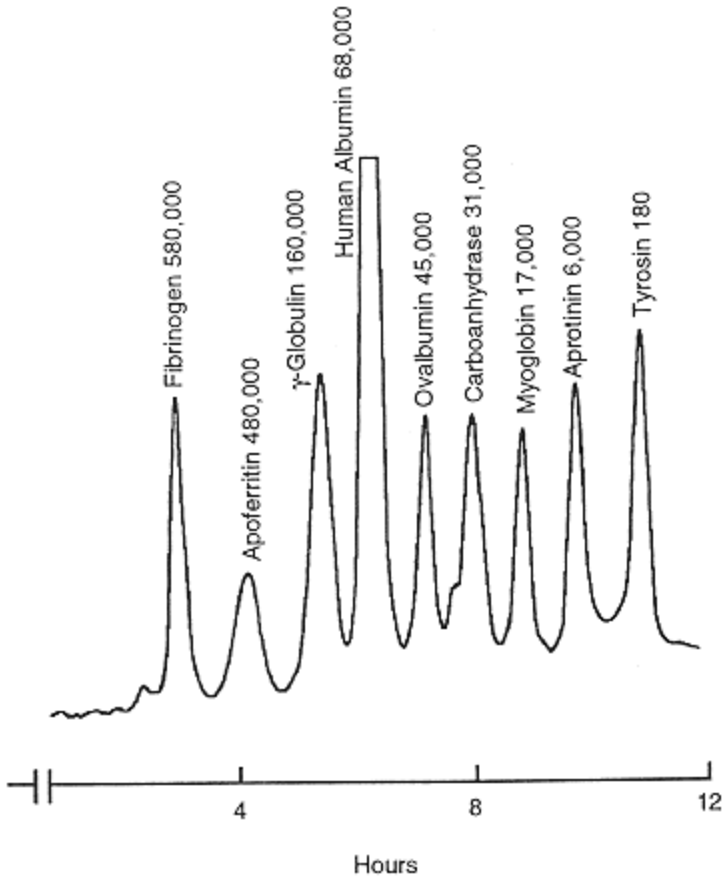

Figure 1.
Analysis of proteins at very low flow rate. Column, TSKgel G3000SW, 10 µm, 60 cm × 7.5 mm; mobile phase, 0.1 M sodium dibasic phosphate, pH 6.8, + 0.1 M sodium chloride; flow rate, 50 µl/minute; detection, 280 nm, UV; temperature, 22 °C; injection, 75 µl; sample, 5–10 µg each protein.

typical values and the range of values for each of the properties discussed here. Table 4 provides general data for controlled pore glasses, which have been used extensively for biopolymer analyses but are not available in particle sizes typically used for HPLC separations. Porous glass is produced from a ternary system of silica (50–75%), sodium oxide (1–10%), and boric acid (to 100%), and such substances as alumina or lime are added to obtain better hydrolytic stability or larger pore sizes (39).

Table 3 Properties of SEC Silica Gels

Property	Common values	Range
Particle size, µm	10	5–10
Particle shape	Spherical	Spherical, irregular
Pore size, Å	125, 250, 500	60–4000
Specific pore volume, ml/ml [a,b]	0.40	0.30–0.50
Pore volume, ml/g[c]	1.2	0.9–1.8
Interparticle porosity, %[a]	40	35–45
Particle porosity, %[a]	60	55–80
Surface modification	Diol	Diol-polyether

[a]Data from Reference 34.

[b]Specific pore volume expressed as ml pore volume per ml column volume.

[c]Pore volumes (ml/g) of several commercial SEC silica gels:

Pore size (Å)	SW TSK-GEL	SW_{XL} TSK-GEL	Beckman	Bio-Rad
125	1.25	1.00	0.95	0.9
250	1.55	1.30	1.35	1.2
500	1.85	1.50	1.55	1.2

Data kindly provided by Dr. Paul Shieh (Beckman) and Wai-Kin Lam (Bio-Rad).

Silica and its bonded phases are characterized by a variety of techniques, including chemical, physical, spectroscopic, and chromatographic methods. A discussion of these techniques can be found in References 40 and 41.

Particle Morphology

As mentioned, reducing particle size was crucial in making liquid chromatography a high-performance technique. Early in the development of HPLC, small silica particles were obtained by grinding and sieving larger silica gels used in the purification of natural products by open-column liquid chromatography. Once the potential of “high-pressure” LC had been demonstrated (42,43), columns packed with 10 µm irregularly shaped silica became readily available. Although such particles are still widely used in routine analyses, most analyses and column development work in academia and industry is performed with spherical 5 µm particles. In recent years, 5 µm particles have become widely available for gel filtration of proteins. The use of even smaller particle sizes in SEC has been advocated by Guiochon and Martin (37) and Engelhardt and Ahr (44), who investigated the optimum particle size

for analyzing proteins.

One of the main advantages of a column packed with spherical particles is that the pressure drop is lower by as much as a factor of 2 compared with a

Table 4 Properties of Controlled Porosity Glasses for SEC

Property	BIORAN[a]	CPG[b]
Pore size, Å	300–4000	75–3000
Specific pore volume, ml/g	0.5–1.2	0.4–0.8
Specific surface area, m^2/g	10–300	7–340
Particle size, μm	30–250	37–177
Surface modification	Diol	Diol

Source: Adapted from Reference 39.

[a]BIORAN: Schott Glaswerke BioTech, Mainz, Germany.

[b]CPG: for address see Reference 21.

column packed with irregular particles of the same average size. Also, although the hardness of silica depends mainly on the size of the pores together with the pore volume per particle, there is some evidence for the widely held belief that irregular particles are more prone to breakage during the column packing process (45). It is also considered more difficult to prepare a well-packed column with irregular particles (46). Particle shape does not influence the kinetic and thermodynamic properties that describe the chromatographic process.

The relationship between particle size and column efficiency is now well understood, although the exact form of the equations, including the Knox equation [see Equation (3)], is still debated (47). The 3–5 μm particle size of modern HPLC columns allows fast analysis of small molecular weight compounds at near optimal column efficiency. As discussed, larger molecular weight compounds, because of their smaller diffusion coefficients, require much lower flow rates to elute with maximum column efficiency. Because of the usual variation in polymer molecular weight, it is not possible to operate the column at the optimal speed for all components in the sample.

Column Dimensions

A common internal diameter for a SEC column is 7.5 or 7.8 mm versus 4.6 mm for non-SEC columns. The length of an SEC column has traditionally been 30 cm, but 60 cm columns have also been available for 10 μm packings. Initial packing studies showing higher efficiencies for larger bore columns contributed to the choice of 7–8 mm as the internal diameter for most high-performance SEC columns (48,49). Advantages of such larger ID columns are (1) a reduction of the importance of extracolumn contributions to the volume of the sample band, (2) increased sample capacity for preparative purposes, and (3) the ability to operate at a flow rate that can easily be maintained with the available HPLC instrumentation. Recent studies have demonstrated that capillary SEC columns

can be packed with equivalent or higher efficiency than SEC columns of standard dimensions. An example is shown in Figure 2, in which the efficiency of 28 and 50 μm ID columns were evaluated using bovine serum albumin (BSA), chicken ovalbumin, and bovine α-chymotrypsinogen as test solutes at linear velocities (based on a totally excluded solute) varying from 0.01 to 0.9 mm/s (50). The microcolumns were packed with 4.5 μm, 150 Å, Zorbax GF-250XL particles that were treated with a zirconium salt and derivatized with a diol functionality. The diffusion coefficients ($\times 10^{-7}$ cm^2/s) for these proteins, ranging in molecular weight from 69,000 to 43,000 and 26,000, were experimentally determined to be 5.65, 6.68, and 8.23, respectively. Note that the optimum reduced plate height was as low as 2 for BSA and as high as 4 for α-chymotrypsinogen. In all cases, the reduced velocity at h_{min} was approximately 5. As measured by the half-height method, the efficiency of a 30 cm × 50 μm ID column compared favorably with that of a standard 25 cm × 9.4 mm ID column filled with the same packing material, and the performance of the capillary column was much better when calculated by statistical moments or based on the Dorsey-Foley equation (51).

Because of the larger ID when operating a standard diameter SEC column at a flow rate of 1 ml/minute, the linear velocity is 2.5 times lower than when the same flow rate is used on a 4.6 mm ID column. Thus, an SEC column is operated closer to the velocity at which the column performs at optimal efficiency. As discussed, however, at least a 10-fold drop in flow rate is required for the column to perform near its optimum for most proteins. This effect is illustrated in Figure 3, in which a protein test mixture is separated at various flow rates on a 25 cm × 4.1 mm ID column packed with 10 μm, 250 Å, amidebonded silica (52). Clearly, resolution improves with decreasing flow rate: the optimum efficiency had not yet been reached at a flow rate of 65 μl/minute or a linear velocity at 0.13 mm/s.

According to Equation (2), reduced velocity is inversely proportional to the solute diffusion coefficient. Under the same conditions, solutes of varying molecular weight show optimal column performance at different flow rates. This is illustrated in Figure 4. The relationship between the logarithm of molecular weight (MW) and the optimal flow rate is plotted for 50 peptides and glycine (MW 50–10,000) analyzed under denaturing mobile-phase conditions (53). As shown, the optimal flow rate is inversely and linearly related to log MW. Over the narrow molecular weight range, the optimum flow rate decreases roughly 2-fold for a 10-fold increase in molecular weight.

Porosity

Except for nonporous particles, all packing materials contain a variation of pore sizes around a mean value. This pore size distribution determines the range of

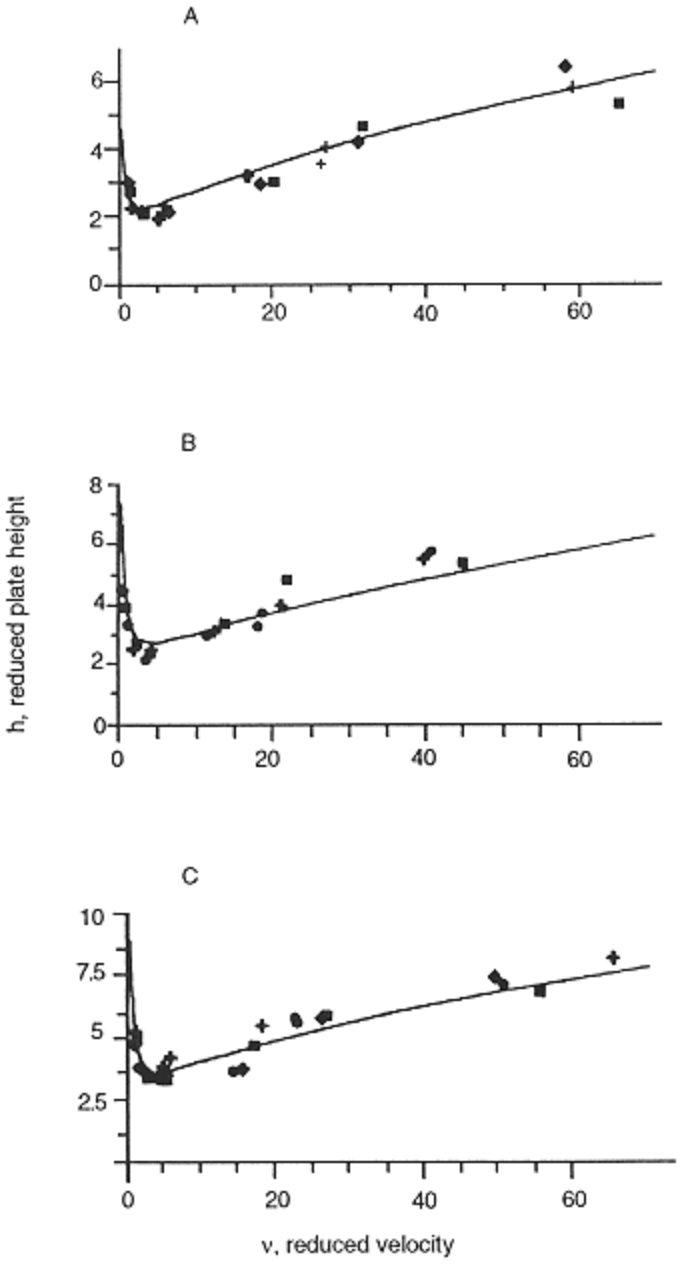

Figure 2.
Column efficiency for 28 and 50 µm ID SEC columns. Column, Zorbax GF-250, 4.5 µm, 30 cm × 28 µm (pluses) or 50 µm (squares, diamonds, and circles); mobile phase, 0.25 M sodium sulfate and 0.1 M sodium phosphate, pH 7.0; linear velocity, 0.001–0.09 cm/s; detection, fluorescence, excitation 254 nm, emission 340 nm; sample (A) bovine serum albumin, (B) ovalbumin, (C) α-chymotrypsinogen A.

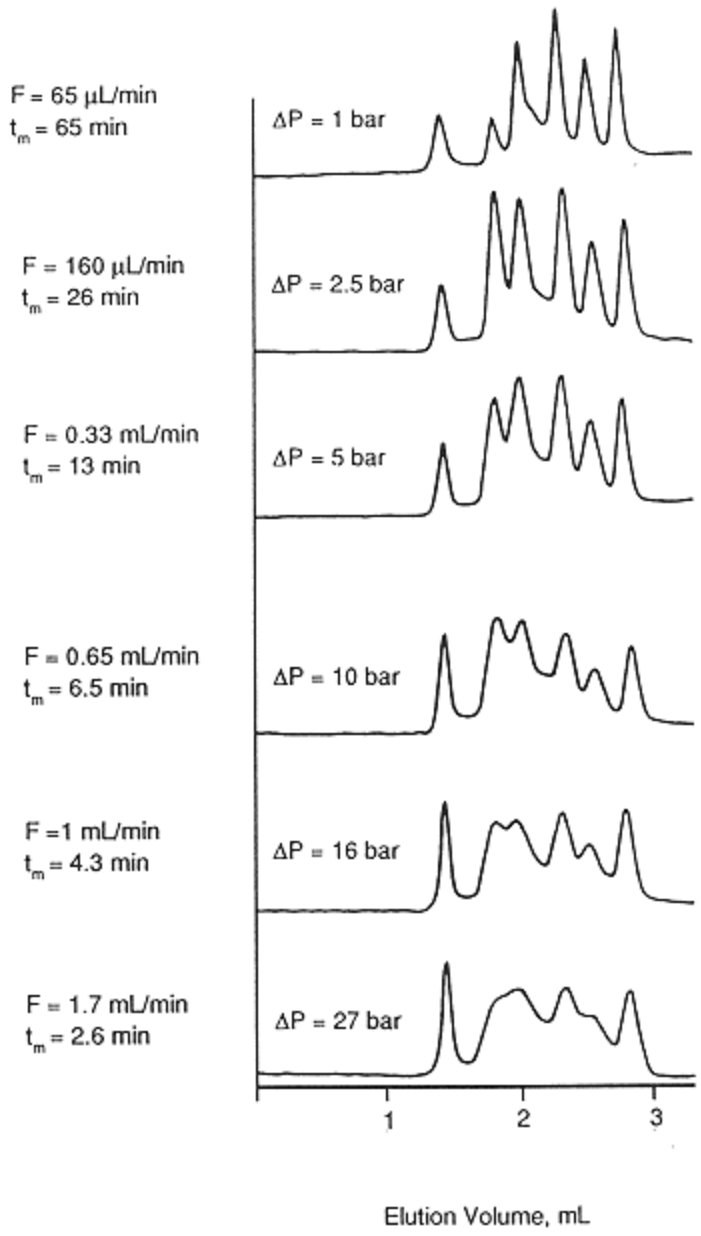

Figure 3.
Efficiency of amide-bonded SEC columns as a function of flow rate. Column, amide-bonded Grace 250 A silica, 10 µm, 25 cm × 4.1 mm; mobile phase, 0.1 M Tris, pH 7, + 0.4 M sodium chloride; detection, 280 nm, UV; elution order, thyroglobulin, alcohol dehydrogenase, conalbumin, myoglobin, cytochrome c, and dinitrophenylglutamic acid.

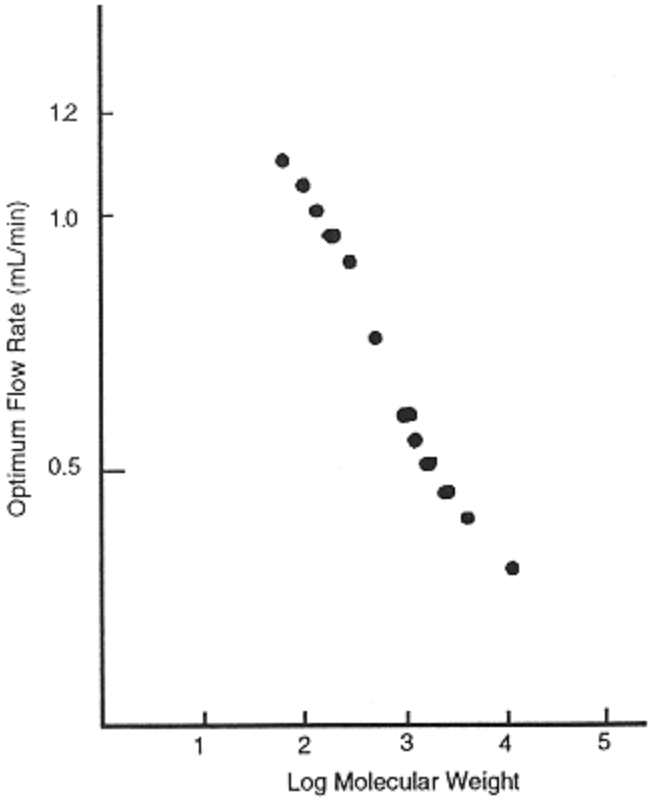

Figure 4.
Optimum flow rate as a function of peptide molecular weight. Column, TSKgel G3000SW, 10 µm, 60 cm × 7.5 mm; mobile phase, 0.15 M phosphate, pH 7.4, + 1 M sodium chloride, 20% methyl Cellosolve, and 1% SDS; detection, fluorescence, o -phthalaldehyde method (J. Benson and P. Hare, Proc. Natl. Acad. Sci. USA, 72: 619, 1979); temperature, 22°C; injection, 0.2 nmol peptide.

molecular weights that can be separated, and the available pore volume throughout the pore size distribution determines the quality of the separation. In general, the larger the volume of the pores per unit column volume, the better the resolution.

As shown in Equation (4), the pore volume V_p is equal to the empty column volume V_C minus the sum of the interparticle or interstitial volume V_i and the volume of the solid particle matrix V_S.

$$V_p = V_C - (V_i + V_S) \quad (4)$$

The pore volume per unit column volume can be maximized by decreasing the interparticle volume and/or by decreasing the volume of the solid matrix. For mechanically stable packing materials, such as silica, the interparticle volume occupies about 40% of the empty column volume. Irregular particles can give rise to larger interparticle volumes than spherical particles because of particle bridging (54), although V_i values as low as 35% of the column volume have been found, presumably caused by smaller particles fitting tightly between larger particles (55). Note that because silica is a rigid support, the interparticle volume cannot be reduced by deforming the particles, an approach successfully demonstrated by Hjerten and Liao for reducing the interparticle volume of soft gel agarose-composite particles (56).

The comparison of SEC columns that differ in length and diameter is simplified by converting the relevant volumes to porosities, dimensionless parameters defined in Equations (5) through (8):

$$\epsilon_i = \frac{V_i}{V_C} \qquad \text{interparticle or interstitial porosity} \tag{5}$$

$$\epsilon_P = \frac{V_P}{V_C} \qquad \text{intraparticle or internal porosity} \tag{6}$$

$$\epsilon_S = \frac{V_S}{V_C} \qquad \text{fraction filled by solid packing} \tag{7}$$

$$\epsilon_T = \epsilon_i + \epsilon_P \qquad \text{mobile-phase porosity} \tag{8}$$

The mobile-phase porosity ϵ_T represents the fraction of the column occupied by mobile phase between the particles and in the pores; it is readily calculated from Equation (9):

$$\epsilon_T = \frac{4Ft_0}{\pi d_C^2 L} \tag{9}$$

where F is the flow rate, t_0 the elution time of an (unretained) small molecular weight molecule, and d_C and L are the column internal diameter and length. Also commonly used is the particle porosity ϵ_{SP}

$$\epsilon_{SP} = \frac{V_P}{V_P + V_S} \tag{10}$$

Equation (10) can also be expressed as the ratio $V_{SP}/(V_{SP} + V_{SS})$, in which V_{SP} is the specific pore volume (ml/g adsorbent) and V_{SS} is the volume of pure solid per gram. Equation (11) presents the relationship between particle porosity and internal porosity:

$$\epsilon_P = \epsilon_{SP}(1 - \epsilon_i) \tag{11}$$

The range for the interparticle porosity ϵ_i listed in Table 3 is largely based on data from Reference 34. It was found that GFC columns packed with spherical particles have interparticle porosities ranging from 0.35 to 0.39, but columns packed with irregular particles showed V_i values as high as 0.47. These values are in reasonable agreement with earlier findings from Giddings (54), who reported ϵ_i values in the range 0.37–0.43. Experiments by the authors with spherical 5 µm, 100 Å pore size silicas have repeatedly found a value of 0.40 for the interparticle porosity and 0.75–0.80 for the mobile phase porosity. Values as low as 0.34 for ϵ_i were measured when these silicas were more fragile and had mobile-phase porosities ϵ_T of 0.80–0.84. Examples of these two types of silicas are shown later. Engelhardt reported 0.42 for the interstitial porosity of solid glass beads and 0.80–0.88 for the mobile-phase porosity of totally porous supports (57).

For particles with very large pores, pore volume is sometimes sacrificed for mechanical stability. For example, when particles varying in pore size from 10 to 385 nm, but with nearly identical porosities, were subjected to pressure tests, those with the largest pore sizes collapsed at lower pressure drops (see Reference 23, p. 174). Thus, the mechanical stability of larger pore size particles can only be maintained by reducing the pore volume. Alternatively, larger pore size particles must be slurry packed at lower pressures, thereby decreasing the stability and lifetime of the packed bed.

Chemical modification of the silica surface results in a loss of pore volume. Thus, the bonded phase layer must be optimized to reduce effectively interactions with silanol groups while minimizing the thickness of the bonded layer to avoid reducing the pore volume and preventing slow transport kinetics in the stationary phase. For example, the thickness of the stationary phase layer was estimated as 0.56 nm for a C3-alkyl functional group and 2.45 nm for C18-alkyl, assuming that the ligands stand upright on the surface (58). This assumption is thought to be correct under conditions that fully solvate the stationary phase layer, which is the case in GFC as well as GPC, in which the stationary and mobile phases have similar polar or nonpolar characteristics, respectively. Under such conditions, however, the bonded phase layer can be partially penetrated by the solutes and, thus, the loss of pore volume is smaller than expected based on the volume of the bonded-phase layer. Henry recently showed the shift in the pore diameter distribution for a polyethyleneimine phase with a layer thickness of 0.85 nm (26).

The average pore size of modern analytical HPLC packings is 100 Å, range 60–120 Å. Figure 5 shows the internal surface area versus pore diameter for four commercial 5 µm silicas with pore sizes ranging from 60 to 120 Å as determined by mercury porosimetry (33). This technique can measure pore diameters down to 30 Å, which is the upper limit of the size range for micropores. Note that the data in Figure 5 are biased toward the smallest pore sizes, which

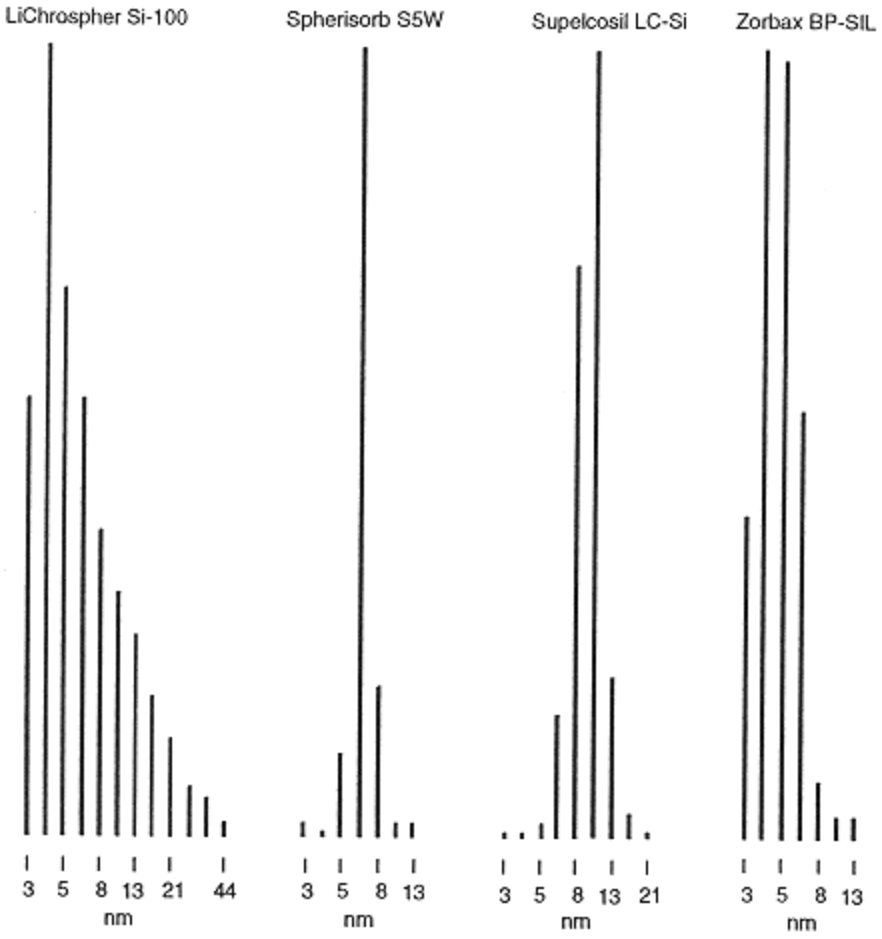

Figure 5.
Pore size distributions of HPLC silicas. Internal surface area versus pore diameter for four commercial 5 µm silicas were determined by mercury intrusion using Micromeritics Autopore II 9200 at pressures up to 60,000 psi (400 MPa). Packing materials, LiChrospher Si-100 (Lot 602F659316), Spherisorb S5W (Lot F5259), Supelcosil LC-Si (Lot 180-86), and Zorbax BP-Sil (Lot 20357-58).

by virtue of their number can contribute significantly to the total surface area while representing a relatively smaller fraction of the total pore volume. It is clear, however, that Spherisorb and Supelcosil have narrower pore size distributions than Zorbax and, particularly, LiChrospher.

The application of the silicas shown in Figure 5 in SEC is demonstrated in Figure 6, in which six narrow molecular weight polystyrene standards ranging

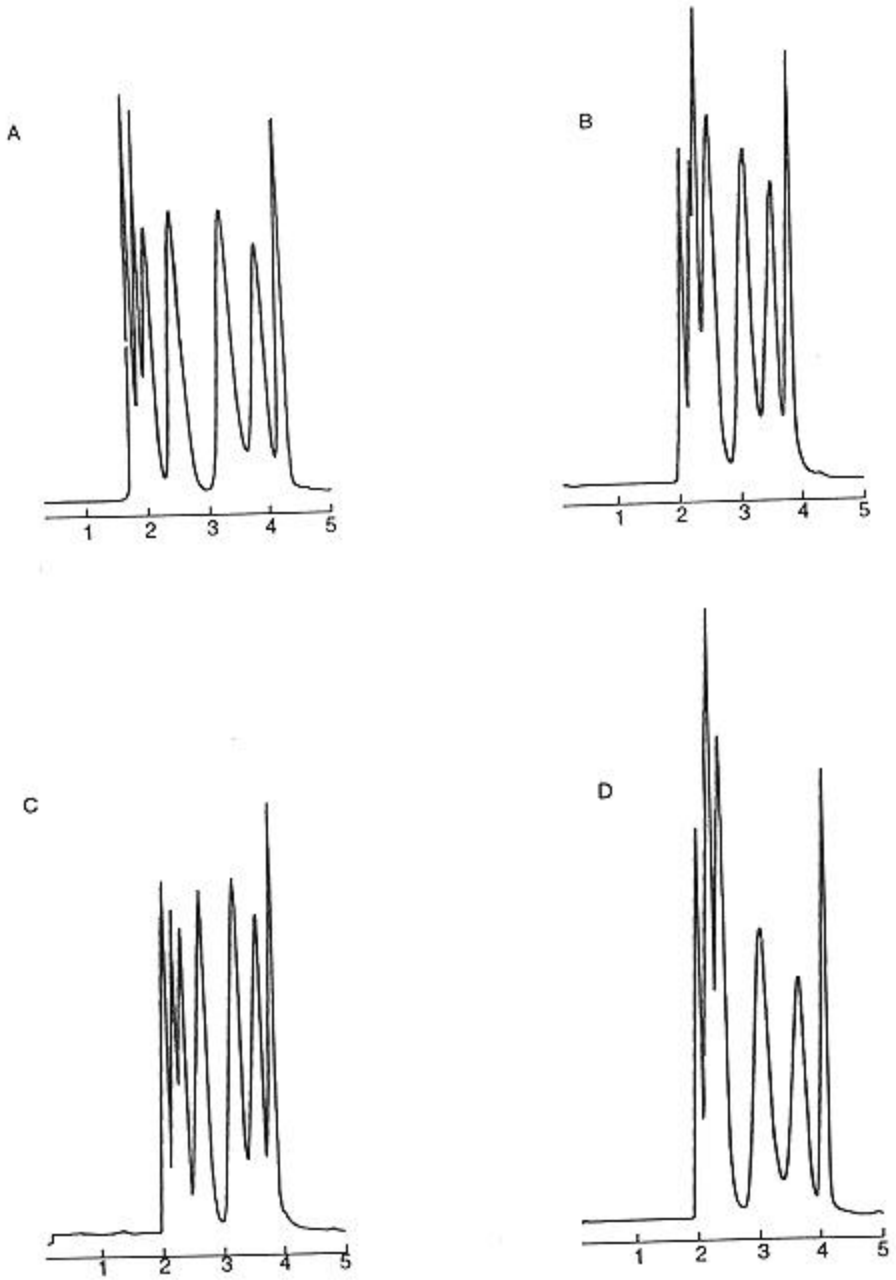

Figure 6.
Separation of polystyrenes on small pore size silica columns. Columns LiChrospher Si-100 (A), Spherisorb SSW (B), Supelcosil LC-Si (C), and Zorbax BP-Sil (D). Lot numbers as in Figure 5, 15 cm × 4.6 mm; mobile phase, methylene chloride; flow rate, 0.5 ml/minute; detection, 254 nm, UV; temperature, 35°C; sample, polystyrenes, MW 4,480,000, 450,000, 50,000, 17,500, 4000, and 890 dalton, and toluene (92), time scale in minutes.

from 4,480,000 to 890 dalton are separated on 15 cm X 4.6 mm ID columns packed with 5 µm LiChrosorb Si-100, Spherisorb S5W, Supelcosil LC-Si, and Zorbax BP-SIL, respectively (33). Toluene is included in the mix to mark the total inclusion volume. The calibration curves for the four silicas, as well as for Nucleosil 120-5 and YMC-GEL SIL 120A S5, are shown in Figure 7 (33). To simplify the comparison of the different packing materials, normalized retention volume V_E/V_i - 1, is plotted on the *x*-axis instead of elution volume. The normalized retention volume, which is zero for a totally excluded solute, is a direct measure of the retention of a compound beyond the interstitial volume.

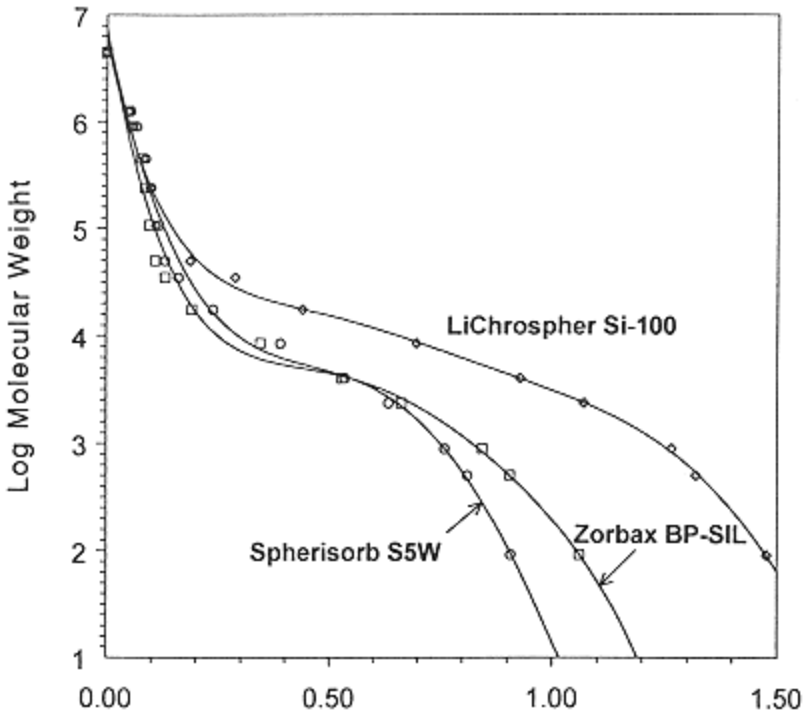

Figure 7.
Polystyrene calibration curves for small pore size silicas. Columns, 5 µm, LiChrospher Si-100, Spherisorb S5W, Zorbax BP-SIL, YMC_GEL SIL 120A S5 (Lot 600327), Supelcosil LC-Si, and Nucleosil 120-5 (Lot 4101), 15cm X 4.6 mm; sample, polystyrenes as in Figure 6 plus MW 1,260,000, 900,000, 240,000, 107,000, 35,000, 8500, 2350, and 500 dalton; other conditions as in Figures 5 and 6.

It is evident from the chromatograms in Figure 6 that of all the columns, LiChrospher provides the best separation for polystyrenes above 17,500 dalton molecular weight, followed by Supelcosil. LiChrospher is also the best choice for separations below 17,500 dalton molecular weight, followed closely by Zorbax. This last result is expected based on the large number of small pores that were measured for LiChrospher and Zorbax in Figure 5. In support of the data shown in Figure 5, the calibration curve for LiChrospher Si-100 in Figure 7A also confirms the presence of pores much larger than 100 Å. In terms of the available pore volume, both the LiChrospher and the YMC silicas are considerably more porous than the other silicas shown in Figure 7. Although this property is particularly attractive for their use in SEC, silicas with large pore volumes are more fragile, as shown later in this section. It is interesting to note

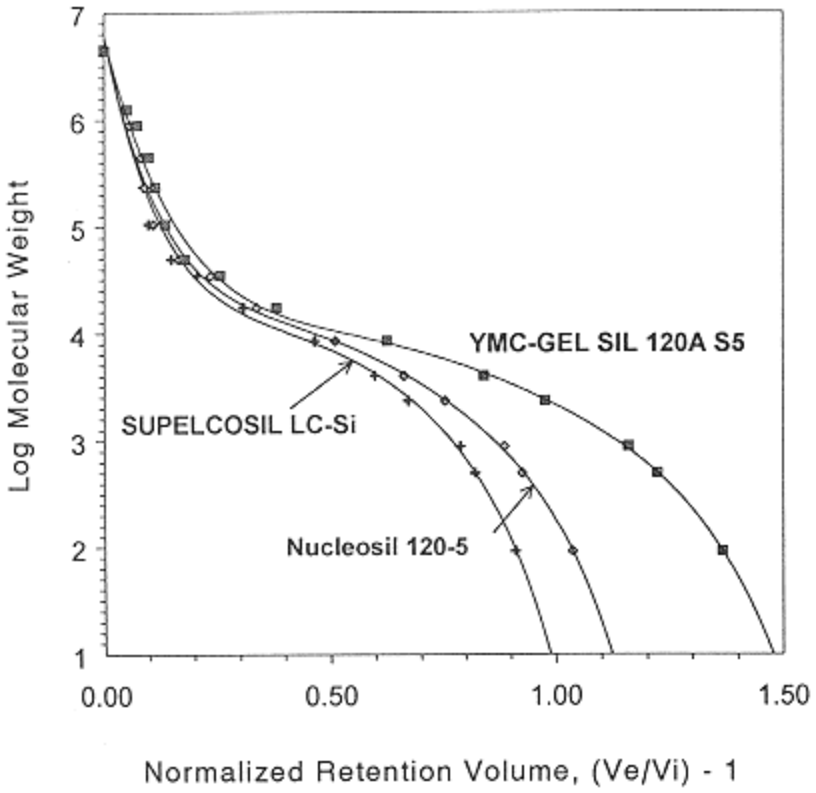

Figure 7.
Continued

that the interparticle porosity for both high pore volume silicas was only 34% of the empty column volume, but that of the other silicas was 40%. A low interparticle porosity can result when a silica has a broad particle size distribution such that the smallest particles can occupy the interparticle space between the larger particles. It is also possible that some particle fracturing took place during column packing. The backpressure for the LiChrospher column was about 25% higher than that for the more robust Spherisorb, Supelcosil, Nucleosil, and Zorbax columns, and the backpressure for the YMC column was twice as high. In comparison with the stronger silicas, the efficiency for the 15 cm LiChrosorb and YMC columns was about 7000 versus 10,000 theoretical plates and the peak asymmetry factor was 0.6 versus 0.9, respectively. Despite these lower values for the column performance parameters, it is clear from Figure 6 that good overall peak shape and resolution were obtained for the polystyrene test mixture on the more fragile LiChrospher silica. Note also that all silicas shown in Figures 5 through 7 were primarily developed for analyzing small molecular weight compounds. Although, as shown in Figure 7, even small solutes are partially excluded from entering all pores, silicas with pores in the range 60–120 Å are large enough to be fully accessible for the molecular weight range (below 2000 dalton) of most organic compounds analyzed by HPLC.

Unlike silica, polymer-based particles are readily available in smaller pore sizes. Small pore size silicas, such as Merck 40 or Davisil 20, are not commercially available in the 5–10 μm particle size range suitable for high-performance SEC. Syloid 63, a food additive produced by W. R. Grace, is an irregular 9 μm particle size silica with 22 Å pores and 0.4 ml/g pore volume. Its broad particle size distribution does not make it readily suitable for high-performance SEC of small molecules.

Table 5 lists two lines of commercially available silica-based gel permeation columns. The selection was limited to the Zorbax and LiChrospher silicas because these materials were specifically developed for gel permeation chromatography. Zorbax silica has a 6 μm particle size for optimum efficiency. The pore sizes were chosen such that a linear calibration curve is obtained when coupling columns of different pore sizes. In addition to plain silicas, Zorbax silicas are also available derivatized with trimethylchlorosilane, providing a surface that is less adsorptive for certain organic soluble polymers. Several important water-soluble industrial polymers, such as polyacrylamide, polyacrylic acid, and polyvinyl alcohol, do not require deactivation of the silica surface to obtain ideal size exclusion behavior. LiChrospher silicas are 10 μm in size; they vary in pore size from 100 to 4000 Å to allow the separation of very large polymers.

Table 6 summarizes the most well-known silicas used in gel filtration chromatography. Note that all the silicas are derivatized. The diol functionality, or some variation thereof, is the most widely used. Because most proteins have molecular weights well below 1 million dalton, they can be separated on silica-

Table 5 Selected Silica-Based Columns for Gel Permeation Chromatography

Column description	Supplier/manufacturer	Stationary phase	Dimensions (cm × mm)	Particle size (μm)	Pore size
Zorbax	Mac-Mod	C_1, also silica	25 × 6.2	6	60
PSM-60					300
PSM-300					1000
PSM-1000					
LiChrospher	Merck	Silica	25 × 4	10	100
Si 100				10	300
Si 300				10	500
Si 500				10	1000
Si 1000				10	4000

[a]Polyethylene glycol.

Table 6 Selected Silica-Based Columns for Gel Filtration Chromatography

Column description	Supplier/manufacturer	Stationary phase	Dimensions (cm × mm)	Particle size (μm)	Pore size (Å)	Ex
UltraSpherogel	Beckman	Polyether				
SEC 2000			30 × 7.5	5	140	
SEC 3000				5	230	
SEC 4000				5	350	
Bio-Sil	Bio-Rad	—				
SEC 125			30 × 7.8	5	125	
SEC 250				5	250	
SEC 400				5	400	
Zorbax	Mac-Mod	Diol on				
GF-250, 250XL		Zr-clad	25 × 9.4	6, 4	150	
GF-450, 450XL		silica		6, 4	300	
LiChrospher	Merck	Diol				
Si 100 DIOL			25 × 4	10	100	P
Si 300 DIOL				10	300	
Si 500 DIOL				10	500	
Si 1000 DIOL				10	1000	
Si 4000 DIOL				10	4000	

(table continued on next page)

(table continued from previous page)

Column description	Supplier/manufacturer	Stationary phase	Dimensions (cm × mm)	Particle size (μm)	Pore size (Å)	E:
Protein-Pak	Waters	Diol				
Protein-Pak 60			30 × 7.8	—	60	
Protein-Pak 125				—	125	
Biosep-SEC	Phenomenex	—				
S2000			30 × 7.5	5	145	
S3000				5	290	
S4000				5	500	
SynChropak	SynChrom	Diol				
GPC Peptide			25 × 4.6, 30 × 7.8	5	50	
GPC100				5	100	
GPC300				5	300	
GPC500				7	500	
GPC1000				7	1000	
GPC4000				10	4000	
TSKgel	Tosoh/TosoHaas, Supelco, others	Glycol ether				
2000SW and SW_{XL}			SW: 30, 60 × 7.5	10, 5	130	
3000SW and SW_{XL}			SW_{XL}: 30 × 7.8	10, 5	240	
4000SW and SW_{XL}				13, 8	450	

Table 7 Separation Ranges for Polymers on TSK-GEL SW Columns

Sample and mobile phase	TSK-GEL G2000SW	TSK-GEL G3000SW	TSK-GEL G4000SW
Polyethylene glycol, water	500–15,000	1,000–35,000	2,000–250,000
Dextran, water	1,000–30,000	2,000–70,000	4,000–500,000
Globular proteins[a]			
Common buffers[b]	5,000–100,000	10,000–500,000	20,000–7,000,000
6 M guanidine-HCl[c]	1,000–25,000	2,000–70,000	3,000–400,000
0.1% SDS[d]	15,000–25,000	10,000–100,000	15,000–30,000
Common buffers[e]	<30,000	30,000–500,000	>500,000
6 M guanidine-HCl[e]	<10,000	10,000–70,000	>70,000
0.1% SDS[e]	—	<60,000	>60,000
RNA[f]	70,000	150,000	1,500,000
DNA[g]	50,000	100,000	300,000

[a]Data from Reference 59.

[b]Examples: 0.05 M sodium phosphate buffer (pH 7.0) containing 0.3 M NaCl, or 0.05 M Tris-HCl containing 0.2 M NaCl, or 0.2 M disodium (or dipotassium) hydrogen phosphate and 0.2 M sodium (or potassium) dihydrogen phosphate.

[c]Guanidine hydrochloride (6 M) in 0.1 M sodium phosphate, pH 6.0.

[d]Aqueous sodium dodecyl sulfate (0.1%) in 0.1 M sodium phosphate, pH 7.0.

[e]Optimum separation range.

[f]Exclusion limit in 0.1 M phosphate buffer (pH 7.0) containing 0.1 M NaCl and 1 mM EDTA (60).

[g]Exclusion limit for double-stranded DNA in mobile phase listed in Note d (60).

based SEC columns with pore sizes of 500 Å or less. Table 7 shows the fractionation ranges for globular proteins in common buffers and under denaturing conditions on TSK-GEL SW columns varying in pore size from 125 to 500 Å (59). Table 7 also shows the fractionation ranges for double-stranded DNA fragments (60). Note that globular proteins are more compact in solution than double-stranded DNA fragments. Using acrylic-based TSK-GEL PW_{XL}, columns, DNA fragments of up to 10 times this size can be separated (61).

Surface Area

Independent of other qualities, surface area is a crucial parameter in the development of an adsorbent because it determines its capacity for purifying or drying chemicals or for catalyzing a reaction. In contrast to the techniques used in interactive chromatography or catalysis, an ideal size exclusion support is not

chemically or physically attractive to any sample component. Size exclusion requires the presence of pores, and thus surface area is still a critical factor in the design of SEC packing materials. A discussion of hydrodynamic size exclusion chromatography, in which polymer particles are separated by size on the external surface of the (porous or nonporous) particles, falls outside the scope of this chapter (62).

The surface area of a 60 Å silica is approximately 500 m^2/g; that of a 500 Å silica is about 50 m^2/g. The packing density of silica, although dependent on the type, is approximately 0.5 g/ml. Thus, a 25 cm × 4.6 mm column contains about 2 g silica, which, depending on the pore size, has a surface area from 100 to 1000 m^2. Equation (12) shows that surface area is inversely proportional to pore diameter (see Reference 23, p. 37):

$$D_P = 4 \times 10^3 \frac{V_{SP}}{S_{BET}} \quad (12)$$

D_P is the mean pore diameter (nm), V_{SP} is the specific pore volume (ml/g), and S_{BET} is the surface area (m^2/g). In theory, pore volume does not change when preparing silicas of different pore diameter by the same procedure. As discussed, the relationship between pore size and surface area is at best approximate because a balance must be struck between particle strength and pore volume. Given the same pore volume, large-pore particles are more brittle than those with small pores. Operation under HPLC conditions requires that the particles withstand the high pressures required for packing. Although small-particle SEC packings are usually operated at low linear velocity, silica-based columns must be packed at relatively high pressures to ensure physical stability of the column. Figure 8 shows the results of a simple test to determine the pressure at which particles fracture (63). The experiment was performed with a constant pressure pump. After filling the column for 5 minutes at 3000 psi, the pressure was increased in 1000 psi increments to 12,000 psi, at which point the hysteresis was determined by lowering the pressure to 4000 psi. Note that the relationship between flow rate and pressure for 100 Å Supelcosil LC-Si silica is linear over the entire pressure range, but that the pressure-flow rate curve for LiChrospher Si-100 starts to deviate from linearity at 6000 psi. Flow rates at higher pressures are lower than expected, and the decline in permeability is permanent. Similar results (not shown) were found for YMC-GEL 120A silica, which started to deviate from linearity at 5000 psi. It was shown earlier that the pore volumes of LiChrospher Si-100 and YMC-GEL SIL 120A S5 were considerably higher than that for Supelcosil LC-Si. A standard procedure to strengthen silica is to sinter the particles at high temperature (23,64). As a result, the distribution of the pores shifts toward larger sizes, and if performed in the presence of a high-melting salt, pore volume can be maintained.

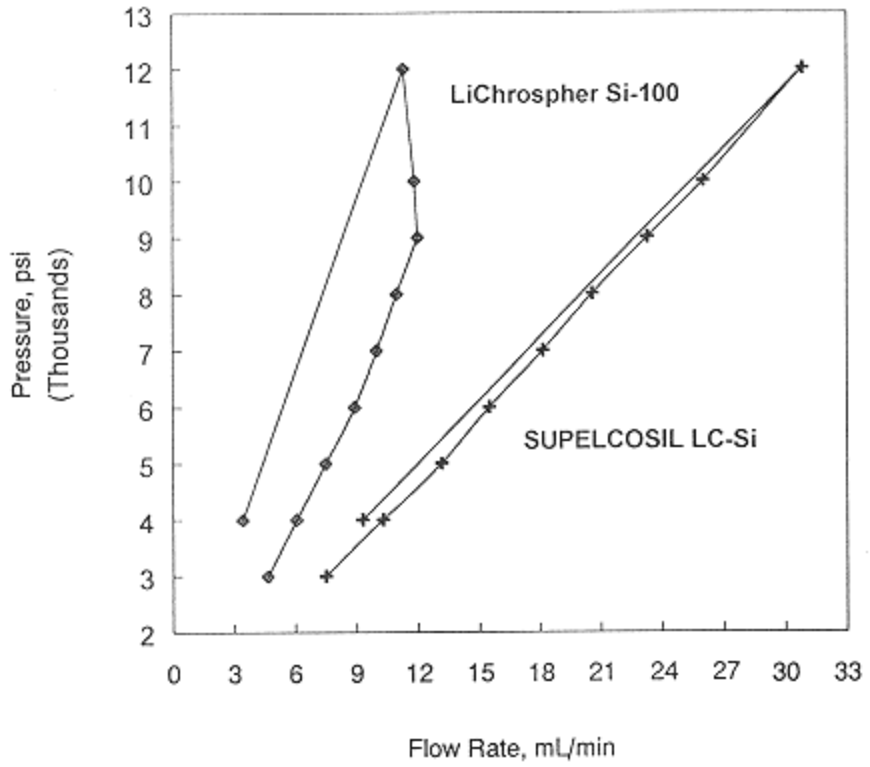

Figure 8.
Stability of HPLC silicas during column packing. Packing materials, 2.25 g of 5 µm Supelcosil LC-Si and 1.35 g of 5 µm LiChrospher Si-100; columns, 15 cm × 4.6 mm; extension, 10 cm × 4.6 mm; slurry reservoir, 35 ml; Haskel pneumatic amplifier Model DSTV-122C; slurry and driving solvent, methanol; see text for details.

Silanol Groups

The strong affinity of silica toward polar solutes, which makes it an excellent choice as an adsorbent in adsorption chromatography, is responsible for it being a less than ideal column packing material for size exclusion chromatography. The amorphous nature of silica is reflected in the random distribution of various chemical structures on the surface, as shown in Figure 9 (23). Free silanols are isolated from other hydroxyl groups by an O-O bond distance larger than 0.30 nm, that is, the average bond distance between two hydrogen-bonded silanol groups. Vicinal and geminal silanols are not commonly discriminated and are referred to as *bound silanols.* Because silica is hygroscopic at room temperature, it contains physically adsorbed water. Heating under vacuum at 473 K for sev-

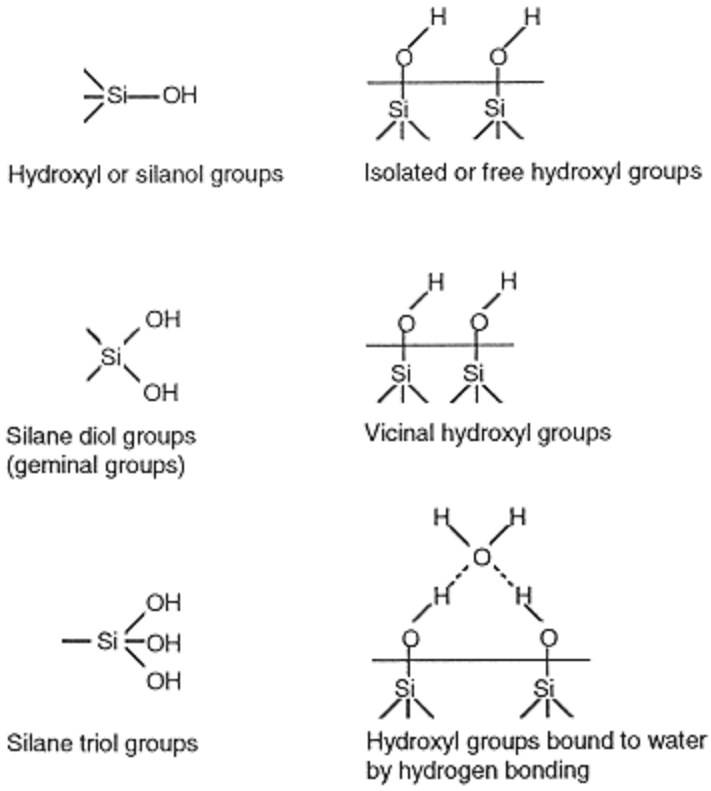

Figure 9.
Silanol groups on silica surface.

eral hours drives off most of this water. At higher temperatures, however, condensation of bound silanols results in the formation of *siloxane bonds.* The total concentration of silanol groups (free and bound) on silica is about 8 μmol/m^2. Of these groups, the free silanol groups constitute the premier adsorption and reaction sites. The bound silanol groups play a secondary role in the adsorption process.

It is well known in HPLC that silica-based packings have two important shortcomings: the silica matrix is not stable at alkaline pH, and most silane-bonded phases can be cleaved at a pH below 2. After chemical modification, approximately 4 μmol/m^2 of silanol groups remains unbonded. These residual silanol groups are negatively charged above pH $\simeq$ 3 and, when accessible, may interact with positive charges on a polymer surface. Because of the use of organic solvents in GPC, chemical stability of the silica is not a concern. The

limited stability at high pH, however, is a potential problem in GFC. In general, proteins are most stable at pH 7–8, which is the upper limit of the accepted pH range for silica-based packing materials. By removing metal impurities in the starting material, several manufacturers have been able to produce highly purified silicas, although it is not yet clear whether ultrapure silica particles have the same chemical stability as standard silica particles. Taking the opposite approach, silica particles when covered with 1 μmol/m^2 of zirconium oxide before performing the diol bonding reaction, allowed extended operation at pH 8 or greater without degrading the column performance (65). An alternative approach involves the preparation of polymerized bonded phases. The bonded layer makes the ≡Si-O-Si bond less accessible to nucleophilic attack, and it requires cleavage of multiple bonds to cause loss of bonded phase. The performance of polymer bonded or encapsulated phases have been reported for a C18-silicone polymer bonded to high-purity silica (28), but this approach has not been extended to the development of silica-based SEC packing materials.

Deactivation

The use of mobile-phase additives to deactivate silanol groups is the most practical way to make them inaccessible to solute molecules. This approach is based on the well-known observation from adsorption chromatography that the activity of silica gel is strongly dependent on the presence and amount of water in a (largely) nonaqueous mobile phase. Thus, in adsorption chromatography, the retention of sample components can be varied by adjusting the amount of water in the mobile-phase. (Because sometimes a variation of as little as 10 ppm water can make the difference between a good separation and no separation at all, alcohol is frequently used to modify retention, which requires a larger volume and is thus easier to control.)

Early successful attempts at reducing the activity of silanol groups on porous glass supports included the use of mobile-phase modifiers (66) and coating the surface with 20,000 dalton polyethylene oxide (67). A more permanent way to deactivate silanol groups is to convert them through chemical reaction. Regnier and Noel first demonstrated that by reacting controlled porosity glass beads with glycidoxypropyltrimethoxysilane, followed by opening the epoxide ring under acid conditions, resulted in a hydrophilic surface suitable for analysis of proteins, nucleic acids, and polysaccharides by a size exclusion mechanism (5). Other examples of modifications are discussed here.

Chemical Modification

As mentioned in the introduction, the explosive growth of HPLC would not have taken place without the recognition that instead of coating the stationary phase to the silica surface, a permanent bonded phase would do away with some

important limitations of physically held phases (68–70). Among these limitations were slow equilibration, decreasing retention as a function of time, and the inability to inject samples dissolved in solvents that were miscible with the stationary phase. Early investigations in bonded phase synthesis (69,70) employed esterification of surface silanols to form an ≡Si-O-C bond, which, however, was found to hydrolyze in aqueous solutions (71). It was replaced by the silylation reaction, leading to the formation of the more stable ≡Si-O-Si-C bond (72). Initial bonded phase columns did not have the required physical stability and reproducibility of retention and selectivity. Development of improved packing and bonding procedures (73–75) corrected these weaknesses, resulting in the design of reliable, automated HPLC-based analyzers (76).

It is interesting to note that the first prepared HPLC bonded phase, named C18 after the octadecylsilane bonding reagent, soon became the most popular column type. According to a 1991 survey, this continues to be the case today with almost half of all HPLC analyses being performed on this column type (77). Chemical modification of the silica surface with long-chain alkyl groups creates a nonpolar, hydrophobic surface that interacts with sample molecules through weak dispersion (van der Waals) forces. Retention is in direct proportion to the hydrophobic surface area of the molecule, and elution is accomplished with a mobile phase consisting of a mixture of water and an organic solvent, such as methanol or acetonitrile. The use of an aqueous mobile phase has greatly simplified the injection of samples studied in the life and food sciences and related industries (particularly the pharmaceutical industry), as well as in the chemical industry. Because the polarities of the mobile and stationary phases were the opposite of those in adsorption chromatography, this mode of liquid chromatography is generally referred to as reversed phase LC.

Several polar bonded phases were developed based on the same bonding chemistry used to prepare C18, C8, and other alkyl bonded phases. Cyanopropyldimethylchlorosilane, 1,2-epoxy-3-propoxypropyltriethoxysilane, and amino-propyltriethoxysilane were reacted to obtain cyano, diol, and amino polar bonded phases, respectively. The cyano phase is a weaker adsorbing surface than plain silica, but it shares the benefit of bonded phases in that equilibrium is reached within minutes and retention is not strongly affected by traces of water in the mobile phase. Because of the presence of the propyl anchor group, the cyano phase has also been used as a weak alkyl bonded phase with aqueous/organic mobile phases. Under such conditions, the cyano group imparts special polar selectivity, such as seen in the analyses of tricyclic antidepressants and PTH (phenylthiohydantoin) amino acids. The amino phase has mainly been applied to the analysis to carbohydrates using water/acetonitrile mobile phases. The separation mode resembles adsorption (normal phase) chromatography in that an increase in the percentage of water decreases retention. Although the diol phase has been applied as a substitute for silica in the analysis of steroids,

for example, its main use has been as a support in gel filtration chromatography, as discussed later in more detail. Columns packed with cyano, amino, or diol bonded phase silica are more popular in adsorption chromatography than plain silica columns (77).

Figure 10 shows the type of chemistry for the preparation of the diol bonded phase, the usefulness of which was first demonstrated for SEC by Regnier and Noel (5). The 1,2-epoxy-3-propoxypropyltriethoxysilane reagent is bonded to the silica following a reaction in toluene at 120°C for 12 h. After a washing step, the epoxide ring is opened by heating the bonded silica in strong acid for 1 h. In aqueous mobile phases, unreacted ethoxy groups are converted into silanol groups that can contribute to extra retention and adsorption effects. The bonding chemistry shown in Figure 10 for preparing GFC phases is similar to the standard procedures for preparing deactivated phases for GPC. In this case, trimethylchlorosilane is bonded with silica in the presence of toluene as a solvent. Usually the reaction is repeated to maximize the coverage of trimethylsilyl groups. This “end-capping” step is also used as a second reaction in the preparation of reserved-phase packing materials but is not common for most polar bonded phases.

The diol functional group has been commercialized by several manufacturers (see Table 6), but other functional groups are worth mentioning. Engelhardt and coworkers have investigated the properties of, in particular, the amide bonded

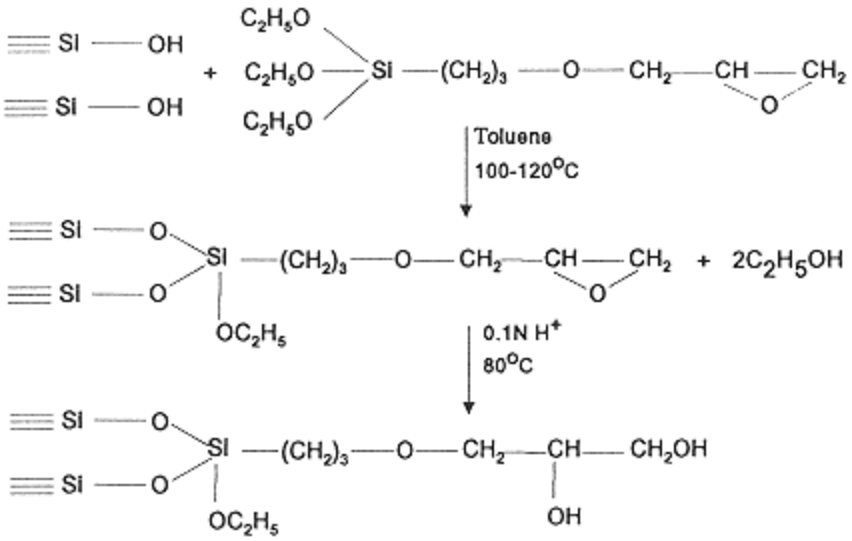

Figure 10.
Diol bonding reactions.

phase, which is prepared by reacting *N*-(3-triethoxysilylpropyl)acetamide with silica under similar conditions as used for the diol phase (52,78). In a related paper, the same authors demonstrated the fractionation of milligram quantities of polypeptides and proteins up to 50,000 dalton molecular weight, with excellent recovery of biological activity on amide columns prepared from LiChrosorb Si-100 silica (79). Miller et al. synthesized an ether bonded phase of the general formula $\equiv$ Si-O-Si$(CH_2)_3$-O-$(CH_2$-CH_2-O$)_n$-R, where n = 1, 2, or 3 and R = methyl, ethyl or n-butyl (80). Resulting phases allowed the separation of proteins under hydrophobic interaction or SEC conditions. Functional groups were bonded to the silica as trialkoxysilane reagents. The reaction was performed in the presence of water to control the formation of a bonded phase network that is more stable in aqueous solutions than those produced from di- or monofunctional silanes (81). When operated in the SEC mode, an ether bonded phase column showed stable elution volumes for basic proteins in high ionic strength (0.5 M ammonium acetate, pH 6.0) mobile phase after flushing the column for 40,000 column volumes. At low ionic strength (0.05 M ammonium acetate, pH 6.0), the retention of lysozyme increased twofold during the same experiment. Recently, Poppe et al. discussed the inertness and stability of a maltose stationary phase (82). Effective shielding of the silica surface was obtained by reacting maltose to aminopropyl bonded silica. Stability against hydrolysis greatly improved by using acid-washed silica, by adding a small amount of water to the silica before bonding with amniopropylsilane, and by polymerizing the glucose units in the maltose groups at 100°C under vacuum. The hydrophilic nature of the "polymaltose" phase allowed the exclusion of all but the most basic proteins. The chemistry of the popular TSK-GEL SW columns has not been described in the open literature. The SW stationary phase has been referred to as a "glycol ether-type bonded phase" similar in nature to the diol phase (83), containing the structure -CH_2C(OH)HCH_2O- (14).

Calibration

As mentioned in the introduction, in high-performance gel filtration chromatography, silica- rather than resin-based packing materials are more widely used for biopolymer separations. This is true for peptides, proteins, and possibly also for nucleic acids, although size exclusion is not a common technique for determining the molecular weight or for isolating this class of compounds. Polymer-based packings are the material of choice for most other water-soluble polymers, including oligo- and polysaccharides and the many examples of natural and synthetic polymers discussed in other chapters.

GPC is routinely used for determining the average molecular weight of an organic soluble polymer and the distribution of the molecular weights around

this mean. Although desirable, it is often not possible to obtain a reliable value for the molecular weight of a protein by GFC. Despite elaborate bonding procedures, all available silica-based (and polymer-based) packings show some deviation from ideal size exclusion behavior for proteins. Unreacted and accessible silanol groups are responsible for secondary retention mechanisms, resulting in inaccurate MW estimates. This section discusses calibration curves for proteins and other biopolymers. A review of the various parameters responsible for non-ideal elution behavior follows.

Under ideal SEC conditions, all solutes elute at a retention volume V_E that is larger than the interparticle volume V_i but smaller than the mobile-phase volume V_T (which is the sum of V_i and the pore volume V_P). The distribution coefficient K_D for elution by ideal SEC is given by Equation (13), in which K_D varies from zero for a fully excluded solute to one for a small molecular weight solute capable of penetrating all the pores:

$$V_E = V_i + K_D V_P \quad (13)$$

The selectivity curve of a packing material is obtained by plotting the elution volume, or some function of V_E, versus an expression of the solute size. It is known that the size for a random coil of a linear polymer is correlated with its molecular weight. Thus, for polystyrene standards of known molecular weight, a unique pore diameter can be assigned at which the polymer is excluded from the pores of a packing material. With dextrans, the relative volume of the random coil is smaller because of the higher relative molecular mass per unit chain length. As a result, dextrans possess larger elution volumes than polystyrenes of identical molecular weights. Proteins, more dense than random coils, elute as even "smaller" molecules, and their calibration curves are displaced from polystyrene and dextrans of the same molecular weight. Figure 11 (84) shows this effect for calibration curves of polyethylene glycols, dextrans, and proteins on TSK-GEL SW columns containing spherical 10 µm particles with pore sizes of 130 Å (G2000SW), 240 Å (G3000SW), and 450 Å (G4000SW). The data in Figure 11 emphasize that calibration should occur with standards possessing the same shape and hydrodynamic volume characteristics as the solute.

Several references have outlined the various methodologies for obtaining correct calibration curves (8,17,18,46,85,86). The simplest is the *peak position calibration* method. It can be used for macromolecules that have a unique molecular weight (such as proteins) or a narrow distribution of molecular weights. The logarithm of the molecular weight for a series of known molecular weight standards ($M_W/M_N \leq 1.1$, where M_W and M_N are the weight- and number-average molecular weights) is plotted versus their elution volumes. In the absence of secondary (i.e., non-SEC) retention mechanisms, the resulting calibration curve is the well-known S-shaped curve containing a linear portion. Thus, a column is selected for which the solutes of interest elute on the linear portion of the

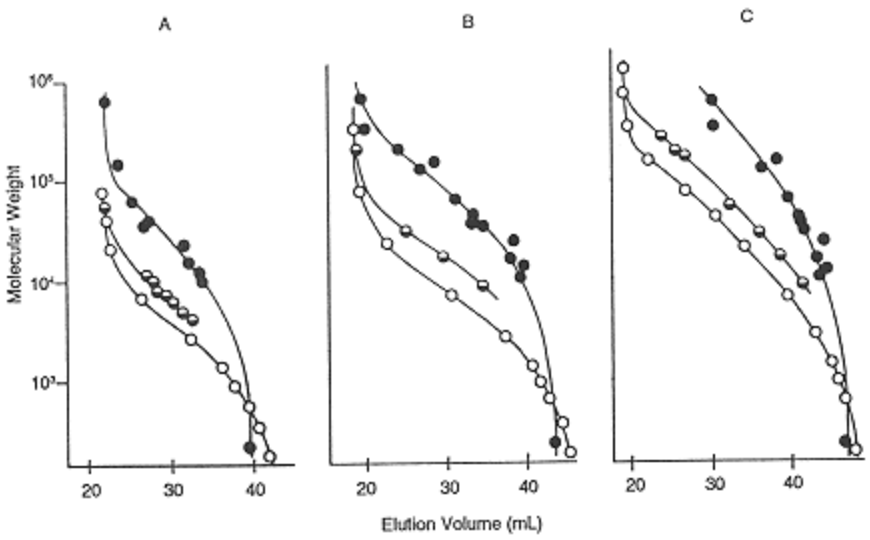

Figure 11.
Calibration curves for proteins (closed circles), polyethylene glycols (open circles), and dextrans (half-closed circles). Columns, TSKgel SW, 10 µm, 60 cm × 7.5 mm, two in series. (A) G2000SW, (B) G3000SW, (C) G4000SW. Mobile phase, proteins: 0.1 M phosphate, pH 7, + 0.3 M sodium chloride; dextrans and polyethylene glycols: distilled water; flow rate, 1.0 ml/minute; detection, 220 nm, UV.

curve. This method requires narrow distribution standards and samples that have the same molecular conformation as the standards. Without appropriate standards, the calculated molecular weight for an unknown can be in error by two- to threefold and up to an order of magnitude under the most unfavorable conditions (46).

The effect of pore diameter upon K_D values for globular proteins was investigated by Gooding and Freiser (11). For the same protein, the K_D value was approximately 0.2 units lower on a 100 Å material versus a 300 Å material. The slope of the linear portion of the calibration curve indicates the homogeneity of the pore structure. The smaller the slope, the more pores there are of the same size and the higher the potential for resolution of two solutes with similar molecular weight (10,19,34). The steeper the slope, the larger the variety of pores of different size and the broader the range of molecular weights that can be separated.

When no narrow molecular weight distribution standards are available, then the *single broad standard calibration* or integral molecular weight distribution method provides the most accurate molecular weight measurements. Reference 8 outlines this method, which requires knowledge of the complete molecular weight distribution [i.e., weight- (M_W) and number-averaged (M_N) molecular

weights] for a single broad molecular weight polymer. Unlike narrow standard methods, calibrations obtained by broad standard methods are affected by instrumental peak broadening. Without corrections, this calibration error can cause errors in the molecular weight analysis of polymer samples. The GPC calibration curve is obtained by matching those molecular weight and elution volume values that correspond to the same value of sample weight fraction on the molecular weight distribution and GPC elution curves (8).

Approximate molecular weights can be obtained when the single broad standard method or universal calibration method is not feasible (8,46). The accuracy of this method depends upon the unknown polymer having the same structure and molecular weight distribution as the standard.

The *universal calibration method* can be utilized for the molecular weight determination of known polymers. This method is valid when polymer retention is determined only by its hydrodynamic volume. In this case, a plot of the logarithm of the intrinsic viscosity times molecular weight, log [η] MW versus the elution volume of the polymer provides a calibration curve that applies to all polymers. The resulting universal calibration curve is approximately the same for all polymers (random coil, rigid rod, or spherical). First, a peak position calibration is performed for the molecular weight range of interest using narrow molecular weight standards, such as polystyrene, providing a value for M_2. After obtaining values for k_1, k_2, and α, the unknown molecular weight M_1 can be calculated from Equation (14):

$$M_1 = \left(\frac{k_2}{k_1}\{M_2^{\alpha_2+1}\}\right)^{1/\alpha_1} \quad (14)$$

where M_2 is the molecular weight determined by the peak position calibration curve method, k_1 is the coefficient of the analyzed polymer, k_2 is the coefficient of the molecular weight standard, and α_1 and α_2 are the second coefficients of the polymer and the molecular weight standard, respectively. Equations (15) and (16) show how k and α are calculated:

$$k = 6.19 \times 10^{\circ} K^{1/3} \quad (15)$$

$$\alpha = \tfrac{1}{3}(1 + a) \quad (16)$$

KK and *a* are Mark-Houwink constants that account for the molecular weight dependence of the intrinsic viscosity. The universal calibration method is broadly applicable given the availability of Mark-Houwink constants. Reference 87 summarizes Mark-Houwink constants for a number of common polymers. Sources of error for the universal calibration method are discussed in References 8, 86, and 88. As can be expected, serious errors occur if mechanisms other than size exclusion are at work. Cassassa stated that [η]MW is not a true universal elution parameter, although both theory and experience indicate good results for species

of similar type (89). Based on theoretical considerations, Cassassa predicted a common [η]MW dependence, however, between random coil polymers and rod-like structures over a narrow range of molecular weight. Indeed, a good fit to universal calibration for dextrans and some native proteins was found over a narrow (1×10^6 to 1.2×10^7) molecular weight range (90).

It was mentioned earlier in this section that the hydrodynamic volume and shape of the standards, in addition to their molecular weight, plays a role in calibration. A claim can be made that the elution behavior of a protein is better related to its Stokes radius R_S than to its molecular weight (91). However, this relationship is not widely employed. The plot of R_S versus the inverse error function erf^{-} of 1 - K_D can be linear if the pore distribution is Gaussian with respect to the Stokes radii of the macromolecules. Work with detergent-soluble membrane proteins emphasizes the need to calibrate with similar standards and the effectiveness of R_S plots (91). Different standards are required for water-soluble globular and detergent-soluble membrane proteins. Often the membrane proteins may be excluded or retarded. A smooth, although nonlinear, relationship was obtained for the plot of R_S versus erf^{-}(1 - K_D), and a scatter of points was observed for log MW versus K_D. Detergent-bound proteins behave differently, and their Stokes radii may be off by 10–30% when calibration curves are based on the elution volumes of water-soluble proteins. Figure 12 (91) shows the selectivity curve for water-soluble and detergent-soluble membrane proteins. All the points for the water-soluble proteins lie on a sigmoid curve (except fibrinogen, which has different behavior as a result of its asymmetrical shape). The membrane proteins clearly fall outside the calibration curve for water-soluble proteins, so that the Stokes radii estimated from this curve are high by 10–30%.

Himmel and Squire (85) found significant improvement in the determination of protein molecular weight using denaturing conditions. Their study reconciles the size parameters of proteins and random coils by determining $F_{(v)}$ in Equation (17):

$$F_{(v)} = \left(\frac{V_E^{1/3} - V_i^{1/3}}{V_T^{1/3} - V_i^{1/3}} \right) \quad (17)$$

Much less error for the molecular weight determination is found when plotting $F_{(v)}$ versus MW$^{1/3}$ than K_D versus log MW, R_S versus MW$^{1/3}$, or $K_D^{1/3}$ versus MW$^{1/3}$. Tarvers and Church (92), working with TSKgel G3000SW columns, utilized both native and denatured proteins to compare plots of $F_{(v)}$ versus erf^{-}(1-$F_{(v)}$, R_S versus erf^{-}(1 - $F_{(v)}$), and R_S versus erf^{-}(1 - K_D) and confirmed plots of $F_{(v)}$ versus MW$^{1/3}$ provided a better estimate of protein molecular weight. The method of Himmel and Squire (e.g., $F_{(v)}$ versus MW$^{1/3}$) has been used to produce linear curves with native proteins (93–95), denatured proteins (96), and, independently, globular proteins (97).

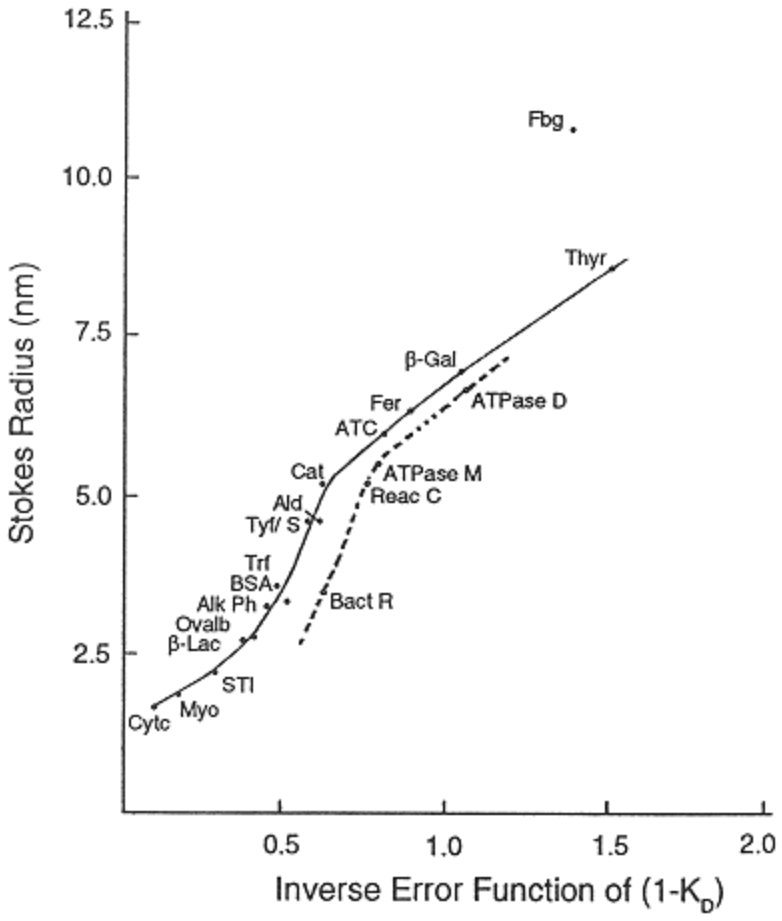

Figure 12.
Calibration curves for water-soluble proteins (closed circles) and detergent-soluble membrane proteins (open circles). Column, TSKgel G3000SW, 10 μm, 30 cm × 7.5 mm; mobile phase, 200 mM sodium acetate, 10 mM imidazole, 30 mM HEPES, and 0.1 mM calcium chloride, pH 7.0, and 0.5 mg/ml of $C_{12}E_8$; detection, 280 nm, UV; injection, 20–250 μl containing 1 μg to 2 mg. Abbreviations: Fbg, fibrinogen; Thyr, thryoglobulin; β-Gal, β-galactosidase; Fer, ferritin; ATC, aspartate transcarbamylase; Cat, catalase; Ald, aldolase; Tyr/S, tyrosyl-tRNA synthetase; Trf, transferrin; BSA, bovine serum albumin; Alk Ph, alkaline phosphatase; Ovalb, ovalbumin; β-Lac, β-lactoglobulin; STI, soybean trypsin inhibitor; Myo, myoglobin; Cytc, cytochrome c; ATPase D, Ca^{2+}-ATPase dimer M, Ca^{2+}-ATPase monomer; Reac C, reaction center; Bact R, bacteriorhodopsin.

Denaturing gel filtration with 0.1% sodium dodecyl sulfate (SDS) or 6 M guanidine hydrochloride results in better resolution, increased accuracy, and an extended linear range. This provides a simple, rapid, and sensitive means of separating protein mixtures and determining protein molecular weights that deviate only 5–7% from reported values measured by gel filtration, sedimentation equilibrium, or SDS-polyacrylamide gel electrophoresis (98). On TSKgel G3000SW (Figure 13), the linear part of the calibration curve for proteins denatured in guanidine hydrochloride extends from molecular weight 9000 to 43,000. Using the same column, the calibration curve for SDS-denatured proteins is linear from 9000 to 93,000, and nondenaturing conditions provide a linear curve from 30,000 to 93,000 with no resolution below 30,000. Similar work by Kato (59) provided the optimum separation ranges presented in Table 7. Good agreement on protein behavior was seen between the various studies for G3000SW columns.

Secondary Retention

Schmidt et al. showed how retention volumes of globular proteins varied on silica-based diol bonded phase columns depending on the pH and ionic strength of the mobile phase and their effective charge (99). Because most proteins elute within the interstitial pore volume, size exclusion is the dominant effect; other possible mechanisms are secondary order effects (100). Pfankoch et al. investigated the importance of secondary retention mechanisms for several commercial GFC columns (34). As discussed, after derivatization with a hydrophilic bonded phase, silica-based packings exhibit residual and accessible silanol groups that dissociate within the usable pH range as a function of the pretreatment of the base silica. It was found that the pH of a solution of TSKgel G3000SW packing material in 0.5 M NaCl was slightly below 5 and that the number of dissociated silanol groups reached 0.013 meq/ml packing material at pH 8 (101). As a consequence, a basic solute, such as arginine, or a protein, such as lysozyme, is retained longer than expected because of interaction with the negatively charged silanol groups; acid proteins or small acids, such as citric acid, are repelled from the surface and elute earlier than expected based on their size. This is illustrated in Table 8, in which the distribution coefficients for citric acid and arginine are listed for various commercial columns as a function of the ionic strength of a pH 7.05 phosphate buffer (34). Normal SEC behavior for citric acid and arginine, that is, elution from the column in the void volume, can be expected on most commercial columns when operated at a mobile phase ionic strength of 0.24 or above. That the behavior of small molecular weight compounds does not always extrapolate to that for proteins is shown in Figure 14, in which the distribution coefficient K_D for lysozyme is plotted as a function

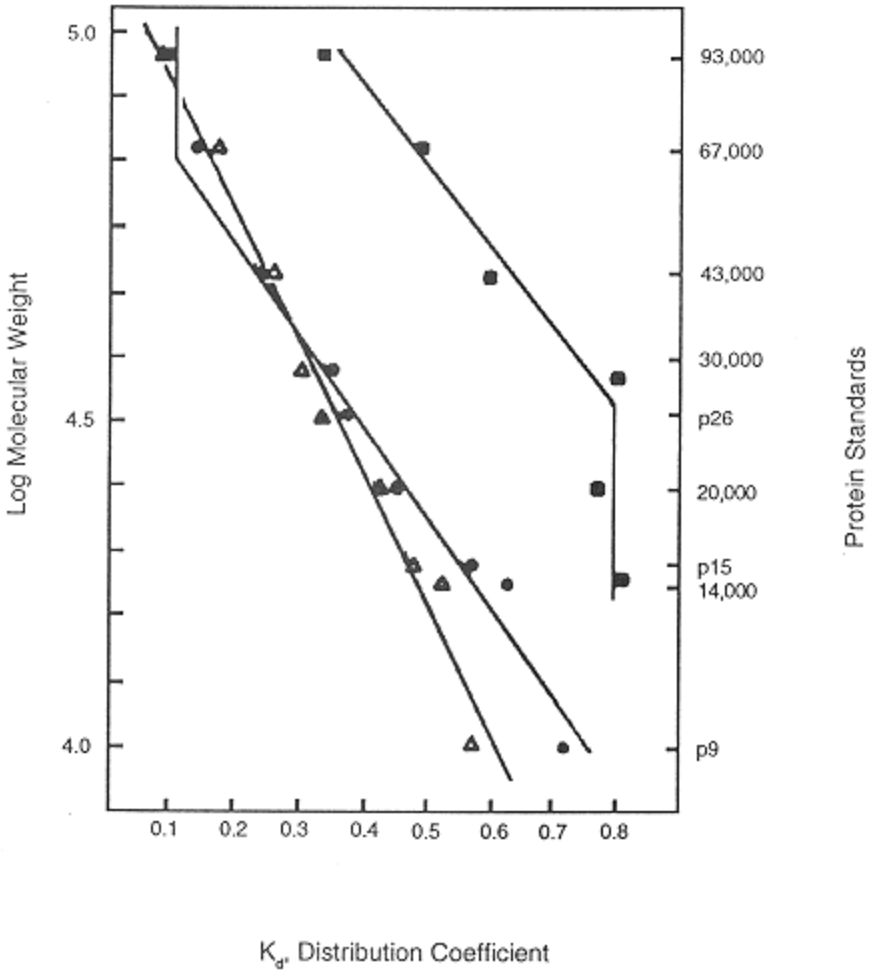

Figure 13.
Protein calibration curves for denaturing and nondenaturing conditions. Column, TSKgel G300SW, 10 µm, 30 cm × 7.5 mm; mobile phase, (circles), 20 mM sodium phosphate, pH 6.5, + 6 M guanidine hydrochloride; (triangles) 50 mM sodium phosphate, pH 6.5, + 0.1% SDS; (squares) 50 mM sodium phosphate, pH 6.5; flow rate, 0.2–0.4 ml/minute; detection, 280 nm, UV; temperature, 25 °C, sample, 1 mg/ml of each protein. Sample preparation: (circles) 20 mM sodium phosphate, pH 6.5, + 8 M guanidine hydrochloride and 1% 2-mercaptoethanol, heated at 100 °C for 2 minutes; (triangles) 10 mM sodium phosphate, pH 7.2, + 1% SDS, heated at 100°C for 2 minutes; (squares) 50 mM sodium phosphate, pH 6.5.

Table 8 K_D Values for Citrate, Arginine, and Phenylethanol as a Function of Ionic Strength for Commercial Silica-Based Gel Filtration Columns[a]

Solute and ionic strength	TSKgel G3000SW	LiChrosorb Diol	SynChropak GPC 100	TSKgel G2000SW	Waters I-125
Citrate					
μ = 0.026	0.66	0.54	0.46	0.43	0.39
0.12	0.89	0.81	0.76	0.75	0.72
0.24	0.92	0.95	0.89	0.84	0.79
2.40	0.94	0.99	0.91	0.88	0.88
Arginine					
μ = 0.026	1.30	1.53	1.35	1.57	1.70
0.12	1.05	1.15	1.06	1.06	1.23
0.24	1.02	1.05	1.01	1.02	1.16
0.60	1.00	0.99	—	0.99	1.08
2.40	0.98	1.07	0.98	0.98	1.00
Phenylethanol					
μ = 0.026	1.47	2.49	1.44	1.95	1.83
0.12	1.50	2.56	1.49	2.02	1.88
0.24	1.53	2.64	1.53	2.10	1.88
0.60	1.61	2.93	1.63	2.30	2.03
1.20	1.81	3.52	1.81	2.71	2.29
2.40	2.35	5.31	2.35	4.01	3.03

[a]The distribution coefficient K_D (or K_{SEC}) is defined by $V_E = V_i + K_D V_P$, in which V_E is the solute retention volume, V_i the interparticle or interstitial volume, and V_P the pore volume. Mobile phase: pH 7.05 phosphate buffer of indicated ionic strength.

Source: Data from Reference 34.

of ionic strength for the same set of commercial columns discussed in Table 8 (34). Based on the data in Table 8, it was expected that the TSKgel G3000SW and SynChropak GPC 100 columns would show similar behavior, but larger K_D values were expected for the remaining columns. Instead, lysozyme shows similar retention on the TSKgel and the LiChrosorb columns and much longer retention on SynChropak and Waters columns.

The importance of hydrophobic interactions as another secondary retention mechanism is also illustrated in Table 8, in which the distribution coefficient for phenylethanol is listed as a function of ionic strength for the same set of commercial GFC columns (34). Indicative of hydrophobic interaction, K_D values increase with increasing ionic strength for this uncharged solute. Thus, a balance must be stuck between the need to increase ionic strength to reduce ionic interactions and to decrease ionic

strength to limit hydrophobic interaction. In practice, hydrophobic interaction is not a strong component of protein retention in size exclusion chromatography because the hydrophobic side chains of the

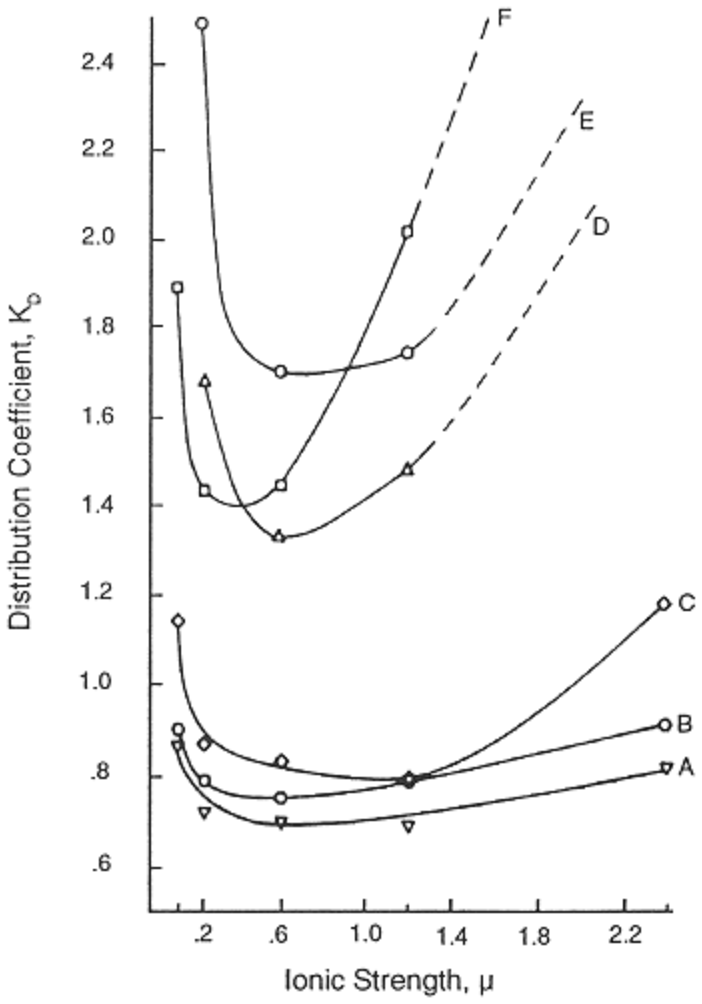

Figure 14.
K_D of lysozyme for commercial hydrophilic bonded silicas. Columns, 10 μm: (A) TSKgel G2000SW, 30 cm × 7.5 mm; (B) TSKgel G3000SW, 30 cm × 7.5 mm, (C) LiChrosorb Diol, 24 cm × 4.1 mm, (D) Shodex OH Pak B-804, 50 cm × 8 mm; (E) Waters I-125, 30 cm × 7.8 mm; (F) SynChropak GPC 100, 25 cm × 4.6 mm; mobile phase, phosphate, pH 3.0; detection 254 nm, UV.

amino acids are predominantly located in the interior of the protein. The addition of 5–20% of a nondenaturing solvent, such as ethylene glycol, to a high ionic strength mobile phase was shown to eliminate the hydrophobic interaction of globular proteins on a diol bonded phase column (99). In contrast to proteins, hydrophobic interaction can be significant in SEC of peptides, some of which may require high concentrations of organic solvents to obtain retention dominated by size exclusion (102,103). Mant et al. demonstrated the effectiveness of 0.1% trifluoroacetic acid or addition of organic solvents to overcome hydrophobic interactions (104). Additionally, the advantageous use of nonideal SEC behavior is detailed.

Kato and coworkers recommend the use of 0.05 M sodium phosphate buffer (pH 7.0) containing 0.3 M NaCl to obtain true size exclusion behavior for most proteins on 5 μm TSK-GEL SW$_{XL}$ columns (7). Not surprisingly, Mori and Kato recommend a very similar mobile phase, 0.1 M phosphate and 0.1 M NaCl at pH 7.0, for size exclusion on diol-bonded porous glass columns (105). Okazaki and Hara (106) recommend 0.15 M NaCl with lipoproteins, but various aqueous buffers with salts are satisfactory as long as the pH is less than 8.5. Salt concentration, buffering, and pH all may alter the lipoprotein separation and improve resolution. Increasing the buffering substance or salt concentration leads to peak broadening, indicating a salting-out effect.

Practical Considerations

Extracolumn Effects

Since the advent of high-performance liquid chromatography, it has been emphasized that the analyst be aware of the influence of the HPLC system components on column efficiency. In a chromatographic system, the observed column efficiency is caused not only by dispersion processes in the column. The peak volume is also broadened by dispersion outside of the column, including broadening of the sample band by the injector, injection volume, the detector cell, detector time constant, and connecting tubing. Once an HPLC system has been assembled, the extracolumn effects are constant factors that may or may not take away from the quality of the separation obtained in the column, depending on the column dimensions and the relative importance of each of the individual extracolumn effects.

The volume in which a band elutes from an HPLC column V_{PV} is defined as four peak standard deviations σ. The relationship between peak volume, retention volume V_E and efficiency of the peak N is given by the equation

$$V_{PV} = \frac{4V_E}{N^{1/2}} \quad (18)$$

in which V_E (earlier described as $V_i + K_D V_P$) can be expressed as a function of the column volume as shown in Equation (19):

$$V_E = 1/4\pi(d_c)^2 L(1 + K_D) \quad V_E = 1/4\pi(d_c)^2 L(1 + K_D)\epsilon_i \quad (19)$$

Substitution of Equation (19) in Equation (18) gives the following expression for the peak volume:

$$V_{PV} = \pi(d_c)^2 L(1 + K_D) \quad V_{PV} = \pi(d_c)^2 L(1 + K_D)\epsilon_i N^{-1/2} \quad N^{-1/2} \quad (20)$$

It is clear from Equation (20) that peak volumes are directly proportional to the volume of the column and that samples elute with smaller peak volumes from the same column when filled with a more efficient, that is, smaller size, packing material. The more efficient the column, the narrower are the sample bands and the more important is the effect of extracolumn band broadening. Wider columns provide for more peak volume, and this reduces the importance of extracolumn band broadening.

In ideal SEC, K_D ranges from zero for an fully excluded solute to one for a fully included solute. Unlike that in interactive liquid chromatography, in which efficiency is roughly independent of the retention factor, the highest efficiency in SEC is obtained for the smallest molecular weight compound that elutes last from the column, that is, in the total mobile-phase volume. Larger compounds that are partially excluded from the pores have broader peaks as a result of slower and restricted diffusion into the pores. The relative importance of extracolumn band broadening diminishes with increasing peak volume. Thus, in SEC, the contribution of the system to extracolumn band broadening is best studied for a small molecular weight solute that elutes in the total inclusion volume.

Sternberg (107) first showed that the variance of the chromatographic output function can be written as the sum of the variances of the distributions of the individual dispersion processes inside and outside the column, as shown in Equation (21):

$$\sigma^2_{obs} = \sigma^2_{col} + \sigma^2_{inj} + \sigma^2_{det} + \sigma^2_{ct} = \sigma^2_{col} + \Sigma\sigma^2_{ec} \quad (21)$$

where σ^2_{obs} is the observed variance or output variance and σ^2_{col} is the variance owing to column band broadening. The other variances represent the contributions from injector, capillary tubing, and detector, respectively, and $\Sigma\sigma^2_{ec}$ is the sum of extracolumn variances. If needed, Equation (21) can be extended with other variances, such as those caused by the electronics of the recording system. The validity of Equation (21) is limited to random dispersion processes that give rise to a Gaussian distribution. This condition is generally assumed in chromatographic applications. The equations describing the individual contributions from extracolumn band broadening are discussed in detail elsewhere (107–111).

Although ideally the observed variance is equal to the column variance, most HPLC systems detract from the column efficiency. Equation (22) can be used to calculate the importance of extracolumn effects:

$$\sigma^2_{obs} = \sigma^2_{col} + \sigma^2_{ec} = \sigma^2_{col} + \theta^2\sigma^2_{col} \quad (22)$$

where θ^2 is the fractional increase of the column variance caused by extracolumn effects. A 10% loss of column efficiency (or a 5% increase in band width) as a result of extracolumn effects, $\theta^2 = 0.1$, is considered acceptable in practice.

Injection effects as a result of mass and volume overloading or the injection technique can detract from column efficiency. As with other extracolumn effects, injection effects become more critical with smaller bore columns, which require smaller injection volumes and low flow rates; refer to Reference 110 for a discussion of extracolumn effects in microcolumn systems.

Equation (23) relates the maximum injection volume to the column dimensions, particle size d_p, mobile-phase porosity ϵ_T, θ, and reduced plate height (111). The constant K_{inj} depends on the injection technique; $K^{2inj} = 12$ for plug flow injection and varies from 2 to 9 for most commercial injectors (75). Equation (23) is valid for a small molecular marker that elutes in the total mobile-phase volume:

$$(V_{inj})_{max} = 1/4\pi K_{inj}\epsilon_T\theta(d_c)^2(Lhd_p)^{1/2} \quad (23)$$

For a reasonably efficient ($h \simeq 8$) 30 cm × 7.5 mm, 10 μm, SEC column, Equation (23) predicts a maximum injection volume of 165 μl for $K_{inj} = 3$, $\theta^2 = 0.1$, and $\epsilon_T = 0.8$. Figure 15 shows experimental data for the effect of injection volume on column efficiency for bovine serum albumin on a 30 cm × 7.5 mm, 10 μm, TSKgel G3000SW column (84). For a 0.5 mg sample load, column efficiency does not decline until the injection volume increases above 250 μl, or 2% of the empty column volume, in reasonable agreement with the predicted value. Note that mass overloading can be detrimental at much lower injection volumes. As demonstrated, dilution of the sample actually improves efficiency beyond the injection volume at which volume overload becomes apparent.

The construction of the detector cell and detector electronics can seriously detract from the efficiency of the column. Although generally some capillary tubing is contained in the detector, we assume that this can be neglected in comparison with the amount of capillary tubing used to connect the column to the injector and detector. This assumption is not valid when the column effluent is directed through a large-volume heat exchanger before entering the detector cell, as in most refractive index detectors. To minimize the band broadening of early peaks, the volume of the cell should be less than one-tenth the volume of the peak of interest (8,46).

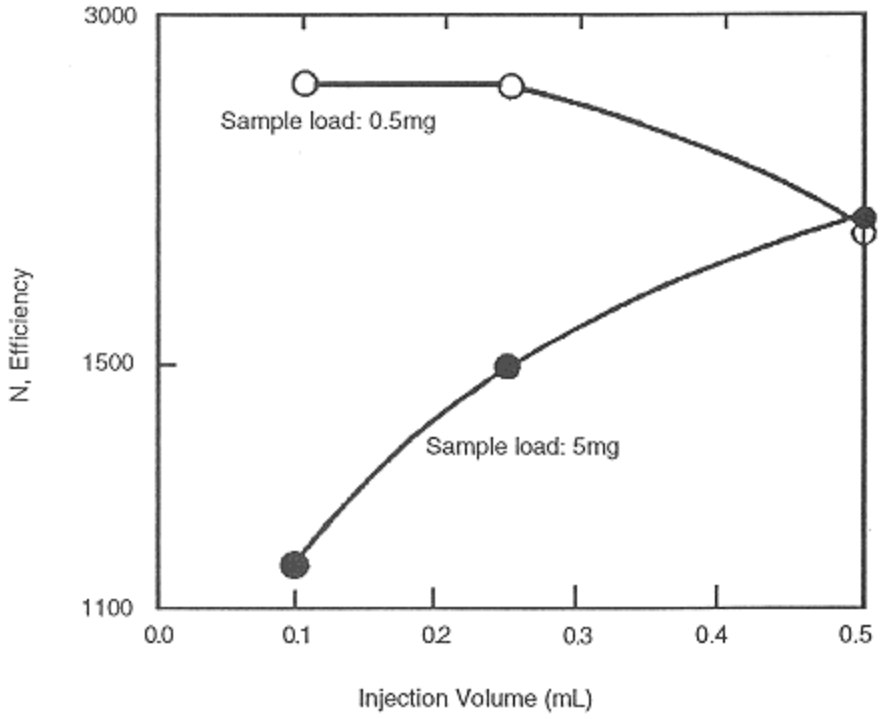

Figure 15.
Effect of sample volume on column efficiency. Column, TSKgel G3000SW, 10 µm, 60 cm × 7.5 mm; mobile phase, 0.1 M phosphate and 0.2 M sodium chloride, pH 7.0; flow rate, 1.0 ml/minute; detection, 280 nm, UV. (Adapted from Reference 83.)

The detector time constant can distort column efficiency when the peak width (in time units) becomes of the same order of magnitude as the response time. High-efficiency columns produce very sharp peaks, and detectors with response times greater than 0.5 s can contribute significantly to band broadening. Electronic filtering can increase response time and cause measurable broadening of sharp peaks. Refer to Reference 109 for an exhaustive discussion of extra-column effects in detector systems.

Capillary tubing should be kept as narrow and short as possible, while remaining practical. The length of tubing for a maximum band width increase of 5% can be calculated from Equation (24), taken from Reference 46:

$$L = \frac{40 V_E^2 D_m}{\pi F N d_{ct}^4} \quad (24)$$

in which D_m is the solute diffusion coefficient in cm^2/s, F is the flow rate in ml/s, d_{ct} is the ID of the capillary in cm, N is the plate number, and the retention volume (V_E) was earlier given by Equation (19). Equation (24) can also be used to calculate the dimensions of a detector cell for the ideal situation in which no mixing occurs in the cell, that is, the plug flow model. Bending, coiling, or deforming the tubing permits longer lengths with the same degree of band broadening as shorter lengths of straight tubing (112).

Sample

As discussed, there is a limit to how much can be injected into an HPLC column in terms of sample mass and volume at which the resolution deteriorates beyond acceptable levels. SEC has the lowest loading capacity (g sample/g packing material) for high-performance HPLC techniques because the separation is performed under isocratic mobile-phase conditions and because the separation takes place within the interstitial pore volume, that is, in the absence of a stationary phase. In general, samples are injected as a large volume of a dilute solution. As the increasing concentration overloads the inlet, asymmetrical and broad peaks are seen and resolution decreases. Gooding et al. (113) derived Equation (25) to calculate the theoretical protein load in milligrams for a 25 cm long column:

$$C \simeq \frac{r^2}{4.4} \quad (25)$$

where C is the loading capacity and r is the column radius in mm. Thus, for a column ID of 7.5 mm, the protein loading capacity is ~3.2 mg/injection. Kirkland and Antle (114) determined that 0.1 mg of a 4800 dalton polystyrene polymer could be injected per gram packing material in GPC on 47 Å silanized silica. Roumeliotis and Unger (100) found that 0.1 mg protein can be loaded per g LiChrosorb Diol material. They demonstrated that load is proportional to the cross-sectional area of the column regardless of particle size. They determined 1 and 8 mg, respectively, for 60 cm × 7.5 mm (10 g packing) and 60 cm × 21.5 mm (80 g packing) TSKgel G3000SW columns. Freiser and Gooding (115) reported loads of 2–4 mg without band broadening on a 300 × 7.8 mm SynChropak GPC 100 column. For best resolution, it is recommended that samples be 0.01–0.5% (wt/vol). However, very dilute samples (<10 μg) sometimes lead to skewed peaks and/or poor recovery (59). For preparative protein purification, loads are usually 10–20 mg/ml (15). The concentration dependence of polymers is a special case and is discussed next.

For macromolecules, the sample size may be limited by viscosity. As a rule of thumb, the sample injected should have a viscosity no greater than twice the viscosity of the mobile-phase. For proteins, this equals 70 mg/ml in a dilute

aqueous mobile phase (9). Thus, viscosity of the sample is seldom an issue with proteins, although it can be a problem when glycerol or sucrose is used as stabilizing agent or ethylene glycol is present to prevent protein adsorption. Increasing viscosity causes restricted diffusion and irregular flow patterns, which lead to broad and tailing peaks (116). With high molecular weight synthetic polymers, a sample concentration $\leq$ 0.1% is often required to eliminate undesirable effects on both molecular coil dimensions and sample viscosity (8). As the sample load increases, the polymer elutes at higher elution volumes (117). The concentration dependence can be attributed to contraction of polymer coils with increasing concentration. It may also be accounted for by the combined effects of coil contraction and sample viscosity in the interstitial pore volume. The viscosity effect can be operative to different extents, depending upon the column system. Viscosity can drastically affect retention volume and peak width (for molecules that elute within the interstitial pore volume), accounting for 80% of the total concentration effect. With other systems, coil contraction can account for 50–80% of the total concentration effect (117).

For small volumes, peak height increases with increasing sample volume, but retention time and resolution are not affected. At some critical volume, a noticeable decrease in retention time occurs (see Figure 15), as well as loss of resolution and efficiency. Theoretically, the maximum injection volume for protein SEC is equal to the separation volume between two proteins of interest, but in practice, microturbulence, nonequilibrium between stationary phase and mobile phase, and long diffusion lead to additional band broadening (116). As a general rule, the maximum injection volume is 1–2% of the total column volume (e.g., 265–530 µl for a 60 cm × 7.5 mm column), which agrees with the data shown in Figure 15. Injection volumes less than 1% of the column volume do not necessarily improve resolution. The manufacturer of TSK-GEL SW columns recommends injection volumes up to 0.5% of the analytical column volume (59).

Mobile Phase

A mobile phase is primarily chosen for its effectiveness in solubilizing and stabilizing the sample. Because of the short contact time related to the isocratic conditions, proteins remain stable if the appropriate mobile phase and column are used. As discussed earlier, nonideal SEC behavior may be observed on silica-based columns. Mobile phase considerations therefore play an important role in SEC. Elimination of protein adsorption is crucial, but the effect of the eluant on protein structure must also be considered. Additionally, polyelectrolytes expand and condense with changes in macroion concentration within the buffer (118).

Aqueous buffers around pH 6–8 are a good environment for many proteins and are suitable for silica-based SEC columns. The most common nondenaturing

aqueous buffers are phosphate (pK_a = 7.2) and tris(hydroxymethyl)aminomethane (pK_a = 8.1) (19,116). Phosphate buffer is most utilized because of the pH 2–7 limitation for silica-based materials. An ionic strength of 0.1–0.5 M is typically sufficient to prevent adsorption to the weakly anionic silica surface while avoiding hydrophobic effects. Hagel (19) suggested the use of Good's buffers (119) if the buffer capacity of phosphate is too low or its properties are incompatible with the sample; phosphate is known to inhibit certain enzymes (120). It has also been noted that borate may interact with glycopeptides (121). The type of buffer anion has a significant influence on adsorption of proteins to silica. Polyvalent anions, such as sulfate and phosphate, are more effective in preventing adsorption than monovalent anions (chlorine, perchlorate, and acetate). However, sulfates may salt-out proteins and promote hydrophobic interactions with the matrix. In those cases, chaotropic ions, such as perchlorate, can be used to increase the ionic strength of the buffer (19), if sodium chloride is undesirable because of its corrosive properties in the presence of stainless steel components.

Nonionic interactions can be eliminated by reversing the conditions used to prevent ionic interactions (i.e., increase pH and/or decrease ionic strength) or by adding a small amount of ethylene glycol, glycerol, organic modifier, or detergent. These additives do not affect the physical properties of silica-based matrices. This stability is an advantage over less rigid SEC supports. Kelner and coworkers (122) examined enzyme recovery from TSKgel G3000SW columns. The addition of glycerol reduces hydrophobic interactions and lessens denaturation. A more pronounced effect was seen for the recovery of α-amylase, and a striking increase in activity was found for adenosine deaminase. Increasing sodium chloride concentration led to a marked decrease in enzyme recovery as a result of hydrophobic interactions. Protein denaturation was more pronounced on the polymer-based TSKgel G3000PW column. The addition of glycerol did not overcome the observed lower mass or activity recoveries. Sykes and Flatman (123) report the use of organic modifier to decrease hydrophobic interactions of human calcitonin gene-related peptide to a TSKgel G2000SW$_{XL}$ column. Acetonitrile-trifluoroacetic acid eluants are attractive for reducing hydrophobic interactions and because of the volatile nature and ultraviolet (UV) transparency of this mobile phase. Protein resolution is dependent upon the acetonitrile concentration and requires the low pH trifluoroacetic acid provides. However, a severe limitation is the low solubility of proteins larger than 15,000 dalton in the 30–45% acetonitrile needed for optimum resolution. This low solubility leads to severe protein aggregation and limits the use of this mobile phase to peptides and low-molecular-weight proteins.

Detergents may be utilized to stop protein hydrophobic interactions with silica matrices. Some detergents are mild and allow nondenaturing conditions (e.g., sodium deoxycholate, Triton, and Nonidet P40). Deoxycholate is the most versatile detergent, with little absorbance at 280 nm. Triton and Nonidet P40

both exhibit strong absorbance in the UV range. The detergent binds to the hydrophobic portion of the protein without forming large micelle structures (this is controlled with the critical micelle concentration, CMC, of each detergent). Triton and Nonidet form large micelles that decrease resolution. Typically, deoxycholate can be used at 0.1%, pH 7.6–8.0, without forming large micelles (116). Detergents, such as SDS, may cause multisubunit proteins to divide into individual subunits, may change the protein quaternary structure from globular to elongated, or, through adsorption, may increase the size of the protein. SDS is always used at its CMC, and the amount of SDS bound is sensitive to the buffer concentration within the range 0.1–0.4 M (124).

The use of denaturing mobile phases is particularly helpful in the analysis of the composition of oligomeric structures (i.e., cell organelles, viruses, and multimeric enzymes), because they disrupt most noncovalent protein-protein interactions. Most common denaturing conditions utilize 0.1% SDS or 6 M guanidine hydrochloride. As mentioned earlier, denaturing conditions may be advantageous for molecular weight determination and lead to in increase in resolution. The use of SDS provides much better resolution than phosphate-guanidine hydrochloride systems because of the extended and uniform conformations of proteins. Takagi et al. (124) and Konishi (125) report the effect of salt concentration (phosphate) on complexes of SDS and polypeptides. Takagi found good resolution within the phosphate concentration range 0.05–0.15 M, although, in general, retention is a strong function of buffer concentration in SDS systems. This effect can only partially be explained by the change in the effective size of the complexes as a result of their polyelectrolyte-like nature. Ion exclusion appears to be at play for the lower concentrations. The complexes were totally excluded at lower buffer concentrations, repelled by the negative charges on residual and accessible silanol groups. Konishi found a linear relationship between log MW and K_D for polypeptides ranging from 1000 to about 80,000 dalton when eluted in a 0.20 M phosphate buffer in the presence of 0.1% SDS (125). At lower phosphate concentrations, the calibration curves were steep, but linear, up to 15,000 dalton and less steep and still linear at higher molecular weights. Furthermore, although the slope of the curves at high molecular weight were independent of salt concentration, below 15,000 dalton the slope became steeper with decreasing phosphate concentration. No marked effect of SDS concentration was detected for polypeptides 10,000 dalton or higher. For polypeptides with molecular weight less than 10,000 dalton, the plot in 1% SDS lost linearity and became steeper.

If SEC is being performed for preparative purification or desalting, such volatile buffers as ammonium bicarbonate or acetate may be preferred because they are readily removed by freeze drying. Organic modifiers, such as acetonitrile, are volatile but may lead to protein aggregation. Triethylamine formate,

pH 3.0, is also a volatile denaturing agent. Reference 120 lists more volatile buffer systems.

As shown in Figure 3, mobile phase flow rate has a strong influence on resolution. For larger molecules (polynucleotides and proteins), the mass transfer term is much larger and the flow rate must be correspondingly decreased. Typical flow rates are 0.5–1.0 ml/minute for 7.5 mm ID columns, and although better resolution can be obtained at much lower flow rates (see Figure 1), these rates represent the best compromise between separation efficiency and time.

Temperature

Although most SEC applications are run at room temperature, increased temperature may be utilized to improve the resolution of difficult separations or to decrease the viscosity. As long as the macromolecule is well dissolved, the influence of temperature on the slope and position of a molecular weight calibration curve is relatively minor (8). Some high molecular weight polyolefins and polyamides require temperatures of 100–135°C because the samples are not soluble at lower temperatures (46). With low molecular weight molecules, increasing the temperature may decrease adsorption. The extent and rate of formation of aggregates was investigated by Watson and Kenney using SEC at elevated temperatures (126). They found that the formation of aggregated species was the main reason for loss of monomer for interleukin-2 analog and γ-interferon.

References

1. J. Porath and P. Flodin, *Nature, 183:* 1657 (1959).

2. J. Moore, *J. Polym. Sci., Part A, 2:* 835 (1964).

3. J. Giddings, *Anal. Chem., 35:* 2215 (1963).

4. J. Kirkland, *J. Chromatogr., 125:* 231 (1976).

5. F. Regnier and R. Noel, *J. Chromatogr. Sci., 14:* 316 (1976).

6. K. Fukano, K. Komiya, H. Sasaki, and T. Hashimoto, *J. Chromatogr., 166:* 47 (1978).

7. Y. Kato, Y. Yamasaki, H. Moriyama, K. Tokunaga, and T. Hashimoto, *J. Chromatogr., 404:* 33 (1987).

8. *Modern Size-Exclusion Liquid Chromatography* (W. Yau, J. Kirkland, and D. Bly, eds.), John Wiley & Sons, New York, 1979.

9. K. Unger, in *Methods in Enzymology, Vol. 104, Part C: Enzyme Purification and Related Techniques* (W. Jakoby, ed.), Academic Press, New York, 1984, Ch. 7.

10. K. Gooding and F. Regnier, in *HPLC of Biological Macromolecules* (K. Gooding and F. Regnier, eds.), Marcel Dekker, New York, 1990, Ch. 3.

11. K. Gooding and H. Hagestam Freiser, in *High Performance Liquid Chromatography of Peptides and Proteins: Separation, Analysis, and Conformation* (C. Mant and R. Hodges, eds.), CRC Press, Boca Raton, FL, 1991.

12. G. Welling and S. Welling-Wester, in *HPLC of Macromolecules. A Practical Approach* (R. Oliver, ed.), IRL Press, Oxford, 1989, Ch. 3.

13. A Preneta, in *Protein Purification Methods. A Practical Approach* (E. Harris and S. Angal, eds.), IRL Press, Oxford, 1989, Ch. 6.

14. J. Dawkins, in *Packings and Stationary Phases in Chromatographic Techniques* (K. Unger, ed.), Marcel Dekker, New York, 1990, Ch. 7.

15. R. Scopes, *Protein Purification. Principles and Practice,* 2nd ed., Springer, New York, 1987, Ch. 6.

16. E. Stellwagen, in *Methods in Enzymology, Vol. 182: Guide to Protein Purification* (M. Deutscher, ed.), Academic Press, New York, 1990, Ch. 25.

17. K. Makino and H. Hatano, in *Aqueous Size-Exclusion Chromatography* (P. Dubin, ed.), Elsevier, Amsterdam, 1988, Ch. 9.

18. *Gel Chromatography. Theory, Methodology, Applications* (T. Klemmer and L. Boross, eds.), John Wiley & Sons, Chichester, 1979.

19. L. Hagel, in *Protein Purification. Principles, High Resolution Methods, and Applications* (J.-C. Janson and L. Ryden, eds.), VCH Publishers, New York, 1989, Ch. 3.

20. H. Barth and B. Boyes, *Anal. Chem., 64:* 428R (1992).

21. *Bibliography on Controlled-Pore Glass Chromatography and Related Subjects,* CPG, Inc., 32 Pier Lane West, Fairfield, NJ 07006, 1986.

22. G. Alexander, *Silica and Me,* ACS, Washington, DC, 1973.

23. K. Unger, *Porous Silica,* Elsevier, Amsterdam, 1979.

24. R. Iler, *The Chemistry of Silica,* Wiley, New York, 1979.

25. A. Berthod, *J. Chromatogr., 549:* 1 (1991).

26. M. Henry, *J. Chromatogr., 544:* 413 (1991).

27. M. Verzele, M. de Potter, and J. Ghysels, *J. HRC & CC, 2:* 151 (1979).

28. Y. Ohtsu, Y. Shiojima, T. Okumura, J.-I. Koyama, K. Nakamura, O. Nakata, K. Kimata, and N. Tanaka, *J. Chromatogr., 481:* 147 (1989).

29. J. Kohler, D. Chase, R. Farlee, A. Vega, and J. Kirkland, *J. Chromatogr., 352:* 275 (1986).

30. M. Nystron, W. Hermann, D. Sanchez, and P. Moller, *Kromasil, a New High Performance Silica for Liquid Chromatography,* EKA Nobel, S-44501, Surte, Sweden.

31. K. Komiya, H. Moriyama, and Y. Kato, Poster, Pittsburgh Conference, New Orleans, LA, 1993.

32. T. Nyhammer, Pharmacia Biotech AB, Uppsala, Sweden, personal communication (1992).

33. R. Eksteen, unpublished results (1986).

34. E. Pfankoch, K. Lu, F. Regnier, and H. Barth, *J. Chromatogr. Sci., 18:* 430 (1980).

35. J. Knox and M. Saleem, *J. Chromatogr. Sci., 7:* 614 (1969).

36. P. Bristow and J. Knox, *Chromatographia, 10:* 279 (1977).

37. G. Guiochon and M. Martin, *J. Chromatogr., 326:* 3 (1985).

38. J. Sjodahl and A. Winter, *Protides* in Vol. 30 (H. Peeters, ed.). *Biol. Fluids, Proc. Colloq.*, 1982, p. 693.

39. R. Schnabel and P. Langer, *J. Chromatogr., 544:* 137 (1991).

40. L. Sander and S. Wise, *Crit. Rev. Anal. Chem., 18:* 299 (1987).

41. K. Unger, *Packings and Stationary Phases in Chromatographic Techniques,* Marcel Dekker, New York, 1990.

42. J. Huber and J. Hulsman, *Anal. Chim. Acta, 38:* 305 (1967).

43. L. Snyder, *Anal. Chem., 39:* 698; *39:* 705 (1967).

44. H. Engelhardt and G. Ahr, *J. Chromatogr., 282:* 385 (1983).

45. T. Wilson and D. Simmons, Poster 116, HPLC' 92, Baltimore, MD, 1992.

46. L. Snyder and J. Kirkland, *Introduction to Modern Liquid Chromatography,* 2nd ed., Wiley, New York, 1979.

47. R. Scoot, *Liquid Chromatography Column Theory,* Wiley, New York, 1992.

48. J. Kirkland, *J. Chromatogr., 125:* 231 (1976).

49. D, Herman, L. Field, and S. Abbott, *J. Chromatogr. Sci., 19:* 470 (1981).

50. R. Kennedy and J. Jorgenson, *J. Microcol. Sep., 2:* 120 (1990).

51. B. Bidlingmeyer and J. Warren, *Anal. Chem., 56:* 1583A (1984).

52. H. Engelhardt and U. Schon, *Chromatographia, 22:* 388 (1986).

53. Y. Shioya, H. Yoshida, and T. Nakajima, *J. Chromatogr., 250:* 341 (1982).

54. J. Giddings, *Dynamics of Chromatography,* Marcel Dekker, New York, 1965.

55. C. Dewaele and M. Verzele, *J. Chromatogr., 260:* 13 (1983).

56. S. Hjerten and J. Liao, *J. Chromatogr., 457:* 165 (1988).

57. H. Engelhardt, *Practice of High Performance Liquid Chromatography,* Springer, New York, 1986.

58. G. Berendsen, Thesis, Delft University, Delft, The Netherlands, 1980, Ch. 5.

59. Y. Kato, *LC.GC, 1:* 540 (1983).

60. Y. Kato, H. Parvez, and S. Parvez, in *Progress in HPLC,* Vol. 1 (H. and S. Parvez, eds.), VNU Science Press, Utrecht, The Netherlands, 1985.

61. Y. Kato, Y. Yamasaki, and T. Hashimoto, *J. Chromatogr., 320:* 440 (1985).

62. G. Stegeman, J. C. Kraak, and H. Poppe, *J. Chromatogr., 550:* 721 (1991).

63. G. Huntzinger and R. Eksteen, Poster 508, HPLC'86, San Francisco, CA, 1986.

64. J. van de Venne, J. Rindt, G. Coenen, and C. Cramers, *Chromatographia*, *13:* 11 (1980).

65. R. W. Stout and J.J. DeStefano, *J. Chromatogr., 326:* 63 (1985).

66. T. Mizutani and A. Mizutani, *J. Chromatogr., 111:* 214 (1975).

67. H. Crone, R. Dawson, and E. Smith, *J. Chromatogr., 103:* 71 (1976).

68. G. Howard and A. Martin, *Biochem. J., 56:* 32 (1950).

69. I. Halasz and I. Sebastian, *Angew. Chem. Int. Ed., 8:* 453 (1969).

70. J. Kirkland and J. DeStefano, *J. Chromatogr. Sci., 8:* 309 (1970).

71. A. Pryde, *J. Chromatogr. Sci., 12:* 486 (1974).

72. R. Majors and M. Hopper, *J. Chromatogr. Sci., 12:* 767 (1974).

73. J. Kirkland, *J. Chromatogr. Sci., 9:* 206 (1971).

74. R. Majors, *Anal. Chem., 44:* 1722 (1972).

75. R. Eksteen, Thesis, Northeastern University, Boston, MA, 1984, Ch. 1 and 2.

76. J. Dolan, R. Gant, N. Tanaka, R. Giese, and B. Karger, *J. Chromatogr., 16:* 616 (1978).

77. R. Majors, *LC-GC, 9:* 686 (1991).

78. H. Engelhardt and D. Mathes, *J. Chromatogr., 142:* 311 (1977).

79. H. Engelhardt, G. Ahr, and M. Hearn, *J. Liq. Chromatogr., 4:* 1361 (1981).

80. N. Miller, B. Feibush, and B. Karger, *J. Chromatogr., 316:* 536 (1985).

81. T. Waddell, D. Leyden, and M. DeBello, *J. Am. Chem. Soc., 103:* 5305 (1981).

82. R. Huisden, T. Ooms, J. Kraak, and H. Poppe, *Chromatographia, 31:* 263 (1991).

83. T. Alfredson, C. Wehr, L. Tallman, and F. Klink, *J. Liq. Chromatogr., 5:* 489 (1982).

84. H. Watanabe, M. Umino, and T. Sasagawa, *Sci. Rep. Toyo Soda, 28:* 1 (1984).

85. M. Himmel and P. Squire, *Int. J. Peptide Protein Res., 17:* 365 (1981).

86. M. Himmel and P. Squire, in *Aqueous Size-Exclusion Chromatography* (P. Dubin, ed.), Elsevier, Amsterdam, 1988, Ch. 1.

87. *Polymer Handbook,* 3rd ed. (J. Brandrup and E. Immergut, eds.), Wiley Interscience, New York, 1989.

88. J. Janca, in *Advances in Chromatography,* Vol. 19 (J. Giddings, E. Grushika, J. Cazes, and P. Brown, eds.), Marcel Dekker, New York, 1981, Ch. 2.

89. E. Cassassa, *Macromolecules, 9:* 182 (1976).

90. R. Frigon, J. Leypoldt, S. Uyeji, and L. Henderson, *Anal. Chem., 55:* 1349 (1983).

91. M. LeMaire, L. Aggerbeck, C. Monteilhet, J. Andersen, and J. Moller, *Anal. Biochem., 154:* 525 (1986).

92. R. Tarvers and F. Church, *Int. J. Peptide Protein Res., 26:* 539 (1985).

93. P. Squire, *J. Chromatogr., 210:* 433 (1981).

94. T. Burcham, D. Osuga, H. Chino, and R. Feeney, *Anal. Biochem., 139:* 197 (1989).

95. M. Dennis, C. Lazure, N. Seidah, and M. Chretien, *J. Chromatogr., 266:* 163 (1983).

96. C. Lazure, M. Dennis, J. Rochemont, M. Seidah, and M. Chretien, *Anal. Biochem., 125:* 406 (1982).

97. J. Bindels and H. Hoenders, *J. Chromatogr., 261:* 381 (1983).

98. R. Montelaro, M. West, and C. Issel, *Anal. Biochem., 114:* 398 (1981).

99. D. Schmidt, R. Giese, D. Conron, and B. Karger, *Anal. Chem., 52:* 177 (1980).

100. P. Roumeliotis and K. Unger, *J. Chromatogr., 218:* 535 (1981).

101. Y. Kato and T. Hashimoto, *JHRC & CC, 6:* 45 (1983).

102. S. Lau, A. Taneja, and R. Hodges, *J. Chromatogr., 317:* 192 (1984).

103. A. Taneja, S. Lau, and R. Hodges, *J. Chromatogr., 317:* 1 (1984).

104. C. Mant, J. Parker, and R. Hodges, *J. Chromatogr., 397:* 99 (1987).

105. S. Mori and M. Kato, *J. Liq. Chromatogr., 10:* 3113 (1987).

106. M. Okazaki and I. Hara, in *Aqueous Size-Exclusion Chromatography* (P. Dubin, ed.) Elsevier, Amsterdam, 1988, Ch. 11.

107. J. Sternberg, *Adv. Chromatogr., 2:* 205 (1966).

108. B. Karger, M. Martin, and G. Guiochon, *Anal. Chem., 46:* 1640 (1974).

109. R. Scott, *Liquid Chromatography Detectors*, 2nd ed., Elsevier, Amsterdam, 1986.

110. *Introduction to Microscale High Performance Liquid Chromatography* (D. Ishii, ed.), VCH, Weinheim, Germany, 1988.

111. G. Guichon and H. Colin, in *Macrocolumn High Performance Liquid Chromatography* (P. Kucera, ed.), Elsevier, New York, 1984.

112. E. Katz and R. Scott, *J. Chromatogr., 268:* 169 (1983).

113. K. Gooding, K. Lu, G. Vanecek, and F. Regnier, 4th International Symposium on Column Liquid Chromatography, Boston, MA, 1979.

114. J. Kirkland and P. Antle, *J. Chrom. Sci., 15:* 137 (1977).

115. H. Freiser and K. Gooding, *J. Chromatogr., 544:* 125 (1991).

116. R. Montelaro, in *Aqueous Size-Exclusion Chromatography* (P. Dubin, ed.), Elsevier, Amsterdam, 1988, Ch. 10.

117. O. Chiantore and M. Guaita, *J. Liq. Chromatogr., 7:* 1867 (1984).

118. B. Stenlund, in *Advances in Chromatography*, Vol. 14, Marcel Dekker, New York, 1976, Ch. 2.

119. N. Good, G. Winget, W. Winter, T. Connoly, S. Izawa, and R. Singh, *Biochemistry, 5:* 467 (1966).

120. D. Perrin and B. Dempsey, *Buffers for pH and Metal Ion Control*, Chapman & Hall, London, 1976.

121. R. Rothman and L. Warren, *Biochim. Biophys. Acta, 955:* 143 (1988).

122. D. Kelner, J. Mayhew, and J. Hobbs, *American Biotechnology Laboratory, 40,* February, (1989).

123. A. Sykes and S. Flatman, poster, Tenth International Symposium on the HPLC of Proteins, Peptides, and Polynucleotides, Wiesbaden, Germany, 1990.

124. T. Takagi, K. Takeda, and T. Okuno, *J. Chromatogr., 208:* 201 (1981).

125. K. Konishi, in *Progress in HPLC*, Vol. 1 (H. and S. Parvez eds.), VNU Science Press, Utrecht, The Netherlands, 1985.

126. E. Watson and W. Kenney, *J. Chromatogr., 436:* 289 (1988).

4
Molecular Weight-Sensitive Detectors for Size Exclusion Chromatography

Christian Jackson and Howard G. Barth E. I. du Pont de Nemours and Company, Wilmington, Delaware

Introduction

Size exclusion chromatography (SEC) provides a rapid, high-resolution method for determining molecular weight distributions (MWD) of macromolecules. In the conventional mode, the molecular weight is determined by calibrating the column to determine the relation between elution volume and molecular weight. The size exclusion separation mechanism is based on the effective hydrodynamic volume of the molecule, not the molecular weight, and as a result the system must be calibrated using standards of known molecular weight and homogeneous chemical composition. The chemical composition must be the same as the standards to be analyzed, and the calibrated molecular weight range must be greater than the range of molecular weights to be analyzed. The calibration curve is thus specific to a given polymer-solvent system.

For many commercial polymers the columns cannot be calibrated because well-characterized standards are unavailable. The situation is further complicated for branched polymers or copolymers, for which there is no single calibration curve relating elution volume to molecular weight (1).

An additional potential source of error is the sensitivity of the calibration curve to alterations in the experimental conditions. Anything that alters the elution time of a given molecular weight species, such as changes or fluctuations in flow rate, column degradation, or enthalpic interactions with the column packing, can lead to serious errors in the measurement of molecular weight.

Because of these limitations, it is clearly desirable to measure the molecular weight, or some property related to molecular weight, directly as the sample elutes from the columns. This is generally done by connecting either a light-scattering detector or a viscometer to the SEC system. The eluting polymer flows through the detector cell as it leaves the column and before it reaches the concentration detector. In a light scattering detector, the excess light scattered by the eluting polymer is proportional to molecular weight. For an on-line viscometer, the specific viscosity can be used to calculate the molecular weight either in conjunction with the Mark-Houwink coefficients of the polymer solution or by using the method of universal calibration.

This chapter reviews the principles and methodology of molecular weight determination by light scattering and viscometry in conjunction with SEC. The emphasis is on those aspects of molecular weight measurement relevant to SEC analysis; more detailed general treatments of light scattering, viscometry, and polymer solutions are available elsewhere (2–10). Applications of both methods are discussed with particular emphasis on molecular weight determination of polymers that are heterogeneous in composition or architecture; it is in these areas that molecular weight-sensitive detectors offer the greatest advantage over conventional SEC.

Principles

Viscometry

At a constant flow rate, the pressure drop across a capillary tube P is proportional to the viscosity of the liquid flowing through the tube. For a polymer solution, the ratio of this pressure to the pressure for the pure solvent P_0 is equal to the relative viscosity η_r of the solution,

$$\frac{P}{P_0} = \frac{\eta}{\eta_0} = \eta_r \quad (1)$$

where η is the solution viscosity and η_0 is the solvent viscosity. The specific viscosity is defined as

$$\eta_{sp} = \frac{\eta - \eta_0}{\eta_0} = \eta_r - 1 \quad (2)$$

which is a measure of the increase in viscosity caused by the addition of the polymer to the solvent. The reduced viscosity η_r/c, where c is the polymer concentration, is a measure of the specific capacity of the polymer to increase the solution relative viscosity. In the limit of infinite dilution this quantity is

known as the intrinsic viscosity:

$$[\eta] = \left(\frac{\eta_{sp}}{c}\right)_{c \to 0} \quad (3)$$

The reduced viscosity has a concentration dependence in dilute solutions described by the Huggins equation,

$$\frac{\eta_{sp}}{c} = [\eta] + k'[\eta]^2 c \quad (4)$$

where *k'* is the Huggins constant. In SEC the concentration of the solute is usually low, so that the assumption of infinite dilution is generally valid and the conditions for Equation (3) hold. Thus, the intrinsic viscosity of an eluting polymer can be determined from measurements of the specific viscosity and concentration of the eluting polymer solution at each elution volume.

The intrinsic viscosity of a polymer solution is related to its molecular weight by the empirical relation known as the Mark-Houwink equation:

$$[\eta] = KM^a \quad (5)$$

where *K* and *a* are the Mark-Houwink coefficients, which depend on the polymer, solvent, and temperature.

Measurement of the specific viscosity requires that both the solution and the solvent viscosity be measured at the same flow rate. This can be achieved by measuring the solvent viscosity baseline before and after the polymer peak elutes or by measuring the solution viscosity as the peak elutes using a reference capillary. An example of such a flow-referenced viscometer is shown in Figure 1 (6). This is a fluid analog of the electrical circuit known as a Wheatstone bridge. With only solution flowing through the viscometer, the flow resistances R1, R2, R3, and R4 are balanced and the differential pressure transducer signal is zero. When a polymer solution enters the viscometer, it fills capillaries R1, R2, and R3, but the reservoir prevents it from reaching the fourth capillary, R4, which still contains flowing solvent. A pressure transducer measures the resultant difference in pressure between the two sides of the bridge. The specific viscosity η_{sp} is calculated from the ratio of this differential pressure to the pressure drop across the bridge. Other types of viscometers include a single-capillary (7) and referenced dual-capillary (8) designs. A listing of commercial instrumentation is given in the appendix.

Figure 2 shows the viscometer and refractometer tracings as a function of elution volume for a mixture of equal amounts of three nearly monodisperse polystyrene standards. Note that the refractometer is proportional to concentration *c;* the signal from the viscometer is proportional to $[\eta]c$. By dividing the viscometer output by the refractometer signal, we can then determine $[\eta]$ at each elution volume increment.

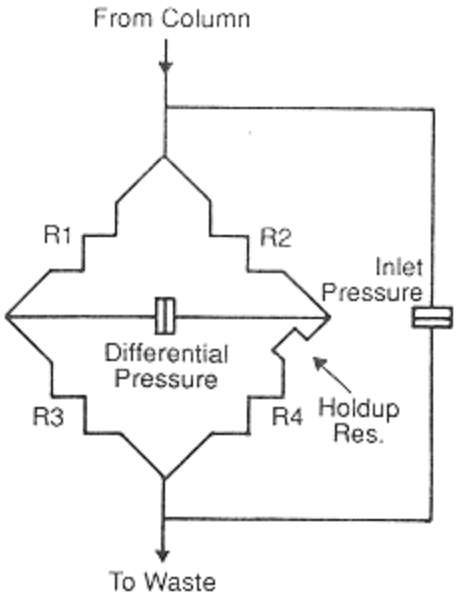

Figure 1.
"Bridge design" flow-referenced capillary viscometer. See text for details. (Adapted from Reference 6 and used with permission from John Wiley and Sons, Publishers.)

Light Scattering

The intensity of the light scattered by a polymer solution, above that scattered by the pure solvent, is related to the molecular weight of the polymer by (9)

$$\frac{K^*c}{R(\theta)} = \frac{1}{M_w P(\theta)} + 2A_2c \qquad (6)$$

where

c = polymer concentration
M_w = weight-average molecular weight of the polymer
A_2 = second virial coefficient of the polymer-solvent system
$R(\theta)$ = measured excess scattering intensity of the solution over that of the pure solvent, the Rayleigh ratio
$P(\theta)$ = particle scattering function as a function of angle relative to the incident beam

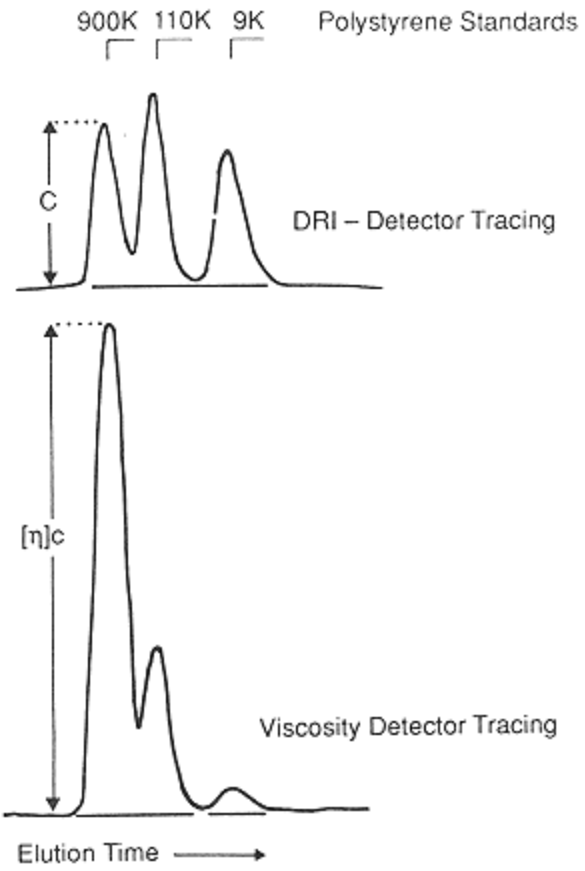

Figure 2.
SEC chromatogram of a mixture of three polystyrene standards showing the outputs of both a differential refractometer (top) and a viscometer (bottom).

and K^* is an optical constant for the scattering system, given by

$$K^* = \frac{4\pi^2 n_0^2 (dn/dc)^2}{\lambda_0^4 N_A} \quad (7)$$

where:

n_0 = refractive index of the solvent
dn/dc = specific refractive index increment of the solution
λ_0 = wavelength of the incident light in a vacuum
N_A = Avogadro's number

The particle-scattering function describes the angular variation of the scattered light intensity and depends upon the polymer size and shape. At low scattering angles it can be approximated by

$$\frac{1}{P(\theta)} = 1 + \left(\frac{4\pi}{\lambda}\right)^2 \sin^2\left(\frac{\theta}{2}\right) \frac{\langle Rg^2\rangle_z}{3} \quad (8)$$

where λ is the wavelength of the incident light in the solution and $\langle Rg^2\rangle_z$ is the mean square radius of gyration of the molecules in solution.

Figure 3 shows a simplified schematic of a light-scattering photometer. In a typical instrument, a laser light source, vertically polarized, irradiates a sample solution. The intensity of the scattered light is measured at a given angle with respect to the forward direction. Instrumentation is available (see appendix) that utilizes a single angle measurement at <10° (10) or 90° (11); two angles (12); or multiangles (13,14).

The weight-average molecular weight, the radius of gyration, and the second virial coefficient can be determined by measuring the scattered intensity as a function of angle for a series of different dilute concentrations. These parameters are determined from a Zimm plot of $K^*c/R(\theta)$ against $\sin^2 \theta/2 + kc$ for these data (Figure 4), where k is an arbitrary constant used to spread out the data. A value of $k = 1/c_{max}$, where c_{max} is the maximum concentration used, has been found to work well (2). The data are extrapolated to zero angle and zero concentration, and the double extrapolation to zero angle and zero concentration intercepts the $K^*c/R(\theta)$ axis at a value equal to the inverse of the molecular weight,

$$\left(\frac{K^*c}{R(\theta = 0)}\right)_{c\to 0} = \frac{1}{M_w} \quad (9)$$

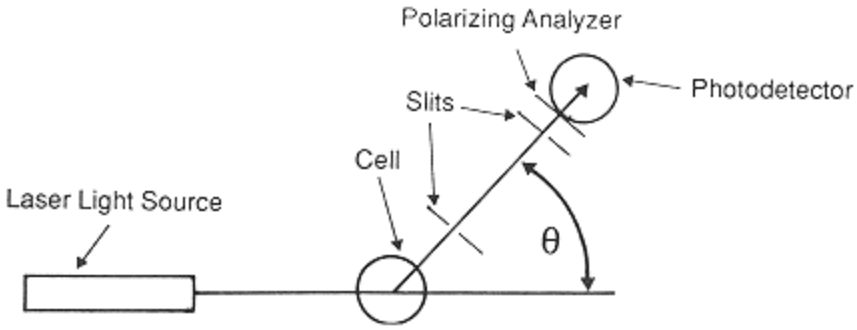

Figure 3.
A light-scattering photometer. Polymer solution in cell is irradiated with an incident beam, and scattered light intensity is measured at angle θ.

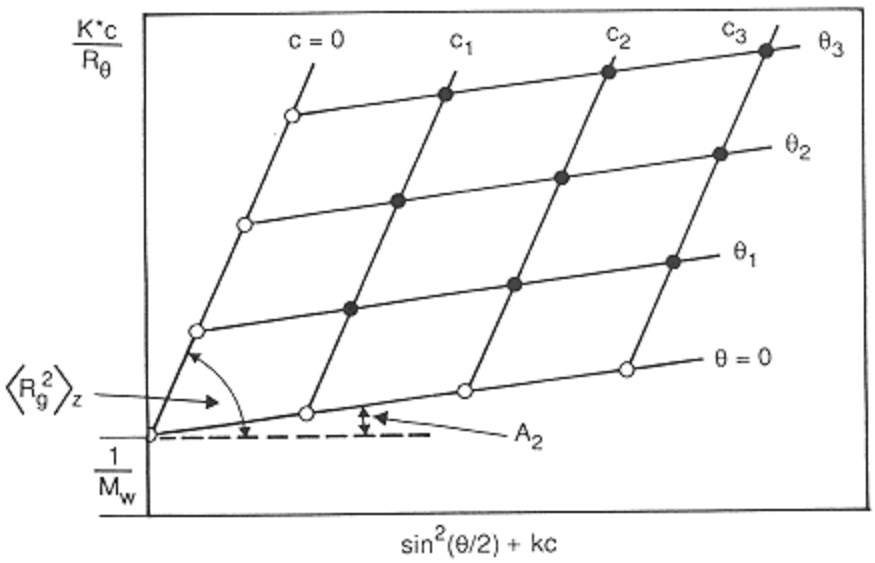

Figure 4.
Zimm plot, which is a double-extrapolation procedure used in light-scattering measurements for determining the second virial coefficient A_2, mean square radius of gyration $\langle R_g^2 \rangle$, and weight-average molecular weight M_w.

The initial slope at zero angle is proportional to the second virial coefficient, and the initial slope of the graph at zero concentration, divided by the intercept, is proportional to the mean square radius of gyration.

When combined with SEC, the light-scattering intensity can only be measured at a single concentration for each molecular weight fraction eluting from the column. Thus, to determine molecular weight, the second virial coefficient must be known beforehand or must be assumed to be zero. In most cases, setting the second virial coefficient to zero is a valid approximation because the eluting polymer concentration is usually low. In general, the resultant error is less than experimental error. Making this approximation and measuring the scattered light intensity at a number of angles, we can determine the molecular weight and mean square radius of gyration for each elution slice by extrapolation to zero angle. The data points thus obtained approximate to the zero concentration points in Figure 4. In practice, the radius of gyration can only be determined for molecules greater than about 20 nm in diameter; below this size it is extremely difficult to measure variation in scattered intensity with angle.

If a single low-angle scattering intensity is measured, typically < 10°, then for most polymer molecules scattering intensity in this region this can be

considered a valid approximation to the zero-angle intensity and no extrapolation is required. The molecular weight is then proportional to the scattered intensity divided by the concentration.

Methodology

Viscometry

Universal Calibration

Benoit and coworkers (15) showed that size exclusion chromatography separates polymer molecules by hydrodynamic volume. The hydrodynamic volume can be expressed as the product of intrinsic viscosity and molecular weight:

$$hv = [\eta]M \quad (10)$$

It is therefore possible to generate a universal calibration curve of polymer hydrodynamic volume against elution volume that is valid for different types of polymers as well as copolymers and branched polymers (Figure 5). This is achieved by using narrow molecular weight distribution standards with known molecular weights and known intrinsic viscosities, either measured or calculated from the Mark-Houwink coefficients. The calibration curve is then constructed from a plot of log $[\eta]M$ against the measured elution volume. The molecular weight of each fraction of an unknown eluting polymer can then be calculated from the universal calibration curve and either the measured polymer intrinsic viscosity or the Mark-Houwink coefficients:

$$M = \frac{hv}{[\eta]} = \left(\frac{hv}{K}\right)^{1/(a+1)} \quad (11)$$

If the intrinsic viscosity of the eluting unknown polymer is measured at each elution volume using an on-line viscometer, universal calibration can be used to calculate the molecular weight at each volume, and thus the molecular weight distribution, without knowledge of the Mark-Houwink coefficients.

For branched polymers or copolymers, the molecules eluting at a given volume may be polydisperse in molecular weight. Molecules with the same hydrodynamic volume but different structure or composition have different molecular weights. In this case the molecular weight in a given elution volume increment measured by universal calibration is the number-average molecular weight M_n (16).

Universal calibration is valid only when there are no enthalpic interactions between the polymer sample and the column packing and the separation is entirely a result of the size exclusion mechanism. Furthermore, chromatographic concentration effects must be absent. Another consideration is that the molecular

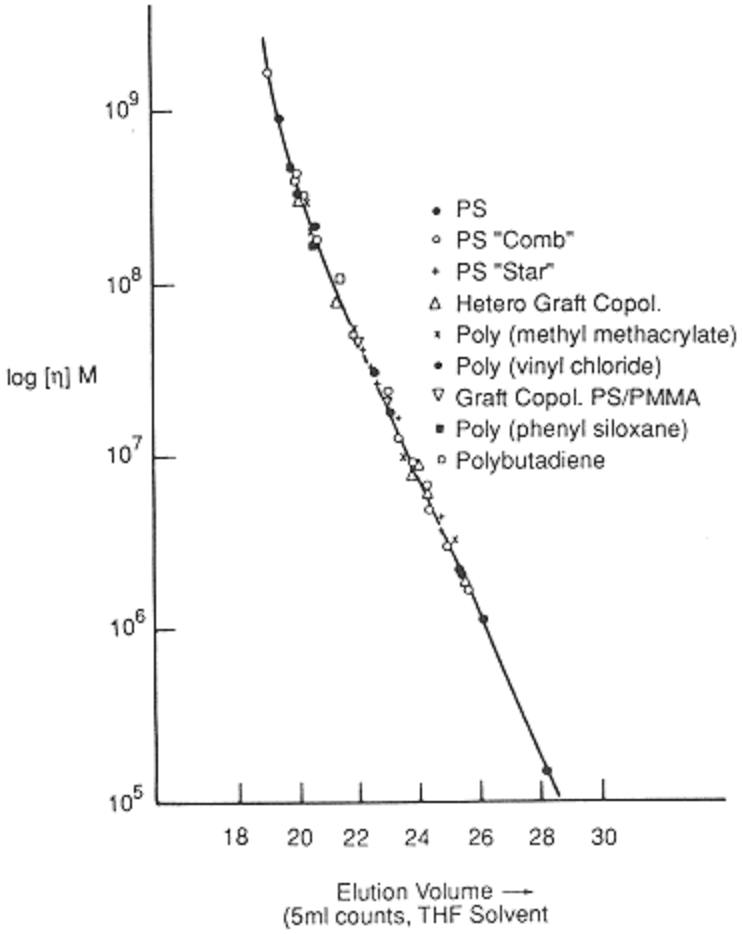

Figure 5.
SEC universal calibration curve demonstrates that molecular hydrodynamic volume [η]M governs the separation mechanism. [Reprinted with permission from John Wiley and Sons, Publishers (15).]

weight of the standards used to construct the universal calibration curve must be known accurately.

SEC-Viscometry Without a Concentration Detector

SEC-viscometry combined with universal calibration can provide measurements of molecular weight distribution even when it is not possible to use a concen-

tration method (17), for example at temperatures at which a concentration detector can no longer operate or in solvents in which there is no measurable difference between solution and solvent refractive index, such as polyolefins in decalin.

The method requires that the Mark-Houwink exponent *a* for the polymer-solvent system and the sample amount injected be known. The concentration at each elution slice is then calculated from the viscometer output η_{sp}, the universal calibration curve, and the Mark-Houwink exponent. From the Mark-Houwink equation and the definition of hydrodynamic volume in universal calibration, it can be shown that the concentration at each elution volume increment is given by (18)

$$c_i = \frac{(\ln \eta_r)_i}{(K^{1/a}(hv)_i)^{a/(a+1)}} \quad (12)$$

where

$$K = \frac{\sum(\ln \eta_r)_i}{\sum c_i}\left(\frac{\sum(\ln \eta_r)_i/hv_i}{\sum c_i}\right)^{1/a} \quad (13)$$

and

$$\sum c_i = m\,\Delta V \quad (14)$$

where *hv* is the hydrodynamic volume at each slice from the calibration curve, *m* is the total sample amount injected, and ΔV is the retention volume increment between data points.

A special case of this approach is the method of calculating the number-average molecular weight from the viscometer output, the universal calibration curve, and the sample amount injected (19):

$$M_n = \frac{\sum c_i}{\sum (\ln \eta_r)_i/hv_i} \quad (15)$$

In this case the Mark-Houwink exponent is not required, and thus this method can be used when the Mark-Houwink exponent is unknown or when it may vary with elution volume, as for copolymers and polymer blends.

Intrinsic Viscosity Distribution

Another approach to the SEC-viscometry data is that of Kirkland et al. (20). The intrinsic viscosity is a fundamental property of the polymer sample in solution, and thus polymers may be characterized in terms of their intrinsic viscosity distribution (IVD) without attempting to convert this into a molecular weight distribution. Moments of the IVD may be calculated similar to those for the MWD (21). The advantage is that the intrinsic viscosity distribution is di-

rectly measured and is not subject to the errors introduced when universal calibration is used to calculate molecular weight.

If the Mark-Houwink coefficients for the polymer-solvent system are known, then the IVD measured by SEC-viscometry can be converted into the molecular weight distribution using the Mark-Houwink relation. This should give greater precision in the measurement of molecular weight distribution than SEC-viscometry with universal calibration, because the IVD measurement is much less sensitive to experimental conditions than a calibration curve.

Radius of Gyration Measurement

If universal calibration is used with SEC-viscometry, it is also possible to calculate the radius of gyration for linear polymers at each elution volume using the Flory-Fox equation (22),

$$R_g = \frac{1}{\sqrt{6}} \left(\frac{M[\eta]}{\Phi} \right)^{1/3} \quad (16)$$

where

$$\Phi = 2.55 \times 10^{21}(1 - 2.63\epsilon + 2.86\epsilon^2) \quad (17)$$

and

$$\epsilon = \frac{2a - 1}{3} \quad (18)$$

The ϵ parameter [Equation (18)] is used to take into account deviations from θ conditions (23). This approach has been evaluated with good success using polystyrene samples (21,24). If a viscosity detector is used in series with a right-angle light-scattering detector, Equation (16) can be used in an iterative procedure to correct for angular asymmetry (see p. 116).

Light Scattering

Determination of the Specific Refractive Index Increment and Solvent Refractive Index

The accuracy of the light-scattering measurement depends on prior determinations of the solvent refractive index and of the specific refractive index increment *dn/dc* of the sample in the solvent [Equation (7)]. The solvent refractive index can be measured with a conventional refractometer or values found in the literature. The *dn/dc* value can be measured using either a differential refractometer or, less frequently, an interferometer. Measurements should be made at the same temperature as the light-scattering measurement and ideally at the same wavelength. Because of the dependence of the optical constant on the square of

dn/dc, extreme care must be taken with the measurement because any error is doubled in the calculated molecular weight. Detailed discussions of the measurement principles and methods can be found in References 2 and 25.

A comprehensive tabulation of experimental values for *dn/dc* has been published (26). Many of these values are at different wavelengths, and the value at the desired wavelength can be obtained by extrapolation of a plot of *dn/dc* against the inverse of the wavelength squared using the relationship

$$\frac{dn}{dc} = k' + \frac{k''}{\lambda^2} \quad (19)$$

where *k'* and *k''* are the intercept and slope, respectively.

Values of *dn/dc* have a nearly linear dependence on solvent refractive index, so that if values are not available in the solvent to be used it can also be determined by extrapolation from other solvent systems. If the polymer refractive index n_p and the partial specific volume of the polymer in the solvent v_p are known, then *dn/dc* can be estimated by the Gladstone-Dale rule (2),

$$\frac{dn}{dc} = \bar{v}_p(n_p - n_0) \quad (20)$$

It should be noted that *dn/dc* also varies with molecular weight. Typically, the *dn/dc* value increases with increasing molecular weight and reaches an asymptotic limit for molecular weights greater than approximately 20,000 g/mol. For polymers with fractions in this low-molecular-weight regime, this effect should be taken into consideration because it generally leads to an error in the measurement of the low-molecular-weight region of the distribution; that is, the number-average molecular weight is most affected. For example, if *dn/dc* decreases with molecular weight, then the molecular weight at each elution volume is overestimated, especially M_n. If the entire polymer MWD is below 20,000, then *dn/dc* values should be determined separately for the required molecular weight range.

One other consideration is the effect of ionic groups on synthetic polyelectrolytes and biopolymers. To measure a reliable value for *dn/dc,* the polymer solution, containing electrolyte, must be dialyzed against the solvent system until a constant chemical potential is obtained. Details on the determination of *dn/dc* of polyelectrolytes can be found in References 2, 25, and 27.

Instrument Calibration

Determination of the Rayleigh ratio from the scattered light intensity requires that the light-scattering detector be calibrated to account for detector sensitivity,

cell geometry, and so on. Utiyama (28) discusses calibration procedures and standards for light-scattering measurements. Because procedures vary depending upon instrument and cell design, discussion of instrument calibration is not presented here and the reader is advised to consult manufacturers' instruction manuals.

Measurement of Molecular Weight Distribution

When *dn/dc* and n_0 have been determined, and the instrument calibrated, the molecular weight can be calculated from the light-scattering intensity and the concentration at each elution volume [Equation (9)]. These values can then be used to determine the molecular weight distribution. If there is any polydispersity at a given elution volume caused by heterogeneity of composition or structure, the calculated value is a weight-average molecular weight.

Measurement of Sample M_w

It can be shown that the weight-average molecular weight can be determined from the ratio of the area of the light-scattering intensity measured at low angle, <10°, and the concentration chromatograms, corrected for their respective calibration constants (29):

$$M_w = \frac{\Sigma M_i c_i}{\Sigma c_i} = \frac{\Sigma R_{\theta i}/K^*}{\Sigma c_i} \quad (21)$$

Thus, an accurate M_w value can be obtained from the light-scattering signal alone if the injected mass is known. Alternatively, the area measurement can be used instead of a point-by-point summation of calculated molecular weights to avoid the effect of baseline noise at the peak edges. This method has been shown to give greater precision than the summation of individual values at each elution volume (30,31). This approach can also be used for samples that contain a high-molecular-weight fraction that is detected only by the light scattering detector, not by the concentration detector.

The inverse problem occurs at the low-molecular-weight end of many distributions, at which the light-scattering signal is too small to determine a reliable molecular weight estimate but there is still a signal from the refractometer. In this case, extrapolation of the column calibration curve from measured data can improve the accuracy of M_n, as shown in Figure 6.

SEC-Light Scattering with Universal Calibration

Light scattering can also be used in conjunction with universal calibration to obtain an estimate of the intrinsic viscosity of the sample (see p. 135). Because

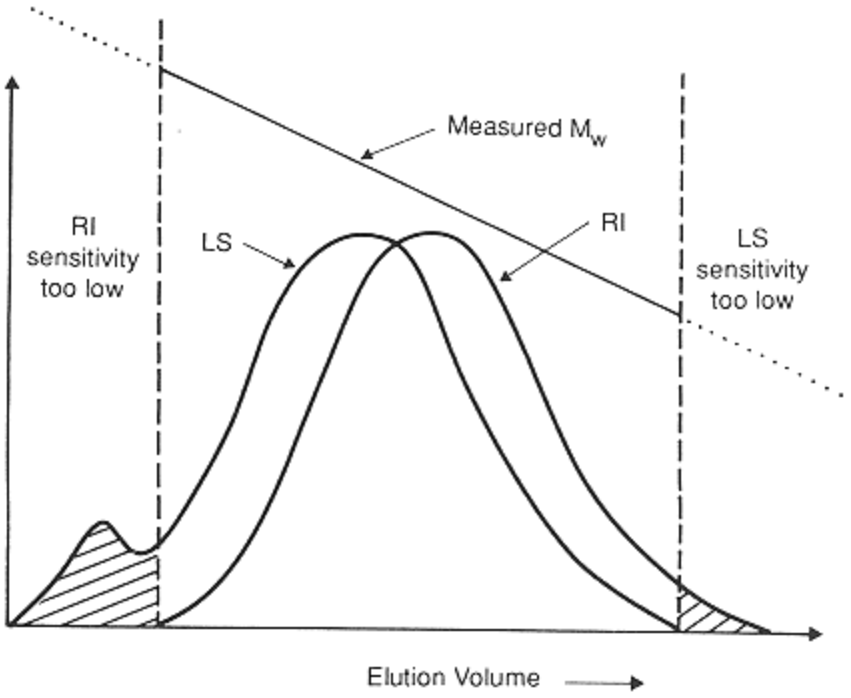

Figure 6.
SEC tracings from light-scattering and differential refractive index detectors showing the low sensitivity of each detector at the ends of a hypothetical distribution.

of the greater complexity of the measurement and the lower light-scattering sensitivity for many samples compared with viscometry, this approach is rarely used.

Right-Angle Laser Light Scattering

Haney et al. (11) used a right-angle light-scattering (LS) detector combined with SEC-viscometry to measure directly both the intrinsic viscosity and molecular weight of each elution slice. For molecules with molecular weights less than about 100,000 g/mol, there is no measurable scattering asymmetry and the right-angle intensity provides a good measurement of the molecular weight. For higher molecular weights, the Flory-Fox equation [Equation (16)] is used in an iterative procedure to correct for any asymmetry in the scattering and thus determine a good approximation to the correct molecular weight. Thus, with this approach, both molecular weight and the radius of gyration [Equation (16)] can

be determined. The method gave accurate molecular weights for polystyrene in THF up to 3×10^6 g/mol.

Concentration Measurement

One of the advantages of conventional SEC is that the absolute concentration of the sample at each elution slice is not required to calculate the MWD. With both SEC-LS and SEC-viscometry it becomes necessary to determine an absolute concentration measurement if the MWD is to be determined.

There are two approaches to determining the concentration: one is to use the injected sample mass, and the other is to calibrate the concentration detector. In the following discussion it is assumed that a refractometer is being used to determine concentration, but the same applies to ultraviolet (UV) detectors, except that the UV absorbance of a sample replaces the *dn/dc* value.

In the first method, the area under the concentration detector chromatogram is taken to be proportional to the total sample mass injected *m:*

$$k = \frac{m}{\Delta V \Sigma h_i} \quad (22)$$

and thus the concentration at each elution slice c_i may be calculated from the detector output at each slice h_i by $c_i = kh_i$.

The advantages of this method are that it is straightforward and is not affected by different *dn/dc* values for different samples. The disadvantage is that the injected amount of sample must be known accurately. This implies that the injection volume is known accurately.

In the second method, the concentration detector is calibrated with a series of solutions of different concentrations and known refractive indices. This provides a calibration constant for the detector k' that converts the signal into a change in refractive index, such that for each chromatogram slice,

$$c_i = \frac{k'}{dn/dc} h_i \quad (23)$$

This avoids the problems with the peak mass not corresponding to the injected mass and thus increases the measurement precision, but it means that *dn/dc* for the sample must be known. Because *dn/dc* must be known for the light-scattering calculation, this clearly does not require any additional work for SEC-light scattering. Furthermore, once the concentration detector is calibrated, *dn/dc* for unknown polymers can be determined using Equation (23) if the injected mass is known. With this approach it is best to use a monochromatic light source for the refractometer having the same wavelength as the light source used for the light-scattering experiment.

Interdetector Delay Volume

When a molecular weight-sensitive detector is added as a second detector to an SEC system, it is essential that the dead volume in the connecting tubing between the measurement points of the two detector cells be known precisely. If this is not done, the calculated values contain significant errors. In particular, the measured polydispersity and Mark-Houwink coefficients are extremely sensitive to errors that may be incurred in the interdetector dead volume.

A number of approaches can be used to determine the interdetector volume. The obvious procedure is to calculate the geometric offset volume from the connection volume between detectors. As discussed by Bruessau (32) and Lecacheux and Lesec (33), however, these calculated values are not correct because they do not take into account peak shape changes that can occur. The most commonly used approach for determining interdetector volume for either viscometers or light-scattering detectors is to measure peak maxima differences of a narrow molecular weight distribution polymer standard or a monodisperse solute, such as a protein. In a viscometer, a solute, such as methanol, can be employed for aqueous SEC (34). Measurement of peak onset difference, as well as the peak maxima difference of an excluded polymer peak, has been reported (35).

A different procedure was used by Lecacheux and Lesec (33) for determining interdetector volume for both a viscometer and a light-scattering detector. In this approach, an excluded monodisperse polymer standard is injected. When the correct interdetector volume is selected, the calculated intrinsic viscosity, or molecular weight, is equal to the expected value and remains constant as a function of elution volume.

To determine the interdetector delay volume for a viscometer, a broad molecular weight distribution standard can be injected and a Mark-Houwink plot, that is, log $[\eta]$ versus log M, generated using universal calibration. The interdetector volume is adjusted until the expected Mark-Houwink exponent is obtained (36).

Another approach to determining the interdetector volume of a viscometer is first to establish an $[\eta]$ versus elution volume calibration curve using a series of narrow polymer standards of known intrinsic viscosities. A broad molecular weight standard is then injected and the interdetector volume is adjusted to obtain superimposition of the intrinsic viscosity calibration curve (37).

With a light-scattering detector, a log M versus elution volume calibration curve is constructed from a series of narrow molecular weight distribution polymer standards. A broad molecular weight distribution standard is then injected, and an iterative procedure finds the interdetector volume that superimposes the broad MWD standard calibration curve onto the one established by the narrow standards (38).

Finally, a spectrophotometric method has been proposed in which a low-angle laser light-scattering (LALLS) detector is used as an absorption photometer (35). Interdetector volume is then determined by injecting a solute that absorbs radiation from the LALLS detector. Mourey and Miller (35) used copper cyclohexanebutyrate as the solute and determined interdetector volume using the peak onsets of the LALLS detector and refractometer.

Band Broadening

SEC does not provide infinite resolution of species with different hydrodynamic volumes; as a result each slice has some residual polydispersity. This is primarily the result of the finite time required for a given polymer to diffuse into and out of the stationary phase. The effect can be compounded by extra dead volume in the detectors or connecting tubing. In conventional SEC, band broadening leads to an overestimate of sample polydispersity. This is because the eluting peak is broadened so that it appears to cover a wide molecular weight range.

If a light-scattering detector is used as a detector, then the true molecular weight at each elution volume can be directly measured. If there is any band broadening, each elution volume is polydisperse in molecular weight, and the measured quantity is a weight average. The slope of the measured M_w against elution volume is flatter than the calibration curve for the molecular weight because of band broadening, and the sample appears less polydisperse. Although the weight-average molecular weight for the sample can still be measured correctly, the number-average molecular weight is overestimated because of the lack of resolution. As a result, polydispersity is underestimated. The error introduced to molecular weight parameters as a function of band broadening is given in Figure 7. These results are based on computer simulation studies (39).

The measured polydispersity can be corrected for band broadening using the method of He et al. (40). For columns with a linear calibration curve in log MW with slope D_2, the true polydispersity is given by

$$\left(\frac{\overline{M}_w}{\overline{M}_n}\right)_{\text{TRUE}} = e^{D_2 D_2'(1-D_2'/D_2)\sigma_T^2} \left(\frac{\overline{M}_w}{\overline{M}_n}\right)_{\text{SEC-LALLS}} \quad (24)$$

where D'_2 is the experimental calibration curve measured by the light-scattering detector and σ^2_T is the variance of the experimental concentration chromatogram. A more general form of the correction, which does not assume a Gaussian peak shape, has been developed by Lederer et al. (41) and Billiani and coworkers (42–44). The same correction also applies to the intrinsic viscosity distribution, the width of which is also underestimated.

In SEC-viscometry with universal calibration, as in conventional SEC, the effect of band broadening is an apparent increase in polydispersity as the peak

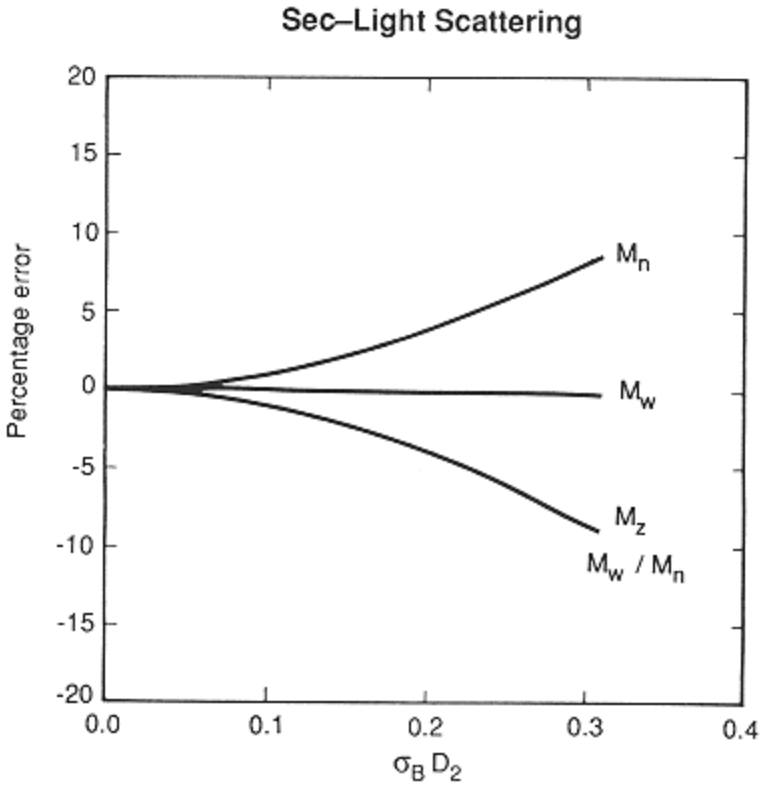

Figure 7.
Effect of band broadening for a polymer with polydispersity 2 on the measured moments of the molecular weight distribution by light scattering, where D_2 is the slope of log molecular weight and elution volume and σ_B is the peak variance caused by band broadening (39).

broadens (Figure 8). Although the true intrinsic viscosity is measured at each slice, the effect of band broadening means that the molecular weight profile no longer has a one-to-one correspondence to the intrinsic viscosity elution profile, from which the universal calibration curve is determined. The corrected intrinsic viscosity, without band broadening, can be calculated using the method of Hamielec (45):

$$[\eta](V) = \frac{F(V)}{F(V - E_2\sigma^2)} e^{1/2(E_2\sigma)^2} [\eta](V)_{exp} \quad (25)$$

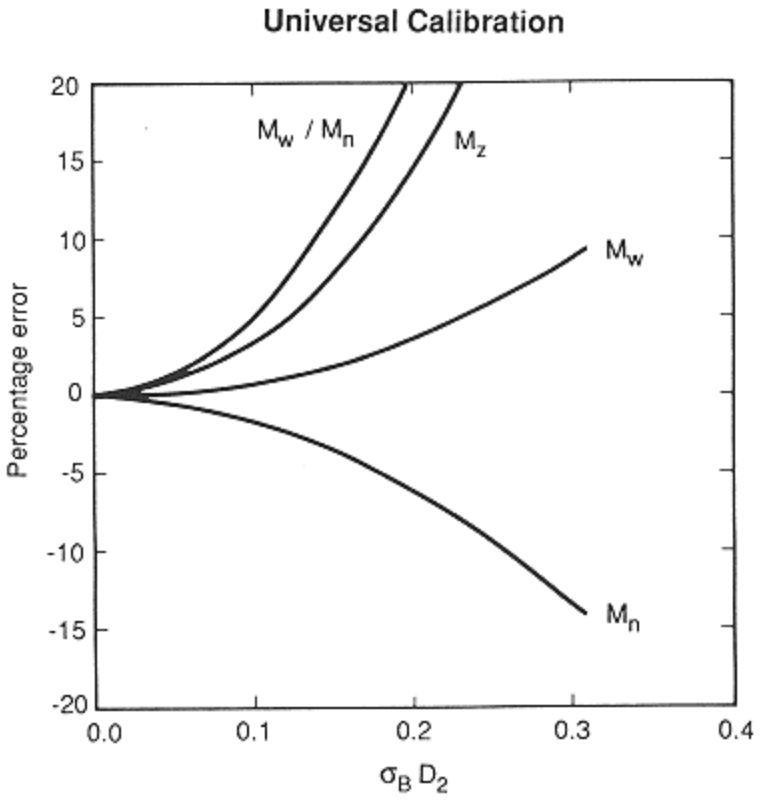

Figure 8.
Effect of band broadening for a polymer with polydispersity 2 on the measured moments of the molecular weight distribution by viscometry and universal calibration, where D_2 is the slope of log molecular weight and elution volume and σ_B is the peak variance caused by band broadening (39).

where $[\eta](V)$ is the corrected intrinsic viscosity at each elution volume V and $[\eta](V)_{exp}$ is the experimentally determined intrinsic viscosity at each elution volume, F is the concentration chromatogram, σ is the Gaussian band-broadening parameter, and E_2 is the slope of the intrinsic viscosity calibration curve

$$[\eta](V) = E_1 e^{-E_2 V} \quad (26)$$

From this, the true molecular weight calibration curve can be determined and can then be used to calculate the correct MWD.

In general, band-broadening corrections are still required if a molecular weight-sensitive detector is added to SEC, especially if the molecular weight

distribution or the Mark-Houwink coefficients are being determined. As mentioned, some average values of the distribution M_w by SEC-LS and [η] by SEC-viscometry are unaffected. In SEC-LS and SEC-viscometry used with Mark-Houwink coefficients, the errors in the determination of the MWD are less than in conventional SEC. In SEC-viscometry with universal calibration, these errors are greater, as shown in Figure 8. A detailed discussion on the effect of band broadening with viscometers and light-scattering detectors can be found in Reference 39.

One related problem is that of interdetector band broadening. Detectors with larger cell volumes, if placed after other detectors in the SEC system, exhibit a broader peak than other detectors. In SEC-LS, for example, the light-scattering peak is generally narrower than the concentration-sensitive detector peak because of the smaller cell volume. This can lead to a mismatch of the two detector signals, even with correct compensation for the interdetector volume. In the SEC-LS example, this mismatch leads to an overestimate of the molecular weight in the center of the peak and an underestimate at the leading and tailing edges. If molecular weight is plotted as a function of elution volume for a narrow MWD sample, it appears as an *n*-shaped curve rather than a nearly flat line. The weight-average molecular weight in this example is unaffected, but the number and *Z* averages are distorted (39).

This effect can be corrected by injecting a narrow MWD sample and measuring the variance of the peaks in each detector. Because the peak shape is nearly Gaussian, it should, ideally, be the same for all detectors. If it is not, the additional variance can be calculated for one of the detectors. In subsequent data analysis, the narrower peak can be digitally broadened using Gaussian band spreading to correct for this mismatch.

Applications

Viscometry

Molecular Weight Distribution

SEC-viscometry and universal calibration has been widely used to determine the MWD of synthetic polymers, and selected applications are listed in Table 1. On-line viscometers have been successfully used at high temperatures: Pang and Rudin (50) measured the MWD of polyolefins dissolved in 1,2,4-trichlorobenzene at 145°C, and Stacy (17) measured the MWD of polyphenyl sulfide in 1-chloronaphthalene at 220°C.

SEC-viscometry has also been applied to natural polymers with more complex molecular weight distributions. Timpa (61) used universal calibration and on-line viscometry to measure the MWD of cotton fibers to evaluate different

Table 1 Measurement of Molecular Weight Distribution by SEC-Viscometry: Selected Applications

Macromolecule	References
Homopolymers	
Polystyrene	36, 46–48
Polymethyl methacrylate	36, 47–49
Polyolefins	50
Polyvinyl chloride	36, 47
Polyvinyl acetate	47
Polyvinyl alcohol	51
Polyallylamine	52
Polyethylene oxide	53
Polyamides	54, 55
Polyphenylene sulfide	56
Copolymers	
Ethylene-vinyl acetate	57
Natural polymers and derivatives	
Lignin	58–60
Cotton	61
Starch	62
Pectin	63, 64
Biopolymers	
Proteins	65, 66

fiber strains by determining the relationship between molecular composition and fiber strength and length.

Copolymer Molecular Weight Distribution

The difficulty with copolymer analysis is in the measurement of the concentration of each elution volume. On-line viscometers measure the correct specific viscosity for copolymers. If universal

calibration holds, the problem with which we are faced is converting the specific viscosity into an intrinsic viscosity. Only if there is no compositional drift with elution volume does the output from a refractometer or UV detector correspond directly to concentration. If there are compositional changes, then the signal reflects these changes through changes in the detector response factor. If the composition changes with molecular weight, then a second detector can be used that is sensitive to only one component of the copolymer (67). This method was used recently by Grubisic-Gallot et al. (68) to characterize polystyrene-b-methyl methacrylate block copolymers. A UV detector set at 262 nm, at which wavelength polymethyl methacrylate

does not absorb, was used to measure the polystyrene content, and the refractometer was used to measure the total change in refractive index. The UV signal was then used to correct for changes in polymer refractive index and allow the concentration of both components at each elution volume to be calculated. Figure 9 shows the weight fraction of styrene for two samples as a function of elution volume.

Another approach is to use a method proposed by Goldwasser (19). This is applicable to copolymers and polymer blends and allows the number-average molecular weight to be calculated if the sample injected mass is known without a concentration detector. Figure 10 shows chromatograms from blends of equal concentrations of polystyrene and polymethyl methacrylate (21). The measured M_n is in good agreement with the value calculated from the known molecular weight of the two components. Note that the refractometer response is twice as sensitive to the polystyrene because of the larger *dn/dc*.

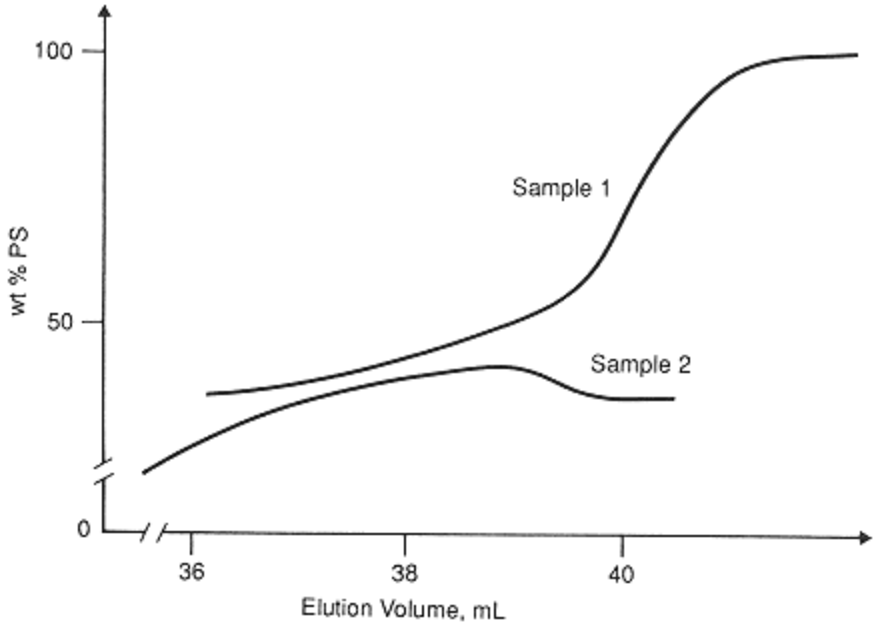

Figure 9.
Weight fraction of polystyrene versus elution volume for two samples of polystyrene-b-methyl methacrylate. Sample 1 contains residual polystyrene homopolymer in the low-molecular-weight region of the distribution. (Adapted from Reference 68 and used with permission from Springer-Verlag Publishers.)

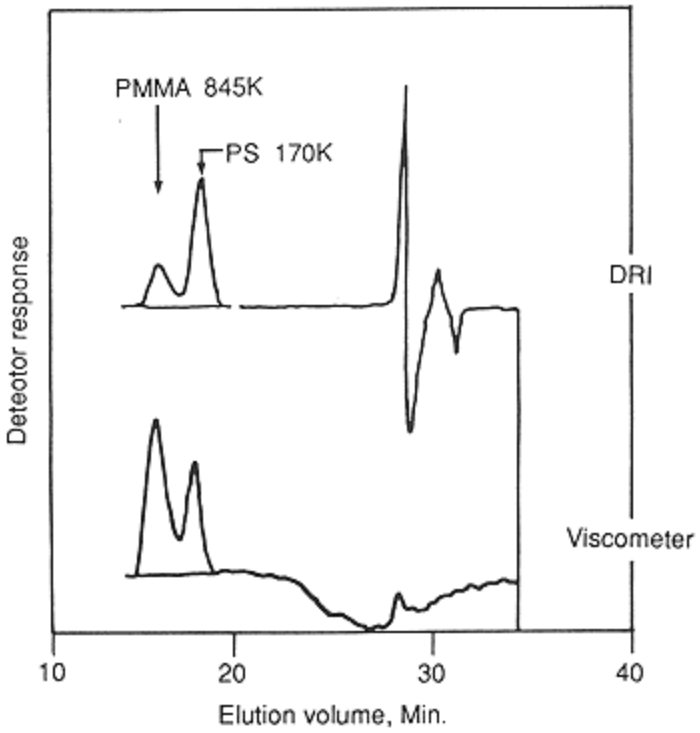

Figure 10.
Differential refractometer (DRI) and viscometer outputs for a 1:1 mixture of 845,000 g/mol of polymethyl methacrylate and 170,000 g/mol of polystyrene. With this method [Equation (15)], the determined M_n was 265,000 g/mol, compared with an expected value of 283,000 g/mol. (Adapted from Reference 21 and used with permission from John Wiley and Sons, Publishers.)

Branching

One of the most important applications of molecular weight-sensitive detectors is in the characterization of branched polymers. A branched molecule in solution has a smaller size than a linear molecule of the same molecular weight. This smaller size also means a correspondingly smaller intrinsic viscosity. By comparing the measured intrinsic viscosity of the branched molecule at each elution volume increment to the intrinsic viscosity of the linear molecule with the same molecular weight, a branching factor g', defined as

$$g' = \left(\frac{[\eta]_b}{[\eta]_l}\right)_M \quad (27)$$

can be determined, where the subscripts *b* and *l* correspond to the branched and linear polymers, respectively. For a linear polymer *g′* is unity. For a branched polymer it decreases as the number of branch points per molecule increases.

Zimm and Stockmayer (69) determined the extent of the relative decrease in the radius of gyration under θ conditions for a given number and type (trior tetrafunctional) of branch points. This is defined in terms of another branching factor,

$$g = \left(\frac{Rg_b^2}{Rg_l^2}\right)_M \quad (28)$$

Where Rg^2 is the mean square radius of gyration. For different branching architectures, *g* can be related to the number of branches per molecule (4).

This branching factor *g* is related to the intrinsic viscosity branching factor *g′* by

$$g' = g^{\epsilon} \quad (29)$$

where ϵ is a structure factor not specified by the theory. Typical values for ϵ range from 0.5 to 1.5. Experimentally determined values for a variety of polymer-solvent systems have been tabulated (70). Because of the uncertainty in ϵ and because SEC measurements are always made in good solvents, whereas *g* is defined for θ conditions, there is too much uncertainty to use *g′* to obtain the number of branch points per molecule. In many cases, only the branching ratio *g′* is reported, where it serves as a useful measure of the relative degree of branching and is a useful parameter for comparing variations among polymer samples.

Kuo et al. (36) used this method to study randomly branched and star polystyrene, as well as branched polyvinyl acetate. Figure 11 shows the Mark-Houwink plots for the linear and branched polystyrenes and a plot of the branching index *g′* for the branched polystyrene as a function of molecular weight. As expected, *g′* for randomly branched polystyrene decreases with increasing molecular weight. Siochi et al. (71,72) used this method to study model graft polymethyl methacrylates and found that in this case, *g′* increased with increasing molecular weight. They speculated that this was possibly caused by a difference between macromer and the backbone monomer polymerization kinetics.

Note that the intrinsic viscosity-molecular weight data for the corresponding linear polymer are required to calculate *g′*. Ideally this should be determined from a linear sample analyzed by SEC-viscometry. Alternatively, literature values for the Mark-Houwink parameters for the linear polymer may be used. If neither of these data are available, the least branched sample or a secondary linear standard can be used as the control. Table 2 lists selected references on the use of SEC-viscometry for branching studies.

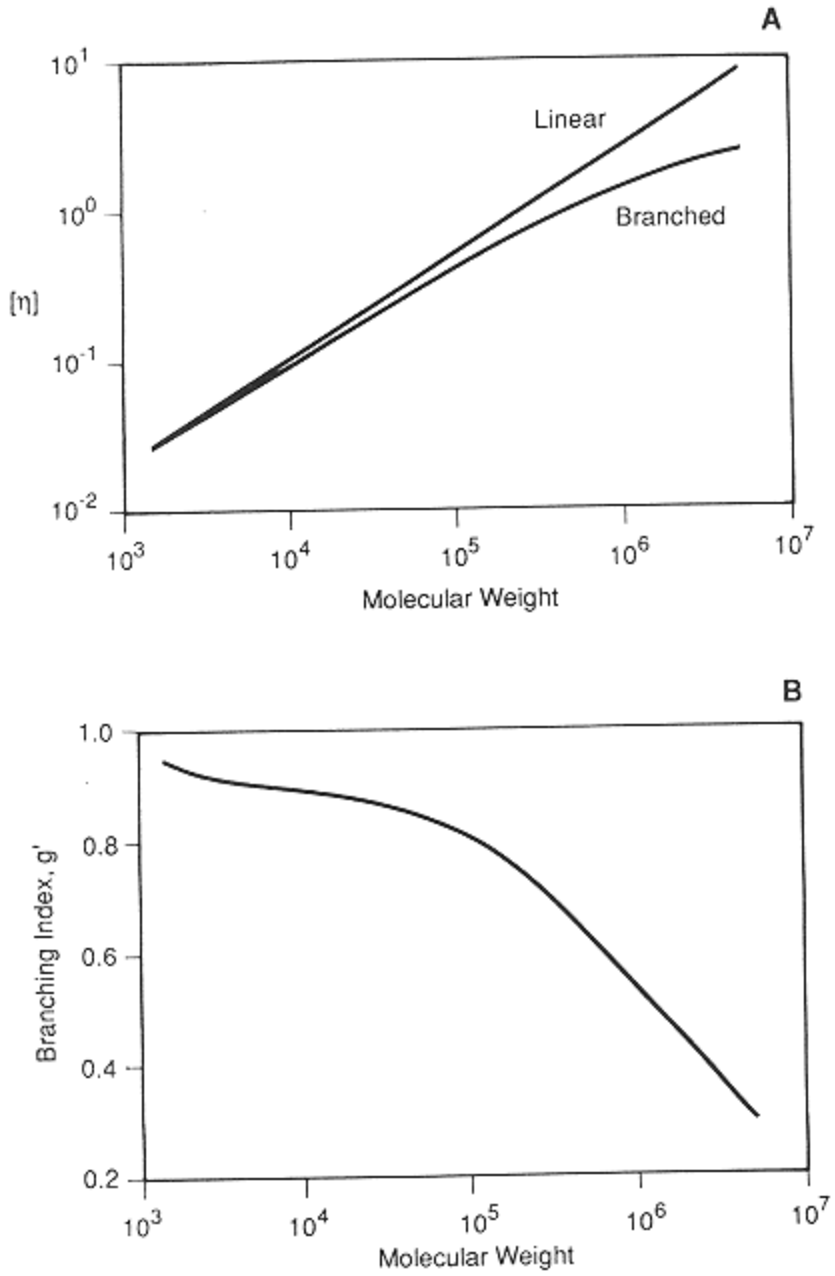

Figure 11.
(A) Mark-Houwink plot of log [η] versus log M for a linear and a branched polystyrene. (B) Plot of branching index g' as a function of molecular weight for the randomly branched polystyrene. (Adapted from Reference 36 and used with permission from the American Chemical Society.)

Table 2 Measurement of Branching by SEC-Viscometry: Selected Applications

Macromolecule	References
Polystyrene	36
Polyvinyl acetate	36, 47, 73
Polyethylene	74–77
Acrylic polymers	71, 72, 78
Polybutadiene	79, 80

Mark-Houwink Coefficients

An important application of SEC-viscometry in conjunction with universal calibration is to determine the Mark-Houwink coefficients for a given polymer system. The coefficients can provide information about solvent quality and molecular conformation. In addition, once the coefficients for a polymer-solvent system are known, that polymer can then be characterized using conventional universal calibration without an on-line viscometer. All references listed in Table 1 report the Mark-Houwink coefficients for the systems studied.

Biopolymer Characterization

In our laboratory, SEC-viscometry has been used to estimate the aspect ratio of proteins (81). This ratio, which describes the shape of proteins, is calculated from the Scheraga-Mandelkern β function (82). To determine this function, the intrinsic viscosity of the protein must be known accurately. Through the use of SEC-viscometry, proteins can be separated from interfering conformers and associated species, and intrinsic viscosities can be determined accurately.

Light Scattering

Molecular Weight Distribution

SEC-LS is used to measure molecular weight distribution directly as a polymer elutes from the SEC without universal calibration. For each polymer-solvent system, the specific refractive index increment *dn/dc* is required, and for most instruments the solvent refractive index is also needed. Table 3 lists selected papers describing SEC-LS measurements of synthetic polymers, copolymers, polysaccharides, cellulosics, and related polymers.

SEC-LS has been used at temperatures of 145°C, for example, for polyolefin analysis. It has also been used with aqueous mobile phases. In the latter case

Table 3 Measurement of Molecular Weight Distribution by SEC-LS: Selected Applications

Macromolecule	References
Homopolymers	
Polystyrene	83–87
Polyolefins	44, 88–93
Polyamides	94–98
Acrylic polymers	99–104
Polyphosphazines	105
Polyvinyl butyral	106
Polyquinolines	107
Urea-formaldehyde resins	42
Polyesters	108–110
Polyvinyl alcohol	111
Polycarbonate	95, 112
Phenolic resins	113
Polyethers	110
Polyethylene oxide	99
Polyethylene terephthate	109
Polybutadiene/polyisoprene	114–117
Copolymers	
Polyacrylates	118, 119
Styrene based	120–125
Polyesters	110,
Others	126
Polysaccharides	
Carrageenans	127
Dextran	99, 128, 129
Guar gum	130
Heparin	131
Pectin	132, 133
Starch	134–137
Xanthan	138, 139
	140–144

particulate contamination of the mobile phase is a serious problem, and the solvent requires careful filtration before use.

Aggregation has been studied by SEC-LS (see later) as well as the polyelectrolyte effect. Schorn et al. (95) used SEC-LS to illustrate how electrolyte was required to suppress the polyelectrolyte effect for nylon 6 in hexafluoroisopropanol. Without the electrolyte, bimodal peaks were observed by conventional SEC.

Copolymer Molecular Weight Distribution

The analysis of copolymers by SEC-LS is complicated by the compositional heterogeneity of the sample in two ways: first is in the determination of the concentration at each elution volume fraction, and second is the effect of the copolymer *dn/dc* on the light scattering signal. If the composition is heterogeneous, an apparent weight-average molecular weight M_w* is measured, which depends on the solvent refractive index n_0. To determine the true molecular weight, the light-scattering intensity must be measured in at least three solvents with different refractive indices (2, 158). This can be understood from Equation (7), which shows that the scattered intensity depends on $(dn/dc)^2$, for two components this is the sum of the respective *dn/dc* values squared. The measured *dn/dc,* however, is merely a straight summation. In an extreme case, the solvent refractive index may lie between the refractive indices of the two components and the *dn/dc* could be zero. However, such a copolymer would still scatter light and M_w* would be infinite. If the composition distribution is homogeneous, as in a random copolymer, or if the refractive indices of the two components are equal, then M_w* is equal to M_w. When these conditions are obtained, SEC-LS can be applied successfully to copolymers.

Grubisic-Gallot et al. (68) studied block copolymers of ethyl methacrylate and deuterated methyl methacrylate by SEC-LALLS. The *dn/dc* values in tetrahydrofuran were nearly equal, 0.084 and 0.079 ml/g, respectively. They found good agreement between the measured molecular weight and the theoretical value obtained using the molecular weights of the blocks. Malihi et al. (125) used static measurements of a styrene-butylacrylate emulsion copolymer in a series of solvents with different refractive indices to obtain the correct M_w and also to find the best solvent for SEC-LS. The best solvent is that in which M_w* is closest to M_w as determined from the multiple solvent measurements, that is, when the component *dn/dc* values are relatively closest. They found good agreement between SEC-LS results and static measurements.

Dumelow (123) used SEC-LALLS with dual concentration detectors to study the variation in compositional heterogeneity with molecular weight in polystyrene-polydimethylsiloxane block copolymers. The results showed that some of the copolymers were in fact blends. The largest errors in the analysis

were found to arise if it were assumed that there was no molecular weight distribution at each elution slice. By avoiding this assumption the results were improved.

The relationship between the radius of gyration and the light-scattering asymmetry is also dependent on copolymer composition and is not the same as for homopolymers. Unless *dn/dc* is equal for both components, the spatial distribution of the component that scatters the most dominates the angular distribution of scattered light and thus the measured radius of gyration (158).

Branching

Light scattering has been widely used to study branching. The molecular weight of the branched polymer M_b is measured for each elusion slice, and the size information is derived from universal calibration. Equation (27) can be rewritten as

$$g' = \left(\frac{M^*}{M_b}\right)^{a+1} \quad (30)$$

where M^* is the molecular weight of the linear molecule with the same hydro-dynamic volume as the branched molecule calculated from universal calibration and a is the Mark-Houwink exponent for the linear molecule. Figure 12 illustrates the effect of branching on the molecular weight calibration curve.

The value of M_b in Equation (30) is a number-average molecular weight, and because light scattering measures the weight-average molecular weight, values of g' do not agree with those measured by viscometry if there is significant polydispersity at each elution slice. This occurs when species with different degrees of branching have the same hydrodynamic volume.

Selected applications are listed in Table 4. One of the most widely studied branched polymers is polyethylene. Rudin and coworkers (167,168) used SEC-LALLS to study branching in polyethylene in conjunction with intrinsic viscosity measurements. They found no appreciable difference between the two methods, indicating that there was little molecular weight polydispersity in each elution volume. They also compared SEC-LALLS results with static LALLS results and found that the latter were significantly larger, possibly because of the poor refractometer signal at the high-molecular-weight end of the distribution. This is because of the molecular weight sensitivity of LS, which makes it especially sensitive to small amounts of highly branched material, or “microgel,” which are either filtered out by the SEC columns or give too low a signal in the refractometer.

Biopolymers

Studies relating to the use of SEC-LS for several classes of polysaccharides and cellulosics are listed in Table 3. In addition, Dean and Rollings (185) studied

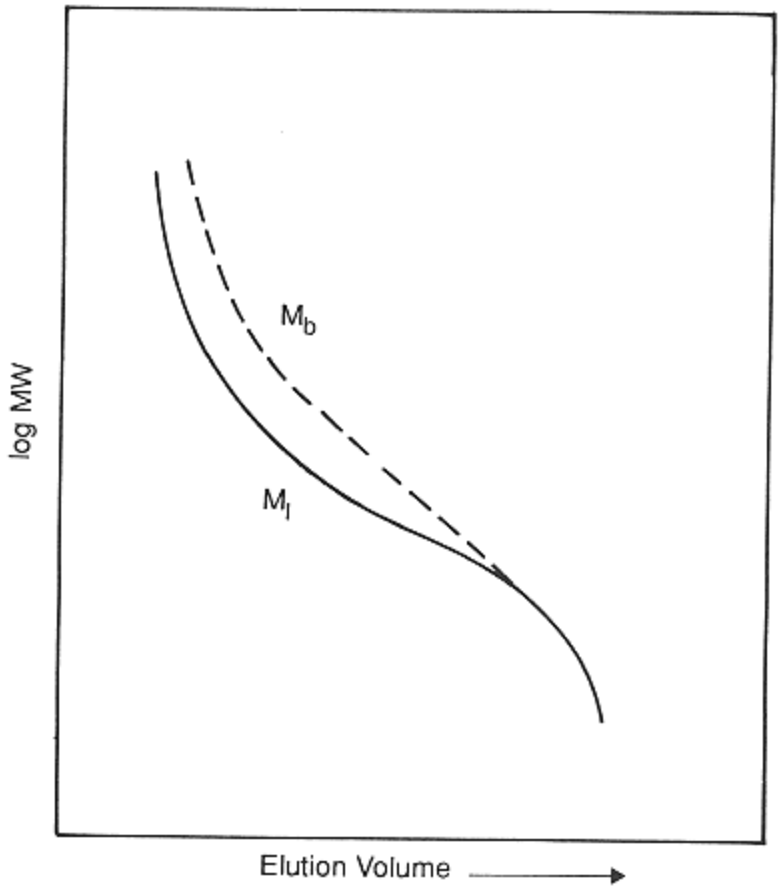

Figure 12.
Typical SEC calibration curves for linear and branched polymers.

polysaccharide depolymerase activity in fermentation with SEC-LS. Agarose and agarose-type polysaccharides, within a molecular weight range 80,000–140,000 g/mol, were also analyzed by SEC-LS (144).

Table 5 lists selected applications of SEC-LS for biopolymers, mainly proteins. An earlier review of SEC-LS of biopolymers can be found in Reference 210. It is of interest that there has been only one reported study on the use of SEC-LS for the analysis of nucleic acids (209).

For protein characterization, SEC-LS has been used as an analytical procedure for determining the molecular weights of unknown samples and also for studying protein association. In using an on-line light-scattering detector for SEC

Table 4 Characterization of Branched Polymers by SEC-LS: Selected Applications

Macromolecule	References
Polyolefins	159–170
Polyvinyl chloride	168
Polyvinyl alcohol	171–174
Polychloroprene	173
Polystyrene	172, 175, 176
Polyoctenamer	177
Polybutadiene/polyisoprene	120, 178–180
Polysaccharides	181, 182
Dextran	129
Polymethyl methacrylate	183
Polyesters	184

of proteins, it seems logical to use assigned *dn/dc* values for individual proteins, determined off-line using purified samples. In many cases, however, purified standard proteins are not available, there is limited sample availability, or the identity of proteins in a sample is not known. Because of the uncertainty in *dn/dc* values, many investigators have used both a differential refractometer and a UV spectrophotometer, in series with a light-scattering detector, to determine *dn/dc* values of eluting species. For example, Maezawa and Takagi (200) used this approach to determine the molecular weights of glycoproteins. A light-scattering-UV-DRI (differential refractive index) detection system has also been used for determining molecular weights of ATPases (194,208) and membrane proteins (210). Recently, Krull and coworkers (187,211) investigated the advantages of using the LS-UV-DRI approach for protein characterization and found

Table 5 Molecular Weight Distribution by SEC-LS: Biopolymers: Selected Applications

Macromolecule	References
Proteins	99, 186–200
Membrane proteins	200–206
Enzymes	207, 208
Nucleic acids	209

that on-line *dn/dc* measurements were in good agreement with off-line measurements. Furthermore, these investigators demonstrated the use of gradient elution high-performance liquid chromatography (HPLC) with an on-line light-scattering detector and applied this technique to examine aggregation of bovine alkaline phosphate (188,212), ribonuclease A (188), lysozyme (188), and pituitary and recombinant human growth hormones (186).

Dollinger et al. (213) used an HPLC fluorimeter as a 90° light-scattering detector for proteins analyzed by reversed-phase HPLC. The excitation and emission wavelengths were both set to 467 nm. Because of the small size of the proteins, there was no measurable scattering asymmetry for molecular weights below 1×10^6 g/mol, and the scattered intensity at 90° was found to be proportional to molecular weight. The light-scattering method was further simplified, in this case, by assuming that the second virial coefficient was neg-

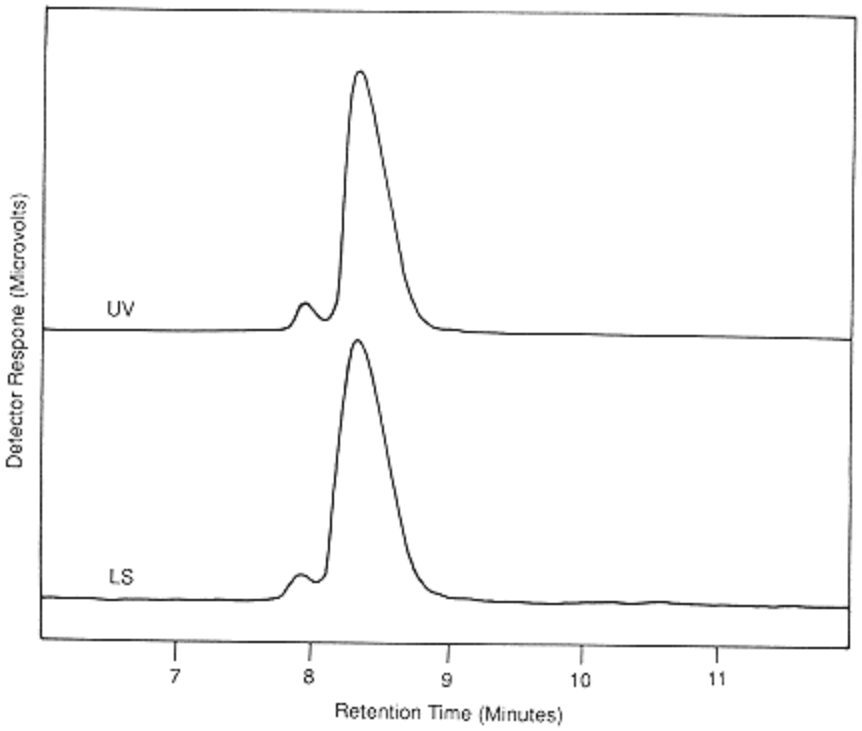

Figure 13.
Gradient reversed-phase HPLC of lysozyme showing two conformers in both the UV and light-scattering tracings. Light scattering was measured using an HPLC fluorimeter at 90°. [Used with permission from Elsevier Science Publishers (213).]

ligible under HPLC conditions and that *dn/dc* values for all proteins under similar chromatographic conditions were equal. Figure 13 shows the LS and UV responses for lysozyme analyzed by reversed-phase HPLC. The double peaks have the same molecular weight and correspond to different conformers rather than aggregates.

Special Applications

Cotts (107) showed that SEC-LALLS could be combined with universal calibration to determine the intrinsic viscosity at each elution volume increment. As in SEC-viscometry with universal calibration, the accuracy of the calculated values depends upon the chromatograms being corrected for axial dispersion. In addition, the Mark-Houwink coefficients can be determined from a plot of molecular weight and intrinsic viscosity at each elution volume for the whole molecular weight distribution. However, it was noted that the values obtained were also sensitive to axial dispersion. Another source of error arises from the poly-dispersity in individual elution volume increments, because universal calibration requires that the number-average molecular weight be used to calculate intrinsic viscosity.

By measuring the scattered intensity at more than one angle, both the radius of gyration and the molecular weight can be determined for each elution volume. Jackson et al. (214) used multiangle LS to determine the radius of gyration of monodisperse and polydisperse polystyrenes. For the nearly monodisperse standards, measurements for radii greater than 10 nm were possible. For the poly-disperse sample the lower limit was 18 nm. A similar LS detector was used to determine the relationship between radius of gyration and molecular weight for linear polyethylene (89), cross-linked polystyrene (215), and polyamic acid (216). Figure 14 shows a plot of R_g versus M_w for a polyamic acid.

The combination of a light-scattering detector and an on-line viscometer with SEC provides a method of directly measuring MWD and intrinsic viscosity distribution, as well as MWD, from universal calibration in a single experiment. Such a combined instrument has been used by Lesec and Volet (217,218) to characterize a range of linear and branched synthetic polymers. Tinland and coworkers (219) used an SEC-viscometry-LS instrument to characterize xanthan and dextran. Grubisic-Gallot et al. (68) added a second concentration detector to an SEC-viscometry-LS instrument to characterize block copolymers. Pang and Rudin (50) showed how each detector (light scattering, viscometer, and DRI) provided useful information in the analysis of linear polyolefins at high temperature. They also demonstrated, for the polymer studied, that no single detector was able to give a complete picture of the MWD because of different sensitivity ranges. Jackson and coworkers (220) showed that the Mark-Houwink exponent

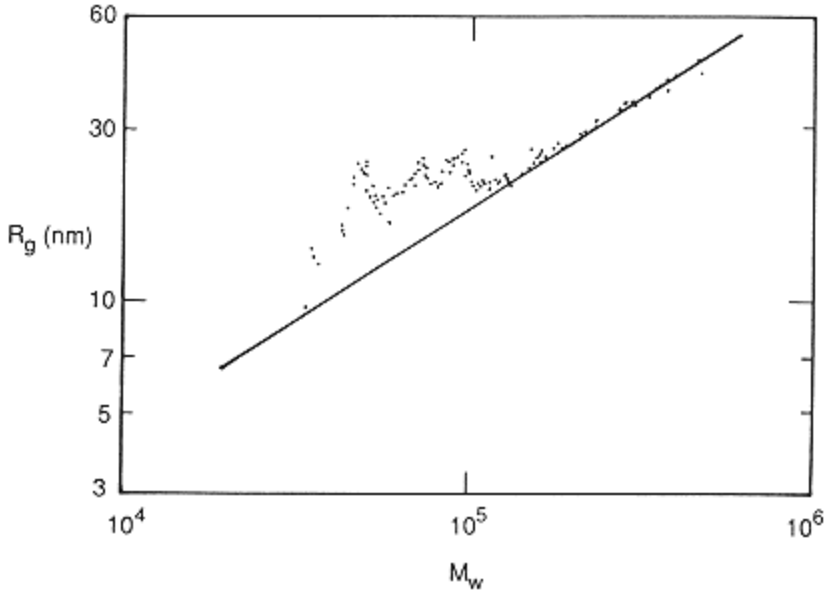

Figure 14.
Radius of gyration R_g versus weight-average molecular weight of a diethyl ester of a polyamic acid as determined using SEC with an on-line multiangle laser light-scattering detector. The line through the data is the linear regression fit for molecular weight greater than 10^5 g/mol. (Adapted from Reference 215 and used with permission from John Wiley and Sons, Publishers.)

of polystyrene in toluene could be measured with a relative standard deviation of less than 1% with a single injection of a broad MWD standard.

As discussed earlier, a combination of a right-angle laser light-scattering detector and a viscometer has proved to be a useful system for determining not only molecular weight and intrinsic viscosity data but also radius of gyration of linear polymers (11). Light-scattering measurements made at 90° simplify the design of light-scattering instrumentation and, in principle, give a less noisy signal by reducing spikes from particle contamination and stray light. In fact, a commercially available HPLC fluorescence detector can be employed for these measurements (213).

Summary

The use of molecular weight-sensitive detectors has increased dramatically the information content that can be obtained from an SEC analysis. With these

detection systems, accurate measurements of fundamental molecular parameters, both average and distributed values, can be determined readily. Furthermore, the use of light-scattering detectors, and viscosity detectors for IVD, eliminates the need of column calibration, which greatly increases the precision and reliability of these measurements. However, as in any other analytical instrumental procedure, good chromatographic practice must be exercised: signal-to-noise ratio of detector outputs must be maximized, defined polymer solutions injected, and instrument calibration parameters and proper interdetector volumes established.

In addition to applications in the area of synthetic polymers, we foresee exciting uses of molecular weight-sensitive detectors for biopolymer characterization and with interactive modes of separation, such as reversed-phase gradient elution or ion-exchange chromatography. Finally, the combination of on-line spectroscopic detectors, including UV-diode array, Fourier transform infrared, mass spectrometry and possibly nuclear magnetic resonance with molecular weight-sensitive detectors represent a significant breakthrough for the characterization of complex polymeric materials.

Acknowledgments

The authors gratefully acknowledge the valuable input and discussions with our colleague Wallace W. Yau. We also thank the Corporate Center for Analytical Sciences of the DuPont Company for giving us opportunity to prepare this chapter.

Appendix: Instrument Companies

Light-Scattering Detectors for SEC

LDC Analytical, 3681 Industrial Park Road North, Riviera Beach, FL 33404: low-angle laser light-scattering detector.

Polymer Laboratories, Inc., Amherst Fields Research Park, 160 Old Farm Road, Amherst, MA 01002: low-angle laser light-scattering detector.

Precision Detectors, Inc., 358 North Pleasant Street, Amherst, MA 01002: dual-angle laser light-scattering detector.

Tosoh Corporation, 707, 1-Chome, Akasaka, Minato-ku, Tokyo, Japan: low-angle laser light-scattering detector.

Viscotek Corp., 1032 Russell Drive, Porter, TX 77365: right-angle light-scattering detector.

Wyatt Technology Corp., 802 East Cota Street, Santa Barbara, CA 93103: multiangle (15 and 3) laser light-scattering detectors.

Viscometers for SEC

Viscotek Corp., 1032 Russell Drive, Porter, TX 77365: four-capillary and two-capillary differential viscometers.

Waters Chromatography Division, Millipore Corp., 34 Maple Street, Milford, MA 01757: single-capillary viscometer.

References

1. W. W. Yau, J. J. Kirkland, and D. D. Bly, *Modern Size Exclusion Liquid Chromatography*, John Wiley and Sons, New York, 1979.

2. P. Kratochvil, *Classical Light Scattering from Polymer Solutions,* Elsevier, New York, 1987.

3. M. Bohdanecky and J. Kovar, *Viscosity of Polymer Solutions,* Elsevier, New York, 1982.

4. H. Yamakawa, *Modern Theory of Polymer Solutions,* Harper and Row, New York, 1971.

5. H. Fujita, *Polymer Solutions,* Elsevier, New York, 1990.

6. M. A. Haney, *J. Appl. Polym. Sci.,* 30:3023 (1985); 30:3037 (1985).

7. J. L. Ekmanis and R. A. Skinner, *J. Appl. Polym. Sci., Appl. Polym. Symp.,* 48: 57 (1991).

8. W. W. Yau, S. D. Abbott, G. A. Smith, and M. Y. Keating, *ACS Symp. Ser.,* 352: 80 (1987).

9. B. H. Zimm, *J. Chem. Phys.,* 16:1093 (1948).

10. M. L. McConnell, *Am. Lab.,* 10(5):63 (1978).

11. M. A. Haney, C. Jackson, and W. W. Yau, in *Proc. Int. Gel Permeation Chromatography Symp. 1991,* San Francisco, 1993, p. 49.

12. Precision Detectors, Application Notes, Amherst, MA.

13. P. J. Wyatt, D. L. Hicks, C. Jackson, and G. K. Wyatt, *Lab.,* 20(6):108 (1988).

14. P. J. Wyatt, C. Jackson, and G. K. Wyatt, *Am. Lab.,* 20(5):86 (1988).

15. Z. Grubisic, P. Rempp, and H. Benoit, *J. Polym. Sci., Part B, Polym. Lett.,* 5:753 (1967).

16. A. E. Hamielec and A. C. Ouano, *J. Liq. Chromatogr.,* 1:111 (1978).

17. C. J. Stacy, *J. Appl. Polym. Sci.,* 32:3959 (1986).

18. M. A. Haney, personal communication.

19. J. M. Goldwasser, *Proc. Int. Gel Permeation Chromatography Symposium 1989,* Newton, MA, 1990, p. 150.

20. J. J. Kirkland, S. W. Rementer, and W. W. Yau, *J. Appl. Polym. Sci.,* 48:39 (1991).

21. W. W. Yau, *Chemtracts-Macromol. Chem.,* 1:1 (1990).

22. P. J. Flory and T. G. Fox, Jr., *J. Am. Chem. Soc.,* 73:1904 (1951).

23. O. B. Ptitsyn and Y. E. Eizner, *Sov. Phys. Tech. Phys.,* 4:1020 (1960).

24. H. G. Barth and W. W. Yau, in *Proc. Int. Gel Permeation Chromatography Symp. 1989,* Newton, MA, 1990, p. 26.

25. M. B. Huglin (ed.), *Light Scattering from Polymer Solutions,* Academic Press, New York, 1972, Ch. 6.

26. M. B. Huglin, in *Polymer Handbook,* 3rd ed., J. Brandrup and E. H. Immergut (eds.), John Wiley and Sons, New York, 1989.

27. H. Eisenberg, *Biological Macromolecules and Polyelectrolytes in Solution,* Clarendon Press, Oxford, 1987.

28. H. Utiyama, in *Light Scattering from Polymer Solutions,* M. B. Huglin (ed.), Academic Press, New York, 1989, Ch. 4.

29. M. Martin, *Chromatographia,* 15:426 (1982).

30. O. Prochazka and P. Kratochvil, *J. Appl. Polym. Sci.,* 3:919 (1986).

31. O. Prochazka and P. Kratochvil, *J. Appl. Polym. Sci.,* 34:2325 (1987).

32. R. Bruessau in *Liquid Chromatography of Polymers and Related Materials-II,* J. Cazes (ed.), Marcel Dekker, New York, 1983, p. 73.

33. D. Lecacheux and J. Lesec. *J. Liq. Chromatogr.,* 5:2227 (1982).

34. H. G. Barth and C. Jackson, manuscript in preparation.

35. T. H. Mourey and S. M. Miller, *J. Liq. Chromatogr.,* 13:693 (1990).

36. C.-Y. Kuo, T. Provder, M. E. Koehler, and A. F. Kah, *ACS Symp. Ser.,* 352:130 (1987).

37. S. T. Balke, P. Cheung, L. Jeng, and R. Lew, *J. Appl. Polym. Sci., Appl. Polym. Symp.,* 48:259 (1991).

38. T. H. Mourey, S. M. Miller, and S. T. Balke, *J. Liq. Chromatogr.,* 13:435 (1990).

39. C. Jackson and W. W. Yau, *J. Chromatogr.,* 645:209 (1993).

40. Z. He, X. Zhang, and R. Cheng, *J. Liq. Chromatogr.,* 5:1209 (1982).

41. K. Lederer, G. Imrich-Scwarz, and M. Dunky, *J. Appl. Polym. Sci.,* 32:4751 (1986).

42. J. Billiani, D. K. Lederer, and M. Dunky, *Angew. Makromol. Chem.,* 180:199 (1990).

43. J. Billiani, I. Amtmann, T. Mayr, and K. Lederer, *J. Liq. Chromatogr.,* 13:2973 (1990).

44. J. Billiani and D. K. Lederer, *J. Liq. Chromatogr.,* 13:3013 (1990).

45. A. E. Hamielec, in *Steric Exclusion Liquid Chromatography of Polymers,* Chromatographic Science Series, Vol. 25, J. Janca (ed.), Dekker, New York, 1984, Ch. 3.

46. M. A. Haney, J. E. Armonas, and L. Rosen, *ACS Symp. Ser.,* 352:119 (1987).

47. M. G. Styring, J. E. Armonas, and A. E. Hamielec, *ACS Symp. Ser.,* 352:104 (1987).

48. F. B. Malihi, C. Y. Kuo, M. E. Koehler, T. Provder, and A. F. Kah, *Org. Coat. Appl. Polym. Sci. Proc.*, 48:760 (1983).

49. F. B. Malihi, C. Y. Kuo, M. E. Koehler, T. Provder, and A. F. Kah, *ACS Symp. Ser.,* 245:281 (1984).

50. S. Pang and A. Rudin, *Polymer*, 33:1949 (1992).

51. D. J. Nagy, *Int. GPC Symp.* '87, 1987, p. 250.

52. D. J. Nagy and D. A. Terwilliger, *J. Liq. Chromatogr.*, 12:1431 (1989).

53. D. J. Nagy, *J. Liq. Chromatogr.,* 13:677 (1990).

54. G. Marot and J. Lesec, *Int. GPC Symp.,* '87, 1987, p. 113.

55. G. Marot and J. Lesec, *J. Liq. Chromatogr.,* 11:3305 (1988).

56. T. Housaki and K. Satoh, *Polym. J. (Tokyo),* 20:1163 (1988).

57. D. Lecacheux, J. Lesec, C. Quivoron, R. Prechner, and R. Panaras, *J. Appl. Polym. Sci.,* 29:1569 (1984).

58. M. E. Himmel, K. Tatsumoto, K. K. Oh, D. K. Johnson, and H. L. Chum, *ACS Symp. Ser.,* 397:82 (1989).

59. M. E. Himmel, K. Tatsumoto, K. Grohmann, D. K. Johnson, and H. L. Chum, *J. Liq. Chromatogr.,* 498:93 (1990).

60. E. J. Siochi, M. A. Haney, W. Mahn, and T. C. Ward, *ACS Symp. Ser.,* 397:100 (1989).

61. J. D. Timpa, *J. Agric. Food Chem.,* 39:270 (1991).

62. B. P. Wasserman and J. D. Timpa, *Starch/Staerke,* 43:389 (1991).

63. M. L. Fishman, D. T. Gillespie, S. M. Sondey, and R. A. Barford, *J. Agric. Food Chem.,* 37:584 (1989).

64. M. L. Fishman, D. T. Gillespie, and S. M. Sondey, *Carbohydr. Res.,* 215:91 (1991).

65. P. K. Dutta, *J. Chromatogr. Sci.,* 28:119 (1990).

66. P. K. Dutta, K. Hammons, B. Willeby, and M. A. Haney, *J. Chromatogr.,* 536:113 (1991).

67. H. E. Adams, in *Gel Permeation Chromatography,* K. H. Altgelt and L. Segal (eds.), Dekker, New York, 1971, p. 391.

68. Z. Grubisic-Gallot, J. P. Lingelser, and Y. Gallot, *Polym. Bull.* (Berlin), 23:389 (1990).

69. B. H. Zimm and W. H. Stockmayer, *J. Chem. Phys.,* 17:1301 (1949).

70. J. Roovers, in *Encyclopedia of Polymer Science and Technology,* 2nd ed., J. Wiley and Sons, New York, Vol. 2, 1989, p. 478.

71. E. J. Siochi, J. M. DeSimone, A. M. Hellstern, J. E. McGrath, and T. C. Ward, *Polym. Prepr. (Am. Chem. Soc., Div. Polym. Chem.),* 30(1):141 (1989).

72. E. J. Siochi, J. M. DeSimone, A. M. Hellstern, J. E. McGrath, and T. C. Ward, *Macromolecules,* 23:4696 (1990).

73. C. Kuo, T. Provder, and M. E. Koehler, *Polym. Mater. Sci. Eng.,* 65:142 (1991).

74. F. M. Mirabella, Jr., and L. Wild, *Polym. Mater. Sci. Eng.,* 59:7 (1988).

75. D. G. Moldovan, *Int. GPC Symp.,* '87, 1987, p. 129.

76. D. Lecacheaux, J. Lesec, and C. Quivoron, *J. Appl. Polym. Sci.,* 27:4867 (1982).

77. D. Lecacheux, J. Lesec, and C. Quivoron, *Polym. Prepr. (Am. Chem. Soc., Div. Polym. Chem.),* 23 (2):126 (1982).

78. P. J. Wang and R. J. Rivard, *J. Liq. Chromatogr.,* 10:3059 (1987).

79. C. Jin, S. Sun, and S. Sui, *Yingyong Huaxe,* 3:50 (1986).

80. C. Jin, S. Sun, R. Hou, and R. Cheng, *Gaofenzi Xuebao,* (2):113 (1987).

81. B. E. Boyes, H. G. Barth, and W. W. Yau, 200th ACS National Mtg., Washington, D.C., August 1990, Dn. Agr. Food Chem., Abstract 147.

82. K. E. van Holde, *Physical Biochemistry,* Prentice-Hall, Englewood Cliffs, NJ, 2nd ed., 1985.

83. W. Zhang, M. Wang, J. Sun, X. Zhang, and Z. He, *Yingyong Huaxue,* 7(3):57 (1990).

84. F. Schosseler, H. Benoit, Z. Grubisic-Gallot, C. Strazielle, and L. Leibler, *Macromolecules,* 22:400 (1989).

85. W. G. Rand and A. K. Mukherji, *J. Appl. Polym. Sci., Polym. Lett. Ed.,* 20:501 (1982).

86. A. Lapp and C. Strazielle, *Makromol. Chem.,* 184(9):1877 (1984).

87. Y. Tsukahara, K. Tsutsumi, Y. Yamashita, and S. Shimada, *Macromolecules,* 23: 5201 (1990).

88. J. G. Rooney and G. Ver Strate, *Liquid Chromatography of Polymers and Related Materials III,* J. Cazes (ed.), Marcel Dekker, New York, 1981, p. 207.

89. T. Housaki and K. Satoh, *Makromol. Chem., Rapid Commun.,* 9:257 (1988).

90. A. W. Degroot, *J. Appl. Polym. Sci., Appl. Polym. Symp.,* 43:85 (1989).

91. V. Grinshpun, K. F. O'Driscoll, and A. Rudin, *Org. Coat. Appl. Polym. Sci. Proc.,* 48:745 (1983).

92. V. Grinshpun, K. F. O'Driscoll, and A. Rudin, *J. Appl. Polym. Sci.,* 29:1071 (1984).

93. V. Grinshpun and A. Rudin, *J. Appl. Polym. Sci.,* 30:2413 (1985).

94. G. Pastuska, J. Just, and H. August, *Angew. Makromol. Chem.,* 107:173 (1982).

95. H. Schorn, R. Kosfeld, and M. Hess, *J. Chromatogr.,* 353:273 (1986).

96. D. J. Goedhart, J. B. Hussem, and B. P. M. Smeets, *Chromatogr. Sci.,* 13*(Liq. Chromatogr. Polym. Relat. Mater.,* 2):203 (1980).

97. P. J. Wang and B. S. Glassbrenner, *J. Liq. Chromatogr.,* 11:3321 (1988).

98. A. Huber, *Biochem. Soc. Trans.,* 19:505 (1991).

99. M. Fukutomi, M. Fukuda, and T. Hashimoto, *Toyo Soda Kogyo K.K.* Japan, 24: 33 (1980).

100. C. J. Kim, A. E. Hamielec, and A. Bendek, *J. Liq. Chromatogr.,* 5:1277 (1982).

101. W. M. Kulicke and N. Boese, *Colloid Polym. Sci.,* 262:197 (1984).

102. G. Muller and C. Yonnet, *Makromol. Chem., Rapid Commun.,* 5:197 (1984).

103. T. Kato, T. Tokuya, T. Nozaki, and A. Takahashi, *Polymer,* 25:218 (1984).

104. R. Jenkins and R. S. Porter, *J. Polym. Sci., Polym. Lett. Ed.,* 18:743 (1980).

105. R. De Jaeger, D. Lecacheaux, and P. Potin, *J. Appl. Polym. Sci.,* 39:1793 (1990).

106. E. E. Remsen, *J. Appl. Polym. Sci.,* 42:503 (1991).

107. P. M. Cotts, *J. Polym. Sci., Part B, Polym. Phys.,* 24:1493 (1986).

108. A. Kinugawa and Y. Kise, *Kobunshi Ronbushu,* 45:531 (1988).

109. S. Berkowitz, *J. Appl. Polym. Sci.,* 29:4353 (1984).

110. D. B. Cotts, *Org. Coat. Appl. Polym. Sci. Proc.,* 48:750 (1983).

111. D. J. Nagy, *Polym. Sci. Part C, Polym. Lett.,* 24:87 (1986).

112. C. Bailly, D. Daust, R. Legras, J. P. Mercier, C. Straziell, and A. Lapp, *Polymer,* 27:1410 (1986).

113. J. D. Wellons and L. Gollob, *Wood Sci.,* 13:68 (1980).

114. S. Bo and R. Cheng, *J. Liq. Chromatogr.,* 5:1404 (1982).

115. T. Honma and M. Tazaki, *Nippon Gomu Kyokaishi,* 60:636 (1987).

116. S. A. Gusev, I. B. Tsvetkovski, and V. I. Valuev, *Kauch. Rezina* 3:32 (1984).

117. X. Wang, X. Zhang, and Z. He, *Yingyong Huaaxue,* 2:77 (1985).

118. C. S. Wu and L. Senak, *J. Liq. Chromatogr.,* 13:851 (1990).

119. F. C. Lin and G. D. Getman, *Int. GPC Symp.,* '87, 225 (1987).

120. R. C. Jordan, S. F. Silver, R. D. Sehon, and R. J. Rivard, *Org. Coat. Appl. Polym. Sci. Proc.,* 48:755 (1983).

121. R. J. Cramer, Report 1987, NWC-TP-6774, SBI-AD-E900674; Order No. AD-A182149, Avail. NTIS.

122. T. Dumelow, S. R. Holding, L. J. Maisey, and J. V. Dawkins, *Polymer*, 27:1170 (1986).

123. T. J. Dumelow, *Macromol. Sci., Chem.,* A26:125 (1989).

124. R. Murakoe, R., *Petrotech (Tokyo),* 10:175 (1987).

125. F. B. Malihi, C. Y. Kuo, and T. Provder, *J. Appl. Polym. Sci.*, 29:925 (1984).

126. V. Grinshpun and A. Rudin, *Polym. Mater. Sci. Eng.*, 54:174 (1986).

127. D. Slootmaekers, J. A. P. P. Van Dijk, F. A. Varkevisser, and C. J. Bloys Van Treslong

128. C. J. Kim, A. E. Hamielec, and A. Bendek, *J. Liq. Chromatogr.*, 5:425 (1982).

129. J. A. P. P. Van Dijk, F. A. Varkevisser, and J. A. M. Smit, *J. Polym. Sci., Part B, Polym. Phys.*, 25:149 (1987).

130. B. R. Vijayendran and T. Bone, *Carbohydr. Polym.*, 4:299 (1984).

131. D. Lecacheaux, Y. Mustiere, and A. Denis, *Spectra 2000,* 122:57 (1987).

132. M. G. Kontominas and J. L. Kokoni, *Lebensm-Wiss. Technol.,* 23:174 (1990).

133. W. E. Hennink, J. W. A. Van den Berg, and J. Feijen, *Thromb. Res.,* 45:463 (1987).

134. A. Heyraud and M. Rinaudo, *ACS Symp. Ser.,* 458 (Biotechnol. Amylodextrin Oligosaccharides):171 (1991).

135. K. Lederer, C. Huber, M. Dunky, J. K. Fink, H. P. Ferber, and E. Nitsch, *Arzneim.-Forsch.,* 35:610 (1985).

136. S. Hizurkuri and T. Takagi, *Carbohydr. Res.,* 134:1 (1984).

137. T. Takagi, *Kagaku Zokan (Kyoto),* 102:253 (1984).

138. J. A. Hunt, T. S. Young, D. W. Grenn, and G. P. Willhite, *SPE Reservoir Eng.,* 3:835 (1988).

139. F. Lambert, M. Milas, and M. Rinaudo, *Polym. Bull. (Berlin),* 7:185 (1982).

140. A. Corona and J. E. Rollings, *Sep. Sci. Technol.*, 23:855 (1988).

141. D. Lecacheaux, R. Panaras, G. Brigand, and G. Martin, *Carbohydr. Polym.*, 5:423 (1985).

142. D. Lecacheaux, Y. Mustiere, R. Panaras, and G. Brigand, *Carbohydr. Polym.*, 6:447 (1986).

143. M. Miya, R. Iwamoto, S. Yoshikawa, and S. Mima, *Kobunshi Ronbushu*, 43:83 (1986).

144. C. Rochas and M. Lahaye, *Carbohydr. Polym.*, 10:129 (1989).

145. J. M. Lauriol, P. Froment, F. Pla, and A. Robert, *Holzforschung,* 41:109 (1987).

146. J. M. Lauriol, J. Comtat, P. Froment, F. Pla, and A. Robert, *Holzforschung*, 41:165 (1987).

147. J. M. Lauriol, J. Comtat, P. Froment, F. Pla, and A. Robert, *Holzforschung*, 41:215 (1987).

148. J. J. Cael, K. J. Cietek, and F. J. Kolpak, *J. Appl. Polym. Sci.,* Appl. Polym. Symp. 37:509 (1983).

149. T. Kato, T. Tokuya, and A. Takahasi, *Kobunshi Ronbunshu*, 39:293 (1981).

150. W. D. Eigner, J. Biliani, and A. Huber, *Papier*, 41:680 (1987).

151. A. Wirsen, *Makromol. Chem.,* 189:833 (1988).

152. P. J. Wood, J. Weisz, and W. Mahn, *Cereal Chem.,* 68:530 (1991).

153. J. T. Cheng and M. J. Langsam, *Macromol. Sci. Chem.,* A21:403 (1984).

154. A. Wirsen and E. Helleday, Report 1986, FOA-C-20602-D-1; Order No. PB86-188067/(GAR, (Sweden). Avail. NTIS from Gov. Rep. Announce. Index (USA) 1986, 86(16), Abstract No. 635,623.

155. A. F. Cunningham, C. Heathcote, D. E. Hillma, and J. I. Paul, *Chromatogr. Sci.,* 13(Liq. Chromatogr. Polym. Relat. Mater., 2):175 (1980).

156. D. S. Argyropoulos and H. I. J. Bolker, *Wood Chem. Technol.* 7:1 (1987).

157. E. S. Olson and J. W. Diehl, *J. Chromatogr.*, 349:337 (1985).

158. H. Benoit in *Light Scattering from Polymer Solutions,* M. B. Huglin (ed.), Academic Press, New York, 1972.

159. F. J. Kolpak, D. J. Cietek, W. Fookes, and J. J. Cael, *J. Appl. Polym. Sci., Appl. Polym. Symp.,* 37:491 (1983).

160. D. E. Axelson and W. C. Knapp, *J. Appl. Polym. Sci.,* 25:119 (1980).

161. B. D. Dickie and R. J. Koopmans, *J. Polym. Sci., Part C, Polym. Lett.,* 28:193 (1990).

162. W. Zhang, M. Wang, J. Sun, and Z. He, *Yingyong Huaxue,* 7(3):48 (1990).

163. T. B. MacRury and M. L. McConnell, *J. Appl. Polym. Sci.,* 24:651.

164. L. I. Kulin, N. L. Meijerink, and P. Starck, *Pure Appl. Chem.,* 60:1403 (1988).

165. D. C. Bugada and A. Rudin, *Eur. Polym. J.,* 23:847 (1987).

166. V. Grinshpun, A. Rudin, K. E. Russel, and M. V. Scammell, *J. Polym. Sci., Part B, Polym. Phys.,* 24:1171 (1986).

167. V. Grinshpun and A. Rudin, *Makromol. Chem. Rapid. Commun.,* 6:219 (1985).

168. A. Rudin, V. Grinshpun, and K. F. O'Driscoll, *J. Liq. Chromatogr.,* 7:1809 (1984).

169. S. Shiga and Y. Sato, *Nippon Gomu Kyokaishi,* 57:811 (1984).

170. S. Shiga, *Nippon Gomu Kyokaishi,* 59:162 (1986).

171. A. E. Hamielec, A. C. Ouano, and L. I. Nebenzahl, *J. Chromatogr.,* 1:527 (1978).

172. Z. Gallot, *Chromatogr. Sci.,* 13 (Liq. Chromatogr. Polym. Relat. Mater., 2):113 (1980).

173. R. C. Jordan and M. L. McConnell, *ACS Symp. Ser.,* 138 (Size Exclusion Chromatogr.):107 (1980).

174. S. H. Agarwal, R. F. Jenkins, and R. S. Porter, *J. Appl. Polym. Sci.,* 27:113 (1982).

175. A. Hasegawa, T. Nakamura, and S. Teramachi, *Kogakuin Daigaku Kenkyu Hokoku,* (60):25 (1986).

176. Z. He, M. Yuan, X. Zhang, X. Wang, X. Jin, J. Huang, C. Li, and L. Wang, *Eur. Polym. J.,* 2:597 (1986).

177. T. Usami, Y. Gotoh, and S. Takayama, *Eur. Polym. J.,* 21:885 (1985).

178. X. Zhang, X. Wang, and Z. He, *Shiyou Huagong*, 15:349 (1986).

179. E. P. Piskareva and G. G. Kartasheva, *Kauch. Rezina*, (1):27 (1988).

180. R. C. Jordan, S. F. Silver, R. D. Sehon, and R. J. Rivard, *ACS Symp. Ser.*, 2245:295 (1984).

181. L. P. Yu and J. E. Rollings, *J. Appl. Polym. Sci.*, 33:1909 (1987).

182. L. P. Yu and J. E. Rollings, *J. Appl. Polym. Sci.*, 35:1085 (1988).

183. P. Lang and W. Burchard, *Makromol. Chem., Rapid. Commun.*, 8:451 (1987).

184. B. L. Neff and J. R. Overton, *Polym. Prepr. (Am. Chem. Soc., Div. Polym. Chem.),* 23(2):130 (1982).

185. S. W. Dean and J. E. Rolling, *Biotechnol. Tech.*, 3:161-185 (1989).

186. H. H. Stuting and I. S. Krull, *J. Chromatogr.*, 539:91 (1991).

187. H. H. Stuting and I. S. Krull, *Anal. Chem.*, 62:2107 (1990).

188. R. Mhatre, I. S. Krull, and H. H. Stuting, *J. Chromatogr.*, 502:21 (1990).

189. W. Flapper, P. J. M. Van den Oetelaar, C. P. M. Breed, J. Steenbergen, and H. J. Hoenders, *Clin. Chem.* (Winston-Salem, NC), 32:363 (1986).

190. T. Takagi, Proc. 30th Colog. Proteides Biol. Fluids (Brussels, 1982), H. Peeters (ed.), Pergamon Press, Oxford, 1982; pp. 701–704.

191. T. Takagi, *Tanpakushitsu Kakusan Koso*, 27:1526 (1982).

192. T. Takagi and S. J. Hizukuri, *Biochem. (Tokyo)*, 95:1459 (1984).

193. T. Takagi, *Prog. HPLC*, 1(Gel Permeation Ion-Exch. Chromatogr. Proteins Pept): 27 (1985).

194. T. Takagi, S. Maezawa, and Y. J. Hayashi, *Biochem. (Tokyo)*, 101:805 (1987).

195. A. Kato and T. Takagi, *J. Agric. Food Chem.*, 35:633 (1987).

196. J. G. Bindels, B. M. DeMan, and H. J. Hoenders, *J. Chromatogr.*, 252:255 (1982).

197. J. G. Bindels and H. J. Hoenders, *Chromatographia*, 15:475 (1982).

198. J. G. Bindels, B. M. De Man, H. Bloemendal, and H. J. Hoenders, *Lens. Res.*, 1:89 (1983).

199. K. Kameyama, T. Nakae, and T. Takagi, *Biochim. Biophys. Acta*, 706:19 (1982).

200. S. Maezawa and T. Takagi, *J. Chromatogr.*, 280:124 (1983).

201. J. G. Bindels and H. J. Hoenders, *J. Chromatogr.*, 261:381 (1983).

202. J. G. Bindels, G. J. J. Bessems, B. M. De Man, and H. J. Hoenders, *Comp. Biochem. Physiol. B*, 76B:47 (1983).

203. Y. Hayashi, H. Matsui, and T. Takagi, *Methods Enzymol.*, 172(Biomembranes, Pt. S):514 (1989).

204. Y. Hayashi, K. Mimura, H. Matsui, and T. Takagi, *Biochim. Biophys. Acta*, 983:217 (1989).

205. S. Maezawa, Y. Hayashi, T. Nakae, J. Ishii, K. Kameyama, and T. Takagi, *Biochim. Biophys. Acta*, 747:291 (1983).

206. T. Fujitani, G. Maeki, and T. Nakao, *Kenkyu Nenpo-Tokyo-toritsu Eisei Kenkyusho*, 34:406 (1983).

207. T. Nakao, T. Ohno-Fujitani, and M. J. Nakao, *Biochem.* (Tokyo), 94:689 (1983).

208. Y. Hayashi, T. Takagi, S. Maezawa, and H. Matsui, *Biochim. Biophys. Acta*, 748:153 (1983).

209. T. Nicolai, L. Van Dijk, J. A. A. P. Van Dijk, and J. A. M. Smit, *J. Chromatogr.*, 389:286 (1987).

210. J. N. Ishii, T. Takagi, K. Kameyanna, and T. Nakae, *J. Exp. Clin. Med.*, 7(supplement):157 (1982).

211. H. H. Stuting, I. S. Krull, R. Mhatre, S. C. Krzysko, and H. G. Barth, LC-GC, 7:402 (1989).

212. I. S. Krull, H. H. Stuting, and S. C. Krzysko, *J. Chromatogr.*, 442:29 (1988).

213. G. Dollinger, B. Cunico, M. Kunitani, D. Johnson, and R. Jones, *J. Chromatogr.*, 592:215 (1992).

214. C. Jackson, L. M. Nilsson, and P. J. Wyatt, *J. Appl. Polym. Sci., Appl. Polym. Symp.*, 45(Polym. Anal. Charact., 2):191 (1990).

215. S. H. Kim, P. M. Cotts, and W. Volksen, *J. Polym. Sci., Part B, Polym Phys.,* 30:177 (1992).

216. C. Johann and P. Kilz, *J. Appl. Polym. Sci., Polym. Symp.* 48 (Polym. Anal. Charact., 3):111 (1991).

217. J. Lesec and G. Volet, *J. Appl. Polym. Sci., Appl. Polym. Symp.,* 45*(Polym. Anal. Charact.,* 2):177 (1990).

218. J. Lesec and G. Volet, *J. Liq. Chromatogr.,* 13:831 (1990).

219. B. Tinland, J. Mazet, and M. Rinaudo, *Makromol. Chem., Rapid Commun.,* 9:69 (1988).

220. C. Jackson, H. G. Barth, and W. W. Yau, *Proc. Int. Gel Permeation Chromatography Symposium 1991,* San Francisco, 1993, p. 751.

5
Determination of Molecular Weight Distributions of Copolymers by Size Exclusion Chromatography

Alfred Rudin University of Waterloo, Waterloo, Ontario, Canada

Size exclusion chromatography (SEC) of copolymers can be particularly complicated, compared with that of homopolymers. The special problems in analyses of copolymers apply also to mixtures of materials. Because SEC always produces numerical results, it is important that those who generate and use such information be aware of instances in which the analytical results may be compromised by the chemical heterogeneity of the sample.

In this chapter, we first review the particular difficulties that copolymers may present in SEC analyses and then summarize various solutions that have been proposed to these problems.

Universal Calibration

To illustrate these points, consider the raw data from a SEC experiment expressed in the form of a chart record, as in Figure 1. For present purposes, we confine our attention to a technique employing universal calibration. Consideration is given here to variations in the method in which the molecular weights of the eluting species are measured by such devices as a low-angle laser lightscattering (LALLS) photometer or a continuos viscometer (CV). In the simplest mode of operation, universal calibration, the *y* axis of the chart represents the

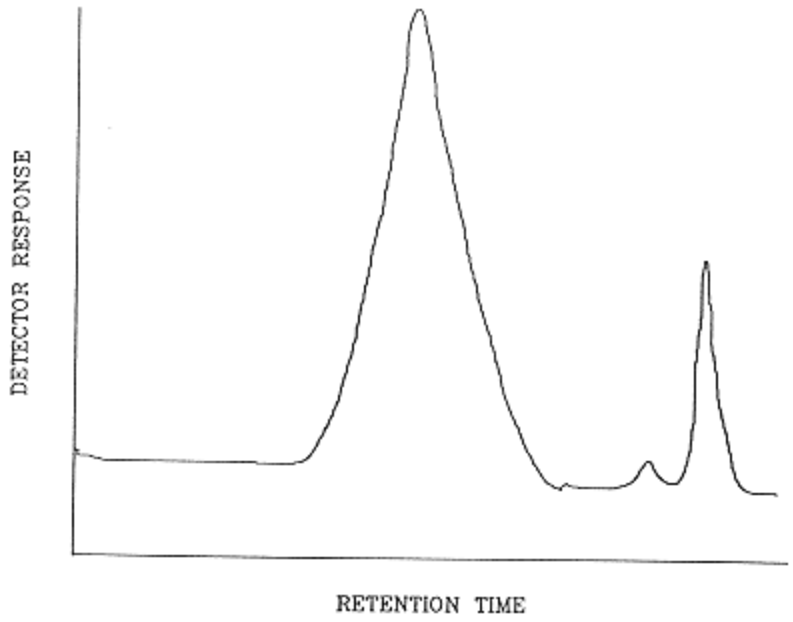

Figure 1.
Typical SEC raw data.

relative concentrations of the eluting species in terms of detector response. Most such concentration detectors at present measure the differential refractive index (DRI) of the polymer solution. Others include fixed-wavelength infrared detectors, evaporative detectors, densimeters, and other devices. The DRI is by far the most common. The assumption implicit here is that the detector response is directly proportional to the mass concentration of the eluting species at a particular retention time (*x* axis variable).

This is a generally useful assumption for the DRI detector with homopolymers, provided the degree of polymerization exceeds a certain minimum value. In about the oligomer range of molecular sizes, the refractive index of a polymer solution decreases with diminishing polymer molecular weight (1). The minimum molecular weight for an effectively constant solution refractive index may be a function of the solvent as well as the polymer. For anionic polystyrenes, for example, solutions in toluene exhibit a reasonably constant specific refractive index increment (i.e., change in refractive index of solution per unit change in polymer solute concentration) at polystyrene molecular weights greater than about 20,000. Dichloroethane solutions are much more sensitive to polymer molecular weight in this region (2). As a result, in SEC analyses of homopoly-

mers, the DRI concentration detector tends to underestimate the relative importance of the low-molecular-weight tail of a broad distribution sample.

Other concentration detectors may be less prone to this error (3). The error mentioned here is real but is generally considered a weak effect. Analyses of compositionally heterogeneous samples introduce another, potentially more serious flaw into the application of a DRI detector to measure polymer concentration in the SEC eluant. This problem applies to copolymers in which the chemical composition is not uniform across the molecular weight distribution, as well as to mixtures of polymeric species in general. Depending on the particular composition, the DRI concentration detector may respond to chemical composition as well as to solute concentration. As a consequence, a normalized plot of mass fraction versus elution volume may be in error.

Even more serious problems are encountered in connection with the *x* axis, that is, retention time, in the raw SEC chromatogram. Retention times in SEC analyses are a function of hydrodynamic size of the eluting species in the analytical solvent. The sizes of the solvent-swollen polymer species in turn are a function of molecular size (which the SEC analysis attempts to determine), as well as the extent of swelling by the solvent. The latter effect depends on the thermodynamic interactions between the solute and solvent (4). Translation of the retention time (or elution volume) into molecular weight using the universal calibration method (5,6) requires knowledge of the Mark-Houwink constants of the particular copolymer. Such information is usually not available, although there are techniques for the fairly rapid determination of these parameters (e.g., Ref. 7). However, none of these methods are of any avail if the chemical composition of the materials to be analyzed is not uniform across the range of molecular sizes. In this case, polymer-solvent interactions can vary with solute size. This variation is generally unpredictable, a priori, and the universal calibration technique cannot be applied with any degree of certainty.

Direct Measurement of Polymer Molecular Weight

As an alternative to universal calibration, one can measure the molecular weight of the eluting species on-line using a detector that responds continuously to the size of the solute. The two most common detectors used for this purpose are the LALLS detector and the CV detector. Various designs of both detectors have been reported (8–14). It should be noted first that these detectors obviate the necessity for universal calibration to translate the SEC retention time into molecular weight, but they do not remove problems that may exist with regard to the response of the concentration detector, which, as mentioned, is usually a DRI or an infrared instrument.

We return now briefly to consideration of alternative concentration detectors that may be less sensitive to the chemical composition of the eluant than the two that were just mentioned. We then review the effects of polymer chemical heterogeneity on the responses of the CV and LALLS molecular weight detectors.

The so-called mass detector, which is more correctly termed an evaporative detector (15), has been reported to be less sensitive than the DRI to chemical composition and molecular weight (3). A disadvantage is its relative insensitivity at low solute concentrations. This can be overcome to some extent by increasing the polymer concentration in the injected sample, but such expedients should be adopted with great caution. Higher concentrations can produce other problems in the analysis (16).

A continuous densimeter can be used as a concentration detector (17,18). This detector has been shown to be less sensitive than a DRI chemical composition of styrene-methyl methacrylate copolymers (19). Present models appear to suffer from a lack of general sensitivity, however. Spectrophotometric detectors have also been employed as SEC concentration detectors. Such instruments may obviously be sensitive to the chemical composition of the eluant and cannot be generally useful as concentration detectors for compositionally heterogeneous materials. Mention is made later of specific uses for identification of the compositions of copolymers.

At the time of writing, SEC practitioners lack a concentration detector whose response is insensitive to composition of the eluting polymers but is adequately sensitive to concentration to provide good values for the low-concentration tails of the molecular weight distribution. Most analyses of copolymers are performed using a DRI concentration detector, with the pious hope (which may be true in many cases) that the resulting errors are not very serious. At the end of this chapter, mention is made of a technique that does not require the use of a concentration detector.

To keep matters in perspective, the reader is reminded that imperfections in concentration measurements with a DRI detector are a cause for concern only if the refractive index increment of the copolymer varies with composition. This is not a problem, for example, with copolymers of ethylene and 1-olefins or styrene and α-methylstyrene.

We have seen that universal calibration techniques are not generally applicable to chemically heterogeneous polymers. Direct measurement of the molecular weight of the eluting species with a LALLS detector may likewise provide misleading information. The basic equation relating scattered light intensity to polymer molecular weight is (20)

$$\frac{32\Pi^3 n_0^2 (dn/dc)^2}{3\lambda^4 L}\frac{c}{\tau} = \frac{1}{\overline{M}_w} + 2A_2 c \qquad (1)$$

Here n_0 is the refractive index of the solvent with light of wavelength λ, *dn/dc* is the specific refractive index of the polymer solution, which has concentration *c*, and *L* is Avogadro's number. A_2 is the second virial coefficient of the polymer solution. Because A_2 is a weakly inverse function of molecular weight, it can be set equal to zero without serious error. The measured turbidity τ is a function of the angle between the incident light and photomultiplier detector, but this dependence is effectively eliminated by using a laser light source at a very low angle to the detection direction. The concentration *c* at a particular retention time is derived from the output of the concentration detector, which is usually a differential refractometer, as mentioned. The only term in Equation (1) that need concern us here is $(dn/dc)^2$, in which the specific refractive index of the polymer solution enters as a squared term. It has long been known that measurement of the correct weight-average molecular weight $\overline{M}_w$ of a copolymer that is heterogeneous as to chemical composition can be obtained in principle by measuring scattered light intensity in at least three solvents that differ in refractive index (21–23). Evidently, use of these solvents is not a palatable procedure in SEC analyses. As a consequence, LALLS detection of absolute molecular weights is not valid for compositionally heterogeneous copolymers and mixtures. Even copolymers of styrene and butadiene, which are quite bland in terms of chemical heterogeneity, do not provide accurate $\overline{M}_w$ values from light-scattering measurements in a single solvent (2). As a general precaution, LALLS techniques should not be used with copolymers unless these materials are either chemically homogeneous (e.g., ethylene-vinyl acetate copolymers) or are such that *dn/dc* is insensitive to chemical composition (e.g., ethylene copolymers with other olefins).

Continuous viscometer detectors are not subject to the same limitation as LALLS instruments. The reasons for this are as follows. If one represents a polymer molecule in solution as an equivalent hydrodynamic sphere (4), then the intrinsic viscosity of the solution $[\eta]$ is defined according to the Einstein viscosity equation as

$$[\eta]M = 0.025LV_h \quad (2)$$

where *M* is the polymer molecular weight and V_h is the hydrodynamic volume of the dissolved polymer. [We note in passing that if the contents of the detector cell are heterogeneous with respect to molecular weight, then the *M* in Equation (2) is $\overline{M}_n$ of the mixture (24).] For present purposes, and in the usual practice, one takes the detector cell contents to be monodisperse. We have already mentioned that SEC separation is on the basis of hydrodynamic volume V_h and, this, then, is directly related to the product $[\eta]M$. The continuous viscometer detector measures $[\eta]$ directly. In practice, one usually calibrates the SEC columns using the CV detector and the familiar anionic polystyrene standards. The molecular weight of each standard polystyrene is known, and CV provides its intrinsic

viscosity [η]. Again, in normal practice, a concentration detector is needed together with the CV. The column calibration curve consists of corresponding [η]*M* and retention time values, if concentrations of the standards are not too high (25). When an unknown polymer or copolymer is analyzed, the CV again provides [η] values that can be related to *M* data from the calibration curve at the corresponding retention time. Thus the CV is generally applicable to direct measurement of the molecular weights of chemically heterogeneous polymers. As before, the relative concentrations of the measured various species may be compromised if the concentration detector responds to composition as well as to concentration. A method that may detect such problems is discussed next. This is a special case of the more general procedure described at the end of this chapter.

If one calibrates the SEC columns using the CV detector, it is possible to use this universal calibration relation and the CV detector to measure the number-average molecular weight of the polymer without reference to the DRI or other concentration detector. This method, which is due to Goldwasser (26), is based on the following identities:

$$\overline{M}_n = \frac{1}{\sum \frac{w_i}{M_i}} = \frac{\sum c_i}{\sum (c/M)_i} = \frac{\sum c_i}{\sum [(c/V_h)/[\eta]]_i} = \frac{\sum c_i}{\sum (c[\eta]/V_h)_i} \tag{3}$$

where w_i is the weight fraction of species *i* (with molecular weight M_i) in the polymer. This species exits from the SEC columns with concentration c_i and hydrodynamic volume V_{hi}. Its intrinsic viscosity is $[\eta]_i$. Now,

$$[\eta] = \frac{1}{c} \ln \frac{\eta}{\eta_0} = \frac{1}{c} \ln \eta_r \tag{4}$$

at infinite dilution (27); then,

$$\overline{M}_n = \frac{\sum c_i}{\sum (\ln \eta_r/V_h)_i} = \frac{sample\ amount}{\sum (\ln \eta_r/V_h)_i} \tag{5}$$

The CV measures the relative viscosity η_r at each slice of the SEC chromatogram, and $\overline{M}_n$ of the sample is obtained by dividing the known amount of sample injected by the sum of the quotients of η_r and the corresponding hydrodynamic volume. $\overline{M}_n$ obtained in this manner can be compared with the same average molecular weight from measurements by a CV and concentration detector. If the two disagree significantly, this is evidence that the concentration detector was affected by the heterogeneous chemical composition of the polymer sample. The Goldwasser procedure is impervious to the heterogeneity of the sample, but of course it provides only $\overline{M}_n$ not the molecular weight distribution. See later for

a description of a recent technique that generalizes this method, subject to certain assumptions.

A similar procedure can be employed with a LALLS detector to measure $\overline{M}_w$ of the whole sample without using a concentration detector (28,29), but this procedure is not applicable to mixtures or nonuniform copolymers for reasons already mentioned.

In many cases the analyst does not know *a priori* whether the particular polymer is compositionally uniform. Some information on this point can be obtained from a CV detector in-line with the SEC apparatus. As explained earlier, universal calibration with the CV and narrow molecular weight distribution polymers provides a relation between $[\eta]M$ and elution volume. The CV measures $[\eta]$ of the unknown polymer, from which M can be derived. A log-log plot of the measured values of $[\eta]$ versus the corresponding M data provides the parameters of the Mark-Houwink expression

$$[\eta] = KM^a \quad (6)$$

If the measured values do not fall on a straight line in such a plot, this is evidence that the solvent-polymer interactions are not uniform across the molecular weight distribution (30). One cause for this could be compositional heterogeneity of the sample.

The following procedure to reduce errors in measuring the molecular weights of heterogeneous samples can be used to advantage when a continuous viscometer detector is not available in-line for direct measurement of molecular weights of the eluting species. This yields a single average molecular weight, rather than the description of the entire molecular weight distribution that can be obtained from chemically homogeneous samples.

In the absence of on-line measurements of molecular weight, one relies on universal calibration. All species with the same hydrodynamic volume elute from the SEC columns with the same retention time. From Equations (1) and (6) it can readily be shown that the molecular weights of two polymers that have the same retention time are related by (5,20)

$$\ln M_2 = \frac{1 + a_1}{1 + a_2} \ln M_1 + \frac{1}{1 + a_2} \ln \frac{K_1}{K_2} \quad (7)$$

where the subscripts refer to polymer 2 (unknown) and polymer 1 (calibration standard) and a and K are the constants in the Mark-Houwink Equation (5).

The size of solvated polymer molecules and hence the Mark-Houwink constants (31) depend on solvent interactions with the various monomer residues in copolymers (6,32,33). In some cases, as when the copolymer structure tends toward alternation, the influence of hetero segments may predominate. As a consequence, the values of the Mark-Houwink constants are relatively insensitive to composition, within certain limits. When the copolymer composition

tends to be less uniform, however, or when the sample is a mixture of copolymers or homopolymers, the overall degree of solvation changes effectively with blend composition at a given molecular weight, and the use of a single set of Mark-Houwink constants produces false molecular weight parameters from SEC data.

Techniques Designed for Heterogeneous Polymer Samples

A new molecular weight average $\overline{M}_x$ has been proposed to characterize polymer samples of heterogeneous composition by SEC (34) when a single set of Mark-Houwink constants is unsatisfactory. $\overline{M}_x$, the hydrodynamic volume average, is defined according to

$$\overline{M}_x = \frac{\sum w_i[\eta]_i M_i}{\sum w_i[\eta]_i} = \frac{\sum w_i[\eta]_i M_i}{[\eta]} \quad (8)$$

where w_i and $[\eta]_i$ are the weight fraction and intrinsic viscosity, respectively, of all species that exit the SEC columns with elution volume Ve_i. The denominator in Equation (8) is equal to the intrinsic viscosity $[\eta]$ of the whole sample in the gel permeation chromatography (GPC) solvent. This parameter can be measured separately and off-line. The values in the numerator are available from the SEC chromatogram. At infinite dilution of the species in the sample, the product $[\eta]_i M_i$ can be read directly from the universal calibration curve and w_i is equated to the ratio of the area of the SEC detector response at elution volume Ve_i to the total area under the chromatogram. This molecular weight average is particularly useful for mixtures of homopolymers or for copolymers in which composition may vary with molecular weight.

The value of $\overline{M}_x$ falls between $\overline{M}_w$ and $\overline{M}_n$ of the sample. Substitution of Equation (6) into Equation (8) gives

$$\overline{M}_x = \frac{\sum w_i K M_i^{a+1}}{\sum w_i K M_i^a} = \frac{\sum w_i M_i^{a+1}}{\sum w_i M_i^a} \quad (9)$$

When $a = 1$,

$$\overline{M}_x = \frac{\sum w_i M_i^2}{\sum w_i M_i} = \overline{M}_z \quad (10)$$

and when $a = 0$,

$$\overline{M}_x = \frac{\sum w_i M_i}{\sum w_i} = \overline{M}_w \quad (11)$$

For most random coil polymers in the relatively nonpolar solvents that are commonly used, $0.5 \leq a \leq 0.8$ (31) and $\overline{M}_z < \overline{M}_v < \overline{M}_n$. Because of its dependence on the Mark-Houwink exponent a, $\overline{M}_v$ of a homopolymer will be somewhat solvent dependent. The more familiar $\overline{M}_v$ also exhibits some solvent dependence, for similar reasons.

Some of the difficulties mentioned in analyses of nonuniform copolymers can be circumvented by use of the $\overline{M}_z$ average, which can be estimated from the GPC chromatogram and the intrinsic viscosity of the polymer without calibration for their components. It may be useful when $\overline{M}_z$ is used to characterize a copolymer or polymer blend that both the parameters $\overline{J}_w$, which is proportional to the weight-average hydrodynamic volume of the sample, and the standard deviation σ_J should also be reported:

$$\overline{J}_w = \sum w_i[\eta]_i M_i \quad (12)$$

$$\sigma_J = \left[\sum w_i (J_i - \overline{J}_w)^2\right]^{1/2} \quad (13)$$

where $J_i = [\eta]_i M_i$. This procedure provides a molecular weight average to characterize the sample and a measure of the mean and breadth of the distribution of hydrodynamic volumes in the sample.

It is evident from Equation (7) that application of universal calibration procedures to copolymers requires knowledge of the Mark-Houwink constants of the copolymers. Runyon and coworkers (35) and Chang (36) suggested methods for the calculation of molecular weight distributions of copolymers from SEC data. These require the calibration curves or Mark-Houwink constants of the constituent homopolymers and knowledge of the copolymer composition. Gold-wasser and Rudin (37) suggested the following procedure, which is equivalent in application to an extension of Chang's hypothesis.

The procedure entails calculation of the copolymer Mark-Houwink constants from knowledge of the copolymer composition and the Mark-Houwink constants of the contributing segments. It can be shown (37) that the hydrodynamic volume of a polymer coil is given by

$$V_h = \frac{4\pi}{3\phi''}\left\{\sum w_i[K_i M_c^{[(a_i+1)]}]^{2/3}\right\}^{3/2} \quad (14)$$

where ϕ'' is Flory's (4,31,37) universal constant [which may be taken = 6.3067×10^{24} (cgs units) for present purposes], w is a weight fraction, the subscript i refers to any identified group of monomer units, K and a are the corresponding Mark-Houwink constants [Equation (6)], and M_c is the molecular weight of the entire polymer chain.

For an A-B block copolymer, there can be only two segments, poly-A and poly-B, and the influence of A-B units can be taken to be minimal (6) and may

be ignored. For statistical copolymers, however, one must take account of A-B heterointeractions, which have been noted to contribute to coil size (6,38). Hence three segments would be included in the calculation: poly-A, poly-B, and A-B units.

The application of Equation (13) to block copolymers is relatively simple if the copolymer composition is known. It is more difficult with statistical copolymers, however.

The fractions of homo- and heterodiads may be calculated from the reactivity ratios and feed composition assuming a simple copolymer (39) or other copolymerization model (40). It is still necessary to estimate Mark-Houwink constants for the hetero segments. A method has been suggested for this (37), but the entire procedure is quite tedious and is unlikely to be applied unless there is a need for many analyses of a particular copolymer.

We turn now to a recent method for SEC analysis of nonhomogeneous polymers using an on-line viscometer, without a concentration detector (41). This evidently applies also to copolymers with nonhomogeneous chemical compositions. The method is a generalization of the Goldwasser technique (26) for $\overline{M}_n$ determinations, which was mentioned earlier. To wring more information from the SEC chromatogram one must make certain assumptions, of course. In this case, a general distribution shape is assumed and fit to the chromatogram data. The result is a number of estimated molecular weight averages rather than an independently measured molecular weight distribution. Nevertheless, the procedure appears to be quite robust, not subject to the potential errors mentioned earlier in analyses of nonhomogeneous samples.

Readers are referred to the original source (41) for details of the method. In essence, the CV is used alone to determine a “viscosity distribution” of the polymer in terms of corresponding molecular weight times intrinsic viscosity $w_i[\eta]_i$ and $M_i[\eta]_i$ values. The latter product is related directly to hydrodynamic volume [Equation (2)] and is obtained from a “universal” calibration with standard polymers, using the CV. The intrinsic viscosity [η] and $\overline{M}_n$ can be obtained directly from the viscosity distribution, outlined earlier, in connection with Equation (3). Now, a Mark-Houwink exponent [Equation (6)] can be approximated. The ratio $\overline{M}_w$ n can then be estimated from the viscosity distribution when the molecular weight distribution is set equal to either a log normal or the even more widely applicable generalized exponential distribution. The parameters characteristic of either assumed molecular weight distribution are easily fit from the moments of viscosity distribution. Once this is done, all average molecular weights can be estimated in principle. Because of analytical uncertainties in the high-molecular-weight tails of the distributions of most synthetic polymers, however, it is wise to confine these estimates to $\overline{M}_n$, $\overline{M}_w$, and $\overline{M}_n$ (42,43). This method is not very sensitive to the choice of the value of the Mark-Houwink exponent

and is believed to be potentially useful in the case of nonhomogeneous copolymers, because any errors in concentration detection are avoided.

Considerable effort is being exerted currently to determine the compositional and molecular weight distributions of copolymers. The basic idea behind these techniques is fractionation of the copolymer by composition and subsequent measurement of molecular weight distributions of chemically uniform fractions by SEC. The problems with SEC characterizations that have been mentioned are circumvented if the samples are indeed compositionally uniform.

A number of studies have also been made in which SEC is used for the first separation and the chemical composition of the various SEC fractions is then analyzed. It should be remembered that SEC separations provide samples that are uniform in hydrodynamic volume, barring side effects. These may not necessarily have the same molecular weight. The first procedure mentioned is therefore probably preferable.

Details of the techniques that have been applied here are beyond the scope of this chapter. Suffice it to say that the most promising current method to measure chemical and molecular weight distributions of copolymers is SEC followed by gradient high-performance liquid chromatography (44,45).

The need for augmentation of molecular weight distribution data with composition properties is particularly strong with ethylene-olefin copolymers. It is well known that branching (i.e., olefin comonomer) distribution differences can produce very significant differences between different polymers with practically identical molecular weight distributions (46). In such cases, temperature rising elution fractionation (47,48) is used to fractionate such materials according to their branch contents, and these fractions are characterized for molecular weight by SEC.

There are many reports in the literature in which chemical and molecular weight distributions have been estimated concurrently by employing multiple detectors to sense the SEC eluant. An example is the use of an ultraviolet detector, which is sensitive to the residues of monomers like styrene but does not “see” acrylate or methacrylate monomer residues. For reasons already discussed, the success of such analyses depends on whether the SEC separation has actually been on the basis of molecular weight and whether the relative concentrations of the eluting species were measured independently of possible variations in their compositions. This probably varies from case to case.

References

1. M. B. Huglin, Light Scattering from Polymer Solutions, Academic Press, Orlando, FL, 1972, Chapter 6.

2. T. C. Chau and A. Rudin, Polymer (London), *15*, 593 (1974).

3. S. S. Huang and H. G. Barth, SPE ANTEC, *31*, 277 (1985).

4. P. J. Flory, Principles of Polymer Chemistry, Cornell University Press, Ithaca, NY, 1953.

5. Z. Grubisic, P. Rempp, and H. Benoit, J. Polym. Sci. Part B, *5*, 753 (1967).

6. A. Dondos, P. Rempp, and H. Benoit, Makromol. Chem., *175*, 1659 (1974).

7. C. J. B. Dobbin, A. Rudin, and M. F. Tchir, J. Appl. Polym. Sci., *25*, 2985 (1980); *27*, 1081 (1982).

8. A. C. Ouano and W. Kaye, J. Polym. Sci., Polym. Chem. Ed., *12*, 1151 (1974).

9. P. J. Wyatt, I. Izisel, R. G. Park, and G. K. Wyatt, Int. GPC Sympos., 1987, Waters Chromatography Div., Milford MA, 1987, p. 168.

10. A. C. Ouano, J. Polym. Sci. Part A-1, *10*, 2169 (1972).

11. D. Lecacheux, J. Lesec, and C. Quivoron, J. Liq. Chromatogr., *3*, 427 (1980).

12. F. B. Malihi, C. Kuo, M. E. Koehler, T. Provder, and A. F. Kah, ACS Symp. Ser., *245*, 281 (1984).

13. M. A. Haney, J. Appl. Polym. Sci., *30*, 3037 (1985).

14. W. W. Yau, S. D. Abbott, G. A. Smith, and M. Y. Keating, ACS Symp. Ser., *352*, 80 (1987).

15. D. L. Ford and W. Kennard, J. Oil Colour Chem. Assoc., *49*, 299 (1966).

16. W. L. Elsdon, J. M. Goldwasser, and A. Rudin, J. Polym. Sci. Part B, *19*, 483 (1981).

17. O. Kratky, H. Leopold, and H. Stalinger, Angew. Phys., *27*, 273 (1969).

18. B. Trathnig and C. Jorde, J. Chromatogr., *24*, 147 (1982).

19. W. L. Elsdon, J. M. Goldwasser, and A. Rudin, J. Polym. Sci., Polym. Chem. Ed., *20*, 3271 (1982).

20. A. Rudin, The Elements of Polymer Science and Engineering, Academic Press, Orlando, FL, 1982.

21. W. H. Stockmayer, L. D. Moore, Jr., M. Fixman, and B. N. Epstein, J. Polym. Sci., *16*, 517 (1955).

22. W. Bushuk and H. Benoit, Can. J. Chem., *36*, 1616 (1958).

23. H. Benoit and D. Froelich, in Light Scattering from Polymer Solutions, Academic Press, Orlando, FL, 1972.

24. A. E. Hamielec, A. C. Ouano, and L. L. Nebenzahl, J. Liq. Chromatogr., *1*, 527 (1978).

25. H. K. Mahabadi and A. Rudin, Polym. J., *11*, 123 (1979).

26. J. M. Goldwasser, Int. GPC Symp., Waters Chromatogr. Div., Newton MA, 1989, p. 150.

27. E. O. Kraemer, Ind. Eng. Chem., *30*, 1200 (1938).

28. O. Prochaska and P. Kratochvil, J. Appl. Polym. Sci., *31*, 919 (1986).

29. S. Pang and A. Rudin, J. Appl. Polym. Sci., *46*, 263 (1992).

30. S. Pang and A. Rudin, Polymer (London), *33*, 1949 (1992).

31. P. J. Flory and T. G. Fox, J. Am. Chem. Soc., *73*, 1904 (1951).

32. T. Kotaka, Y. Murakami, and H. Inogaki, J. Phys. Chem., *72*, 829 (1968).

33. A. Dondos and H. Benoit, Makromol. Chem., *118*, 165 (1968).

34. J. M. Goldwasser, A. Rudin, and W. L. Elsdon, J. Liq. Chromatogr., *5*, 2253 (1982).

35. J. R. Runyon, D. E. Barnes, J. F. Rudd, and L. H. Tung, J. Appl. Polym. Sci., *13*, 2359 (1969).

36. F. S. C. Chang, J. Chromatogr., *55*, 56 (1971).

37. J. M. Goldwasser and A. Rudin, J. Liq. Chromatogr., *6*, 2433 (1983).

38. T. Kotaka, T. Tanaka, H. Onhumi, Y. Murakami, and H. Inagaki, Polym. J., *1*, 245 (1970).

39. F. R. Mayo and F. M. Lewis, J. Am. Chem. Soc., *66*, 1594 (1944).

40. A. Rudin, K. F. O'Driscoll, and M. S. Rumack, Polymer, *22*, 740 (1981).

41. R. A. Sanayei, K. G. Suddaby, and A. Rudin, Makromol. Chem., *194*, 1953 (1993).

42. W. J. Tchir, A. Rudin, and C. A. Fyfe, J. Polym. Sci., Polym. Phys. Ed., *20*, 1443 (1982).

43. S. T. Balke, Quantitative Column Liquid Chromatography, Elsevier, Amsterdam, 1984.

44. S. Teramichi, Y. Hasegawa, K. Shigekuni, K. Zenta, and M. Hashimoto, Appl. Polym. Symp., *45*, 87 (1990).

45. G. Glockner, M. Stickler, and W. Sunderlich, Anal. Chem., *328*, 76 (1987).

46. E. Karbashewski, A. Rudin, L. Kale, W. J. Tchir, and H. P. Schreiber, Polym. Eng. Sci., *31*, 1581 (1991).

47. L. Wild, T. R. Ryle, D. C. Knobeloch, and I. R. Peat, Am. Chem. Soc. Div. Polym. Chem. Polym. Prepr., *18*, 182 (1977).

48. M. G. Pigeon and A. Rudin, J. Appl. Polym. Sci., *51*, 303 (1994).

6
Size Exclusion Chromatography of Polyamides, Polyesters, and Fluoropolymers

Paul J. Wang 3M Center, St. Paul, Minnesota

Introduction

Size exclusion chromatography (SEC) of semicrystalline polyamides, polyesters with high melting point, and certain fluoropolymers is reviewed in this chapter. Because of their semicrystalline nature, polyamides are hard to dissolve in common chromatographic solvents. The SEC of nylons, or different types of polyamides with strong intermolecular H bonding, is reviewed based on the types of solvents in which they are soluble. These solvents are high-temperature *m*-cresol (neat or blended with other solvents), certain common solvents after trifluoroacetylation of the polymers, and fluorocarbon solvents, such as trifluoroethanol and hexafluoroisopropanol. The merits and limitations of each solvent systems are discussed here.

Semicrystalline polyesters usually have an aromatic ring in the repeating unit, causing high crystalline melting temperatures that hinder solubility in common solvents. To destroy crystallinity in the polymer, the high-temperature solvents *m*-cresol, *o*-chlorophenol/chloroform, and nitrobenzene/tetrachloroethane must be used. An alternative room temperature solvent is the polar hexafluoroisopropanol or blends.

Only those fluoropolymers that are soluble in uncommon solvents are reviewed here. One of these is perfluoroether polymer, which can be chromatographed in 1,1,2-trichloro-1,2,2-trifluoroethane (Freon 113). SEC of poly(bistrifluoroethoxyphosphazenes) was successfully conducted in cyclohexanone in the presence of tetrabutylammonium nitrate (TBAN). Polytrifluorochloroethy-

lene or Kel-F resin, because of its superior vapor barrier properties, has gained renewed interest recently. This polymer can be converted to tetrahydrofuran (THF)-soluble polytrifluoroethylene by reacting with tri-*n*-butyltin hydride and then chromatographed in common THF.

SEC of Polyamides

Because of their high melting temperatures (for example, 265°C for nylon 6,6) and strong intermolecular H bonding interactions between amide linkages, nylons have an excellent combination of high strength, flexibility, toughness, abrasion resistance, dyeability, low creep, and resistance to solvents. Based on chemical structure, nylons are characterized by their crystalline amide linkages and may be classified into two categories:

1. Aliphatic polyamides

2. Aromatic polyamides

Aliphatic polyamides generally fall into two types:

1. Nylon 4,6, nylon 6,6, nylon 6,9, nylon 6,10, and nylon 6,12

2. Nylon 6, nylon 11, and nylon 12

Class 1 nylons are usually polymerized from a stoichiometrically balanced condensation reaction of a diacid with a diamine. Nylon 6,6 is the most common and is used in fiber, specialty plastic, and electrical applications. Class 2 nylons are usually synthesized from the ring-opening polymerization of cyclic amides or lactams. For instance, nylon 6 is polymerized from ϵ-caprolactam. Cyclic aliphatic polyamides normally have better thermal stability than their linear counterparts.

Aromatic polyamides, depending on the position of the reactive site in the reactants, form polymers known as Nomex (flameproof protective clothing) or Kevlar (high fiber strength tire cord) (1).

The chemical structures of a few of the aforementioned nylons are as follows:

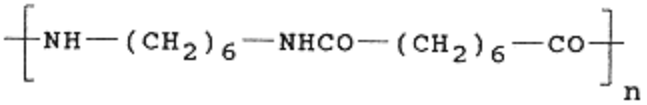

Nylon 6/6

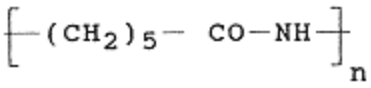

Nylon 6

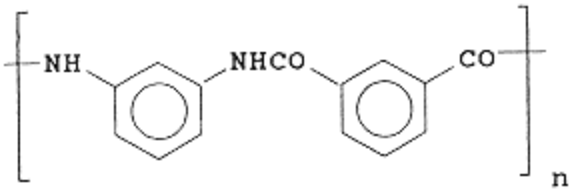

Nomex™

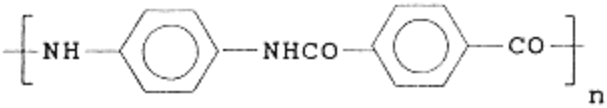

Kevlar™

For the molecular weight measurement of any polymers by SEC, the first requirement is that the polymers or its derivatives be soluble in a chromatographic solvent. Of the different types of nylons, only a few noncrystalline aliphatic polyamides are soluble in common solvents. The majorities of aliphatic polyamides, however, are soluble in common solvent only after trifluoroacetylation (2). A literature search did not find any work related to aromatic polyamides, and therefore they are not included here.

The solvent systems used for nylon SEC work fall into three categories (3):

1. High-temperature solvents, such as *m*-cresol at above 100°C, *m*-cresol/chlorobenzene at 43°C, *m*-cresol/chloroform at 25°C, and hexamethylphosphoramide (HMPA) at 105°C

2. Common solvent, such as THF, CH_2Cl_2, and CH_2Cl-CH_2Cl after reaction of the polymers with trifluoroacetylation (TFA)

3. Room temperature fluorocarbon-containing solvents, such as 2,2,2-trifluoroethanol (TFE) and hexafluoro-2-isopropanol (HFIP)

Each of these solvent systems has some drawbacks. For instance, *m*-cresol used at 130°C may cause polymer degradation; it also may be difficult to separate oligomers from additives (4). In the method of destroying the crystallinity of the polyamide with trifluoroacetic anhydride, Biagini et al. (5) reported significant differences in the molecular weight (MW) distribution of nylon 6 de-

pending on the degree of acetylation. When using trifluoroethanol as solvent, Wang and Rivard (6) observed the inability of this solvent to dissolve nylon 6,10, 6/12, 11, and 12. For HFIP, the high price of the solvent (>U.S.$1000 per liter) and low plate count for polystyrene-based columns (7) are the main reasons that chromatographers refrain from using it.

Other factors complicating the direct SEC analysis of nylons in fluorinated solvents are the selection of calibration standards and the polyelectrolyte effect (7) in fluorinated solvents. Another consideration is column durability under high-temperature conditions and in fluorinated solvents. Regarding commercial nylon standards, broad molecular weight nylon standards have only become available from American Polymer Standard Corporation (Mentor, Ohio) in the 1980s. A series of nylon 6,6 standards with molecular weight ranging from 27,000 to 110,000 is now obtainable from commercial suppliers.

Because the solubility of nylons is the key issue, we therefore review the literature based on the solvents in which the SEC work was done.

High-Temperature Solvents and Mixed Solvents

In the early 1970s, Dudley (8) quantitatively characterized nylon 6,6 of various dispersities using *m*-cresol at 130°C. A *Q* factor can be defined as the ratio of monomer molecular weight to its extended chain length, derived from bond length and valence angles or simply as molecular weight per angstrom. He validated the *Q* factor value of 13.9 by proving that nylon 6,6 molecules assume an extended chain configuration in *m*-cresol at 130°C by having the Mark-Houwink α value of 1.0. The limiting viscosity number and nylon fractions of known number-average M_n from osmometry were used to calculate the Mark-Houwink α value. After band broadening and viscous fingering correction, the calculated M_w from SEC showed good agreement with those determined from light scattering.

Possible degradation of nylons and the inconvenience of operation using *m*-cresol at high temperature led Ede (9) to reduce the operation temperature to 43°C by using equal volumes of chlorobenzene and *m*-cresol. The mixed solvent had to be distilled and corrected to the 50:50 vol/vol ratio for reuse. Benzoic acid (0.25% wt/wt) was required in the eluant to prevent adsorption. Although Ede claimed that good agreement was obtained between number-average MW determined by SEC and by end-group analysis, concern remains about the effect on the hydrodynamic volume of the nylon molecules of compositional changes in the mixed solvent. Other concerns raised by using a mixed solvent are whether the mobile phase composition is the same in the pore as in the stream, how much the refractive index sensitivity varies with mixed mobile-phase changes, and do the hydrodynamic volumes of calibration standards have the same degree of change as samples?

Pastuska and Just (10) used benzyl alcohol with a silica column but observed strong solvent-column H bonding interaction. To get around this interaction problem, Marot and Lesec (11) measured MW of nylon 6, 11, 12, and copolymers using a cross-linked polystyrene column in benzyl alcohol, polytetrahydrofuran standards, and dual detectors, that is, refractometer and on-line continuous viscometer. The MW results show excellent agreement with samples measured in HFIP via the static light-scattering method. The universal calibration method using polytetrahydrofuran as the column calibration standard was employed to obtain the true MW of these nylons. The column calibration standards for polystyrene and polyethylene oxide failed to give correct MW because of their interaction with packing. Addition of an infrared detector to the dual detection setup permitted the simultaneous study of copolymer composition (polyether-amide block copolymer synthesized from polyamide 12 and polytetramethylene glycol prepolymers) as a function of molecular weight.

Petit et al. (12) used hexamethylphosphoramide at 105°C for SEC work but gave no details on molecular weight accuracy. Panaris and Pallas (13) used HMPA at 85°C but gave no comparison between the nylon MW determined from polystyrene standards and a *Q* factor correction, and the MW determined by an absolute method. Goedhart et al. (14) reported frequent gelation of polyamides and column plugging in HMPA. In the Marot and Lesec (11) paper, however, examples were given using HMPA as the chromatographic solvent to compare with results with SEC in benzyl alcohol and with static light scattering in HFIP. It appeared that Marot and Lesec did not experience the same problem as described by Goedhart et al. when using HMPA as the SEC solvent.

Common Solvents After Trifluoroacetylation

In 1980, Jacobi et al. (15) used trifluoroacetic anhydride, $(CF_3CO)_2O$, to functionalize polyamides (replacing H in the amide group with CF_3CO) into polymers soluble in common solvents. Completion of the TFA reaction can be shown by the disappearance of N-H absorption (at 3300 and 3080 cm^{-1}) and the amide II band (at 1540 cm^{-1}) in the infrared. The authors claimed that no considerable amount of polymer degradation occurred by comparing IR spectra of the virgin polyamides to polyamides after trifluoroacetylation reaction and subsequent hydrolysis reaction. They cautioned, however, about avoiding the contact of TFA-polyamides with water, alcohols, or any other reagent able to cause scission of the $N\text{-}COCF_3$ bond. Several samples of TFA-polyamides were run using methylene chloride as the eluant with more sensitive UV detection and Styragel columns.

Regarding the trifluoroacetylation reaction, Biagini et al. (16) investigated the degree of substitution of TFA by titrating trifluoroacetic acid, a by-product formed during the functionalization reaction. It was found that a homogeneous

phase can be achieved after 90–95% conversion, which is independent of the MW of the starting materials. However, the reaction rate depends on the dimensions or mesh size of the polyamide. Evidence of degradation was found with a nylon 6 sample after TFA reaction, hydrolysis, and refunction cycle compared with simple trifluoroacetylation of the same polymer. It is speculated that strong trifluoroacetic acid may cause the degradation in the hydrolysis reaction. They also reported that universal calibration does not seem to be applicable to TFA-nylons because of high-polarity -$COCF_3$ side groups. Because of less bubble formation and low moisture sensitivity, 1,2-dichloroethane was used as the eluant in place of methylene chloride.

Roerdink and Warnier (17) characterized nylon 4,6 in *m*-cresol and in methylene chloride after TFA. Analysis in *m*-cresol was done at 110°C using two silanized Zorbax (DuPont) bimodal columns (PSM 60 and 1000 Å) with a refractive index (RI) detector, whereas the TFA-nylon work was performed using three micro-Styragel columns at 254 nm of ultraviolet (UV) detection. Good agreement was obtained between the MW determined by high-temperature SEC and light-scattering values. The calibration procedure was not mentioned at all in the article, however.

Weisskopf (18) studied MW of nylon 6 and Trogamid in THF after trifluoroacetylation using direct calibration with polydisperse standards and universal calibration methods. In the direct calibration method, the plot of log M_w versus peak maximum (V_{max}) led to the best results compared with M_w from light scattering and M_n from osmometry. The MW of TFA-nylon computed from universal calibration was higher; the same trend is observed with Trogamid. The interaction between the gel matrix and the polar TFA groups on nylon may be responsible for the discrepant universal calibration results.

Dark (4) found agreement between the SEC measurements of various nylons dissolved in *m*-cresol at 100°C with detection by differential refractive index and TFA-nylon in chloroform at room temperature with UV detector. The various nylons included nylon 6, 11, 6, 6, 6, 9, 6, 10, and 6, 12. The better reproducibility of weight-average MW of TFA-nylon (3–4%) than nylons in *m*-cresol (7–9%) was also reported.

Ogawa and Sakai (19) proved that trifluoroacetylated nylon 12 followed the universal calibration curve of polystyrene in dichloromethane. Fractions of nylon 12 were prepared by column elution using benzyl alcohol and decalin as the solvent/non-solvent pair. Weight-average and number-average MW of these fractions were determined by low-angle laser light-scattering and vapor-phase osmometry (VPO) in HFIP/toluene (2:8). The peak MW M_p of these fractions was calculated according to the equation

$$M_p = M_n D^{1/2}$$

where M_n is from VPO and D is equal to M_w/M_n (g/g). The M_w and M_n are

"polystyrene equivalent weight-average and number-average MW" calculated from SEC. The intrinsic viscosities were measured by a Ubbelohde viscometer. It was reported that TFA-nylon 12 solution is stable 48 h after preparation. The authors did not offer any explanation about the agreement of TFA-nylon 12 with universal calibration as opposed to the cases described by Biagini et al. (16) and Weisskopf (18).

Using RI and UV detectors, Ogawa and Sakai (20) were able to determine the compositional heterogeneity of certain copolymers: (1) nylon 12 and polytetramethylene ether glycol and (2) nylon 6 and natural rubber. Dichloromethane was employed as the eluant for copolymer 1, with a UV detector set at 230 nm, and 1,1,2,2-tetrachloroethane was used for copolymer 2 at 260 nm.

Room Temperature Fluorinated Solvents, Such as 2,2,2-trifluoroethanol and Hexafluoro-2-isopropanol

Because of their high polarity and hydrogen bonding, fluorinated solvents, such as TFE and HFIP, are able to dissolve crystalline nylons at ambient temperature. In 1971, Provder et al. (21) used TFE as the solvent and a secondary calibration method for nylon 6. The method employed a hydrodynamic volume calibration curve based on polystyrene in THF, along with an integral distribution curve for polymethyl methacrylate (PMMA) in THF and in TFE for the generation of a HDV calibration curve in TFE. PMMA is used as test polymer soluble in both THF and TFE. The integral distribution curves of elution volume for the test polymer were constructed for the transformation. The multistep whole-calibration generation method may be simplified now using commercially available PMMA narrow fractions, which unfortunately did not exist in 1971.

Wang and Rivard (6) used a mixed-bed styrene-based column interfaced with a Chromatix low-angle laser light-scattering (LALLS) detector and a refractive index detector for MW measurement of nylon 6, nylon 4,6, and nylon 6,6. The column was custom packed in a rather polar solvent acetone to prevent column voiding when using TFE as the solvent. A small amount of lithium bromide or sodium acetate was needed in the eluant to reduce column adsorption effects. Figure 1 shows the chromatogram of a commercial nylon 6,6 run in trifluoroethanol + 0.1% sodium acetate.

Recently, Veith and Cohen (3) analyzed nylon 6 in TFE using the universal calibration method and peak retention data from narrow PMMA fractions. Silanized silica columns obviate the solvent incompatibility problem of TFE with styrene-based packings and give reproducible results. The accuracy of the calculated nylon 6 molecular weights was cross-checked with an independent end-group analysis (for M_n) and intrinsic viscosity measurement (for M_v).

As mentioned previously, HFIP is expensive but appears to be a better solvent for different types of nylons than TFE. Drott (7) reported the use of

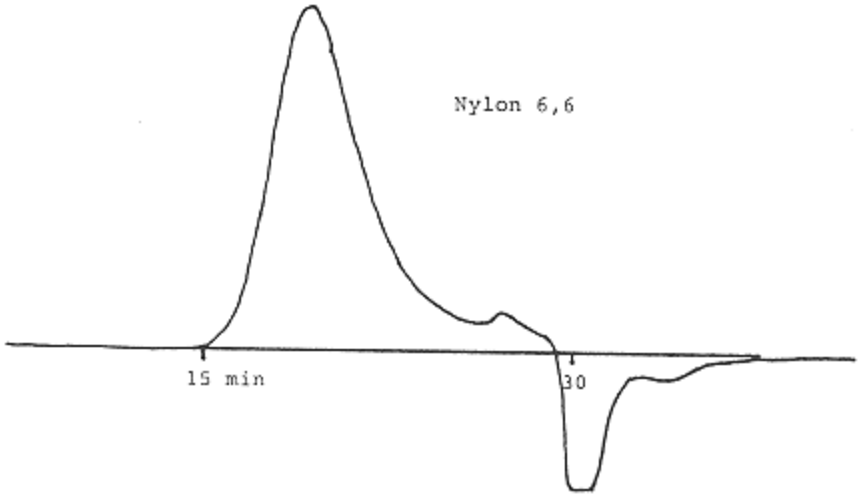

Figure 1.
Nylon 6,6 in trifluoroethanol eluant. Column, Jordi mixed bed; eluant, trifluoroethanol + 0.1% sodium acetate; flow rate, 1 ml/minute; detector, HP1037 A, RI.

HFIP for nylons and polyesters with DuPont porous glass columns and Water's μ-Styragel columns (10 μm beads). For μ-Styragel columns, column efficiency (1400 plates/column set) has remained stable for 2 years. No column stability problems were seen with glass columns, but the high-molecular-weight exclusion limit is lower than that for gel columns. In addition, sodium trifluoroacetate must be added to HFIP to suppress the polyelectrolyte effect of nylons. Strict exclusion of water is necessary to avoid the formation of corrosive products. Direct calibration was obtained by trial-and-error adjustment of the coefficients of a cubic polynomial equation until intrinsic viscosities for the samples calculated from SEC data (using the Mark-Houwink equation) agreed with experimentally measured values.

Schorn et al. (22) also proved that it is feasible to use HFIP with sodium trifluoroacetate, unmodified silica columns, and low-angle laser light-scattering detection for direct MW measurement of nylon 6. They also showed that spikes can be minimized in the LALLS signal by water exclusion, filtration, and a data-smoothing technique.

Ogawa et al. (23) used a HFIP/toluene (20:80) mixture as the eluant for nylon 12. Column fractionation of the same polymer was also performed using benzyl alcohol/decalin as the solvent/nonsolvent pair. They were able to demonstrate that in the HFIP/toluene mixture, polystyrene narrow standards and nylon 12 narrow fractions were in compliance with the universal calibration

curve. The same universal calibration curve was also followed for broad polystyrene and nylon 12 if $(M_n M_w)^{1/2}$ was used as the MW in the log MW (IV) expression. The M_w was the weight-average MW determined by LALLS, and the M_n was the number-average MW determined by vapor-phase osmometry.

Fractionations of nylon 12 by column fractionation and by preparative-scale SEC in HFIP/CF_3COONa and in HFIP/toluene (20:80) mixtures were carried out by Ogawa and Sakai (24). They found that SEC fractionation in HFIP/toluene (20:80) is more effective than in HFIP/CF_3COONa. Column fractionation using benzyl alcohol and decalin as the solvent/nonsolvent pair is more practical in producing large quantities of narrow fractions, however. Molecular weight characterization of the fractions was accomplished by analytical SEC in HFIP/toluene (20:80) and by static LALLS work in straight HFIP.

SEC of Polyester

Like their nylon counterparts, aromatic polyesters are polar polymers with relatively high crystalline melting points and are soluble in only two classes of solvents, high-temperature solvent blends and HFIP blends. The high-temperature solvents or blends are *m*-cresol, *o*-chlorophenol/chloroform, and nitrobenzene/tetrachloroethane. The fluorinated solvents or blends include HFIP, HFIP/methylene chloride (30:70), HFIP/pentafluorophenol, and HFIP/chloroform (1:9).

Polyethylene terephthalate (PET), known by the trade names Mylar, Dacron, and Terylene, has good mechanical strength up to 150–175°C as well as good chemical and solvent resistance. PET can be blended with cotton fiber to give better crease resistance, and it can also be used as tire cord, magnetic tape, and x-ray and photographic film, to name only a few applications. The structure is

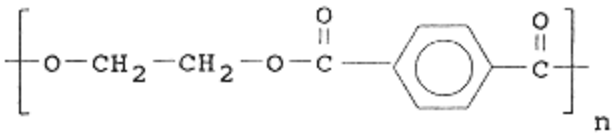

Poly(ethylene terephthalate)

Another group of polyesters soluble in chloroform are aliphatic polyesters and copolymers of aromatic polyesters. The incorporation of a comonomer serves to break the regularity of crystallinity, thus making aromatic polyester copolymers soluble in chloroform. In all the published work, only infrared detection was utilized in chloroform to monitor the ester carbonyl group. Birley et al. (25) employed SEC to identify oligomers prepared by the polyestification of terephthalic acid with excess 1,2-propylene glycol. Tymczynski and Sek (26)

used SEC to measure the molecular weight of an aromatic polyester copolymer, that is, poly-(4,4'-dihydroxyldinaphthyl-1,1'-terephthalate-bisphenol A terephthalate copolymer. For this copolymer, neither of the homopolymers is soluble in any known solvent. Polyethylene glycol sebacate, number-average MW less than 2500, was also characterized by Mori (27) using SEC after functionalizing of the polymer's end group. Polyesters with hydroxyl and carboxyl end groups were characterized at different infrared (IR) absorption wavelengths. In a recent publication, Xu et al. (28) cross-fractionated polyethylene terephthalate-tetramethylene ether copolymer. The individual fractions were then analyzed via SEC for compositional hetergeneities and MW distribution using dual detectors (RI and UV). Analogously, SEC analysis of aromatic polyesters is reviewed according to the classes of solvents in which they are soluble.

High-Temperature Solvent Blend

The *o*-chlorophenol/chloroform (25:75) solvent system was initially developed for PET by Screaton and Cullen (29) on a Waters 200 chromatograph and later reported in more detail by Jabarin and Balduff (30). The polymer solution was prepared by adding *o*-chlorophenol (OCP) to PET at 110°C with agitation until the polymer dissolved (10–30 minutes). The solution was then cooled to room temperature, at which time the chloroform was then added to make the final solution. SEC was run at ambient conditions with the mixed solvent. Using this system, Jabarin and Balduff were able to quantify the amount of cyclic trimer in PET.

There were no reported problems with baseline stability in these two articles. In practice, extreme difficulty with obtaining a stable baseline was experienced in our laboratory. Moreover, OCP is a brownish liquid containing tars that must be removed by distillation before use as SEC solvent. The solvent also has an excessively strong odor and is corrosive as well toward the instrument components. Therefore, the use of OCP/chloroform was abandoned and the method developed by Paschke et al. (31) was tried. Essentially, PET was run at room temperature in a mixed eluant of nitrobenzene (NB) and tetrachloroethane (TCE) at a ratio of 0.5 to 99.5%. The sample was first dissolved in nitrobenzene at 180°C and then quickly diluted with nearly boiling TCE to make a 1% solution. Paschke et al. showed that the sample preparation conditions did not degrade PET by comparing the inherent viscosity of the initial sample and that of the recovered PET. AT 3M, we also proved that the sample dissolution process did not degrade PET from the following two experimental approaches.

First, two noncrystalline PET samples, PE100 and PE200 from Aldrich Chemical, readily soluble in the mixed solvent without heating, were run under

the preceding conditions. Basically no difference was seen in MW between samples prepared with and without heating.

Second, another noncrystalline PET, a 80:20 mixture of terephthalate/isophthalate polymerized with ethylene glycol, was dissolved in ambient chloroform versus dissolved under the preceding condition. Identical results were obtained, further indicating that no degradation had occurred.

In the dissolution process, we found that some PET solutions remained clear for 2–3 days but became cloudy afterward. Recrystallization of the PET at ambient conditions was believed to be the cause. Reheating the solution to 145°C for 15 minutes clears it again.

Because only 0.5% NB is added in TCE, the baseline stability is excellent. Separation of cyclic trimer from major polymer also is good evidence. Although nitrobenzene is highly carcinogenic, good ventilation in the sample preparation area minimizes the hazard. Therefore, we think the NB/TCE is a practical way to measure MW of PET.

In the same article, Paschke et al. (31) also demonstrated that *m*-cresol at 130°C for 3 h degraded and narrowed the MW distribution of PET. The degradation was probably a result of the acid-catalyzed hydrolysis reaction.

Uglea et al. (32) fractionated polyethylene terephthalate-ethylene isophthalate copolymer with the coacervate extraction technique, that is, successive extractions of the precipitated polymer using a solvent/nonsolvent pair, with an increasing solvent amount in the next round of the extraction process. The fractioned samples were dissolved in phenol/TCE (3:2, wt/wt) at ambient, and the SEC was later run in TCE-nitrobenzene (95:5, vol/vol) at 100°C. Elevated temperature (100°C) was used, probably to increase the solubility of the copolymers in the eluant.

HFIP Blend

Slagowski et al. (33) demonstrated the feasibility of HFIP as the SEC eluant for several polytetramethylene terephthalate polymers. Because polystyrene is not soluble in HFIP, no MW values were reported. In the same year Drott (7) used HFIP as SEC solvent for both nylons and polyesters. A polyelectrolyte effect had been observed for nylons but it was not a problem for polyesters. Drott also indicated that no polymer degradation occurred in HFIP by comparing the intrinsic viscosities of the initial and recovered PET samples. The direct calibration method was used by trial-and-error adjustment of the coefficients of a cubic polynomial until intrinsic viscosities of the samples calculated from SEC data (using the Mark-Houwink equation) agreed with experimentally measured values.

Overton and Browning (34) used methylene chloride/HFIP (70:30) as the solvent in two DuPont Bimodal IIS columns. The advantage of this mixed solvent is that it is a solvent for polystyrene and it forms a low-boiling azeotrope. They observed faster dissolution of PET by this solvent blend than by straight HFIP and speculated that $MeCl_2$ swells the amorphous regions of PET, providing HFIP with easy access to the crystalline regions. A solvent system of $CHCl_3$/HFIP, with less HFIP content (9:1) was also used at 3M to analyze PET with UV detection.

A mixed solvent system of HFIP/pentafluorophenol was used by Berkowitz (35) to carry out SEC + LALLS work to obtain absolute MW of PET without using calibrant. By combining MW information and intrinsic viscosity measurement on several broad MW samples, the Mark-Houwink coefficients were determined.

Another way of using HFIP for polyester SEC work is to dissolve the polyester sample in 1 ml HFIP for 1 or 2 h and then add 9 ml chloroform to make the sample solution. SEC work can be carried out in chloroform. The polyester remains soluble in chloroform as long as it is rendered soluble in HFIP initially. With this method, much less expensive HFIP is required for each sample. Figure 2 shows the chromagram of a commercial crystalline polyester run in chloroform, with good resolution of cyclic trimer from the main polymer peak.

Miller et al. (36) studied the MW distribution of polycarbonates and aromatic polyesters blends using two solvents selectively. A blend of methylene chloride/HFIP (70:30) dissolves both polymers, but THF dissolves only polycarbonate. Separations were performed on a column set comprising a PL gel 5 μm mixed bed, a 100 Å column, and a 5 μm precolumn. Although these two polymers coeluted, use of a diode array UV detector set at 285 nm allowed detection of the polyester because absorption is 20 times greater for PET versus polycarbonate.

SEC of Fluoropolymers

There are numerous articles in the literature describing the synthesis and characterization of polymers with their main chains or side groups partially substituted by fluorine atoms. These low-fluorine polymers are usually soluble in common solvents and therefore are not included in this review. Only a few commercial fluoropolymers, which are soluble in uncommon solvents, are reviewed. These polymers include polyvinylidene fluoride, polyperfluoroethers, poly(bis-trifluoroethoxyphosphazenes), and polytrifluoroethylenes, and Kel-F polymer.

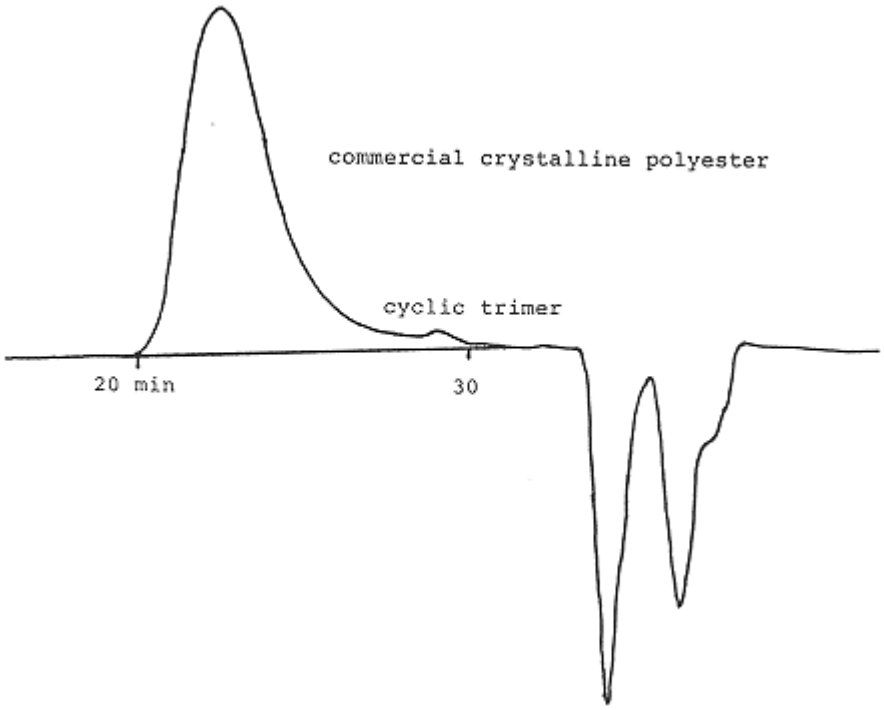

Figure 2.
Crystalline polyester dissolved in HFIP but run in chloroform.
Column, Jordi mixed bed + 100 Å; eluant, chloroform; flow rate,
1 ml/minute; detector, HP 1037 A.

Polyvinylidene fluoride is used extensively in the electronics industry because of its piezoelectric and pyroelectric properties. Only two room temperature solvents, *n*-methylpyrrolidone and dimethyl acetamide, have been found. Still-wagon (37) used *n*-methylpyrrolidone as the solvent for low-angle laser light-scattering measurement because of the larger refractive index increment value *(dn/dc)* in that solvent. No SEC work in these solvents was mentioned.

Polyperfluoroethers are viscous liquids with exceptional chemical and physical properties that are used widely in industry as lubricants, dielectric fluids, and, because of their high oxygen solubility, blood substitutes. There are two articles describing their MW measurement using 1,1,2-trichloro-1,2,2-trifluoroethane (Freon 113) as the solvent. Korus and Rosser (38) were able to use porous silica-packed columns and UV detection to separate five distinct peaks, which can be attributed to monomer, dimer, trimer, tetramer, and pentamer. Perfluo-

roether oligomers made in their laboratory provided a means of column calibration up to a MW of approximately 12,000.

Cantow et al. (39) also used a KMX-6 LALLS apparatus and six DuPont porous silica columns in Freon 113 to analyze a series of fractions from two structurally different types of perfluoroether polymers:

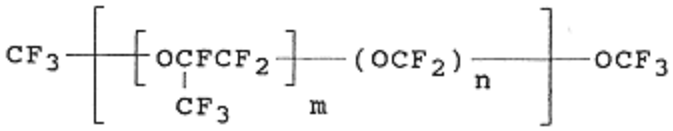

Fomblin Y

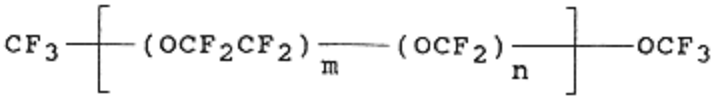

Fomblin Z

They experienced some difficulty in making LALLS measurement because of the chemical similarity of the solute and the solvent. They also found that *dn/dc* decreases with increasing MW as a result of an end-group effect in the low-MW chains. Molecular dimensions were determined in two ways. The first method involved measurement of limiting viscosity numbers and the application of a theory of the hydrodynamic properties of linear polymers in solution to calculate the root-mean-square (RMS) end-to-end distance of a molecule. The second method utilized the universal calibration principle by running a series of polystyrene standards in THF and perfluoroether polymers in Freon 113 using the same column set. The perfluoroether calibration is thus established from the RMS end-to-end distance of the standards. Molecular weights of perfluoroethers from 1000 to 9000 were measured.

In our laboratory at 3M, we similarily have tried to use silica columns to analyze perfluoroether polymers. Severe adsorption was observed, probably caused by extensive use of the column set for other polymers, which may have caused polymer-packing interactions. A styrene-based column custom packed by Jordi Associate was then used. To overcome the tendency of Freon 113 (poor solvent for polystyrene) to collapse styrene columns, the column was initially packed in a less swelling solvent, such as pentane. A void-free column was obtained after displacing pentane with Freon. Figure 3 shows the chromatogram

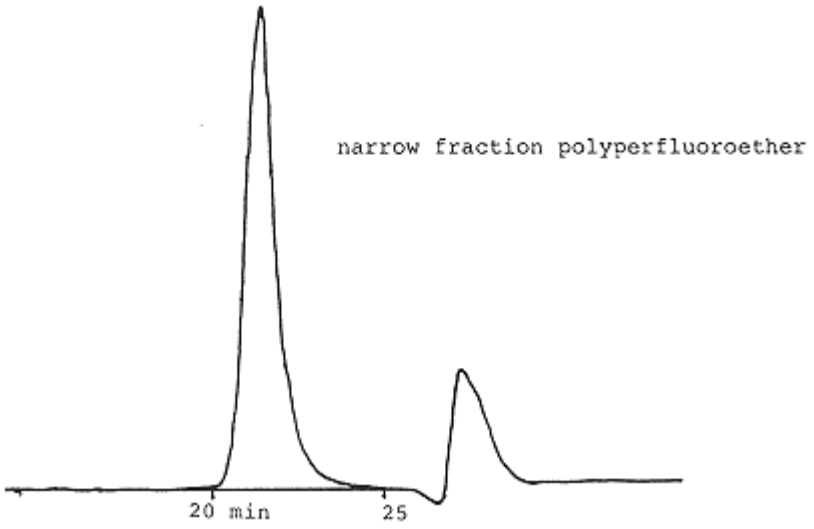

Figure 3.
Polyperfluoroether in Freon 113 eluant. Column, Jordi mixed bed; eluant, Freon 113; flow rate, 1 ml/minute; detector, HP 1037 A, RI.

of a narrow fraction polyperfluoroether in Freon 113 using a refractive index detector.

In recent years, the characterization of poly(bis-trifluoroethoxyphosphazenes),

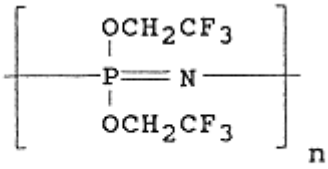

Poly[bis(trifluoroethoxy)phosphazene]

has gained increasing attention because of the commercial development of synthetic processes for noncrystalline longer chain fluorinated elastomers. Mourey et al. (40) examined the dilute solution viscosities of this polymer in acetone, THF, and cyclohexanone in the presence of tetrabutylammonium nitrate. Although THF and acetone are better solvents, a rather poor solvent, cyclohexane, was chosen as the SEC eluant. The better solvents were rejected, because for THF, the refractive index difference between polymer and solvent is too small, and for acetone, concentration-induced chain compression was observed down

to the concentration range of the injected samples. For the true MW measurement, LALLS and a differential viscometer were connected to SEC along with a concentration detector. Narrow MW polystyrene, polymethyl methacrylate, and polytetrahydrofuran gave a good universal calibration fit in cyclohexanone and 0.01 M TBAN. Poly(bis-trifluoroethoxyphosphazenes) was shown to have a bi-modal MW distribution with lower MW mode, possessing a different set of Mark-Houwink constants than the main, high-MW portion of the distribution.

Dejaeger et al. (41) used a styrene-based column in THF with the addition of LiBr to minimize the polyelectrolyte effect of polytrifluoroethyoxyphosphazenes. SEC interfaced with LALLS was also tried despite low detector response caused by a low *dn/dc* value. The authors also demonstrated that the polyphosphazene counterparts containing no fluorine, that is, polydiphenoxy- and polyaryloxyphosphazenes, follow the universal calibration concept despite their unique backbone structure.

Of all the polytrifluoroethylenes, polytrifluoro-chloroethylene, or Kel-F resin, which was invented in the early 1950s, has gained renewed interest because of its superior vapor barrier properties. Kaufman and Muthana (42) used chlorofluorobutane as solvent for membrane osmometry measurement of Kel-F with MW ranges between 56,000 and 100,000. In the following year, Hall (43) carried out light-scattering work on Kel-F using mesitylene but reported insufficient solubility of high-MW material in mesitylene. Initially we used mesitylene as the SEC solvent in styrene-based column but with no success. The injected Kel-F was adsorbed by the column and resulted in a delayed elution peak a few minutes after the solvent peak. Recently Cais and Kometani (44) indirectly measured MW of Kel-F via SEC by quantitative reductive dechlorination to polytrifluoroethylene. The Kel-F resin is suspended in THF with excess tri-*n*-butyltin hydride as the reductive agent. As the Kel-F is converted to polytrifluoroethylene, it becomes soluble in the THF. We used this method to analyze several Kel-F resins, the results correlating well with no strength temperature (NST) testing method. The NST test involves the preparation of a double V-notched molded specimen and the measurement of the temperature at which the specimen breaks with a given weight attached to one end.

Appendix: SEC Conditions

Polymer	Column	Mobile phase	Co
Nylon 6	Styragel	*m*-Cresol/chlorobenzene (1:1)	RI, operated at 4
Nylon 6	Styragel	2,2,2-Trifluorethanol	Secondary calibr
Nylon 6,6	Four columns	*m*-Cresol at 130 °C	Use PS calibratic corrections to ge
Nylon 6,6	μ-Styragel DuPont glass column	HFIP, ambient	Direct nylon cali fitting to match r
All commercial nylons	μ-Styragel	Methylene chloride UV above 300 nm	First article on tr
Nylon 6, oligomers high-MW gels	μ-Styragel	Dichloroethane after trifluoro-acetylation UV, 254 nm	Universal calibra NTFA nylon

(Table continued on next page)

(Table continued from previous page)

Appendix: SEC Conditions *(Continued)*

Polymer	Column	Mobile phase	
Nylon 6	Unmodified Si columns LiChrospher	HFIP + NaTFA	LALLS, s
Nylon 4,6	μ-Styragel	Dichloroethane after trifluoro-acetylation UV, 254 nm	Compares *m*-cresol
Nylon 12	Preparative ToyoSoda HMHG	GFIP and HFIP/toluene (2:8)	Efficiency LALLS ir
Nylon 12	Analytical GPC -ToyoSoda, GMHG	HFIP and HFIP/toluene (2:8), RI detector	Universal
Nylon 12, Nylon 6	Shodex AD -80/S	Methylene chloride and tetrachloroethane	UV and R
Nylon 6, aromatic; nylon 6,3, Trogamid	μ-Styragel	THF, UV	Direct cali
Nylon 6, 6/6, 6/9, 6/10, 6/12, 11	μ-Styragel	Chloroform 254 nm	TFA resul
Nylon 6, 4/6, 6/6	Jordi gel	Trifluoroethanol + LiBr	On-line L
Nylon 6, 11, 12	μ-Styragel	Benzyl alcohol at 135 °C Poly-THF standards	On-line vi

(table continued on next page)

(table continued from previous page)

Polymer	Column	Mobile phase	Comn
Nylon 12	Shodex AD-80/S	Methylene chloride RI and UV	Universal calibration TFA-nylon and polys
Nylon 6	Silanized Zobax bimodal	Trifluoroethanol	PMMA narrow standa calibration for true M
Polyethylene terephthalate	Styragel columns	Tetrachloroethane/nitrobenzene (99.5:0.5)	Gel permeation chron room temperature cor in nitrobenzene at 18(with boiling TCE
Polyethylene terephthalate	Styragel columns	*o*-Chlorophenol/chloroform at 25°C	RI, excessive odor an
Polyethylene terephthalate-ethylene isophthalate copolymer	Styragel columns	Tetrachloroethane/nitrobenzene (99.5:0.5) at 100°C	Samples dissolved in phenol/tetrachloroeth
Aliphatic polyester	Shodex A802	Chloroform with infrared detector	Oligomers with MW

Appendix: SEC Conditions *(Continued)*

Polymer	Column	Mobile phase	Com
Polyethylene terephthalate-polytetra-methylene ether copolymer	TSK 3000H, 4000H	Chloroform with infrared and UV detectors	Compositional heter distribution
Polytetra-methylene terephthalate	Styragel columns	HFIP with RI	Polystyrene standarc No reported MW
Polyethylene terephthalate	μ-Styragel DuPont glass column	HFIP, ambient	Direct PET calibrati match measured IV
Polyethylene terephthalate	DuPont bimodal IIs	Methylene chloride/HFIP (70:30)	Fast dissolution of F soluble in the mixed
Polyethylene terephthalate	DuPont SE columns	GPC + LALLS in HFIP + pentafluorophenol (50:50)	Determine Mark-Ho
Polyester/polycarbonate blend	PL gels	Methylene chloride/HFIP (70:30) and THF	Diode array UV at 2 when coeluting with
Polyvinylidene fluoride		Use *N*-methylpyrrolidone for LALLS	No GPC work

(table continued on next page)

(table continued from previous page)

Polymer	Column	Mobile phase	Com
Polyperfluoro ether	Silica columns	Use Freon 113 and UV	Resolve monomer, d and pentamer to MV
	DuPont silica columns	Freon 113, LALLS	Some difficulty witl *dn/dc;* use polystyre universal calibration
Poly(bis-trifluoro-ethoxyphosphozene	PL gels	Cyclohexanone + 0.01 M tetrabutyl ammonium nitrate LALLS and differential viscometer	Bimodal MW distrit PMMA, and poly-T
Poly(bis-trifluoroethoxy-phosphozene	Styrene columns	THF + LiBr, SEC/LALLS	Low LALLS respon universal calibration
Poly(trifluoroethystyrene)		THF after dechlorination	Dechlorination is th

References

1. G. Odian, *Principle of Polymerization*, John Wiley & Sons, New York, pp. 106, 152, 534.

2. K. Weisskopf and G. Meyerhoff, *Polymer 24,* 72 (1983).

3. C.A. Veith and R.E. Cohen, *Polymer 30,* 942 (1989).

4. W.A. Dark, in *Proceedings of the International GPC Symposium,* Chicago, May 11–13, 1987.

5. E. Biagini, E. Gattiglia, E. Pedemonte, and S. Russo, *Makromol. Chem. 184,* 1213 (1983).

6. P.J. Wang and R. Rivard, *J. Liq. Chromatogr. 10*(14), 3059 (1987).

7. E.E. Drott, in International Symposium on Liquid Chromatographic Analysis of Polymers and Plastics, 1977, pp. 41–50.

8. M.A. Dudley, *J. Apply. Polym. Sci. 16,* 493 (1972).

9. P.S. Ede, *J. Chromatogr. Sci. 9,* 275 (1971).

10. G. Pastuska and U. Just, *Ang. Makromol. Chem. 81,* 11 (1979).

11. G. Marot and J. Lesec, *J. Liq. Chromatogr. 11*(16), 3305 (1988).

12. D. Petit, R. Jerome, and P. Teyssie, *J. Polym Sci., Polym. Chem. Ed. 17,* 2903 (1979).

13. R. Panaris and G. Pallas, *J. Polym. Sci., Polym. Lett. 8,* 441 (1970).

14. D.J. Goedhart, J.B. Hussem, and B.P.M. Smeets, in *Liquid Chromatography of Polymers and Related Materials,* Vol. 13, Ed. by J. Cazes and X. Delaware, Marcel Dekker, New York, 1977, p. 203.

15. E. Jacobi, H. Schuttenberg, and R.C. Schulz, *Makromol. Chem., Rapid Commun. 1,* 397 (1980).

16. E. Biagini, E. Gattiglia, E. Pedemonte, and S. Russo, *Makromol. Chem. 184,* 1213 (1983).

17. E. Roerdink and J.M.M. Warnier, *Polymer 26,* 1582 (1985).

18. K. Weisskopf, *Polymer 26,* 1187 (1985).

19. T. Ogawa and M. Sakai, *J. Polym. Sci., Part A, Polym. Chem. 26,* 3141 (1988).

20. T. Ogawa and M. Sakai, *J. Liq. Chromatogr. 8*(6), 1025 (1985).

21. T. Provder, J.C. Woodbery, and J.H. Clark, *Separation Sci. 16,* 493 (1972).

22. H. Schorn, R. Kosfeld, and M. Hess, *J. Chromatogr. 282,* 579 (1983).

23. T. Ogawa, M. Sakai, and W. Ishtobi, *J. Polym. Sci., Poly. Chem. 24,* 109 (1985).

24. T. Ogawa and M. Sakai, *J. Polym. Sci., Poly. Chem. 23,* 1109 (1985).

25. A.W. Birley, J.V. Dawkins, and D. Kyriacos, *Polymer 21,* 631 (1980).

26. R. Tymczynski and D. Sek, Polish *J. Chem. 54,* 1815 (1980).

27. S. Mori, *Anal. Chim. Acta 17,* 189 (1986).

28. Z. Xu et al., *J. Appl. Polym. Sci. 37,* 3195 (1989).

29. R.M. Screaton and P.F. Cullen, in Molecular Weight Distribution of Polyethylene Terephthalate by GPC, GPC Symposium, 1976.

30. S.A. Jabarin and D.C. Balduff, *J. Liq. Chromatogr. 5,* 10 (1982).

31. E.E. Paschke, B.A. Bidlingmeyer, and J.G. Bergmann, *Polymer Prepr. 17,* 440 (1976).

32. C.V. Uglea, S. Aizicovici, and A. Mihaescu, *Eur. Polym. J. 21*(7), 677 (1985).

33. E.L. Slagowski, R.C. Gebauer, and G.J. Gaesser, *J. Appl. Polym. Sci. 21,* 2293 (1977).

34. J.R. Overton and H.L. Browning, Jr., *Org. Coat, Appl. Polym. Sci. Proc. 48,* 940 (1983).

35. S. Berkowitz, *J. Apply. Polym. Sci. 29,* 4353 (1984).

36. R.L. Miller, R.V. Brooks, and J.E. Briddell, *Polym. Eng. Sci. 59,* 30 (1990).

37. L.E. Stillwagon, *ASC Preprint, Div. Organic Coating,* 1983, p. 780.

38. R.A. Korus and R.W. Rosser, *Anal. Chem. 50*(2), 249 (1978).

39. M.J.R. Cantow, et al., *Makromol. Chem. 187,* 2475 (1986).

40. T.H. Mourey, S.M. Miller, W.T. Ferrar, and T.R. Molaire, *Macromolecules 22,* 4286 (1989).

41. R. De Jaeger, D. Lecacheux, and P. Potin, *J. Appl. Sci. 39,* 1793 (1990).

42. H.S. Kaufman and M.S. Muthana, *J. Polym. Sci.,* 251 (1950).

43. H.T. Hall, *J. Polym. Sci. 4,* 443 (1951).

44. R.E. Cais and J.M. Kometani, *Macromolecules 17,* 1932 (1984).

7
Size Exclusion Chromatography of Natural and Synthetic Rubber

Terutake Homma and Michiko Tazaki Kanagawa Institute of Technology, Atsugi, Japan

Introduction

In the early years of the rubber industry, only natural rubber was the material used for final products, and there was no need to know the molecular characteristics, such as average molecular weights and molecular weight distribution, precisely. However, since the introduction of various kinds of synthetic rubbers to the rubber industry, efforts have been devoted to understanding the correlations between their molecular weight characteristics and the physical properties and processability. Apart from this technological point of view, considering the reaction of the chemical modification of present rubbers or the synthesis of new rubbers, elucidation of the molecular characteristics is the first necessary step for development. Until the introduction of gel permeation chromatography (GPC) to the method of polymer characterization in 1964 by Moore (1), a tedious molecular weight fractionation method or ultracentrifugal analysis was employed for these measurements. However, since then, GPC has been recognized as an invaluable method for the study of the molecular characterization of rubbers. At present, the term “size exclusion chromatography” (SEC) is more frequently used than GPC, and this is becoming much more refined in both hardware and software, as described elsewhere.

It is always necessary to dissolve the rubber sample in SEC solvents before SEC analysis. Natural rubbers as well as many synthetic rubbers are mainly composed of diene and vinyl units and are in an amorphous solid state. Therefore, in general, no problems are encountered when performing SEC measure-

ments. Many data for SEC for rubbers have been obtained. In this chapter these data are listed in the Appendix to provide SEC experimental conditions, and some consideration is given here to the SEC analysis of rubbers.

Classification of Rubbers

In addition to natural rubber, today many synthetic rubbers are commercially available. Although there are several ways to classify these rubbers, the American Society for Testing and Materials (ASTM) Standard D1418-85 gives the classification and designation of rubbers based on their chemical composition. Therefore, in this chapter, the classification and naming of rubbers are based on this standard. For convenience, the nomenclature is reproduced in Table 1, extracted from the standard.

As pointed out earlier, rubber must be dissolved in SEC solvent when SEC analysis is attempted. Almost all final rubber products, however, are produced by vulcanization in which raw rubbers tend to become completely insoluble. Therefore, SEC of rubbers is limited to raw rubbers only. This criterion, however, is not obeyed for SEC of low-molecular-weight compounds in vulcanized rubbers. Vulcanized rubbers contain many additives, such as curatives, antiox-

Table 1 Abbreviation of Rubbers According to ASTM D 1418–85

ABR	acrylate-butadiene
BR	butadiene
CIIR	chloro-isobutene-isoprene
CR	chloroprene
IIR	isobutene-isoprene
IR	isoprene, synthetic
NBR	nitrile-butadiene
NCR	nitrile-chloroprene
NIR	nitrile-isoprene
NR	natural rubber
SBR	styrene-butadiene
SCR	styrene-chloroprene
SIR	styrene-isoprene rubbers
Z	polyorganophosphazene
Q	polysiloxane rubber
FKM	fluoro rubber of polymethyrene type having substituent fluoro and perfluoroalkoxy groups on the polymer chain

idants, and modifiers. These additives can be easily analyzed by SEC if their forms are soluble in the SEC solvents, as demonstrated by Zimbo et al. (34) for the SEC analysis of the extender oil bloom on EPDM (terpolymer of ethylene, propylene, and a diene) vulcanizates.

General Remarks

To manifest the particular property of rubber—high elasticity—rubbers have high molecular weights with a broad molecular weight distribution compared with other polymeric materials. This is seen typically in the molecular weight distribution curve for NR, shown in Figure 1. Synthetic commercial rubbers were initially produced after natural rubber, and their molecular weight distributions were also almost the same as that of natural rubber. Therefore, the SEC characteristics of the various rubbers are considered together.

The convenience of SEC for the determination of molecular weight data of a wide variety of synthetic rubbers was appreciated early after the introduction of SEC. One of the reasons is that they are generally easily soluble in SEC solvents and need no specific SEC experimental condition, such as high temperature.

In some cases, however, it is difficult to perform SEC analysis, especially when attempting SEC of new rubbers. An example is polyorganophosphazene rubber (30,31). For SEC, the choice of SEC conditions should be made first.

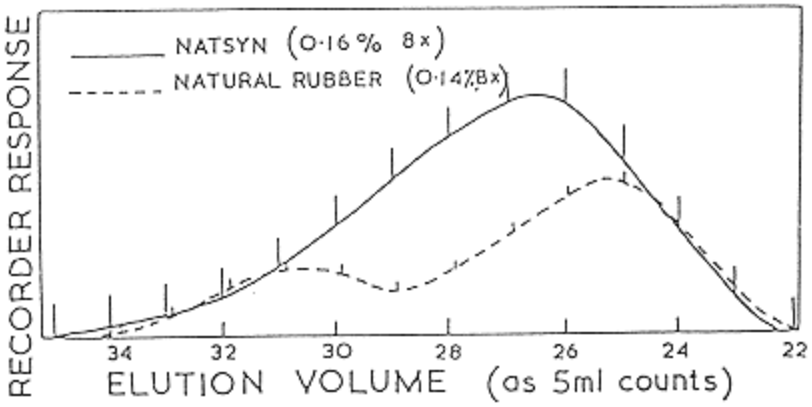

Figure 1.
Chromatograms of Natsyn 400 and natural rubber. Instrument: Waters Model 200. Column: 10^6, 10^5, 5×10^4, 10^3 Å porosities. Mobile phase: THF (0.05% wt/vol antioxidant). Flow rate: 0.91, 0.95 ml/minute. Temperature: 35°C. [From A. Subramaniam (1972) (8).]

The SEC/low-angle laser light-scattering (LALLS) or SEC/LALLS/viscosity detector coupling systems give effective results. By these techniques, the dilute solution properties of the rubber polymer, which are closely related to their behavior in SEC, are understood simultaneously. Cooperative data from SEC and dilute solution properties give information on molecular branching, molecular weight distribution, and compositional heterogeneity so that more precise molecular characterization can be obtained.

Solvents of Rubber for SEC

SEC is a separation technique based on the difference of molecular sizes in solution. The most essential condition in the SEC of rubbers is that they be dissolved completely in SEC solvents. Solvents used for the SEC of rubbers are summarized in Table 2. The most common solvent is tetrahydrofuran (THF).

There are so-called organic solvent-resistant rubbers and heat-resistant rubbers. Also, there are rubbers that contain microcrystalline parts or molecular associations even in their solution state. NBR, CR, Z, Q, FKM, and EPDM are examples. An example of SEC analysis of these rubbers is seen in phosphazene rubbers (30,31). In the SEC of such rubbers, difficulties arise in finding suitable SEC solvents. In principle, such methods as increasing the temperature to enhance the solubility are needed for these rubbers. In EPDM or EPM (copolymers of ethylene and propylene), for instance, once normal room temperature SEC was used, but today use of a high-temperature SEC is the most common because these may contain some crystalline parts depending on the block of C_2 or C_3 segments. Choice of other solvents depends on the required sensitivity of the detectors.

Care should be taken when handling rubber solutions because rubbers have considerable amounts of unsaturated double bonds and are prone to oxidation by the peroxide in THF or even by the oxygen in air. The addition of suitable antioxidants is very common to reduce the incidence of such oxidative degradation. Also, the solution should not be exposed to light or high storage temperature. Common antioxidants used in SEC for rubbers are shown in Table 3.

Presence of Gel

Both natural and synthetic rubbers normally have a gel component, which is a part that remains undissolved in a solvent (61,62). The gel component is probably produced by chain branching during the polymerization process or by slight cross-linking when handling rubbers. The most common example is seen in unmilled natural rubbers. When such a component is present, SEC analysis affords only the molecular weight data on the soluble fraction, excepting the gel fraction. In this case, to understand the viscoelastic properties of the rubbers connected with the SEC data is not appropriate because the gel contributes to these properties. Studies of the influence of the gel fraction on the mechanical properties of natural

Table 2 Various Solvents and Operating Temperatures in the Literature for SEC Analysis of Rubbers[a]

Polymer	Solvent	Temperature (°C)	References
EPDM	TCB	135	70
	THF		39
EVA (high VA)	THF	Ambient	70
EVA (low VA)	ODCB	140	70
NR	Toluene	80	70
	THF	24	5
	THF	27	6
	THF	35	7, 9
	THF	40	3
	THF		10
Polyacrylonitrile	DMF	80	70
Polybut-1-ene	TCB	140	70
BR	Toluene	80	70
	THF	40	29
	THF		22, 24, 28
Q	Toluene	80	70
	THF	Ambient	70
Polyurethane	THF	Ambient	70
	DMF	80	70
SBR	Toluene	80	70
	THF	40	21
	THF		20
IR	THF	Ambient	58
	Toluene	80	70
Z	THF	30	30
	Acetone + cyclohexane		31

[a]EVA, polyethylene + vinyl acetate; TCB, 1,2,4-trichlorobenzene; ODCB, 1,2-dichlorobenzene.

rubber are listed in a relevant article (61). The suggestion is that, in natural rubber, the gel tends to be soluble in SEC solvents when suitably masticated.

A common practice in SEC is to filter the sample solution through an approximately 0.5 μm filter used for the injection. This means that the gel or aggregates that cannot pass through the filter are removed from the SEC columns.

SEC Calibration

As is well known, a SEC system should be calibrated by plotting the elution volume V_e of the peak maxima of a series of calibrants with narrow molecular weight distribution against the log molecular weight M before SEC analysis is made. Commonly, standard polystyrenes are used for the calibrants. The cali-

bration curve log M versus V_e for the polystyrene calibrants is valid only for SEC analysis of linear polystyrene samples. For rubbers, rubber standards of the same type of rubber in question should be used. The difference in the calibration curves between polystyrene and polyisoprene standards is depicted in Figure 2 (6). However, only a limited number of commercial rubber standards are available, as shown in Table 4.

Table 3 Antioxidants Used for SEC Analysis of Rubbers

Antioxidant	Concentration (%)	References
4,4-Thiobis-3-methyl-6-*tert*-butylphenol (Santonox)	0.1 wt/vol	40, 61
2,4-Di-*tert*-butylphenyl phosfite (D-13 168)	0.1 wt/vol	61
2,6-Di-*tert*-butyl-4-methylphenol (Ionol)	0.03	30
	1 for polymer	44
	0.05 wt/wt	43

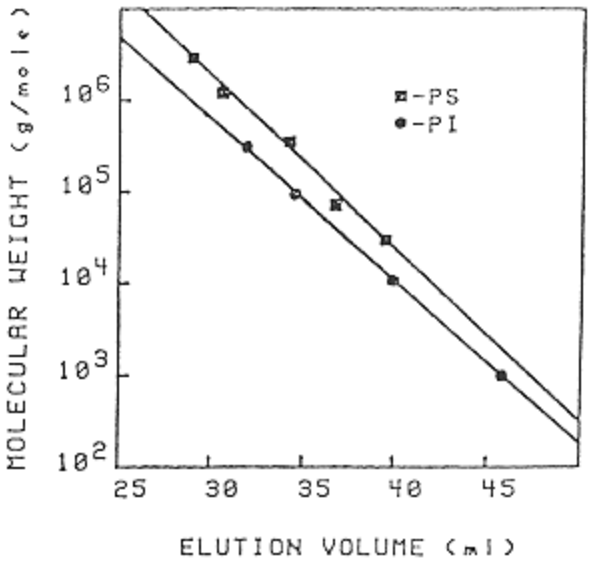

Figure 2.
Typical GPC calibrations with PS (Q = 60.4 g/ Å) and PI molecular weight standards. Instrument: Waters Model 244. Column: 10^6, 10^5, 10^4, 10^3, 500 Å porosities. Mobile phase: THF. Flow rate: 1 ml/minute. Temperature: 27 °C. Detector: RI. [From G. L. Swanson et al. (1986) (6).]

An alternative approach to calibrating an SEC system has been to use a single broad molecular weight distribution calibrant. However, this method is not common.

A method to overcome this is Benoit's universal calibration plot (63) of log [η] M against V_e, where [η] is intrinsic viscosity. However, this method needs the constants from the Mark-Howink [η]M relationships for the rubber samples to be analyzed in the SEC solvents before the SEC analyses. However, a literature survey showed that few constants for rubbers are available, as shown in Table 5. Another method is to use the Q factor (64), which is defined as the ratio of the extended chain length between polystyrene and rubber samples. This method is valid only for vinyl polymers and is empirically crude (6).

A much more satisfactory calibration method is to use LALLS coupling with the usual refractive index (RI) detector in the SEC system so that the molecular weight corresponding to each elution volume can be obtained directly (30,38). The molecular weight distributions of the polyorganophosphazenes have

Table 4 Molecular Weight Standards for SEC Analysis of Rubbers

Polybutadiene

Polyisoprene

Polyisobutylene

Polystyrene-isoprene diblock

Polystyrene-butadiene diblock

Polystyrene-butadiene star block

Source: From Reference 71.

Table 5 Mark-Houwink Viscometric Constant for Rubbers Used for SEC

Polymer	Solvent	Temperature (°C)	$K \times 10^{-4}$	α	Reference
Natural rubber	THF	25	1.09	0.79	72
Polybutadiene	THF	25	2.36	0.75	72
Polyisoprene	THF	25	1.77	0.735	72
SBR (28% styrene)	THF	25	4.51	0.693	72
Polybutadiene	ODCB	135	2.7	0.746	72
Polydimethylsiloxane	ODCB	135	3.83	0.57	72
	$CHCl_3$	30	0.54	0.77	72
Polyaryloxyphosphazene	THF	30	0.0119	0.649	30

been obtained by this method; they cannot be obtained with other methods because of their complex behavior in SEC solvent.

It is not always necessary to calculate the correct molecular weight distribution to obtain information from SEC chromatograms. Simple inspection of chromatograms often reveals important information, as shown in Figure 3. The comparison is valid only for data obtained under the same SEC conditions, however, because a SEC chromatogram is a function of molecular weight distribution as well as the SEC system, including columns and instrumentation. Although the fingerprinting method is qualitative, it is the most frequently used method for the design of syntheses of new rubber polymers. SEC chromatograms indicate polymerization recipes and polymerization conditions (47,50,52).

SEC of Molecular Branching

Both natural rubber *(Hevea)* and synthetic rubbers have molecular chain branching. The presence of branched molecules effect the SEC behavior to a great

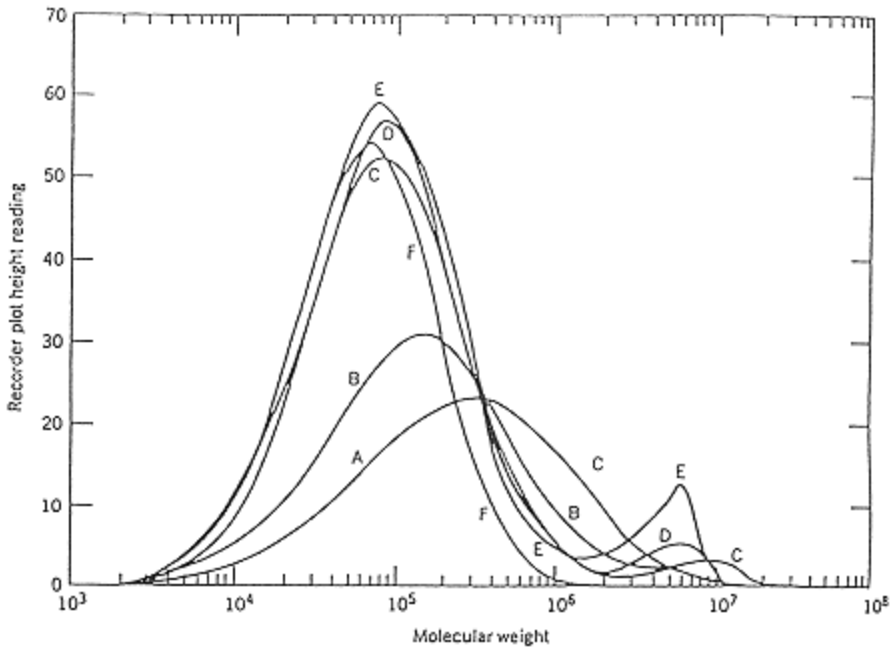

Figure 3.
Gel permeation chromatograms showing the effect of NR mastication. (A) 8 minutes milling time; (B) 21 minutes; (C) 38 minutes; (D) 43 minutes; (E) 56 minutes; and (F) 76 minutes. [From J. F. Johnson (1985) (65).]

extent, because a branched molecule has a smaller hydrodynamic volume than a linear chain molecule of the same molecular weight and is eluted later. Therefore, when branched molecules are present, an erroneous molecular weight distribution curve results by analyzing the SEC curve as if there are all linear molecules. Subramaniam (8) has shown an example in the SEC analysis of NR.

Many modern SEC systems include LALLS. As described earlier, this gives information about both the molecular weight distribution and the extent of chain branching in the same SEC analysis time. It is convenient for simultaneous determination of chain branching and molecular weight distribution. Even when LALLS is not used, a combination of SEC and viscometric measurements can estimate chain branching using the universal hydrodynamic calibration method (63). Fuller and Fulton (3) studied the relation between molecular branching and the mechanical behavior of NR.

SEC of Copolymer Rubbers and Blends

As can be seen in Table 1, several rubbers have a copolymer structure. The physical properties of the copolymers are affected not only by the molecular weight distribution but also by the compositional distribution. Therefore, it is desirable to know the compositional distribution in addition to the molecular weight distribution. This type of analyses is often performed by SEC systems having more than two detectors.

When one of the constituents *A* or *B* of a copolymer has ultraviolet (UV) absorption and the other does not, a UV-RI dual-detector system can be used for the detection of the chemical heterogeneity of the copolymer. Like molecular weight distribution, 1:1 eluant-eluant composition against the retention volume V_e is calculated from the two chromatograms, and a compositional variation is plotted as a function of molecular weight. However, the response factors of the two components in the two detectors must be calibrated first. This method has been applied to the determination of chemical heterogeneity for styrene-butadiene copolymers (14,59). SBR is one of the most widely used synthetic rubbers. In the earliest stage of introduction of SEC for SBR, the molecular weights and molecular weight distribution were only included in the analysis by RI detection. However, by using a UV absorption detector, additional comonomer styrene UV maxima can be obtained separately. If a UV photodiode array detector is used, various low-molecular-weight additives that have different UV maxima can be detected at one time (14).

Other detection methods, such as turbidometric titration (19) and Fourier transform infrared spectrometry (35), have been used for compositional detection in copolymer rubbers.

Recently rubbers have been modified by blending or by chemical reaction to suit specific needs for the product. In these cases, the compositional analysis

is very important. The same SEC analysis is used as an effective companion method.

For the SEC of rubber blends, it is crucial that SEC equipped with two or three properly selected detectors, instead of the conventional single RI detector, be used (65).

Preparative SEC for Rubbers

From the beginning, preparative SEC was applied to the preparation of narrow molecular weight samples of a specified rubber polymer. Nevertheless, the literature survey shows that only a few studies have been reported. The reason, as Chaturcedi and Patel (43) describes, is that the preparative SEC method is tedious and time consuming compared with the conventional prefered precipitation method.

Fractionation of *trans*-1,4-polyisoprene by preparative SEC was reported by Chaturcedi and others (43). However, they obtained only three fractions that could be measured by further viscometry.

Typical Applications of Sec Rubbers

SEC for NR and IR

Although the molecular weight distribution of NR has been studied extensively, different results have been reported. The reason appears to be that there is a variation between different samples of NR depending on both the origin of trees and processing methods. Also, samples of NR have additional complication as a result of oxidation and gelation that take place in the bulk state or even in solution.

In 1972, Subramaniam (8) reported a comprehensive study on the molecular weight distribution of selected samples of NR by SEC. Solutions of NR were prepared on fresh latex obtained from six clones of *Hevea brasiliensis.* Figure 1 shows the SEC chromatogram of the purified natural rubber sample. It can be seen in this curve that NR has a very broad molecular weight distribution with a distinctive bimodal curve. Comparing this to that obtained on a sample of synthetic polyisoprene (IR), Natsyn 400, the bimodality can be seen more clearly. Using the universal calibration method (63), he showed that the integral molecular weight distribution curves for six clones of NR ranges from 10^4 to 10^7. However, the average molecular weights derived from SEC curves are too low compared with values obtained conventionally. He pointed out that this error was a result of not considering chain branching. By this method chain branching was not completely detected. Further study is needed to use SEC/LALLS or other relevant methods.

Subramaniam also described difficulty with the practice of SEC for NR. This difficulty was the partial blockage of the columns experienced with some

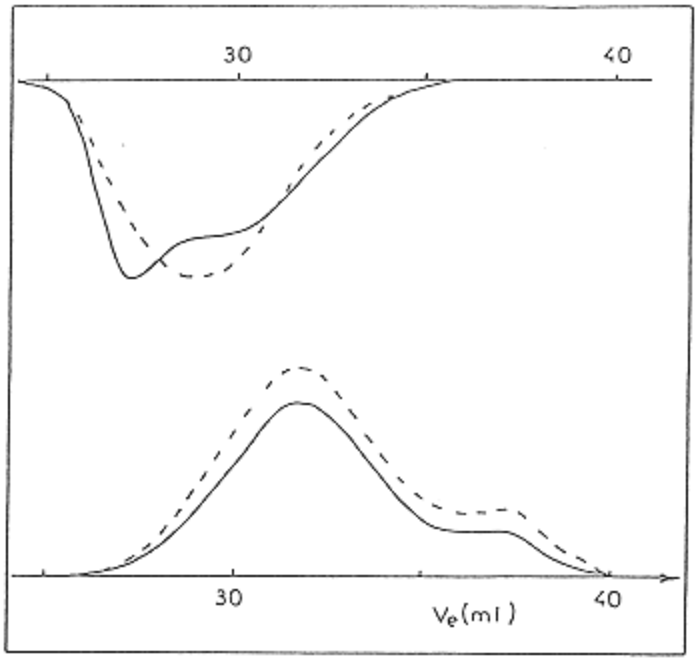

Figure 4.
Comparison of two polydiphenoxyphosphazene samples of very similar RI chromatogram (lower trace). The LALLS detector seems to reveal some aggregates. Instrument: Waters Model 150 ALC/GPC. Column: Shodex 80M. Mobile phase: THF (0.03% antioxidant, 2,6-di-tert-butyl-4-methylphenol). Flow rate: 1 ml/minute. Temperature: 30°C. Detector: RI, LALLS. [From R. De Jaeger et al. (1990) (30).]

concept, and examination of dilute solution viscosity behavior is a simple method of screening a potential solution for SEC analysis.

When using SEC to study rubber samples having the same unusual characteristics, properly selected dual or triple detectors yield much more comprehensive information on molecular characteristics. Otherwise, the use of single detector in SEC for such samples may lead to erroneous conclusions. Commercially available detectors are LALLS, UV, infrared, and evaporative detector (ED) photometers with conventional RI detectors.

Special Applications of SEC for Rubbers

SEC is used for the characterization of the molecular weight parameters of rubbers; however, there is an inverse SEC consideration in which the determi-

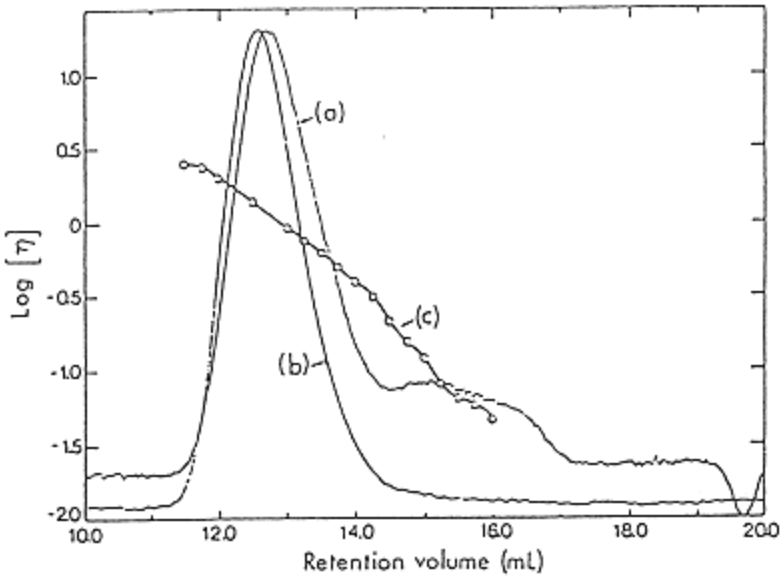

Figure 5.
Chromatograms of polybistrifluoroethoxyphosphazene using different detectors: (a) differential refractometer, (b) differential viscometer, and (c) intrinsic viscosity. Column: PLgel mixed bed. Mobile phase: acetone, cyclohexanone. Temperature: 30°C, 40°C. [From T. H. Mourey et al. (1989) (31).]

nation of the porous structure of the column packings (if the packings are vulcanized rubber) might be elucidated by examining the retention data for polymers having known molecular weights. This technique is called inverse SEC. This seems to be a natural extension of inverse gas chromatography (68).

In 1984, Haidar and others (39) reported their inverse SEC results for the elucidation of structural differences in networks prepared by chemical and photochemical reactions of EPDM. They used conventional GPC for their inverse SEC, except for the columns, in which fine powders of cross-linked EPDM were packed. Polystyrenes of various molecular weights were used as the probe.

Their elution data for standard polystyrenes from EPDM packed columns showed clearly the differences presented between two vulcanizing methods: one was photo-cross linked and the other was peroxide-cured EPDM. From this study they concluded that the M_c, the molecular weight between cross-linking junctions, was different for the two samples.

In 1985, Capillon and others (69) criticized that the inverse SEC gives erroneous results when used in gels that swell too much, such as vulcanized rubbers.

Subsequently, very little work has been done using inverse SEC for the characterization of the network structure of rubbers.

Conclusion

Rubber based on dienes can easily be analyzed for their molecular characterization by SEC; however, special rubbers, such as polyorganophospazenes, show some difficulty because of their imperfect dissolution in SEC solvents. Fluororubbers are hard to dissolve in solvents. The application of SEC to such rubbers is not covered in the literature cited in Table 5.

Recent application trends of SEC to rubbers are multidetector systems to obtain much more information on the molecular characteristics in a single SEC run. A properly arranged SEC system gives almost a complete molecular characterization of rubbers if the rubbers are dissolved in SEC solvents.

For the Appendix we could not find a role for SEC in the quality control of rubber production processes despite its technological importance. Furthermore, we expect that much work on the correlation between SEC analysis and mechanical properties of rubbers is in development.

Appendix: SEC Conditions for Rubbers

Polymer	Columns	Mobile phase	Comments	Reference
NR (masticated)				2
NR (not cross linked)	Two 60 cm mixed bed columns (Polymer Laboratories)	THF 0.5 ml/minute 40 °C	UV (215 nm) Polystyrene standard	3
NR	10^6, 10^5, 10^3, 100, 50 Å PLgel	0.8 ml/minute 70 °C	UV, RI Polyisoprene standard Polystyrene (PS) standard	4
Guayule Parthenium		THF 1 ml/minute 24 °C	Polyisoprene standard	5
Guayule	10^6, 10^5, 10^4, 10^3, 500 Å µStyragel	THF 1 ml/minute 27 °C	RI Polystyrene standard Polyisoprene standard	6

(table continued on next page)

(table continued from previous page)

Polymer	Columns	Mobile phase	Comments	Reference
Guayule	10^7, 10^6, 5×10^5, 1×10^5-3×10^5 5×10^3-1×10^4 Å Styragel	THF 1 ml/minute 35°C	Water Ana-Prep chromatograph RI Universal calibration	7
NR IR	10^5, 5×10^4, 1.5×10^4, 10^3 Å 10^6, 10^5, 5×10^4, 10^3 Å	$C_6H_5CH_3$ THF 0.91 ml/minute 0.95 ml/minute 35°C	Polystyrene standard Toluene a good solvent for NR and quite stable, but refractive index increment between it and NR small	8
NR, IR, SBR, BR masticated NR, IR, SBR, BR	10^7, 10^6, 10^5, 10^4 Å 7×10^7, 10^6, 10^4 Å	THF 1 ml/minute 35°C		9
NR latex (modified with peracetic acid epoxidation)		THF	Solubility decreases with increasing level of epoxidation because of higher gel content	10
Copolymer of NR and nylon 6	Two Shodex AD-80M/S	1,1,2,2-Tetrachloroethane ($CH_2Cl_2CH_2Cl_2$) 1.0 ml/minute ambient temperature	RI + UV (260 nm) (37% nylon 6 mechanically blend)	11
NR (lightly masticated)	10^6, 10^5, 10^4, 10^3, 5×10^2 Å	THF 1 ml/minute	UV	12
IR (lightly masticated) BR (lightly asticated)			Graft copolymers	
SBR VSBR (vinyl styrene butadiene rubber)			Molecular weight distribution (MWD) bimodal, each peak with a narrow MWD	13

(table continued on next page)

(table continued from previous page)

Polymer	Columns	Mobile phase	Comments	Reference
SBR	Ultrastyragel linear column	THF 1.0 ml/minute	RI Photodiode array detector	14
SIR Styrene-ethylene-butadiene copolymer Styrene-butyl-methacrylate copolymer	Ultrastyragel 500 Å (Waters)	38°C		
SBR (ozonolysis)	Styrene-divinylbenzene gel (21.2 mm inner diameter, ID, 60 cm, three)	Chloroform 2 ml/minute	UV (254 nm)	15
SBR lattices	Bimodal-S kit (DuPont)	THF BHT (butylated hydroxytoluene)	UV, RI Vistex solution	16
SBR (ozonolysis) BR (ozonolysis)	Styrene-divinylbenzene gel (7.5 mm ID, 500 mm)	Chloroform	UV	17
PS-BR-THF ternary system PS-BR-tetralin ternary system	Styragel, 5×10^6, $1.5-1.7 \times 10^5$, $1.5-5 \times 10^4$, $2-5 \times 10^3$ Å	THF 1 ml/minute Tetralin	Ternary-phase studies (blend) Phase diagram determination	18
BR			RI + UV 254 nm	
Anionic polymerized	Styragel (Waters)	THF (0.3% $NaNO_3$)	Compositional distribution	19
Dimethylformamide	10^7, 10^6, 10^5, 10^4 Å	0.5 ml/minute		
SBR	(0.1% Ionol)	26°C	Universal calibration	
SBR		THF	(Waters Associates, Inc.)	20
SBR	Glaskugel	THF	RI, UV	21
BR		40°C		

(table continued on next page)

(table continued from previous page)

Polymer	Columns	Mobile phase	Comments	Reference
BR (OH terminated)	Analytical GPC μStyragel 10^4, 10^3, 500, 100 Å preparative GPC Styragel 10^4, 10^3 Å	THF 2 ml/minute THF 10 ml/minute	RI, UV Universal calibration	22
1,4-BR-b-1,2-BR	PLgel columns (2) 10^5, 10^3 Å	chloroform 1 ml/minute	RI Polystyrene standard	23
BR Waste rubber	μBondagel E linear columns	THF	Mixture of 1,4-BR, 1,4-trans, and 1,2-vinyl polybutadiene	24
Phosphorus-terminated BR	Divinylbenzene cross-linked polystyrene bead (10 μm) 10^5-10^2 Å		RI Universal PS calibration	25
BR *Cis*-1,4-polybutadiene (branched)	Waters 200 GPC		Determination of long-chain branching	26
ω-Functional group terminated BR (liquid polymer)			Polymers polymerized with different kinds of initiator were measured (different organometallic initiators)	27
BR	Silicagel Lichrospher	THF 0.5 ml/minute	Polystyrene standard	28
Cis-BR (Taktene 1220)		THF 3 ml/minute (two columns) 1 ml/minute (four columns) 40°C	Polystyrene standard	29

(table continued on next page)

(table continued from previous page)

Polymer	Columns	Mobile phase	Comments	Reference
PZ (polyorgano phosphazene) FZ (polyfluoro phosphazene)	Two Shodex 80 M (stabilized with 0.03% 2,6-di-*tert*-butyl-4-VCmethylphenol)	THF + LiBr 0.1 Mol/l, + ethyleneglycol, or + diethylene glycol 1 ml/minute 30 °C	LALLS-RI in series Aggregates form because of the presenceof P-Cl, P-O bonds or P-OH, P-O, and N-H bonds	30
FZ Polydichloro-phosphazene Z	Polystyrene-divinylbenzene	Acetone + cyclo-hexanone, 30°C, 40° C, Ammonium nitrate	Dilute solution properties in acetone, THF, cyclohexane in the presence of TBAN (tetrabutyl-ammonium butyrate) examined to choose optimum eluant conditions for SEC; acetone in SEC caused concentration-induced chain compression; poorer solvent, cyclohexane, reduced this effect	31
Modified phosphazenes	µBondagel	THF with 0.01 N tetra-*n*-butyl ammonium bromide (added to break up polymer association)	Anomalies in GPC data attributed to separation by chemical heterogeneity as well as molecular size	32

(table continued on next page)

(table continued from previous page)

Polymer	Columns	Mobile phase	Comments	Reference
PZ	Five 4 ft/ in. Styragel columns of porosity rating 5×10^6, two of 1.5-7 $\times 10^5$, 10^5, 1.5-5 $\times 10^4$ Å	THF 1 ml/minute	Polystyrene standard	33
Extender oil bloom on the surface of EPDM vulcanizates	100 Å UltraStyragel (300, 7.8 mm ID)	THF 1.0 ml/minute 30°C	Dissolution part in hexane RI	34
EPM (copolymers of ethylene and propylene)	Shodex columns 802, 803, 804, 805	TCB 0.5 ml/minute 135°C	Composition drift collecting solvent-free polymer film from a high-temperature GPC	35
EP (C_3 = mol% 51-36) M_w/M_n 3.2-12.9	Styragel 10^7, 10^6, 10^5, 10^4, 10^3 Å 10^7, 10^6, 10^4, 10^3 Å	ODCB 1 ml/minute 135°C	Double peaks	36
EPM-g-SAN, (styreneacrylonitrile copolymer)	Styragel (5×10^3, 10^7 Å)	THF 1 ml/minute	UV RI	37
EPM	µStyragel (500, 10^6 Å)			
EPM	Styragel 10^6, 10^5, 10^4, 10^3 Å	1,2,4-Trichlorobenzene	GPC-LALLS RI	38
EPDM	Waters	140°C		
EPDM	Packed with polymer pieces of cross-linked elastomer (EPDM)	THF 0.4 ml/minute	Inverse GPC	39
EPDM	11 × 300 mm PLGel column (2×10^6, 1×10^3 Å)	Trichlorobenzene 1 ml/minute 135°C	LALLS (ED, DRI (differential refractive index))	40

(table continued on next page)

(table continued from previous page)

Polymer	Columns	Mobile phase	Comments	Reference
IR	DuPont Z or latex PSM	THF	M_w of complex polymer can be determined by SEC on-line viscometry detector	41
IR	μStyragel	THF 25°C	Polyisoprene standard No indication of aggregates found Association behavior in end-functionalized polymer	42
Trans-1,4-IR	10^6, 10^5, 10^4, 10^3 Å	Toluene 2 ml/minute 30°C		43
Hydroxytelechelic polybutadiene	For analytical GPC Styragel 1000, 500, 100, 50 Å	THF	30 g Arco-R45M fractionated into five fractions; fractions recovered from solutions by vacuum and characterized by nuclear magnetic resonance, VPO, and GPC RI (Waters R401) Polystyrene standard Polybutadiene standard	44
U (thermoplastic)	PI-Gel 10μm	THF (250 ppm BHT) 1.0 ml/minute 40°C	RI	45

(table continued on next page)

(table continued from previous page)

Polymer	Columns	Mobile phase	Comments	Reference
U	Not given	Not given	GPC curves of fragments obtained by decomposition of U in n-$BuNH_2$/dimethylsulfoxide solution shown	46
Polyisobutyrene (PIB) isoprene living polymerization telechelic living PIB			Polymerization Polyisobutadiene standard Polystyrene standard RI	47
Cyclopolyisoprene cy-PIP/PIB multiblock (tr-1,4-PIP)-b-PIB-b-(tr-1,4-PIP) (PIB is a thermoplastic elastomer) (PIB is a thermoplastic elastomer)			For MW determination	
NBR (low conversion) Acrylonitrile in polymer 20, 26, 34, 37, 50 wt%	Cross-linked 2-chloro-acrylonitrile gel Shodex H-2005	Chloroform/*n*-hexane (gradient) 0.5 ml/minute Chloroform 3.5 ml/minute	Evaporative mass detector (Model 750/14ACS Co.) Mixture of three commercial NBR of different AN contents separated	48
Antioxidant in CR (chloroprene) (methylene-4426-s,KY-405, phenothiazine)	MCH-5N-CAP	MeOH-$CHCl_2$-H_2O		49

(table continued on next page)

(table continued from previous page)

Polymer	Columns	Mobile phase	Comments	Reference
Triflate ($-OSO_2CF_3$) terminated PIB	μStyragel 10^5, 10^4, 10^3, 500, 100 Å	THF 1 ml/minute	Synthesize triblock and star-block copolymers consisting of central PIB and external PTHF (polytetrahydrofuran); polystyrene standard UV, RI	50
Polyether-amide block copolymer Thermoplastic elastomer	μStyragel 10^5, 10^4, 10^3, 500 Å	Benzyl alcohol (0.5% di-*t*-butyl-paracresol)	RI IR	51
Polyisobutyrene Living polymerization	UltraStyragel 10^5, 10^4, 10^3, 500, 100 Å	THF 1 ml/minute 1 ml/minute	Living polymerization of IB polymerization conditions followed by SEC	52
S-B-S, S-I-S triblock copolymers Their ozonolysis products	Polystyrene gel Preparative column 3×10^3 Å Analytical column 7×10^5, 2×10^5, 1×10^5, 5×10^4 Å	Chloroform 2 ml/minute (preparation) 1 ml/minute (analytical)	Polystyrene standard Commercial S-B copolymer KX-65, Solprene-411, Clearen 530-L Commercial S-I block copolymer Kraton-1107, TR-1112 Chemical composition distribution determined by high-performance liquid chromatography using acrylonitrile gel of hexanechloroform mixture	53

(table continued on next page)

(table continued from previous page)

Polymer	Columns	Mobile phase	Comments	Reference
Polystyrene-polydimethylsiloxane block copolymer PS-PDMS (polysimethylsiloxane) blend	Four 30 cm 10 µm packings (Polymer Laboratories 10^6, 10^5, 10^4, 10^3 Å)	$C_2H_2Cl_4$ (tetrachloroethylene) quoted pore size concentration 5×10^{-3} g/cm^{-3} or less	RI, LALLS (dual detector) Compositional heterogeneity correlation with MWD	54
Toluene diisocyanate Diphenylmethane diisocyanate in polyurethane polymers	500, 100, 100 Å Styragel	CH_2Cl_2 1 ml/minute 30 cm × 78 mm ID	Urethane	55
Polyepichlorohydrin	TSKgel (two G2000H8, G3000H8, G40000H8)	THF 40°C	RI UV (254 nm)	56
Polyurethane-based copolymer with polyether and polyamide	TSK G3000HXL, G4000HXL	THF	Polystyrene standard	57
Polyorganosiloxane-polyarylester block copolymers (perfectly alternating) functional siloxane oligomers	50, 10^6, 10^5, 10^4 Å µStyragel	THF 1.0 ml/minute	RI, UV Step growth reactions of the two oligomers confirmed from SEC chromatograms	58
SB (styrenebutadiene copolymer)	10^6, 10^5, 10^4, 10^3, 800 Å	THF	UV, RI Polystyrene standard Polybutadiene standard	59
Polyalkenylenes	Not given	Not given	Bimodal molecular weight distribution curve of polyoctenylene shown	60

References

1. J. C. Moore, *J. Polym. Sci., A2:* 835 (1964).

2. H. Bartels, M. L. Hallensleben, G. Pampus, and G. Sholz, *Angew. Macromol. Chem., 180:* 73 (1990).

3. K. N. G. Fuller and W. S. Fulton, *Polymer, 31:* 609 (1990).

4. H. Bartels, M. L. Hallensleben, G. Pampus, and G. Scholz, *Angew. Makromol. Chem., 180:* 73 (1990).

5. J. West and E. Rodriguez, *Rubber Chem. Technol., 60:* 888 (1987).

6. C. L. Swanson, M. E. Carr, and H. C. Nielsen, *J. Polym. Mater., 3:* 211 (1986).

7. T. Hager, A. MacArthur, D. McIntyre, and R. Seeger, *Rubber Chem. Technol., 52:* 693 (1979).

8. A. Subramaniam, *Rubber Chem. Technol., 45:* 346 (1972).

9. T. Homma, N. Tagata, and H. Hibino, *Nippon Gomu Kyokaishi, 41:* 242 (1968).

10. I. R. Gelling, *Rubber Chem. Technol., 58:* 86 (1985).

11. T. Ogawa and M. Sakai, *J. Liq. Chromatogr., 8*(6): 1025 (1985).

12. D. S. Campbell and A. J. Tinker, *Polymer, 25:* 1146 (1984).

13. R. R. Rahalkar, *Polymer, 31:* 1028 (1990).

14. J. K. Del Rios, *Am. Lab., 20:* 78, 80 (1988).

15. Y. Tanaka, H. Sato, and J. Adachi, *Rubber Chem. Technol., 59:* 16 (1986).

16. D. L. Bender, J. J. Beres, and R. B. Timmer, *Int. GPC Symp. '87,* 1 (1987).

17. Y. Tanaka, H. Satou, and Y. Nakafutami, *Polymer, 22:* 1721 (1981).

18. D. R. Lloyd, V. Narasimhan, and C. M. Burns, *J. Liq. Chromatogr., 3*(8): 1111 (1980).

19. M. Hoffmann and H. Urban, *Makromol. Chem., 178:* 2683 (1977).

20. Y. Minoura and Y. Hatanaka, *Nippon Gomu Kyokaishi, 43:* 838 (1970).

21. H. J. Cantow, J. Probst, and C. Stojanov, *Kautschuk Gummi, 21:* 609 (1968).

22. K. N. Ninan, V. P. Balagangadharan, and K. B. Catherine, *Polymer, 32:* 628 (1991).

23. S. Poshyachinda, H. G. M. Edwards, and A. F. Johnson, *Polymer, 32:* 334 (1991).

24. G. Adam, A. Sebenik, U. Osredkar, Z. Veksli, and F. Ranogajec, *Rubber Chem. Technol., 63:* 660 (1990).

25. W. E. Lindsell, K. Radha, I. Soutar, and M. J. Stewart, *Polymer, 31:* 1374 (1990).

26. J. Chunshan and G. Qipeng, *J. Appl. Polym. Sci., 41:* 2383 (1990).

27. R. A. Livigni, I. G. Hargis, H. J. Fabris, and J. A. Wilson, *J. Appl. Polym. Sci., Appl. Polym. Symp., 44:* 11 (1989).

28. L. MrKvickova, I. Kucharikova, S. Pokorny, and J. Cermak, *Plaste Kautsch, 34:* 17 (1987).

29. G. Kraus and C. J. Stacy, *J. Polym. Sci., A-2, 10:* 657 (1972).

30. R. De Jaeger, D. Lecacheux, and P. Potin, *J. Appl. Polym. Sci., 39:* 1793 (1990).

31. T. H. Mourey, S. M. Miller, W. T. Ferrar, and T. R. Molaire, *Macromol., 22:* 4286 (1989).

32. W. T. Ferrar, A. S. Marshall, E. C. Flood, K. E. Goppert, and D. Y. Myers, *Polm. Prepr. (Am. Chem. Soc., Div. Polym. Chem.), 28*(1): 444 (1987).

33. G. L. Hagnauer and B. R. LaLiberte, *J. Polym. Sci., Polym. Phys. Ed., 14:* 367 (1976).

34. M. Zimbo, L. M. Skewes, and A. N. Theodore, *J. Appl. Polym. Sci., 41:* 835 (1990).

35. A. H. Dekmezian and T. Morioka, *Anal. Chem., 61:* 458 (1989).

36. K. Q. Wang, S. Y. Zhang, J. Xu, and Y. Li, *J. Liq. Chromatogr., 5:* 1899 (1982).

37. A. De Chirico, S. Arrighetti, and M. Bruzzone, *Polymer, 22:* 529 (1981).

38. B. J. R. Scholtens and T. L. Welzen, *Macromol. Chem. Phys., 182:* 269 (1981).

39. B. Haider, A. Vidal, H. Balard, and J. B. Donnet, *J. Appl. Polym. Sci., 29:* 4309 (1984).

40. V. Grinshpun and A. Rudin, *J. Appl. Polym. Sci., 32:* 4303 (1986).

41. W. W. Yau and S. W. Rementer, *J. Liq. Chromatogr., 13*(4): 627 (1990).

42. N. S. Davidson, L. J. Fetters, W. G. Funk, W. W. Graessley, and N. Hadjichristidis, *Macromol., 21:* 112 (1988).

43. P. N. Chaturcedi and C. K. Patel, *J. Polym. Sci. Polym. Phys., 23:* 1255 (1985).

44. I. Descheres, O. Paisse, J. N. Colonna-Ceccaldi, and Q. T. Pham, *Macromol. Chem., 188:* 583 (1987).

45. D. J. Keller and E. G. Kolycheck, *J. Liq. Chromatogr., 13*(10): 2035 (1990).

46. K. Murakami, H. Oikawa, and T. Nagai, Nichon Reoroji Gakkaishi, *17:* 77 (1989).

47. G. Kaszas, J. E. Puskas, and J. P. Kennedy, *J. Appl. Polym. Sci., 39:* 119 (1990).

48. N. Asada, H. Hosozawa, A. Toyoda, and H. Sato, *Rubber Chem. Technol., 63*(2): 181 (1990).

49. Y. Wang and Y. Peng, *Sepu* (China), *7*(6): 391 (1989).

50. A. Gadkari and J. P. Kennedy, *J. Appl. Polym. Sci., Appl. Polym. Symp., 44:* 19 (1989).

51. G. Marot and J. Lesec, *J. Liq. Chromatogr., 11:* 3305 (1988).

52. G. Kaszas, J. Puskas, and J. P. Kennedy, *Makromol. Chem., Macromol. Symp., 13/14:* 473 (1988).

53. Y. Tanaka, H. Sato, and J. Adachi, *Rubber Chem. Technol., 60:* 25 (1987).

54. T. Dumelow, S. R. Holding, L. J. Maisey, and J. V. Dawkins, *Polymer, 27:* 1170 (1986).

55. K. Taymaz, *J. Liq. Chromatogr., 9*(15): 3347 (1986).

56. S. Kohjiya, S. Ohta, and S. Yamashita, *Polym. Bull., 5:* 463 (1981).

57. H. Kazama, M. Hoshi, H. Nakajima, D. Horak, Y. Tezuka, and K. Imai, *Polymer, 31:* 2207 (1990).

58. P. J. A. Brandt, C. L. S. Elsbernd, N. Patel, G. York, and J. E. McGrath, *Polymer, 31:* 180 (1990).

59. J. R. Runyon, D. E. Barnes, J. F. Rudd, and L. H. Tung, *J. Appl. Polym. Sci., 13:* 2359 (1969).

60. A. Draxler, *Handbook of Elastomers* (A. K. Bhowmick and H. L. Stephens, eds.), Marcel Dekker, New York, p. 665 (1988).

61. K. N. G. Fuller, Chapter 5, *Rheology of Raw Rubber in Natural Rubber Science and Technology*, (A. D. Roberts, ed.) Oxford, New York, 1988.

62. D. C. Blackley, *Synthetic Rubbers, Their Chemistry and Technology*, Elsevier Applied Science (England), 1983.

63. Z. Grubisic, P. Rempp, and H. Benoit, *J. Polym. Sci., Part B, 5:* 753 (1967).

64. F. W. Billmeyer, Jr., *J. Paint Technol., 41:* 209 (1969).

65. S. Mori, in *Size Exclusion Chromatography* (B. J. Hunt and S. R. Holding, eds.), Blackie, Glasgow and London, p. 100 (1989).

66. J. F. Johnson, in *Encyclopedia of Polymer and Engineering* (J. I. Kroschwitz, ed.), Vol. 3, Wiley, New York, p. 520 (1985).

67. T. Homma, et al., *Nippon Gomu Kyokaishi, 41:* 242 (1968).

68. D. R. Lloyd, T. C. Ward, and H. P. Schreiber (eds.), *Inverse Gas Chromatography*, ACS Symposium Series 391, Washington, D.C., 1989.

69. J. Capillon, R. Audebert, and C. Quivoron, *Polymer, 26:* 575 (1985).

70. B. J. Hunt and S. R. Holding (eds.), *Size Exclusion Chromatography*, Blackie, Glasgow and London, 1989, p. 277.

71. B. J. Hunt and S. R. Holding (eds.), *Size Exclusion Chromatography*, Blackie, Glasgow, 1989, p. 275.

72. B. J. Hunt and S. R. Holding (eds.), *Size Exclusion Chromatography*, Blackie, Glasgow, 1989, p. 279.

8
Size Exclusion Chromatography of Asphalts

Richard R. Davison, Charles J. Glover, Barry L. Burr, and Jerry A. Bullin Texas A & M University, College Station, Texas

Introduction

Early researchers in the application of size exclusion chromatography (SEC) to asphalt (1–7) noted that SEC (also called GPC, gel permeation chromatography) was very sensitive to differences in asphalts and to changes in composition. This was exploited by Adams and Holmgreen (8) to show differences between various asphalts and between asphalts from the same supplier at different locations. Glover et al. (9,10) used SEC to show how asphalts from a number of suppliers changed with the seasons. It has been used to compare fractions produced by preparative SEC and other methods (9,11–16).

SEC can be quite sensitive to contamination by material of low molecular weight or narrow molecular weight distribution. This was used by Burr et al. (17) to prove incomplete solvent removal by standard American Society for Testing and Materials (ASTM) extraction and recovery procedures.

Bynum and Traxler (4) were the first to use SEC to study road aging. SEC is very sensitive to the changes that occur when an asphalt hardens. Minshull (5) and Haley (18) showed that the large molecular size material increased greatly following air blowing. A series of studies on Texas test sections (8,9,19,20) showed a progressive growth in large molecular size (LMS) material. This material is usually defined as that comprising about the first third of the chromatogram elution time. Similar results are reported for oven aging (12,21,22) and for aging during the hot-mix operation (22–24). Asphalts also change when in contact with solvents, and this is detected by an increase in the LMS region (25).

Many tests have been proposed for simulating hot mix and road aging, and SEC may be used to compare laboratory and field aging (23,26). The effectiveness of recycling agents in restoring aged asphalt for reuse has also been studied by comparing the SEC chromatograms of the old, new, and restored asphalts (14,26–28).

Since Bynum and Traxler (4) there have been a number of attempts to relate road performance to SEC results. Plummer and Zimmerman (29) studied test sections in Michigan and Indiana and found that a greater LMS percentage seemed to correlate with cracking. Jennings and coworkers (14,26,30–34) conducted a major study relating cracking of roads to higher percentage LMS, primarily in Montana but also in other regions of the country. Both Jennings and Pribanic (33) and Hattingh (21) showed that low-percentage LMS can result in rutting.

There have been a number of not particularly successful attempts to correlate asphalt physical properties to chemical properties, including SEC (10,19,35–40). Chollar et al. (41) attempted to relate a number of chemical and physical properties, including percentage LMS, with poor results. Huynh et al. (42) divided asphalt into a number of fractions by preparatory SEC and showed that the glass transition temperature (not precisely defined for asphalts), in moving from one fraction to the next, first decreased with increasing molecular size and then increased. Beazly et al. (43) used SEC and nuclear magnetic resonance (NMR) to estimate asphalt yields and viscosity from crude oil; Woods et al. (44) used SEC fractions to study differences in maltenes from tar sand bitumens.

The measurement of molecular weight by SEC, as with other methods, is greatly complicated by the tendency of the more polar asphalt constituents to associate. Girdler (45) and Speight et al. (46) report large ranges of molecular weights measured by various methods. SEC molecular weight curves must be calibrated by some external standard, such as against vapor pressure osmometry (VPO) measurements of preparative SEC fractions of the asphalt (1,12,47–51). The results are thus limited by the accuracy of the standard, and these methods are very dependent on the solvent and concentration. Markedly different retention times for molecules of different structure but the same molecular weight are a major complicating factor (9,12,46,47,49–51), and data of Bergman and Duffy (52) with model compounds indicate that this is very solvent dependent. A number of researchers have used intrinsic viscosity data in an attempt to eliminate the effect of structurally dependent elution volumes (12,47,49,51,53), but it has been demonstrated (54) that the assumption of a constant relation between molecular volumes and elution volumes does not apply to the differing structural types in asphalt.

Because of the tendency of asphalts to associate and also to be adsorbed on the column (7,10,26,47,55,56), the choice of solvent is very important. Jennings et al. (26) reported that the relative percentage of LMS between asphalts could be reversed by using chloroform instead of tetrahydrofuran (THF). Altgelt

and Gouw (55) report that 5% methanol in chloroform or benzene is an excellent solvent. Brulé (12) compared several solvents: the greater the polarity, the smaller the LMS region. Although increasing polarity tends to decrease the percentage LMS, this is not automatic and depends on the specific interactions. Jennings et al. (57) showed 5% MeOH in THF increasing the percentage of LMS. Done and Reid (56) and Donaldson et al. (58) compared THF and toluene. Higher concentrations and higher flow rates can both cause an increase in the LMS region (12,59,60). A lengthy residence time of asphalt in a solvent also causes a growth in the LMS region (12,25).

Asphalt Chemistry

Asphalt is probably the most complex material routinely studied by SEC. Asphalt is the residual left when practically everything that can be recovered from crude oil by high-vacuum, high-temperature distillation has been vaporized. Alternately, the residuum may be propane extracted to remove even more material and the resulting very hard asphalt may be cut back with lighter fractions. Regardless of how it is produced, the result is a sticky, near solid containing a vast array of high-molecular-weight compounds varying from paraffins to highly condensed aromatics. Included within these compounds, especially in the more condensed material, are the so-called heteroatoms, O, N, S, and metals, especially Ni and V.

To simplify asphalt analysis, a common practice is to fractionate the material to divide it into groupings of simpler constitution. A large number of methods have been proposed, but most are based on either selective solvent extraction or chromatographic separation or, frequently, a combination of solvent precipitation and chromatographic separation.

One of the most used procedures, an ASTM standard, D4124, was developed by Corbett (61) and separates asphalt into four fractions. Asphaltenes are precipitated by heptane, and the remaining solution is divided into saturates, naphthene aromatics, and polar aromatics by a series of successively more polar solvents on an alumina column. Similar procedures produce fractions variously known as asphaltenes, resins, and oils or saturates, aromatics, resins, and asphaltenes, for example. Although similar, the methods are not identical and produce fractions that overlap those of other methods.

Corbett (61,62) used a densometric procedure coupled with molecular weight determination by VPO at 37°C to determine the structure of his fractions, as shown in Table 1. Asphaltenes could not be characterized completely because of the difficulties in molecular weight determination as a result of asphaltene molecular association.

Table 1 Fractions Obtained Using Corbett Analysis

Group	Wt% range	Average MW	Fraction aromatic	Rings/mole Naphthene	Rings/mole Aromatic	Descriptic
Saturates	5-15	650	0	3	0	Pure parafins + pure nap paraffin-naphthenes
Naphthene aromatics	30-45	725	0.25	3.5	2.6	Mixed paraffin-naphther sulfur-containing compo
Polar aromatics	30-45	1150	0.42	3.6	7.4	Mixed paraffin-naphther multiring structures + su nitrogen-containing com
Asphaltenes	5-20	3500	0.5	-	-	Mixed paraffin-naphther polycyclic structures + s nitrogen-containing com

Source: From L. W. Corbett, *Anal. Chem.,* 41(4):576-579 (April, 1969).

Table 2 (63) shows additional structural data estimated for the fractions. These results are all dependent on the composition of the source crude oil, particularly heteroatom content and metals. Both Ni and V are found primarily in the heptane-precipitated asphaltenes and are evenly distributed without regard to molecular size. They seem to be interchangeable in structure in that in fractions of a given asphalt the ratio of V to Ni is constant over wide ranges of composition. These metals often exist in porphyrin structures and have been implicated in higher rates of asphalt oxidation.

Heteroatoms are important because of an inordinate contribution to properties. Large increases in asphalt hardening occur with the uptake of only 1 wt% oxygen. Petersen (64,65) has done extensive work on heteroatom analysis. A typical analysis is shown in Table 3 (65). When asphalt oxidizes, the principle increase is in ketones and sulfoxides. Carboxylic acids and anhydrides tend to concentrate at the aggregate surface in asphalt concrete and may produce sensitivity to water damage.

Studies have shown that increases in asphalt viscosity with oxidation can be correlated with increases in carbonyl formation (20). Almost certainly this hardening results from hydrogen bonding between heteroatom groups in asphaltene molecules and also between polar aromatics, which then may become asphaltenes (66–69). This association strongly impacts attempts to measure molecular size by SEC or colligative properties.

There is considerable evidence that, contrary to the data in Tables 1 and 2 and much published data, the single asphaltene molecule is actually no larger than those of other fractions. Figure 1 shows an SEC chromatogram of a badly

Table 2 Elemental Characterization of Corbett Fractions

	Average number of atoms per molecule in			
Element	Saturates	Naphthene aromatics	Polar aromatics	Asphaltenes
Carbon				
Paraffin chain	31	21	24	85
Naphthene ring	14	17	18	29
Aromatic ring	0	13	25	115
Hydrogen	85	94	105	350
Sulfur	0	0.5	1	4
Nitrogen	0	0	1	3
Oxygen	0	0	1	2.5
Average molecular weight	625	730	970	3400

Source: From L. W. Corbett, *Proc. AAPT, 39:* 481-491 (1970).

Table 3 Distribution of Functional Groups in Fractions from Corbett Separation[a]

	Concentration in fraction (M)				
	Whole asphalt	Saturates	Naphthene Aromatics	Polar Aromatics	Asphaltenes
Ketones	0	0	0	0.11	Trace
Carboxylic acids	0.027	0	0	0	0.034
Anhydrides	0	0	0	Trace	Trace
2-Quinolone types	0.021	0	0	0.023	0.046
Sulfoxides	0.019	0	Trace	0.12	0.09
Pyrrolics	0.17	0	0	0.21	0.23
Phenolics	0.035	0	0	0.055	0.075

[a]Yield of fractions based on whole asphalt were saturates, 9.9%; naphthene aromatics, 25.3%; polar aromatics, 38.1%; asphaltenes, 21.6%; loss (which should be added to polar aromatics), 5.1%.

Source: From J. C. Petersen, *Trans. Res. Rec., 1096:* 1-111 (1986).

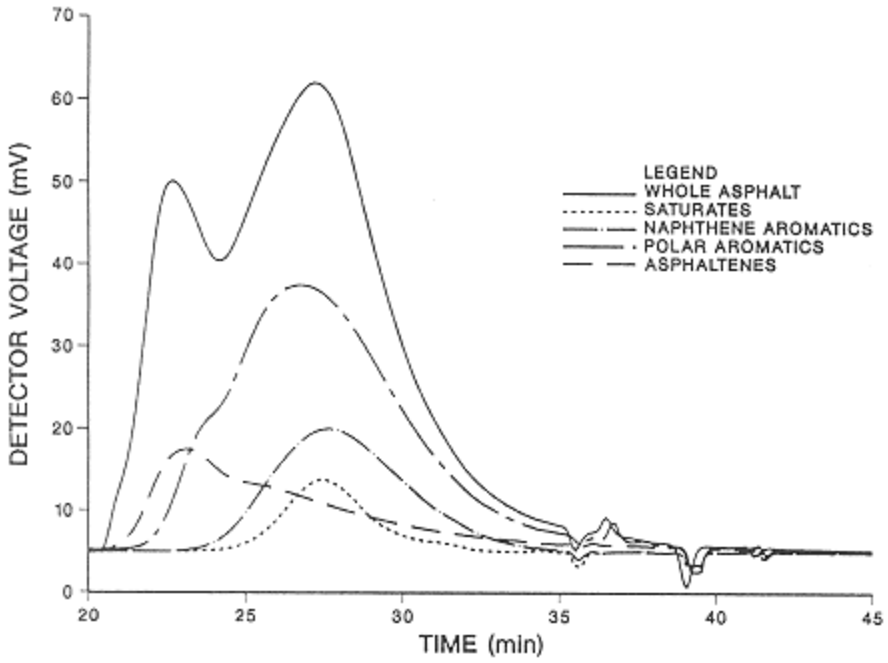

Figure 1.
SEC analyses of an aged asphalt and its Corbett fractions (500/50 Å 60 cm PLgel, THF at 1 ml/minute, 100 µl, RI detector). The whole asphalt is analyzed using a 7 wt% solution; the Corbett fractions are adjusted according to their weight fraction.

oxidized asphalt from a road core along with chromatograms of its Corbett fractions. It is seen that the saturates appear slightly larger than the naphthene aromatics. There is a shift to larger size with the polar aromatic fractions and a greater shift with asphaltenes, but it is these latter fractions that tend to associate, thereby giving a false impression of molecular size.

Boduszynski et al. (70,71), using field ionization mass spectroscopy (FIMS), obtained average molecular weights from 873 to 1231 for the Corbett fractions, with asphaltenes actually the smallest molecules. The VPO value for asphaltenes was over 4000. The values obtained for polar aromatics was 1020 by FIMS and over 1400 by VPO. Results for naphthene aromatics and saturates were quite close by the two methods. It should be realized that the designation of asphaltenes is arbitrary, depending on the precipitating solvent (72,73). Propane precipitates most of the polar aromatics, and pentane asphaltenes can be nearly twice the heptane asphaltenes.

Many of the properties of asphalt are determined by the variety of chemical types and their divergent properties. The asphaltenes and saturates are immiscible. Mixtures of asphaltenes and naphthene aromatics are highly non-Newtonian at 100°F, but polar aromatics and asphaltene mixtures are Newtonian (63). It has long been proposed (74,75) that asphalt exists as asphaltene micelles or clusters solubilized by polar aromatics.

Yen and associates (76–79), based on x-ray analysis, proposed that asphaltenes and resins (polar aromatics) existed as flat, condensed aromatic disks to which alkyl and naphthenic side chains were attached, forming a unit sheet. Through π bonding between aromatic sheets, and no doubt hydrogen bonding between heteroatom groups, the unit sheets arrange themselves in stacks, forming a particle or cluster. Unless two sheets are connected by a side chain, the unit sheet weight is approximately the molecular weight. In asphalt, polar aromatic sheets can combine in a stack with asphaltene sheets and, being less condensed, help to solubilize the asphaltenes in the remaining, less miscible fractions. When an asphalt is dissolved in a solvent, the polar aromatics may be extracted from the stack, causing the depleted asphaltene particles to clump, increasing apparent molecular weight and perhaps causing precipitation. Although Yen's work involves a number of structural assumptions, his unit sheet weights are similar to those obtained by FIMS and, like FIMS, yield higher molecular weights for resins than for asphaltenes.

Others (48,49,80–83), using nuclear magnetic resonance and elemental analysis with certain structural assumptions, have obtained very similar results for unit sheet weights. Several researchers have applied this procedure to asphalt fractions produced by preparative SEC. The unit sheet weights are always less than SEC- or VPO-determined molecular weights. Kiet et al. (49) found nearly constant sheet weights for his large molecular size fractions, which exhibited an over fourfold change in VPO molecular weights that he attributed to an increas-

ing number of sheets per stack in the heavier fractions. Haley (18) hardened preparative SEC fractions by air blowing: VPO molecular weights showed a considerable increase. The unit sheet weights increased for the heavier fractions, reflecting an increase in aromaticity and some cross-linking, but considerably less than the VPO molecular weights. It is clear that the tendency of both asphaltenes and polar aromatics to associate, which is affected by other asphalt constituents and the polarity of carrier solvents, has a number of implications for SEC analysis.

Applications of SEC to Asphalts

Asphalt Fingerprinting, Compositional Analysis, and Aging

Asphalt from each source crude oil has its own characteristic chromatogram that usually changes only slightly with grade. For this reason SEC is a very effective tool for detecting changes in asphalt as a result of processing changes, crude source, or contamination. Glover et al. (9) ran monthly SEC chromatograms on 11 asphalts for a period of a year. Each asphalt exhibited its characteristic shape, but some of these showed considerable seasonal change, probably reflecting processing changes. It must be emphasized that characterizations of this kind require that all SEC parameters be held constant. This is a major disadvantage, making comparisons difficult between laboratories and even over time. An asphalt standard should be run periodically to confirm constant operating parameters.

Low-molecular-weight contaminants, or any material having a narrow molecular weight range, produce a peak on the chromatogram and are easily detected, often at very low concentrations. Before asphalts from roads or hot-mix plants can be studied chemically, they must be separated from the aggregate. There are standard ASTM procedures for extracting the asphalt and then removing the extracting solvent. Burr et al. (17) showed that the standard procedures often left sufficient solvent in the asphalts to affect properties significantly. The literature is replete with work that has been marred in this manner. By using SEC, the solvent can be detected at low concentrations, and Burr et al. developed methods to assure complete solvent removal. It is prudent to use SEC routinely to assure complete solvent removal from recovered asphalt.

SEC analysis can be used very effectively in combination with Corbett separation, solvent or supercritical solvent fractionation, and other fractionation procedures for the purpose of understanding asphalt composition and aging. Figure 2 shows chromatograms for an asphalt cut into a 60% top fraction and a 40% bottom fraction by supercritical pentane (15). The top 60% was fractionated into four fractions by supercritical pentane (Figure 3), and the bottom

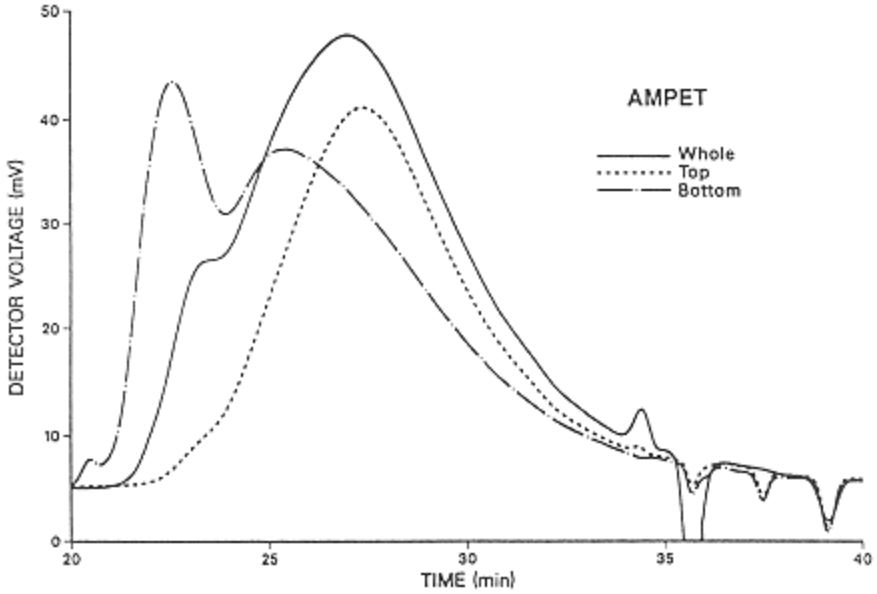

Figure 2.
SEC analyses of an asphalt and its light (top, 60%) and heavy (bottom, 40%) supercritically separated fractions (500/50 Å 60 cm PLgel, THF at 1 ml/minute, 100 µl of 5 wt% solution, RI detector).

40% was fractionated into four fractions by pentane and pentane-cyclohexane mixtures under ambient conditions. The slight hump in fraction 4 probably results from the small amount of asphaltenes in this fraction. Figure 4 show saturates and Figure 5 polar aromatics from the supercritically separated top fractions. The saturate curves are typical, being symmetrical and having relatively little variation in molecular size from one fraction to the next. The polar aromatics, in contrast, grow progressively higher in molecular size in heavier fractions and show signs of considerable association in the higher molecular size fractions by the growing hump in the LMS region. Asphaltenes (Figure 6) from fraction 4, separated from the top material, are markedly lower in size than the material from the fractions of the bottom 40%.

As asphalts age, the characteristic change to the SEC chromatogram is growth in the LMS region, which sometimes changes shape in the process. Figure 7 shows tank asphalts and cores for a single asphalt used in test sections at three Texas locations. The difference in the cores is primarily the percentage of air voids in the finished concrete. In 1987, the air voids at Lufkin were 1.8% and the 60°C viscosity was 5400 P. At Dumas it was 8.5% and 55,000 P, and

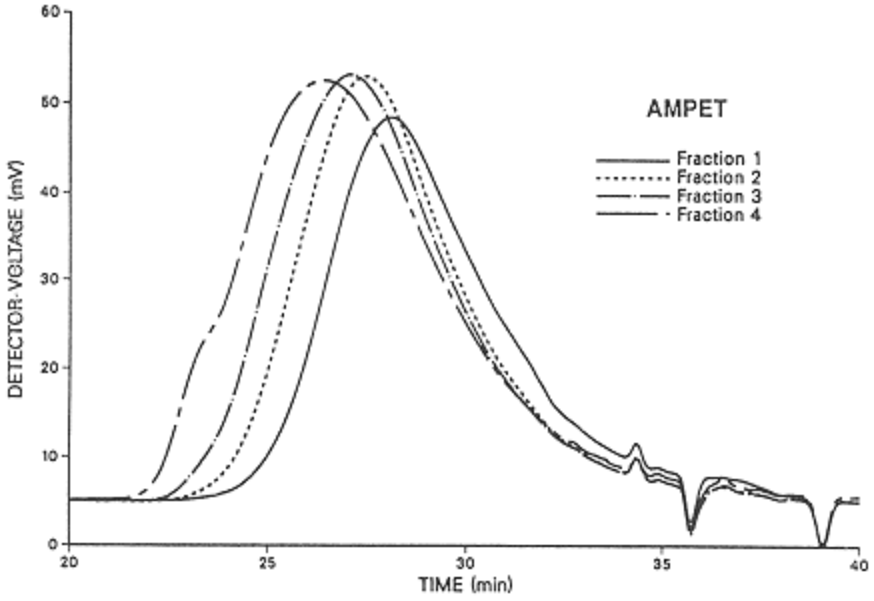

Figure 3.
SEC analyses of an asphalt's supercritical fractions 1–4 (500/50 Å 60 cm PLgel, THF at 1 ml/minute, 100 µl of 5 wt% solution, RI detector).

at Dickens it was 11% and 376,000 P. These differences are clearly shown in the chromatograms.

This percentage LMS growth is directly related to oxidation but may be highly asphalt dependent. Figure 8 shows the change in percentage LMS with growth in the carbonyl peak, an excellent measure of oxidation effects. The open circles in this figure include the data in Figure 7 and show a steady growth in the LMS region with carbonyl increase, but it is seen that with some asphalts, the growth in percentage LMS is small until higher levels of oxidation are reached.

Several tests, including SEC, were used to compare two standard oven aging tests (the thin-film oven test, TFOT, ASTM D 1754, and the rolling thin-film oven test, RTFOT, ASTM D 2872) and to determine their accuracy in simulating the changes that occur in the hot-mix plant (23). The tests were also performed at extended times, and these data are designated ETFOT and ERTFOT. Asphalts and hot-mix were taken from nine plants using six different suppliers and with two grades from one supplier. The asphalts were aged in the oven tests and compared using six parameters. Figure 9 shows the agreement in the percentage of LMS, and similar agreement was obtained for the other parameters, confirm-

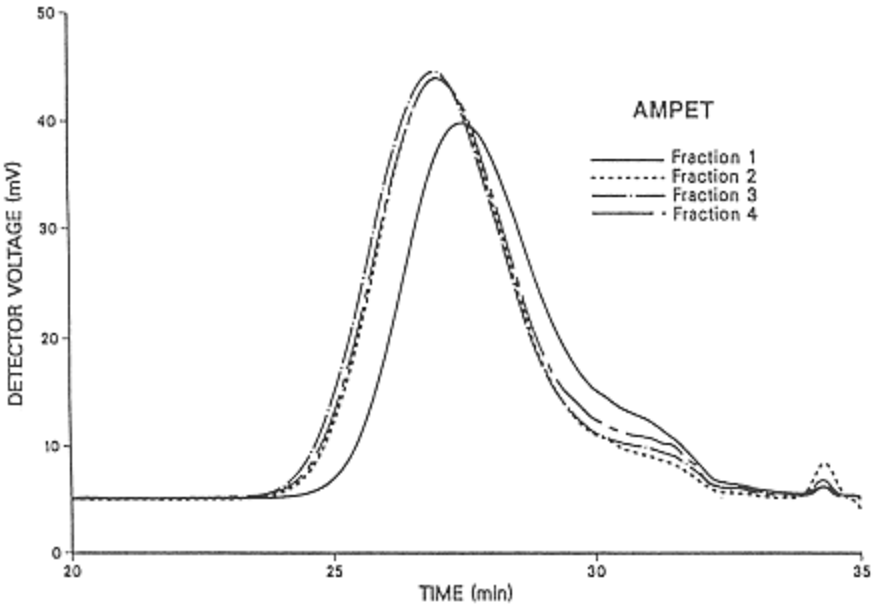

Figure 4.
SEC analyses of the saturates from an asphalt's supercritical fractions 1–4
(500/50 Å 60 cm PLgel, THF at 1 ml/minute, 100 µl of 5 wt% solution, RI detector).

ing that the oven tests are interchangeable. The oven tests were then compared to asphalts from the extracted hot mixes. Figure 10 shows the disagreement between the oven tests and the recovered hot-mix asphalts, disagreements confirmed by the other parameters as well. The tests were designed to reproduce the 60°C viscosity and does this reasonably well, but obviously not by the same mechanisms.

Asphalts also tend to age on contact with solvents, and this is manifested by both viscosity and LMS increases. Simply dissolving an asphalt in a good solvent and recovering it immediately produces about a 10% viscosity increase; 2 days contact at room temperature causes a 50% or greater increase in viscosity. If samples are made and run immediately or within hours at room temperature, the effect on the SEC chromatogram is negligible, but days or even hours at a higher temperature can produce significant growth in the LMS region.

The Corbett analysis of an asphalt is also altered by aging. In Figure 11 chromatograms are shown of Corbett fractions of a tank asphalt and a 1984 core from one of the Texas test sections. As expected, there is no change in the saturates. There is a decrease in quantity but not in elution time for naphthene aromatics. The polar aromatics change little in quantity as material is gained

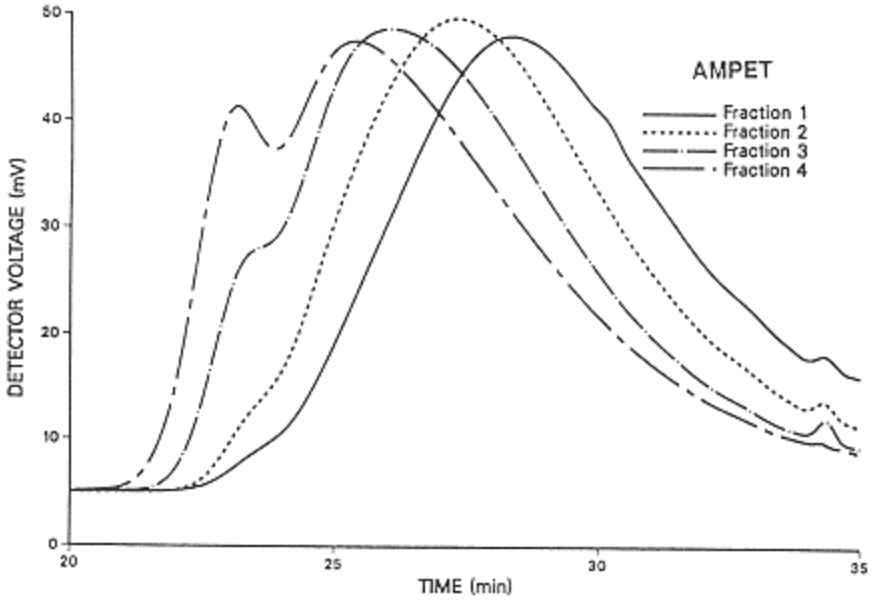

Figure 5.
SEC analyses of the polar aromatics from an asphalt's supercritical fractions 1–4
(500/50 Å 60 cm PLgel, THF at 1 ml/minute, 100 µl of 5 wt% solution, RI detector).

from the naphthene aromatic fraction and lost to the asphaltenes. Despite this considerable shifting of material, the elution time is little changed. There is an increase in the asphaltene content and a slight shift to shorter elution times. This reflects a higher oxygen content and greater association. The large tailing effect with asphaltenes is probably caused by column adsorption.

Use of SEC to Predict Pavement Performance

Plummer and Zimmerman (29) studied roads in Michigan and Indiana and found that an increase in the LMS region correlated with increased cracking. Hattingh (21) found that in the hot South African climate roads with a low asphaltene content and a small LMS region were subject to bleeding. By far the most extensive effort of this kind is that of Jennings and coworkers, conducted primarily in Montana but extended nationwide. The principal road problem addressed was that of cracking.

A total of 39 roads in Montana constructed with asphalt from four refineries were cored, extracted, and analyzed by SEC (26,31). The condition of the roads was noted and categorized as excellent, good, poor, or bad based on both the age of the pavement and the extent of cracking. A 19-year-old road in excellent

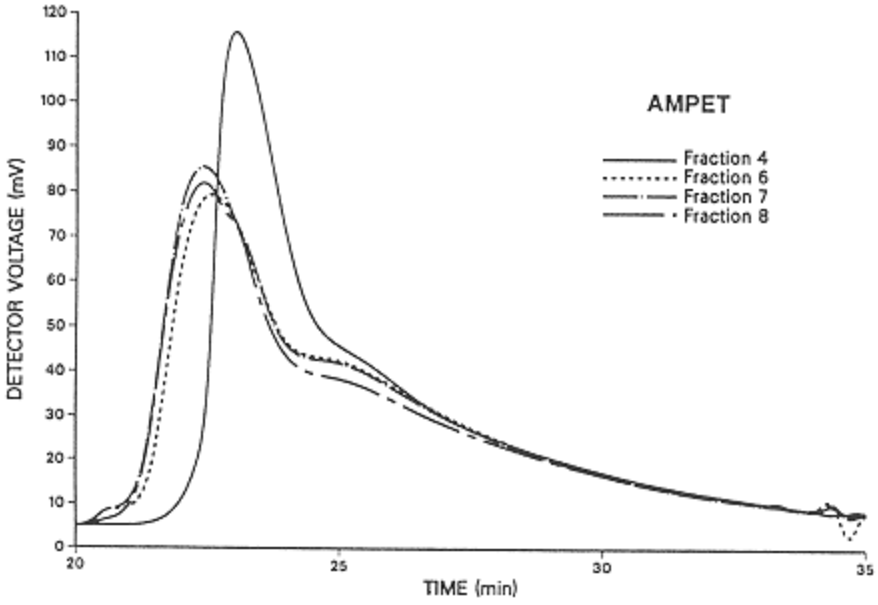

Figure 6.
SEC analyses of the asphaltenes from an asphalt's fractions 4 and 6–8 (500/ 50 Å 60 cm PLgel, THF at 1 ml/minute, 100 µl of 5 wt% solution, RI detector).

condition was chosen as a standard. It had a low LMS region, and a high degree of correlation was found between the condition of the other roads and the similarity of their SEC chromatograms to that of this standard, particularly in the LMS region. This is clearly seen in Figures 12 and 13, in which the standard is labeled Gallatin Gateway-South. A correlation with the percentage of asphaltenes was also found, which is not surprising because the percentage asphaltenes and percentage LMS region are strongly correlated, although not all asphalts fit. Based on these results, a range of the LMS region from 8 to 10% and an asphaltene content from 12.5 to 16.5% was recommended for Montana roads.

Jennings and Pribanic (34) expanded this study to include samples from 15 other states. The nation was divided into zones of similar climate, and the condition of roads within each zone was compared on the basis of the molecular size distribution. In general, in each zone there was a percentage of LMS above which all roads were poor or bad, and most of the good and excellent roads were those of lower percentage LMS. However, there was a very large difference between the percentage of LMS that could be tolerated in warm zones and that in very cold zones. Furthermore, there was evidence from the warm zones that too low a percentage of LMS correlated with rutting.

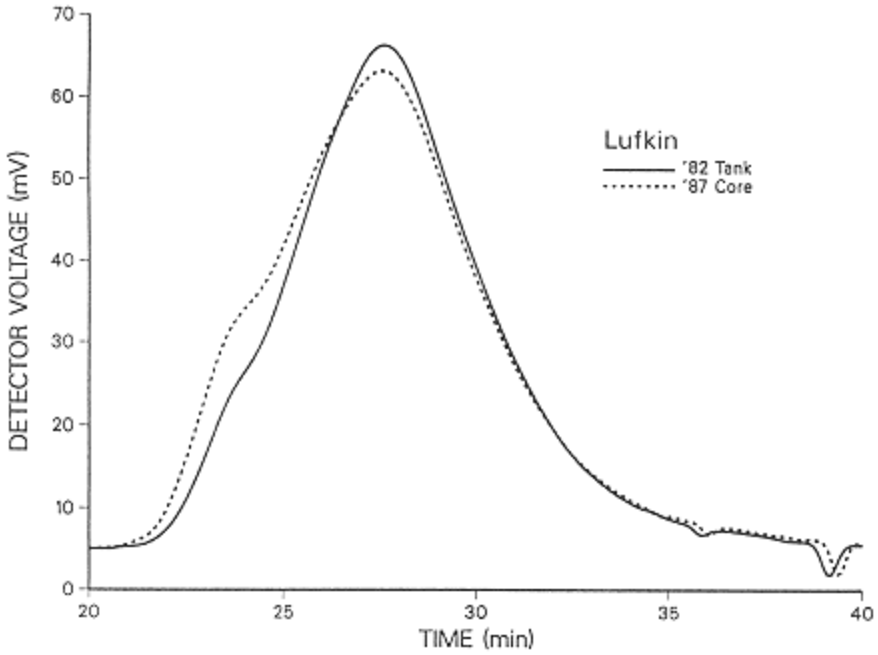

Figure 7.
SEC analyses of an unaged asphalt and its aged binder recovered from highway test pavements at three locations (500/50 Å 60 cm PLgel, THF at 1 ml/minute, 100 µl of 7 wt% solution, RI detector).

There were many exceptions, particularly poor and bad roads with low percentage LMS, but of course there are many factors unrelated to asphalt quality that can cause road failure. Jennings presented evidence that some asphalts failed because of poor viscosity temperature susceptibility even though having a satisfactory percentage of LMS.

There have been objections to this approach (16), partly because of the arbitrariness of the procedure in which the percentage of LMS is very much an artifact of the SEC operating parameters. It is also thought that it is the mechanical properties that cause failure, and these do not correlate well with chemical properties, such as SEC; thus if ex post facto measurements are to be used, they may as well be the physical properties of the old asphalt. There are several studies that indicate that there is a limiting ductility below which all roads fail (84,85). It has been suggested (86) that penetration at 4°C, a good predictor of the limiting stiffness temperature, be used to predict the tendency to crack.

There are other problems in that some asphalts with a very high percentage of LMS do not fit at all; the black circles in Figure 8 are for a good-performing

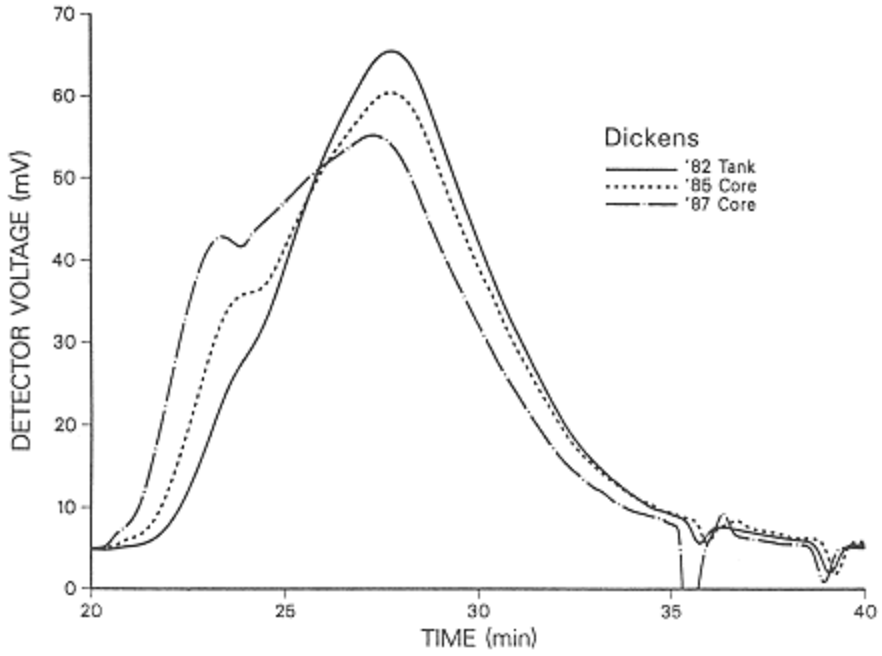
Dickens
'82 Tank
'85 Core
'87 Core
DETECTOR VOLTAGE (mV)
TIME (min)
0
10
20
30
40
50
60
70
20
25
30
35
40

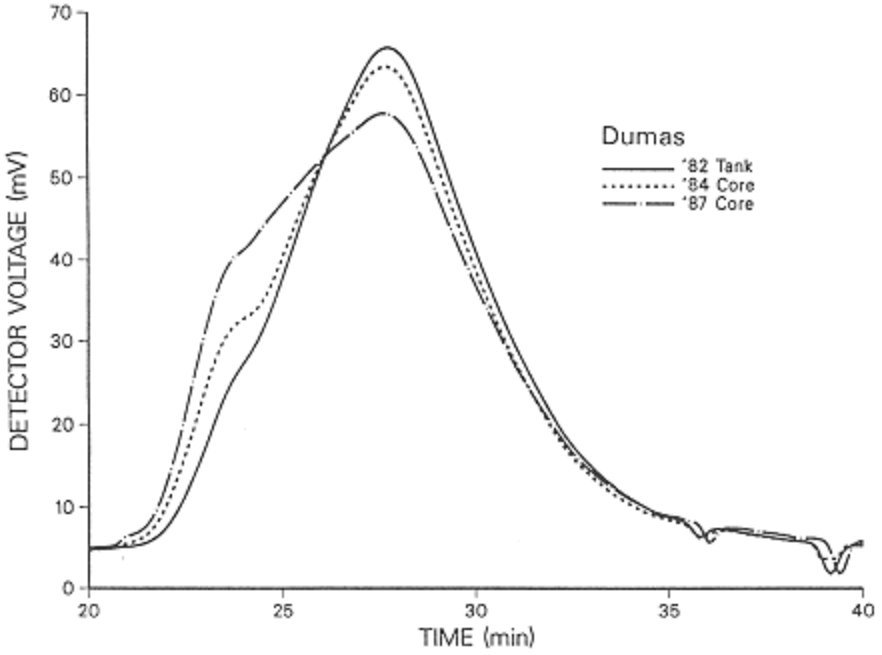
Dumas
'82 Tank
'84 Core
'87 Core
DETECTOR VOLTAGE (mV)
TIME (min)
0
10
20
30
40
50
60
70
20
25
30
35
40

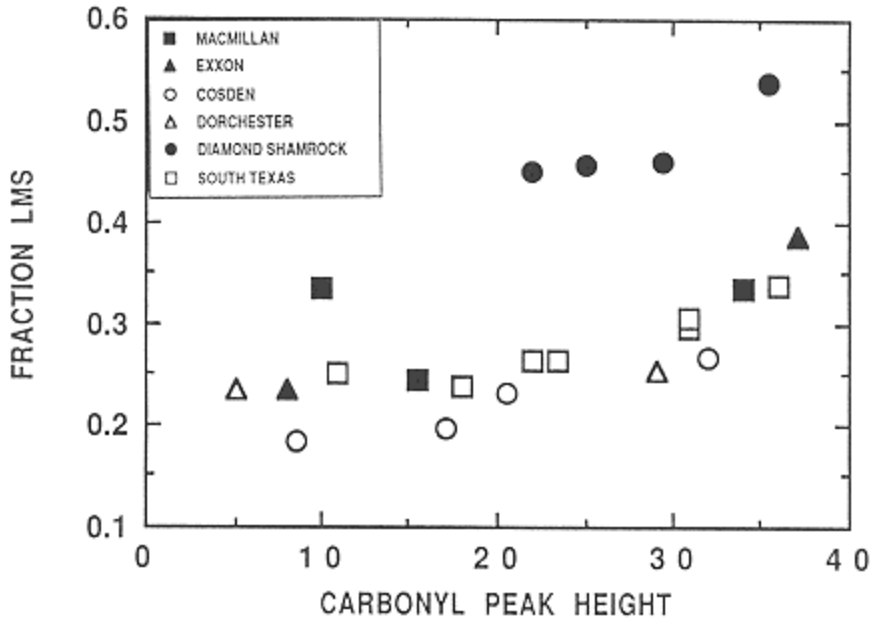

Figure 8.
SEC LMS fraction versus Fourier transform infrared spectroscopy carbonyl peak height for asphalts recovered from aged pavement cores (500/50 Å 60 cm PLgel, THF at 1 ml/minute, 100 µl of 7 wt% solution, RI detector).

asphalt of very high percentage LMS. The use of old road data is also a problem, whether for percentage LMS or physical properties. Figure 7 shows that the same asphalt can have greatly different percentages of LMS at the same age depending on nonasphalt factors. High-percentage LMS is an indication of aging without regard to what caused it. In the Texas study, the asphalts at Lufkin all had lower percentage LMS because they were not aging. The same asphalts had much higher percentage LMS at the other locations. Even so, Jennings' results are too impressive to be ignored.

As noted, Jennings also found some connections between rutting and a low LMS region. This is confirmed by the data in Figure 14. Here six asphalts have been rated by users according to “tenderness” (slow setting that can result in rutting). A high score indicates tenderness. Clearly there is a correlation between the tenderness rating and the size of the LMS region.

Jennings has also done some work with asphalt recycling. In this process old road material in bad condition is stripped from the roadway, mixed with a softening agent, and relaid. Sufficient new material is generally added to restore viscosity and ductility to levels approximating those of new asphalt. This does

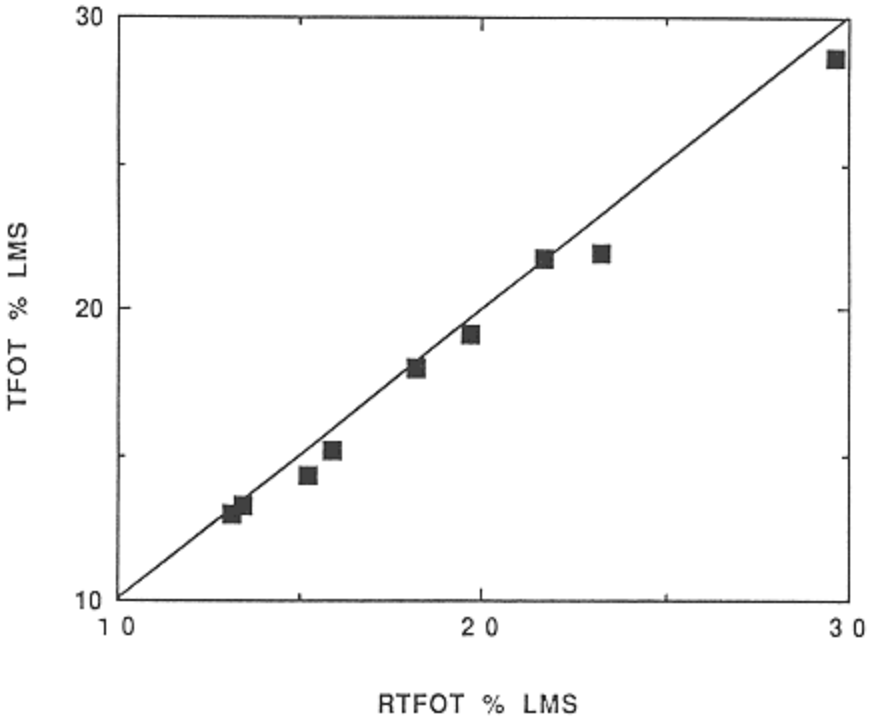

Figure 9.
Comparison of percentage LMS for TFOT- and RTFOT-aged asphalts
(500/ 50 Å 60 cm PLgel, THF at 1 ml/minute, 100 µl of 7 wt% solution,
RI detector).

not usually reduce the percentage of LMS to that of new asphalt. One roadway done with a commercial recycling agent having 0% LMS showed a high percentage of LMS even though the resulting mixture was quite soft. Unfortunately, there are not as yet any performance results from these roads.

Correlating Physical Properties with SEC Results

Attempts to correlate asphalt physical properties with chemical properties have not been particularly successful. This no doubt is primarily the result of the lack of uniqueness in the chemical properties that are used. For instance, a Corbett fraction from one asphalt may have very different physical properties from those of the same fractions from another asphalt. Also, two asphalts with similar physical properties can have radically different SEC chromatograms.

Bishara et al. (39,40) report good correlation of viscosity temperature susceptibility and LMS to medium molecular size ratio.

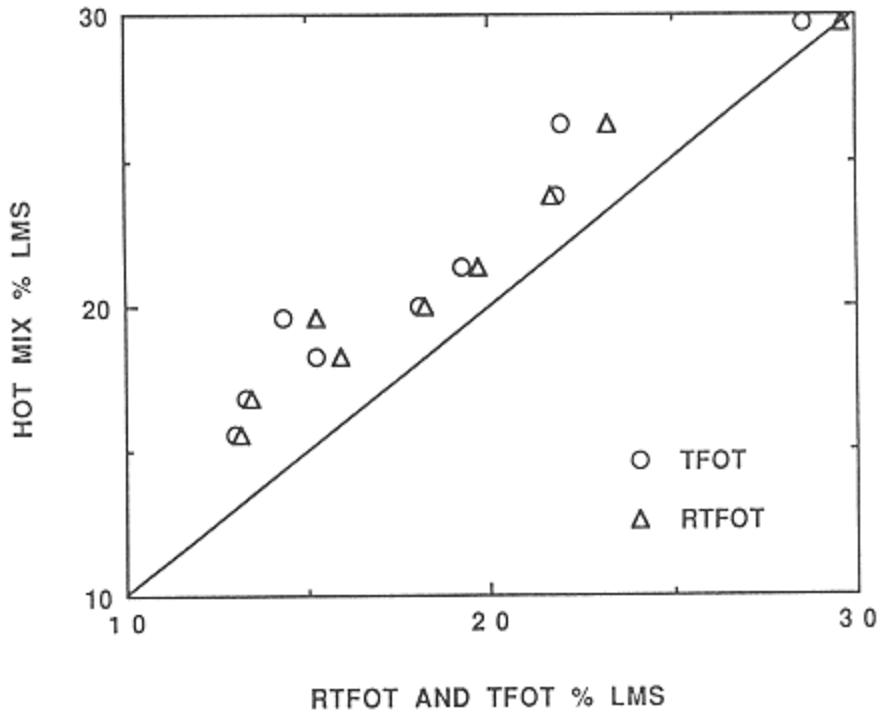

Figure 10.
Comparison of percentage LMS for hot-mix and oven-aged asphalts (500/ 50 Å 60 cm PLgel, THF at 1 ml/minute, 100 µl of 7 wt% solution, RI detector).

The viscosity temperature susceptibility from 60 to 135°C of the Texas test section tank asphalts were correlated with percentage LMS and percentage small molecular size using both THF and toluene as carriers. The penetration index would not correlate, and later attempts to extend this to aged asphalts were not successful. Inclusion of other parameters can improve results. For instance, the viscosities of all the asphalts represented in Figure 8, except the anomalous Diamond Shamrock (black circles), were correlated by log viscosity at 60°C = $A + B$ (% LMS)$^{-0.6}$ + C(IR)$^{0.9}r^2 = 0.968$, in which IR is the area of the carbonyl peak. Infrared carbonyl area and Heithaus parameters (a measure of asphalt compatibility) were more successful in correlating other properties than percentage LMS. The carbonyl peak was one of the best parameters, and because it is strongly cross-correlated with percentage LMS, the efficiency of the latter is affected.

Because of the crudeness of representing the shape of the SEC chromatograph by three sections, Garrick and coworkers (36–38) divided the total area

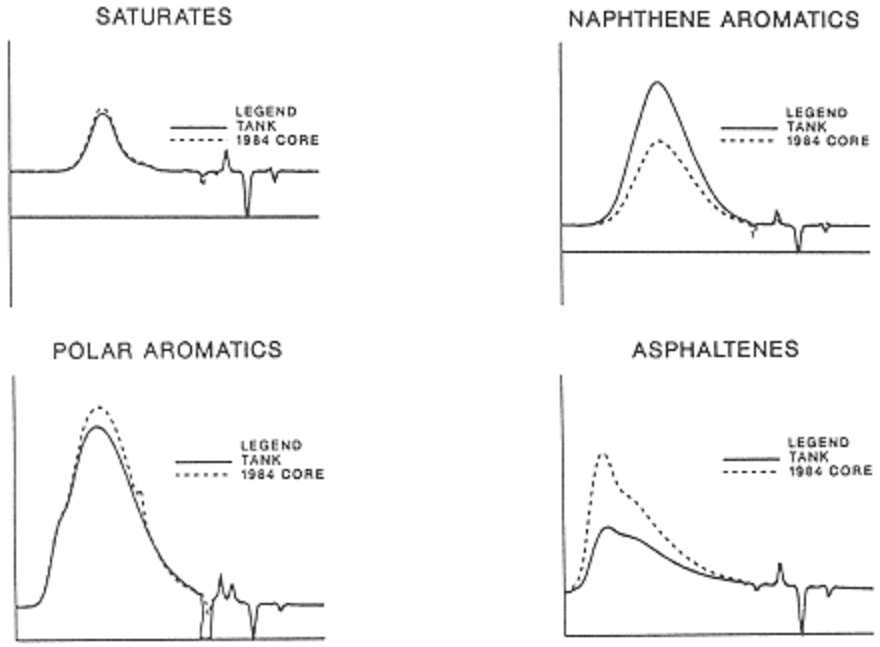

Figure 11.
Comparison of SEC chromatograms of Corbett fractions for an unaged and aged (recovered pavement binder) asphalt (500/50 Å 60 cm PLgel, THF at 1 ml/minute, 100 µl, RI detector). The solution concentrations are adjusted according to each Corbett fraction's weight fraction in the asphalt.

into eight sections. Correlations are then attempted using some or all of the sections as parameters. Some reasonably good correlations were obtained, but the number of parameters is large, the choice of correlating sections seems almost random, and the range of variables is not very great. The question remains as to what extent this is an artifact of the procedure both as to choice of correlating parameters and SEC operating conditions.

Determination of Asphalt Molecular Weight Distribution

Because SEC responds directly to apparent molecular size, it appears to be a simple method for obtaining the molecular weight distribution of asphalt. However, it turns out not to be a straightforward determination for a number of reasons. The first, already discussed, is that some asphaltic fractions associate in solution. These same fractions also may tend to be adsorbed in the column. A final factor is the chemical complexity of asphalt. It is well known that the order of elution of polar and nonpolar compounds can be considerably altered

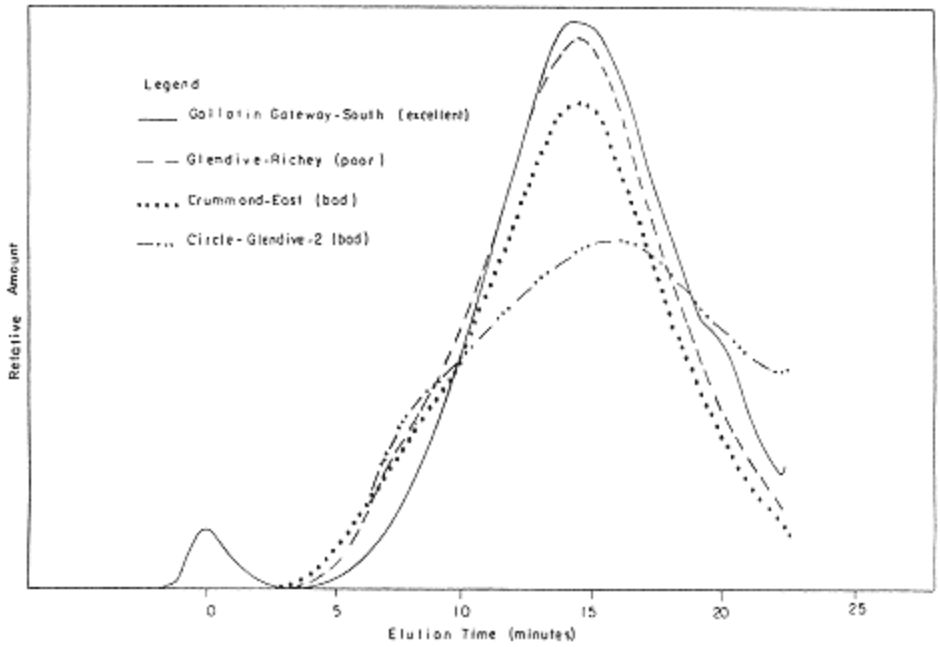

Figure 12.
Comparisons of SEC chromatograms using a refractive index detector of asphalt from Montana roads for the chosen standard and three poorly or bad-performing pavements. The small peak at zero time is a polystyrene standard. (Reproduced from Reference 31, p. 23, by courtesy of the authors.)

by changing solvents, so it is difficult to choose calibrating compounds for such a complex mixture.

The common calibration procedure for asphalt depends on preparative SEC fractionation. Fractions thus obtained are then subjected to analytical SEC analysis to obtain mean elution values, and the fraction molecular weights are determined by an independent method, such as VPO. In general, a single plot of molecular weight versus elution volume holds rather well for most asphalts (12), but upon aging asphalts by air blowing, a series of such curves is produced for different degrees of hardening (18).

Molecular weight-elution volume curves are actually very sensitive to composition. Champagne et al. (51) plotted molecular weight versus retention time for a series of pure compounds along with polystyrenes, obtaining separate and distinct curves for the polystyrenes, long-chain asphaltenes, and nonfused polyaromatics. For fused polyaromatics scatter was obtained.

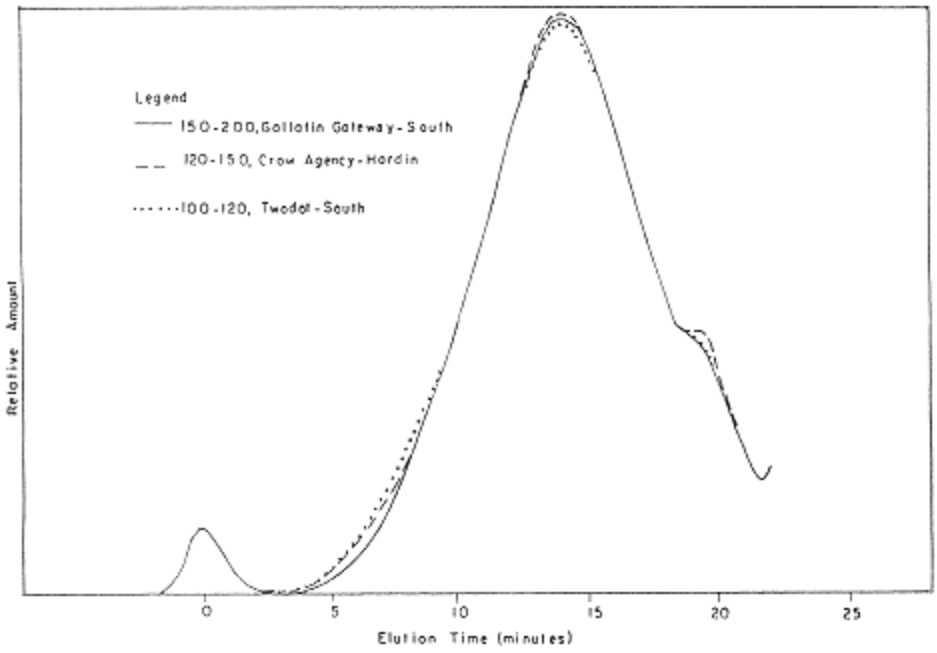

Figure 13.
Comparisons of SEC chromatograms using a refractive index detector of asphalts from Montana roads for the chosen standard and two excellent- or good-performing pavements. The number range for each sample is the binder penetration grade, and the small peak at zero time is a polystyrene standard. (Reproduced from Reference 31, p. 29, by courtesy of P. W. Jennings.)

The SEC elution times are dependent on molecular hydrodynamic volume rather than molecular weight, *M*, as is the intrinsic viscosity, [η]. Thus the idea of a universal calibration curve is proposed (53) in which log [η]*M* is plotted versus the elution volume. Brulé (12) shows a single curve for a number of asphalts, although it still deviates from the universal curve established for polystyrene or other polymers (49). In fact, there is considerable deviation from the universal curve for aromatic and highly condensed compounds (54,87).

There are a variety of limitations for any SEC asphalt calibration procedure. First, it is no better than the method used to establish the fraction molecular weights. This in turn is affected by the solvent, the concentration, and the temperature, with no certainly that complete dissociation has been attained. The SEC chromatogram is also affected by all these conditions plus others imposed by the column and detector.

Both Girdler (45) and Speight (46) published data showing an enormous range of asphalt molecular weights determined by various methods. Table 4 shows a summary of some of these data in which the entries are average molecular weights for 14 asphalts measured by VPO. Molecular weights so determined usually decrease with decreasing concentration; elution times for large, associating material tend to increase with greater dilution. However, Moschopedis et al. (88) show that even if the molecular weight does not decrease with

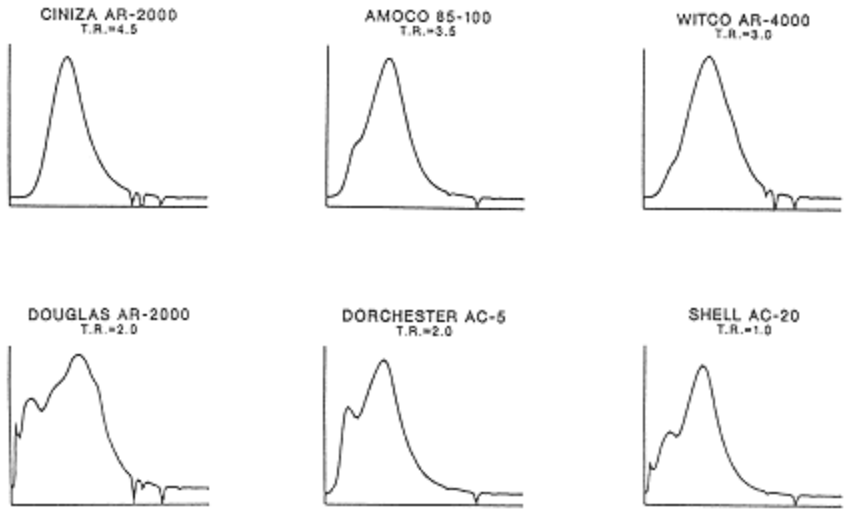

Figure 14.
Comparison of SEC chromatograms to tenderness rating for six asphalts (500/50 Å 60 cm PLgel, THF at 1 ml/minute, 100 µl of 7 wt% solution, RI detector).

Table 4 VPO Molecular Weight Variations with Solvent Properties

Solvent	Temperature (°C)	Molecular weight
C_6H_6	37	5047
CH_2Br_2	37	4015
C_2H_5N	37	2766
$C_6H_5NO_2$	100	1900
$C_6H_5NO_2$	115	1857
$C_6H_5NO_2$	130	1798

Source: From Reference 88.

dilution in one solvent, it may still show a much lower molecular weight in another. Thus, regardless of how measured, molecular weights for associating species are dependent on the parameters used in the procedure. The same is equally true for the shape of the SEC chromatograms.

Generally, the parameter set in the molecular weight determination that yields the lowest value is preferred, bearing in mind that any method based on colligative properties is very sensitive to low-molecular-weight contaminants, such as solvents. Similarly, the SEC parameters giving the largest elution volume should be preferred, except that column adsorption will increase the elution volume. Fortunately, solvents that minimize association also tend to minimize adsorption. Thus, using a very good solvent for the associating species at a low concentration may give molecular weight values approaching complete dissociation. The lowest values in Table 4, for instance, are still about twice the values obtained by Boduszynski et al. (70) using FIMS.

The chief utility of SEC in molecular size distribution measurements is not to obtain absolute values but to measure the degree of association in asphalts of different properties and composition, particularly to note the changes that occur during aging. It is likely that the effect of solvent power on the change in apparent molecular size carries information about the internal stability of the asphalt.

Solvent and Concentration Effects

Choice of the solvent system is of great importance, particularly with a complex material like asphalt. The solvent system includes not only the solvent but also the concentration, temperature, sample size, and even the flow rate because of effects apart from the effect on column performance. All these factors interact to determine the solution characteristics on which the column must act. The key factors are the tendency of polar materials in asphalt to associate and to be adsorbed on the column. To a lesser, but still important extent, the results are also affected by interactions with the solvent that affect the apparent hydrodynamic volume. For instance, associating substances, such as asphaltenes, show much higher molecular size in a poor solvent, but a smaller size polar substance, such as a C_{12}–C_{18} normal alcohol, shows a considerably larger elution time (smaller size) in, say, toluene than in THF, even though the latter is a better solvent for alcohols.

Association is such an important characteristic of asphalts, believed by many to be an indicator of asphalt performance, that attempts have been made to use poorer solvents to emphasize this feature. Unfortunately, poorer solvents lead to column fouling and bad tailing of the adsorbed material. Figure 15 is an extracted core asphalt and its Corbett fractions run in toluene and is similar to

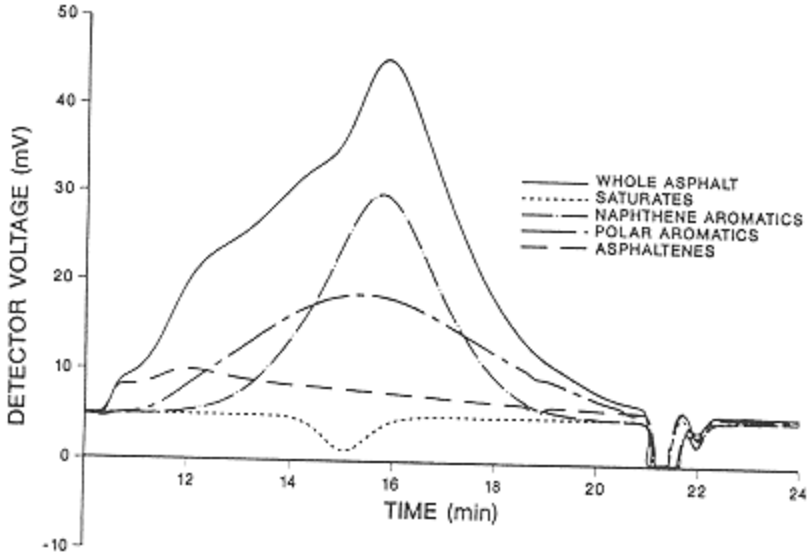

Figure 15.
SEC analyses of the same samples as in Figure 1 with a toluene carrier solvent (500 Å 60 cm PLgel, toluene, 1 ml/minute, 100 µl, RI detector). The whole asphalt is analyzed using a 7 wt% solution; the Corbett fractions are adjusted according to their weight fraction.

the material in Figure 1. In both instances the asphaltenes tail badly, but in toluene this is the predominant effect, largely displacing the larger material to much lower apparent size.

All the evidence discussed previously indicates that if SEC is to be employed in molecular weight determinations the best solvent system for the associating material should be used. These include data at low concentrations and extrapolation to infinite dilution. Elevated temperatures probably help, but the choice of solvent is especially important.

There are two particularly useful schemes for choosing solvents. The oldest is the solubility parameter method of Hildebrand and Scott (89) with the modifications of Hansen and colleagues (90–92). Hildebrand's solubility parameter is based on the internal pressure, defined as the square root of the molar internal energy of vaporization divided by the molar volume. Strictly speaking, the formulation applies only to solutions having an ideal entropy of mixing, but in fact it is also remarkably good for a wide range of nonpolar and weakly polar mixtures. In the modification of Hansen it is assumed that the effective solubility parameter can be divided into three factors resulting from dispersion forces,

polarity, and hydrogen bonding. The dispersion forces were estimated from the hydrocarbon homomorph. The polar factor was calculated from theoretical considerations based on measurements of dielectric constant, dipole moment, and refractive index. It is then assumed that the measured parameter is the sum of the dispersive, polar, and hydrogen bonding components, and the latter is calculated from the difference. The parameter has found many applications and was applied to asphalt by Hagen et al. (93). In this treatment the polar and hydrogen bonding components were combined and solubility correlated on a two-dimensional scale. They found that asphalt solubility correlated on a two-dimensional plot. The maximum solubility occurred in a region occupied by such solvents as THF, chloroform, and toluene. That these solvents are far from equal shows the imperfections in the system, but they also found that as the asphalts aged, the maximum solubility moved in the direction of an increasing hydrogen bonding parameter.

The significance is that the material exhibiting maximum association is also the most oxidized material, and the solvent should be chosen for this material, not the whole asphalt. Thus with increasing oxidation, a solvent of increasing hydrogen bonding should be chosen. This is seen in the data of Cipione et al. (94), in which the highly oxidized material, which is most tightly bound to the aggregate in aged asphalt concrete, is much better extracted if ethanol is added to the solvent.

A second useful treatment is that of Snyder (95), in which solvents are evaluated on the basis of a polarity index calculated from the solvent interaction with three test solutes, dioxane, ethanol, and nitromethane. Figure 16 (12) shows an SEC chromatogram of an asphalt for the four solvents indicated. The results show significant decrease in association at 800 Å as one goes from tetraline to benzonitrile. Although tetraline has the lowest dielectric constant and benzonitrile the highest, the order is reversed for THF (E = 7.25) and chloroform (E = 4.806). On the basis of Snyder's polarity parameter P', however, the order is THF (P' = 4.2) chloroform (P' = 4.4), and benzonitrile (P' = 4.6), which agrees with the 800 Å order.

As with any system, the effect of sample size depends on the response characteristics of the detector, but with asphalt this is complicated by the greater association in more concentrated solutions and the dissociation kinetics following injection. There is usually a decrease in the percentage of LMS as lower concentrations are injected.

Flow rate has much the same effect. Brulé (12) injected the same sample size at different flow rates and found that the percentage of LMS increased with flow rate. Despite the great dilution in the carrier solvent, the dissociation rate is sufficiently slow that the results largely reflect the state in the injected solution. Thus the faster the flow, the less dissociation had occurred.

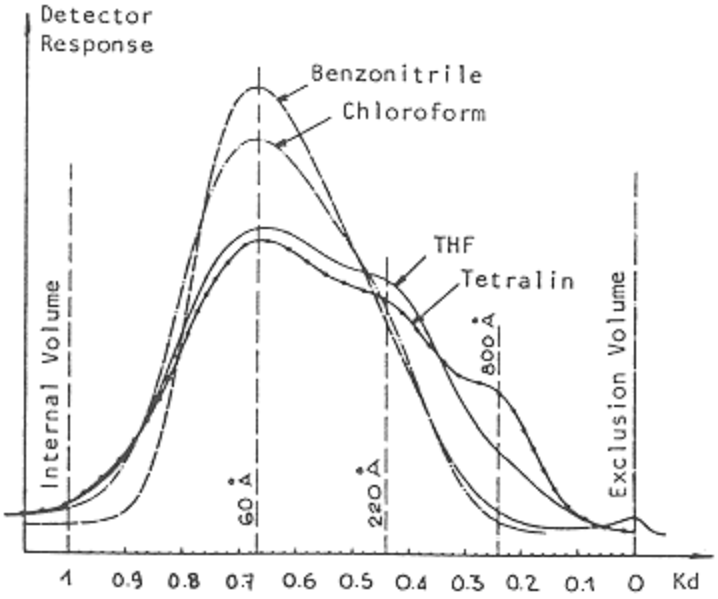

Figure 16.
Comparisons of asphalt SEC chromatograms using four different carrier solvents. (Reprinted from Reference 12, p. 225, by courtesy of Marcel Dekker, Inc.)

Brulé also ran asphalt samples at extended intervals following preparation: 4 h and 7, 14, and 21 days. In these samples the LMS region increased with aging. This involves the phenomenon of solvent hardening that occurs, particularly in dilute solutions, in all solvents and increases rapidly with increasing temperature. Burr et al. (25) gave results for a variety of solvents and asphalts, but of particular significance is the infrared spectra for five asphalts after 2 days at room temperature in 15% ethanol in trichloroethylene. The viscosity of the recovered asphalts increased from 50 to 90%, and all but one of the asphalts showed significant changes in infrared spectra. The changes were different for each asphalt, however, and were not correlated with the viscosity changes. Because the exposure to solvent changes the SEC chromatograms with time, samples should generally be run the same day they are prepared.

Detectors and “Mass Detection”

Researchers have used a wide variety of detectors to analyze asphalts in GPC studies. Generally, the aim is to characterize rapidly the molecular or, more correctly, the apparent size distributions. This implies the need to determine the

concentration of asphalt in the eluant, which in turn requires a detector having uniform sensitivity to mass at all retention times and for all types of asphalts, regardless of differences in the materials' functionalities and degrees of molecular association. Such an ideal detector would be a true mass detector. Because of asphalt's complicated structure and composition, all detectors used to analyze asphalts by GPC fall short of being true mass detectors (46,96,97). Consequently, no single detector has gained universal appeal.

By far, the most popular on-line detectors for asphalt GPC are the differential refractive index (RI) and the ultraviolet absorption (UV) detectors. The RI detector measures differences in refractive index between the pure carrier solvent and the GPC eluant. These differences are related to the amount of solute in the eluant. The UV detector measures the eluant's absorbance of UV light at a selected wavelength. Here also, the response is related to sample concentration for a given solute.

Asphalt contains many different compounds that vary not only in molecular, or particle, size but also in UV absorptivity or refractive index. Figure 17 shows the relation between detector response per unit mass and apparent molecular size for some asphalts (12). Neither detector is uniform, as a mass detector would be. The UV detector is much less uniform than the RI detector. This is mainly because paraffinic hydrocarbons, known as saturates, which comprise roughly 10–20% of a typical asphalt, are very weak absorbers of UV light, and the aromatic components in the asphalt are strong UV absorbers. Consequently, a

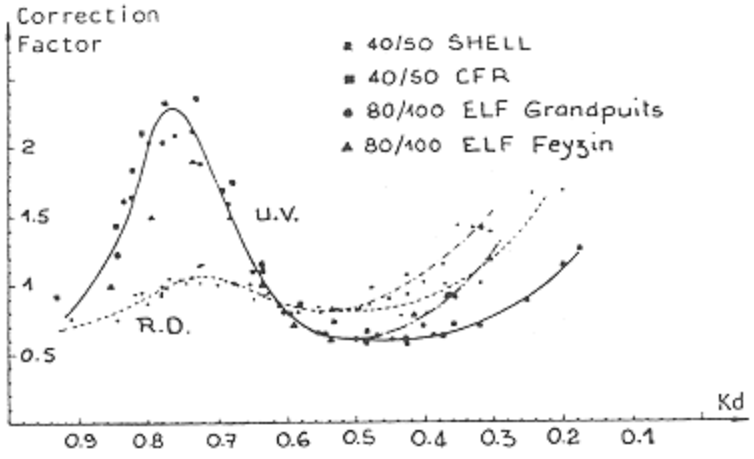

Figure 17.
Comparison of the response of UV and RI detectors to materials of different apparent molecular size. (Reprinted from Reference 12, p. 239, by courtesy of Marcel Dekker, Inc.).

UV detector's response to a saturate is much less than to an aromatic compound (96,98). The effect of molecular association (which occurs in the large molecular size region) on detector sensitivity is probably significant but is not well understood (46,57,59).

The RI and UV detectors are popular because they are commonly used in other high-performance liquid chromatography applications, relatively inexpensive, reliable, and easy to operate. The UV detector is preferred by some because it has much lower detection limits, whereas others prefer the RI detector because it has more uniform response across the entire range of asphalt constituents. The multiple-wavelength UV detector simultaneously scans several wavelengths in the UV and visible spectra. Spectra from this detector provide information about which size of molecules, or particles, contain certain UV-sensitive functionalities. Vanadyl porphyrins, for instance, have specific UV absorbances at 410 nm and are suspected of affecting asphalt aging processes. The multiple-wavelength UV detector shows (Figure 18) that the vanadyl porphyrins are present at all molecular sizes but are concentrated in the small molecular size region (99).

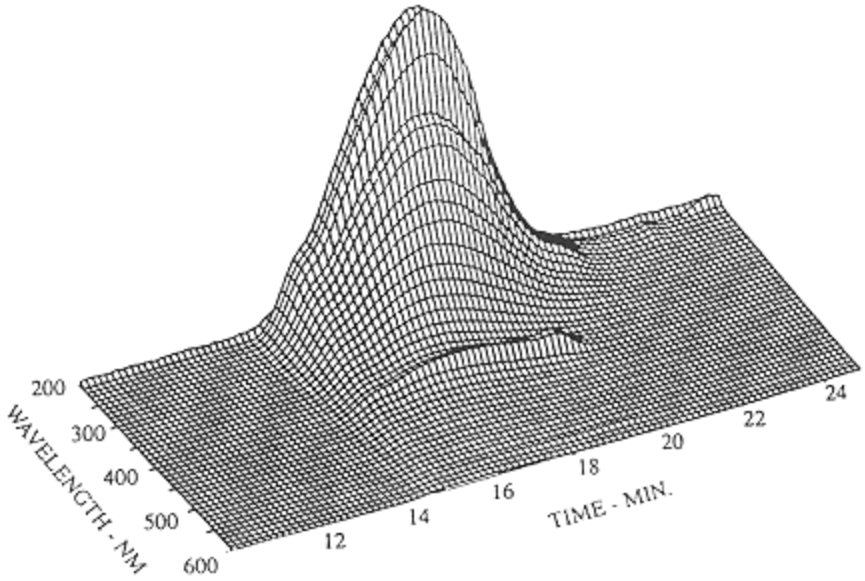

Figure 18.
SEC chromatogram for an asphalt using a multiple-wavelength UV detector
(Reprinted from Reference 99, p. 172, by courtesy of Joan A. Pribanic.)

Recently, several evaporative on-line detectors have been developed and reported to be true mass detectors. However, when applied to asphalts and heavy petroleum fractions, these detectors' responses show signs of being solute dependent.

Two types of evaporative flame ionization detectors (FID) are the moving wire (100,101) and the rotating disk detectors (102–104). These convey the eluant along a wire or quartz disk into an evaporation chamber, where the volatile carrier solvent is removed. The nonvolatile sample is then passed through an FID. Any unburned sample is removed in an ashing chamber before the wire or disk returns to its eluant-collecting position.

The FIDs rely only on the amount of combustible material present, rather than light absorption or refraction characteristics of the solvent. This should make them respond more uniformly to mass over the particle size spectrum than RI or UV detectors. However, the literature indicates that nonuniformities are still a problem. Saturates and aromatics gave different response factors, possibly as a result of different carbon-hydrogen ratios in the materials. The differences in response were comparable to those in RI or UV detectors. These detectors are generally more expensive and more difficult to operate than RI or UV detectors, however.

Another evaporative on-line detector is the evaporative light-scattering detector (ELSD) (97,104–107). In the ELSD, the eluant is nebulized with an inert gas to form an aerosol. The solvent in the dispersed eluant droplets is evaporated and removed in a heated chamber. The resulting solute particles fall through a light-scattering detector. The scattered light is related to the amount of mass in the particles, which in turn corresponds to the amount of solute in the eluant.

The light scattering is supposed to be minimally dependent upon the structure and functionality of the solutes. The sparse literature pertaining to asphalt and heavy petroleum fractions indicates that the detector's response varies with different solutes, however. Pentane solubles gave markedly lower response than asphaltenes and benzene insolubles. The response to pentane solubles also varied with evaporator temperature, which is usually a sign of solute loss by evaporation. This seems unlikely with a material as nonvolatile as asphalt. Like the evaporative FIDs, the ELSD is more expensive and more difficult to operate than the RI or UV detectors.

“Universal” detectors, which combine continuous RI and intrinsic viscosity (IV) detection, propose to remove some of the error caused by chemical functionality differences within a sample. GPC columns separate on the basis of hydrodynamic volume, or the volume a molecule or association of molecules occupies in solution. Hydrodynamic volume is converted to molecular weight using calibrations of standard molecular weight molecules, such as polystyrene. However, molecules having the same molecular weights can have

considerably different hydrodynamic volumes because of differences in molecular structure. Linear molecules, such as paraffins, have higher hydrodynamic volumes than branched molecules, like polar aromatics, of the same weight. Therefore, in GPC with conventional concentration detection, these molecules elute at different times and appear to have different molecular weights. Intrinsic viscosity detection gathers information on molecular structure (degree of branching or compactness), which is used to convert hydrodynamic volumes to molecular weights.

The only universal detector sensitive enough to detect asphalt (because of its relatively low molecular weight) is the Viscotek differential viscometer (108,109). It utilizes a Wheatstone bridge flow resistance scheme that measures intrinsic viscosity differences between the column eluant and the carrier solvent. Other viscosity detectors measure absolute intrinsic viscosity of the eluant and are not as precise. In Figure 19, several supercritically refined asphalt fractions having a variety of molecular weights *(M_w)* are seen to have similar RI and IV

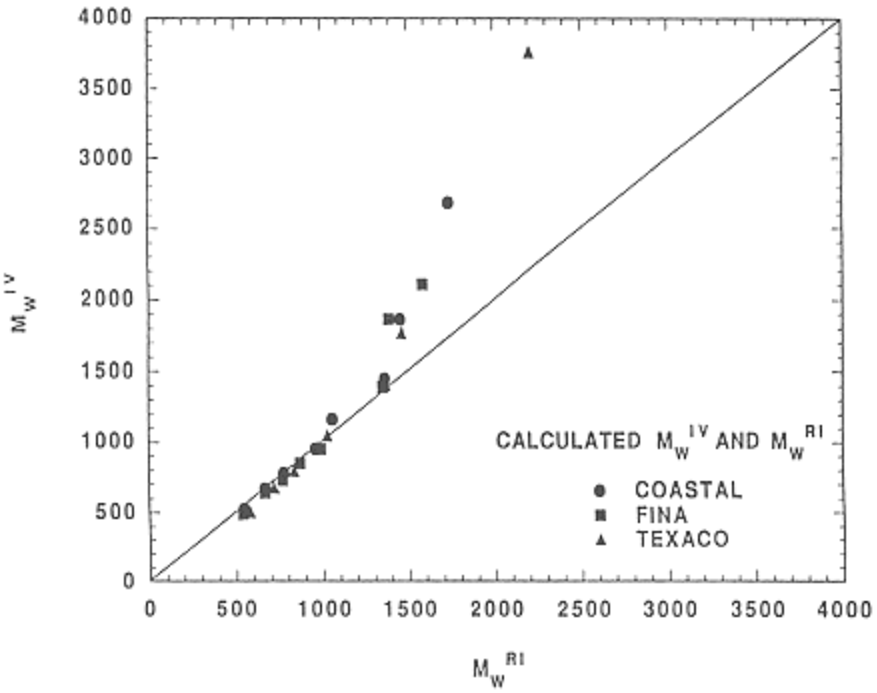

Figure 19.
Comparisons of apparent molecular size as determined by intrinsic viscosity (IV) and refractive index (RI) detectors.

molecular weights in the low-molecular-weight regions (110). In high-molecular- weight regions, where fractions have higher asphaltene contents, viscosity detection results in higher molecular weights than RI detection. This is because asphaltenes are much more compact than polystyrene, have lower hydrodynamic volumes relative to molecular weight, and therefore elute at the same time as a smaller polystyrene molecule. Maltenes and polystyrene seem to have similar compactness. The detector still cannot account for errors caused by tailing or molecular associations in solution. At present, there are no instances of universal detection providing improved characterization in terms of chemical composition or performance properties.

Other on-line detectors receive rare mention in the literature and are used for specialty applications. Nickel and vanadium detectors have been used to detect the distribution of metal porphyrins in asphalts (111). Fluorescence detectors have been used to detect cut points between associated and nonassociated constituents.

While searching for a mass detector, it must be remembered that other chromatographic problems still prevent the determination of asphalt molecular size distributions. Large, polar molecules tend to interact with the column packing and cause adsorption-desorption tailing in the chromatograms. Therefore, material that appears to have low molecular size may actually be of very large molecular size. Also, asphalt forms associations of molecules that may individually be of average size but collectively appear to be very large molecules. A mass detector may determine how much material is in the form of large particles but does not reveal the true size of the particles' component molecules. If different asphalts form molecular associations to different degrees, then it is pointless to draw conclusions on asphalt molecular size distributions purely from GPC.

Summary

Size exclusion chromatography has been used extensively for the study of asphalts. Conditions that have been reported in the literature are summarized in Table 5. SEC of asphalts is especially useful for observing differences between asphalts, changes that occur to an asphalt upon oxidative aging, and for detecting low molecular size contaminants. Correlations of SEC chromatograms with physical properties, although aggressively sought, have been elusive, undoubtedly because of the role of other factors besides size, such as the chemical nature of the molecules and the compatibility of the many components in the asphalt blend. Nevertheless, SEC of asphalts is established as an important analytical technique, especially when used in concert with other methods.

Table 5 Reported Conditions for SEC Determinations of Asphalt and Related Materials[a]

Polymer	Column type/ pore sizes (Å)	Mobile-phase solvent/flow rate (ml/minute)	Detector	Comments (µl)/c
Asphalt[b]	PS/—[c]	Bz + 10% MeOH/1.5	Prep	10 ml/1
	PS/10^4 + 2 at 400 + 100	THF/1	RI	—/0.5
	PS/10^4 + 10^3 + 500 + 50	THF/—	RI	—/1.08
	PS/—	Bz/—	Prep	—
	PS/—	Bz + 5% MeOH/—	Prep	—
	PS/—	THF/—	RI	—
	PS/500 + 50	THF/1	RI	100/7
	PS/500 + 50	Tol/1	RI	100/7
	PS/—	Bz + 10% MeOH/250	Prep	300 g/0
	PS/10^3 + 10^4 + 10^5 + 10^6 or PS/10^3 + 10^4	THF, $CHCl_3$, Bznt, Tet/several	RI; UV (254) UV (350)	Several
	PS/10^4 + 10^3	THF/3.5	RI; UV (350)	15/2
	—	THF/—	—	50 to 2
	PS/500 + 50	THF/1	RI	100/5
	PS/—	Bz + 10% MeOH/2	Prep	5 ml/2(
	—	THF/—	Prep	—
	PS/10^3 + 500 + 100	—	UV (—)	—
	PS/10^5 + 10^3 + 4 at 500	Several	UV (254)	Several
	S/—	THF/2	RI	0.5 ml/
	PS/10^3 + 3 at 500 + 10^5 + 100	THF/3	RI	1 ml/2
	PS/10^3 + 2 at 500	THF/0.9	RI; UV (340)	100/0.5
	PS/10^3 + 3 at 500 + 10^5 + 100	THF/2	RI; UV (254)	1 ml/2
	PS/10^3 + 3 at 500 + 10^5 + 10^6	THF/2	RI	0.5 ml/
	PS/10^3 + 2 at 500	THF/1	UV (290)	50/0.5
	PS/3 at 500 + 10^3 + 100	THF/2	UV (340)	—/2

(table continued on next page)

(table continued from previous page)

Polymer	Column type/ pore sizes (Å)	Mobile-phase solvent/flow rate (ml/minute)	Detector	Comments (µl)/c
	PS/50% 100-50% 250 + 2 at 10^3 + 10^4	$CHCl_3$ + 5% MeOH/2	UV (370)	0.02 g/
	PS/60 + 100 + 10^3 + 5 × 10^3 + 10^5	THF/1	RI	—/0.25
	PS/10^4 + 3 × 10^3 + 800 + 250 + 100	THF/1	RI	2 ml/0.
	PS/10^4 + 10^3 + 500 + 100	THF/1.5	RI, UV (—)	—
	—	Several	—	—
	PS/—	Bz + 5% MeOH/10	Prep	—
	PS/60	THF or Tol/1.15	RI	10–30/
	PS/10^3 + 10^4	THF/3.5	UV (350)	10/10
	PS/10^3 + 10^4	—	—	—
	PS/8500 + 10^3 + 500 + 70	THF/1	—	—/0.5
	PS/400 + 100	Bz/1	Prep	1.7 g
	PS/500	THF + 5% Pyr	RI; UV/(354)	100–20
	PS/4000 + 40 + 4	THF/1	MW UV visible	50/0.5
	Several	Several	RI; UV (313 + 365); MW-FID	Severa
	PS/1000 + 500 + 100	THF/1.2	RD-FID; ELSD; RI	—
	Bio-Beads SX-1/170	Tol/3.6	Fluorescence	150 ml
	PS/10^4 + 0–1000 Mixed bed + 150	Xyl + 20% Pyr + 0.5% Crs/1	ICP	100/0.1
Asphalt 25, 35°C	PS/10^5 + 2 at 10^4 + 10^3	THF/—	—	—/0.25
Asphalt 30°C	PS/3 × 10^3 + 500 + 250 + 60	THF/—	Prep	—
Asphalt 90°C	S/60	THF/1	UV (220)	25/0.05

[a]Analyses are at 25°C or room temperature unless otherwise noted. PS = polystyrene; S = silica; THF = tetrahydrofuran; Tol benzene; $CHCl_3$ = chloroform; Bznt = benzonitrite; Tet = tetraline; Pyr = pyridine; Xyl = xylene; Crs = cresol; RI = refractiv = preparative SEC, detector not used; ELSD = evaporative light-scattering detector; RD-FID = rotating disk FID; MW-FID = coupled plasma; MW UV = multiwavelength UV visible.

[b]May include aged asphalt material, air-blown residue, asphalt fractions, or crude oils.

[c]Data not reported.

[d]Crude oil or its fractions.

[e]Nickel and vanadium determinations.

References

1. K. H. Altgelt, *J. Appl. Polymer Sci., 9:* 3389–3393 (1965).

2. K. H. Altgelt, *Makromol. Chem., 88:* 75–89 (1965).

3. W. B. Richman, *Proc. AAPT, 36:* 106–113 (1967).

4. D. Bynum, Jr., and R. N. Traxler, *Proc. AAPT, 39:* 683–702 (1970).

5. J. A. Minshull, *Australian Road Res. Board, 428:* 1468–1476 (1968).

6. J. J. Breen and J. E. Stephens, *AAPT, 38:* 706–712 (1969).

7. C. A. Stout and S. W. Nicksic, *Separation Science, 5*(6): 843–854 (December 1970).

8. C. K. Adams and R. J. Holmgreen, FHWA/TX-86/287-4F (1986).

9. C. J. Glover, J. A. Bullin, J. W. Button, R. R. Davison, G. R. Donaldson, M. W. Hlavinka, and C. V. Philip, FHWA/TX-87/419-1F (1987).

10. C. J. Glover, R. R. Davison, J. A. Bullin, J. W. Button, and G. R. Donaldson, *Trans. Res. Rec., 1171:* 71–81 (1988).

11. K. H. Altgelt and E. Hirsch, *Separation Science, 5*(6): 855–862 (December 1970).

12. B. Brulé, in *Liquid Chromatography of Polymers and Related Materials II* (J. Cazes and X. Delamare, eds.), Marcel Dekker, New York, 1980, pp. 215–248.

13. C. Such, B. Brulé, and C. Baluja-Santos, *J. Liq. Chromatogr., 2:* 437–453 (1979).

14. P. W. Jennings, *Proc. AAPT, 54:* 635–651(1985).

15. J. R. Stegeman, A. L. Kyle, B. L. Burr, H. B. Jemison, R. R. Davison, C. J. Glover, and J. A. Bullin, *Fuel Sci. Tech., 10:* 767–794 (1992).

16. J. L. Goodrich, J. E. Goodrich, and W. J. Kari, *Trans. Res. Rec., 1096:* 146–167 (1986).

17. B. L. Burr, R. R. Davison, C. J. Glover, and J. A. Bullin, *Trans. Res. Rec., 1269:* 1–8 (1990).

18. G. A. Haley, *Anal. Chem., 47*(14): 2432–2437 (December 1975).

19. R. R. Davison, J. A. Bullin, C. J. Glover, B. L. Burr Jr., H. B. Jemison, A. L. G. Kyle, and C. A. Cipione, FHWA/TX-90/458-1F (1990).

20. K. L. Martin, R. R. Davison, C. J. Glover, and J. A. Bullin, *Trans. Res. Rec., 1269:* 9–19 (1990).

21. M. M. Hattingh, *Proc. AAPT, 53:* 197–215 (1984).

22. C. J. Glover, R. R. Davison, S. M. Ghoreishi, H. B. Jemison, and J. A. Bullin, *Trans. Res. Rec., 1228:* 177–182 (1989).

23. H. B. Jemison, R. R. Davison, C. J. Glover, and J. A. Bullin, *Trans. Res. Rec., 1323:* 77–84 (1991).

24. B. H. Chollar, J. A. Zenewitz, J. G. Boone, K. T. Tran, and D. T. Anderson, *Trans. Res. Rec., 1228:* 145–155 (1989).

25. B. L. Burr, R. R. Davison, H. B. Jemison, C. J. Glover, and J. A. Bullin, *Trans. Res. Rec., 1323:* 70–76 (1991).

26. P. W. Jennings, J. A. Pribanic, and K. R. Dawson, FHWA-MT-82/001 (June 1982).

27. D. E. Newcomb, B. J. Nusser, B. M. Kiggundu, and D. M. Zallen, *Trans. Res. Rec., 968:* 66–77 (1984).

28. A. S. Noureldin and L. E. Wood, *Trans. Res. Rec., 1228:* 191–197 (1989).

29. M. A. Plummer and C. C. Zimmerman, *Proc. AAPT, 53:* 138–159 (1984).

30. P. W. Jennings, FHWA-MT-7927 (December 1977).

31. P. W. Jennings, J. A. Pribanic, W. Campbell, K. R. Dawson, and R. B. Taylor, FHWA-MT-7930 (March 1980).

32. P. W. Jennings and J. A. S. Pribanic, *Big Timber Test Section Report,* Montana State University, Bozeman, Montana (August 1984).

33. P. W. Jennings and J. A. S. Pribanic, FHWA/MT-85/001 (April 1985).

34. P. W. Jennings and J. A. S. Pribanic, *Fuel Sci. Technol., 7*(9): 1269–1287 (1989).

35. E. L. Dukatz, Jr., D. A. Anderson, and J. L. Rosenberger, *Proc. AAPT, 53:* 160– 185 (1984).

36. N. W. Garrick and L. E. Wood, *Trans. Res. Rec., 1096:* 35–41 (1986).

37. N. W. Garrick and R. R. Biskur, *Trans. Res. Rec., 1269:* 26–39 (1990).

38. N. W. Garrick and L. E. Wood, *Proc. AAPT, 57:* 26–40 (1988).

39. S. W. Bishara, R. L. McReynolds, and E. R. Lewis, *Trans. Res. Rec., 1323:* 1–9 (1991).

40. S. W. Bishara, and R. L. McReynolds, *Trans. Res. Rec., 1342:* 35–49 (1992).

41. B. H. Chollar, J. G. Boone, W. E. Cuff, and E. F. Bailey, *Public Roads, 49*(1): 7– 12 (June 1985).

42. H. K. Huynh, T. D. Khong, S. L. Malhotra, and L. P. Blanchard, *Anal. Chem., 50*(7): 976–979 (June 1978).

43. P. M. Beazly, L. E. Hawsey, and M. A. Plummer, *Trans. Res. Rec., 1115:* 46–50 (1987).

44. J. R. Woods, L. S. Koflyar, D. S. Montgomery, B. D. Sparks, and J. A. Ripmeester, *Fuel Sci. Technol., 8*(2): 149–171 (1990).

45. R. B. Girdler, *Proc. AAPT, 34:* 45–79 (1965).

46. J. G. Speight, D. L. Wernick, K. A. Gould, R. E. Overfield, B. M. L. Rao, and D. W. Savage, *Rev. Inst. Fr. Petrole, 40*(1): 51–61 (January-February 1985).

47. L. R. Snyder, *Anal. Chem., 41*(10): 1223–1227 (August 1969).

48. G. A. Haley, *Anal. Chem., 43*(3): 371–375 (March 1971).

49. H. H. Kiet, L. P. Blanchard, and S. L. Malhotra, *Separation Science, 12*(6): 607–634 (1977).

50. H. Reerink and J. Lijzenga, *Anal. Chem., 47*(13): 2160–2167 (November 1975).

51. P. J. Champagne, E. Manolakis, and M. Ternan, *Fuel, 64:* 423–425 (March 1985).

52. J. G. Bergman and L. J. Duffy, *Anal. Chem., 43*(1): 131–133 (January 1971).

53. Z. Grubisic, P. Rempp, and H. Benoit, *J. Polymer Sci., Part B, 5:* 753–759 (1967).

54. H. H. Oelert, D. R. Latham, and W. E. Haines, *Separation Science, 5*(5): 657– 668 (October 1970).

55. K. H. Altgelt and T. H. Gouw, *Adv. Chromatog., 13:* 71–175 (1975).

56. J. N. Done and W. K. Reid, *Separation Science, 5*(6): 825–842 (December 1970).

57. P. W. Jennings, M. A. Desando, M. F. Raub, J. O. Hoberg, R. Moats, and F. F. Stewart, in *Symposia of Chemistry and Characterization of Asphalts* (J. Youtcheff and T. Mill, co-chairmen), American Chemical Society, Washington, D.C., *35*(3): 440–444 (July 1990).

58. G. R. Donaldson, M. W. Hlavinka, J. A. Bullin, C. J. Glover, and R. R. Davison, *J. Liq. Chromatogr., 11*(3): 749–765 (1988).

59. B. Brulé, G. Ramond, and C. Such, *Trans. Res. Rec., 1096:* 22–34 (1986).

60. I. Ishai, B. Brulé, J. C. Vaniscote, and G. Ramond, *Proc. AAPT, 57:* 65–93 (1988).

61. L. W. Corbett, *Anal. Chem., 41:* 576–579 (1969).

62. L. W. Corbett, *Anal. Chem., 36*(10): 1967–1972 (September 1964).

63. L. W. Corbett, *Proc. AAPT, 39:* 481–491 (1970).

64. J. C. Petersen, *Trans. Res. Rec., 999:* 13–30 (1984).

65. J. C. Petersen, *Trans. Res. Rec., 1096:* 1–11 (1986).

66. R. V. Barbour and J. C. Petersen, *Anal. Chem., 46*(2): 273–277 (1974).

67. J. C. Petersen, *Fuel, 46:* 295–305 (1967).

68. S. E. Moschopedis and J. G. Speight, *Fuel, 55:* 187–192 (1976).

69. J. F. McKay, P. J. Amend, T. E. Cogswell, P. M. Harnsberger, R. B. Erickson, and D. R. Latham, in *Analytical Chemistry of Liquid Fuel Sources* (P. C. Uden and S. Siggia, eds.), Advances in Chemistry Series 170, American Chemical Society, Washington, D.C., pp. 128–142 (1978).

70. M. M. Boduszynski, J. F. McKay, and D. R. Latham, *Proc. AAPT, 49:* 123–143 (1980).

71. M. M. Boduszynski, in *Chemistry of Asphaltenes* (J. W. Bunger and N. C. Li, eds.), Advancement in Chemistry Series 195, American Chemical Society, Washington, D.C., pp. 119–135 (1981).

72. D. L. Mitchell and J. G. Speight, *Fuel, 52:* 149–152 (1973).

73. J. G. Speight, R. B. Long, and T. D. Trowbridge, *Fuel, 63:* 616–620 (1984).

74. F. J. Nellensteyn, *J. Inst. Petrol. Technol., 14:* 134–138 (1928).

75. J. Ph. Pfeiffer, and R. N. J. Saal, *Phys. Chem., 44:* 139–149 (1940).

76. T. F. Yen, J. G. Erdman, and S. S. Pollack, *Anal. Chem., 33*(11): 1587–1594 (October 1961).

77. J. P. Dickie and T. F. Yen, *Anal. Chem., 39*(14): 1847–1852 (December 1967).

78. T. F. Yen and J. P. Dickie, *J. Inst. Petrol. Technol., 54*(530): 50–53 (February 1968).

79. T. F. Yen, in *Symposia of Chemistry and Characterization of Asphalts* (J. Youtcheff and T. Mill, co-chairmen), American Chemical Society, Washington, D.C., *35*(3): 314–319 (July 1990).

80. S. W. Ferris, E. P. Black, and J. B. Clelland, *Ind. Eng. Chem. Prod. Res. Dev., 6*(2): 127–132 (June 1967).

81. F. E. Dickson, B. E. Davis, and R. A. Wirkkala, *Anal. Chem., 41*(10): 1335–1337 (August 1969).

82. F. E. Dickson, R. A. Wirkkala, and B. E. Davis, in *Gel Permeation Chromatography* (K. H. Altgelt and L. Segal, eds.), Marcel Dekker, New York, 1971, pp. 579–591.

83. G. A. Haley, *Anal. Chem., 44*(3): 580–585 (March 1972).

84. W. J. Halstead, *Proc. AAPT, 32:* 247–270 (1963).

85. P. S. Kandhal and W. C. Koehler, *Trans. Res. Rec. 999:* 41–50 (1984).

86. J. L. Goodrich and L. H. Dimpfl, *Proc. AAPT, 55:* 57–91 (1986).

87. H. J. Coleman, J. E. Dooley, D. E. Hirsch, and C. J. Thompson, *Anal. Chem., 45:* 1724–1737 (1973).

88. S. E. Moschopedis, J. F. Fryer, and J. G. Speight, *Fuel, 55:* 227–232 (1976).

89. J. Hildebrand and R. Scott, *Solubility of Non-Electrolytes,* 3rd ed., Reinhold, New York, 1949.

90. C. M. Hansen and K. Skaarup, *J. Paint Technol., 39*(511): 511–514 (August 1967).

91. C. M. Hansen, *Ind. Eng. Chem. Prod. Res. Dev., 8*(1): 2–11 (March 1969).

92. C. M. Hansen and A. Beerbower, in *Encyclopedia of Chemical Technology,* (R. E. Kirk and D. F. Othmer, eds.), 2nd ed., Supplement Volume, John Wiley and Sons, New York, 1971, pp. 889–910.

93. A. P. Hagen, R. Jones, R. M. Hofener, B. B. Randolph, and M. P. Johnson, *Proc. AAPT, 53:* 119–137 (1984).

94. C. A. Cipione, R. R. Davison, B. L. Burr, C. J. Glover, and J. A. Bullin, *Trans. Res. Rec., 1323:* 47–52 (1991).

95. L. R. Snyder, *J. Chromatogr., 92:* 223–230 (1974).

96. H. V. Drushel, *J. Chromatogr. Sci., 21:* 375–384 (1983).

97. K. D. Bartle, N. Taylor, M. J. Mulligan, D. G. Mills, and C. Gibson, *Fuel, 62:* 1181–1185 (1983).

98. S. W. Bishara and R. L. McReynolds, *Trans. Res. Rec., 1269:* 40–47 (1990).

99. J. A. S. Pribanic, M. Emmelin, and G. N. King, *Trans. Res. Rec., 1228:* 168–176 (1989).

100. H. V. Drushel, in *Analytical Chemistry of Liquid Fuel Sources* (P. C. Uden and S. Siggia, eds.), Advances in Chemistry Series 170, American Chemical Society, Washington, D.C., pp. 295–306 (1978).

101. E. W. Albaugh and P. C. Talarico, *J. Chromatogr., 74:* 233–253 (1972).

102. J. B. Dixon, *Chimia, 38*(3): 82–86 (March 1984).

103. C. D. Pearson and S. G. Gharfeh, *Anal. Chem., 58:* 307–311 (1986).

104. S. Coulombe, *J. Chromatogr. Sci., 26:* 1–6 (1988).

105. T. H. Mourey and L. E. Oppenheimer, *Anal. Chem., 56:* 2427–2434 (1984).

106. M. Righezza and G. Guiochon, *J. Liq. Chromatogr., 11*(9/10): 1967–2004 (1988).

107. K. D. Bartle, M. Burke, D. G. Mills, S. Pape, and S. Lu, in *Symposia of Chemistry and Characterization of Asphalts* (J. Youtcheff and T. Mill, co-chairmen). American Chemical Society, Washington, D.C., 35(3):415–420 (July 1990).

108. M. Haney, *American Laboratory,* March and April (1985).

109. M. Haney, U. S. Patent No. 4,463,598, *Official Gazette, 54* (August 7, 1984).

110. H. B. Jemison, Texas A&M University, Department of Chemical Engineering, Ph.D. Thesis, 1991.

111. C. D. Pearson and J. B. Green, *Fuel, 68:* 465–474 (1989).

112. J. F. Branthaver, J. J. Duvall, and J. C. Petersen, in *Symposia of Chemistry and Characterization of*

Asphalts (J. Youtcheff and T. Mill, co-chairmen), American Chemical Society, Washington, D.C., *35* (3): 407–414 (July 1990).

9
Size Exclusion Chromatography of Acrylamide Homopolymer and Copolymers

Fu-mei C. Lin Calgon Corporation, Pittsburgh, Pennsylvania

Introduction

Acrylamide monomer is a white crystal, available commercially as a 50 wt % aqueous solution. Acrylamide monomer can be polymerized to a very-high-molecular-weight (10^6–10^7 g/mole) homopolymer, copolymer, or terpolymer. Polyacrylamide (PAM) is a nonionic polymer. The anionic polyacrylamide species can be obtained from the hydrolysis of the amide (—$CONH_2$) functional group of the homopolymer, or from the copolymerization of acrylamide with an anionic monomer, such as acrylic acid (AA) or 2-acrylamino 2-methyl propane sulfonic acid (AMPS). Acrylamide can be copolymerized with a cationic monomer, such as dimethyl diallylammonium chloride (DMDAAC) or acryloyloxyethyl trimethyl ammonium chloride (AETAC), to form the cationic acrylamide polymer. Acrylamide can simultaneously react with anionic and cationic monomers to form a polyampholyte. The acrylamide homopolymer, copolymers, and terpolymers are synthesized (1–20) by free radicals via solution or emulsion or other polymerization methods. F. A. Adamsky and E. J. Beckman (21) reported the inverse emulsion polymerization of acrylamide in supercritical carbon dioxide. The product classes of acrylamide polymers include liquid, dry, and emulsion.

The nonionic, anionic, and cationic acrylamide polymers have been used for many industrial applications (1, 2, 3, 13, 22, 23). The polymer selection for a particular application depends upon the desired chemical structure, chemical composition, molecular weight (MW), and molecular weight distribution (MWD). Some applications of acrylamide polymers are shown in Table 1. Size

Table 1 Applications of Acrylamide Polymers (1, 2, 3, 13, 22, 23)

Application	Polymer	Charge (%)	Molecular weight
Liquid/solid separation			
Process water clarification	Anionic PAM	High	High
Filtration aid	PAM	None	High
	Anionic PAM	High	High
Primary waste water clarification	PAM	None	High
	Anionic PAM	High	High
	Cationic PAM	Medium	High
Secondary waste water clarification	Cationic PAM	High	High
Sludge thickening and sludge dewatering for biological waste	Cationic PAM	High	High
Sludge thickening and sludge dewatering for mineral	PAM	None	High
	Anionic PAM	High	High
Retention/drainage aid	Cationic PAM	Medium to high	High
	Anionic PAM	Low to medium	High
Dry strength aids for paper	Anionic PAM +	Low	Medium
	Polyamine	High	Low
Wet strength aids for paper	Gloxated cationic PAM (lightly Crosslinked PAM)	Low	Medium
Hair and skin conditioners in personal care applications	Cationic PAM	Medium to high	High
	Amphoteric	Low (net charge)	High
Oil field applications			
Mobility control	Anionic PAM	Low-high	High
Recovery of petroleum	PAM gel or powder	None	High
	PAM + 5% HYPAM	Low	High
Lubricant-coolant	Ethylene/maleic	None	Medium
	Anhydride + PAM		
Reducing friction losses	PAM	None	Medium to high
	Anionic PAM		
	Cationic PAM		

exclusion chromatography (SEC) is an excellent technique to determine MW and MWD. Yau, Kirkland, and Bly (24) have discussed the SEC technique. Barth (25) has reported a practical approach to steric exclusion chromatography of water-soluble polymers. However, SEC is not easily carried out for the subject polymers because of the high molecular weight (10^6–10^7 g/mole) and the poly-electrolyte characteristics of the charged polymers. In order to obtain meaningful SEC data, the columns, mobile phase, concentration of polymer solution, sample preparation method, flow rate, and shear degradation of the polymer should be considered in an SEC experiment.

Several authors (26, 27, 28, 29) have discussed concentration effects in SEC. Barth and Carlin (30) have proposed mechanisms and possible sources of polymer shear degradation in SEC. Giddings (31) determined the shear degradation of PAM. Omorodion, Hamielec and Brash (32) studied the effects of pH, ionic strength, and nonionic surfactants on polymer dimensions and elution volume for aqueous SEC of PAM with controlled-pore glass (CPG) columns. Onda et al. (33, 34) analyzed PAM by SEC using CPG columns in formamide and aqueous media. They also studied the effects of salt addition on the retention volume. Klein and Westerkamp (35) separated PAM, acrylamide/sodium acrylate copolymers, dextrans, and poly(sodium styrene sulfonates) by using CPG columns. They investigated the thermal degradation of PAM at 50 and 75°C. Letot, Lesec, and Duivoron (36) used polyvinylpyrrolidone-coated silica columns and pure water to chromatograph PAM and other water-soluble polymers. El-Awady and co-workers (37) investigated the MW and MWD of PAM in side chains and in homopolymer by SEC during grafting of cellulose acetate with acrylamide monomer. McCormick and Park (38) studied the effects of Fe(II), H_2O_2, acrylamide, and dextran concentration on the hydrodynamic volumes of dextrangrafted acrylamide copolymers by SEC. Muller and Yonnet (39) studied a high MW hydrolyzed polyacrylamide (HYPAM) and a 74/26 mole % AM/AA high MW copolymer by SEC, static low-angle laser light scattering (LALLS) and photon correlation light scattering. Huang (40) evaluated the chemical structural heterogeneity of cationic acrylamide copolymers by high performance liquid chromatography. Abdel-Alim and Hamielec (41) used a broad MWD PAM standard A to create a linear calibration curve that covers the molecular weight range from 10^3 to 10^7 g/mole. This calibration was used to characterize two other broad-MWD standards B and C.

The Micropak TSK Gel PW, TSK Gel PWXL and Shodex OHpak Q-800, B-800, and KB-800 series are more recently available columns developed for analyzing the acrylamide polymers and other water-soluble polymers in aqueous SEC. The TSK columns have been evaluated by Barth (25), Alfredson et al. (42), Sasaki et al. (43), and Lin and Getman (44). Showa Denko K. K. (45) reported the SEC analysis of PAM by Shodex OHpak columns. The narrow MWD polyacrylamide standards ($\overline{M}w$ = 1.2E4 to 9.0E6 g/mole) produced by

the American Polymer Standards Corporation are listed in Table 2. However, some acrylamide copolymers and terpolymers are heterogeneous (40) in terms of chemical structure and MW, and the standards having chemical structures similar to the samples are not commercially available. The absolute MW and MWD of these polymers are difficult to determine using conventional SEC with a single refractive index (RI) detector and using narrow MWD standards for calibration. The on-line dual or multidetectors were used in an SEC system to solve the above problems.

Kim and coworkers (46) developed a methodology for using RI/LALLS dual detectors to establish the MW calibration curve and peak broadening parameter for a wide range of MW for PAM. Lin and Getman (44) determined the absolute MW and MWD of PAM, HYPAM, acrylamide/acrylic acid (AM/AA), and acrylmide/dimethyldiallylammonium chloride (AM/DMDAAC) copolymers by Micropak TSK Gel PW and PWXL columns with an RI/LALLS dual detecting system. Also, the authors determined the molecular weight reduction and mass loss of degraded AM/AA copolymer in a boiler by SEC with RI detector. Lesec and Volet (47) applied RI/LALLS/on-line viscometer triple detectors to determine the absolute MW and MWD of PAM.

A Calgon in-house computer simulation program developed by Min and Cha (48) has been applied to construct a conventional calibration curve. This program is written in Fortran. It needs two standards for a linear fit and four

Table 2 Polyacrylamide Standards (Reported by American Polymer Standards Corporation)

Nonionic, 100% water soluble powder

Catalog #	$\overline{M}w$ (g/mole)	*Mp* (g/mole)	$\overline{M}n$ (g/mole)	IV[a] (dl/g)
PAAM9000K	9,000,000	6,500,000	4,250,000	14.600
PAAM6000K	5,500,000	3,695,000	2,460,000	10.385
PAAM1000K	1,140,000	725,000	465,300	3.800
PAAM500K	524,000	331,000	209,600	2.250
PAAM350K	367,000	193,400	141,000	1.650
PAAM80K	79,000	50,500	44,400	0.645
PAAM60K	58,400	46,100	36,500	0.545
PAAM20K	21,900	17,300	13,700	0.255
PAAM10K	11,530	7,950	7,600	0.160

*IV = Intrinsic viscosity in dl/g in 0.05 M sodium sulfate at 30 °C

$[\eta] = kM^a$

$a = 0.66$

$k = 0.000373$

standards for a third-order fit. The required parameters are the $\overline{M}w$ and $\overline{M}n$ (number-average molecular weight) of each standard. The different weighted factor (0 to 1) can be entered into the program to specify the degree of importance of the given $\overline{M}w$ or $\overline{M}n$ value.

Rand and Mukherji (49) reported a MW calibration technique with the assistance of a computer program to handle the routine analysis of a specific polymer with a special set of columns, identical mobile phase, and identical SEC experiment. This method deals with modifying the previous calibration curve by shifting the retention times of the upper and/or lower limits to obtain a new calibration curve for the current experiment.

A list of the SEC conditions used in the above references will be compiled in the appendix of this chapter.

The methodology and applications of SEC for characterizing acrylamide polymers will be discussed in this chapter from a practical point of view.

Experimental

Column and Mobile Phase

The selections of columns and mobile phase depend on the chemistry and molecular weight of the polymer to be analyzed. Important factors (31, 32) such as chemistry, pore size, particle size, ionic group, and adsorptive properties of the stationary phase, the resolving power, molecular weight separation range, solvent compatibility, lifetime, sample loading capacity, and temperature stability should be considered before selecting a column. When a high-molecular-weight (>10^6 g/mole) polymer is analyzed, the shear degradation of the polymer in the columns is an important factor which influences the accuracy of the MW and MWD determinations. Giddings (31) reported the reduction in intrinsic viscosity of polyacrylamide solution ($\overline{M}w$ = 6.25 × 10^6 g/mole) after passing through a CPG-10 column (3000 Å pore size and 39–75 micrometer particle size) at a flow velocity as low as 0.025 cm/sec. The experiment was carried out by Dr. Lyle Bowman at Calgon Center.

When an anionic or cationic acrylamide polymer is analyzed, the ionic group of the stationary phase should be considered before selecting a column. Sasaki (43) reported that the TSK Gel PWXL columns have small amounts of weakly anionic groups. Lin and Getman (44) observed the adsorption of a high MW acrylamide/DMDAAC cationic polymer in the TSK Gel PWXL columns. Therefore, the TSK Gel PW columns are recommended for analyzing cationic and amphotoric acrylamide polymers.

Simple salts such as sodium chloride or sodium sulfate are added to the mobile phase to minimize the polyelectrolyte effect of the charged acrylamide

polymers. The optimal ionic strength of the mobile phase can be determined by measuring the intrinsic viscosity [η] of the polymer solutions with increasing concentration of simple salt until the intrinsic viscosity becomes constant. If a linear calibration curve is desired, the different pore sizes of columns should be investigated for a particular range of MW. If a very slow flow rate such as 0.1– 0.3 ml/minutes is required for a very-high-molecular-weight sample in a narrow MW range, a single column may be used to reduce the analysis time. Research should be conducted to provide adequate information for selecting columns and mobile phase. The columns and mobile phases that have been used to analyze polyacrylamide and its copolymers and terpolymers are summarized in a list of SEC conditions, which are compiled in the appendix at the end of this chapter.

Sample Preparation

Sample preparation is a very important step for SEC analysis. The MW of a polymer can be changed unintentionally during sample preparation. Use the mobile phase to prepare samples. If the low MW tail of the chromatogram overlaps with the salt peak, replace the mobile phase with an appropriate amount of water to obtain a negative polarity salt peak. The quantity of water to be used depends on the concentration to be prepared and the percentage of active polymer in the sample. It can be determined from a series of SEC experiments with varying amounts of water added to the sample until a negative polarity salt peak is obtained. The optimum concentration of SEC sample depends on the MW of the polymer. Lundy and Hester (50) suggested that the polymer solution injected into the columns should not be greater than one-half the reciprocal of its intrinsic viscosity. If an unusual pressure trace caused by a high viscosity of a solution is observed during the injection, reduce the concentration and remove the pre-column filter, if such a filter is present.

Filter size selection depends on the MW and solution concentration. Use an appropriate size of filter to prepare polymer solutions, so the large molecules will not be excluded by the filter. If there is no information about the MW of the polymer, a large size filter of 5, 8, or 10 micrometers is recommended. Examples are shown below.

Weight-average molecular weight $\overline{Mw}$ (g/mole)	Concentration (g/100 ml)	Filter size (micrometers)
10^2–10^4	0.1–0.15	0.22
10^5	0.1	0.45
10^6	0.05–0.08	1.2–3.0
$>10^6$	0.03–0.05	5.0–10.0

The mixing method can change the actual MW and MWD. In this work, different methods were used to prepare three types of samples:

For Solution Samples

The magnetic stirring method at low speed is recommended.

For Solid Samples

It is very difficult to dissolve high MW solid PAM or its copolymers in a high-ionic- strength mobile phase directly. A special process is recommended as follows:

Pour about 60 ml filtered water into a bottle and stir the water with a magnetic stir bar at high speed. Sprinkle the correct amount of solid sample into the bottle. When the solid sample disperses homogeneously in the water, cap the bottle tightly and place the bottle containing sample in a shaker with low speed at 50°C overnight. Remove the sample from the shaker when the solid sample is dissolved completely. Add the correct amount of salt to the above sample solution and adjust the total volume to 100 ml by adding filtered water. Mix the solution very well and filter the solution with an appropriate size of filter. Degas the polymer solution in a flask, then transfer the polymer solution to a 4 ml vial.

For Emulsion Samples

Dilute the emulsion sample with xylene or hexane, then precipitate the dilute solution into isopropyl alcohol (IPA) or acetone. Filter the mixture to obtain the solid sample. Dry the precipitated sample in a vacuum oven at 40°C overnight to remove the residual IPA or acetone. A solution of the precipitated sample for SEC analysis can be prepared by the same method used for preparing solid samples.

Results and Discussion

Chromatographic System

PAM, HYPAM and AM/AA copolymers can be analyzed by TSK Gel PWXL (44), TSK Gel PW (25, 44), Shodex OHpak (25, 45), CPG (31, 32, 33, 34, 38, 41, 46), Sephacryl S1000 (39), polyvinylpyrrolidone-coated silica columns (36) with an appropriate mobile phase. For cationic acrylamide copolymers, the Gel TSK PW columns (44) have a better separation capability than the Gel PWXL columns. This is probably due to the higher number of residual anionic sites found in PWXL columns (44). When a cationic polyacrylamide is analyzed,

conditioning the columns is very important. This process can be achieved by injecting the lower MW solution (or first sample) that has the same chemical structure as the samples into the columns before data are collected for analysis. The MW range that can be separated by TSK PW or TSK PWXL columns is 10^3–10^7 g/mole.

The high-ionic-strength mobile phase creates some difficulty in maintaining a constant flow rate during the SEC experiment. About 0.025 to 0.05 minutes fluctuations in retention time at 1 ml/minute flow rate have been observed in 50 minute run times. The consistency of flow rate during the SEC analysis can be evaluated by comparing the elution times of salt peaks among chromatograms of samples. Data generated from inconsistent flow rates will give incorrect MW information. Lundy and Hester (51) designed a syringe pump to obtain 0.15 ml/minute consistent flow rate for characterizing large water-soluble macro-molecules.

Figure 1 shows the chromatograms of PAM and HYPAM from TSK PWXL columns and AM/DMDAAC copolymer from TSK PW columns. The MW of five PAM samples will be discussed later. The narrower line width of the chromatogram of the highest MW sample (PAM 1, $\overline{M}w = 6 \times 10^6$ g/mole) is probably due to the insufficient separation capability of the columns (TSK Guard column + G6000 + G5000 + G4000 PWXL). Figure 2 shows the chromatogram of a very broad-MWD PAM standard, which was obtained by mixing these five PAM samples. The MW information, which is summarized in Table 3, was determined from five PAM samples using peak MW calibration techniques. Using this single broad-MWD standard rather than several PAM standards can save SEC analysis time for routine samples. The 50/50 wt % monomer charge ratio of AM/DMDAAC contains a narrow high MW portion and low MW tail [negative skewness defined by Chen and Hu (52)]. The high and low MW portions have been separated by precipitating the copolymer solution in isopropyl alcohol (IPA). Both precipitated solid (high MW portion) and supernatant (low MW portion) were dried in a vacuum oven at 40°C. The dried samples were redissolved in H_2O and analyzed by proton NMR spectroscopy. Based on the copolymer composition determined from proton NMR analysis, the high MW portion is acrylamide-rich AM/DMDAAC copolymer, and the polymer in the low MW fraction is DMDAAC-rich AM/DMDAAC copolymer. The copolymer composition of AM/DMDAAC copolymer is a function of MW. This phenomenon is caused by the different copolymer reactivity ratios of acrylamide and DMDAAC ($r_{AM} = 2.36$, $r_{DMDAAC} = 0.046$) monomers. Again, the narrow line shape of the high MW portion may be due to the poor separation capability of the columns at the upper MW end (about 5×10^6 g/mole). M. A. Langhorst and co-workers (53) stated that the combination of hydrodynamic chromatography (HDC) and LALLS detection can be applied to determine MW and MWD of partially hydrolyzed PAM up to $\overline{M}w = 9 \times 10^6$ g/mole.

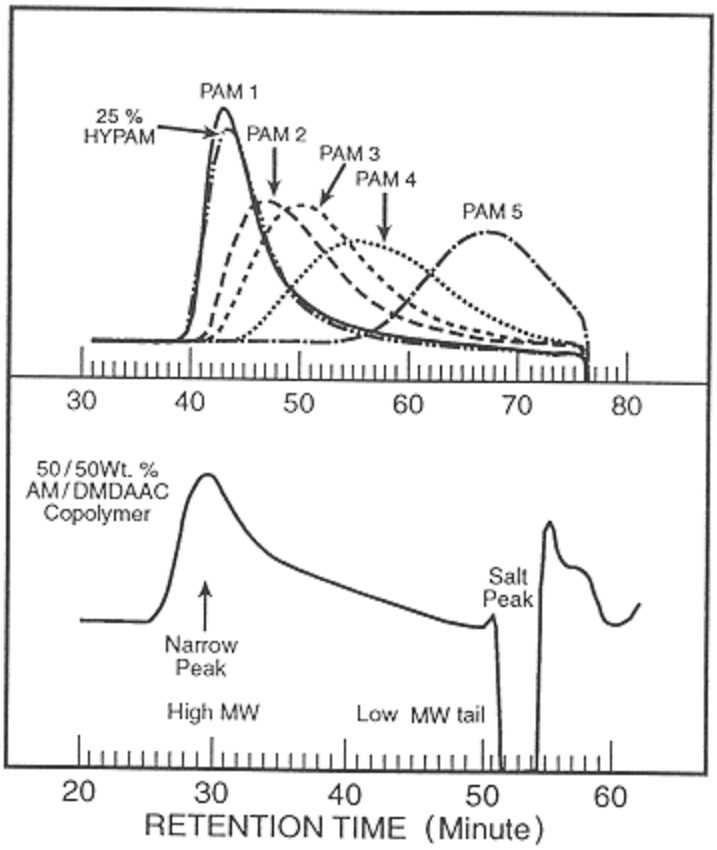

Figure 1.
Size exclusion chromatograms of PAM, HYPAM, and AM/DMDAAC copolymer (raw data).

Figure 3 shows two chromatograms of low MW 90/10 wt % AM/DMDAAC copolymer samples with solvent peaks of different polarity. The low MW tail of the chromatogram overlaps with the salt peak. Therefore, the final processing time is difficult to determine and the $\overline{M}w$, $\overline{M}n$ and $\overline{M}w/\overline{M}n$ values depend on the choice of the final process time. With the positive salt peak, a significant amount of area was eliminated in the MW and MWD determination. This results in an narrower polydispersity. With the negative salt peak, a small area of the salt peak was included in the MW and MWD determination. This results in a broader polydispersity.

The RI, UV, LALLS and viscometer detectors have been successfully used in this work. The FTIR detector has been applied to study protein by Remsen

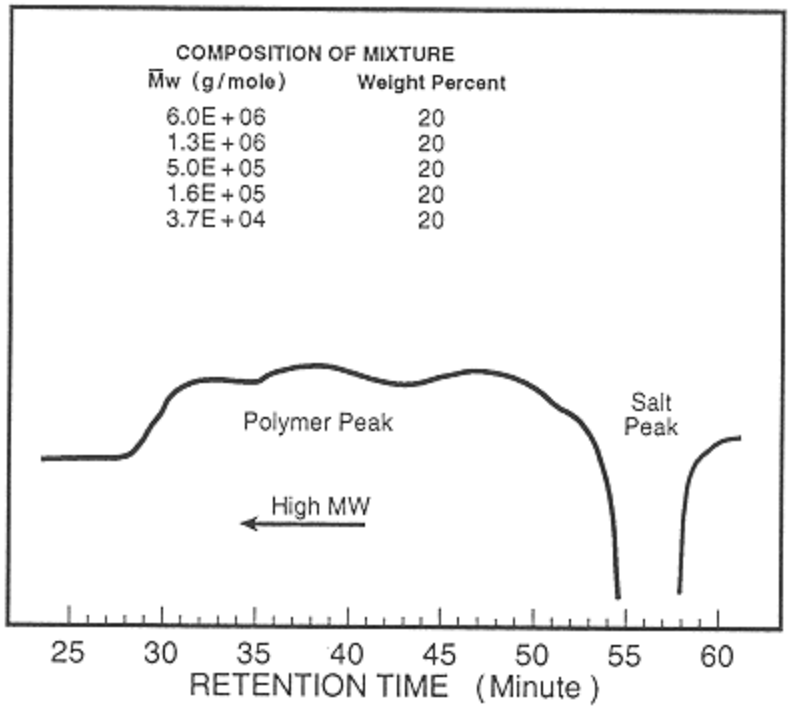

Figure 2.
A broad-MWD PAM standard obtained from five individual PAM samples.

and Freeman (54). It is difficult to obtain a strong signal from the conductivity detector (Waters Model 430) because of the high-ionic-strength mobile phase.

Characterization of Molecular Weight Standards

Static LALLS Experiment

This experiment determines the absolute $\overline{M}w$ of a polymer in solution. It requires the specific refractive index increment [$(dn/dc)_{T,\lambda,\mu}$] (55, 56, 57) of the polymer solution in order to calculate $\overline{M}w$.

The *dn/dc* measurement should be carried out under the same temperature (T) and same wavelength (λ) as the LALLS experiment and at a constant chemical potential (μ). The conditions for a constant chemical potential can be achieved by dialyzing the polymer solution against the filtered mobile phase until the *dn/dc* of the polymer solution becomes constant. In addition, the final concentration of the polymer solution should be

Table 3 MW and MWD of a Broad-MWD PAM Standard Shown in Figure 2

PAM Standards: PAM 1, PAM 2, PAM 3, PAM 4, PAM 5, and PAM 6 ($\overline{M}w$ = 3.7E + 04 to 6.0E + 6 g/mole)

$\overline{M}w$ = 1.1E + 06 g/mole

$\overline{M}n$ = 5.2E + 04 g/mole

$\overline{M}w/\overline{M}n$ = 24

Cumulative wt%	Slice MW (g/mole)
0.045	34,409,572
0.432	16,696,033
1.622	8,682,435
6.391	2,829,109
12.761	1,140,318
21.184	544,627
38.745	224,933
56.957	106,853
68.643	65,451
74.720	50,499
86.133	28,440
94.563	14,351
97.324	9,653
99.183	6,216
100.000	3,812

Columns: Guard column + TSK G6000 PW + G5000 PW + G3000 PW

Mobile phase: 0.15 M Na_2So_4 + 1% acetic Acid, pH = 3.1

Temperature: 35°C

determined after dialysis. It was found that when a 0.1 g/100 ml-high MW PAM solution was dialyzed against 2000 ml of mobile phase with a 1000 MW cut-off dialysis membrane, it took about three to four days to obtain a constant *dn/dc* and resulted in a 3 to 5 wt % mass loss. The concentration of polymer solution was decreased from 0.1 g/100 ml to 0.097 g/100 ml to 0.095 g/100 ml. Other parameters that may affect the *dn/dc* value are the molecular weight of the polymer and the temperature of the experiment. Research should be conducted to define the correct conditions for the *dn/dc* measurement. Also, it should be noted that the measured *dn/dc* of an acrylamide copolymer is an average of its components.

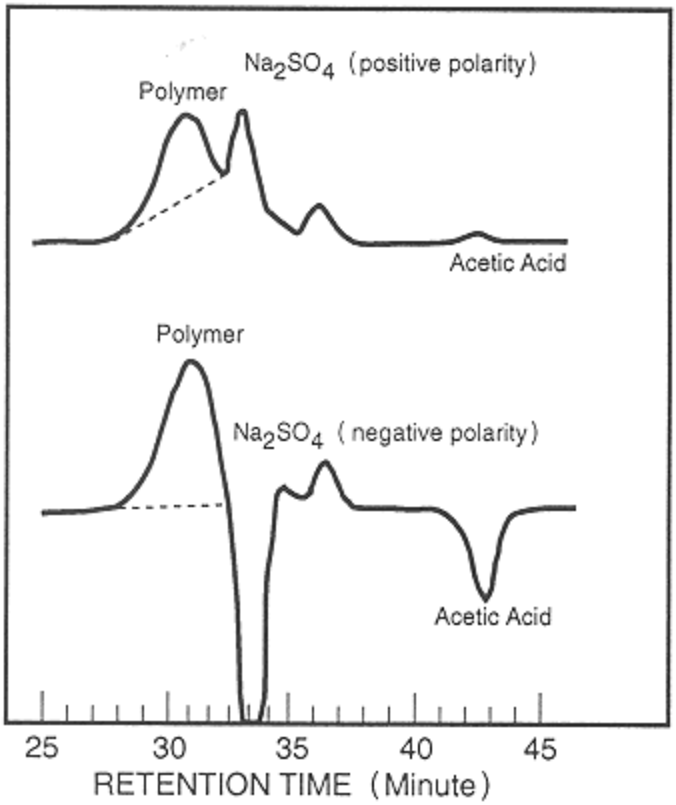

Figure 3.
Size exclusion chromatograms of low MW 90/10 wt %
AM/DMDAAC copolymer with positive or negative salt peak.

SEC Analysis with RI/LALLS Dual Detectors

This type of analysis provides the absolute MW and MWD without standards (44, 46, 47). The $\overline{Mw}$, $\overline{Mn}$, polydispersity, and molecular weight versus cumulative % area of polymer can be obtained. $(dn/dc)_{T,\lambda,\mu}$ of the polymer solution should be used for MW determination. Samples characterized by this technique can be used as SEC MW standards.

The LALLS detector is insensitive to low MW and low concentration species. Therefore, the $\overline{Mn}$ determined by this method may be erroneously high. Another commercially available MW detector is a Multi Angle Laser Light Scattering (MALLS) photometer. It should be noted that a good chromatographic

system is required for obtaining a meaningful MW and MWD, even if a MW detector (LALLS or MALLS) is used. In other words, the MW detector cannot solve chromatographic problems.

Intrinsic Viscosity Determination

The intrinsic viscosity and Mark-Houwink constants of standards can be determined from a static capillary viscometer or an on-line viscometer detector in an SEC system. If the intrinsic viscosity is to be used for constructing a universal calibration curve, it is important to use the identical conditions in performing the SEC analysis and the intrinsic viscosity measurement. A Mark-Houwink plot for five PAM standards and one PAA standard is shown in Figure 4. The intrinsic viscosity of PAM may decrease with time and becomes constant after about one week. It is recommended that the PAM solution be analyzed while still fresh.

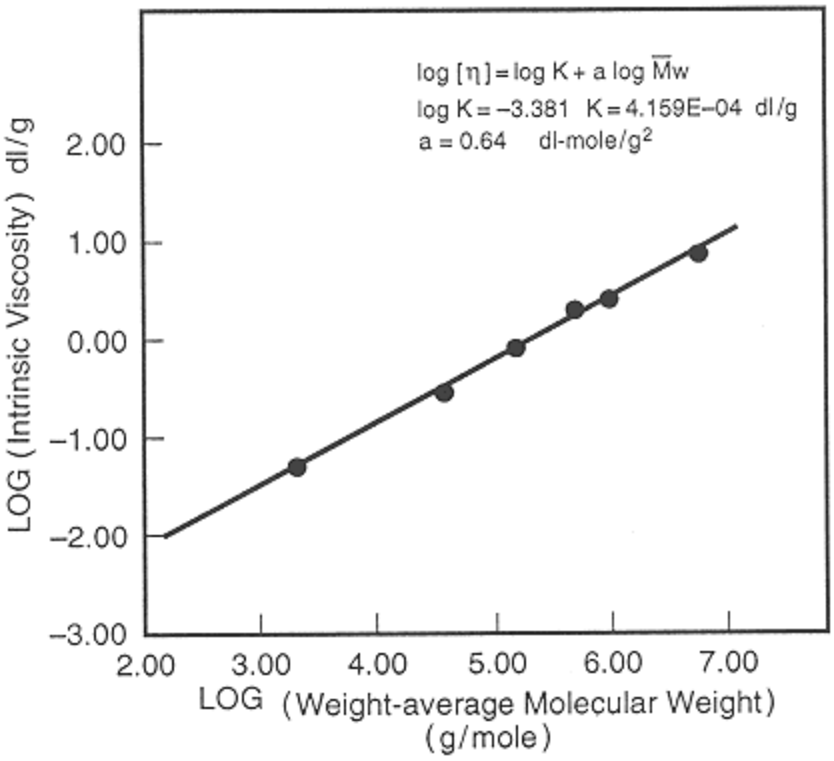

Figure 4.
Mark-Houwick plot of five polyacrylamides and one polyarcylic acid.

Factors Influencing the MW Determination

MW and Chemical Structure of Standards

Table 4 shows the average molecular weights and polydispersities of four 80/ 20 w/w AM/DMDAAC high MW copolymers. It appears that the use of poly (DMDAAC) as a standard results in the reporting of a higher molecular weight and polydisperity of the copolymer. It is also important to note that the chain microstructure (stereostructure, end groups, or monomer sequence distribution) of a polymer may affect the molecular size when in solution. Every effort should be made to use a polymer with a similar chain microstructure for standardization when determining MW. Otherwise, erroneous values may be obtained because even though a polymer may have the same chemistry, it may have a different chain microstructure and behave differently in solution. When comparing relative MW, the same MW standards must be used for all determinations.

MW and Calibration Technique

Table 5 shows the given $\overline{M}w$ (determined by LALLS) and intrinsic viscosities determined from an on-line viscometer (Viscotek Model 110) and the measured $\overline{M}w$ determined by different calibration techniques for six samples. The deviations {[(measured $\overline{M}w$ - given $\overline{M}w$)/(given $\overline{M}w$)] × 100} between the measured $\overline{M}w$ and those given $\overline{M}w$ for PAM are -10% to +15% by universal calibration and -8% to +4% by peak position calibration. The universal calibration technique gives relatively higher deviations, probably due to the fact that the intrinsic viscosity was determined from a single point (58) or the universal calibration curves included two different types of polymers (five PAM and one low MW polyacrylic acid) as shown in Figure 5, or the polydispersity of PAM is not narrow (59). Bose and co-workers (60) found that the universal calibrations of polystyrene sulfonate and dextrans do not coincide. For a 25% hydrolyzed PAM, its absolute $\overline{M}w$ (1.8×10^6 g/mole) determined from universal calibration is

Table 4 Molecular Weight of 80/20 W/W Acrylamide/DMDAAC Copolymers

	Relative to poly (DMDAAC) standards			Relative to polyacrylamide standards		
Sample	$\overline{M}w$	$\overline{M}n$	$\overline{M}w/\overline{M}n$	$\overline{M}w$	$\overline{M}n$	$\overline{M}w/\overline{M}n$
Copolymer 1	6.13E6	1.57E6	3.90	3.06E6	8.45E5	3.62
Copolymer 2	7.59E4	1.18E4	6.43	7.16E4	3.48E4	2.06
Copolymer 3	2.66E5	3.13E4	8.50	1.58E5	6.76E4	2.34
Copolymer 4	1.85E6	8.38E4	22.1	8.47E5	1.48E5	5.72

Table 5 Weight-Average Molecular Weight ($\overline{M}w$) and Intrinsic Viscosity of PAM and 25% Hydrolyzed PAM

			Measured $\overline{M}w$ (g/mole) (Relative to PAM Standards)	
Sample	[η] dl/g	Given $\overline{M}w$ (g/mole) by LALLS	Universal calibration	Peak position calibration
HYPAM	16.483	—	1.8E + 06	5.0E + 06
PAM 1	8.095	6.0E + 06	5.4E + 06	5.9E + 06
PAM 2	2.975	1.3E + 06	1.5E + 06	1.2E + 06
PAM 3	2.210	5.0E + 05	5.4E + 05	5.2E + 05
PAM 4	0.896	1.6E + 05	1.8E + 05	1.6E + 05
PAM 5	0.312	3.7E + 04	3.4E + 04	3.7E + 04

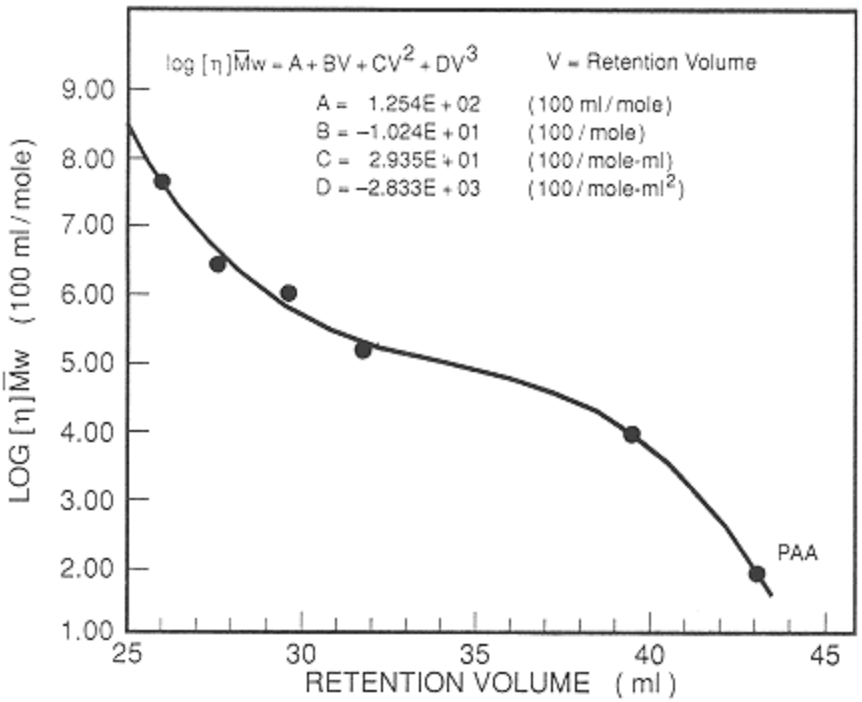

Figure 5.
Universal calibration curve of five PAM and one PAA samples.

about one-third of its relative $\overline{M}w$ (5.0×10^5 g/mole) determined from PAM standards. The high relative $\overline{M}w$ is due to the intrinsic viscosity (16.483 dl/g). Only the universal calibration technique can provide the correct information.

MW and Column Pore Size Distribution

Table 6 shows the $\overline{M}w$ determined from two column pore size distributions and two mobile phases. The $\overline{M}w$ values determined from two systems for four PAM samples 1, 2, 3 and 5 agree very well. Also, their $\overline{M}w$ values agree with the given values. However, for sample 4, the $\overline{M}w$ (1.6×10^5 g/mole) determined from four columns (TSK G6000/5000/4000/3000 PWXL) and the neutral pH mobile phase agrees with the given $\overline{M}w$ while the $\overline{M}w$ (2.0×10^5 g/mole) determined from three columns (TSK G6000/5000/3000 PW) and the acidic pH (3.1) mobile phase is about 25% higher than the given $\overline{M}w$ (1.6×10^5 g/mole). It seems that the pore size of a TSK G4000PWXL column gives a better separation for the MW range of 1.0×10^4 to 2.0×10^5 g/mole.

Applications of Sec

SEC is mainly used for determining MW and MWD simultaneously. Other applications of SEC technique for various studies in industry have been reported in references 25, 37, 38, and 40. The additional projects, which were carried out by the author, will be discussed in this section.

Table 6 Weight-Average Molecular Weight ($\overline{M}w$) and Polydispersity ($\overline{M}w/\overline{M}n$) of Polyacrylamides

		Measured $\overline{M}w$ and $\overline{M}w/\overline{M}n$ (relative to PAM Standards)			
		Determined from Column Set 1		Determined from Column Set 2	
Sample	Given $\overline{M}w$ by LALLS (g/mole)	$\overline{M}w$ (g/mole)	$\overline{M}w/\overline{M}n$	$\overline{M}w$ (g/mole)	$\overline{M}w/\overline{M}n$
PAM 1	6.0E + 06	5.85E + 06	3.83	5.78E + 06	3.87
PAM 2	1.3E + 06	1.18E + 06	3.99	1.16E + 06	3.95
PAM 3	5.0E + 05	5.15E + 05	2.92	5.23E + 05	3.38
PAM 4	1.6E + 05	1.64E + 05	1.93	2.02E + 05	2.44
PAM 5	3.7E + 04	3.70E + 04	2.03	3.66E + 04	1.93

Column Set 1: TSK G6000/5000/4000/3000/PWXL 0.3 M NaCl + 0.1 M KH_2PO_4, pH = 7.0

Column Set 2: TSK G6000/5000/4000 PW 0.15 M Na_2SO_4 + 1% (v/v) acetic acid, pH ~ 3.1

For Anionic Acrylamide Polymers

Monitoring the MW and MWD of Products for Manufacturing

Figure 6(a) shows three lots of 65/35 wt % AM/AA having a consistent MW and MWD. Figure 6(b) shows that an abnormal lot of product contains high MW species compared to a normal product. By comparing the raw chromatograms of any lots of product to a control, the abnormal lot of product can be easily identified.

Determining Percent Active Polymer in Solution Product

Figure 7(a) shows the chromatograms obtained using a RI single detector for five low MW AM/AA solutions. The injected mass of the five solutions varies from 9.48E-06 to 1.90E-04 grams. A calibration curve that relates the injected mass and total area of the polymer peak for the five solutions is shown in Figure 7(b). Utilizing the calibration constant (4.90E-10 g/unit area) obtained from Figure 7 (b), the active polymer in the copolymer sample has been determined to be 30.2%. It is about 0.6% higher than the expected value (29.6%).

Determining the Molecular Weight Reduction and Mass Loss of Degraded Polymer

Figure 8 shows SEC chromatograms of 75/25 wt % AM/AA copolymer treated at various conditions (44). The 4000 ppm solution treated in an autoclave at 350°C and 2400 psi pressure has about 82% $\overline{M}_w$ reduction and about 71% mass loss. This mass loss can be determined from the reduction of area for the degraded polymer in each sample. Both proton and carbon-13 NMR analyses indicated that the lost mass was converted to the low MW degradation products. It appears that the hydrolysis of AM and chain scissoring of the polymer chains occurred during the heating process in an autoclave. The molecular weight of the degradation product is lower than the separation limit (MW is about 600 g/mole) of the columns at the low molecular end.

For Cationic Acrylamide Polymers

Providing a Guideline for Process Development in the Polymer Synthesis Area

Studying Structure/Performance Relationship

Figure 9 shows the chromatogram of two precipitated samples of AM/AA/DMDAAC emulsion terpolymers. The high MW and narrow peak width in chro-

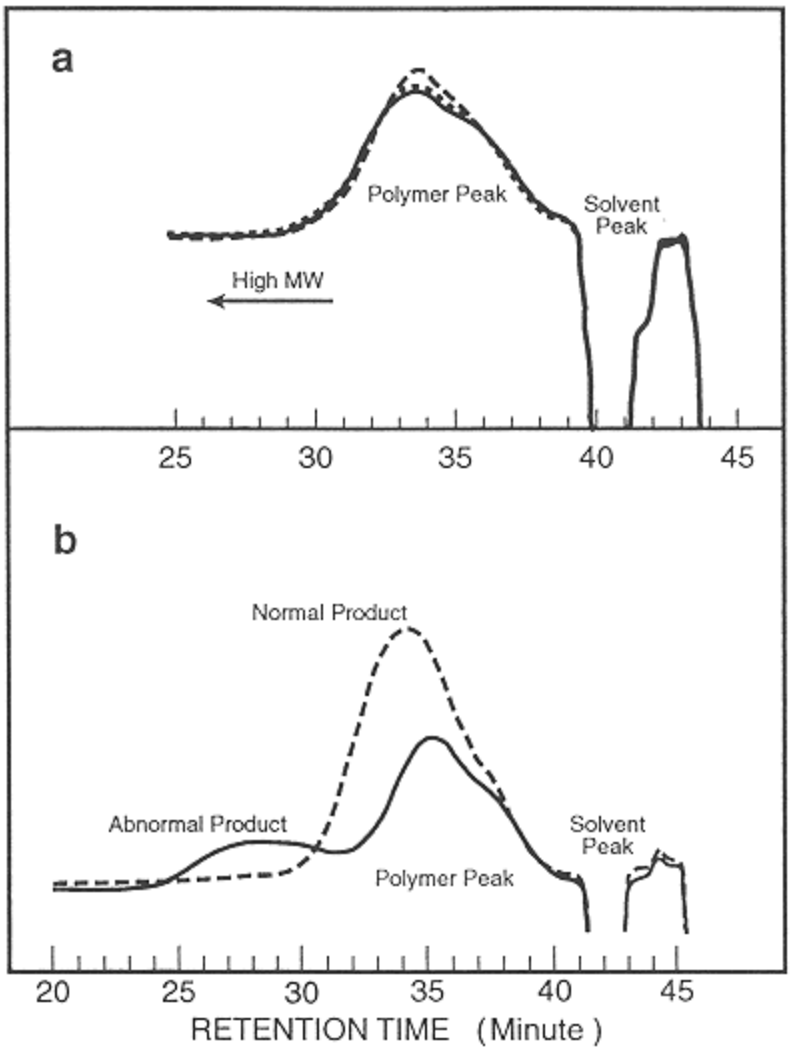

Figure 6.
(a) Size exclusion chromatograms of three lots of 65/35 wt % AM/AA copolymers which have a consistent MW and MWD. (b) Comparison between the size exclusion chromatograms of a normal and an abnormal products of 65/35 wt % AM/AA copolymers.

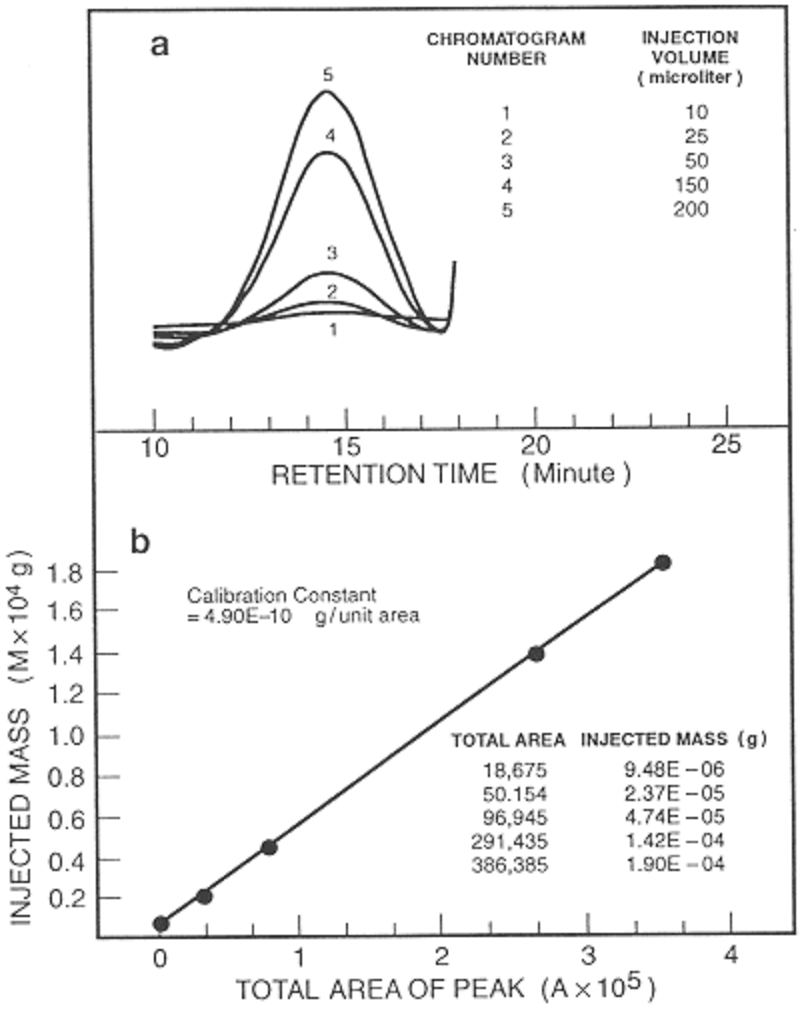

Figure 7.
Size exclusion chromatograms and concentration calibration curve of low MW AM/AA copolymer ($\overline{M}_w$ = 8,000 g/mole).

matogram (1) is due to cross-linked species in the sample. The same phenomenon is not observed in chromatogram (2). This structure difference leads to different behaviors in a paper industrial application. The partially cross-linked terpolymer performs well and the non-cross-linked terpolymer performs poorly. Based on this information, a cross-linking agent may be added during the polymerization process to modify the structure until the desired structure is obtained.

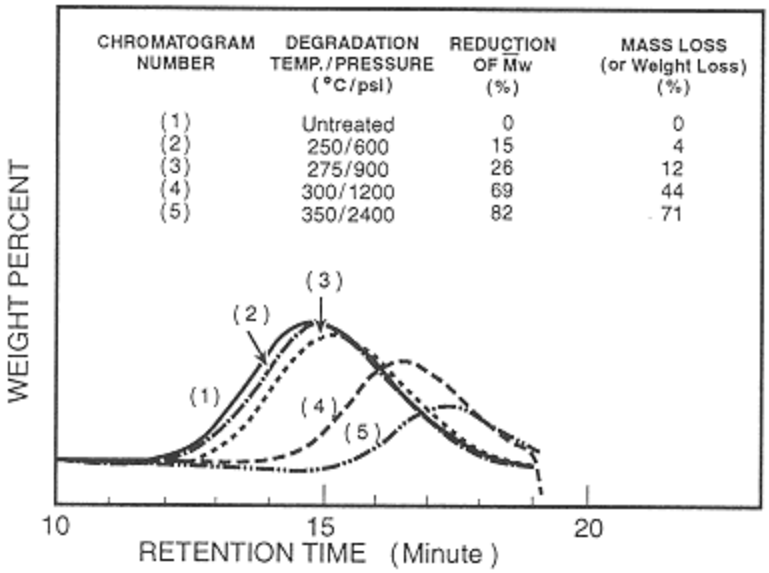

Figure 8.
Size exclusion chromatograms of A 75/25 wt % AM/AA copolymer treated at various conditions (4000 ppm solution). (Courtesy of Millipore Corporation).

Studying the Kinetics of a Chemical Reaction

Four 90/10 wt % AM/DMDAAC copolymers were synthesized with different initiator levels. The correlation between log $\overline{M}_w$ and initiator level for four copolymers is a third order equation as shown in Figure 10. For a desired MW range, the required initiator level can be predicted from Figure 10.

Studying the Distribution of Dansyldiallylamine Incorporation Along an AM/DMDAAC Copolymer

Figure 11 shows the RI and UV scans of dansyldiallylamine tagged AM/DMDAAC (50/50 w/w monomer charge ratio) copolymers. No UV signal can be observed for the copolymer synthesized at pH 6.5, so dansyldiallylamine did not incorporate into this copolymer chain. However, the chromatograms of UV and RI scans for a copolymer synthesized at pH 3.0 are similar. This indicates that the dansyldiallylamine has been incorporated evenly throughout the entire copolymer chain.

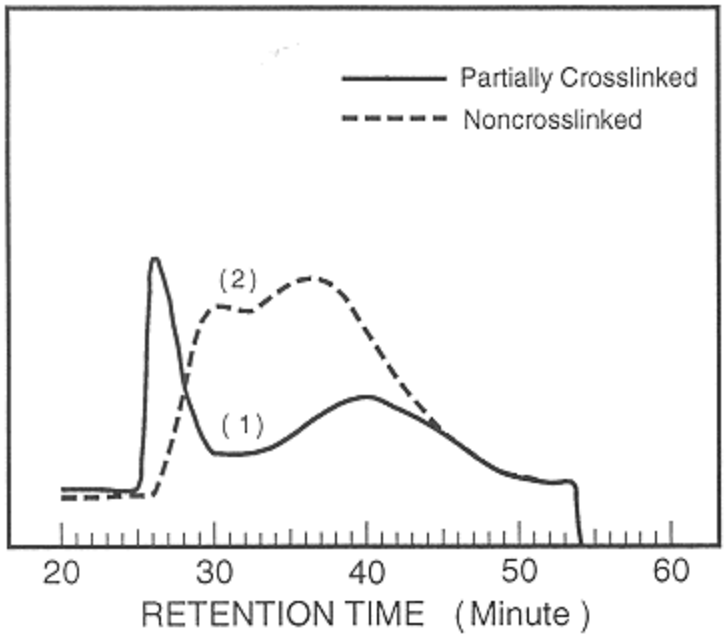

Figure 9.
Size exclusion chromatograms of two precipitated AM/AA/DMDAAC emulsion terpolymers: (1) partially crosslinked terpolymer; (2) noncrosslinked terpolymer.

Studying Formulation of Polymer Blends

In Figure 12, chromatogram (a) is a blend of 90/10 w/w AM/AA copolymer and epichlorohydrin polyamine. The composition determined by NMR spectroscopy for this polymer blend is 65/35 wt % copolymer/polyamine. Based on this information, the higher MW peak is AM/AA copolymer and the lower MW peak is polyamine. Chromatogram (b) is a formulated blend of 92.5/7.5 wt % AM/AA copolymer and polyamine. In a comparison of the two chromatograms, the molecular size of the copolymer in the formulated blend is found not to be as large as the molecular size of the copolymer in the desired blend. In industrial applications, these two polymer blends may behave differently. The area ratio of two overlapping chromatographic peaks can be more easily determined by using a deconvolution technique reported by R. A. Vaidya and R. D. Hester (61).

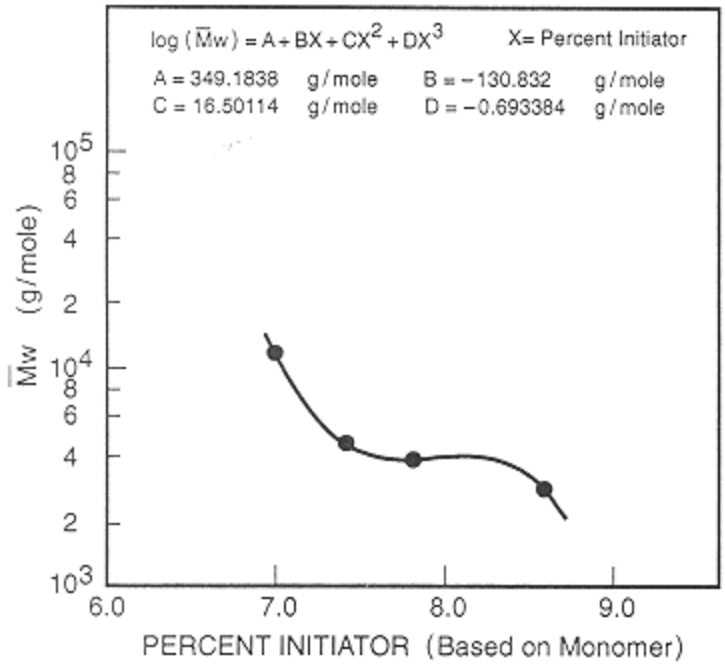

Figure 10.

log $\overline{M}_w$ (relative to PolyDMDAAC standards) versus % initiator for 90/ 10 wt % AM/DMDAAC copolymers.

Conclusions

SEC is a very powerful tool for characterizing polymers and studying the relationship of their various properties and performances in industrial applications. Additionally, the SEC technique demonstrates the capability for guiding process development in the polymer synthesis and studying the kinetics of a chemical reaction. The combination of SEC and NMR techniques is especially useful for studying the formulation of polymer blends and the degradation of polymers. However, the high-molecular-weight ($\overline{M}_w$) acrylamide polymers are difficult to separate efficiently by the commercially available columns at the present time. The chromatographic systems, sample preparation, characterization of MW standards, and calibration technique affect the SEC MW and MWD determination. Therefore, values obtained for SEC MW and MWD should be interpreted carefully.

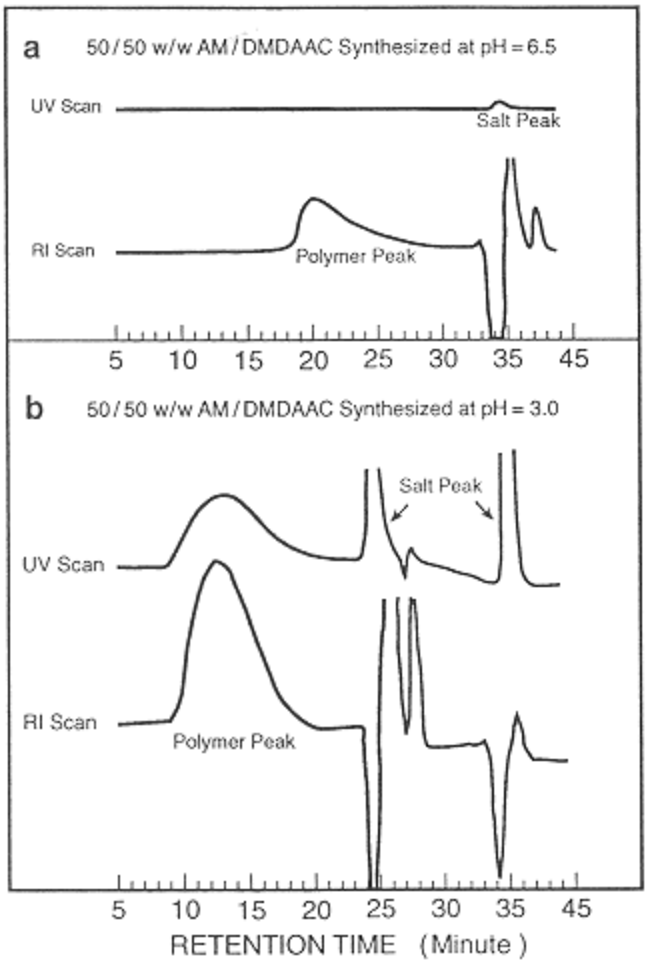

Figure 11.
Size exclusion chromatograms (raw data)
of dansyldiallylamine tagged 50/50 wt % AM/DMDAAC
copolymers.

Acknowledgement

The author expresses her appreciation to Calgon Corporation for its permission to publish this article and for its support on all research work.

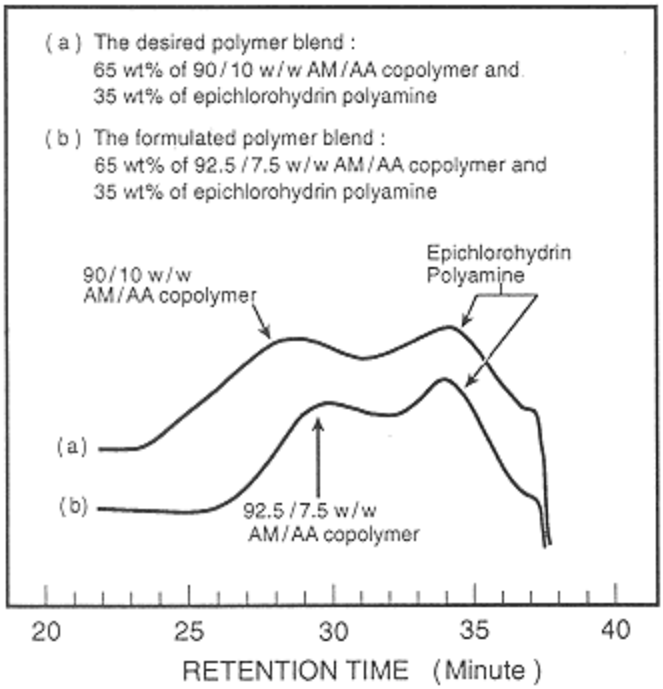

Figure 12.
Size exclusion chromatograms of polymer blends.

Appendix: SEC Experimental Conditions

Polymer	Column	Mobile phase	Comments	Chapter/ reference
Polyacrylamide	Controlled-porosity glass (CPG-10)Mean pore diameter: 3000, 3000, 2000, 1000 and 729 Å Column size = 4 ft × 3/8 in. I.D.	Aqueous solution Contains Na_2SO_4 (ionic strength = 0.25), 0.025 g/L polyethylene oxide, 1.5 g/24L Tergitol, 2.5% CH_3OH, pH = 7.0	RI detector	32

(table continued on next page)

(table continued from previous page)

Polymer	Column	Mobile phase	Comments	Chapter/ reference
Polyacrylamide	Controlled-porosity glass Mean pore diameter: 3125, 486, 255, and 75 Å Column size = 4 ft × 3/8 in I.D.	Formamide with 10^{-1} M to 5×10^{-3} M KCl	RI detector	33
Polyacrylamide	Controlled-porosity glass Mean pore diameter: 3125, 2000, 973, 493, 240 and 123 Å Column size = 4 ft × 3/8 in I.D.	Aqueous solution with 0.005 M KCl	RI detector	34
Polyacrylamide Acrylamide/ sodium acrylate copolymer Dextrans, polystyrene sulfonated	Controlled-porosity glass Mean pore diameter: 16.4–300 nm Column size: 620 mm long 7 mm I.D.	Aqueous solution with 0.1 M Na_2SO_4, which contained 10 ppm biocide Kathon WT	RI detector Cubic B-spline calibration technique	35
Polyacrylamide Polyethylene oxide Polyvinyl alcohol Hydroxyethyl cellulose	Polyvinylpyrrolidone Water (PVP)-coated silica Mean pore diameter: 100, 500, 1000 and 4000 Å Column size: 30 cm length 48 mm ID	Water	RI detector Universal calibration	36
Hydrolyzed polyacrylamide, 26/74 mole %	Wet-packed Sephacryl S 1000 superfine (Pharmacia Fine Chemicals) Column size: 2.6 cm diameter 70 cm or 100 cm bed height	Aqueous solution with 1 M NaCl	Collected fractions and analyzed by LALLS.	39
Acrylate/acrylamide copolymer			Determined diffusion coefficients by photon correlation light scattering	

(Table continued on next page)

(Table continued from previous page)

Appendix: (Continued)

Polymer	Column	Mobile phase	Comments	Chapter/ reference
Cellulose acetate -grafted acrylamide copolymer	CPG-10 Mean pore diameter: 2023, 1223, 723, 129 Å Column size: 90 cm × 9 mm I.D.	Water	RI and UV detectors	37
Dextran-grafted acrylamide copolymer	Porous glass Mean pore diameter: 300, 1400, 700, 350, 240, 170 Å Column size: 60 × 0.762 cm I.D.	Aqueous solution with 0.05 M potassium biphthalate	RI detector	38
Polyacrylamide CPG-10 2000 Å,	Bio glass 2500 Å, 125/240/370 Å Porasil DN 400/800 Å Porasil CX 200/400 Å	Water	RI detector	41
Polyacrylamide	Dry-packed controlled porosity glass Mean pore diameter: 700, 1000 and 3000 Å Particle size: 200/400 mesh Column size: 3.8 in. I.d. 4 –6.5 ft long	Aqueous solution with 0.2 M Na_2SO_4 + 1 g/25 L Tergital NPX (Union Carbide Corp.)	DRI/LALLS dual detectors	47
Polyacrylamide hydrolyzed polyacrylamide Acrylamide/ acrylic acid copolymers	TSK columns: Guard+ G6000 PWXL + G5000 PWXL + G4000 PWXL + G3000 PWXL	Aqueous solution with 0.3 M NaCL + 0.1 M KH_2PO_4 adjusted pH = 7.0 by 50/50 w/w NaOH	RI/LALLS dual detectors	44
Polyacrylamide Acrylamide/ dimethyl diallylammonium chloride copolymers	TSK columns: Guard+ G6000 PW + G5000 PW + G3000 PW	Aqueous solution with 0.3 M Na_2SO_4 + 1% acetic acid pH = 3.1	RI/LALLS dual detectors	44

(table continued on next page)

(table continued from previous page)

Polymer	Column	Mobile phase	Comments	Chapte referen
Polyacrylamide	Shodex OH -Pak or Ultrahydrogel	Pure water or 0.5M $LiNO_3$ aqueous solution	LALLS/Viscometer/RI triple detectors	46
Methacryloxy-ethyl trimethylammonium chloride/AM copolymer, diallyldimethyl ammonium chloride copolymer	TSK PWH guard column + TSK PWXL mixed-bed column	0.24 M aqueous sodium formate pH 3.7	RI	40

References

1. *Acrylamide polymers,* in *Encylopedia of Science and Technology,* 1st Ed., Vol. 1, 177–197, and references therein by W. M. Thomas, American Cyanamid Company. Interscience Publishers, New York (1964).

2. *Acrylamide polymers,* in *Encyclopedia of Science and Engineering,* 2nd Ed., Vol. 1, 169–211, and references therein by W. M. Thomas, American Cyanamid Company. John Wiley & Sons, New York (1985).

3. D. N. Schulz, *Kinetic and Practical Aspects of Water Soluble Polymer Synthesis,* Water Soluble Short Course sponsored by The University of Southern Mississippi, Dept. of Polymer Science, Feb. 24–25, 19

4. R. A. M. Thomson, Methods of polymerization for preparation of water soluble polymer, in *Chemistry and Technology for Water Soluble Polymer,* 31–70, C. A. Finch, Ed., Plenum, New York (1983).

5. N. M. Bikales, *Water soluble polymers,* in *Polymer Science and Technology,* Vol. 2, 213–225, N. M. Bikales, Ed.,: Plenum, New York, (1973).

6. N. Yoshida, Y. Ogana, and R. Handa, U.S. Patent 4,306,045. Assigned to Nitto Chemical Company, Dec. 15, 1981.

7. K. Plochoka, *J. Makromol. Sci. Rev. Macromol. Chem., C20*(1), 67 (1981).

8. K. Y. Park, E. R. Santee, and H. J. Harwood, *ACS Polym. Prepr. 27*(2), 81 (1986).

9. U.S. Patent 4,022,731, May 10, 1977. Assigned to American Cyanamide Company.

10. U.S. Patents 3,624,019, Re28,474, July 8, 1974. Assigned to Nalco Chemical Co.

11. D. N. Schulz, J. J. Mauer, and J. Bock, U.S. Patents 4,463,151 and 4,463,152. Assigned to Exxon, Ju 31, 1984.

12. W. M. Kulicke, R. Kniewske, and J. Klein, *Prog. Polym. Sci. 8*, 373 (1982).

13. R. H. Yocum and E. B. Nyquist, Ed., *Functional Monomers,* Vol. 1, Ch. 1, 23–52, and references therein, Marcel Dekker, Inc., New York (1973).

14. R. Schulz, G. Renner, H. Henglien, and W. Kern, *Makromol. Chem., 12,* 20 (1954).

15. W. B. Crummett and R. A. Hummell, *J. Amer. Waterworks Ass., 55,* 209 (1963).

16. Thomas Chung-li Shen, *Controlled Polymerization of Acrylamide to Produce Copolymers with Unique Solution and Viscosity Properties,* Ph.D. Dissertation, University of Southern Mississippi, University of Microfilms International (1977).

17. Muyen Michael Wu, *Polymerization of Acrylamide in Water-In-Oil Microemulsion,* Ph.D. Dissertation, University of Akron, University Microfilms International (1983).

18. R. A. M. Thomson, A kinetic study of the adiabatic polymerization of acrylamide, *J. Chem. Educ.*, *63*(4), 362–364 (1986).

19. T. Ishige and A. E. Hamielec, *J. of Appl. Poly. Sci., 17,* 1479–1506 (1973).

20. W.-C. Hsu, C.-Y. Chen, J.-F. Kuo, and E. M. Wu, *Polymer*, *35*(4), 849–856 (1994).

21. F. A. Adamsky and E. J. Beckman, Inverse emulsion polymerization of acrylamide in supercritical carbon dioxide, *Macromolecules, 27*(1), 312–314 (1994).

22. Y. L. Meltzer, *Water-Soluble Resins and Polymers Technology and Applications,* 14–44, Moyes Data Corp., New Jersey (1976).

23. J. A. Caskey, *The Effect of Polyacrylamide Molecular Structure on Flocculation Activity of Domestic Sewage,* Final report to National Science Foundation Thermodynamic and Mass Transfer Division of Engineering for Research Grant, July 15, 1977.

24. W. Yau, J. Kikland, and D. Bly, *Modern Size Exclusion Chromatography,* John Wiley & Sons, New York (1979).

25. H. G. Barth, *J. of Chrom. Science, 18,* 409–429 (September, 1980).

26. O. Chiantore and M. Guaita, *J. of Liq. Chrom. (*9), 1867–1885 (1984).

27. M. Song and G. Hu, *J. of Liq. Chrom. 8*(14), 2543–2556 (1985).

28. M. Song and G. Hu, *J. of Liq. Chrom. 11*(2), 363–381 (1988).

29. S. Pokorny, J. Zábranský, and M. Bleha, *J. of Liq. Chrom. 7*(9), 1887–1901 (1984).

30. H. G. Barth and F. J. Carlin, Jr., *J. of Liq. Chrom. 7*(9), 17 (1984).

31. J. C. Giddings, *Adv. in Chromatogr., 20* (Ch. 6), 217–258 (1982).

32. S. N. E. Omorodion, A. E. Hamielec, and J. L. Brash, *ACS Symposium Series 138, Size Exclusion Chromatography* (GPC), 267–284, (1980).

33. N. Onda, K. Furusawa, N. Yamaguchi, and S. Komuro, *J. of Appl. Poly. Sci., 23,* 3631–3638 (1979).

34. N. Onda, K. Furusawa, N. Yamaguchi, M. Tokiwa, and Y. Hirai, *J. of Appl. Poly. Sci., 25,* 2363–2372 (1980).

35. J. Klein and A. Westerkamp, *J. of Poly. Sci., Poly. Chem. Edition, 19,* 707–718 (1981).

36. L. Letot, J. Lesec, and C. Duivoron, *J. of Liq. Chrom., 4*(8), 1311–1322 (1981).

37. N. I. El-Awady, N. A. Ghanem, W. B. Pedersen, and K. Singer, *European Polymer Journal, 15,* 1017–1024 (1979).

38. C. McCormick and L. Park, *J. of Appl. Poly. Sci., 26,* 1705–1717 (1981).

39. G. Muller and C. Yonnet, *Makromol. Chemi., Rapid Commun., 5,* 197–201 (1984).

40. Shyhchang S. Huang, *J. of Chrom., 536,* 203–209 (1991).

41. A. H. Abdel-Alim and A. Hamielec, *J. of Appl. Poly. Sci., 18,* 297–300 (1974).

42. T. V. Alfredson, C. T. Wehr, L. Tallman, and F. Klink, *J. of Liq. Chrom., 5*(3), 489–524 (1982).

43. H. Sasaki, T. Matsuda, O. Ishikawa, T. Takamatsu, K. Tanaka, Y. Kato, and T. Hashimoto, *Scientific Report of Toyo Soda Manufacturing Company, Ltd., 29*(1), 37–54 (1985).

44. F. C. Lin and G. D. Getman, *Internal GPC Symposium '87,* Millipore Corp. 225–245.

45. K. K. Dhowa Denko, Shodex application data on Shodex aqueous GPC columns.

46. C. J. Kim, A. Hamielec and A. Bendek, *J. of Liq. Chromatog., 5*(7), 1277–1294 (1982).

47. J. Lesec and G. Volet, *Internal GPC Symposium '89,* Millipore Corp. 386–405.

48. K. Min and C. Cha, Technical Report, Calgon Corporation (1981).

49. W. Rand and A. Mukerji, *J. of Liq. Chromatog., 5*(5), 841–851 (1982).

50. C. E. Lundy and R. D. Hester, *J. of Liq. Chrom. 7*(10), 1911–1934 (1984).

51. C. E. Lundy and R. D. Hester, *J. of Poly. Sci., Part A: Polymer Chemistry, 24,* 1829–1839 (1986).

52. S. A. Chen and H. C. Hu, *J. of Poly. Sci., Polymer Chemistry Edition, 21,* 3373–3380 (1983).

53. M. A. Langhorst, F. W. Stanley, Jr., S. S. Cutie, J. H. Sugarman, L. R. Wilson, D. A. Hoagland, and R. K. Prud'homme, *Anal. Chem., 58*(11) Sept., 2242–2247 (1986).

54. E. E. Remsen and J. J. Freeman, *Applied Spectroscopy, 45*(5), 868–873 (1991).

55. Th. G. Scholte, *Techniques and Methods of Polymer Evaluation,* Vol. 4, Ch. 8, 542–547, Marcel Dekker Inc., New York (1975).

56. M. B. Huglin, *Determination of molecular weight by light scattering, in Top. Curr. Chem. 77 (Inorg. Phys. Chem.),* 155–208, Springer-Verlag (1979).

57. J. Stejskal and J. Horska, *Makromol. Chem., 183,* 2527–2535 (1982).

58. K. K. Chee, *J. of Appl. Poly. Sci., 34,* 891–899 (1987).

59. D. Lecacheux, J. Lesec and C. Quivoron, *J. of Liq. Chrom., 5*(2), 217–228 (1982).

60. A. Bose, J. Rollings, J. Caruthers, M. Okos and G. Tsao, *J. of Appl. Poly. Sci., 27,* 795–810 (1982).

61. R. A. Vaidya and R. D. Hester, *J. of Chrom., 287,* 231–244 (1984).

10
Aqueous Size Exclusion Chromatography of Polyvinyl Alcohol

Dennis J. Nagy Air Products and Chemicals, Inc., Allentown, Pennsylvania

Introduction

Polyvinyl alcohol (PVA) is the largest volume, synthetic, water-soluble polymer resin produced in the world. PVA, a polyhydroxy polymer, is synthesized commercially by the hydrolysis (or methanolysis) of polyvinyl acetate (PVAc). As a result of keto-enol tautomerism, the vinyl alcohol monomer does not exist in the free state, and only traces have been detected (1–3). PVA was discovered in 1924 by Herrmann and Haehnel, who added alkali to a clear solution of PVAc and obtained the ivory-colored resin, PVA (4).

Today, PVA is used in a wide range of applications because of the excellent physical properties of the resin. Primary end uses of PVA include adhesives, fibers, textile and paper sizing, emulsion polymerization, and the production of polyvinyl butyral. Significant volumes of PVA are also used in joint cements for building construction; water-soluble films for hospital laundry bags; cold water-soluble packaging for herbicides, pesticides, and fertilizers; temporary protective films; emulsifiers in cosmetics; and photoprinting plates. PVA is an excellent adhesive and possesses superb solvent, oil, and grease resistance. Films of PVA have high tensile strength, good abrasion resistance, and excellent oxygen barrier properties at low humidity. Because of low surface tension, the emulsification and protective colloid properties of PVA are excellent. PVA is also biodegradable (1). An interesting application of PVA is its use as a hydrophilic packing material for size exclusion chromatography (SEC) (5–8).

Commercial production of PVA from PVAc is carried out via a continuous process. PVAc is polymerized with a free radical initiator in methanol, usually between 55 and 85°C. Molecular weight is controlled by the residence time in the reactors, monomer feed rate, solvent concentration, initiator concentration, and polymerization temperature. Direct hydrolysis or catalyzed alcoholysis converts the PVAc into the corresponding PVA, a water-soluble polymer (1). The degree of hydrolysis can be controlled to yield various grades of PVA: super-hydrolyzed (>99 mol%), fully hydrolyzed (98 mol%), and partially hydrolyzed (88 mol%). There are also specialty grades less than 80 mol%. The annual worldwide capacity of PVA is about 750 million pounds.

The physical properties of PVA depend to a greater extent on the method of synthesis than do those of most other polymers. This is because the final properties are affected by the polymerization of the parent PVAc, hydrolysis conditions, drying, and grinding (1). For example, the degree of hydrolysis determines the final glass transition temperature of PVA, usually between 58 and 85°C.

The molecular weight and molecular weight distribution affect many of the physical properties of PVA. These include solution viscosity, tensile strength, block resistance, water and solvent resistance, adhesive strength, and dispersing power. These effects are well documented (1,9–11). Reliable and accurate methods are required to understand the effect of molecular weight on physical properties and, ultimately, the performance of PVA in any application or process.

The discussions in this chapter review prior work for the molecular weight characterization of PVA. The major emphasis is on recent studies utilizing low- angle laser light scattering (LALLS), multiangle laser light scattering (MALLS), and differential viscometry (DV) as molecular weight-sensitive detectors for aqueous SEC of fully and partially hydrolyzed PVA. The advantages and disadvantages of using each of these techniques are summarized.

Historical Review of Aqueous SEC of PVA

Early Aqueous SEC Characterization of PVA

Characterization of PVA by SEC has closely followed the advances in column and detection technology. Aqueous SEC, in particular, presents a number of challenges as a result of frequently encountered secondary, non-size exclusion effects. These effects, common to aqueous SEC, have been reviewed by Barth (12).

Although PVA is a water-soluble polymer, early molecular weight characterization involved the reacetylation of the resin to PVAc and subsequent SEC analysis in tetrahydrofuran or toluene (10,13). Direct analysis of PVA by aque-

ous size exclusion chromatography was first reported in 1969 by Bombaugh et al. using deactivated porous silica (Porasil) as the column support material (14). Four columns, each 4 feet in length, were employed with water as the mobile phase at 65°C. Dextrans were used as calibration standards. Using pyridine and valeric acid, the authors demonstrated the deactivation of the silica packing and its suitability for steric size separations. PVA, which was permanently retained on unmodified Porasil, was reproducibly fractionated on the deactivated material with no evidence of adsorption. The differences in molecular weight distribution of PVA prepared by various polymerization methods (bulk, solution, and suspension) are shown as concentration chromatograms in Figure 1. The time frame for these separations was over 2 h (14).

Belenkii et al. described the aqueous SEC of PVA along with dextran, polyvinyl pyrrolidone, and polyethylene oxide using Sephadex G-75 and G-100 packing (15). Plots of log (intrinsic viscosity × molecular weight) versus elution volume exhibited significant deviations from Benoit's principle of universal calibration (16). It was suggested that this behavior was caused by different degrees of thermodynamic compatibility of the eluted polymers with the sorbent matrix.

The use of μBondagel as a column support material for the separation of PVA was demonstrated by Vilvilecchia et al. in 1977 (17). This was the first example of the use of high-performance columns for the fractionation of PVA.

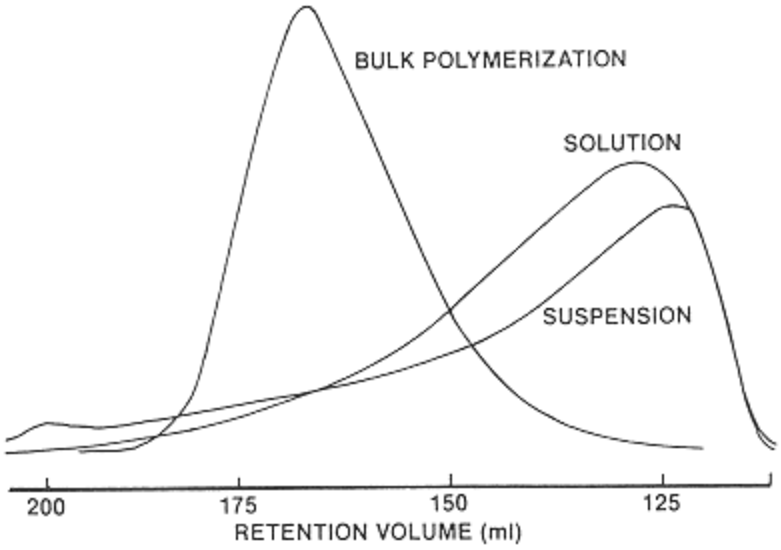

Figure 1
SEC chromatograms of PVA from various methods of producting using deactivated Porasil (14). (Courtesy of Waters/Millipore Corporation.)

These columns yielded 15,000–30,000 theoretical plate counts per meter, with separations of the order of 5–20 minutes. µBondagel is a silica-based support with a particle size of about 10 µm. PVA was successfully fractionated using water as a mobile phase with a µBondagel E-Linear column. Detection was with a differential refractive index (DRI) detector and an ultraviolet (UV) photometer at 254 nm (Figure 2). The authors attributed the increase in the UV absorption of the "used" PVA as a probable indication of polymer oxidation.

SEC of PVA with Hydrophilic Polymer Gels

In 1978, TSK gel type PW column supports became commercially available from Toyo Soda Manufacturing Company, Ltd., Japan. The first reported use of these new packings for the SEC characterization of PVA was by Hashimota et al. (18). These supports, which have gained wide popularity for SEC of water-

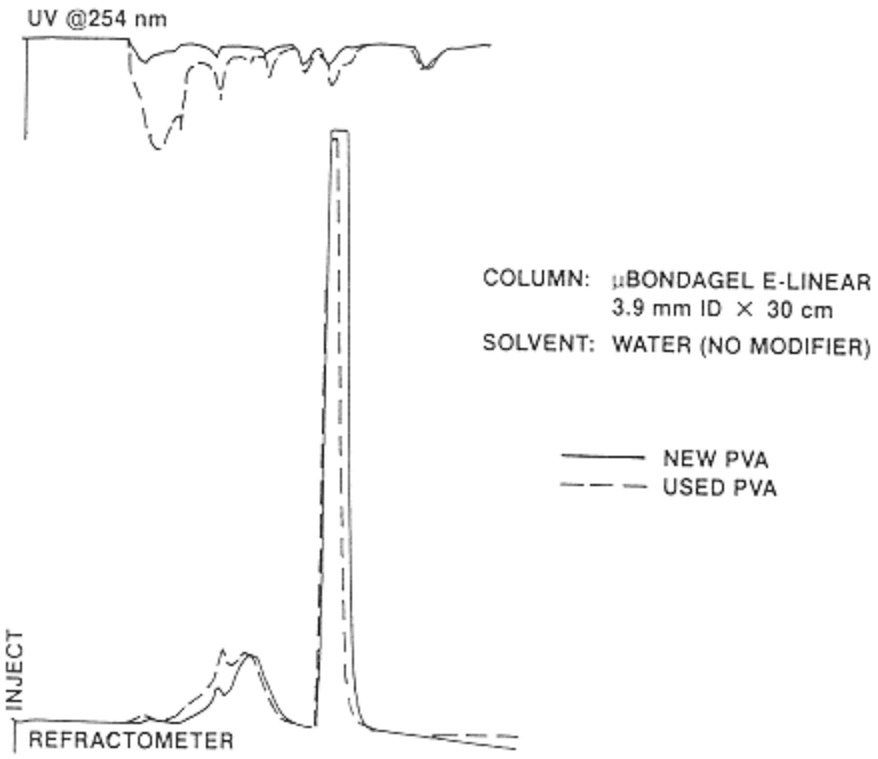

Figure 2
Separation of PVA samples using a µBondagel E-Linear column (17). (Courtesy of Waters/Millipore Corporation.)

soluble polymers, contain a polyether gel (-$CH_2CHOHCH_2O$-) and residual carboxylate functionality on the packing surface (19,20). The TSK-PW columns contain a high number of theoretical plates and are available in a range of pore sizes.

These authors demonstrated the separation of dextrans, polyvinyl pyrrolidones, polyacrylamide, polyethylene glycol, and PVA on a column set consisting of one G3000 PW and two G5000 PW columns using 0.08 M Tris-HCl buffer solution at pH 7.94 and 1.0 ml/minute. PVA of 86.5–89.0% hydrolysis was efficiently separated by size. One of the highest molecular weight PVA resins commercially available (GH-23 from Nippon Gohsei) eluted within the separation range of the column set used. A drop-counting apparatus was employed to measure elution volume (every 20 drops) and mark the chart recording. The authors noted a distinct narrowing of the elution interval near the peak maximum in PVA. This was attributed to the lowering of the surface tension of the water in the mobile phase (18).

In the late 1970s, low-angle laser light scattering became commercially available as a detection method for size exclusion chromatography. LALLS detection provided a new dimension to SEC analysis of polymers as a result of the measurement of absolute molecular weight, not relative molecular weight. A more detailed discussion of LALLS detection for PVA follows in the next section.

In 1980, Fukutomi et al. reported on the application of LALLS detection for proteins, enzymes, and a variety of synthetic water-soluble polymers, including PVA (21). A differential refractometer was used as the concentration detector in tandem with the LALLS photometer. TSK-PW columns were used for the separations.

In 1981, Herman et al. published results for the separation of PVA and other synthetic, water-soluble polymers on silica-bonded diol size exclusion column supports (22). The diol bonded-phase packings were produced by reaction of glycidoxypropyltrimethoxysilane reagent with bare silica (10 μm LiChrospher), followed by acid hydrolysis of the bonded epoxide to give the diol functionality. PVA of 2000 molecular weight was separated using a monomeric diol bonded phase and an eluant of 50% methanol-water. The methanol was required to optimize recovery of the PVA through the columns. Without an organic modifier, PVA loss on the columns was attributed to hydrophobic interactions with the diol phase. The authors demonstrated that polymer recoveries and plate counts were similar to the recently commercialized TSK-PW columns (22).

Two more investigations were published in 1985 dealing with the separation of PVA materials on TSK-PW columns. The first, by Gebben et al., described the characterization of PVA cross-linked with glutaraldehyde (23). The authors wanted to study the possibility of preparing monodisperse, low-deformability polymers by the intramolecular cross-linking of linear, high-molecular-weight

PVA. This included both partially hydrolyzed and fully hydrolyzed PVA of 82,000–101,000 molecular weight (μw). TSK-PW G3000 and G4000 columns were connected in series with a Chromatix KMX-6 LALLS photometer for absolute molecular weights. The authors found surprising results by SEC and LALLS. The reaction product was not homogeneous but consisted of a mixture of PVA, which may have been both intra- and intermolecularly cross-linked. The intramolecularly cross-linked, single PVA molecules were smaller than the initial polymer molecules, and their size decreased with increasing degree of cross-linking. They concluded that intramolecular cross-linking of PVA made the molecule less deformable. After cross-linking, temperature no longer had any effect on the intrinsic viscosity of the cross-linked polymer sample (23).

That same year, Kato et al. reported the use of a new column, TSKgel GMPW, for the separation of water-soluble polymers, such as PVA (24). GMPW columns are packed with a mixture of TSKgels G2500 PW, G3000 PW, and G6000 PW. This column exhibits a wide linear calibration using polyethylene glycol, extending from several million to less than 100 molecular weight. PVA was successfully eluted on GMPW columns using 0.1 M sodium nitrate. In this paper, the authors also describe the problem they encountered with non-size exclusion behavior, specifically, hydrophobic interaction between polymer and packing. Two examples were polyvinyl pyrrolidone and anionic sulfonated polystyrene. Sulfonated polystyrene did not elute with the 0.1 M sodium nitrate mobile phase but was successfully separated with the addition of an organic modifier, acetonitrile, to the eluant (80:20 volume ratio). This result using an organic modifier is significant because the authors make no mention of the fractionation of partially hydrolyzed PVA (the more hydrophobic form of PVA). It is assumed that the data they discussed for PVA using 0.1 M sodium nitrate were for a fully hydrolyzed type. A discussion follows, in the section on aqueous SEC-differential viscometry, which describes the problems of hydrophobic interactions of partially hydrolyzed PVA on TSK columns. The resulting non-universal calibration behavior must be taken into consideration for accurate molecular weight analyses.

Aqueous SEC of PVA Using On-Line Light Scattering

Low-Angle Laser Light Scattering

Aqueous SEC/LALLS circumvents the problems of SEC calibration for PVA because it measures *absolute* molecular weight on-line. SEC/LALLS was successfully used to measure the absolute molecular weight of fully and partially hydrolyzed PVA over a wide range of molecular weights by this author (25,26). This was the first reported use of aqueous SEC/LALLS for absolute molecular

Table 1 Experimental Conditions for Aqueous SEC of PVA

SEC System	150 GPC, Waters/Millipore Corp.
Columns	Toyo Soda TSK-PW, 7.5 mm inner diameter × 30 cm, set of 1000, 2000, 3000, 4000, 5000, 6000 Å pore size
Mobile phase	0.05 M $NaNO_3$ for LALLS/MALLS 0.10 M $NaNO_3$, 0.10 M $NaNO_3$/CH_3CN (80:20, vol/vol), H_2O/CH_3CN (80:20, vol/vol) for DV (all solutions contain trace of NaN_3)
Temperature	27°C for LALLS/MALLS; 35°C for DV
LALLS	LDC/Milton Roy CMX-100 (632 nm), used with a 0.22 µm prefilter
MALLS	Wyatt DAWN F (632 nm)
Viscometer	Viscotek Model 100, parallel configuration with 150C
Flow rate	1.0 ml/minute (nominal)
Injection volume	0.500 ml for LALLS/MALLS; 0.200 ml for DV
Software	Viscotek GPC-LS Version 3.01 for LALLS Wyatt ASTRA Version 2.0 for MALLS Viscotek UNICAL Version 3.02 for viscometry
dn/dc	LDC/Milton Roy KMX-16 laser differential refractometer (632 nm)
Standards	Polyethylene glycol: 975-18,000 daltons, American Polymer Standards Corp. Polyethylene oxide: 20,000-800,000 daltons, American Polymer Standards Corp. Polyacrylamide: 8000-725,000 daltons, American Polymer Standards Corp. Polysaccharide: 6000-850,000 daltons, Polymer Laboratories
PVA grades	Fully hydrolyzed and partially hydrolyzed grades, Air Products and Chemicals, Inc.
PVA sample preparation	90°C for 30 minutes in aqueous mobile phase, prefiltered through 0.45 µm Millex-HV filter, Millipore Corp.

weight characterization for PVA over a broad range of molecular weights and various degrees of hydrolysis. Details of the experimental conditions are summarized in Table 1.

Weight-average molecular weights $\overline{M}_w$, measured by SEC/LALLS for low- and medium-molecular-weight grades (fully and partially hydrolyzed PVA), range from 36,000 to 127,000 (Table 2). For these analyses, the LALLS detector was an LDC/Chromatix CMX-100 using a measuring angle of 5–7° with a 632 nm wavelength. A 0.22 μm prefilter was used for the LALLS. This prefilter is required to minimize particulate noise and "spikes" common to low-angle laser detection. Also, summarized in Table 2 are values for the weight-average molecular weight $\overline{M}_w$ obtained from static LALLS measurements using an LDC/ Chromatix KMX-6 LALLS photometer. There is good agreement between the SEC/LALLS M_w and static LALLS $\overline{M}_w$ values for these PVA grades (25,26). From multiple determinations, the precision of the SEC/LALLS measurements was found to be ±3% (25).

Water exhibits a low value for the Rayleigh factor R_0 compared with many organic solvents. However, PVA exhibits a reasonably high value for the specific refractive index increment *dn/dc* and the polymer optical constant *K,* which enables characterization under aqueous conditions for a wide range of molecular weights. For fully hydrolyzed PVA, *dn/dc* = 0.1501 ml/g and $K = 1.632 \times 10^{-7}$ mol-cm^2/g^2. For partially hydrolyzed PVA, *dn/dc* = 0.1429 ml/g and $K = 1.478 \times 10^{-7}$ mol-cm^2/g^2. These values were measured at 27°C in 0.05 M $NaNO_3$. The assumption was made that a single value for *dn/dc* is valid for an 88% degree of hydrolysis PVA, which is in effect a copolymer of vinyl alcohol and vinyl acetate. Any significant degree of copolymer inhomogeneity as a function of molecular weight distribution (vinyl alcohol/vinyl acetate) would invalidate this assumption (25,26).

Table 2 Molecular Weight of PVA[a]

		SEC/LALLS			Static LALLS
PVA type	MW	$\overline{M}_n$	$\overline{M}_w$	$\overline{M}_w/\overline{M}_n$	$\overline{M}_w$
FH	Low	17,400	36,500	2.1	35,000
FH	Medium	60,400	111,000	1.8	107,000
PH	Low	23,400	43,500	1.9	42,800
PH	Medium	59,800	127,000	2.1	138,000

[a]FH, fully hydrolyzed; PH, partially hydrolyzed.

Source: From References 24 and 25.

The SEC/LALLS described here for PVA has some inherent limitations that must be recognized. Even with the use of high-efficiency TSK-PW packings, the polymer fraction analyzed by the LALLS is not truly monodisperse. This leads to a slight underestimation of the width of the molecular weight distribution because the calculated number-average molecular weight is biased high. A Dextran T-70 (from Pharmacia) was analyzed nine times to characterize the extent of this bias. The dextran is a broad standard with well-characterized values for molecular weight: $\overline{M}_w$ = 64,400 and $\overline{M}_n$ = 41,100. Average values from LALLS were $\overline{M}_w$ = 63,300 and $\overline{M}_n$ = 45,200. The number-average molecular weight shows a positive bias of at least 10% (25).

On the other hand, one of the advantages of using LALLS detection is the increased sensitivity to high molecular weights. Fortunately, this means that high-molecular-weight PVA requires less mass injected onto the columns (compared with low molecular weight) to achieve the necessary sensitivity. This greatly reduces the possibility of high viscosity effects (viscous fingering). The strong dependence of the LALLS detector signal on molecular weight allows characterization of PVA molecular weight abnormalities. One example is the presence of gels, undissolved PVA, or contamination by high-molecular-weight material present in very small quantities. A medium-molecular-weight, fully hydrolyzed PVA clearly illustrates this effect, as seen in the LALLS and concentration (DRI) chromatograms (Figure 3). A peak is clearly evident before the main distribution in the LALLS chromatogram. This material is not detected by the DRI detector because of its low concentration in the sample.

Multiangle Laser Light Scattering

Multiangle laser light scattering provides a means to characterize superhigh-molecular-weight grades of PVA easily. Superhigh-molecular-weight PVA is often difficult to analyze by LALLS because of sample entrapment as the polymer passes through the 0.22 µm prefilter used with the LALLS (lower molecular weight grades of PVA do not present this problem). The use of a larger 0.45 µm prefilter eliminates the sample loss problem but introduces excessive noise and particulate spikes. However, this problem is eliminated by the use of a multiangle laser light-scattering detector. A MALLS chromatogram for a super- high-molecular-weight PVA illustrates this effect at a scattering angle of 90° (Figure 4). It is important to note that the MALLS chromatogram was obtained *without* the use of a prefilter. The data were taken on a Wyatt Technology Dawn Model F MALLS in a mobile phase of 0.05 M sodium nitrate at 27°C.

The absolute molecular weights calculated from MALLS for the superhigh-molecular-weight PVA are $\overline{M}_w$ = 264,000 and $\overline{M}_n$ = 135,000 ($\overline{M}_w/\overline{M}_n$ = 2.0). A total of 15 scattering angles (21.73–158.27°) were used for the calculations. For absolute molecular weight from MALLS, a Debye plot of the scattered inten-

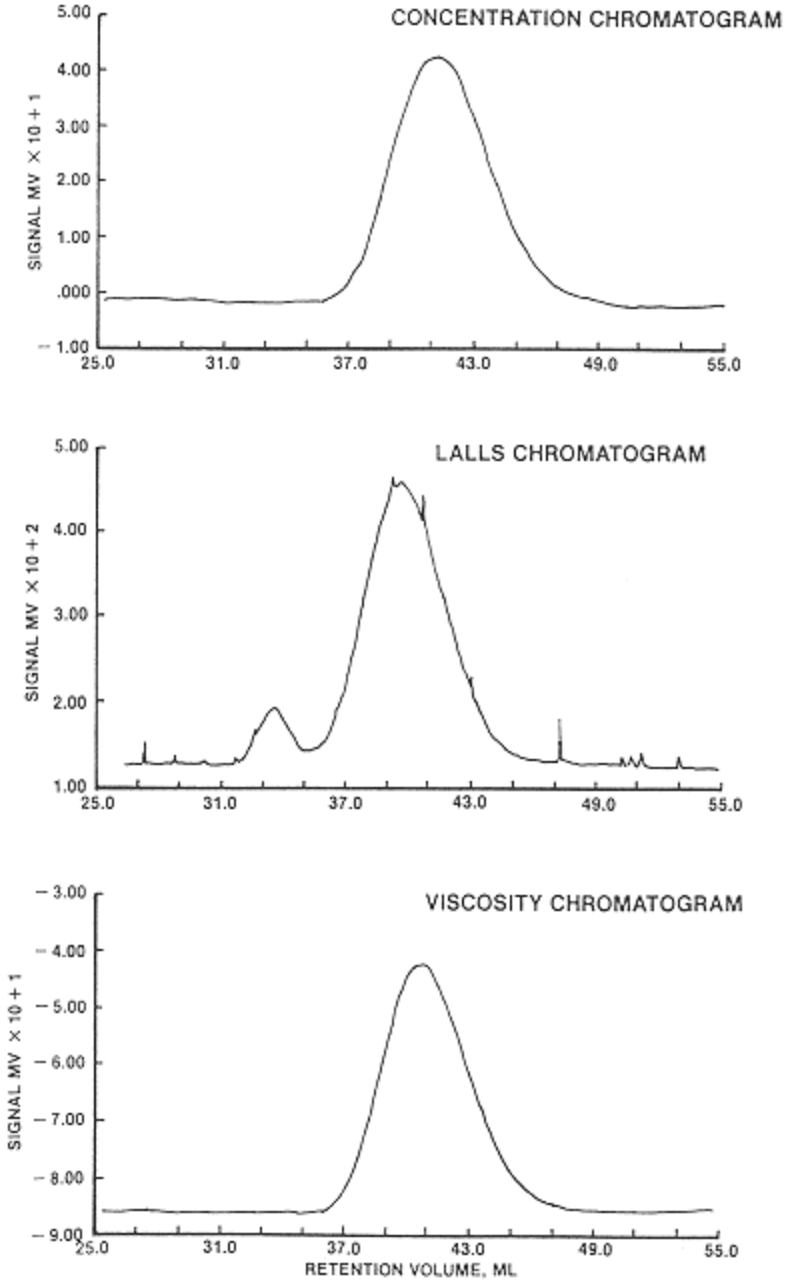

Figure 3
Concentration (DRI), LALLS, and viscometry chromatograms
for medium molecular-weight, fully hydrolyzed PVA.

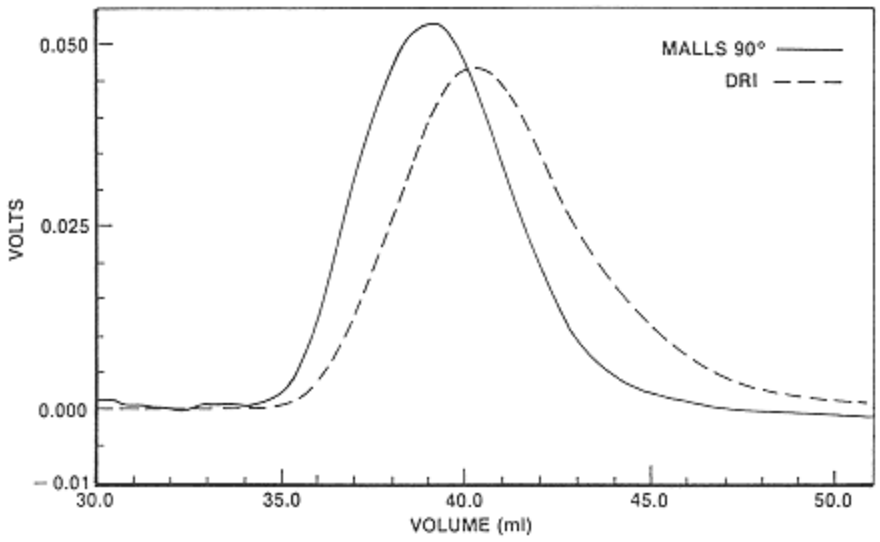

Figure 4
Concentration (DRI) and MALLS (scattering angle = 90°) chromatograms for a superhigh-molecular-weight PVA.

sities measured at *each* of the 15 angular detectors at a given elution time is used to extrapolate to the scattering at zero degrees (27). This procedure circumvents the particulate and noise problem common to low-angle detection and is a major advantage to using MALLS.

Aqueous SEC of PVA Using On-Line Viscometry

Fully Hydrolyzed PVA

SEC-viscometry provides a means to measure the absolute molecular weight distribution of fully hydrolyzed PVA via universal calibration. It can be thought of as both a complementary and supplementary technique to LALLS.

For SEC-viscometry analysis, the TSK-PW columns were calibrated using a mobile phase of 0.10 M $NaNO_3$ with four water-soluble standards: polyethylene glycol (PEG); polyethylene oxide (PEO), polysaccharide (PSC), and polyacrylamide. Molecular weights range from 975 for PEG to 850,000 for PSC (Table 1). Universal calibration was observed for these four standards from a plot of log (intrinsic viscosity × molecular weight) versus retention volume (Figure 5). The four polymer types fall closely on a single curve, indicating the validity of universal calibration conditions, and this demonstrates that separation

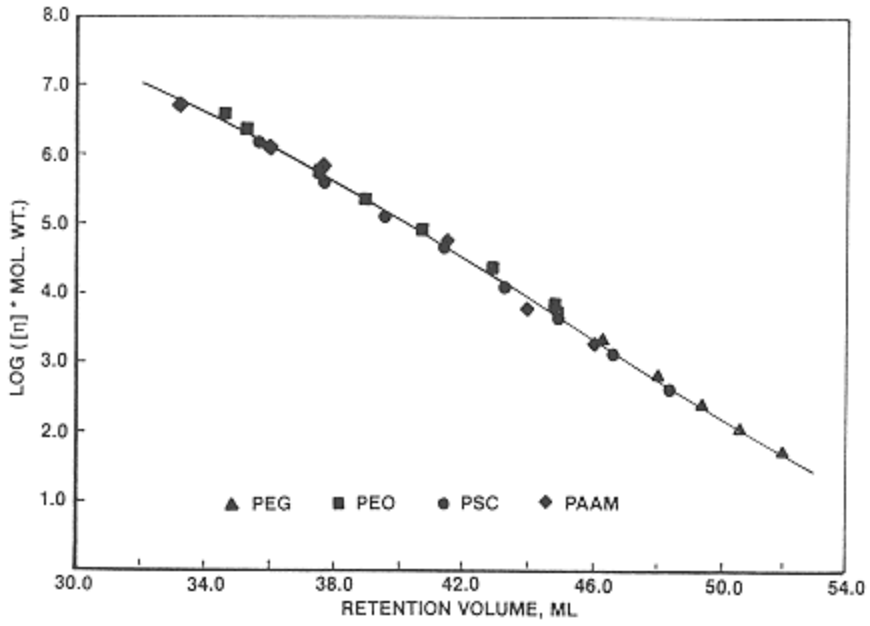

Figure 5
Universal calibration plot for polyethylene glycol, polyethylene oxide, polysaccharide, and polyacrylamide in 0.10 M sodium nitrate at 35°C.

is by a true size exclusion mechanism (28). This calibration was used for subsequent molecular weight calculations by viscometry. Universal calibration using TSK-PW columns has also been verified using an aqueous mobile phase with acetonitrile as an organic modifier (29).

The viscometry chromatogram for a fully hydrolyzed, medium-molecular-weight PVA is shown in Figure 3 (along with the concentration DRI and LALLS chromatograms). As described earlier, the small peak at the high-molecular-weight end in the LALLS chromatogram is probably caused by some aggregated or incompletely dissolved PVA. The DV response, which overall exhibits a cleaner signal, is not sensitive to this contaminant because it exhibits little or no specific viscosity.

A comparison of DV and LALLS chromatograms for a superlow-molecular-weight PVA of identical sample injection mass shows a dramatic difference in signal response (Figure 6). The LALLS chromatogram exhibits poor sensitivity for this molecular weight (approximately 10,000 daltons). This illustrates the superior sensitivity of viscometry compared with LALLS for low-molecular-weight material. Typically, for LALLS, low-molecular-weight or superlow-molecular-weight PVA require increased sample concentrations to provide reason-

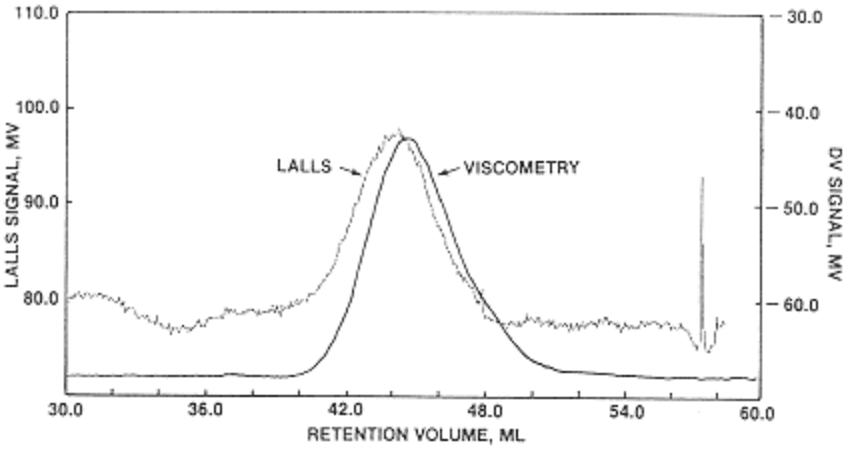

Figure 6
Comparison of viscometry and LALLS chromatograms for a superlow-molecular-weight, fully hydrolyzed PVA.

ably good signal-to-noise ratios (28). For low-molecular-weight PVA, viscometry is estimated as three to five times more sensitive than LALLS. The advantage of using viscometry for better detection of low-molecular-weight fractions in a distribution becomes obvious.

Absolute molecular weights $\overline{M}_w$ calculated by viscometry for fully hydrolyzed PVA compare favorably to LALLS (Table 3). Data from MALLS are also included for a medium-molecular-weight PVA. The viscometry results were obtained with the same mobile phase, 0.10 M $NaNO_3$, used for universal calibration. Data for LALLS were obtained in 0.05 M $NaNO_3$, as previously described. There is excellent agreement for $\overline{M}_w$ between these two methods for grades of superlow, low, medium, and high molecular weight. Some of the molecular weight values reported in Table 3 for LALLS vary slightly from those summarized in Table 2 for the same PVA type and molecular weight grade. This is caused by sample variability. The results summarized in these tables are for demonstrative purposes only and should not be considered exact product specifications for these PVA grades.

Our estimated precision for viscometry is ±5%. The peak parameters (detector offset, σ, $\tau[v]$, and $\tau[c]$) required by the Viscotek software for molecular weight calculations were calculated from a polyethylene oxide standard of molecular weight 80,000.

Also included in Table 3 are intrinsic viscosity data from differential viscometry and Ubbelohde viscometry. There is excellent agreement between the

Table 3 Comparison of Molecular Weights for Fully Hydrolyzed PVA

PVA type	$\overline{M}_n$	$\overline{M}_w$	$\overline{M}_w/\overline{M}_n$	[η]
High molecular weight				
DV (0.10 M $NaNO_3$)	55,000	149,000	2.7	1.50
LALLS (0.05 M $NaNO_3$)	66,000	139,000	2.1	1.00[a]
Medium molecular weight				
DV (0.10 M $NaNO_3$)	44,000	100,000	2.3	0.85
LALLS (0.05 M $NaNO_3$)	48,000	97,000	2.0	0.82[a]
MALLS (0.05 M $NaNO_3$)	68,000	107,000	1.6	-
Low molecular weight				
DV (0.10 M $NaNO_3$)	10,000	26,000	2.6	0.41
LALLS (0.05 M $NaNO_3$)	14,000	28,000	2.0	0.40[a]
Superlow molecular weight				
DV (0.10 M $NaNO_3$)	5,900	19,000	3.2	0.31
LALLS (0.05 M $NaNO_3$)	10,000	20,000	2.0	0.33[a]

[a][η] at 35°C in 0.10 M $NaNO_3$ by Ubbelohde viscometry.

intrinsic viscosity determined on-line by SEC and off-line with Ubbelohde viscometry.

It should be noted that the calculated number-average molecular weights from viscometry are slightly lower than those from LALLS. This type of effect has been previously reported (26,28). This illustrates the increased sensitivity of viscometry for low-molecular-weight material. The resulting polydispersity values from viscometry reflect this, because these values are slightly higher than those from LALLS. A comparison of molecular-weight distributions from viscometry and LALLS for a medium-molecular-weight PVA shows fairly good agreement, although it is not perfect (Figure 7). The polydispersity obtained from viscometry better accounts for the low-molecular-weight end of the molecular weight distribution.

Weight-average molecular weights calculated from SEC-viscometry for a superhigh-molecular-weight PVA, discussed in the previous section, compare favorably to those from MALLS (Table 4). The agreement for $\overline{M}_w$ is within the expected precision of the two methods. However, we see once again that the number-average value from light scattering is biased high compared with viscometry. This reflects the decreased sensitivity of MALLS to the low-molecular-weight material in the distribution. Both methods, however, are still excellent choices for the characterization of this type of PVA.

Viscometry measurements allow the calculation of the Mark-Houwink constants under conditions used for the analysis. The K and α values for PVA over

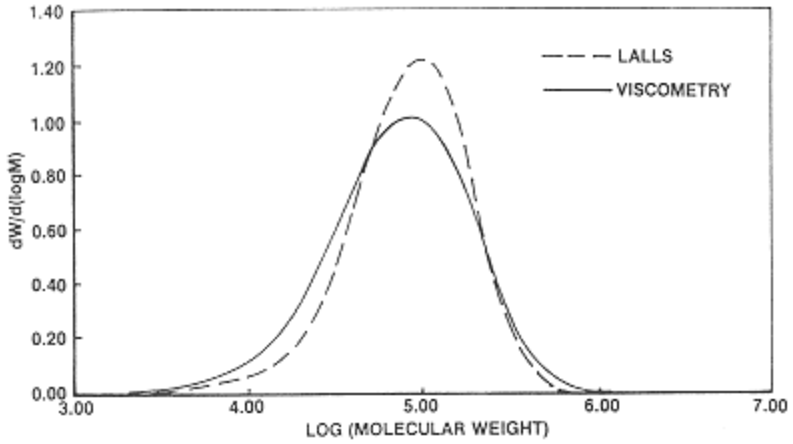

Figure 7
Comparison of molecular weight distributions obtained from viscometry and LALLS for a medium-molecular-weight, fully hydrolyzed PVA.

Table 4 Comparison of Molecular Weights for Superhigh-Molecular-Weight PVA

	$\overline{M}_n$	$\overline{M}_w$	$\overline{M}_w/\overline{M}_n$
DV (0.10 M $NaNO_3$)	91,600	249,000	2.7
MALLS (0.05 M $NaNO_3$)	135,000	264,000	2.0

Table 5 Mark-Houwink Constants for Fully Hydrolyzed PVA in 0.10 M $NaNO_3$ at 35 °C

Molecular weight	α	log *K*
Superhigh	0.570	-2.899
High	0.567	-2.870
Medium	0.560	-2.863
Low	0.569	-2.902
Superlow	0.517	-2.687

the range from superhigh to superlow molecular weight are given in Table 5 at 35°C in 0.10 M $NaNO_3$. These results are average values from six independent determinations [for α, % relative standard deviation (SD) = 2.5%; for log *K*, % relative SD = 2.6%]. The α values are within the expected range of 0.5–0.8 for random-coil polymers and are essentially constant over the entire range of molecular weights. The superlow-molecular-weight PVA shows a slightly lower value. This may reflect that the excluded volume diminishes and the polymer chains become stiffer at low molecular weights. The Mark-Houwink *K* and α values for PVA in water have been previously reported (10,30) and are slightly higher than our values in 0.10 M $NaNO_3$. Our work is the first reported use of aqueous SEC-viscometry for determining the Mark-Houwink constants for PVA.

The Mark-Houwink plot of log[η] versus log molecular weight shows a linear relationship for high-molecular-weight PVA (Figure 8). This linear behavior suggests little or no long-chain branching in the PVA. Long-chain branching during the hydrolysis of PVAc to PVA is discussed in the last section of this chapter.

The significance of knowing the *K* and α values is that molecular weight distribution data can be directly calculated using one of two methodologies: (1) the Mark-Houwink method, which requires prior knowledge of *K* and α values for PVA and the calibration standards, such as PEG and PEO, and (2) the intrinsic viscosity distribution (IVD) method as reported by Yau and Rementer

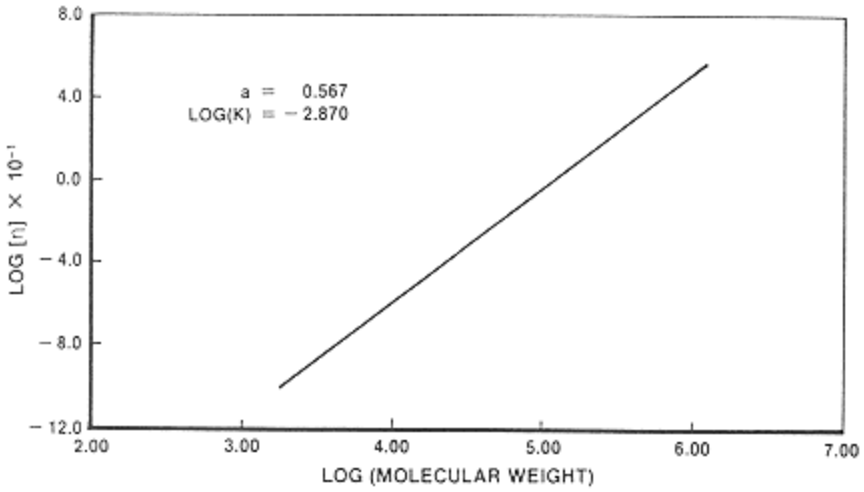

Figure 8
Mark-Houwink plot for high-molecular-weight, fully hydrolyzed PVA in 0.10 M sodium nitrate at 35°C.

(31). The former is a calibration-dependent procedure, and Mark-Houwink constants for the standards are readily obtained from calibration-viscometry measurements. These have been reported for PEG and PEO (29). For the latter method, however, a simple ratio of the concentration signal to the specific viscosity signal in a viscometry analysis yields the IVD (peak parameters, mass injected, and viscometer inlet pressure must be known). The IVD method is a *calibration-independent* procedure. By inputting the Mark-Houwink values, molecular weights can be calculated using the Mark-Houwink relationship. Because this procedure is calibration independent, it may hold significant value for quality or process control applications (28).

Partially Hydrolyzed PVA

A high-molecular-weight, partially hydrolyzed (88 mol%) PVA exhibits excellent signal response, as evidenced by concentration (DRI), LALLS, and viscometry chromatograms (Figure 9). A few particulate spikes are seen in the LALLS chromatogram, which was acquired using a 0.22 μm prefilter on the CMX-100 LALLS.

Using the same conditions as for fully hydrolyzed PVA grades, molecular weight calculations from viscometry for various molecular weight grades of partially hydrolyzed PVA result in values low by 20–30% (compared with LALLS). This was not surprising: partially hydrolyzed is more hydrophobic than the corresponding fully hydrolyzed PVA. It is suspected that secondary, non-size exclusion effects result in retardation of the polymer, longer elution times, and lower molecular weights. Similar types of hydrophobic interactions using TSK-PW columns have been reported for other water-soluble polymers (24). The addition of an organic modifier to the aqueous mobile phase can minimize or eliminate this effect.

Two mobile-phase compositions of H_2O/CH_3CN (80:20, vol/vol) and 0.10 M $NaNO_3/CH_3CN$ (80:20, vol/vol) were used for SEC-viscometry of partially hydrolyzed grades (32). PEO, PEG, and PSC were used for column calibration, and universal calibration was observed (29). Molecular weights by SEC-viscometry for grades of high, medium, low, and superlow molecular weight compare favorably those from SEC-LALLS, especially with the H_2O/CH_3CN mobile phase (Table 6). It is suspected that the nonsalt mobile phase works better to eliminate the hydrophobic interactions and maximize the size exclusion mechanism (32). Intrinsic viscosity values calculated from viscometry for the two acetonitrile mobile-phase compositions and from Ubbelohde viscometry in H_2O/CH_3CN, are also summarized in Table 6.

The Mark-Houwink constants for partially hydrolyzed PVA in H_2O/CH_3CN (80:20) are similar to those for fully hydrolyzed PVA in 0.10 M $NaNO_3$ (Table

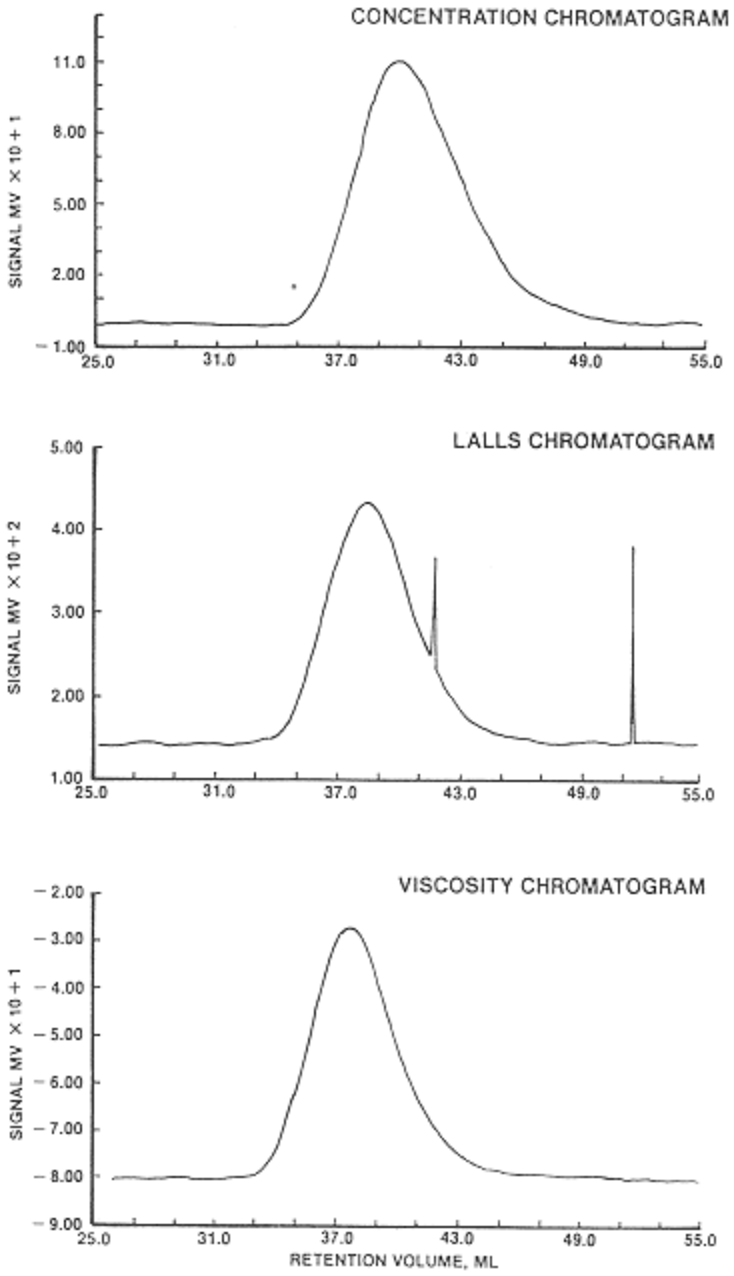

Figure 9
Concentration (DRI), LALLS, and viscometry chromatograms for a high-molecular-weight, partially hydrolyzed PVA.

7). The values have been rounded to two decimal places because they are the result of a single determination. The α values are slightly lower than the values reported for fully hydrolyzed PVA in 0.10 M $NaNO_3$, except for low-molecular-weight PVA (32).

In general, the characterization of partially hydrolyzed PVA needs further investigation to understand better the impact of hydrophobic interactions. The use of other organic, mobile-phase modifiers, such as *N*-methylpyrrolidone or dimethylsulfoxide, is a possible approach.

Table 6 Comparison of Molecular Weights for Partially Hydrolyzed PVA

PVA type	$\overline{M}_n$	$\overline{M}_w$	$\overline{M}_w/\overline{M}_n$	[η]
High molecular weight				
DV (H_2O/CH_3CN, 80:20)	59,000	151,000	2.6	1.13
DV (0.10 M $NaNO_3/CH_3CN$, 80:20)	59,000	144,000	2.4	1.17
LALLS (0.05 M $NaNO_3$)	88,000	160,000	1.8	0.96 [a]
Medium molecular weight				
DV (H_2O/CH_3CN, 80:20)	53,000	123,000	2.3	0.78
DV (0.10 M $NaNO_3/CH_3CN$, 80:20)	48,000	103,000	2.2	0.94
LALLS (0.05 M $NaNO_3$)	63,000	118,000	1.9	0.81 [a]
Low molecular weight				
DV (H_2O/CH_3CN, 80:20)	12,000	39,000	3.3	0.47
DV (0.10 M $NaNO_3/CH_3CN$, 80:20)	14,000	33,000	2.4	0.46
LALLS (0.05 M $NaNO_3$)	18,000	37,000	2.1	0.42 [a]
Superlow molecular weight				
DV (H_2O/CH_3CN, 80:20)	4,700	18,000	3.8	0.34
DV (0.10 M $NaNO_3/CH_3CN$, 80:20)	9,100	18,000	2.0	0.30
LALLS (0.05 M $NaNO_3$)	9,500	20,000	2.1	0.30 [a]

[a] [η] at 35°C in H_2O/CH_3CN (80:20) by Ubbelohde viscometry.

Table 7 Mark-Houwink Constants for Partially Hydrolyzed PVA in H_2O/CH_3CN (80:20) at 35°C

Molecular weight	α	log *K*
High	0.53	-2.64
Medium	0.54	-2.79
Low	0.52	-2.67
Superlow	0.65	-3.19

Long-Chain Branching in the Hydrolysis of PVAc to PVA

The molecular weight of PVAc (the precursor to PVA) can be reliably measured in tetrahydrofuran (THF) using SEC-viscometry (33). The use of differential viscometry and LALLS provides a means to examine long-chain branching in the hydrolysis of PVAc to PVA. It is known that this hydrolysis results in the loss of hydrolyzable, long-chain branches that extend from the ester to the main PVAc backbone (10). Of course, branches formed by hydrogen abstraction and chain transfer to a carbon atom in the PVAc backbone are nonhydrolyzable and remain.

Our examination of branching utilized fully hydrolyzed PVA and the fact that PVA can be reacetylated (with acetic anhydride in pyridine) back to PVAc. The reacetylated PVA can be thought of as the "linear" PVAc and the starting PVAc (referred to as PVAc paste) as the "branched" analog.

A distinct difference is observed in the high-molecular-weight range of the molecular weight distributions for the PVAc paste and the reacetylated PVA (Figure 10 and Table 8). It is readily apparent that the reacetylated PVA is lower in molecular weight. Virtually all of the molecular weight is lost from the high-molecular-weight end of the distribution. This is attributed to the loss of long-chain branches from the PVAc paste during hydrolysis and is seen as a lower value for the polydispersity of the reacetylated PVA. The $\overline{M}_w$ and intrinsic viscosity values also reflect this difference. It is also interesting to note that the change in the Mark-Houwink α value from 0.63 for the PVAc paste to 0.73 for the reacetylated PVA is another indicator of the loss of long-chain branches. The molecular weight of the PVA that was reacetylated to PVAc is also listed in Table 8. These molecular weights were obtained from SEC/LALLS and are consistent with those of the two PVAc types obtained from SEC-viscometry.

Figure 10 also includes an overlay of the Mark-Houwink plots for the PVAc paste and reacetylated PVAc, showing how the PVAc paste curve deviates slightly from linearity because of the presence or branched polymer. The loss of long-chain branches in the hydrolysis and the corresponding decrease in molecular weight of the PVAc are reflected in this small difference in the Mark-Houwink plot.

Summary

Taken as a whole, aqueous SEC-viscometry, LALLS, and MALLS have provided a wealth of molecular weight information for PVA that was not available only a few years ago. All three are excellent methods for the characterization of fully hydrolyzed PVA. Viscometry is more sensitive to low-molecular-weight material but requires adherence to universal calibration for the calculation of

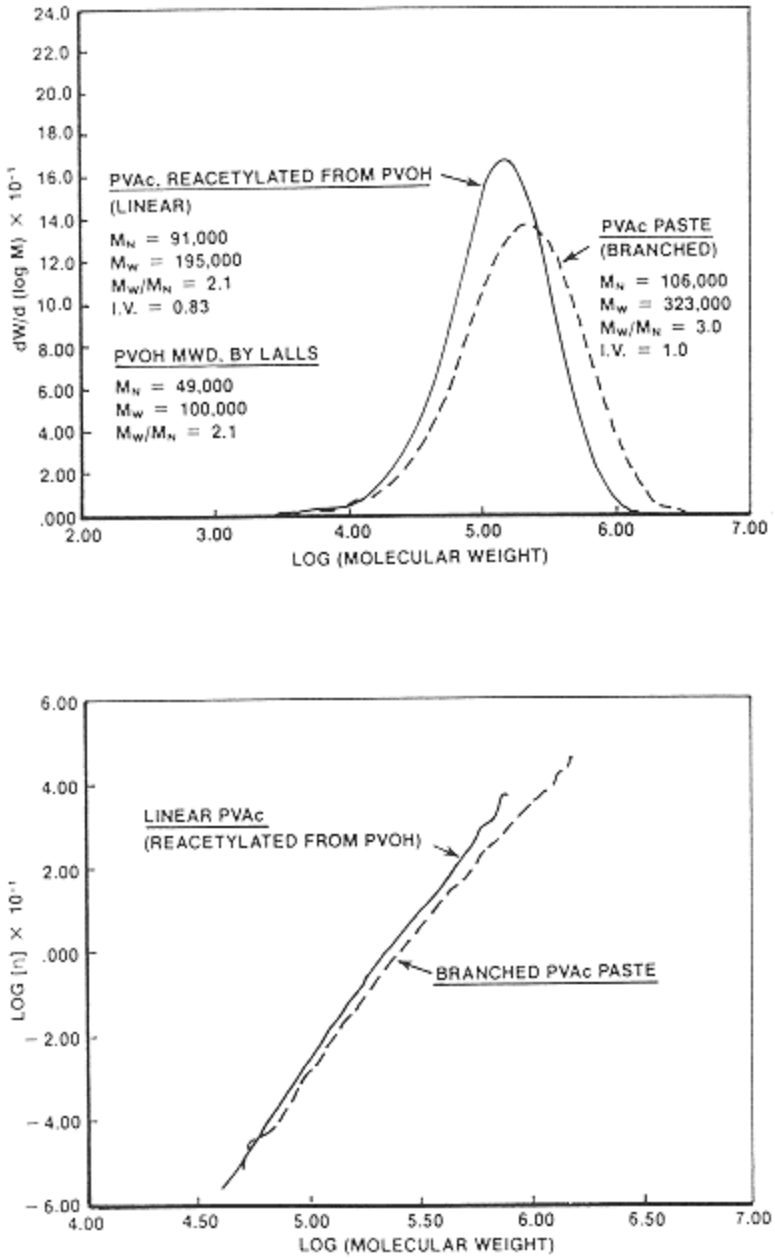

Figure 10
Molecular weight distributions and Mark-Houwink plots of PVAc paste and reacetylated PVA from SEC-viscometry in THF.

Table 8 Molecular Weight and Viscosity Data for PVAc Hydrolysis to PVA

	PVAc paste	PVAc reacetylated	PVA
$\overline{M}_w$	323,000	195,000	100,000
$\overline{M}_n$	106,000	91,000	49,000
$\overline{M}_w/\overline{M}_n$	3.0	2.1	2.1
[η]	1.00	0.83	—
α	0.63	0.72	—
log *K*	-3.44	-3.84	—

absolute molecular weights. Universal calibration behavior is observed using TSK-PW columns in a mobile phase of 0.10 N $NaNO_3$. Mark-Houwink constants have been determined under these conditions over a full range of molecular weights for fully hydrolyzed PVA. Both LALLS and MALLS require prior knowledge of *dn/dc* constants for molecular weight analysis. Viscometry and MALLS work well for superhigh-molecular-weight PVA of approximately 250,000 daltons.

Characterization of partially hydrolyzed PVA by viscometry is complicated by secondary, hydrophobic interaction effects. These effects can be minimized using a suitable aqueous mobile phase with an organic modifier such as acetonitrile.

Long-chain branching can be characterized by SEC-viscometry (in THF) of the starting PVAc used for the hydrolysis to PVA. The Mark-Houwink plot of log [η] versus log molecular weight for fully hydrolyzed PVA supports a linear structure for the polymer.

Acknowledgments

The author thanks Mr. D. A. Terwilliger for providing technical assistance throughout these studies and to Air Products and Chemicals, Inc. for permission to publish this work.

References

1. F. L. Marten, "Vinyl Alcohol Polymers," in *Encyclopedia of Polymer Science,* Volume 17, John Wiley & Sons, New York, 1989, p. 167.

2. J. M. Hay and D. Lyon, *Nature,* 216, 790 (1967).

3. B. Capon, D. S. Watson, and C. Zucco, *J. Am. Chem. Soc.,* 103, 1761 (1987).

4. W. Haehnel and W. O. Hermann, German Patent 450,286 (1924), to Consort. F. elecktrochem., Inc., GmbH.

5. S. Kido, Y. Saito, and T. Iwaeda, U.S. Patent 4,104,208, Toyo Soda Manufacturing Company, Ltd., 1978.

6. S. Mori, *J. Chromatogr.,* 452, 137 (1988).

7. S. Mori, *J. Liq. Chromatogr.,* 11, 1205 (1988).

8. R. Stevenson, K. Noguchi, and Y. Yanigihara, 1991 International GPC Symposium, Waters/Millipore Corporation, San Francisco, CA, October 1991.

9. Airvol Polyvinyl Alcohol, Product Bulletin 1990, Air Products and Chemicals, Inc., Allentown, PA.

10. I. Sakurada, *Polyvinyl Alcohol Fibers,* Marcel Dekker, New York, 1985.

11. C. A. Finch, *Polyvinyl Alcohol, Properties and Applications,* John Wiley and Sons, New York, 1973.

12. H. G. Barth, "Characterization of Water-Soluble Polymers Using Size-Exclusion Chromatography," in *Water-Soluble Polymers,* Advances in Chemistry Series 213, J. E. Glass, Ed., American Chemical Society, Washington, D.C., 1986.

13. W. F. Tiedge, Air Products and Chemicals, Inc., private communication.

14. K. J. Bombaugh, W. A. Dark, and J. N. Little, *Anal. Chem.,* 41(10), 1337 (1969).

15. B. G. Belenkii, L. Z. Vilenchik, V. V. Nesterov, V. J. Kolegov, and S. Y. Frenkel, *J. Chromatogr.,* 109, 233 (1975).

16. Z. Grubisic, P. Rempp, and H. Benoit, *J. Polym. Sci., Part B,* 5, 753 (1967).

17. R. V. Vilvilecchia, B. G. Lightbody, N. Z. Thimot, and H. M. Quinn, *J. Chromatogr. Sci.,* 15, 424 (1977).

18. T. Hashimoto, H. Sasaki, M. Aiura, and Y. Kato, *J. Polym. Sci., Polym. Phys.,* 16, 1789 (1978).

19. P. L. Dubin, C. M. Speck, and J. I. Kaplan, *Anal. Chem.,* 60, 895 (1988).

20. H. Sasaki, T. Matsuda, O. Ishikawa, T. Takamutsu, K. Tanaka, Y. Kato, and T. Hashimoto, *Sci. Rep.,* Toyo Soda Manufacturing Company, Ltd., 29, 37 (1985).

21. M. Fukutomi, M. Fukuda, and T. Hashimoto, *Toyo Soda Kenkyu Hokoku,* 24(1), 33 (1980).

22. D. P. Herman, L. R. Field, and S. Abbott, *J. Chromatogr. Sci.,* 19, 470 (1981).

23. B. Gebben, H. W. A. van den Berg, D. Bargeman, and C. A. Smolders, *Polymer,* 26, 1737 (1985).

24. Y. Kato, T. Matsuda, and T. Hashimoto, *J. Chromatogr.,* 332, 39 (1985).

25. D. J. Nagy, *J. Appl. Polym. Sci., Part C, Polym. Lett.,* 24, 87 (1986).

26. D. J. Nagy, Proceedings of 1987 International GPC Symposium, Waters/Millipore Corporation, Chicago, IL, May 1987.

27. Polymers, Wyatt Technology, Application Note #1: Santa Barbara, CA, 1990.

28. D. J. Nagy, First International GPC-Viscometry Symposium, Viscotek Corporation, Houston, TX, April 1991.

29. D. J. Nagy, *J. Liq. Chromatogr.,* 13, 677 (1990).

30. A. Beresniewicz, *J. Polym. Sci.*, 39, 63 (1959).

31. W. W. Yau and S. W. Rementer, *J. Liq. Chromatogr.,* 13, 627 (1990).

32. D. J. Nagy and D. A. Terwilliger, 1991 International GPC Symposium, Waters/Millipore Corporation, San Francisco, CA, October 1991.

33. B. D. Lawrey, First International GPC-Viscometry Symposium, Viscotek Corporation, Houston, TX, April 1991.

11
Size Exclusion Chromatography of Polyvinyl Acetate

Bruce D. Lawrey Air Products and Chemicals, Inc., Allentown, Pennsylvania

Introduction

Polyvinyl acetate (PVAc) is the largest volume polymer produced from a vinyl ester (1). In 1990, over 2.5 billion pounds of vinyl acetate monomer were produced in the United States alone (2). The bulk of this monomer was used for making PVAc and PVAc copolymers, which are widely used in water-based paints, adhesives, coatings, and binders for nonwoven paper products. PVAc is also the precursor to polyvinyl alcohol (PVA) and polyvinyl butyral, which cannot be made by direct polymerization. Methods of PVAc polymerization vary depending on the end use. Solution polymerizations of vinyl acetate in methanol are generally employed in processes in which PVAc is used as an intermediate in the production of PVA. PVAc latexes are generally made by emulsion polymerization, and PVAc in bead form is often synthesized by suspension polymerization (3,4).

PVAc homopolymer is sold in various grades based on molecular weight. Typical grades are listed in Table 1 (5). Like other thermoplastics, the physical properties and end uses of PVAc are strongly governed by molecular weight. The effects of molecular weight distribution and branching on the rheological properties of PVAc have been reported by Long et al. (6) and Onogi et al. (7,8). Size exclusion chromatography (SEC) techniques used to characterize the molecular weight and branching distributions in PVAc are described below.

Table 1 Typical Grades of Polyvinyl Acetate Homopolymer

M_w	Viscosity (10% in ethyl acetate at 20 °C, mPa s)
15,000	1.2–1.4
47,000	2.5–3.5
91,000	5.0–6.5
150,000	8–11
530,000	~90
1,100,000	>1000

Sec Conditions

Polyvinyl acetate is an atactic, noncrystalline, flexible polymer that is soluble in a wide range of organic solvents. The solvent most often used for SEC is tetrahydrofuran (THF). However, the response factor (chromatogram area/mass injected) obtained from PVAc dissolved in THF with a differential refractive index detector (DRI) is almost four times smaller than that obtained with polystyrene in THF. The DRI detector gain should be increased accordingly to optimize the quality of the chromatograms. Typical SEC operating conditions for characterizing PVAc are summarized in Table 2.

Because of its solubility in both THF and more polar solvents, PVAc has also been used to calibrate systems employing mobile phases that are nonsolvents for polystyrene. Gilding et al. (9) describes a technique for calibrating an SEC system in hexafluoroisopropanol (HFIP) using broad molecular weight distribution (MWD) PVAc standards. HFIP, a nonsolvent for polystyrene, is an excellent solvent for polyamides, polyesters, polyurethanes, and polyglycolic acid.

PVAc produced by emulsion polymerization techniques often contains a significant percentage of THF-insoluble material, chiefly as a result of the presence of polyvinyl alcohol, which is commonly employed as a protective colloid. The extent to which the polyvinyl alcohol grafts onto the PVAc latex particles during polymerization strongly influences the percentage of THF insolubles. In addition, the presence of surfactants, chain-transfer agents, and cross-linking agents may also affect the solubility of the PVAc latex (10). The size of the insoluble fraction is typically determined by performing a Soxhlet extraction, and subsequently, the molecular weight distribution of the soluble fraction is measured by SEC.

Table 2 Typical SEC Operating Conditions for Polyvinyl Acetate

Columns	Cross-linked styrene-divinyl benzene (e.g., Ultrastyragel, PLgel, Phenogel) or cross-linked divinyl benzene (e.g., Jordi DVB)
Solvent	Tetrahydrofuran
Flowrate	1.0 ml/minute
Temperature	35°C
Polymer concentration	2 mg/ml
Injection volume	100 µl
Detector(s)	Differential refractive index (DRI), on-line viscometer (Viscotek Corp., Houston, TX; Waters Chromatography, Millipore Corp., Milford, MA)
Calibration	Universal calibration with narrow MWD polystyrene standards

Universal Calibration

In universal calibration the relationship between hydrodynamic volume and retention volume is independent of polymer type and structure (11). The validity of applying universal calibration to the determination of PVAc molecular weights in THF has been demonstrated in several studies. However, Altgelt found that in studying PVAc in trichloroethylene, the PVAc fractions eluted earlier than polystyrene at a given hydrodynamic volume (12). Incompatibility between the polymer and column packing, as well as aggregation, have been suggested as explanations for this departure from universal calibration (12–14).

Several studies on linear and branched samples of PVAc have been reported in which the outlet of a Waters 200 GPC was coupled to an automatic capillary viscometer (15–18). The results obtained using universal calibration were in good agreement with weight-average molecular weight M_w values determined via static light scattering. More recently, as SEC detection systems consisting of a continuous automatic viscometer in combination with a differential refractometer have come into use, several authors have reported results that further support the universal calibration principle for PVAc (19,20).

A thorough study examining the validity of universal calibration for PVAc was done by Atkinson and Dietz (13). Linear PVAc samples were synthesized, and several fractions were isolated by preparative SEC. The fractions were rigorously characterized for M_w by light scattering, number-average molecular

weight M_n by membrane osmometry, and intrinsic viscosity [η] by off-line viscometry. When the retention volume of each fraction was measured, the resulting calibration curve of log [η]M versus retention volume coincided with results obtained using polystyrene standards. The validity of universal calibration for PVAc was established over a molecular weight range of 17,000–1,200,000. The samples used in this work are available as Certified Reference Materials from the National Physical Laboratory, United Kingdom.

Mark-Houwink Parameters

Goedhart and Opschoor (21) first applied the principle of universal calibration to calculate the Mark-Houwink constants for PVAc in THF. By measuring the intrinsic viscosity of fractions leaving the siphon of a Waters 200 GPC using an automatic capillary tube viscometer, they determined the following Mark- Houwink expression for PVAc in THF at room temperature:

$$[\eta] = 3.5 \times 10^{-4} M_w^{0.63} \quad (1)$$

The M_w and M_n values they reported were in good agreement with results obtained by light scattering and osmometry, respectively. Because information regarding the sample's polymerization temperature, level of conversion, or degree of long-chain branching (LCB) was not specified, the K and α values provided in Equation (1) should be applied judiciously. Although Equation (1) is often cited for PVAc (22,23), it is not possible to assign a single set of Mark-Houwink constants to PVAc because of differences in branching. During the polymerization of vinyl acetate, the branching frequency increases with conversion and temperature (4). Linear PVAc can be produced at low conversions and low temperatures. Several different sets of Mark-Houwink constants that have been reported for linear PVAc are summarized in Table 3. The values reported by Atkinson and Dietz (13) represent the result of analyzing the greatest number of samples, the widest range of molecular weights, and the most thoroughly characterized samples.

Table 3 Mark-Houwink Contants for Linear PVAc in THF

$K \times 10^4$	α	Temperature (°C)	MW range	No. samples	Reference
0.51	0.791	25	302,000–625,000	5	15
1.56	0.708	35	17,000–1,160,000	13	13
0.942	0.737	25	76,000–420,000	6	24
1.60	0.70	25	54,000–499,000	11	25

The intrinsic viscosity behavior of polystyrene (PS) is very similar to that of linear PVAc. The following Mark-Houwink constants are often cited for PS in THF: $\alpha = 0.706$, $K = 0.00016$ (19,22). Therefore, PS and linear PVAc samples of the same molecular weight elute at nearly the same retention volume. Consequently, for certain PVAc products, the increased cost, complexity, and experimental uncertainty associated with analysis of SEC data by universal calibration may not be justified (26).

Light-Scattering Studies

To obtain absolute molecular weight values without the use of a calibration curve, several investigators have interfaced low-angle or multiangle laser light- scattering detectors in series with a concentration detector. Such SEC systems require knowledge of the specific refractive index increment *dn/dc* for a specific polymer, solvent, and temperature. Jordan and McConnell (27) measured a specific refractive index increment *dn/dc* of 0.0517 ml/g for PVAc in THF at 25°C using a Chromatix KMX-16 laser differential refractometer at 632.8 nm. Millaud and Strazielle (28) reported a value of 0.050 ml/g at 632.8 nm using a Brice- Phoenix differential refractometer. The *dn/dc* value of PVAc in THF does not vary significantly with molecular weight. Values of 0.0471 and 0.0502 ml/g were obtained for samples of high ($M_w = 4.66 \times 10^6$) and low ($M_w = 107{,}000$) molecular weight, respectively, at 26°C with a KMX-16 (29). Styring et al. (20) measured the *dn/dc* values of two highly branched PVAc samples under ambient conditions at 632.8 nm, obtaining values of 0.0455 and 0.0528 ml/g for molecular weights of 328,000 (low conversion) and 628,000 (high conversion), respectively. Agarwal et al. (30) reports a value of 0.054 ml/g for a highly branched PVAc sample ($M_w = 750{,}000$). Allowing for experimental uncertainties and sample molecular weight and branching variations, an average value of 0.05 ml/g is reasonable.

Branching

The presence of long-chain branches and the resultant broadening of the MWD both strongly affect the rheology of polymers in shear and extensional flow fields (31). For example, in studies of branched PVAc prepared by graft polymerization, Long et al. (6) observed that samples containing branches that exceed Z_c, the critical length needed for interchain entanglement, exhibit higher melt viscosities than linear PVAc of the same molecular weight. On a molecular level, polymerization of vinyl acetate proceeds by a free radical mechanism but is also characterized by a relatively high degree of chain transfer (3,4). In SEC studies

on branching in free radical polymerizations, PVAc is often preferred over other polymers that exhibit long-chain branching, such as low-density polyethylene (LDPE). Unlike PVAc, LDPE is insoluble in tetrahydrofuran, the most widely used SEC solvent (32). Branching in PVAc can occur through hydrogen abstraction and chain transfer at three different sites (3,4,33): the α and β hydrogens on the chain backbone and the acetate methyl group. Branching through the acetate group can be detected by a reduction in molecular weight that results after hydrolyzing the polymer to polyvinyl alcohol and then reacetylating it back to PVAc.

Coleman and Dawkins (24) prepared linear PVAc by carrying out polymerization reactions to conversions of about 5% at temperatures between 233 and 268 K. They prepared branched PVAc by polymerizing to greater than 80% conversion at 353 K. All samples were analyzed by SEC. Portions of each sample were hydrolyzed and then reacetylated. Following hydrolysis and reacetylation, the linear PVAc had changed in molecular weight by less than 2%, indicating that the material synthesized at low temperatures and low conversions contained no hydrolyzable branches. The PVAc samples polymerized at 353 K showed significant decreases in molecular weight and polydispersity following hydrolysis and reacetylation. After removal of the hydrolyzable long-chain branches present in the high-temperature samples, the samples were found to fall on the same universal calibration curve as the samples of linear PVAc. These results indicated that, if any nonhydrolyzable branches were present, they had no significant effect on the intrinsic viscosity values. Their conclusion that chain transfer through the acetate methyl group greatly exceeds that to the chain backbone is in agreement with other studies (4,30). The results also confirmed that the separation was based strictly on a size exclusion mechanism. The presence of residual hydroxyl groups as a result of incomplete reacetylation can give rise to peak shifts or tailing caused by enthalpic interactions between the polymer and the column packing. Coleman and Dawkins estimated the degree of reacetylation in their experiments as >99.9%.

Foster et al. (31) found that in calculating the molecular weight and branching distributions in PVAc from SEC data, the use of a branching structure factor ϵ equal to 1.0 gave good agreement with Graessley's kinetic model (33). ϵ is the exponent in the equation for the branching factor *G(v)*, described by

$$G(v) = \left\{ \frac{[\eta_b](v)}{[\eta_l](v)} \right\}^{1/\epsilon} \quad (2)$$

where $[\eta_b](v)$ and $[\eta_l](v)$ are the intrinsic viscosities of branched and linear polymer, respectively, eluting at retention volume *v*. *G(v)* can be related theoretically to the number of LCB points per molecule as a function of elution volume by the Zimm-Stockmayer equations (34). SEC-viscometry and SEC- ultracentrifugation data were used by Dietz and Francis (35) to characterize

samples of branched PVAc. Branching factors and molecular weights obtained using the two techniques were in good agreement.

Summary

Because PVAc is a widely used thermoplastic, developments in its characterization have tracked advances in SEC technology as a whole. This chapter outlines procedures and conditions for characterizing the molecular weight and long-chain branching distributions in PVAc. Several studies were discussed, indicating that the principle of universal calibration applies to PVAc in THF.

References

1. F. W. Billmeyer, *Textbook of Polymer Science,* 3rd ed., Wiley, New York, 1984, p. 391.

2. *Chemicalweek,* 148(22), 29 (June 12, 1991).

3. W. Daniels, *Kirk-Othmer Encyclopedia of Chemical Technology,* 3rd ed. (M. Grayson, ed.), Wiley, New York, Vol. 23, 1983, p. 817.

4. M. K. Lindemann, in *Vinyl Polymers,* Vol. I., Part I (G. E. Ham, ed.), Marcel Dekker, New York, 1967, pp. 207–329.

5. Vinnapas Homopolymer Brochure, Wacker-Chemie GmbH, Munich, March 1988.

6. V. C. Long, G. C. Berry, and L. M. Hobbs, *Polymer,* 5, 517 (1964).

7. S. Onogi, S. Kimura, T. Kato, T. Masuda, and N. Miyanaga, *J. Polym. Sci., Part C,* 15, 381 (1966).

8. S. Onogi, T. Masuda, and T. Ibaragi, *Kolloid Z. Z. Polym.,* 222(2), 110 (1968).

9. D. K. Gilding, A. M. Reed, and I. N. Askill, *Polymer,* 22, 505 (1981).

10. C. A. Finch, *Polyvinyl Alcohol—Developments,* John Wiley and Sons, New York, 1992.

11. Z. Grubisic, P. Rempp, and H. Benoit, *J. Polym. Sci. B5,* 753–759 (1967).

12. K. H. Altgelt, *Separation Sci.,* 5(6), 777 (1970).

13. C. M. L. Atkinson and R. Dietz, *Eur. Polym. J.,* 15(1), 21 (1979).

14. J. V. Dawkins, *Polymer,* 19(6), 705 (1978).

15. W. S. Park and W. W. Graessley, *J. Polym. Sci., Polym. Phys. Ed.,* 15(1), 71 (1977).

16. W. S. Park and W. W. Graessley, *J. Polym. Sci., Polym. Phys. Ed.,* 15(1), 85 (1977).

17. *Liquid Chromatography of Polymers and Related Materials II* (J. Cazes and X. Delamare, eds.), Marcel Dekker, New York, 1980, p. 113.

18. Z. Grubisic-Gallot, M. Picot, P. Gramain, and H. Benoit, *J. Appl. Polym. Sci.,* 16, 2931 (1972).

19. C. Y. Kuo, T. Provder, M. E. Koehler, and A. F. Kah, in ACS Symp. Series 352 (T. Provder, ed.),

ACS, Washington, D.C., 1987, p. 130.

20. M. G. Styring, J. E. Armonas, and A. E. Hamielec, in ACS Symp. Series 352 (T. Provder, ed.), ACS, Washington, D.C., 1987, p. 104.

21. D. Goedhart and A. Opschoor, *J. Polym. Sci., Part A-2*, 8, 1227 (1970).

22. W. W. Yau, J. J. Kirkland, and D. D. Bly, *Modern Size-Exclusion Liquid Chromatography*, Wiley, New York, 1979, p. 252.

23. J. Armonas, American Polymer Standards Catalog, Mentor, Ohio, 1991, p. 14.

24. T. A. Coleman and J. V. Dawkins, *J. Liq. Chromatogr.*, 9(6), 1191 (1986).

25. F. Cane and T. Capaccioli, *Eur. Polym. J.*, 14(3), 185 (1978).

26. B. D. Lawrey, First International GPC-Viscometry Symposium, Viscotek Corporation, Houston, TX, April 1991.

27. R. C. Jordan and M. L. McConnell, ACS Symp. Series 138 (T. Provder, ed.), ACS, Washington, D.C., 1980, p. 107.

28. B. Millaud and C. Strazielle, *Makromol. Chem.*, 180, 441 (1979).

29. KMX-16 Application Note LS-7 Appendix 1 (November 1979).

30. S. H. Agarwal, R. F. Jenkins, and R. S. Porter, *J. Appl. Polym. Sci.*, 27, 113 (1982).

31. G. N. Foster, A. E. Hamielec, and T. B. MacRury, in ACS Symp. Series 138 (T. Provder, ed.), ACS, Washington, D.C., 1980, p. 131.

32. A. E. Hamielec, A. C. Ouano, and L. L. Nebenzahl, *J. Liq. Chromatogr.*, 1(4), 527 (1978).

33. W. W. Graessley, R. D. Hartung, and W. C. Uy, *J. Polym. Sci., Part A-2*, 7, 1919 (1969).

34. B. H. Zimm and W. H. Stockmayer, *J. Chem. Phys.*, 17, 1301 (1949).

35. R. Dietz and M. A. Francis, *Polymer*, 20(4), 450 (1979).

12
Size Exclusion Chromatography of Vinyl Pyrrolidone Homopolymer and Copolymers

Chi-san Wu, James F. Curry, Edward G. Malawer, and Laurence Senak International Specialty Products, Wayne, New Jersey

Polyvinyl pyrrolidone (PVP) is a polar and amorphous polymer that is completely soluble in water and some organic solvents, such as alcohols, chlorinated hydrocarbons, dimethylformamide, and *N*-methylpyrrolidone. It is an important polymer in the pharmaceutical, personal care, cosmetic, agriculture, beverage, and other industries.

PVP is a physiologically inert and biologically compatible polymer. PVP is known to reduce significantly the toxicity and irritant effects of many medications. PVP can form complexes with a variety of substances. For example, the PVP-iodine complex in the form of povidone or Betadine aqueous solution is the most widely used antiseptic in hospitals. It significantly reduces the toxicity and staining effect of the tincture of iodine solution but retains the germicidal activity of the iodine.

Because of the excellent solubility of PVP in water, the dissolution rate of many drugs and compounds that are difficult to dissolve can be significantly improved if they are coprecipitated with PVP. PVP is amphiphilic in nature and is slightly surface active. It is frequently used in industries as a suspending aid and a protective colloid for polymers, emulsions, and lattices. PVP is also used as a dye stripper in the textile industry and in detergent formulation to prevent soil and dye redeposition. Because of its good adhesive and cohesive strengths and excellent water solubililty, PVP is one of the most widely used tablet binders

for the pharmaceutical industry. It is also used as the major component in glue sticks and for bonding medical devices to a patient's skin.

The hydrophilic, hydrophobic, and ionic nature of PVP can be modified by copolymerization to enhance the properties of PVP for certain applications. Nonionic, anionic, and cationic VP copolymers have all been commercialized. A wide range of vinyl pyrrolidone and vinyl acetate copolymers, which are non-ionic, have been made with optimized amphiphilicity and solubility in water or alcohol for the cosmetic and pharmaceutical industries. The surface activity of PVP can be further enhanced by copolymerization with acrylic acid. Vinyl pyrrolidone and acrylic acid copolymers, which are anionic in their major applications, with different molar rations have been developed with well-balanced surface, associative, and film-forming properties for industrial applications.

Quaternized copolymers of vinyl pyrrolidone and dimethylaminoethylthacrylate, which is cationic, have been developed for the hair care and skin care industries because of their optimal substantivity, minimum buildup, and ability to form nontacky and continuous films. Other important comonomers include vinyl alcohol, styrene, maleic anhydride, acrylamide, acrylonitrile, crotonic acid, and methyl methacrylate.

Molecular Weight Grades of Important VP-Based Polymers

Many different molecular weight grades of VP-based polymers, characterized by viscosity, are available commercially. The determination of viscosity is historically satisfactory for quality assurance purposes; however, most physical properties of polymers are directly related to molecular weight. For example, the glass transition temperature and tensile strength of amorphous polymers are known to depend on molecular weight. The melt viscosity of polymers and the bulk viscosity of concentrated polymer solutions are also known to depend on molecular weight.

Molecular Weight Grades of PVP Based on K Value

The molecular weights of PVP have traditionally been characterized by the Fikentscher (2) *K* value, which is related to relative viscosity measured at 25°C by

$$\frac{\log \eta_{rel}}{C} = \frac{75K_0^2}{1 + 1.5K_0C} + K_0$$

where $K = 1000K_0$ and C is the solution concentration in g/dl. An increase in η_{rel} corresponds with an increase in K value. Table 1 shows the dependence of

K value on η_{rel} for given values of relative viscosity, measured at 1 g/dl (or 1% wt/vol). As seen from Table 1, a PVP polymer with a relative viscosity of 2 would have a *K* value of 60 and the polymer would be referred to as a K-60. In industry, the *K* value is generally obtained from a table similar to Table 1, with concentrations specified by the U.S. Pharmacopoea (USP) for the different molecular weight grades of PVP. The USP specifies that K-30, K-60, or K-90 should be obtained from 1% solutions and K-15 and K-120 should be obtained from 5 and 0.1% solutions, respectively.

The molecular weight ranges of various commercial *K* value grades of PVP are shown in Table 2. The $\overline{M}_w$ of an unknown PVP sample can be calculated from intrinsic viscosity if the Mark-Houwink equation, which correlates intrinsic viscosity with $\overline{M}_w$, is known from the literature. The unknown PVP sample should be similar in branching and polydispersity to the PVP samples from which the Mark-Houwink equation is derived. Levy and Frank published the following Mark-Houwink equation in 1955 (3) for unfractionated PVP samples in water at 25°C: $[\eta] = 5.65 \times 10^{-2} \times \overline{M}_w^{0.55}$. Senak et al. published the following Mark-Houwink equation in 1987 (4) for unfractionated PVP samples in water-methanol (1:1 vol/vol) with 0.1 M $LiNO_3$ at 25°C: $[\eta] = 1.32 \times 10^{-4} \times \overline{M}_w^{0.65}$.

If a *K* value versus absolute weight-average molecular weight equation or table is available for PVP, then the *K* value can be easily determined from relative viscosity. Such a relationship, developed by Senak et al., is shown in the equation $\log \overline{M}_w = 2.82 \log K + 0.594$ and in Table 3 for commercial grades of unfractionated PVP (5). It should be pointed out here that *K* value is a function not only of molecular weight but also of molecular weight distribution and branching.

Molecular Weights of VP-Based Copolymers

Most VP-based copolymers are also characterized by *K* value. However, the literature on molecular weights of VP copolymers is very sparse. Wu and Senak reported in 1990 (6) the absolute molecular weights of cationic copolymers of quaternized vinyl pyrrolidone and dimethylaminoethyl methacrylate by size exclusion chromatography with low-angle laser light scattering (SEC/LALLS) and SEC with universal calibration (see Table 8). The molecular weights (relative to polyethylene oxide standards) of nonionic copolymers of vinyl pyrrolidone and vinyl acetate, a nonionic terpolymer of vinyl pyrrolidone, dimethylaminoethyl methacrylate, and vinyl caprolactam, and anionic copolymers of vinyl pyrrolidone and acrylic acid were also reported in 1991 (7) by Wu et al. (see Tables 6 and 7).

Table 1 *K* Value versus Relative Viscosity at 1% Concentration (wt/vol)

K value	Relative viscosity	*K* value	Relative viscosity
20	1.120	60	2.031
25	1.175	65	2.258
30	1.243	70	2.527
35	1.325	75	2.846
40	1.423	80	3.225
45	1.539	85	3.678
50	1.677	90	4.219
55	1.839	95	4.870

Molecular Weight Distribution of VP-Based Polymers by Size Exclusion Chromatography

Many important properties of polymers depend not only on molecular weight but also on molecular weight distribution. For example, both viscosity and its dependence on the shear rate of polymer melt and concentrated polymer solution are dependent on molecular weight distribution. SEC is the most practical and the best method for determining the molecular weight distribution of a polymer without going through the tedious classic fractionation procedure using nonsolvent precipitation.

SEC of PVP: Historical Review

The SEC of PVP is not straightforward because of the polar nature of the polymer. Various interactions between PVP and columns, such as adsorption, partition, and electrostatic interactions, must be eliminated by prudent choice of column and mobile phase to obtain true separation by size with 100% recovery and compliance with universal calibration.

Table 2 Molecular Weights of PVP

K value	$\overline{M}_w$	$\overline{M}_n$
K-15	7,000–12,000	~2,500
K-30	40,000–65,000	~10,000
K-60	350,000–450,000	~100,000
K-90	900,000–1,500,000	~360,000
K-120	2,000,000–3,000,000	—

Table 3 *K* Value versus Weight-Average Molecular Weight for PVP[a]

K value	$\overline{M}_w$ (AMU)	*K* value	$\overline{M}_w$ (AMU)
10	2,594	70	626,869
15	8,139	75	761,505
20	18,319	80	913,511
25	34,371	85	1,083,831
30	57,475	90	1,273,397
35	88,771	95	1,483,135
40	129,363	100	1,713,957
45	180,326	105	1,966,770
50	242,714	110	2,242,474
55	317,558	115	2,541,955
60	405,870	120	2,866,099
65	508,646		

[a]The calculations are based on the regression formula $\overline{M}_w = 2.82 \log K + 0.594$.

The SEC behavior of PVP has been of interest to many researchers. In the 10 year period from 1975 to 1984, seven papers, using seven different kinds of columns with various surface modifications and in both aqueous and nonaqueous mobile phases with and without modifiers and salts, were reported for the SEC of PVP with different degrees of success. Some of columns used are commercially available; some are specially made.

Belenkii et al. reported in 1975 (8) the SEC of PVP with unspecified molecular weight using Pharmacia Sephadex G-75 and G-100 columns and a 0.3% sodium chloride solution as the mobile phase. Deviations from universal calibration behavior were noticed from PVP, dextran, polyethylene oxide (PEO), and polyvinyl alcohol. With the development of the important semirigid polymer gel, Toyo Soda TSK-PW columns for water-soluble polymers, Hashimoto et al. reported in 1978 (9) the SEC of PVP K-30 and K-90 using TSK-PW 3000 and two 5000 columns an 0.08 M Tris-HCl buffer (pH = 7.94) as mobile phase and PEO and dextran as calibration standards.

By using an E. Merck LiChrospher SI300 column, modified with an amide group ([NH[CO[CH_3) chemically bonded to the surface, Englehardt and Mathes reported in 1979 (10) the SEC of PVP with molecular weights from 10,000 to 360,000 AMU. A 0.1 M Tris-HCI buffer, pH 8.0, whose ionic strength was adjusted to 0.5 by Li_2SO_4, was used as the eluant. PVP was adsorbed by the column when water or buffer solution was used as eluant; upon the addition of 10% (vol/vol) ethylene glycol to the eluant, however, this interaction was eliminated.

Herman and Field synthesized monomeric diol onto E. Merck Lichrospher SI-500 and reported in 1981 (11) the SEC of PVP with molecular weight 10,000. Poor recovery (0–25%) of PVP was noticed using water as eluant. A 100% recovery was obtained using 40% acetonitrile in 0.01 M KH_2PO_4, pH 2.1. A 100% recovery of PVP was also reported using a TSK-PW-3000 column with 0.08 M Tris buffer. Mori reported in 1983 (12) the SEC of PVP with molecular weights from 11,000 to 1,310,000 AMU using two Shodex AD-80M/S columns with dimethylformamide (DMF) and 0.01 M LiBr as eluant at 60°C. Separation of PVP based on hydrodynamic volume in this SEC system was demonstrated by the applicability of universal calibration using PEO and polyethylene glycol as calibration standards. Domard and Rinaudo grafted quaternized ammonium groups onto silica gels with pore diameters 150, 300, 600, 1250, and 2000 Å and reported in 1984 (13) the SEC of PVP K-15, 25, 30, 60, and 90 using 0.2 M NH_4OAC as the eluant. Some adsorption of PVP K-15, 25, 30, 60 and 90 was noticed by deviation from the universal calibration curve.

In 1984, Malawer et al. (14) did a thorough study on the SEC of PVP K-15, 30, 60, and 90 using diol-derivatized silica gel column sets and aqueous mobile phase modified with various polar organic solvents. A log-linear calibration curve over three decades in molecular weights was obtained on a specially constructed Electronucleonics gylceryl-CPG column set consisting of two 75, 500, and 3000 Å columns and was found to provide better recovery and separation than the commercially available prepacked, 10 μm high-efficiency diol-derivatized silica gel columns. Methanol was found to be a better aqueous mobile-phase modifier to eliminate the adsorption effect than either dimethylformamide or acetonitrile. The best recovery (>90%) and separation were obtained with a mobile phase of 50:50 (vol/vol) methanol-water containing 0.1 M $LiNO_3$.

In summary, when commercially available SEC columns are used, successful SEC separation of PVP without polymer-column interactions has been reported in either an aqueous environment (9) or DMF (12). However, as indicated later, the aqueous environment has the advantage of providing better separation at the low-molecular-weight end of the SEC peak, especially for the lower molecular weight grades, PVP K-30 and K-15. Therefore, the remaining discussion of PVP concentrates on the aqueous environment.

SEC/LALLS and SEC with Universal Calibration for PVP

In a continuation of the earlier work (14), Senak et al. reported in 1987 (4) the most extensive SEC study on PVP to date with the determination of absolute molecular weight and molecular weight distribution by SEC/LALLS and SEC with universal calibration of the four most widely used PVP grades, K-15, K-30, K-60, and K-90. The column set used consists of TSK-PW 6000, 5000,

3000, and 2000 columns and a mobile phase of 50:50 (vol/vol) water-methanol with 0.1 M $LiNO_3$; 100% recovery was reported. The highlights of this paper are reviewed in this section.

Because the principle of SEC with LALLS was discussed in Chapter 4, only the results of SEC with LALLS are presented here. The water-methanol mixed mobile phase used for SEC was also suitable for the determination of molecular weight by LALLS because no preferential solvation of PVP by water or methanol occurred in the mixed mobile phase. This was demonstrated by monitoring the equilibrium concentrations of water and methanol with crosslinked PVP. Furthermore, the differential refractive index increments of PVP in water and PVP in methanol are very close. Lack of preferential solvation in the mixed mobile phase was also demonstrated by the fact that the $\overline{M}_w$ of a PVP K-90 sample was found to be similar, as measured by static LALLS, in the mixed mobile phase (1.43×10^6 AMU) and in water with 0.1 M $LiNO_3$ (1.57×10^6 AMU).

Differential refractive index increments of PVP in the mixed mobile phase were found to be 0.174 ml/g and independent of molecular weight for PVP K-15, K-30, K-60, and K-90. Second virial coefficients of PVP, determined by static LALLS, were found to decrease with increasing $\overline{M}_w$ as expected. The $\overline{M}_w$ of PVP K-60 and K-90 determined by SEC/LALLS were found to be the same as those determined by static LALLS, respectively, indicating no shear degradation of PVP K-60 and K-90 by SEC in the mixed mobile phase.

Based on the SEC with LALLS results, Mark-Houwink constants of both fractionated and commercial unfractionated PVP samples were reported in the mixed mobile phase. The Mark-Houwink constants thus determined were later used in universal calibration to calculate absolute molecular weight and absolute molecular weight distribution. The absolute molecular weights of PVP based on the universal calibration curve calculated from the Mark-Houwink constants of fractionated PVP were found to be similar to those calculated from the Mark-Houwink constants of commercial unfractionated PVP. This indicates that for the purpose of calculating molecular weights by the universal calibration method, the Mark-Houwink constants may be obtained from broad distribution polymers without fractionation, as long as branching is similar for the polymer grades of interest. The molecular weights of PVP by SEC/LALLS and SEC with universal calibration are shown in Table 4. The results showed good agreement in $\overline{M}_w$ from SEC/LALLS and from SEC with universal calibration for PVP K-30, K-60, and K-90. This indicates PVP is separated by hydrodynamic volume in the mixed mobile phase with the TSK-PW column set and confirms the validity of universal calibration.

SEC/LALLS was found to overestimate $\overline{M}_n$ because of the lack of LALLS detector sensitivity in the low-molecular-weight portion of the SEC chromatogram. This overestimation is expected to be more significant for the broad mo-

Table 4 Molecular Weights of PVP Determined by SEC/LALLS and SEC with Universal Calibration

	$\overline{M}_w$		$\overline{M}_n$	
Grade	SEC/LALLS	Universal calibration	SEC/LALLS	Universal calibration
K-15	1.68×10^4	1.12×10^4	1.10×10^4	4.18×10^3
K-30	6.24×10^4	6.19×10^4	3.10×10^4	1.28×10^4
K-60	3.37×10^5	3.40×10^5	1.57×10^5	5.23×10^4
K-90	1.52×10^6	1.24×10^6	6.38×10^5	2.06×10^5

Source: From Reference 4.

lecular weight distribution polymers than for the narrow distribution polymers. The larger difference in $\overline{M}_w$ for PVP K-15 (vis-à-vis the higher K-value grades) could be caused by a combination of lower sensitivity of LALLS at low molecular weight and/or less accuracy of the universal calibration curve at the low-molecular-weight end. Absolute molecular weight distributions for PVP K-90, K-60, K-30, and K-15 grades based on universal calibration are shown in Figure 1.

SEC of Commercial Grades of PVP with a Single Linear Column

One of the most important developments in the technology of semirigid polymeric gels for SEC of synthetic water-soluble polymers in recent years is the availability of the log-linear column with good separation range, from less than 1000 to several million in molecular weight. A linear calibration curve improves both the accuracy and precision of the determination of molecular weight and molecular weight distribution. The commonly used brand names for linear columns for aqueous SEC are Showa Denko Shodex OH pack, Toyo Soda TSK-PW, and Waters Ultrahydrogel. The column packing materials for these columns are all cross-linked, hydroxylated polymethyl methacrylate (PMMA) in nature. Using single linear columns also greatly reduces analysis time and solvent consumption, making SEC a practical method for quality assurance.

Linear PEO calibration curves generated in this laboratory for the Ultrahydrogel linear column in 20:80 methanol-water (vol/vol) with 0.1 M lithium nitrate and in 50:50 methanol-water (vol/vol) with 0.1 M lithium nitrate and for the Shodex KB-80M linear column in 20:80 methanol-water with 0.1 M lithium nitrate are shown in Figures 2, 3, and 4. The effect of methanol-water ratio of the mobile phase on the elution time of PEO standards from a Ultrahydrogel linear column is shown in Table 5.

The PEO standards elute slightly earlier in the 50:50 methanol-water mixture than in the 20:80 methanol-water mixture. Because the viscosity of the 50:

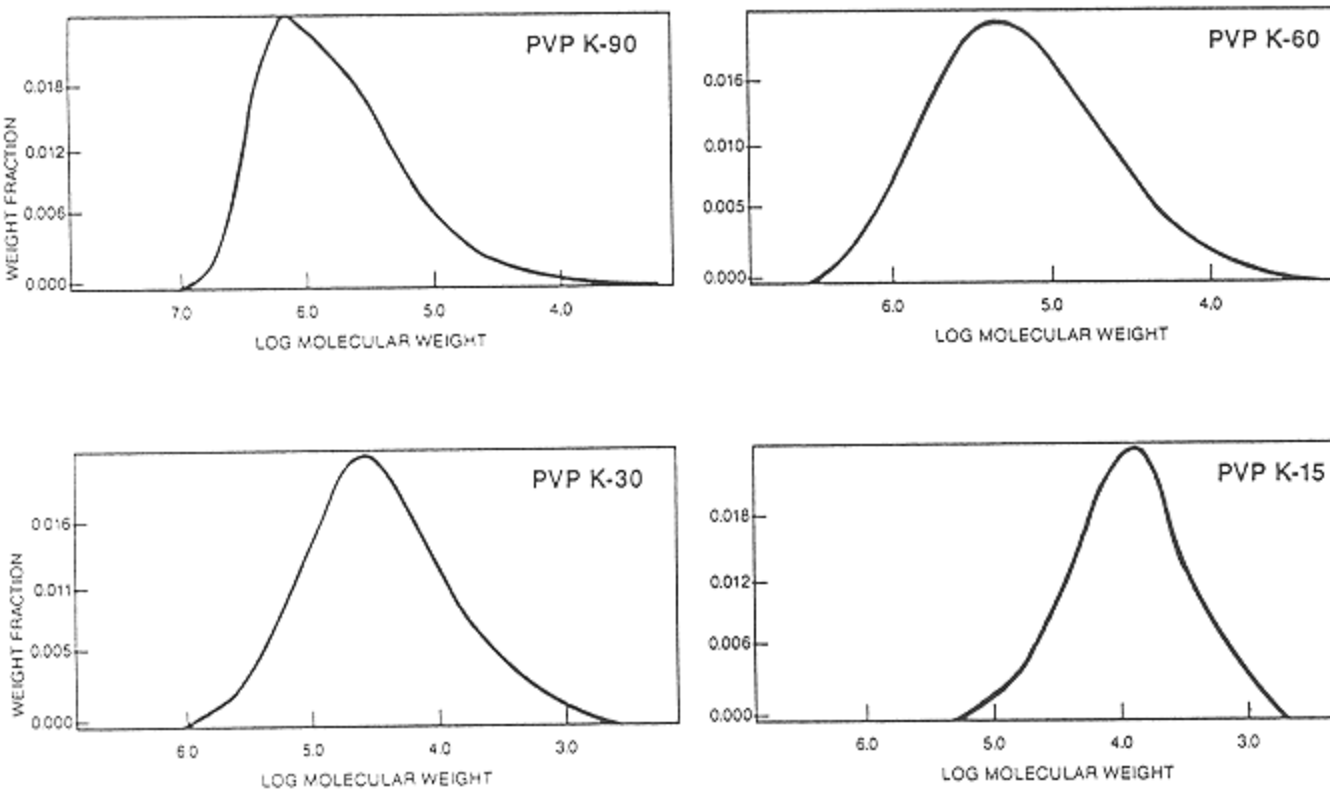

Figure 1
Molecular weight distributions of PVP polymers. (From Reference 4.)

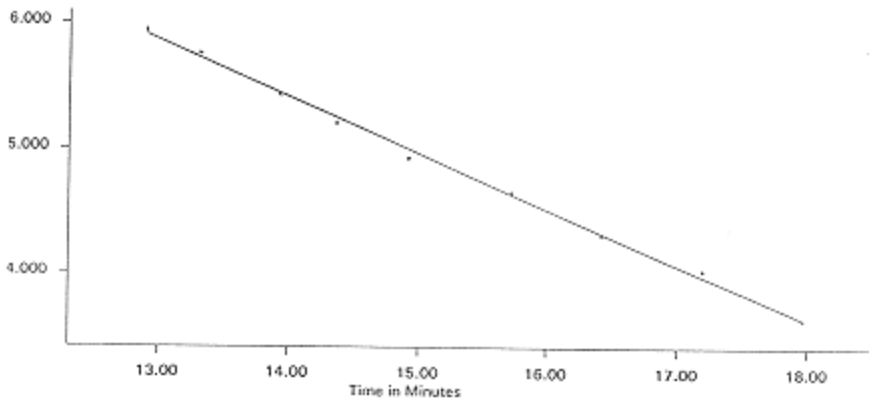

Figure 2
PEO Calibration of Ultrahydrogel linear column in 50:50 (vol/vol) water/MeOH with 0.1 M $LiNO_3$.

50 mixture (1.59 cP at 25°C) is higher than that of the 20:80 mixture (1.30 cP), the retention time in the 50:50 mixture theoretically should be longer than in the 20:80 mixture because of higher viscosity or back-pressure on the column. This indicates the Ultrahydrogel linear column can swell slightly more in the 20:80 methanol-water mixture to generate larger pore sizes and volumes than in the 50:50 methanol-water mixture. As discussed later, the larger pore volume

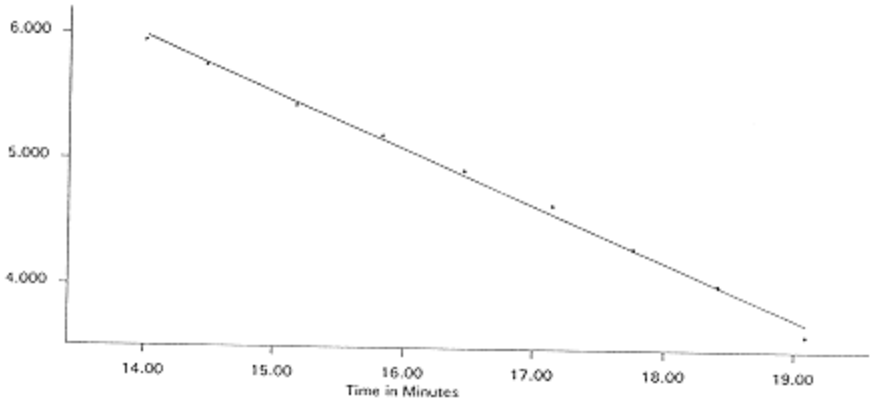

Figure 3
PEO calibration of Shodex KB-80M mixed column in 20:80 (vol/vol) methanol-water with 0.1 M $LiNO_3$.

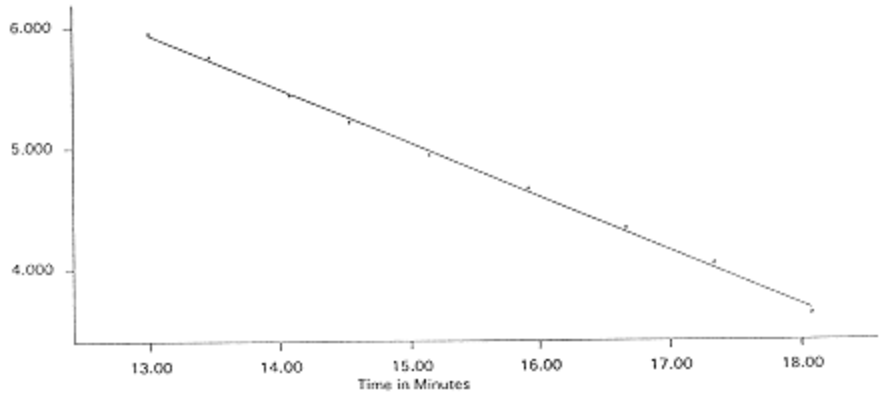

Figure 4
PEO calibration of Ultrahydrogel linear column in 20:80 (vol/vol) methanol-water with 0.1 M $LiNO_3$.

in the 20:80 mixture may provide better separation at the high-molecular-weight end.

Overlays of SEC chromatograms of five commercial grades of PVP using the Shodex KB-80M linear column with a mobile phase of 20:80 (vol/vol) MeOH/H_2O with 0.1 M $LiNO_3$ and the Ultrahydrogel linear column with a mobile phase of either 20:80 (vol/vol) MeOH/H_2O with 0.1 M $LiNO_3$ or 50:50 (vol/vol) MeOH/H_2O with 0.1 M $LiNO_3$ are shown in Figures 5, 6, and 7. Adequate separation of all commercial grades of PVP can be obtained from all three systems.

Table 5 Retention Times of PEO Using Ultrahydrogel Linear Column in Different 0.1 M Lithium Nitrate Mobile Phases

PEO (AMU)	20:80 Water/MeOH	50:50 Water/MeOH
885,000	13.00	12.88
570,000	13.47	13.33
270,000	14.08	13.92
160,000	14.53	14.33
85,000	15.15	14.93
45,000	15.92	15.73
21,000	16.67	16.40
10,750	17.33	17.17
4,250	18.08	17.97

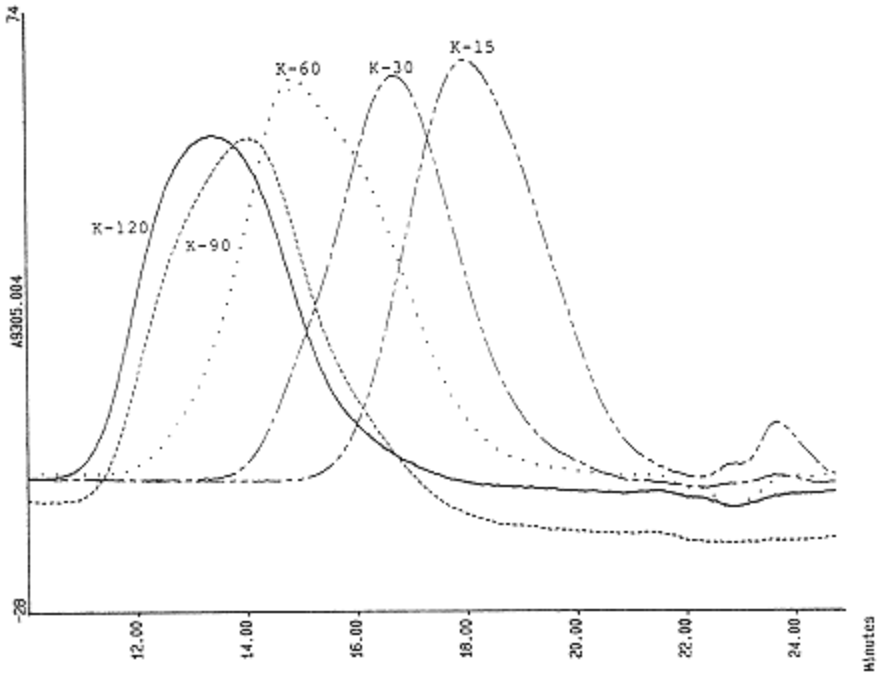

Figure 5
Overlay of gel permeation chromatogram (GPC) of commercial grades of PVP using Shodex KB-80M mixed column and 20:80 (vol/vol) methanol-water with 0.1 M $LiNO_3$ as mobile phase.

The weight-average molecular weights (relative to PEO standards) of the five commercial-grade PVP samples obtained from these three systems with the respective mobile phases are shown in Table 6. Also shown is a Polymer Laboratories polyethylene oxide standard of reported $\overline{M}_w$ of 1,370,000 AMU. Good agreement in weight-average molecular weights were obtained for the low- and medium-molecular-weight grades PVP K-15, 30, and 60 samples among the three systems. However, the Shodex linear column yields higher molecular weight values for the high-molecular-weight grade PVP K-90 and 120 and the PEO standard than the Ultrahydrogel linear column. This indicates the Shodex linear column provides better separation at the high-molecular-weight end than the Ultrahydrogel linear column. The Ultrahydrogel column may also provide better separation at the high-molecular-weight end in the 20:80 methanol-water mobile phase than in the 50:50 methanol-water mobile phase; however, the difference is small.

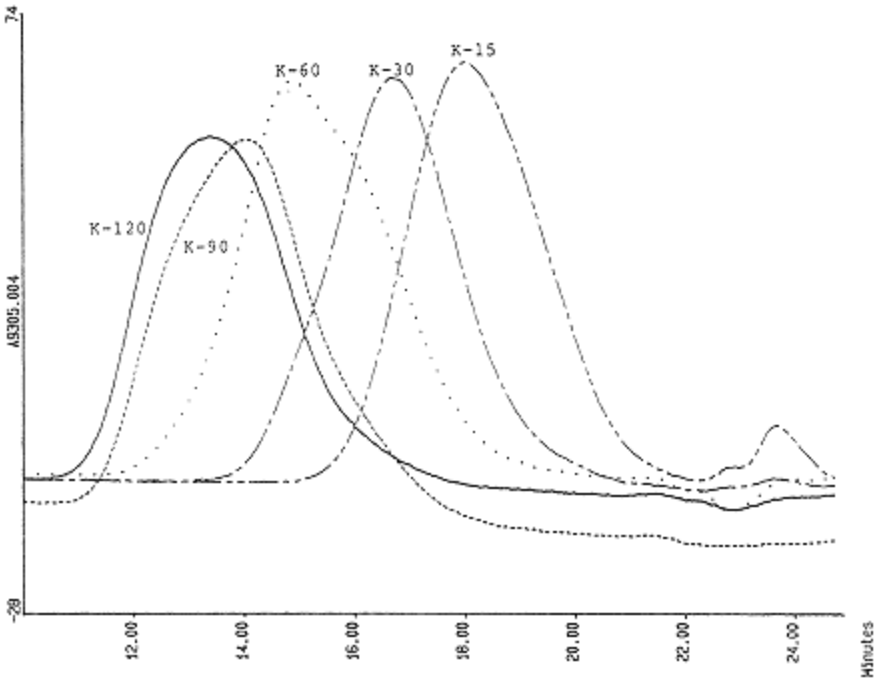

Figure 6
Overlay of GPC chromatograms of commercial grades of PVP using Ultrahydrogel linear column and 80:20 (vol/vol) water/MeOH with 0.1 M $LiNO_3$.

Molecular Weights and Molecular Weight Distributions of VP-Based Copolymers of by SEC

Nonionic Copolymers: Copolymers of Vinyl Pyrrolidone and Vinyl Acetate (VA) and Terpolymer of Vinyl Pyrrolidone, Dimethylaminoethyl Methacrylate (DMAEMA), and Vinyl Caprolactum (VC)

Wu et al. reported in 1991 (7) the SEC of PVP/VA copolymers and PVP/ DMAEMA/VC terpolymer in both aqueous and nonaqueous systems. For the aqueous system the column set consisted of four Waters Ultrahydrogel columns of pore sizes 120, 500, 1000, and 2000 Å, and the mobile phase was 1:1 water-methanol (vol/vol) with 0.1 M $LiNO_3$. Aqueous mobile phase with no organic modifiers, such as methanol, cannot be used because of the poor solubility of some of the nonionic copolymers in pure water and the adsorption of the copolymers by the columns. For the nonaqueous system, the column sets were

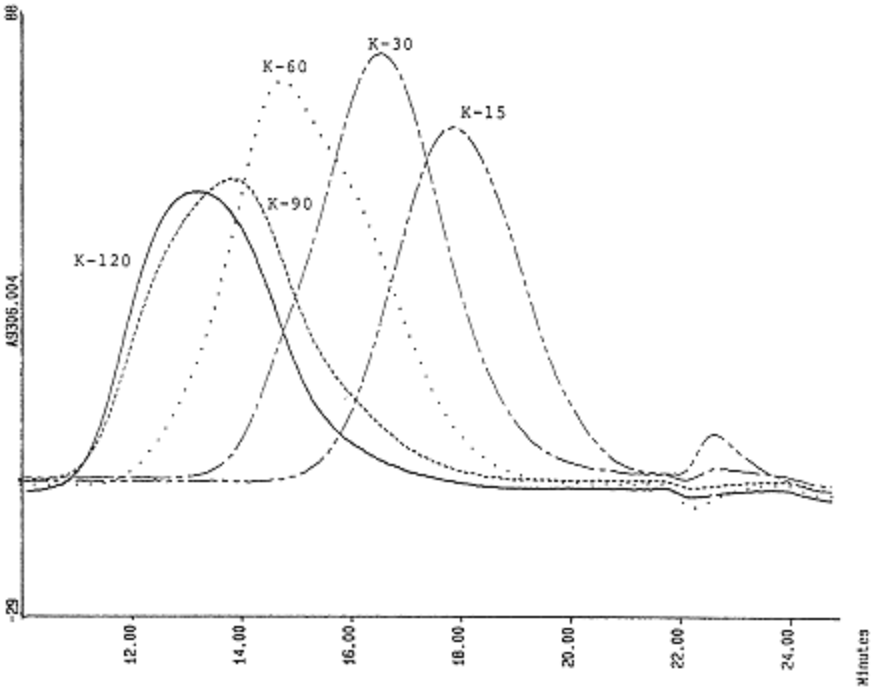

Figure 7
Overlay of GPC chromatograms of commercial grades of PVP using Ultrahydrogel linear column and 50:50 (vol/vol) water/MeOH with 0.1 M $LiNO_3$.

Table 6 Weight-Average Molecular Weights of Five Commercial Grades of PVP and a PEO Standard Obtained from the Shodex Linear Column and the Ultrahydrogel Linear Column

	Weight-Average Molecular Weights (AMU)		
		Ultrahydrogel	
Grade	Shodex	20:80 Water-methanol	50:50 Water-methanol
PEO	1,170,000	1,020,000	934,000
K-120	1,060,000	845,000	810,000
K-90	698,000	597,000	578,000
K-60	160,000	166,000	166,000
K-30	29,700	33,600	32,900
K-15	7,500	7,200	6,780

Shodex KD-80M plus Ultrahydrogel 120 Å, Shodex KD-80M plus PLgel 100 Å, and PLgel 10^4 Å plus 500 Å, and the mobile phase was DMF with 0.1 M $LiNO_3$.

For the nonaqueous systems, the peak shapes are very similar for all three column sets; the Shodex KD-80M plus Ultrahydrogel 120 Å provides slightly better separation of the solvent peak and the low-molecular-weight end of the polymer peak. However, the aqueous system showed the best separation at the low-molecular-weight end, as shown in Figures 8 and 9. The weight-average molecular weights and intrinsic viscosities determined in aqueous and nonaqueous systems (Shodex KD-80M plus Ultrahydrogel 120 Å) are shown in Table 7. A 100% recovery was achieved in both aqueous and nonaqueous systems for PVP/VA in SEC.

Anionic Copolymers: Copolymers of Vinyl Pyrrolidone and Acrylic Acid (AA)

Even though this copolymer is soluble in the water-methanol (50:50, vol/vol) mobile phase with 0.1 M lithium nitrate, no recovery of the copolymer can be obtained in SEC with the Ultrahydrogel columns in this mobile phase. Wu et al. reported in 1991 (7) the SEC of PVP/AA using a 0.1 M pH 9 Tris buffer with 0.2 M $LiNO_3$ as the mobile phase and the Ultrahydrogel 120, 500, 1000, and 2000 Å column set. The PVP/AA samples were first dissolved in 0.25 N

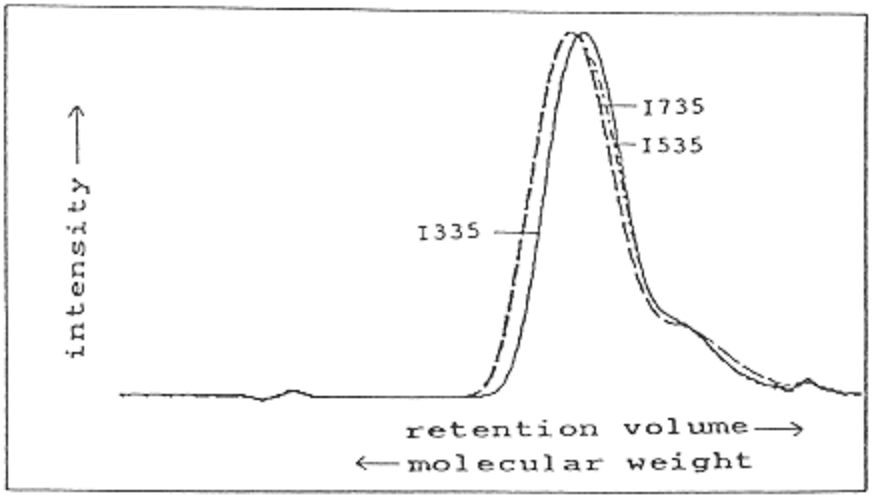

Figure 8
SEC traces of PVP/VA, I series, using the SU2 column set with DMF solvent. (From Reference 7.)

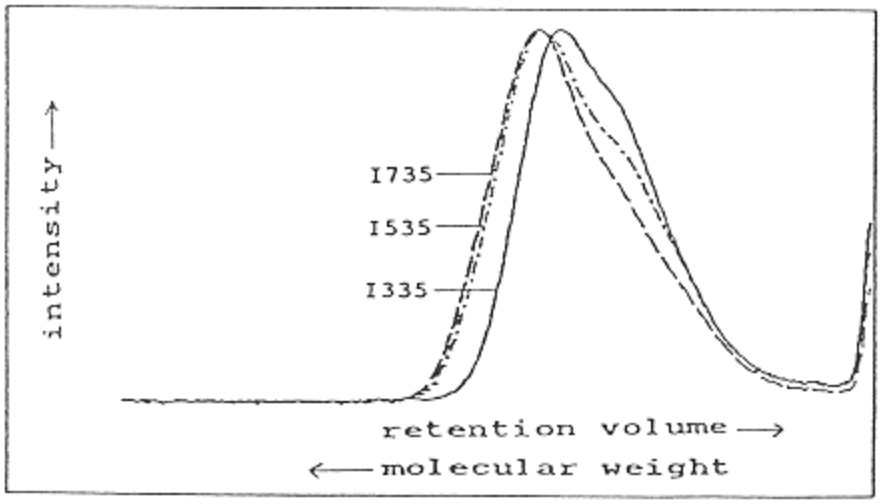

Figure 9
SEC traces of PVP/VA, I series, using the U4 column set with water-methanol solvent. (From Reference 7.)

Table 7 Intrinsic Viscosities and Weight-Average Molecular Weights (Relative to PEO) of PVP/VA and PVP/DMAEMA/VC

		Aqueous system		Nonaqueous system	
Polymer	Composition (% VP)	$\overline{M}_w$	[η] (dl/g)	$\overline{M}_w$	[η] (dl/g)
PVP/VA					
E335	30	28,800	0.265	37,900	0.261
E535	50	36,700	0.363	38,700	0.241
E635	60	38,200	0.330	37,600	0.253
E735	70	56,700	0.429	52,200	0.310
I335	30	12,700	0.176	15,000	0.162
I535	50	19,500	0.222	20,300	0.174
I735	70	22,300	0.261	21,500	0.182
W735	70	27,300	0.265	25,000	0.238
S630	60	51,000	0.424	48,600	0.321
PVP/DMAEMA/VC	—	82,700	0.620	68,200	0.480

Source: From Reference 7.

NaOH (1%, wt/vol) and then diluted with the pH 9 buffer to the proper concentration for analysis. The SEC chromatograms are shown in Figure 10. The separation is reasonably good; however, a baseline separation between the solvent peak and the low-molecular-weight end of the copolymer peak could not be achieved. The weight-average molecular weights (relative to PEO standards) and intrinsic viscosities of PVP/AA are shown in Table 8. A 100% recovery was achieved for PVP/AA in SEC.

Cationic Copolymer: Quaternized Copolymer of Vinyl Pyrrolidone and Dimethylaminoethyl Methacrylate

Wu and Senak reported in 1990 (6) the absolute molecular weights and molecular weight distributions of PVP/DMAEMA by SEC/LALLS and SEC with universal calibration using Waters Ultrahydrogel 120, 500, 1000, and 2000 Å columns and a 0.1 M Tris pH 7 buffer with 0.5 M $LiNO_3$ as mobile phase. The quaternized amino groups on PVP/DMAEMA are responsible for the cationic charge in a pH 7 buffer. Because of the cationic charges on the molecules, a much higher salt content is needed in the SEC mobile phase for the cationic PVP/DMAEMA copolymers (0.5 M $LiNO_3$) than the salt contents for nonionic and anionic copolymers (0.1 and 0.2 M $LiNO_3$) to improve separation and recovery of polymer. As indicated in the earlier discussions, these semi-rigid polymeric gels are hydroxylated PMMA in nature. They can be expected to have a small amount of free carboxyl groups on the gels as a result of hydrolysis, which

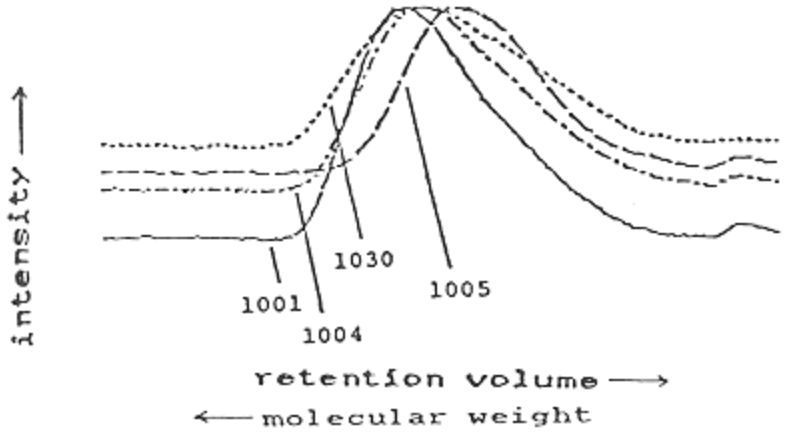

Figure 10
SEC traces of PVP/AA copolymers using the U4 column set with pH 9 solvent.
(From Reference 7.)

Table 8 Weight-Average Molecular Weights and Intrinsic Viscosities of PVP/AA

PVP/AA	$\overline{M}_w$ (AMU)	[η] (dl/g)
1001	318,800	1.33
1004	256,000	1.37
1005	135,000	1.04
1030	277,000	—[a]

[a]Not measurable because of poor solubility at high concentrations.

Source: From Reference 7.

can interact adversely with the cationic polymers. The much higher salt content (0.5 M) is required to neutralize the electrostatic interactions between the cationic polymer and the carboxylate groups on the column. A 100% recovery of the cationic PVP/DMAEMA was achieved in SEC in the pH 7 (0.5 M $LiNO_3$) mobile phase.

This cationic copolymer is also soluble in the 1:1 (vol/vol) water-methanol mobile phase with 0.1 M lithium nitrate, and SEC has been carried out in the past in this laboratory in this mobile phase with the Ultrahydrogel columns, with adequate results. The separation and recovery are generally better in the pH 7 buffer with 0.5 M lithium nitrate than in the water-methanol mixed mobile phase with 0.1 M lithium nitrate with the Ultrahydrogel columns and therefore is the preferred method for the PVP/DMAEMA polymer.

The Mark-Houwink constants K and α for cationic PVP/DMAEMA copolymers in pH 7 buffer were determined as 1.42×10^{-4} and 0.67, respectively. The intrinsic viscosities and absolute molecular weights of PVP/DMAEMA are shown in Table 9. The number-average molecular weights are overestimated by

Table 9 Intrinsic Viscosities and Absolute Molecular Weights of Cationic PVP/DMAEMA Copolymers in pH 7 Buffer, 0.5 M $LiNO_3$

		Absolute molecular weights (AMU)			
		SEC/LALLS		SEC-universal calibration	
Polymer	Intrinsic viscosities	$\overline{M}_w$	$\overline{M}_n$	$\overline{M}_w$	$\overline{M}_n$
734	0.647	300,000	115,000	331,000	110,000
755	2.15	1,630,000	704,000	1,720,000	483,000
755N	2.22	2,020,000	889,000	2,020,000	523,000

Source: From Reference 6.

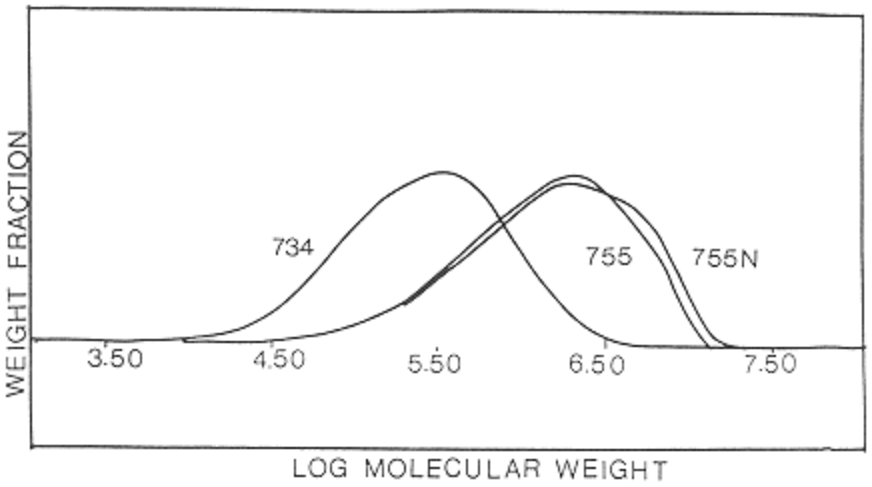

Figure 11
Molecular weight distributions of quaternized polyvinyl pyrrolidone-dimethylaminoethyl methacrylate copolymers. (From Reference 6.)

SEC/LALLS. The weight-average molecular weights determined by SEC/LALLS are the same as those determined by SEC with universal calibration, indicating the cationic PVP/DMAEMA copolymers are separated by hydrodynamic volumes in SEC. The overlays of molecular weight distributions of the cationic PVP/DMAEMA copolymers are shown in Figure 11.

Conclusions

Successful SEC of PVP- and VP-based copolymers in both aqueous and nonaqueous systems using commercially available columns has been reported in the literature. For PVP, separations based on hydrodynamic volume and universal calibration were also reported for both aqueous and nonaqueous SEC systems. In general, the aqueous SEC system (modified with methanol to eliminate polymer-column interactions) provides better separation than the nonaqueous SEC system, especially at the low-molecular-weight end. Therefore, aqueous SEC systems are preferred for PVP and VP-based copolymers in general, as long as the aqueous system is applicable.

For PVP, the optimized SEC system is the Shodex linear column KB-80M with 20:80 water-methanol (vol/vol) and 0.1 M lithium nitrate. For low- to medium-molecular-weight nonionic copolymers, such as PVP/VA, the optimized SEC system is a Shodex linear column KB-80M plus a low-molecular-weight

Shodex KB-802 column and a mobile phase of 50:50 water-methanol (vol/vol) with 0.1 M lithium nitrate. For the anionic copolymers, such as PVP/AA, the optimized SEC system is the Shodex linear column KB-80M and a mobile phase of a pH 9 buffer with 0.2 M lithium nitrate. For the cationic copolymer, PVP/DMAEMA, the optimized SEC system is the Shodex linear column KB-80M and a pH 7 buffer mobile phase with 0.5 M lithium nitrate.

Depending on the molecular weight range of interest, the Shodex linear column KB-80M may have to be replaced with other Shodex OH-pack columns with different pore sizes to optimize separation. Ultrahydrogel columns or TSK-PW columns can also be used interchangeably with the Shodex OH-pack columns for PVP- and VP-based copolymers in the respective mobile phases. However, the Shodex OH-pack columns at the present time provide slightly better separation for high-molecular-weight PVP- and VP-based copolymers than the Ultrahydrogel columns or the TSK-PW columns.

References

1. F.W. Billmeyer, Jr., *Textbook of Polymer Science*, 3rd Edition, Wiley & Sons, New York, 1984, p. 341.

2. H. Fikentscher, *Cellulose-Chem.*, 13, 58 (1932).

3. B. Levy and H.P. Frank, *J. Polym. Sci.*, 37, 247–254 (1955).

4. L. Senak, C.S. Wu, and E.G. Malawer, *J. Liq. Chromatogr.*, 10(6), 1127–1150 (1987).

5. L. Senak, C.S. Wu, and E.G. Malawer, unpublished results.

6. C.S. Wu and L. Senak, *J. Liq. Chromatogr.*, 13(5), 851–861 (1990).

7. C.S. Wu, J. Curry, and L. Senak, *J. Liq. Chromatogr.*, 14(18), 3331–3341 (1991).

8. B.G. Belenkii, L.Z. Vilenchik, V.V. Nesterov, V.J. Kolegov, and S.Y.A. Frenkel, *J. Liq. Chromatogr.*, 109, 223–238 (1975).

9. T. Hashimoto, H. Sasaki, M. Aiura, and Y. Kato, *J. Polym. Sci., Polym. Phys. Ed.*, 16, 1789–1800 (1978).

10. H. Engelhardt and D. Mathes, *J. Chromatogr.*, 185, 305–319 (1979).

11. D.P. Herman and L.R. Field, *J. Chromatogr. Sci.*, 19, 470–476 (1981).

12. S. Mori, *Anal. Chem.*, 55, 2414–2416 (1983).

13. A. Domard and M. Rinaudo, *Polym. Commun.*, 25, 55–58 (1984).

14. E.G. Malawer, J.K. De Vasto, and S.P. Frankoski, *J. Liq. Chromatogr.*, 7(3), 441–461 (1984).

13
Size Exclusion Chromatography of Cellulose and Cellulose Derivatives

Anthony H. Conner U.S. Department of Agriculture Forest Service, Madison, Wisconsin

Introduction

Approximately 2×10^{11} ton biomass is produced on land and in water annually (1). Cellulose is the principal structural material in the cell wall of all plants (2). In addition, cellulose can be found in algae, bacteria, and animals (tunicates). Assuming that the average source contains 50% cellulose (Table 1) (3–5), then approximately 1×10^{11} ton cellulose is formed each year. This makes cellulose the most important renewable resource in the world.

Cellulose and its derivatives have been and are commercially and scientifically important. They are used in the production of paper; textiles and fibers (e.g., rayon); films (e.g., cellophane); gums and thickeners (e.g., cellulose ethers); foods; pharmaceuticals; cosmetics; explosives and propellants (e.g., nitrocellulose); and adhesives. In addition, the hydrolysis of cellulose is actively being studied as raw material for the production of alcohol fuels (6) and chemicals (7). As nonrenewable materials are depleted, the importance of cellulose as a chemical raw material will increase. Analysis and characterization of any

Table 1 Cellulose Content of Natural Sources

Plant source	Cellulose content (%)
Algae (green)	20–40
Bacteria	20–30
Bagasse	35–45
Bamboo	40–55
Bark	20–30
Cotton	90–99
Flax	70–75
Hemp	75–80
Jute	60–65
Kapok	70–75
Mosses	25–30
Ramie	70–90
Straw	40–50
Wood	40–50

Source: From Refs. 3–5

polymeric starting material are important in its production, at intermediate stages in the production of various products from it, and in the characterization and analysis of its derived products; this is no less true with cellulose and its derivatives. Size exclusion chromatography (SEC) has been and will continue to be an important tool in the characterization and analysis of cellulose and cellulosics (8–110). The SEC analysis of cellulose was reviewed in 1975 (91) and covered the literature through about 1972. This review covers the literature from about 1970 to 1991 and thus may overlap with the previously reviewed literature.

Chemical and Macromolecular Structures

Both chemical and macromolecular structures are important determinants in the selection of the SEC method(s) used for the analysis and characterization of cellulose. Each structure is briefly discussed; however, each is also the subject of much research and debate. For detailed discussions, refer to the literature (e.g., Refs. 111–124).

Cellulose is a homopolymer of D-anhydroglucopyranose monomeric units connected through β-(1 → 4)-glycosidic linkages (Fig. 1). As illustrated, every other monomeric unit is rotated by approximately 180° about the long axis of the cellulose chain compared with its two neighboring monomeric units. Because of this, cellobiose is, in the strictest sense, properly considered the repeat unit

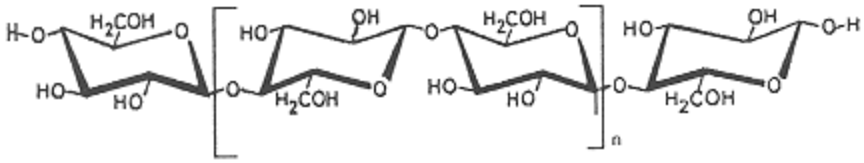

Figure 1.
Chemical structure of cellulose.

of the cellulose polymer. It is apparent from Figure 1 that the cellulose molecule contains two nonequivalent ends. The hemiacetal group at one end can act as a reducing group and is therefore referred to as the reducing end. The opposite end is referred to as the nonreducing end.

In nature, cellulose is generally admixed with and often intimately associated with other substances, including lignin, hemicelluloses, pectins, fats, waxes, and protein. “Native” cellulose (i.e., cellulose as produced by plants) generally exists in the cellulose I crystallographic form, although cellulose II is known to occur in marine algae. Other crystallographic forms (polymorphs) can be produced chemically (118); for example, cellulose II is formed when cellulose I is mercerized or regenerated from solution.

Separation of pure cellulose requires further treatment consisting of steps that include extraction with organic solvents, pulping processes, partial hydrolysis, and dissolution and reprecipitation. Because cellulose reacts with both acids and bases and is subject to oxidation, these isolation procedures can and often do degrade the cellulose.

The degree of polymerization (DP) of cellulose (i.e., the number of anhydroglucose units per chain) varies widely (Table 2) and depends on the source of the cellulose, the extent of cell development within that source, and the methods used for isolation of the cellulose. Cellulose is polydisperse; the DPs reported in Table 2 are weight-average degrees of polymerization (DP_w) that were determined by viscometric methods (assumes $DP_w \simeq DP_v$).

The linear nature conferred upon cellulose as a consequence of the β-(1→4)-glycosidic linkages (Figure 1) results in a rigid, rod-like molecule. As a result of the large number of hydroxyls, cellulose molecules readily form hydrogen bonds with other cellulose molecules to give a fibrillar structure. Electron microscopic examination of mechanically disrupted cellulosic material reveals that the fibrillar structure is composed of structural units generally referred to as microfibrils. The dimensions of microfibrils have been determined both by electron microscopy and by x-ray diffraction (120,121). The length of microfibrils (often several micrometers) may be longer than that estimated from the DP of the cellulose chain because chains end randomly within microfibrils. Their

Table 2 Average Degrees of Polymerization for Cellulose Isolated from a Variety of Sources

Cellulose source	DP_w
Acetobacter xylinum	2000–6000
Bagasse	700–900
Cotton	8,000 (opened)–15,000 (unopened)
Cotton linters	1,000–5,000
Flax	7,000–8,000
Kapok	9,500
Pulp (bleached)	500–2,100
Ramie	9,000–11,000
Rayon	300
Valonia	25,000–27,000
Wood	8,000–9,000

Source: From Refs. 3–4.

width and thickness vary among sources but are generally 10–30 and 5–12.5 nm, respectively, in ramie, algal, and bacterial celluloses. In cotton and most plants, the width and thickness tend to be in the range 3–5 nm.

Crystalline and paracrystalline (amorphous) regions are found throughout the length of the microfibrils, indicated by both well-defined reflections and background scattering in the x-ray diffractograms. Various models have been proposed that account for the presence of crystalline and amorphous regions within the microfibrils of native cellulose. However, discussion of these models is beyond the scope of this chapter.

Cellulose Structure and SEC

Cellulose and cellulose oligomers of DP approximately greater than 7–9 are insoluble in water and most organic solvents, although oligomers of DP up to 15–20 are apparently soluble in dimethylsulfoxide (DMSO). The low solubility is due in part to the crystalline nature of cellulose and the large crystalline packing forces from extensive hydrogen bonding within the cellulose crystallites. This obviously imposes a severe restriction on the ability to conduct SEC analysis of cellulose.

Two general methods have been used to overcome the lack of cellulose solubility: (1) formation of cellulose derivatives that exhibit solubility and (2) dissolution of cellulose using “cellulose solvents.” Both methods have been used to “solubilize” cellulose for SEC analysis and are discussed in this chapter.

Cellulose Derivatives

Each cellulose molecule contains three distinct types of glucose units: those at the reducing end, those at the nonreducing end, and the anhydroglucopyranose monomers in the interior (Figure 1). The anhydroglucopyranose monomeric units within the cellulose molecule each contain three hydroxyl groups—one primary and two secondary hydroxyls. The monomer at the nonreducing end contains four hydroxyls, and that at the reducing end contains a hemiacetal group in addition to three hydroxyls. These hydroxyls react in the same fashion as primary and secondary hydroxyls found in other simpler molecules. Thus, these hydroxyls can be converted to a variety of ethers and esters. These derivatives are often soluble and can in theory be used to carry out SEC analysis of cellulose derivative. It is then assumed that the information obtained on the molecular weight distribution of the cellulose derivative accurately reflects that of the original cellulose after appropriate correction for increased molecular weight caused by derivative formation.

However, the derivatization reactions are more complicated than those for a simple substance, because derivatization reactions nearly always involve heterogeneous reactions. The heterogeneous nature of the reactions exists not only because cellulose is not soluble in the reaction medium but because cellulose itself is heterogeneous. In general, reagents have greater access to the paracrystalline (amphorous) regions than to the highly crystalline regions. In addition, the reactivity of the hydroxyls within the crystalline regions varies, presumably as a result of the hydrogen bonding patterns within the crystalline lattice (125). Thus, two major concerns in using cellulose derivatives for SEC analysis are that the derivatives are not completely formed and that substituents are not uniformly distributed along the cellulose chain length. An additional concern is that the reaction conditions used for forming the cellulose derivative may cause degradation of the cellulose molecule, for example by hydrolysis of the glycosidic linkages or by oxidation.

Cellulose Solvents

Several known systems dissolve cellulose (126–129). These systems range from solutions in protonic acids (e.g., 78% phosphoric acid) to metallic complexes (e.g., cuprammonium). All known methods for dissolving cellulose can be fit into four main categories (128): cellulose acting as a base, cellulose acting as an acid, cellulose complexes, and cellulose “derivatives.” The cellulose derivatives are distinguished from those discussed previously in that dissolution occurs simultaneously with derivative formation and the derivative produced can easily be regenerated (129).

Cellulose solvents have been used as the medium in which cellulose is dissolved and eluted during SEC analysis. However, problems can arise from

adverse effects on cellulose molecule (e.g., hydrolysis or oxidative degradation), from adverse effects on the material used as a packing in the column system used to conduct the SEC analysis (e.g., degradation or swelling of the packing material), or limitations on the range of DP over which the cellulose molecule is soluble.

SEC of Derivatized Cellulose

From an experimental standpoint, it is desirable to conduct the SEC analysis of cellulose directly on the underivatized polymer, thus avoiding any possibility of degradation and minimizing the number of steps involved in the preparation of the sample. As a result of the insolubility of cellulose in the more common solvents, however, it has usually been necessary to derivatize the cellulosic sample to obtain a soluble material for analysis. Cellulose trinitrate and to a lesser extent cellulose acetate have historically been employed as the derivatives of choice. Recently, the tricarbanilate derivative of cellulose has come into common use for conducting SEC analysis and has a number of reported advantages over the nitrate derivative. The use of each of these derivatives is discussed. In addition examples of SEC analysis of other cellulose derivatives are given.

Cellulose Trinitrate

The historical emphasis on the trinitrate ester as the derivative of choice for early experimental work on the SEC analysis of cellulose and cellulosics and the continued use of the trinitrate in this capacity are readily understandable. Cellulose nitrate was known to be soluble in organic solvents, and a “mild” method for its preparation with a high nitrogen content (approximately 13.4% N compared to 14.1% N theoretically) was reported (130). In addition, cellulose trinitrate was extensively used in previous studies of cellulose by viscometry, osmometry, ultracentrifugation, and fractional precipitation. Thus, SEC data could be readily compared with existing data for the trinitrate derivative.

In the mid-1960s, a cross-linked polystyrene gel (Styragel, Waters Associates) was identified as a suitable porous column-packing material for the SEC analysis of cellulose trinitrate (91). The principal solvent used in these studies was tetrahydrofuran (THF) because it readily dissolved the cellulose trinitrate and was compatible with the Styragel.

Typically, a number of columns containing Styragel with differing exclusion limits were connected in series. Because of the large particle size of the Styragel, each column was rather large, approximately 1.2 m long and 0.09 mm inside diameter. Analysis times were lengthy, about 3–4 h or more. This basic setup was used well into the 1980s, until the advent of packing materials of smaller

particle size (e.g., μ Styragel and PLgel, Polymer Laboratories). Table 3 gives information on several systems using these materials for the SEC analysis of cellulose trinitrate.

Many possible complications (29,81) associated with the use of the trinitrate derivative for the SEC analysis of cellulose have been reported. The major complication arises from the distinct possibility of hydrolysis of the polymeric cellulose chain as a result of the acid reaction conditions employed during derivatization. That the derivatization reaction does not give a completely derivatized material and that the cellulose trinitrate is not stable are also complicating

Table 3 Typical Conditions for SEC of Cellulose Trinitrate Using THF as the Eluant

Porous packing material	Exclusion limits of each column (Å)[a]	Temperature (°C)	Flow rate (ml/minute)	References
Styragel	3×10^6 1×10^6 1×10^5 3×10^4	Ambient	1	9, 10
	1×10^6 1×10^5 1×10^4 1×10^3	25	1	32
	1×10^5 1×10^4 3×10^3 1×10^3 400	-	-	63
	5×10^6 1×10^5 3×10^4 3×10^3	-	1	28
μStyragel	1×10^6 1×10^5 1×10^4 1×10^2 or 1×10^3	-	1	22, 66, 93
PLgel	1×10^6 1×10^6 1×10^3	20	1	57

[a]10 Å = 1 nm.

factors. However, the effect of variations in the extent of nitrate substitution of SEC analysis in THF solution was reported to be minimal as long as the final cellulose trinitrate contained at least 12.6–13.3% N (28).

In addition, several complications have been observed when actually conducting the SEC analysis. First, elution volume shifts with changes in sample concentration (28). The shift in elution volume is large even at low concentrations. In previous work, chromatograms were obtained with 1:4 and 1:8 concentrations, and the results extrapolated to zero concentration. This procedure is time consuming. Typically, SEC has been determined at 1:8 concentration. Second, the presence of microgels as a result of small but significant amounts of very high molecular weight cellulose trinitrate was detected using a low-angle laser light-scattering (LALLS) detector (28). However, the microgel was not detected by the refractive index (RI) detector, suggesting that this detector responds as if to a true polymeric solution. Last, a plot of the viscometrically determined DP of cellulose trinitrate compared with elution volume contains three distinct linear regions, requiring separate determination of calibration parameters for each region (93).

In addition to the polystyrene-based materials, several attempts have been made to utilize silica gel as a porous column-packing material (37,38,65). C_8 chain-coated silica gel was used for the SEC analysis of cellulose trinitrate with a DP of approximately 250–2500 (65). The separating power of the system was determined by a comparison of the molecular weight distribution obtained by SEC and fractional precipitation on the same sample. It was determined that in the SEC analysis, the cellulose trinitrate sample was in fact being separated by a size exclusion mechanism.

Silanized silica gel has also been studied for the SEC analysis of cellulose trinitrate (37,38), using THF as the eluant. It was concluded that the elution behavior of the cellulose trinitrate sample was influenced by polyelectrolytic effects and was not based strictly upon size exclusion. The addition of 0.01 mol acetic acid per liter THF suppressed the non-size exclusion effects. Under these conditions, a universal calibration curve relating cellulose trinitrate and polystyrene could be established.

Cellulose Acetate

Interest in the SEC analysis of cellulose nitrate has been primarily as a result of the utilization of the nitrate for the purpose of studying cellulose, not cellulose nitrate per se. However, the reverse is true of cellulose acetate.

Generally, commercial cellulose acetate is not completely derivatized, having a degree of substitution (DS) of about 2–2.5. This product, regarded as the diacetate, is thermoplastic and soluble in acetone. Cellulose triacetate is also

produced commercially, but this material is insoluble in acetone and soluble in dichloromethane.

The SEC analyses of both the diacetate (10,57,60,71,94) and the triacetate (59,72) have been studied. Table 4 outlines typical conditions used in these SEC analyses.

One complication that has been reported in connection with the SEC analysis of cellulose diacetate is the presence of a small, separate peak ("prehump") or shoulder on the high-molecular-weight end of the chromatogram (10,94) obtained from wood pulps. Material isolated from this peak is enriched in mannose and xylose, and the size of the peak can be directly correlated with the amount of hemicellulose in the pulp. The hemicellulosic material causing the prehump can be removed as a small amount of poorly soluble material by fractional precipitation.

Cellulose Tricarbanilate

Since its initial use (131), the tricarbanilate derivative of cellulose has proven to be very valuable for the SEC analysis of cellulose and cellulosics (22,23,28,29,36,40,52,54,57,58,75,76,81,99,108). Table 5 outlines some typical conditions that have been used for the SEC analysis of cellulose tricarbanilate.

The carbanilate derivative of cellulose is reported to have several advantages (29,81) compared with other derivatives, especially the nitrate. These advantages include the stability of the tricarbanilate, that complete substitution of cellulose takes place, that the substitution reaction does not normally cause depolymerization of the starting cellulose, and the ready solubility of the carbanilate. One disadvantage may be the large increase in molecular weight of the material after conversion to the tricarbanilate derivative (36); any SEC system must be capable of handling the higher molecular weights.

One indication that the formation of the trinitrate derivative of cellulose causes depolymerization and the formation of the tricarbanilate does not is that the DPs of cellulose determined as the tricarbanilate are considerably greater than those obtained as the trinitrate (22). Although a plausible explanation for this difference is the depolymerization of cellulose curing formation of the trinitrate derivative, comparison of DP derived from the trinitrate and the tricarbanilate using the same sources of cellulose indicates that this difference may simply be a result of errors in the Mark-Houwink coefficients for cellulose trinitrate in acetone solution (22).

Several solvents have been studied as a medium for the reaction of phenylisocyanate with cellulose. These include dimethylformamide (DMF), pyridine, and DMSO. The rate of derivative formation is affected by the choice of solvent (40), being fastest in DMSO and slowest in DMF. No degradation in the cellulose chain length was observed when the reaction was carried out in pyridine

Table 4 Conditions for SEC of Cellulose Acetates

Cellulose	Porous packing material	Exclusion limits of each column (Å)[a]	Solvent	Temperature	Flow rate (ml/minute)	I
Diacetate	Styragel	3×10^6	THF	Ambient	1	
		1×10^6				
		1×10^5				
		3×10^4				
	PLgel	5 μm mix	THF	20°C	1	
		5 μm mix				
Triacetate	Styragel	7×10^5-5×10^6	Dichloromethane	Ambient	1	
		5×10^3				
		2×10^3-5×10^3				

[a]10 Å = 1 nm.

Table 5 Typical Methods for SEC of Cellulose Tricarbanilate Using THF as the Eluant.

Porous packing material	Exclusion limits of each column (Å)[a]	Temperature	Flow rate (ml/minute)	References
μStyragel	1×10^6 1×10^5 1×10^4 1×10^3	-	1	22
Spherosil				
XOC-005	$>4 \times 10^6$	-	0.7	29
XOB-015	1.5×10^6			
XOB-030	1×10^6			
XOB-030	1×10^6			
XOB-075	4×10^5			
Shodex				
KF806	4×10^7	-	1	40
KF805	4×10^6			
KF804	4×10^5			
PLgel	1×10^6 1×10^6 1×10^3	-	1	40
μBondagel (Three columns)	7×10^6-5×10^3	20°C	0.5	53, 54
TSKgel HXL	4×10^8 4×10^7 4×10^6	-	-	76
Shodex				
KF805	4×10^6	Ambient	1	108
KF803	4×10^4			
μStyragel	100			

[a]10 Å = 1 nm.

at 80°C, but degradation was observed at the higher temperatures used by previous researchers (81).

In some cases (e.g., regenerated celluloses), a considerable amount of solid material is still present after the 48 h reaction period in pyridine-phenylisocyanate. This suggests that these samples were not completely converted to the tricarban-

ilate. These samples must be activated before the reaction. Several activation procedures have been used. These include soaking the sample in water and then solvent exchanging the water with pyridine (108,132), treatment with methylamine (133), and regeneration from DMSO-paraformaldehyde (22). If the derivatization reaction is carried out in DMSO at 70°C, no prior activation is needed.

To recover the cellulose tricarbanilate by precipitation in methanol is common practice. However, this procedure can lead to losses of the methanol-soluble, low-molecular-weight material (107). It was shown that simple evaporation of the reaction mixture gives a material that can be subjected to SEC analysis because the reaction by-products are sufficiently separated from the cellulose tricarbanilate. For further analysis of the cellulose tricarbanilate, such as elemental analysis, these nitrogenous by-products must be removed. An optimized method for recovering the precipitated tricarbanilate has been reported (40).

Researchers (39,41) have investigated the addition of various amines to the carbanilation reaction mixtures to decrease the reaction time needed for derivatization of cellulose, especially the reaction time required for a sample with high molecular weight. In DMSO and DMF, the amines catalyzed the conversion of the phenylisocyanate to its trimer phenylisocyanurate. In addition, several amines actually retarded the carbanilation reaction. Most significant was that the presence of several amines in the DMSO-phenylisocyanate reaction mixture caused depolymerization of the cellulose, especially high-molecular-weight cellulose. In some cases, the depolymerization was severe. All three components (amine, phenylisocyanate, and DMSO) were required for depolymerization to take place.

Other Cellulose Derivatives

In comparison with the nitrate, acetate, and carbanilate, very little is available in the literature that describes the systematic investigation of other cellulose derivatives by SEC analysis. This is surprising, given the number of cellulose derivatives that are available both commercially and experimentally. This may be because these derivatives are often incomplete derivatizations of cellulose, with DS ranging from less than 1 to near 3. Thus, suitable standards are even less readily available than those for the completely derivatized (e.g., DS about 3) cellulose nitrate and tricarbanilate.

Methods for the SEC analysis of ethyl cellulose (21,57); hydroxyethyl cellulose (57,79); cellulose acetate butyrates (80); allylated methylcellulose, triallyl cellulose, and glycidyl cellulose (48); tetrahydropyranyl cellulose, tetrahydropyranyl hydroxyethyl cellulose, and tetrahydropyranyl methylcellulose (14); carboxymethylcellulose (11,91); and cellulose ethers (97) have been described in

the literature. Conditions used for the SEC analysis of these types of derivatives are given in Table 6.

Sec of Underivatized Cellulose

Before the advent of SEC, viscometry was routinely used to determine the DP of cellulose. A number of cellulose solvents have and continue to be used for determining the DP of underivatized cellulose. Thus, it is not surprising that some initial attempts to utilize SEC in the analysis of cellulose and cellulosics centered around the use of cellulose solvents, both to dissolve the cellulose

Table 6 Methods for SEC of Cellulose Derivatives

Cellulose	Porous packing material	Exclusion limits of each column (Å)[a]	Solvent	Temperature (°C)	Flow rate (ml/minute)	Reference
Ethyl	PLgel	Mixed Å	THF	20	1	57
	Styragel[b]	1×10^6 1×10^5 1×10^4 1×10^3	THF[c]	Ambient	1	21
Hydroxyethyl	PLgel	Mixed Å	DMF + LiBr (1% wt/vol)	50	1	57
	TSKgel HN-75F	5×10^5 $>6 \times 10^6$	Water	-	5.2	79
Allylated Methyl Allyl Glycidyl	Styragel	1×10^5 1×10^4 1×10^3 5×10^2 1×10^2	-	-	-	48

[a]10 Å = 1 nm.

[b]Probable material was Styragel.

[c]Methylene chloride was also used as a solvent. Anomalous results were obtained, however, caused by association between residual hydroxyl groups in the ethyl cellulose.

without derivatization and to act as the eluant. Segal (91) reviewed the initial attempts to use cellulose solvents and the difficulties encountered with swelling of the packing materials.

Two cellulose solvents, cadoxen (133) and the more recently discovered *N,N*-dimethylacetamide/LiCl system (134), have shown good promise for use in the SEC analysis of cellulose. The use of these two solvents is described here. In addition, the cellulose solvent systems based on iron-sodium tartrate (8) and DMSO-paraformaldehyde (47,110) have had limited use for the SEC analysis of cellulose.

Cadoxen

Cadoxen, a solution of CdO in aqueous ethylenediamine, is a clear, colorless (which allows detection by RI), and stable solvent for cellulose with DP up to about 10,000. Cellulose can reportedly be dissolved in this solvent for long periods with little to no degradation (135,136). Cadoxen is thought to dissolve cellulose by formation of a complex. The literature contains several reports describing the use of cadoxen for the SEC analysis of cellulose (11,12,17,18,27,85,109).

Several factors have limited the development of cadoxen for SEC analysis of cellulose (12). The high viscosity of solutions of cellulose in cadoxen lead to extensive tailing in the chromatograms as a result of the phenomenon of "viscose fingering." In addition, large quantities of rather expensive cadoxen are required as eluant for each analysis, and cadoxen is difficult and time consuming to prepare.

The major advantage of using cadoxen solutions of cellulose for SEC is that the cellulose need not be derivatized before determination of the SEC. This eliminates the time-consuming step of derivative formation, which in the case of the tricarbanilate derivative requires more than 48 h. In addition, smaller cellulose samples are required and any changes in the cellulose resulting from sample preparation are minimized.

Various packing materials have been used in conjunction with cadoxen solutions of cellulose to obtain SEC. These include polyacrylamide gel (BioGel P-300) (109), agarose gel (BioGel A50m) (11,27), organic gel (Fractogel HW 65 and 75) (85), and carbohydrate-based gel (Sepharose CL-6B) (12). As shown in Table 7, the cadoxen used for eluant can be diluted or replaced altogether, thus lessening the amount of cadoxen required for the complete analysis.

DMAc/LiCI

Several new, often exotic cellulose solvents have been reported since about 1975. Among these is a cellulose solvent consisting of *N,N*-dimethylacetamide (DMAc) and LiCl (134). Cellulose dissolved in DMAc/LiCl is reported to be a

Table 7 Examples of the Use of Cadoxen for SEC of Cellulose

Packing material	Solvent	Temperature (° C)	Flow rate	Reference
BioGel P-300	Cadoxen-water (1:1, vol/vol)	10	-	109
BioGel A-50 m	Cadoxen	-	4-5 ml/h	11
	Cadoxen	25	7.5 g/h	27
Fractogel				
HW-65 HW-75 HW-65 and HW-75	Cadoxen	15	1 ml/minute	85
Fractionated Sepharose CL-6B	0.5 N NaOH	Ambient	6 ml/h	12

true solution, to be stable over a long time, and to exhibit no degradation in chain length during the dissolution process (35,134,137). Also, this cellulose solvent has been reported as reasonably inert with respect to SEC packing materials (51).

As was true for cadoxen, the use of DMAc/LiCl for the SEC analysis of cellulose (35,51,95,96) is less time consuming and nondegradative. Table 8 lists typical conditions for the SEC of cellulose.

The preparation of cellulose solutions suitable for SEC analysis in DMAc/LiCl is reasonably straightforward (35,51). The dissolution process requires preswelling of the cellulose in water or its activation in refluxing DMAc. Evidently, it is important that the pH of the cellulose be neutral initially (51); otherwise, considerable degradation may occur before the dissolution process is complete.

Calibration and Calibration Standards

As previously discussed, cellulose is a polydisperse, naturally occurring polymer. Monodisperse standards of different molecular weights are not available, especially on a commercial basis. Because SEC analysis is not an absolute method, calibration with materials of known molecular weight is required before experimental data can be expressed quantitatively. Thus, the lack of monodisperse standards constitutes a major difficulty in carrying out the SEC analysis of cellulose. When the only interest is in qualitatively evaluating changes that occur during a given process or reaction, the lack of proper standards is less of a problem.

Table 8 Typical Methods for SEC of Cellulose in DMAc/0.5% LiCl Solvent

Porous packing material	Exclusion limits of each column (Å)[a]	Temperature (°C)	Flow rate (ml/minute)	References
Ultrastyragel	1×10^5	80	1	35
	1×10^4			
	1×10^3			
	1×10^6	80	—	95, 96
	1×10^5			
	1×10^4			
	1×10^3			
Styragel	1×10^6	30–45	1	51
	1×10^5			
	1×10^4			
	1×10^3			

[a]10 Å = 1 nm.

Basically, three calibration methods have been used for the SEC analysis of cellulose. These three methods, which by no means are unique to the SEC analysis of cellulose, include (1) the peak position method (i.e., DP versus elution volume), (2) the universal calibration method, and (3) the LALLS method.

Cellulose standards for use in calibration, especially by the peak position method, can be obtained by a number of methods. The most straightforward method is to utilize a series of celluloses from a variety of sources (e.g., pulps, yarns, and avicel) that have a wide range of DPs (15,26). In a second method, celluloses of different DPs are obtained from a single cellulosic source (e.g., cotton) by controlled, acid-catalyzed depolymerization (93). Another method uses fractional precipitation of the appropriate cellulose derivative (10,29). Once obtained, the DP of each cellulose standard can be determined by osmotic and viscometric methods. The SEC calibration curve obtained with these standards is then adjusted numerically until a best fit with the DPs of each of the standards is obtained (93).

Dextran samples of a narrow molecular weight distribution have been used as calibration standards (100). However, dextran is a polymer composed of 1,6-linked glucose units. The glucopyranose rings in this polymer are connected through three bonds, as opposed to the two bonds found in cellulose. Thus, dextran is more flexible than cellulose and, as such, may not accurately represent the hydrodynamic behavior of cellulose.

For the universal calibration technique, commercially available, essentially monodisperse polystyrene of known molecular weight has been used

(28,29,38,81,99,108). As described in Chapter 1, a calibration curve constructed for polystyrene can be used to determine the molecular weight of a second polymer if the Mark-Houwink coefficients of the two polymers in the solvent used for SEC analysis are known. The Mark-Houwink coefficients for cellulose in a variety of solvents have been tabulated (138).

An interesting variation on the universal calibration technique has been reported for determining the molecular weight distribution of underivatized cellulose (95). A commercial viscometer detector coupled with a RI detector can be used to monitor viscosity and concentration simultaneously as polymer elutes from the SEC system (see Chapter 4). The simultaneous determination of viscosity and concentration allows the intrinsic viscosity to be determined as a function of retention volume. Polystyrene fractions of known molecular weight are used to establish a calibration curve that relates hydrodynamic volume (i.e., intrinsic viscosity × molecular weight) and retention volume. Because in the absence of non-size exclusion effects a plot of hydrodynamic volume versus retention volume for all types of polymers using a given column system should fall on the same line, the molecular weight of cellulose eluting at a given retention time can be determined from the intrinsic viscosity measured at that retention volume.

As discussed in Chapter 4, calibration by the LALLS method does not require primary standards. This method has proven very useful as a calibration method for the SEC analysis of cellulose (22,23,28,29,34,36,40,52–54,105).

Conclusion

The size exclusion chromatography of cellulose and cellulosics had its infancy in the early 1960s (91). Although cellulose is insoluble in water and other common organic solvents, methods were devised that allowed SEC analysis of cellulose. Some initial attempts used “cellulose solvent” system to dissolve the cellulose and to act as the eluant. These attempts were frustrated by incompatabilities between the gels used for packing the columns and the cellulose solvents.

The use of cellulose derivatives as the basis for analysis was seen as a means of overcoming the difficulties in using cellulose solvents. Early on, SEC analysis of cellulose as its trinitrate ester became the preferred method. This method continues to be used with success. Although the tricarbanilate derivative was tried in some initial experiments, only recently has this cellulose derivative been extensively used because of several reported advantages over the trinitrate derivative.

The discovery of novel cellulose solvent systems has led to renewed interest in the "direct" SEC analysis of cellulose and cellulosics. It appears that this method will eventually prove to be the method of choice.

As is true of other polymeric substances, the lack of commercially available, monodiperse cellulose standards has also impeded the routine analysis of cellulose by SEC. Newer detection methods, such as LALLS and viscometer detectors, have and will continue to change this by offering "in-line" methods for determining the molecular weight of samples as they elute.

Cellulose is an important renewable, raw material. SEC analysis provides a rapid means for determining the molecular weight distribution of cellulose and its derivatives. As illustrated in the extant literature, SEC will be important in future studies of cellulose structure and its conversion into useful products.

References

1. V. P. Karlivan, In: *CHEMRAWN I: Future Sources of Organic Raw Materials,* L.E. St.-Pierre and G.R. Brown (eds.), Pergamon Press, New York, 1980.

2. R.D. Preston, *The Physical Biology of Plant Cell Walls,* Chapman and Hall, London, 1974.

3. D. Fengel and G. Wegener, *Wood: Chemistry,* Ultrastructure, *Reactions,* Walter de Gruyter, New York, 1984.

4. D.N.-S. Hon, In: *Adhesives from Renewable Resources,* R.W. Hemingway, A.H. Conner, and S.J. Branham (eds.), ACS Symposium Series 385, Am. Chem. Soc., Washington, D.C., 1989.

5. I.S. Goldstein, In: *Organic Chemicals from Biomass,* I.S. Goldstein (ed.), CRC Press, Boca Raton, Florida, 1981.

6. J.F. Harris, A.J. Baker, A.H. Conner, J.L. Minor, R.C. Pettersen, R.W. Scott, E.L. Springer, T.H. Wegner, and J.I. Zerbe, Gen. Tech. Rep. FPL-45, USDA Forest Service, Forest Products Laboratory, Madison, Wisconsin, 1985.

7. S.A. Leeper, T.E. Ward, and G.F. Andrews, Rep. No. EGG-BG-9033, USDOE, Idaho National Engineering Laboratory, 1991.

8. G. Agg and R.W. Yorke, Tappi Conference Papers. 5th International Dissolving Pulps, 1980, p. 190.

9. W.J. Alexander and T.E. Muller, *J. Polym. Sci.,* (Part C), 87–101 (1971).

10. W.J. Alexander and T.E. Muller, *Separ. Sci.,* 6, 47–71 (1971).

11. K.E. Almin, K.E. Eriksson, and B.A. Pettersson, *J. Appl. Polym. Sci., 16,* 2583–2593 (1972).

12. Y.T. Bao, A. Bose, M.R. Ladisch, and G.T. Tsao, *J. Appl. Polym. Sci., 25,* 263–275 (1980).

13. N.R. Bertoniere, S.P. Rowland, and M. Kabir, *Text. Res. J., 54,* 434–437 (1984).

14. S.S. Bhattacharjee and A.S. Perlin. In: *Modified Cellulosics,* R.M. Rowell and R.A. Young (eds.), Academic Press, New York, 1978, pp. 285–301.

15. F.A. Blouin, L.F. Martin, and S.P. Rowland, *Text. Res. J.*, *40*, 809–813 (1970).

16. F.A. Blouin, L.F. Martin, and S.P. Rowland, *Text. Res. J., 40,* 959–964 (1970).

17. O. Bobleter, and W. Schwald, *Papier, 39,* 437–441 (1985).

18. A. Bose, *Diss. Abstr. Int. B, 41,* 3111 (1981).

19. A. Broido, and H. Yow, *J. Appl. Polym. Sci., 21,* 1667 (1977).

20. A. Broido, and H. Yow, *J. Appl. Polym. Sci., 21,* 1677 (1977).

21. A.P. Brookshaw, D.E. Hillman, and J.I. Paul, *Br. Polym. J. 5,* 229–239 (1973).

22. J.J. Cael, D.J. Cietek, and F.J. Kolpak, *J. Appl. Polym. Sci. 37,* 509–529 (1983).

23. J.J. Cael, R.E. Cannon, and A.O. Diggs, *5th Int. Dissolving Pulps Conf.,* (Conf. Paper), 216–223 (1980).

24. M. Chang, *Tappi, 55,* 1253–1257 (1972).

25. M. Chang, *Tappi, 56,* 173–174 (1973).

26. M. Chang, T.C. Pound, and R.S.J. Manley, *J. Polym. Sci., 11,* 399–411 (1973).

27. J.D. Cosgrove, B.C. Head, T.J. Lewis, S.G. Graham, and J.O. Warwicker. In: *Cellulose and Its Derivatives: Chemistry, Biochemistry and Applications,* J.F. Kennedy, G.O. Phillips, D.J. Wedlock, and P.A. Williams (eds.), Horwood, Chichester, UK, 1985, pp. 143–152.

28. A.F. Cunningham, C. Heathcote, D.E. Hillman, and J.I. Paul. In: *Liquid Chromatography of Polymers and Related Materials II,* J. Cazes and X. Delmare (eds.), Marcel Dekker, New York, 1980, pp. 173–196.

29. J. Danhelka, I. Kossler, and V. Bohackova, *J. Polym. Sci., 14,* 287–298 (1976).

30. J. Danhelka, M. Netopilik, and M. Bohdanecky, *J. Polym. Sci.* (Part B), *25,* 1801–1815 (1987).

31. J. Dyer, *ACS Symp. Ser., 10,* 181–194 (1975).

32. J. Dyer and L.H. Phifer, *J. Polym. Sci.* (Part C), 103–119 (1971).

33. J. Dyer and L.H. Phifer, *Separ. Sci., 6,* 89–99 (1971).

34. W.D. Eigner, J. Billiani, and A. Huber, *Papier 41,* 680–684 (1987).

35. J.L. Ekmanis, *American Laboratory News* (January/February), 10–11 (1987).

36. A.E. El Ashmawy, J. Danhelka, and I. Kossler, *Svensk Papperstidning, 77,* 603–608 (1974).

37. T.E. Eremeeva, T.O. Bykova, and V.S. Gromov, *Khim. Drev.,* 108–109 (1988).

38. T.E. Eremeeva, T.O. Bykova, and V.S. Gromov, *J. Chromatogr., 522,* 67–75 (1990).

39. R. Evans, R.H. Wearne, and A.F.A. Wallis, *J. Appl. Polym. Sci., 42,* 813–820 (1991).

40. R. Evans, R.H. Wearne, and A.F.A. Wallis, *J. Appl. Polym. Sci., 37,* 3291–3303 (1989).

41. R. Evans, R.H. Wearne, and A.F.A. Wallis, *J. Appl. Polym. Sci., 42*, 821–827 (1991).

42. K. Fischer, W. Picker, and J. Fritz, *Cellul. Chem. Technol., 23,* 415–428 (1989).

43. H. Goetz, H. Elgass, and L. Huber, *J. Chromatogr., 349,* 357–367 (1985).

44. K. Hamacher, G. Schmid, H. Sahm, and C. Wandrey, *J. Chromatogr, 319,* 311–318 (1985).

45. H. Hatakeyama and T. Hatakeyama, *Mokuzai. Gakkaishi, 24,* 228 (1977).

46. C. Holt, W. Mackie, and D.B. Sellen, *Polymer, 19,* 1421 (1978).

47. D. Kato and A. Takahashi, *Proceedings of TAPPI Int. Dissolving Pulps Conf.* (Geneva), pp. 67–70 (March 24–27, 1987).

48. T. Kondo, A. Ishizu, and J. Nakano, *J. Appl. Polymer Sci., 37,* 3003–3009 (1989).

49. L.N. Konkina, V.D. Ermakova, N.G. Taganov, S.A. Osipov, V.A. Morozov, and S.G. Entelis, *Vysokomol. Soedin.,* Ser. B31, 182–185 (1989).

50. Y. Kusama, E. Kageyama, M. Shimada, and Y. Nakamura, *J. Appl. Polym. Sci., 20,* 1679 (1976).

51. A.L. Kvernheim and E. Lystad, *Acta Chem. Scand., 43,* 209–211 (1989).

52. J.-M. Lauriol, J. Comtat, P. Froment, F. Pla, and A. Robert, *Holzforschung, 41,* 165–169 (1987).

53. J.M. Lauriol, P. Froment, F. Pla, and A. Robert, *Holzforschung, 41,* 215–224 (1987).

54. J.M. Lauriol, P. Froment, F. Pla, and A. Robert, *Holzforschung,* 41, 109–113 (1987).

55. M.A. Lazareva, V.I. Zakharov, and A.K. Ivanov, *Khim. Drev.,* 107–110 (1989).

56. J.B.F. Lloyd, *Anal. Chem., 56,* 1907–1912 (1984).

57. L.L. Lloyd, F.P. Warner, J.F. Kennedy, and C.A. White. In: *Wood and Cellulosics,* J.F. Kennedy, G.O. Phillips, and P.A. Williams (eds.), Wiley and Sons, New York, pp. 203–210 (1987).

58. L.L. Lloyd, C.A. White, A.P. Brookes, J.F. Kennedy, and F.P. Warner, *Br. Polym. J., 19,* 313–318 (1987).

59. F. Mahmud and E. Catterall, *ACS Symp. Series, 245,* 365–375 (1984).

60. R.S.J. Manley, *Text. Res. J., 44,* 401–402 (1974).

61. R.S.J. Manley, *Appl. Polym. Sci., 28,* 693 (1976).

62. R.S. John Manley, *J. Polym. Sci., 11,* 2303–2306 (1973).

63. R.S. John Manley, *J. Polym. Sci., 12,* 1347–1354 (1974).

64. L.F. Martin, N.R. Bertoniere, F.A. Blouin, and M.A.F. Brannan, *Tex. Res. J., 40,* 8–14 (1970).

65. M. Marx-Figini and O. Soubelet, *Polym. Bull.* (Berlin), *6,* 501–508 (1982).

66. M. Marx-Figini and O. Soubelet, *Polym. Bull.* (Berlin), *11,* 281–286 (1984).

67. G. Meyerhoff, *J. Chromatogr. Sci., 9,* 596 (1971).

68. G. Meyerhoff, *Makromol. Chem., 134,* 129 (1970).

69. K. Ogura, *Sen. I. To. Kogyo, 5,* 9–13 (1972).

70. P.A. Okunev, S.P. Dorofeev, K.S. Nikolskii, T.M. Kubaenko, E.S. Kulikova, and R.B. Tsokolaev, *Khim. Volokna* (1971).

71. P.A. Okunev, Z.A. Dorofeev, Z.A. Kudryavtseva, and O.G. Tarakanov, *Vysokomol. Soedin., Ser.* A, *13,* 1680–1683 (1971).

72. P.A. Okunev, O.V. Golubeva, and S.P. Dorofeev, *Sb. Nauch. Tr. Ivanov Energ. Inst., 14*, 236–241 (1972).

73. A.C. Ouano, E.M. Barrall, and A. Broido. *Advan. Chem. Ser., 125,* 187–193 (1973).

74. L.H. Phifer and J. Dyer, *Separ. Sci., 6,* 73–88 (1971).

75. T. Rantanen and J. Sundquist, *Tappi J., 70,* 109–111 (1987).

76. T. Rantanen, P. Farm, and J. Sundquist, *Paperi ja Puu-Papper och Tra, 68,* 634–641 (1986).

77. M. Rinaudo and J.P. Merle. *Eur. Polym. J., 6,* 41–50 (1970).

78. A. Rudin and H.L.W. Hoegy, *J. Polym. Sci.,* Part A-1 *10,* 217–235 (1972).

79. A.M. Safieddine and R.D. Hester, *Polym. Prepr. 30,* 369–370 (1989).

80. C.W. Saunders, Thesis, Virginia Polytech. Inst. and State Univ. Eng., 1990.

81. L.R. Schroeder and F.C. Haigh, *Tappi 62,* 103–105 (1979).

82. J. Schurz and J. Haas, *Cellulose Chem. Technol., 4,* 633 (1970).

83. J. Schurz, J. Haas, and H. Kraessig, *Cellulose Chem. Technol., 5,* 269–284 (1971).

84. J. Schurz, J. Haas, and K. Mueller, *Papier* (Darmstadt), *24,* 691–698 (1970).

85. W. Schwald and O. Bobleter, *J. Appl. Polym. Sci., 35,* 1937–1944 (1988).

86. L. Segal, J.D. Timpa, and J.I. Wadsworth, *J. Polym. Sci.* (Part A-1), *8,* 25–35 (1970).

87. L. Segal, J.D. Timpa, and J.I. Wadsworth, *J. Polym. Sci.* (Part A-1), *8,* 3577 (1970).

88. L. Segal and J.D. Timpa, *Textile Chem. Color, 4,* 66 (1972).

89. L. Segal and J.D. Timpa, *Textile Res. J., 43,* 468 (1973).

90. L. Segal, J.I. Wadsworth, and J.D. Timpa, *Tappi 56,* 172–173 (1973).

91. L. Segal. In: *Advances in Chromatography,* J.C. Giddings, E. Grushka, R.A. Keller, and J. Cazes (eds.), Marcel Dekker, New York, Vol. 12, 1975, pp. 31–59.

92. J. Sjostrom and B. Holmbom, *J. Chromatogr., 411,* 363–370 (1987).

93. O. Soubelet, M.A. Presta, and M. Marx-Figini, *Angew. Makromol. Chem., 175,* 117–128 (1990).

94. L.J. Tanghe, W.J. Rebel, and R.J. Brewer, *J. Polym. Sci.* (Part A-1), *8,* 2935–2947 (1970).

95. J.D. Timpa, *J. Agr. Food Chem., 39,* 270–275 (1991).

96. J.D. Timpa and H.H. Ramey, Jr., *Text. Res. J., 59,* 661–664 (1989).

97. N. Usman, *Polym. Paint Colour J., 177,* 494–495 (1987)

98. A.I. Usov. Sb. Tr., Methody Issled. *Tsellyulozy* (Riga) 205–211 (1981).

99. L. Valtasaari and K. Saarela, *Paperi ja Puu, 57,* 5–10 (1975).

100. M. Van Lancker, *Ann. Sci. Text. Belg., 22,* 169–184 (1974).

101. M. Van Lancker and E. Veirman. *Ann. Sci. Text. Belg., 20,* 21–38 (1972).

102. M. Van Lancker and E. Veirman, *Ann. Sci. Text. Belg., 20,* 98–120 (1972).

103. J.I. Wadsworth, L. Segal, and J.D. Timpa, *Polym. Prepr., 12,* 854–858 (1971).

104. J.I. Wadsworth, L. Segal, and J.D. Timpa, *Advan. Chem. Ser., 125,* 178–186 (1971).

105. A. Wirsen, *Makromol. Chem., 189,* 833–843 (1988).

106. V. Wollny and T. Krause, *Papier, 42,* 117–120 (1988).

107. B.F. Wood, A.H. Conner, and C.G. Hill, *J. Appl. Polym. Sci., 32,* 3703–3712 (1986).

108. B.F. Wood, A.H. Conner, and C.G. Hill, *J. Appl. Polym. Sci., 37,* 1373–1394 (1989).

109. K.-E. Eriksson, F. Johanson, and B. Pettersson. *Sven. Papperstidn. 70,* 610 (1967).

110. J.L. Minor. *J. Liq. Chromatogr.,* 2(3), 309–318 (1979).

111. R.A. Young and R.M. Rowell, eds., *Cellulose: Structure, Modification and Hydrolysis,* Wiley-Interscience, New York, 1986.

112. J.F. Kennedy, G.O. Phillips, and P.A. Williams (eds), *Wood and Cellulosics: Industrial Utilization, Biotechnology, Structure, and Properties,* Halsted Press, New York, 1987.

113. R.M. Rowell and R.A. Young (eds.) *Modified Cellulosics,* Academic Press, New York, 1978.

114. J.F. Kennedy, G.O. Phillips, D.J. Wedlock, and P.A. Williams (eds.), *Cellulose and Its Derivatives: Chemistry, Biochemistry and Applications,* Halsted Press, New York, 1985.

115. R.D. Brown, Jr. and L. Jurasek (eds.), *Hydrolysis of Cellulose: Mechanisms of Enzymatic and Acid Catalysis,* Adv. Chem. Ser. 181, American Chemical Society, Washington, D.C., 1979.

116. J.C. Arthur, Jr. *Cellulose Chemistry and Technology,* ACS Symp. Ser. 48, American Chemical Society, Washington, D.C., 1977.

117. A. Hebeish and J.T. Guthrie, *The Chemistry and Technology of Cellulosic Copolymers,* Springer-Verlag, New York, 1981.

118. T.P. Nevell and S.H. Zeronian (eds.), *Cellulose Chemistry and its Applications,* Halsted Press, New York, 1985.

119. A.F. Turbak, D.F. Durso, O.A. Battista, H.I. Bolker, J.R. Colvin, N. Eastman, T.N. Kleinert, H. Krassig, and R. St. J. Manley. In:*Kirk-Othmer Encyclopedia of Chemical Technology*, 3rd Edition, Vol. 5, 1979, p. 70.

120. M.L. Rollins, A.M. Cannizzaro, and W.R. Goynes. In: *Instrumental Analysis of Cotton Cellulose and Modified Cotton Cellulose,* R.T. O'Connor (ed.), Marcel Dekker, New York, 1972.

121. V.W. Tripp and C. Conrad. In: *Instrumental Analysis of Cotton Cellulose and Modified Cotton Cellulose*, R.T. O'Connor (ed.), Marcel Dekker, New York, 1972.

122. J.W.S. Hearle. In: *Fibre Structure,* J.W.S. Hearle and R.H. Peters (eds.), Butter-worth, London, 1963.

123. F. Shafizadeh and G.D. McGinnis, *Adv. Carbohydr. Chem. Biochem., 26,* 297 (1971).

124. S.G. Shenouda. In: *Applied Fibre Science,* Vol. 3, F. Happey (ed.), Academic Press, New York, 1979.

125. S.P. Rowland and N.R. Bertoniere. In: *Cellulose Chemistry and Its Applications,* T.P. Nevell and S.H. Zeronian (eds.), Halsted Press, New York, 1985.

126. G. Jayme. In: *Cellulose and Cellulose Derivatives,* N.M. Bikales and L. Segal (eds.), Interscience, New York, 1971.

127. B. Philipp, H. Schleicher, and W. Wagenknecht, *Chemtech, 7,* 702 (1977).

128. A.F. Turbak, R.B. Hammer, R.E. Davies, and H.L. Hergert, *Chemtech, 10,* 51 (1980).

129. D.C. Johnson. In: *Cellulose Chemistry and Its Applications,* T.P. Nevell and S.H. Zeronian (eds.), Halsted Press, New York, 1985.

130. W.J. Alexander and R.L. Mitchell, *Anal. Chem. 21*, 1497 (1949).

131. R.J. Brewer, L.J. Tanghe, S. Bailey, and J.T. Burr, *J. Polym. Sci.* (A-1), *6*, 1697 (1968).

132. J. Sundquist and T. Rantanen, *Pap. Puu, 65,* 733 (1983).

133. G. Jayme and K. Neuschaffer, *Makromol. Chem., 23,* 71 (1957).

134. C.L. McCormick, P.A. Callais, and B.H. Hutchinson, *Macromol. 18,* 2394 (1985).

135. G. Jayme and F. Lang. In: *Methods in Carbohydrate Chemistry,* Vol. III, R.L. Whistler (ed.), Academic Press, New York, 1963.

136. G. Jayme. In: *High Polymers,* Vol. V, Interscience, New York, 1971.

137. A.B. Turbak. In: *Agricultural Residues,* E.H. Soltes (ed.), Academic Press, New York, 1983.

138. J. Brandrup and E.H. Immergut (eds.), *Polym. Handb.,* 2nd Edition, Wiley, New York, 1975.

14
Size Exclusion Chromatography of Lignin Derivatives

Michael E. Himmel National Renewable Energy Laboratory, Golden, Colorado

Juraj Mlynár* and Simo Sarkanen University of Minnesota, St. Paul, Minnesota

Introduction

Lignins

Among biopolymers, lignins are second only to cellulose in abundance. As cell wall components in all vascular plants and woody tissues, they embody significant structural variations with species, cell type, and subcellular location (1–3). Lignins are formed by enzyme-catalyzed dehydrogenative polymerization of monolignols that differ only in the methoxyl substituents around the aromatic ring. There are three such precursors, *p*-hydroxycinnamyl (*p*-coumaryl) alcohol, 4-hydroxy-3-methoxycinnamyl (coniferyl) alcohol, and 4-hydroxy-3,5-dimethoxycinnamyl (sinapyl) alcohol; these may be oxidatively coupled to form as many as 10 different interunit linkages when being incorporated into macromolecular lignin structures (4). Nevertheless approximately half of the resulting linkages are the same type, that is, β-*O*-4-alkyl aryl ethers (4). The most

This chapter is Paper No. 20,780 of the Scientific Journal Series of the Minnesota Agricultural Experiment Station, funded through Minnesota Agricultural Experiment Station Project No. 43–68, supported by Hatch funds.

**Permanent affiliation:* Institute of Chemistry, Slovak Academy of Sciences, Bratislava, Slovak Republic.

basic difference between lignins from different tree species is in their monomer composition: lignins in gymnosperms (softwoods) are usually derived primarily from coniferyl alcohol, and those in angiosperm dicotyledons (hardwoods) contain guaiacyl and syringyl units—from coniferyl and sinapyl alcohol, respectively—in roughly equal proportions.

Lignins usually comprise between 25 and 30% wt/wt of woody tissues in hardwoods and softwoods, respectively. Unfortunately, they cannot be removed from the constituent cell walls without concomitant degradation. In this connection difficulties are invariably encountered because the majority of interunit linkages in lignin macromolecules are relatively stable, much more so than those in most other biopolymers. Thus isolated lignin preparations differ from one another in the extent to which they have been modified with respect to the native macromolecules.

For example, extraction of finely divided wood meal with aqueous dioxane furnishes a partial yield of a lignin sample that is relatively little changed from the original biopolymer except in its average degree of polymerization. On the other hand, more complete removal of lignin from wood cell walls requires either acid or basic reagents, whereupon much more extensive modification takes place. Under such circumstances lignin depolymerization may be partly counteracted by the formation of new covalent bonds between previously independent monomer residues; cleavage of, and structural changes in, macromolecular lignin chains may be complicated by repolymerization of some low-molecular-weight components formed during the degradation of the native biopolymer (5,6). This is typically thought to be the case during the industrial delignification of wood chips to produce cellulosic fibers for making paper.

Size Exclusion Chromatography of Lignin Preparations

The most fundamental property of any isolated lignin preparation is of course its molecular weight distribution. The size exclusion chromatographic (SEC) conditions adopted for determining the molecular weight distributions of lignins should be those under which the interactions of solute with solute (association), solute with solvent (solvation), and solute with column packing material (adsorption) are minimized, but it is difficult to discern *a priori* when such circumstances prevail. Consequently, absolute molecular weight calibrations of the size exclusion chromatographic elution profiles are essential for the reliable determination of molecular weight distributions of isolated lignin samples. Association between the individual molecular components in many lignin derivatives is very difficult to defeat completely (7–12), and there is the ever present danger that adsorptive interactions with column packing materials may strongly affect the true molecular weight calibration curve for the sample under investigation (see, for example, Reference 13).

The solvents or solutions being employed as mobile phases should uphold moderate to high solubility for all the species comprising the lignin preparation being studied, and at the same time they should be compatible with optimum column performance. It was reported over 40 years ago that lignin solubility is generally a maximum when the Hildebrand solubility parameter of the solvent or solvent mixture approaches a value of around 11 (14), but this claim has not been the subject of subsequent confirmation or dispute. Nevertheless, dioxane and tetrahydrofuran (THF), which exact little deterioration of polystyrene-divinylbenzene high-performance liquid chromatographic (HPLC) columns (15), typically confer only sparing solubility upon the higher molecular weight species in underivatized lignin samples. Conversely, dimethylformamide (DMF) and dimethylsulfoxide (DMSO), in which most lignin preparations are much more soluble, tend to elicit poorer performance from polystyrene-divinylbenzene columns.

Even careful efforts dedicated to determining reliable molecular weight distributions of lignin preparations may yield disappointing results. The difficulties are aptly illustrated by work published in 1983 (16), in which elution in THF through a polystyrene-divinylbenzene column was adopted for characterizing a softwood kraft lignin (produced industrially by treating wood chips at elevated temperature with an aqueous solution containing NaOH and Na_2S). Absolute molecular weight calibration of the elution profile was accomplished with a KMX-6 low-angle laser light-scattering photometer (LDC Analytical) that was equipped with a narrow band-pass interference filter and connected in series with a differential refractometer to the column outlet. The resulting calibration curve differed from that for polystyrenes by a factor ranging between 5 and 10 at molecular weights of 70,000 and 1100, respectively, for the lignin species. The $\overline{M}_w$ of the kraft lignin calculated from the elution profile was 10,650; the corresponding value determined by light scattering from the sample as a whole was 17,300. The discrepancy may have been caused by associative interactions between the kraft lignin components: the second virial coefficient for the complete sample in THF was negative in magnitude. However, the $\overline{M}_n$ calculated from the elution profile was 6050 but the corresponding value measured by vapor pressure osmometry for the sample as a whole was only 1750. The reason for the pronounced difference between the $\overline{M}_n$ determinations is not clear, but it would have been helpful if the percent recovery of the kraft lignin sample from the column had been reported.

The dangers of carrying out size exclusion chromatographic analyses of lignin samples without the benefit of absolute molecular weight determinations can be quite serious. One such example is illustrated here for a lignin fraction purified from a lignin derivative produced by Repap Technologies (Valley Forge, PA). The profile described by eluting the sample with THF through Polymer Standards Service (PSS) polystyrene-divinylbenzene 10^4 and 10^2 Å pore size columns in series is shown in Figure 1. The (633 nm) light scattered by the

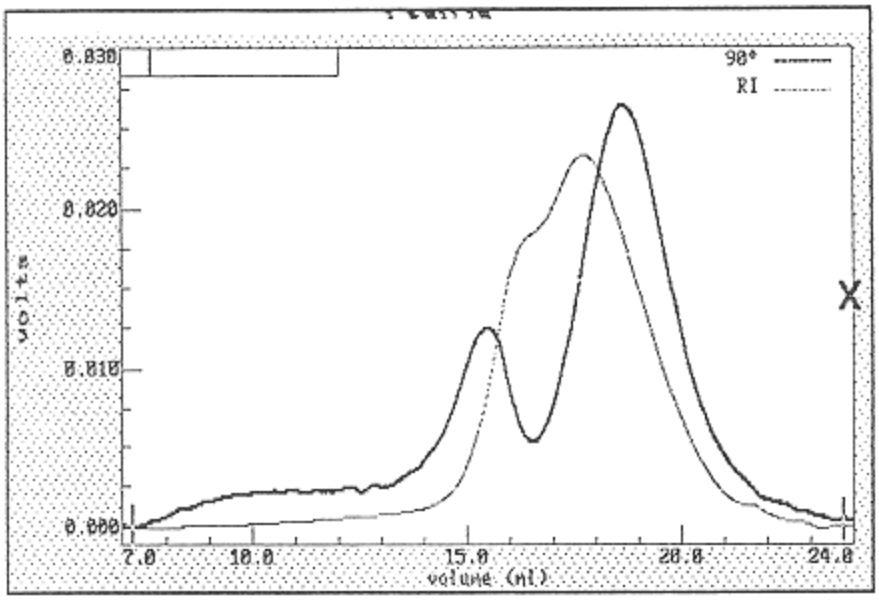

Figure 1
Purified fraction, in THF, from lignin derivative produced by Repap Technologies. Elution profile from PSS polystyrene-divinylbenzene 10^4 and 10^2 Å pore size columns in series monitored with refractometer. Intensity (proportional to voltage) of 633 nm light scattered at 90° measured by Dawn F detector fitted with 10 nm band-pass interference filters. (Data provided by Wyatt Technology Corp.)

eluted species was measured with a Dawn F detector (Wyatt Technology Corp.) fitted with 10 nm band-pass interference filters; the intensity scattered at 90° (proportional to the product of solute molecular weight and concentration) is overlaid on the plot of refractive index versus elution volume in Figure 1. The profile itself consists of three broad peaks, the second and third of which overlap with one another. The absolute molecular weight calibration curve for these features is displayed in Figure 2.

It can be seen that the molecular weights of the lignin species decrease with increasing elution volume in the first two peaks, but a substantial increase in molecular weight with elution volume between 16.5 and 19 ml is evident in the third peak, which represents the majority of the lignin sample. Provided that errors from any possible fluorescence were obviated by the interference filters in the light-scattering detector, reversible adsorption of the lignin species in the third peak to the column packing material presumably masks the size exclusion chromatographic behavior prevailing in the first two peaks. Yet, visually there

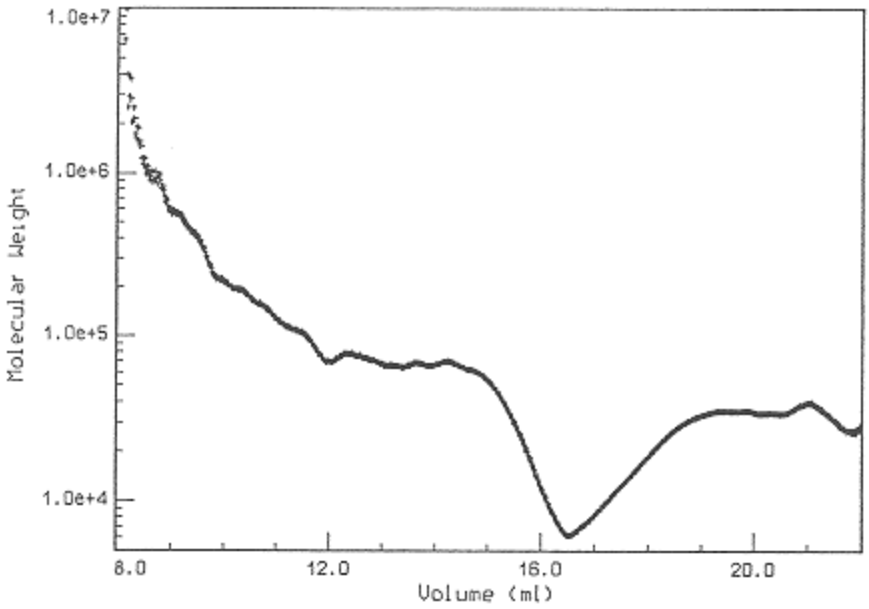

Figure 2
Semilogarithmic plot of weight-average molecular weight versus elution volume for purified lignin derivative fraction produced by Repap Technologies upon elution from PSS polystyrene-divinylbenzene 10^4 and 10^2 Å pore size columns in THF.
(Results furnished by Wyatt Technology Corp.)

is no indication (from pronounced tailing, for example) that the predominant mechanism of chromatographic separation may differ from one region of the profile to another. Certainly column calibration with paucidisperse synthetic polymer standards (such as polystyrenes) would give no hint of the problem.

In contrast, the molecular weight distributions of kraft and Organosolv lignin preparations manifested by elution in aqueous alkaline solution through cross-linked dextran (Sephadex G series) gels packed in open columns are remarkably reliable: a high degree of reproducibility is upheld in the corresponding ultracentrifuge sedimentation equilibrium calibrations of paucidisperse fractions selected from the elution profiles (7,9–11). Under these circumstances, adsorptive interactions between solute species and the column packing material are completely overcome and the lignin samples are totally recovered from the columns. Strong interactions between the solute components persist, however, and the degree of association characterizing the lignin preparation depends upon the conditions of incubation in solution before introducing the sample onto the column (7,9,11,12). Indeed, similar considerations apply to size exclusion chro-

matography of lignins generally. Unfortunately, the Sephadex G/aqueous alkaline solution system suffers from two drawbacks: resolution is inherently lower than that in typical high-performance SEC (HPSEC) columns, and the packing material slowly decomposes on exposure to aqueous 0.10 *M* NaOH (8), so that reproducible column performance is limited to about 3 months at ambient temperatures.

There have, of course, been numerous studies of the molecular weight distributions of lignin preparations by HPSEC using paucidisperse synthetic polymer standards for calibration purposes. These have employed pure organic solvents (12,16–20) and organic solvent mixtures (21,22) as mobile phases for analyzing both underivatized (12,20,22) and acetylated (16–21) lignin samples. Generally speaking, the distributions of species eluted from polystyrene-divinylbenzene columns in DMF and DMSO are multimodal and extend to very high apparent molecular weights, whether or not the lignins are acetylated (12,21). Thus it seems likely that strong noncovalent interactions between the lignin components engender the formation of associated macromolecular complexes under these conditions. On the other hand, the corresponding profiles both in DMF containing dissolved electrolytes (0.10 *M* LiCl or LiBr) and in THF are displaced to higher elution volumes (12,21). Unfortunately, no systematic absolute molecular weight measurements have been undertaken to determine whether such effects arise from an attenuation in the interactions between solute components or an increase in reversible adsorption with the column packing material. It could be worth mentioning that the recovery of acetylated lignin preparations from the polystyrene-divinylbenzene columns is incomplete in both THF and DMF (with or without dissolved electrolyte), but, however that may be, the elution volumes for polystyrene fractions increase substantially with mobile-phase polarity (21). Consequently more than one factor is responsible for the observed changes in elution behavior.

The commercial availability of a flow-through differential viscosimetric detector (Model 100; Viscotek Corp.) allows the determination of molecular weights for unknown polymers using the principle of universal calibration (23–28). The approach is inherently different from light scattering, which employs Debye theory, in the elaboration developed by Zimm and Stockmayer (29), to calculate $\overline{M}_w$ (with the low-angle KMX-6 or multiangle Dawn F photometer) and *z*-average radius of gyration (with the multiangle Dawn F instrument only). The determination of molecular weight distributions for different polymer samples by light-scattering measurements from size exclusion chromatographic elution profiles has been applied in a broad range of contexts (30–33). A critical parameter for calculating $\overline{M}_w$ from scattered light intensities is the differential refractive index *dn/dc* of the macromolecules in the mobile phase being used: its magnitude does not remain constant for polymers that exhibit heterogeneity with respect to molecular weight. As far as lignin derivatives are concerned,

however, the most important concern involves poor signal-to-noise ratios in scattered light intensities from components possessing molecular weights below 10,000. Moreover, it is imperative that errors arising from fluorescence be eliminated with a narrow band-pass interference filter even when the incident light is of long wavelength (633 nm from a He-Ne laser).

The rest of the chapter is dedicated to illustrating how the molecular weight distributions of lignin preparations can be determined by size exclusion chromatography with the viscosimetric detector and by ultracentrifuge sedimentation equilibrium analysis. Thus, later, four different acetylated lignin preparations (34,35) from the hardwood aspen *(Populus tremuloides)* are compared by conventional SEC (using paucidisperse "standard" polymer fractions), universal calibration of their size exclusion chromatographic elution profiles (using the Viscotek Model 100 differential viscometer), and the sedimentation equilibrium behavior of the complete samples (using the Beckman Model E analytical ultracentrifuge). Subsequently, the molecular weight distribution of an underivatized kraft lignin preparation from the softwood Jack pine *(Pinus banksiana)* in aqueous alkaline solution is compared with that of an acetylated methylated derivative in DMF. Here absolute molecular weight calibration is accomplished by employing the Beckman Optima XL-A analytical ultracentrifuge for sedimentation equilibrium analyses of paucidisperse fractions isolated from the corresponding size exclusion chromatographic elution profiles. Unprecedented accuracy has been achieved in fitting the data from the ultracentrifuge with curves that describe the sedimentation behavior of remarkably few ideal solute components.

Molecular Weight Distributions of Acetylated Lignins in THF

Lignin Samples

Four lignin derivatives were isolated from aspen wood by different methods. A milled wood lignin was prepared through a procedure (36) affording a sample with very low residual carbohydrate content; the yield was 10% (wt/wt) of the wood meal after pre-extraction with ethanol-benzene. An alkali-extracted steam-exploded aspen lignin was prepared by successive carbon tetrachloride and aqueous alkali extractions of wood samples (from Iotech Corp.) that had been exposed to a 240°C temperature for 55 s (21). An acid-hydrolyzed aspen lignin was prepared by treating wood meal at 120°C with aqueous 0.05 *N* sulfuric acid (37), whereupon the clarified supernatant was mixed at 25°C with aqueous 1% (wt/wt) NaOH in a Waring blender. Finally, an Organosolv lignin was prepared by extracting aspen wood meal with aqueous 70% methanol at 165°C for 2.5 h in a rocking autoclave. All four lignin samples were then acetylated using a procedure (38) that facilitated quantitative recovery of the resulting derivatives.

Theory of Universal Calibration

The concept of universal calibration, as introduced by Benoit et al. (23,24), is based on the Einstein viscosity law,

$$[\eta] = \frac{\nu_i N \upsilon_h}{M} \quad (1)$$

This equation relates the hydrodynamic volume υ_h of a macromolecule with molecular weight M to its intrinsic viscosity $[\eta]$ in cm^3/g, N is Avogadro's number, and v is a shape factor developed by Simha (39), which has a value of 2.5 for spheres.

The equivalent sphere for a flexible polymer has radius $R_e = \xi R_G$. Thus,

$$\upsilon_h = \frac{4}{3}\pi\xi^3 R_G^3 \quad (2)$$

The radius of gyration R_G is given by $R^{2G} = \alpha^2\beta^2 M/6M_0$, where M_0 is the molecular weight of the polymer chain segment; α is an empirical parameter that is strongly solvent dependent; and β is the effective length per chain segment, which is specific to the polymer in question and dependent on temperature. Hence Equation (1) becomes

$$[\eta] = \frac{10\pi N\alpha^3\beta^3\xi^3 M^{0.5}}{3(6M_0)^{1.5}} \quad (3)$$

For flexible-chain polymers, β and ξ are independent of molecular weight M, when M is large, and can be considered constants. Also, because α can be expressed as a function of the form $\alpha = AM^x$, the familiar relationship first expressed by Mark (40) and Houwink (41) in the 1940s can be deduced:

$$[\eta] = K'M^a \quad (4)$$

where K' and a are known as the Mark-Houwink constants and are particular to a polymer type. For flexible linear polymers, values of a fall within the range 0.50–0.80.

Equation (1) also predicts that all molecules having the same value of $[\eta]M$ would have the same value of υ_h, provided there is no appreciable influence from the shape factor. If υ_h is the parameter that uniquely determines the size exclusion chromatographic elution volume V_e, such molecules should also have the same elution volume. The relationship between υ_h and V_e is not necessarily semilogarithmically linear, and indeed most universal calibration curves shown in the literature that cover four to six decades in M show a definite upward curvature at high values of M (24).

Sources of error in this approach arise on both experimental and theoretical grounds. Modern theories of size exclusion chromatographic retention mecha-

nisms are based on the assumption that penetration into the pores of the column packing material uniquely determines the elution volumes of the solute components. Yet, the possibility of reversible adsorption is difficult to dismiss, and when it occurs, errors in interpretation may easily result. Furthermore, a less obvious error may reside in a consequence of Equation (1), in which the hydrodynamic volume of a macromolecule, which may be a highly deformable random coil, is related to its intrinsic viscosity. This experimental parameter, when properly measured, necessitates extrapolation to infinite dilution and, for many polymers, should be extrapolated to zero shear as well. When size exclusion chromatographic data have been analyzed in this context, Equation (1) has been applied under conditions in which both concentrations and shear rates could be too high. In regard to the general applicability of universal calibration methods, it has been pointed out (42) that, even though the quantity $[\eta]M$ is not a truly universal elution parameter for SEC, both theory and experiment indicate that good results can be obtained for components of a similar type (e.g., rod-like macromolecules of comparable cross-sectional dimension in a restricted size range or linear flexible polymer chains). It has even been suggested that, over restricted ranges of M, a common $[\eta]M$ dependence among random coil polymers and rod-like structures should exist. Divergence often increases, however, in sets of data extending over three orders of magnitude in M (43).

Finally, because SEC separates molecules according to some function of size, one might ask which parameter is most appropriate. Hydrodynamic volume is certainly a reasonable choice, but other parameters related to size have also been considered (44,45), allowing alternative bases for constructing universal calibration curves. The product $[\eta]M$ is related to the radius of an equivalent sphere R_e by the equation

$$[\eta]M = 10N\pi\frac{R_e^3}{3} \quad (5)$$

and to the radius of gyration R_G of a random coil polymer by

$$[\eta]M = 6^{1.5}\phi R^{3G} \quad (6)$$

Here, ϕ is the Flory-Fox (46) constant, having the approximate value 2.4×10^{21} when $[\eta]$ is expressed in dl/g. $[\eta]$ can also be related to the square root of the mean square end-to-end distance $[\eta]M = 6^{1.5}\phi R_G^3$ of a random coil polymer (46) by the equation

$$[\eta]M = \phi\langle h^2\rangle^{1.5} \quad (7)$$

Although Equations (6) and (7) are of considerable interest, only Equation (4) has been applied, through Viscotek Unical software, to the data presented in this section.

SEC with Differential Viscosimetric Analysis

Application of universal calibration to unknown polymers using Viscotek Unical software, once the column system has been calibrated with paucidisperse standards, is quite straightforward. A master calibration file of these paucidisperse standards was developed that incorporates the "peak parameter" values calculated from one (or averaged from several) such well-behaved fraction(s). Chromatographic mismatch of the two detectors (refractive index and differential pressure) used in the system is taken into account, and approximate corrections for peak broadening and peak tailing are included. These peak parameters represent effects specific to the chromatographic system used in each case. The concentration of every sample processed must be known accurately, because this enters into the calculation of reduced viscosity, measured here directly as specific viscosity, and the molecular weight averages. An assumption central to the data processing is that under the chromatographic conditions employed sample dilution is sufficiently high that the reduced viscosity approximates the intrinsic viscosity. The software can be used to create the Mark-Houwink plots ([η] versus *M*) for each standard polymer series. All the polymer standards are then used to construct a universal calibration plot of [η]*M* versus elution volume. The software can also be employed to recalculate the values of $\overline{M}_n$, $\overline{M}_w$, $\overline{M}_n$, and $\overline{M}_{z+1}$ for the paucidisperse standards originally used to construct the curve. This useful exercise typically shows an approximate ±10% deviation (for $\overline{M}_w$) in the recalculated values compared with the values entered initially. Molecular weight averages are found for unknown polymers (accepting the shortcomings mentioned earlier) in a similar way.

Theory of Sedimentation Equilibrium

The expressions that describe the equilibrium concentrations of solutes in the ultracentrifuge cell have been derived from both classic thermodynamics, in which there are few uncertainties, and from material transport theory, in which approximations exist. Svedberg (47,48) derived expressions from the two approaches and showed that identical results can be deduced from both methods for ideal solutions.

At equilibrium, the flux as a result of sedimentation J_{sed} is equal to the flux arising from diffusion J_{diff} at all points in the cell, and no further change in the concentration profile occurs. Therefore,

$$J_{sed} = cA\frac{dr}{dt} \quad (8)$$

where *c* is concentration, *A* is cross-sectional area, *r* is the radial distance from the center of rotation, and *t* is time (cgs units). From transport theory, it can be

shown that

$$M = \frac{Nfs}{1 - \bar{v}_2\rho}$$

and

$$s = \frac{dr/dt}{\omega^2 r}$$

where s is the Svedberg sedimentation coefficient, f is the frictional coefficient, $\bar{v}_2$ is the partial specific volume, ρ is the density of the solution, and ω is the angular velocity of the rotor. These two equations lead to

$$M(1 - \bar{v}_2\rho) = \frac{Nf(dr/dt)}{\omega^2 r} \quad (9)$$

which when combined with Equation 8 gives

$$J_{sed} = \frac{cAM(1 - \bar{v}_2\rho)\omega^2 r}{Nf} \quad (10)$$

J_{diff} is derived from Fick's first law (49) and can be written as

$$-J_{diff} = DA\frac{dc}{dr} = \frac{RT}{Nf}A\frac{dc}{dr}\left(1 + \frac{c\partial \ln \gamma}{\partial r}\right) \quad (11)$$

Here D is the diffusion coefficient of the solute, R is the gas constant, T is the temperature, and γ is the activity coefficient of the solute. The second expression employs the Einstein-Sutherland equation, which may be derived from the thermodynamics of irreversible processes.

Setting Equations (10) and (11) equal and rearranging,

$$M = \frac{RT}{(1 - \bar{v}_2\rho)\omega^2}\frac{1}{rc}\frac{dc}{dr}\left(1 + \frac{c\partial \ln \gamma}{\partial r}\right) \quad (12)$$

Because $(1/rc)(dc/dr) = 2(d \ln c/dr^2)$, Equation (12) may be written in the following form, which is suitable for Rayleigh interference optics in the ultracentrifuge:

$$M = \frac{2RT}{(1 - \bar{v}_2\rho)\omega^2}\frac{d \ln c}{dr^2}\left(1 + \frac{c\partial \ln \gamma}{\partial r}\right) \quad (13)$$

For a two-component system, such as the lignin/THF case under consideration in this section, provided that the assumption of ideality can be made, the term incorporating the solute activity coefficient becomes unity and Equation (13) is reduced to the familiar form of the expression describing sedimentation-

diffusion equilibrium in the ultracentrifuge cell (50):

$$M_{app} = \frac{2RT}{(1 - \bar{v}_2\rho)\omega^2} \frac{d \ln c}{dr^2} \quad (14)$$

If nonideality is suspected in the system under scrutiny, experiments performed at various concentrations of solute lead to the evaluation of M_{app} as

$$\frac{1}{M_{app}} = \frac{1}{M}\left(1 + \frac{c\partial \ln \gamma}{\partial c}\right) \quad (15)$$

For monodisperse systems, plots of ln c versus r^2 should yield straight lines. In general, systems exhibiting polydispersity show upward-sloping curves of ln c versus r^2, whereas monodisperse nonideal systems show downward-sloping curves (51). When solutes are polydisperse, as SEC invariably reveals lignin derivatives to be, it is useful to recognize that the expression in Equation (14) becomes M_{wr}, the weight-average molecular weight at any given radial distance r from the center of rotation (52). Accordingly, the overall weight-average molecular weight $\overline{M}_w$ for the sample as a whole disposed in a sector-shaped ultracentrifuge cell can be deduced from

$$\overline{M}_w = \frac{\int_m^b M_{wr} c \, dr^2}{\int_m^b c \, dr^2} \quad (16)$$

where the limits of integration m and b refer to the meniscus and base of the solution column. It can readily be shown that the z-average molecular weight (53) M_{zr} of the solute components at each point r in the ultracentrifuge cell is given by

$$M_{zr} = M_{wr} + \frac{c \, dM_{wr}}{dc} \quad (17)$$

whence the overall z-average molecular weight $\overline{M}_z$ for the sample as a whole (52) can be obtained from

$$\overline{M}_z = \frac{\int_m^b M_{zr} \, dc}{\int_m^b dc} \quad (18)$$

calculated over the same limits of integration as in Equation (16) for a solution column disposed in a sector-shaped ultracentrifuge cell. The molecular weight

averages $\overline{M}_w$ and $\overline{M}_n$ for the polymer under investigation provide a general indication of the polydispersity of the sample: in a logarithmic-normal molecular weight distribution of solute components, for example, $\overline{M}_z/\overline{M}_w = \overline{M}_w/\overline{M}_n$ (53).

If the sample being studied spans a broad range of molecular weight, however, the values of M_{app} calculated from Equation (14) at the meniscus and base of the solution column in the ultracentrifuge cell can still provide useful information about the molecular weight distribution. Particularly revealing in the determination of molecular weight distributions for polydisperse polymers is the application of multiple rotor speed analysis. This method (54–56) permits the delineation of the overall molecular weight distribution for a sample with high polydispersity from data collected at multiple (7–20) rotor speeds for various heights in the sample solution column. Unfortunately, the approach has been substantially underutilized and has not been adapted directly for use with data collected from the interference optical system described in this section (57).

The Rayleigh interference fringe photographs, which reflect the variation in solute component concentration with radial distance *r,* are aligned in a micro-comparator and analyzed by routine procedures (51,58). Calculation of the overall weight-average molecular weight is based on the assumption that the mass of solute components at equilibrium was conserved with respect to the conditions before ultracentrifugation was initiated (53,59). For the ultracentrifuge work summarized in this section, a specific and limited form of Equation (14) (51) was used:

$$M_{app} = \frac{2RT}{(1 - \bar{v}_2\rho)\omega^2(r_b^2 - r_m^2)} \frac{c_b - c_m}{c_0} \quad (19)$$

where c_b and c_m represent the solute concentrations at the base and meniscus of the solution column upon attainment of equilibrium and c_0 denotes the concentration before the sedimentation process has begun.

Values for $M_{app,m}$, $M_{app,b,}$ and the corresponding $d \ln c/dr_2$ can be found at the appropriate radial positions in the cell (59), that is, r_m at the meniscus and r_b at the base of the solution column. The values of M_{app},b are rarely used, however, because polymer buildup at the cell base at higher rotor speeds often obscures fringe determination at this position.

For the work with lignin derivatives in THF described here, the sedimentation equilibrium data were presented in terms of Rayleigh interference patterns using Equation (14). It was assumed that, at the 1–2 g/liter solute concentrations used, ideal behavior in THF would prevail and therefore the data were collected at one concentration only. It is not currently known, however, what would constitute theta conditions for lignin derivatives in THF.

Owing to the inherent uncertainty in Rayleigh fringe determination at the cell base and the distinct possibility that concentration-dependent processes, such as association, are occurring in that region, $M_{app,m}$ and $M_{app,b}$ are not presented

here for the four lignin samples. Rather, $\overline{M}_w$ values at different rotor speeds are tabulated without any attempt to extrapolate to zero speed because the basis for doing so (54–56) has not been directly adapted to the data generated here.

Molecular Weight Distributions of Acetylated Lignin Derivatives in THF

Molecular Weight Distributions from SEC

The results from "conventional gel permeation chromatography (GPC)" of four acetylated aspen lignin derivatives are shown in Table 1. These data were collected with a sensitive ultraviolet HPLC detector, permitting 0.2 mg column loadings. The values for $\overline{M}_n$, $\overline{M}_w$, and $\overline{M}_n$ (35) proved to be similar to those reported in the literature from other laboratories (17–20), where a polystyrene-divinylbenzene (μStyragel) column was used with THF as the mobile phase. A general pattern evident in these data concerns the similarity in $\overline{M}_w$ among all the acetylated aspen lignin derivatives investigated, except the milled wood lignin, which was distinctly higher in $\overline{M}_w$. The polydispersities $\overline{M}_w / \overline{M}_n$ found from the GPC work were close in magnitude for all samples and possibly identical within experimental error *(i.e.,* 4.0 ± 0.4).

Table 1 also displays the average molecular weights found by the universal calibration approach for the four acetylated lignin derivatives. The relative ordering of these values is very similar to that from conventional GPC in that the milled wood lignin shows the highest average molecular weights. However, the $\overline{M}_n$ from conventional GPC range from values that are identical within experimental error (alkali-extracted steam-exploded lignin) through values that are 35% smaller than those from universal calibration (Organosolv and acid-hydrolyzed lignins), to values from GPC that are half those from universal calibration (milled wood lignin). The values of $\overline{M}_w$ from conventional GPC are 20–40% smaller for all four acetylated aspen lignin derivatives. There is a systematic difference in $\overline{M}_n$ by a factor of about 2 with respect to the values from conventional GPC and universal calibration, the former being always the larger. This may indicate a detector- or software-based bias, because the placement of baselines on the original chromatographic data is especially critical in calculating $\overline{M}_n$ values, which are sensitive to the proportions of high-molecular-weight species. As with the results from conventional GPC, the polydispersities are the same within experimental error for all the acetylated lignin derivatives in THF.

Molecular Weight Distributions from Sedimentation Equilibrium Studies

Average molecular weights were determined for the acetylated lignin samples from sedimentation equilibrium at different rotor speeds and positions in the cell

Table 1 Molecular Weight Distributions of Acetylated Aspen Lignin Derivatives in THF

		SEC through universal calibration				Conventional GPC[a]				Sedimentation equili	
Sample	Loading	$\overline{M}_n$	$\overline{M}_w$	$\overline{M}_z$	$\overline{M}_w/\overline{M}_n$	$\overline{M}_n$	$\overline{M}_w$	$\overline{M}_z$	$\overline{M}_w/\overline{M}_n$	$\overline{M}_w$ (app. 15 krpm)	$\overline{M}_w$ (app. 30 krpm)
Steam exploded	0.2 mg					1,300	5,700	76,000	4.4		
	1 mg	1,100	7,300	3,950	6.7						
	2 g/liter[b]	1,900	7,100	27,000	3.7					9,100	
Organosolv	0.2 mg					760	2,950	38,400	4.0		
	1 mg	1,300	5,200	16,000	4.0						
	2 g/liter[b]	1,000	4,400	18,000	4.4					8,000	3,100
Acid hydrolyzed	0.2 mg					1,100	4,300	80,000	3.8		
	1 mg	2,200	8,100	38,000	3.7						
	2 g/liter[b]	1,300	6,600	34,000	5.0					9,000	4,900
Milled wood lignin	0.2 mg					2,900	11,000	91,000	3.7		
	1 mg	3,600	17,000	46,800	4.7						
	2 g/liter[b]	9,000	22,000	47,000	2.4					10,600	5,200

Source: From References 34 and 35.
[a]UV detection at 260 nm; calibrated with paucidisperse polystyrene fractions.
[b]SEC loading at 2 mg.

solution column using a method incorporating the conservation of mass principle [Equation (19)]. Table
of these experiments at a lignin concentration of approximately 2 g/liter. Without the possibility of accur
the values at different rotor speeds to zero, it may be assumed that the estimate for $\overline{M}_w$ at 15,000 rpm is a
approximation.

The issue of rotor speed variation and its impact on the "intrinsic" $\overline{M}_w$ requires further discussion. Early
clearly indicated the necessity for examining polydisperse samples at a wide range of ultracentrifuge rotc
centrifugal force (proportional to ω^2) is increased in the sample solution column, the apparent distributio
changes as heavier fractions sediment to the cell base (or lie close to this position). Improvements (56) o
(54) were made so that broadly polydisperse polymers could be fully analyzed, but unfortunately these p
were developed for the interpretation of schlieren patterns only. The work presented here was performed
interference optical system so that more dilute solutions could be studied; schlieren optical analysis requi
concentrations in the 3–6 g/liter range. However, it may be inferred (56) that values found for the appare
speeds lie near (and are somewhat lower than) the intrinsic $\overline{M}_w$ for the sample. This assumption is probab
a series of rotor speeds yields $\overline{M}_w$ values that appear to approach a limiting value at low speed. The value
obtained by size exclusion chromatographic methods appear only roughly similar to those calculated at t
speeds in sedimentation equilibrium experiments. Yet, the trend in molecular weight appears conserved
approaches are compared. Future work, then, must be dedicated to determining $\overline{M}_w$ values found from ex
zero concentration and zero rotor speed.

Reconciliation of Results Within the Study

The multidisciplinary approach taken here (34,35) to determining the molecular weight distributions of a
derivatives follows a long-known, but little trod, experimental path. Interesting comparisons (61–63) we
of hydrodynamic data from viscometry, sedimentation velocity, and light-scattering measurements for sp
fractions. From plots of log M versus log [η], these spruce lignin fractions appeared to exhibit behavior i

branched polymers. In the studies summarized here (34,35), three approaches to determining the molecul distributions of four acetylated aspen lignin derivatives were taken: conventional GPC, universal calibrat exclusion chromatographic elution profiles, and sedimentation equilibrium studies. Conventional GPC a columns calibrated with polystyrene standards produced the lowest molecular weight estimates for the fo Universal calibration methodology led to molecular weight estimates higher by factors of

1½–2½ than conventional GPC, and sedimentation equilibrium studies gave values of $\overline{M}_{w,app}$ that were roughly similar to those from universal calibration. These results are not surprising because conventional GPC, relying as it does upon comparison with a series of standard polymers, predicts the effective hydrodynamic volume of the lignin derivative, not its molecular weight. Universal calibration of size exclusion chromatographic elution profiles, however, relies on the conservation of the relationship between the hydrodynamic volume $[\eta]M$ and elution volume for a specific column set throughout a wide range of polymer structures and sizes. Indeed, the finding of higher $\overline{M}_w$ from universal calibration than from GPC is consistent with the possibility that lignins are branched polymers: a branched polymer of higher molecular weight may occupy the same hydrodynamic volume as a linear polymer of lower molecular weight. Universal calibration is dependent upon column elution behavior, and so anomalies caused by adsorption, or, in block copolymers and branched heteropolymers, the contributions from the polymer "core" and "shell" to hydrodynamic behavior must be understood (30,64). The availability of appropriate branched polymer fractions as universal calibration standards could elicit further insight into the configurations of the acetylated aspen lignin derivatives.

An alternative approach to determining the absolute molecular weight distributions of lignin derivatives may be found in direct ultracentrifuge sedimentation equilibrium studies of paucidisperse fractions selected from suitable size exclusion chromatographic elution profiles (7–12). When the sedimentation equilibrium curves (relative solute concentration versus radial distance from center of rotation) are delineated in terms of ultraviolet absorbance, no errors arise from fluorescence through the customary scanner optical system. Moreover, very low solute concentrations (typically between 4×10^{-3} and 8×10^{-3} g/liter) can be chosen so that a particularly close approximation to solution ideality may be achieved. Furthermore, because each lignin derivative fraction occupies only a narrow interval within the overall molecular weight distribution, the necessity for sedimentation equilibrium analyses over a range of different rotor speeds is obviated. Such investigations with the Beckman Optima XL-A analytical ultracentrifuge are the subject of the next section.

Molecular Weight Distributions of Kraft Lignin Derivatives

Kraft Lignin Samples

The parent kraft lignin preparation chosen for these studies was isolated, as previously described (8), by acidification of an industrial "black liquor" produced from Jack pine *(P. banksiana)* by the Boise Cascade Corporation (Inter-

national Falls, MN). The resulting (thoroughly washed) precipitate was redissolved in aqueous solution (on the slightly basic side of neutrality) and desalted by exhaustive ultrafiltration with ultrapure water through a (YC05) 500 nominal molecular weight cutoff membrane (Amicon, Beverly, MA) before freeze drying.

A portion of the parent preparation was incubated (under ambient conditions) at 160 g/liter for 92.5 h in aqueous 0.40 *M* NaOH containing 0.60 *M* NaCl, whereupon association between kraft lignin species in solution (7,9) brings about a slight increase in the proportion of higher molecular weight species observable in aqueous 0.10 *M* NaOH (reference conditions previously adopted for reliable molecular weight determinations of kraft of lignin samples). Upon recovery of the kraft lignin preparation from solution, all alkyl and aryl hydroxyl groups were acetylated (acetic anhydride/pyridine) and any residual carboxylic acid moieties methylated (diazomethane) to preclude those noncovalent interactions that are governed by hydrogen bonding between the individual molecular components.

SEC of Kraft Lignin Derivatives

Upon elution with (carbonate-free) aqueous 0.10 *M* NaOH through Sephadex G-100, the parent kraft lignin preparation exhibited the profile depicted in Figure 3A, which represents complete recovery of the solute. Under such conditions, the distribution of species comprises associated macromolecular complexes and individual components in the higher and lower molecular weight regions, respectively (7,9). (The scale of relative retention volume V_R was correlated with an assignment of 2.0 as a constant value for *p*-nitrophenol.) Nine fractions were selected from the overall Sephadex G-100/aqueous 0.10 *M* NaOH profile and reeluted twice through the same column system before absolute molecular weight determinations. The resulting profiles of these paucidisperse fractions are shown in Figure 3B to approximate reasonably well to Gaussian shapes.

The kraft lignin molecular weight calibration curve deduced from ultracentrifuge sedimentation equilibrium analyses of the fractions is depicted in Figure 4. The graph itself is compiled from a plot of log $\overline{M}_w$ versus $V_{R,\max}$, the relative retention volume at the peak of the profile for each fraction, but it should be remembered that this is only strictly valid for Schulz-Zimm distributions of solute species (65). In regard to the parent kraft lignin preparation, the calibration curve in Figure 4 is applicable only to $\overline{M}_w$ below 50,000: for paucidisperse fractions selected from the region around the excluded limit, values of elution volume at the peak of each profile $V_{e,\max}$ after reelution are greater than the original V_e because of diffusion of the solute species during passage through the column.

For comparison, the acetylated methylated kraft lignin derivative was eluted in DMF through a (600 × 7.5 mm) TSKgel G7000-H6 10^7 Å pore size poly-

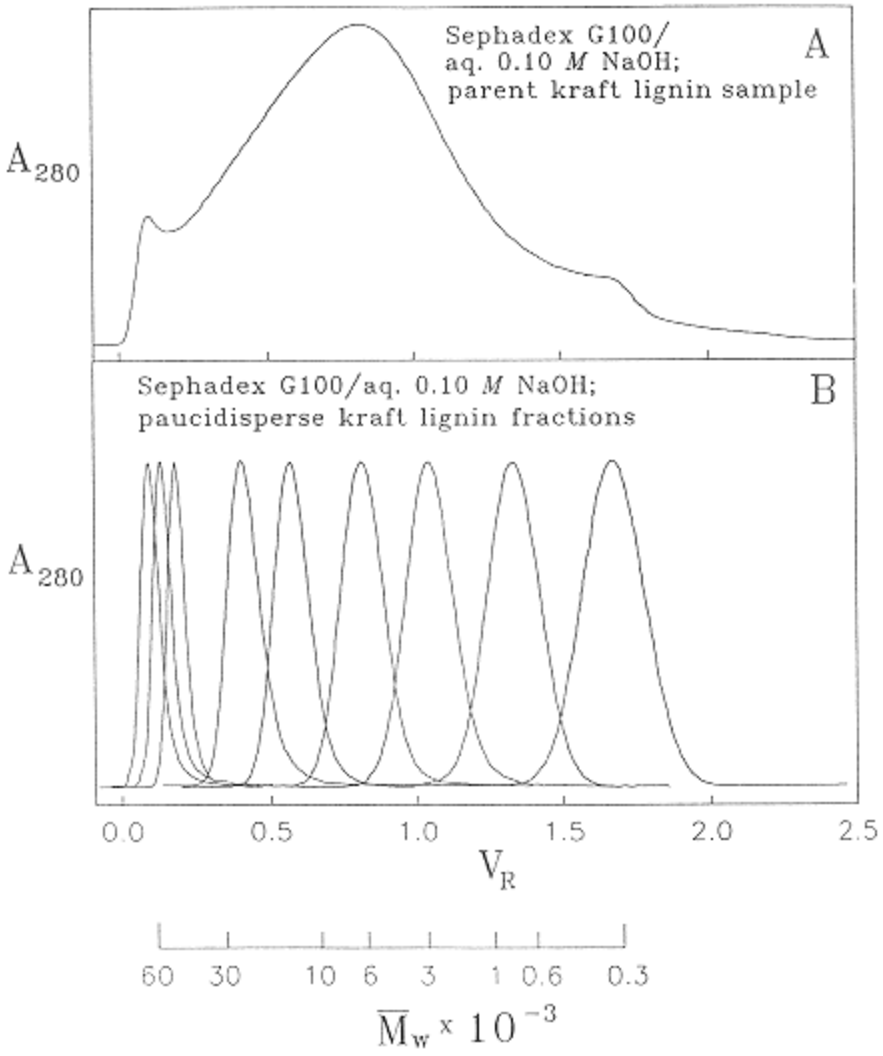

Figure 3
(A) Kraft lignin sample from Jack pine and (B) paucidisperse fractions size exclusion chromatographically produced from parent preparation. Elution profiles in aqueous 0.10 M NaOH from Sephadex G-100 monitored at 280 nm; weight-average molecular weights of paucidisperse fractions deduced from sedimentation equilibrium analyses.

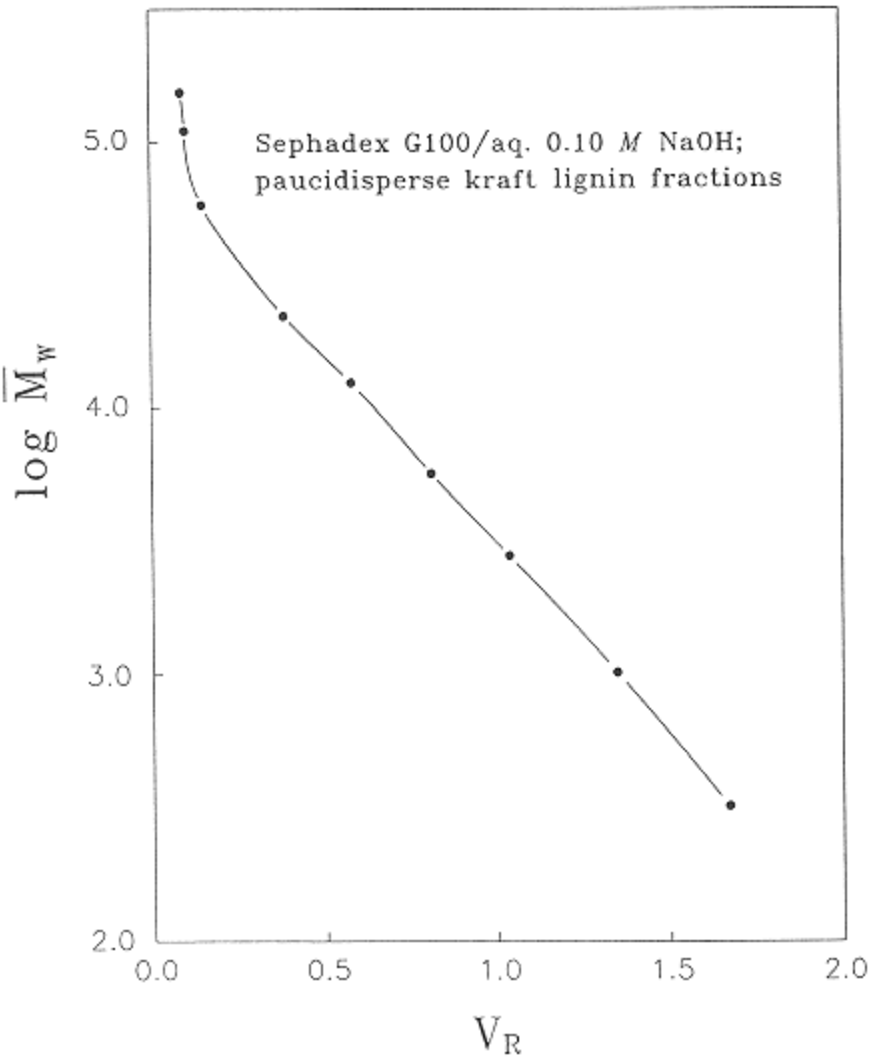

Figure 4
Semilogarithmic plot of weight-average molecular weight versus relative retention volume for paucidisperse kraft lignin fractions eluted from Sephadex G-100 with aqueous 0.10 M NaOH.

styrene-divinylbenzene column, whereupon the profile that was generated (representing 80% recovery of solute species from 0.0034 mg loadings) displayed the form depicted in Figure 5A. The result is very similar to that previously found with a PLgel 10^6 Å pore size polystyrene-divinylbenzene column (66), although in the work described here the distinct features visible earlier in the higher molecular weight region (corresponding to the 10–14 ml range of elution volume) have not been resolved.

Paucidisperse acetylated methylated kraft lignin fractions from the TSKgel G7000-H6/DMF profile were allocated to absolute molecular weight determinations without reelution through the column system. The calibration curve deduced from ultracentrifuge sedimentation equilibrium analyses of these fractions is compared in Figure 5B with the corresponding plot for standard polystyrenes based on the molecular weight data provided by the suppliers (Polymer Laboratories, Inc., Polysciences, Inc., and the Pressure Chemical Co.). It is evident that the distribution of acetylated methylated kraft lignin species in DMF extends to much higher molecular weights (Figure 5B) than the upper bound of the range encompassed by the underivatized kraft lignin preparation in aqueous 0.10 *M* NaOH (Figure 4). Clearly associated macromolecular kraft lignin complexes persist in DMF without the agency of hydrogen-bonded interactions between the individual molecular components.

Perhaps the most remarkable aspect of the results summarized in Figure 5B is in the striking differences between the calibration curves for the polystyrenes and the acetylated methylated kraft lignin sample: at an elution volume of around 15.0 ml, for instance, the acetylated methylated kraft lignin species exhibit molecular weights lower than those for polystyrenes by a factor of more than 50,000! It is inconceivable that this marked disparity could be caused solely by differences in the intrinsic viscosities of the respective solute species; clearly, any attempt to apply universal calibration principles here would engender drastic errors in the resulting molecular weight estimates for the acetylated methylated kraft lignin sample in DMF.

Absolute Molecular Weight Determinations

Paucidisperse acetylated methylated and underivatized kraft lignin fractions were selected for absolute molecular weight determinations at 8×10^{-3} g/liter concentrations in DMF and aqueous 0.10 *M* NaOH, respectively, using the Beckman Optima XL-A analytical ultracentrifuge. The partial specific volumes of the solute species $\bar{v}_2$ (0.744 cm^3/g), and densities ρ of solvent or solution were measured with a Paar 60/602 digital density meter. The sedimentation curves were scanned at two wavelengths (280 and 320 nm) after equilibrium had been reached at more than one suitable rotor speed; the effective baseline at 600 nm was subtracted from each set of sedimentation equilibrium data to correct for

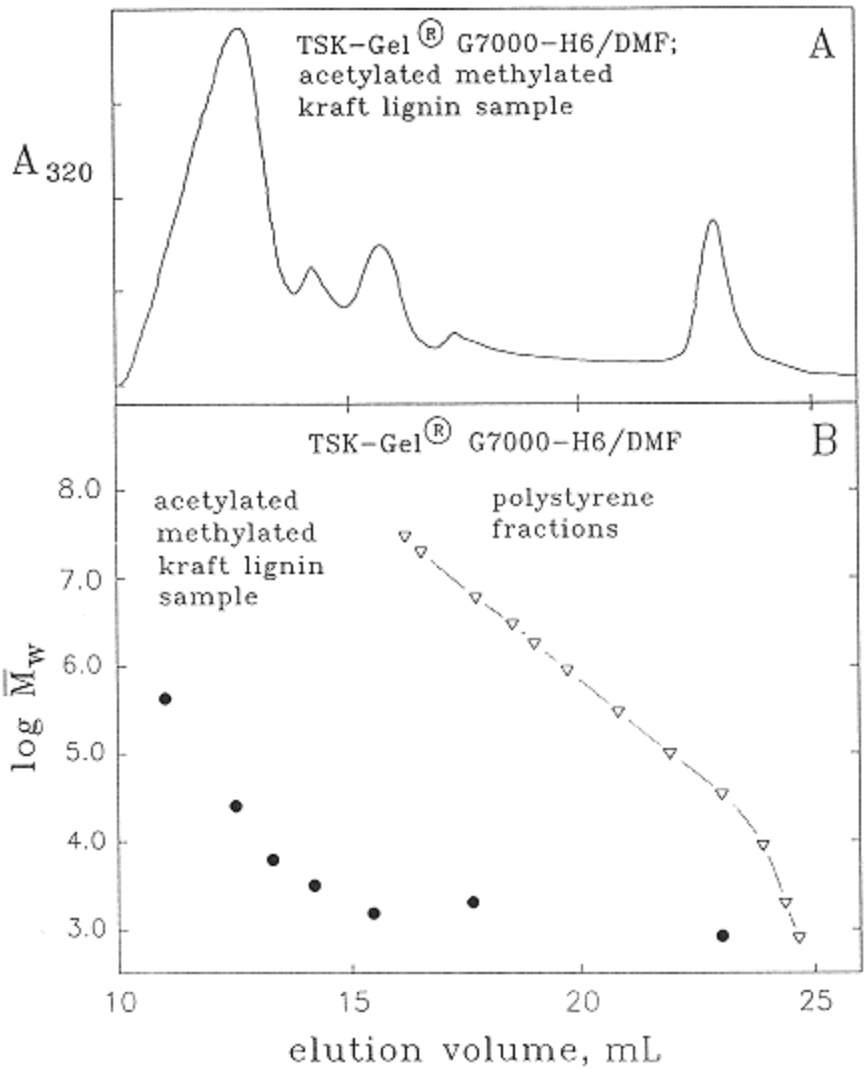

Figure 5
(A) Acetylated methylated kraft lignin derivative. Elution profile in DMF from TSKgel G7000-H6 column monitored at 320 nm; (B) corresponding semilogarithmic plot of weight-average molecular weight versus elution volume (deduced from sedimentation equilibrium analyses) with polystyrene calibration curve for same chromatographic system.

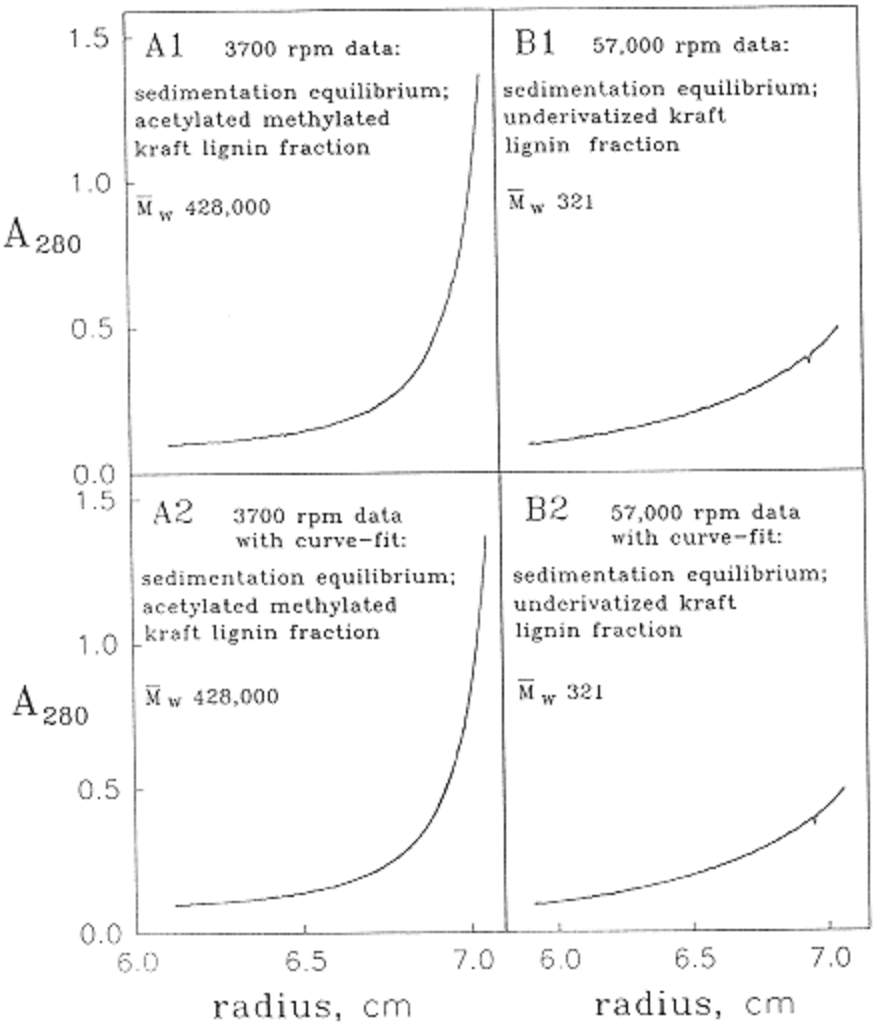

Figure 6
Sedimentation equilibrium analyses of (A) acetylated methylated and (B) underivatized kraft lignin fractions. (1) Variation in solute concentration with radial distance from center of rotation monitored in Beckman Optima XL-A ultracentrifuge; (2) curve fit to data points achieved by sum of terms of the form expressed in Equation (20).

any optical defects that might have been present in the cell assemblies. The resulting plots of absorbance versus radial distance from the center of rotation are exemplified in Figure 6A1 and B1.

The concentrations of kraft lignin species were so low that ideal behavior could, with reasonable confidence, be expected to prevail. Thus, at equilibrium, the concentration c_r of each solute species varies with radial distance r in the solution column according to

$$c_r = c_m \exp\{M[(1 - \bar{v}_2\rho)\omega^2/2RT](r^2 - r_m^2)\} \quad (20)$$

where c_m and r_m are the solute concentration and radial distance, respectively, corresponding to the meniscus. Consequently, Equation (20) describes the entire sedimentation equilibrium curve for any monodisperse sample. On the other hand, the related expression set forth in Equation (19) incorporates the fact that the mass of components at sedimentation equilibrium is the same as before ultracentrifugation has been initiated, but there the calculation of molecular weight rested upon only two data points corresponding to the respective solute concentrations at the base and meniscus of the solution column in the ultracentrifuge cell.

Using SigmaPlot 5.0 (Jandel Scientific, San Rafael, CA), the sets of sedimentation equilibrium data for the paucidisperse acetylated methylated and underivatized kraft lignin fractions were successfully curve fit to functions representing sums of terms of the form expressed in Equation (20). In no case were more than four individual terms required for the fits of unprecedented accuracy that were achieved; these are exemplified in Figure 6A2 and B2. The sums of the areas under the component exponential curves confirmed that the total mass of solute species observed at equilibrium never differed by more than 1% from that present before the sedimentation process began.

The weight-average molecular weights $\overline{M}_w$ calculated directly from the individual values of M in the respective terms of the curve-fitting expression were, to all intents and purposes, identical to those computed from M_{wr} using Equation (16). Furthermore, the values of $\overline{M}_n$ exhibited far less scatter than those calculated previously by curve fitting with orthogonal polynomials (10). The authors are not aware of any previous report documenting the practical implementation of such an approach to analyzing sedimentation equilibrium data.

Reliability of Molecular Weight Distributions for Lignin Derivatives

Clearly, absolute molecular weight determinations are essential for the reliable interpretation of size exclusion chromatographic elution profiles as molecular weight distributions for lignin derivatives. Light scattering is certainly a useful

tool in this regard, provided that fluorescence does not contribute to the intensity measurements, but the technique suffers in accuracy with respect to moderate or low concentrations of solute species with molecular weights below 10,000. The application of universal calibration principles to size exclusion chromatographic elution profiles of lignin derivatives represents a promising alternative, but the approach can lead to serious errors without warning in the kind of empirical results obtained.

Although they have the potential advantage of avoiding SEC altogether, ultracentrifuge sedimentation equilibrium studies of polydisperse lignin derivative samples at multiple rotor speeds have not been developed to the stage at which they can be generally viewed as viable options. Consequently, ultracentrifuge sedimentation equilibrium analyses of paucidisperse fractions from suitable size exclusion chromatographic elution profiles at present provide the most reliable means for determining molecular weight distributions of lignin derivatives. Concentrations of lignin species low enough for ideal solute behavior do not compromise the accuracy of the ultraviolet absorbance data, and the curve fitting routine presented for the first time in this chapter is particularly convenient for the task of computing $\overline{M}_w$ and $\overline{M}_n$. Fortunately, the Beckman Optima XL-A analytical ultracentrifuge is eminently capable of yielding dependable results throughout the molecular weight ranges usually encompassed by lignin derivatives.

Acknowledgments

Acknowledgment for support of this work is made to the *Ethanol from Biomass* Program of the Biofuels Systems Division at the U.S. Department of Energy, the Vincent Johnson Lignin Research Fund at the University of Minnesota, the Minnesota State Legislature at the recommendation of the Legislative Commission on Minnesota Resources, and the Minnesota Agricultural Experiment Station.

References

1. N. G. Lewis and E. Yamamoto, *Annu. Rev. Plant Physiol. Plant Mol. Biol.,* 41, 455–496 (1990).

2. S. Saka and D. A. I. Goring, in Biosynthesis and Biodegradation of Wood Components (T. Higuchi, ed.), Academic Press, New York, 1985, Chapter 3, pp. 51–62.

3. H. Grisebach, in The Biochemistry of Plants—A Comprehensive Treatise; Volume 7: Secondary Plant Products (E. E. Conn, ed.), Academic Press, New York, 1981, pp. 457–478.

4. E. Adler, *Wood Sci. Technol.,* 11, 169–218 (1977).

5. J. Gierer, *Holzforschung,* 36, 43–51 (1982).

6. K. Lundquist, *Appl. Polym. Symp.,* 28, 1393–1407 (1976).

7. S. Dutta, T. M. Garver, Jr., and S. Sarkanen, *ACS Symp. Ser.,* No. 397, 155–176 (1989).

8. T. M. Garver, Jr. and S. Sarkanen, *Holzforschung,* 40 (Suppl.), 93–100, (1986).

9. S. Sarkanen, D. C. Teller, C. R. Stevens, and J. L. McCarthy, *Macromolecules,* 17, 2588–2597 (1984).

10. S. Sarkanen, D. C. Teller, E. Abramowski, and J. L. McCarthy, *Macromolecules,* 15, 1098–1104 (1982).

11. S. Sarkanen, D. C. Teller, J. Hall, and J. L. McCarthy, *Macromolecules,* 14, 426–434 (1981).

12. W. J. Connors, S. Sarkanen, and J. L. McCarthy, *Holzforschung,* 34, 80–85 (1980).

13. T. Iversen, *Wood Sci. Technol.,* 19, 243–251 (1985).

14. C. Schuerch, *J. Am. Chem. Soc.,* 74, 5061–5068 (1952).

15. W. W. Yau, J. J. Kirkland, and D. D. Bly, Modern Size-Exclusion Liquid Chromatography, Wiley, New York, 1979.

16. W. Lange, O. Faix, and O. Beinhoff, *Holzforschung,* 37, 63–67 (1983).

17. D. Meier, O. Faix, and W. Lange, *Holzforschung,* 35, 247–252 (1981).

18. W. Lange, W. Schweers, and O. Beinhoff, *Holzforschung,* 35, 119–124 (1981).

19. O. Faix, W. Lange, and E. C. Salud, *Holzforschung,* 35, 3–9 (1981).

20. O. Faix, W. Lange, and O. Beinhoff, *Holzforschung,* 34, 174–176 (1980).

21. H. L. Chum, D. K. Johnson, M. P. Tucker, and M. E. Himmel, *Holzforschung,* 41, 97–108 (1987).

22. M. E. Himmel, K. K. Oh, D. W. Sopher, and H. L. Chum, *J. Chromatogr.,* 267, 249–265 (1983).

23. H. Benoit, Z. Grubisic, P. Rempp, D. Decker, and J.-G. Zilliox, *J. Chim. Phys. Phys.-Chim. Biol.,* 63, 1507–1514 (1966).

24. Z. Grubisic, P. Rempp, and H. Benoit, *J. Polym. Sci. Part B,* 5, 753–759 (1967).

25. L. Letot, J. Lesec, and C. Quivoron, *J. Liq. Chromatogr.,* 3, 427–438 (1980).

26. F. B. Malihi, C. Kuo, E. Koehler, T. Provder, and A. F. Kah, *ACS Symp. Ser.,* No. 245, 281–294 (1984).

27. M. G. Styring, J. E. Armonas, and A. E. Hamielec, *J. Liq. Chromatogr.,* 10, 783–804 (1987).

28. M. E. Himmel and P. G. Squire, in Aqueous Size-Exclusion Chromatography (P. L. Dubin, ed.), Elsevier, New York, 1988, Chapter 1, pp. 3–22.

29. B. H. Zimm and W. H. Stockmayer, *J. Chem. Phys.,* 17, 1301–1314 (1949).

30. R. C. Jordan, S. F. Silver, R. D. Sehon, and R. J. Rivard, *ACS Symp. Ser.,* No. 245, 295–320 (1984).

31. J. Roovers, N. Hadjichristidis, and L. J. Fetters, *Macromolecules,* 16, 214–220 (1983).

32. S. H. Agarwal, R. F. Jenkins, and R. S. Porter, *J. Appl. Polym. Sci.,* 27, 113–120 (1982).

33. A. E. Hamielec, A. C. Ouano, and L. L. Nebenzahl, *J. Liq. Chromatogr.,* 1, 527–554 (1978).

34. M. E. Himmel, K. Tatsumoto, K. K. Oh, K. Grohmann, D. K. Johnson, and H. L. Chum, *ACS Symp. Ser.*, No. 397, 82–99 (1989).

35. M. E. Himmel, K. Tatsumoto, K. Grohmann, D. K. Johnson, and H. L. Chum, *J. Chromatogr.*, 498, 93–104 (1990).

36. K. Lundquist and R. Simonson, *Sven. Papperstidn.*, 78, 390 (1975).

37. K. Grohmann, R. Torget, and M. Himmel, *Biotech. Bioeng. Symp.*, 17, 135–151 (1986).

38. J. Gierer and O. Lindeberg, *Acta Chem. Scand. B*, 34, 161–170 (1980).

39. R. Simha, *J. Phys. Chem.*, 44, 25–34 (1940).

40. H. Mark, in Der Feste Körper, Hirzel, Leipzig, 1938, pp. 65–104.

41. R. Houwink, *J. Prakt. Chem.*, 157, 15–18 (1940).

42. E. F. Cassassa, *Macromolecules*, 9, 182–185 (1976).

43. R. P. Frigon, J. K. Leypoldt, S. Uyeji, and L. W. Henderson, *Anal. Chem.*, 55, 1349–1354 (1983).

44. J. Janca *, in Advances in Chromatography (J. C. Giddings, E. Grushka, J. Cazes, and R. P. Brown, eds.), Marcel Dekker, New York, 1981, Vol. 19, Chapter 2, pp. 37–90.

45. E. F. Cassassa, *J. Phys. Chem.*, 75, 3929–3939 (1971).

46. P. J. Flory and T. G. Fox, Jr., *J. Am. Chem. Soc.*, 73, 1904–1908 (1951).

47. T. Svedberg, *Kolloid-Z.*, 36, 53–64 (1925).

48. T. Svedberg, *Physik. Chem.*, 121, 65–77 (1926).

49. A. Fick, *Ann. Physik. u. Chem.*, 94, 59–86 (1855).

50. H. K. Schachman, Ultracentrifugation in Biochemistry, Academic Press, New York, 1959.

51. E. G. Richards and H. K. Schachman, *J. Phys. Chem.*, 63, 1578–1591 (1959).

52. E. T. Adams, Jr., in Characterization of Macromolecular Structure, Natl. Acad. Sci. U.S.A., Washington, D.C., 1968, Publication 1573, pp. 84–142.

53. W. D. Lansing and E. O. Kraemer, *J. Am. Chem. Soc.*, 57, 1369–1377 (1935).

54. H. Fujita, Mathematical Theory of Sedimentation Analysis, Academic Press, New York, 1962.

55. H. W. Osterhoudt and J. W. Williams, *J. Phys. Chem.*, 69, 1050–1056 (1965).

56. Th. G. Scholte, *J. Polym. Sci.* A-2, 6, 91–109 (1968).

57. H. Fujita, Foundations of Ultracentrifugal Analysis, Wiley, New York, 1975, pp. 344 ff.

58. C. H. Chervenka, *Anal. Chem.*, 38, 356–358 (1966).

59. E. G. Richards, D. C. Teller, and H. K. Schachman, *Biochemistry,* 7, 1054–1076 (1968).

60. E. T. Adams, Jr., *Proc. Natl. Acad. Sci. USA,* 51, 509–515 (1964).

61. F. Pla and A. Robert, *Holzforschung,* 38, 37–42 (1984).

62. F. Pla and A. Robert, *Cellulose Chem. Technol.,* 8, 3–10 (1974).

63. F. Pla and A. Robert, *Cellulose Chem. Technol.,* 8, 11–19 (1974).

64. L.-K. Bi and L. J. Fetters, *Macromolecules,* 9, 732–742 (1976).

65. H. L. Berger and A. R. Schultz, *J. Polym. Sci.* Part A, 2, 3643–3648 (1965).

66. S. Dutta and S. Sarkanen, *Mat. Res. Soc. Symp. Proc.,* 197, 31–39 (1990).

15
Size Exclusion Chromatography of Starch

Jau-Yi Chuang National Starch and Chemical Company, Bridgewater, New Jersey

Introduction

Starch is one of the most abundant polysaccharides occurring in nature. All organs of higher plants contain starch. Starch granules can be found in pollen, leaves, stems, woody tissues, roots, tubers, fruits, flowers, bulbs, and seeds. Starch can also be found in mosses, ferns, algae, and bacteria.

Starch and its derivatives are used in many industries. Starch paste was one of the earliest adhesives used by human beings. In the food industry, starch is used to promote adhesion, binding, moisture retention, gelling, and form strengthening. It is also used as a flowing aid, clouding reagent, and stabilizer. These functions make starch an indispensable ingredient in bakery products, dairy products, soups, pet foods, salad dressing, beverages, and confectionery products. In the paper industry, modified starches are used as a retention aid to improve retention of fines and fillers and as a draining aid to increase water removal on wire. In the textile industry, starch is used as the sizing reagent. In 1988, it was estimated that about 6 million tons of starch were consumed in the United States, the European Community, Japan, and Taiwan.

Starch is a renewable resource and is biodegradable. It can be an important raw material to make environmentally friendly products. The National Starch and Chemical Co. developed an extrusion process to make dry starch foam. The starch foam behaves like the styrene form and can be used as its replacement in the packing industry. After usage, the starch foam can be dumped into a sink

and washed away with water for simple disposal. The research to make plastics from starch is now actively pursued in many companies.

Starch is a polymer of α-D-glucopyranose. It can be readily extracted from major plant seeds, stems, or roots. Native starch is usually composed of two components. One component, called amylose, is a linear (1 → 4 linkage) or lightly branched (1 → 6 linkage) polymer. Another component, called amylopectin, is highly branched. The ratio of amylose and amylopectin in native starch depends on the type of plant. The starches from waxy corn or waxy rice are essentially 100% amylopectin. The molecular weight of amylose varies from several hundred thousand to a few million. For amylopectin it can be over several hundred million (1). The origin of amylose and amylopectin is not yet fully understood. Some people suggested that the starch in plants is a giant molecule, which was degraded into linear amylose and branched amylopectin during the extraction process (2).

Starch polymers can be hydrolyzed by acid or enzymes. Some enzymes, like isoamylase or pullulanease, hydrolyze specifically at the 1 → 6 branching points; α-amylosase attacks the molecules in a random fashion. It can also be degraded by physical force, such as extrusion. Starch can also be modified by various chemical reagents. It is important to know the molecular weights of the starch after the treatment. Size exclusion chromatography (SEC) has proven to be a valuable tool in studying these chemical modifications.

SEC of polysaccharides was reviewed by Chrums in 1970 (3) and by Whistler and Anisuzzman in 1980 (4). Praznik listed the starch SEC conditions used before 1986 (5). The fundamental size separation mechanism and the application of SEC coupled to low-angle laser light scattering (LALLS) to the characterization of polysaccharides were discussed by Corona and Rollings (6). Rinaudo and Tinland discussed the problems of aqueous SEC of biopolymers (7). Most of the early SEC systems used water, sodium hydroxide solution, or buffer as the mobile phase. Before 1980, the packing materials used most often were Sephadex, Sepharose, or BioGels. More recently, small particle silica-based or synthetic polymeric packing materials have become popular (8–15). the problems associated with aqueous SEC are the degradation of starch in alkali in the presence of oxygen and the retrogradation of amylose in aqueous solution.

Dimethylsulfoxide (DMSO) is known to be a good solvent for starch. Starch characterization using DMSO as the solvent was briefly discussed by Jackson when he studied the solubility of starch in a DMSO and water mixture (16). In 1974, Dintzis and Tobin determined the molecular weight of amylose by using a mixture of 95% DMSO and 5% water as the mobile phase on a porous glass column (17). Since then, pure DMSO or DMSO containing a mobile phase has been used on various kinds of packings (18–29). Starch in DMSO solution is very stable. An autosampler can be used in a DMSO SEC system. Unattended operation is the major advantage of using DMSO as the mobile phase.

Table 1 Summary of SEC Conditions

Polymer	Columns	Mobile phase	Comm
Corn, potato, synthetic amylose, pullulan, dextran	Sephacryl S-400 + S-500 + S-1000	0.005 N NaOH + 0.02% NaN_3	Summary of MW calibrati
Wheat beta-limit dextrin	Sepherogel-TSK 3000SW	H_2O	α-Amylase h study
Amylose (potato, sweet potato, tapioca, kuzu, lily)	TSK G3000 PW G4000 PW + G6000 PW	50 mM phosphate buffer + 0.02% NaN_3	LALLS, MW
Corn, sorghum	Shodex S/806/S + S-805/S + S-804/S + S-803/S	H_2O	Effect of moi extrusion
Corn, Alkali cooked	Shodex S-806/S + S-805/S + S-804/S + S-803/S	H_2O	Structural characterizat
Corn amylose	Fractogel HW-75F TSK G6000 PW + G4000 PW + G3000 PW	50 mM NaCl 50 mM phosphate + 0.02% NaN_3	LALLS, stru characterizat
Hydroxyethylated potato and corn, dextran, pullulan	TSK G5000 PW + G4000 PW	0.05 M NaCl	LALLS, MW
Waxy corn, wheat,	PL-GFC 300A + 2X4000A	0.1 M NaCl	Amylopectin amylose

(table continued on next page)

(table continued from previous page)

Polymer	Columns	Mobile phase	Comm
amylopectin, amylose			separation
Various wheats	Ultrahydrogel 250	H_2O	Characterizat
Various corns	Shodex KS-806 + KS-804 + KS-803 + KS-802	H_2O	Temperature solubility
Amylose, dextran	Porous glass 370A	95% DMSO/5% H_2O	MW, univers calibration
Amylose, dextran	Porous silica gel, 100A + 100–200A + 200–400A	DMSO	MW, univers calibration
Hydroxyethylated, acid-treated, oxidized starch	Bondagel E-1000 + E-125 or SynChropak 1000A + 2 × 500A	DMSO and H_2O mixture with or without buffer	MW, operati study
Hydroxyethylated, oxidized starch	SynChropak 2X500A + 100A	DMSO or DMSO and H_2O mixture with or without buffer	Operation pa study
Wrinkled pea, corn, potato	Sephacryl S-200	40% DMSO and 60% H_2O	Structure bef lintnerisation
Pea (wrinkled, smooth)	Sephacryl S-200	40% DMSO and 60% H_2O	Structural characterizat
	Sephacryl S-1000	40% DMSO and 60% H_2O	MW
	Sepharose CL-2B	0.1 M KOH	
Various corns	Bio-glass 2500 + 500 + 200	DMSO	MW

(Table continued on next page)

(Table continued from previous page)

Table 1 (Continued)

Polymer	Columns	Mobile phase	Comm
Potato amylose, corn amylopectin, tapioca, others	Diol 2X1000A + 100A	DMSO with 15% methanol and 0.5 M ammonium acetate	SEC-LALLS calibration, M
Wheat, corn	Bondagel E-linear + E-1000	DMSO	Amylopectin ratio
Wheat	Zorbax PSM 60s	DMSO	Structural characterizat
Wheat (native and extruded)	Bondagel E-125 + E-500 + E-1000	DMSO	Characterizat
Corn, waxy corn, modified starch (corn, potato)	Bondapak E-High + E-linear + E-1000 + E-125	DMSO or DMSO with 0.03 M $NaNO_3$	Operation pa study, MW
	Aquapore OH-4000 + OH-500 + OH-100 μ-Styragel 500	DMSO + 0.3 M $NaNO_3$ DMSO + 0.03 M $NaNO_3$	
Modified corn	PLgel Mixed	DMSO (0–0.03 M $NaNO_3$)	Eluant ionic effect, MW
Corn	Toyopearl HW-75F	50 mM NaCl	LALLS, stru characterizat
Rice amylose	TSK G6000 PW + G4000 PW + G3000 PW	50 mM phosphate buffer + 0.02% NaN,	LALLS, stru characterizat

(table continued on next page)

(table continued from previous page)

Polymer	Columns	Mobile phase	Comm
Amylopectin (tapioca, potato, kuzu, waxy rice)	TSK G3000 SW + 2XG2000 SW	0.1 M phosphate buffer + 0.02% NaN_3	LALLS, stru characterizat
Rice amylose	TSK G6000 PW + G4000 PW + G3000 PW	0.1 M phosphate buffer + 0.02% NaN_3	LALLS, stru characterizat
Debranched amylopectin (rice, corn, taro, wheat, kuzu, yam, tulip, lotus, potato, lily)	TSK G2000 PW + 2XG3000 PW	10 mM phosphate buffer + 0.02% NaN_3	LALLS, stru
Corn, amylose	Fractogel TSK 40S + 65F	0.5 N NaOH	LALLS, univ calibration, b
Amylopectin, amylose, corn	Fractogel TSK 40S + 65F	0.5 N NaOH	LALLS, amy amylose ratic
Dextran	Fractogel TSK HW-65F + HW-40S	0.42 N NaOH	Universal cal
Sulfonated styrene, polyethylene glycol			Viscometer, development

(Table continued on next page)

(Table continued from previous page)

Table 1 (Continued)

Polymer	Columns	Mobile phase	Comm
Pullulan, dextran, polyethylene oxide	Ultrahydrogel 500A + 1000A + 2000A Shodex OH-Pak B-803 + B-804 + B-805 + B-806	LiOH (0.1 M-0.5 M), 0.1 M $NaNO_3$, 0.1 M NaCl, 0.1 M Na_2So_4	LALLS, visc universal cali operation par
Pullulan, polyethylene oxide	TSK G1000 PW + G2000 PW + G3000 PW + G4000 PW + G5000 PW	0.1 N $NaNO_3$ + 20% CH_3CN	Universal cal viscometer, I
Corn	Ultra-Styragel 10^3 + 10^4 + 10^5 + 10^6	DMAc with 0.5% LiCl	Extrusion fra
Maltodextrin, cyclodextrin, cellodextrin, gentodextrin	BioGel P-2	H_2O	Temperature effect on rete
Starch and oligosaccharides	BioGel P-2	H_2O	Automated c analysis
Starch and its related oligosaccharides	BioGel P-2	0.1 M NaCl	Characterizat molecular sh retention
Oligosaccharides (amylose, dextran,	BioGel P-2	0.1 M NaCl	Separation a identification

(table continued on next page)

(table continued from previous page)

Polymer	Columns	Mobile phase	Comm
Elsinan, Nigeran, Lichenan)			
Glucose oligomer	BioGel P-2	H_2O	Large-scale fractionation
Synthetic amylose, maltodextrin, pullulan, dextran	Superose 6	H_2O or 0.02 M NaCl	MW, eluant s
Kuzu amylopectin	BioGel P-30	H_2O	Characterizat
Potato amylopectin, enzyme treated	BioGel P-60 or P-30	H_2O	Fractionation phosphate gr
Amylose (potato, sweet potato, tapioca, kuzu, lily)	Toyopearl HW-75F	50 mM NaCl	Purity and str characterizat
Amylopectin (various rices)	TSK G3000 SW + 2XG2000 SW	0.1 M phosphate buffer + 0.02% NaN_3	LALLS, stru characterizat
	Toyopearl HW-75F	50 mM NaCl	
Sweet potato	Toyopearl HW-75F	50 mM NaCl	Structural characterizat
	BioGel P-30	H_2O	
Lily	BioGel P-30	H_2O	Structural characterizat
Dextran	TSK G6000 PW + G5000 PW + G4000 PW	H_2O or 0.1 M KNO_3	LALLS, MW effect

(Table continued on next page)

(Table continued from previous page)

Table 1 (Continued)

Polymer	Columns	Mobile phase	Comments[a]	F
Dextran	CPG-10 75A–729A	H_2O or 0.05 M phosphate buffer	LALLS, MW, eluant salt effect	
Dextran, sulfonated polystyrene	Porous glass 1250A + 75A	0.2 or 0.8 M Na_2SO_4	LALLS, universal calibration, MW	
Wheat amylopectin	Sepharose CL-2B + CL-4B	0.01 M NaOH + 0.02% NaN_3	Debranching study	
	BioGel P-10	0.02% NaN_3		
	BioGel P-4	0.02% NaN_3		
Various corn starches	Sephadex G-75	0.02 N NaOH + 0.2% NaN_3	Structural characterization	
Low DE, maltodextrins	BioGel P-2		Characterization	
Oligosaccharide	BioGel P-2	H_2O	Autoanalytical system	
Wheat, corn	Sepharose CL-6B	0.25 N NaOH	Amylopectin-amylose ratio	
Amylose, potato amylopectin	μHydrogel 250 + 2000	50 mM NaOH	On-line iodine complexing detection	

(table continued on next page)

(table continued from previous page)

Polymer	Columns	Mobile phase	Comm
Amylose (rice, corn)	TSK G6000 PW + G4000 PW + G3000 PW	Phosphate buffer + 0.02% NaN_3	LALLS, stru
	Toyopearl HW-65F + HW-60F	H_2O	
Lotus	Asahipak GS-320X2 + TSK Guard + TSK G2000 SW + TSK Guard	0.1 M phosphate buffer + 0.02% NaN_3	LALLS, MW characterizat
	TSK G6000 SW + G4000 SW + G3000 SW	0.1 M phosphate buffer + 0.02% NaN_3	
Pullulan	TSK G3000 PW + G6000 PW	Sodium acetate buffer	LALLS, visc
Synthetic amylose, potato amylose, dextran	Sepharose CL-4B	H_2O	MW
Wheat amylopectin	Asahipak GS-320 + TSK Guard + TSK G2000 SW + TSK Guard	0.1 M phosphate buffer + 0.02% NaN_3	LALLS, stru characterizat

[a]Most of the structural characterizations involved enzyme degradation. MW, molecular weight.

is often added to prevent the growth of microorganisms. There is no systematic study in the literature to suggest which mobile phase is the best. For molecular weight determination, water is probably not a good choice. Praznik et al. found that amylose samples gave different elution profiles when the eluant was changed from pure water to 0.02 M KCl (45). A sample run in pure water usually shows an additional early peak (see Figure 1). The early peak was attributed to the association of amylose molecules. Another explanation is possible. The Hizukuri group found that many starches contain phosphate functional groups (30,46–53). Figure 2 is an elution curve of a debranched sweet potato run with pure water on a BioGel P-30 column. Fraction F-1 was found to contain most of the phosphorus of the original sample. Some molecules of F-1 are smaller

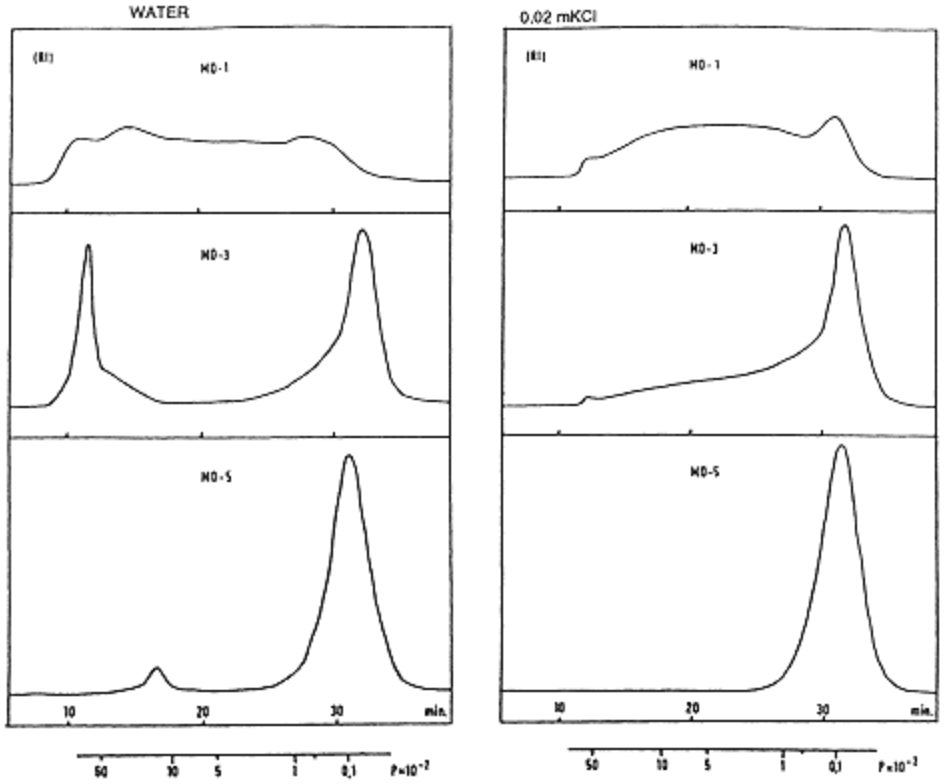

Figure 1
Effect of salt in the mobile phase on the elution profiles of three maltodextrins (45). Column: Superose 6 HR 10/30. Mobile phase: water or 0.02 M potassium chloride. (Reprinted with permission from the publisher, VCH Verelagsgesellschaft mbH, D-6940, Weinheim, Germany.)

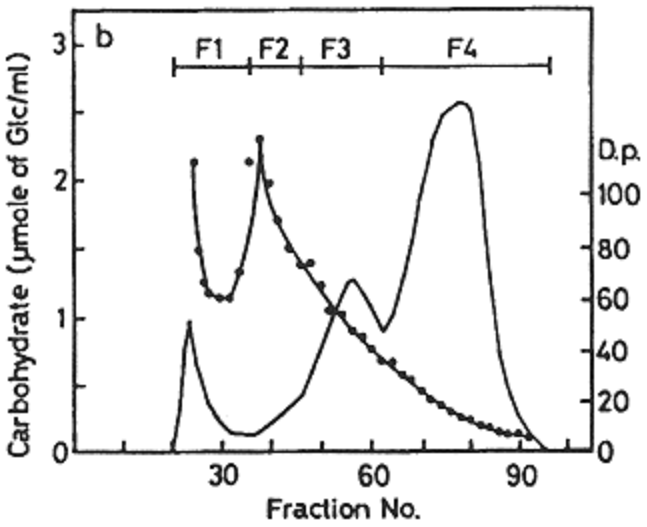

Figure 2
Elution curve for debranched sweet potato with a BioGel P-30 column and water as eluant (52). [Reprinted with permission from the publisher, VCH Verlagsgesellschaft mbH, D-6940, Weinheim, Germany.]

than the late-eluted species. Ion exclusion may be the cause of this nonsize separation of starch molecules. Dextran shows a similar elution behavior when pure water is used as the eluant (54,55).

Sodium hydroxide solution is a frequently used mobile phase in the aqueous starch SEC system. The concentrations range from 0.005 to 0.5 N. The optimum concentration may depend on the packing material used. In aqueous SEC for sulfonated polystyrene, sodium sulfate in the mobile phase can be as high as 0.8 M for porous glass bead columns (56). For Bondagel or Aquapore columns, the salt concentration must below 0.05 M (57).

Detection

Many aqueous SEC users use colorimetric reactions and a differential refractometer to monitor the progress of the separation. The color reagents include phenol-H_2SO_4 (58,59), anthrone-H_2SO_4 (50), orcinol-H_2SO_4 (60,61), and cysteine-H_2SO_4 (62). Most of the colorimetric detections were off-line. The eluants were collected and mixed with the reagent and the absorbance of the mixture determined by a spectrophotometer. On-line colorimetric detection has been used (61,62). Figure 3 shows colorimetric detection using orcinol-H_2SO_4 as the reaction reagent. Colorimetric detection may be sensitive, but all colorimetric reagents involve strong

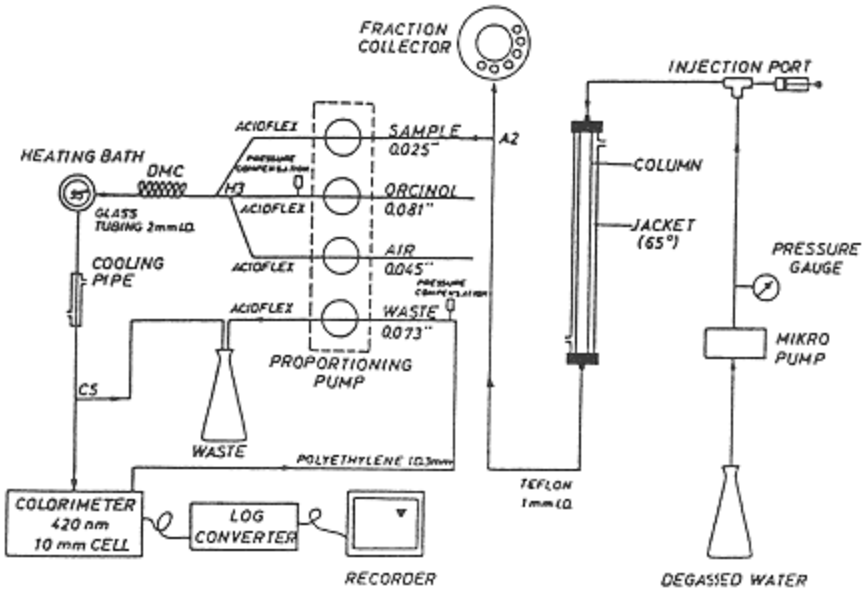

Figure 3
Colorimetric detection system for SEC (61). (Reprinted with permission from the publisher, Elsevier Science Publishers B.V., Netherlands.)

acids, which is not very desirable. The modern refractive index (RI) detector is sensitive enough for most SEC application.

Off-line iodine complexing is a frequently used method to characterize the SEC fractions. Amylose-iodine and iodine-amylopectin complex have a maximum absorbance at about 658 and 546 nm, respectively. Recently, Suortti and Pessa (63) demonstrated that is is possible to do iodine complexing detection on-line, such as that shown in Figure 4. Photodiode array (PDA) ultraviolet (UV) detectors are readily available now. PDA can take the UV spectrum of the eluant on the fly. The information is stored in the computer. After the run, a contour plot or three-dimensional plot can be shown on the screen or printed out. Iodine complexing with PDA detection can be a very useful technique for characterizing starch samples.

Multiple-Detector SEC and Its Application

Light-scattering and intrinsic viscosity measurement are two popular methods for determining the absolute molecular weight of polymers. Figure 5 shows the SEC system with a low-angle laser light-scattering detector used by Hizukuri

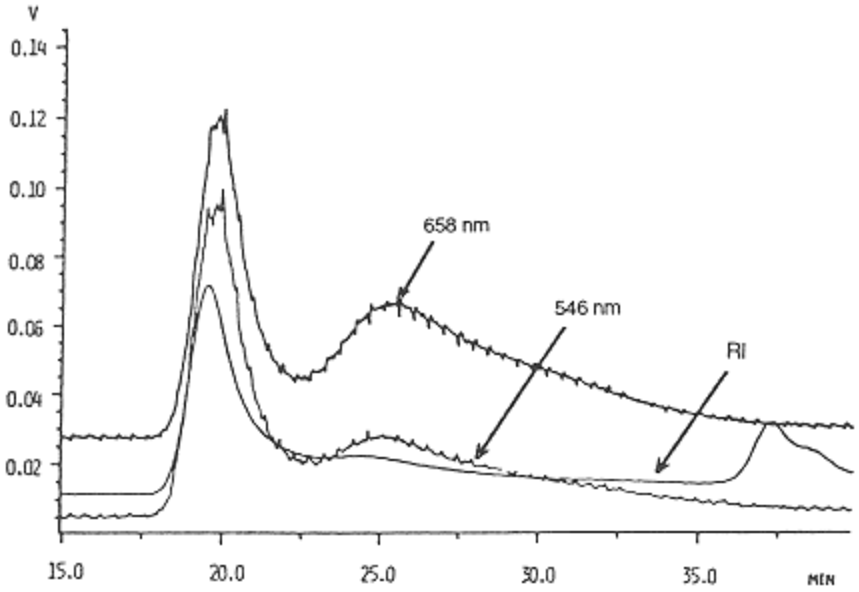

Figure 4
Chromatogram of potato amylopectin. Detection with a refractometer detector (RI) and by spectrophotometry after complexation with iodine (63). (Reprinted with permission from the publisher, Elsevier Science Publishers B. V., Netherlands.)

and Takagi (9,34). Equation (1) is used to calculate the weight-average molecular weight at a given retention time:

$$M_w = k' \frac{\mathrm{LS/RI}}{dn/dc} = k \frac{\mathrm{LS}}{\mathrm{RI}} \quad (1)$$

where LS (light scattering) and RI are the LALLS and refractometer responses, respectively, *dn/dc* is the refractive index increment of the polymer, *k'* is the instrument constant, and *k* is the product of *k'* and *dn/dc*. The value of *k* is calculated from the detector responses of a standard polymer that has the same *dn/dc* as the sample. Narrowly distributed pullulans were said to be suitable standards. Figure 6a is an elution curve of isoamylase-debranched amylopectin from waxy rice. The instrument is able to determine chain length down to about 10 glucose units (Figure 6b). Many types of starches have been characterized by this unit (9,30–34,50,64,65,69).

Yu and Rollings used an LALLS-equipped SEC system (TSK HW-65F, 40S, 0.5 N NaOH mobile phase) and found that universal calibration was valid for dextran, amylose, and sulfonated polystyrene under their conditions (35a). In another study, they proposed to use a SEC system with LALLS and a visco-

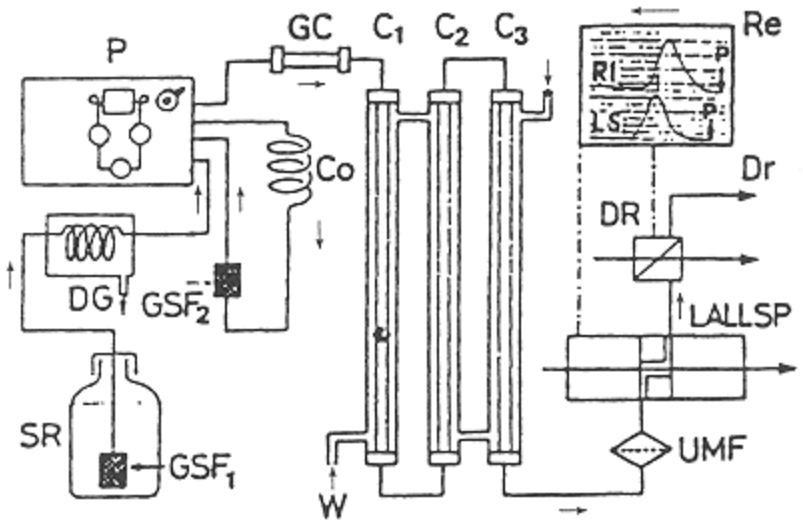

Figure 5
SEC instrument with a LALLS detection system (9). Outline of instrumentation (Toyo Soda Co., unless stated otherwise): SR, solvent reservoir (3.5 liters); GSF_1, sintered stainless steel filter (Umetani Seiki Co., Model SYF); DG, degasser (Elma Optical Works, Model ERC-3310); P, high-speed liquid chromatograph (Model HLC-803D) with a 500 µl sample loop; Co, helical stainless steel tube (0.2ϕ × 6 m); GSF_2, sintered stainless steel filters (Umetani Seiki Co., Model SLF); GC, guard column (Model TSK GSWP, 7.5 × 100 mm); C_1, C_2, and C_3, packed columns (each 7.5 × 600 mm) of TSKgel G3000PW, G4000PW, and G6000PW,respectively; W, circulating water; UMF, ultramembrane filter (two Millipore filters, Type LS-WP 01300, pore size 1 µm, in series); LALLSP, low-angle laser light-scattering photometer (Model LS-8); DR, differential refractometer (Model RI-8); Re, double-pen recorder; P, pen position; Dr, drain; RI and LS, differential refractometer and low-angle laser light-scattering photometer curves, respectively. (Reprinted with permission from the publisher, Elsevier Science Publishers B. V., Netherlands.)

metric detector to determine the weight fraction of branched polymer in a starch sample according to the equation (35b)

$$W_{b,v} = \frac{g_{v(m)}\, g'_{v(m)} - g_{v(m)} - g'_{v(m)} + 1}{g_{v(m)}\, g'_{v(m)} - 2g'_{v(m)} + 1}$$

where $g_{v(m)}$ and $g'_{v(m)}$ are two branching parameters and are defined as

$$g_{v(m)} = \left(\frac{[\bar{\eta}]_m}{[\eta]_\epsilon}\right)_v$$

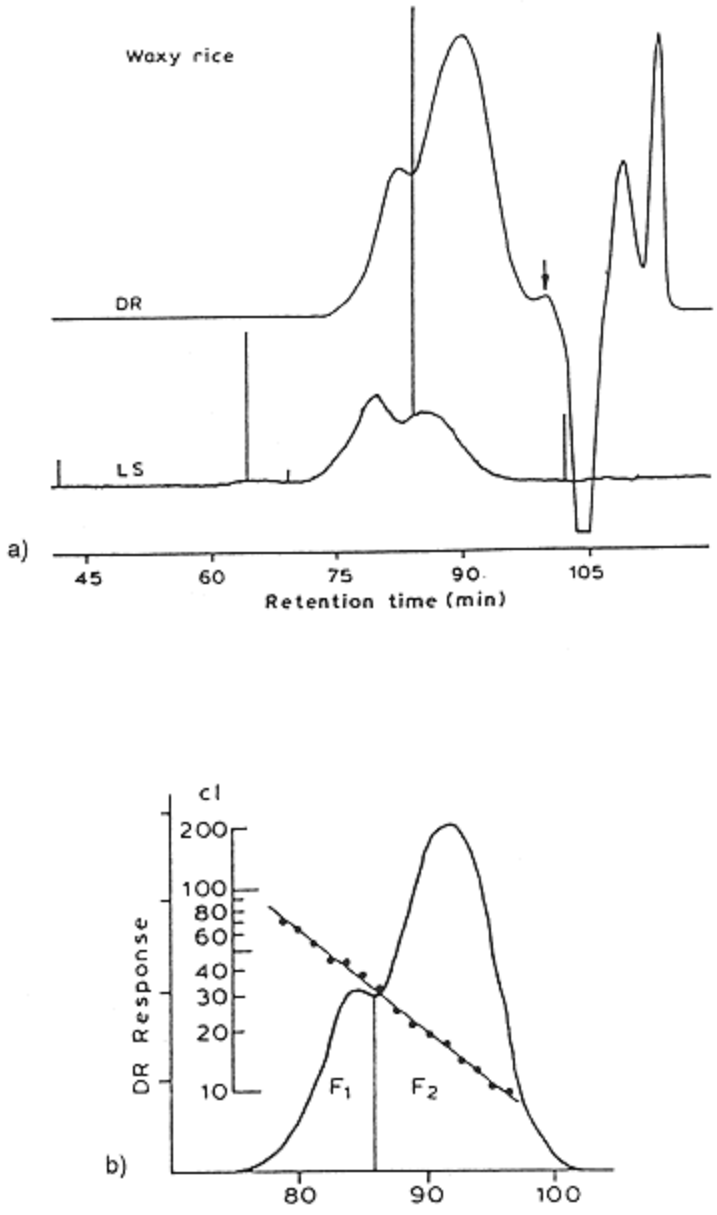

Figure 6
(a) SEC chromatogram of debranched waxy rice with LALLS and refractometer detector (RI) detection. (b) Chain length (CL) versus retention time. (Reprinted from Reference 34 with permission from the publisher, Elsevier Science Publishers B. V., Netherlands.)

the ratio of the intrinsic viscosity of the mixture $\overline{\eta}_m$ and the intrinsic viscosity of the linear polymer $[\eta]_l$ at retention volume *v*, and

$$g'_{v(m)} = \left(\frac{\mathbf{M}_l}{(\overline{M}_w)_m}\right)_v$$

the ratio of the molecular weight of linear polymer M_l and the weight-average molecular weight of the mixture $\overline{M}_{w_m}$ at retention volume *v*.

In principle, the branching parameters $g_{v(m)}$ and $g'_{v(m)}$ can be measured simultaneously by on-line viscometer and LALLS, respectively. The weight fraction of the branched portion in a mixture can be calculated.

Dextran and pullulan are two commonly used calibration standards. Van Dijk et al. (54), Sommermeyer et al. (66), Lesec and Volet (37), and Huber (13) used SEC with multiple detectors to study the elution behavior of these two polysaccharides under various experimental conditions.

Organic-Phase SEC for Starch Characterization

Dimethylsulfoxide or Its Mixture as the Mobile Phase

Packing Materials and Mobile Phase

The packing materials used in a DMSO SEC system include porous glass, silica gel, diol, Bondagel, Sephacryl, and cross-linked polystyrene (the references are listed in Table 1). Porous glass was found to absorb the impurity from DMSO if the solvent is not pure (17). The adsorption eventually changes the character of the column. Samples run on diol columns (Aquapore, DMSO and 0.03 sodium nitrate, 80° C) usually show a broad negative peak at the end of the run. The packing material may interact with the impurity of the sample, but there is no indication that this kind of interaction affects the analysis of starch under the experimental conditions (28). Cross-linked polystyrene columns can last many years if a prefilter (2 μm frit) and a guard column are used.

The addition of salt to the mobile phase has a great effect on the molecular weight determination of starch samples (19,20,28,29). Figure 7 shows the ionic strength effect on the elution curve of a corn starch sample. In a salt-free mobile phase, the sample shows an additional early peak or has a shorter retention time. This is an indication of the change in molecular size or ion exclusion effect. Similar behavior is also observed with waxy corn starch, dextran, and some synthetic amyloses. The relative molecular weights calculated from three salt-containing mobile phases are very close, but those from pure DMSO are much higher. The amount of salt needed to suppress the ionic interaction may depend on how many phosphate groups are in the sample molecules. For waxy corn and corn starches, 0.0003 M sodium nitrate is enough to eliminate this problem

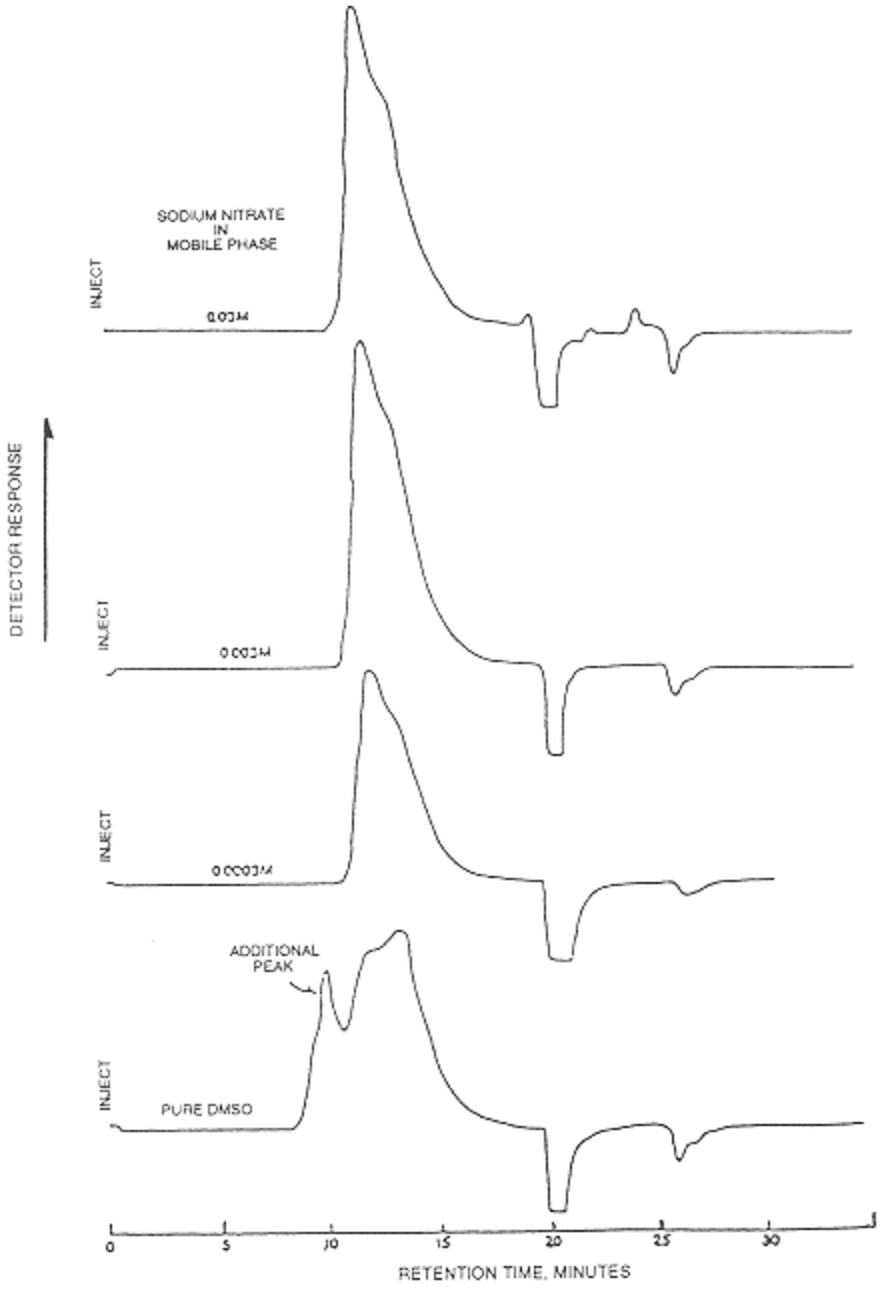

Figure 7
Effect of ionic strength on the elution profile of a modified corn starch with DMSO as the mobile phase at 80°C. The columns are Plgel Mixed (29).
(Reprinted with permission from the publisher, John Wiley & Sons.)

(29). The phosphate groups in starch are found mostly in the amylopectin portion. A mobile phase without salt may be suitable for the determination of amylose molecular weight or amylose percentage in a sample, but it should be used with caution.

Table 1 shows that the water content in a DMSO mobile phase varies from zero to 40%. It is advantageous to use a mobile phase that is a good solvent for starch. Jackson studied the solubility of corn starches in a mixture of DMSO and water and found that maximum solubility was obtained when DMSO with 10% water was used (16). Solubility dropped sharply in pure DMSO. DMSO with 0.03 M $NaNO_3$ has been used as the mobile phase for many years in the author's laboratory (28,29). Table 2 shows the results of a study of the solubility of waxy corn granules, corn granules, and enzyme-degraded waxy corn in DMSO and 0.03 M $NaNO_3$ and in DMSO, 10% water, and 0.03 M $NaNO_3$. The solutions were heated at 80°C for 54 h and then analyzed by SEC. The peak areas were used as measurements of the solubility of starches in the two solvent systems. The results indicate that both solvents are about equal in dissolving starch samples.

Sample Preparation

The is no standard method for preparing the sample solution. Some of the sample preparation methods reported in the literature are listed here.

Young (23): 0.1% starch in DMSO heated at 150°C for 1 h

Table 2 Solubility of Waxy Corn, Corn, and Enzyme-Degraded Waxy Corn in a DMSO-Water Mixture[a]

Sample	Concentration (mg/ml)	Relative area/mg
Corn		
DMSO, 0.03 M $NaNO_3$	1.20	11,545
DMSO, 10% H_2O, 0.03 M $NaNO_3$	1.20	13,068
Waxy corn		
DMSO, 0.03 M $NaNO_3$	1.20	10,750
DMSO, 10% H_2O, 0.03 M $NaNO_3$	1.20	10,073
Enzyme-degraded waxy corn		
DMSO, 0.03 M $NaNO_3$	2.39	38,546
DMSO, 10% H_2O, 0.03 M $NaNO_3$	2.42	37,689

[a]SEC conditions: instrument, Waters ALC/GPC-150C; column, two PLgel mixed; mobile phase, DMSO with 0.03 M $NaNO_3$; temperature, 80°C for injector and column compartments; injection volume, 150 µl.

Stone and Karsow (20): Method 1: 0.5% of starch solution in DMSO heated at 100°C for 30 minutes, diluted to 0.125% with appropriate solvent to match the mobile phase, and filtered through a 0.5 μm filter; method 2: 10% starch slurry heated with a jet cooker and the paste diluted to 0.5% with DMSO

Kobayashi et al. (25,26): 40 mg starch in 2 ml of 90% DMSO heated in a boiling water bath for 5 minutes and the solution centrifuged at 3000 *g* for 5 minutes

Colonna and Mercier (22): 2–3 mg starch in 25 ml DMSO, shaken for 1 h at room temperature

Most starch material, except granular starch, is readily dissolved in DMSO at 80°C within 1 h. For some samples a longer heating time may be necessary. The time required can be found by analyzing the sample periodically during the heating period until constant results are obtained. The starch-DMSO solutions are quite stable. At 80°C, the solutions are stable for at least several days. Granular starches do not completely dissolve in DMSO at 80°C even if the heating period is extended to several weeks. The solution is cloudy, but it passes through the SEC column with a 2 μm frit. The particles in solution appear to be very fragile. The shear force of the flow path gradually degrades the particles, and the system pressure eventually returns to normal. Shaking, stirring, or heating at a higher temperature may increase the solubility of the granules, but degradation may occur (67). Heating under an inert atmosphere may prevent the degradation.

Injector Temperature Effect

When an autosampler is used in a SEC system, the temperature of the injector may affect the analytical results for some samples. Figure 8 shows the elution profiles of a corn starch sample analyzed with the Waters ALC/GPC-150C. The columns were kept at 80°C. The sample injected at 80°C shows three distinguished peaks. A similar elution profile is obtained when the sample solution is shaken and injected immediately at 40°C. The first peak is reduced to a shoulder when the sample is injected at 40°C or below. The results suggest that some starch molecules may settle at the bottom of the sample vial when the sample solution is kept at room temperature.

Absolute Molecular Weight Determination by DMSO SEC

Dintzis and Tobin used a porous glass column with a 95% DMSO and 5% H_2O mobile phase and found that universal calibration was valid for dextran and amylose (17). Universal calibration was also found to be valid for these two polysaccharides with deactivated silica gel and a pure DMSO system (18).

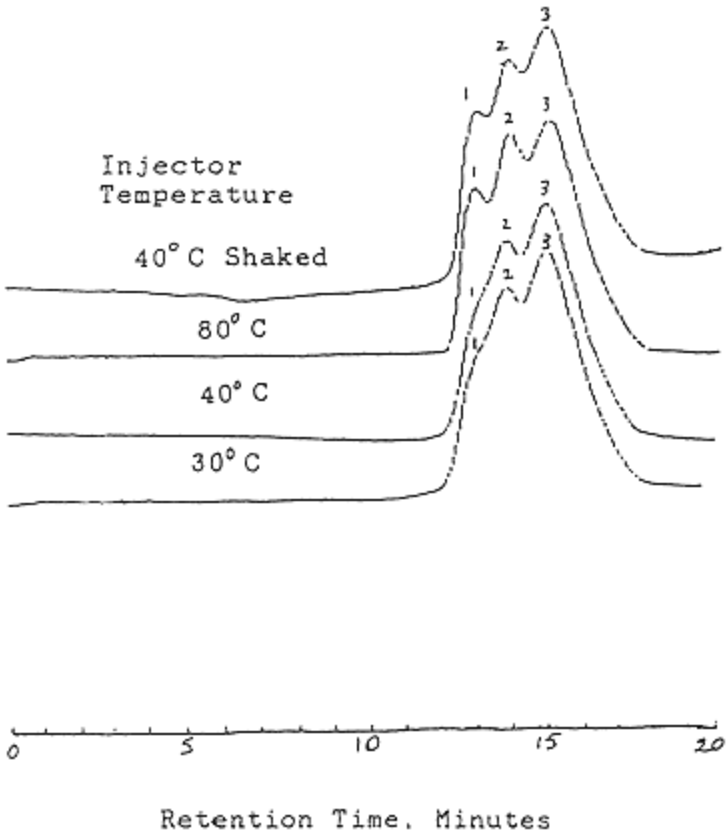

Figure 8
Effect of injector temperature on SEC chromatogram of a nongranular corn starch (unpublished data). Instrument, Waters ALC/GPC-150C; column, two Plgel Mixed; mobile phase, DMSO + 0.03 M sodium nitrate; temperature of column compartment, 80°C; flow rate, 1 ml/minute; injection volume, 150 µl; sample concentration, 0.25%.

Salemis and Rinaudo used an on-line LALLS to determine the molecular weights of various starches (24). A diol column and a mobile phase of DMSO, 15% methanol, and 0.5 M ammonium acetate were used. One of the starches they analyzed was a potato amylose. This is a commercial product. The weight-average molecular weight they found was 2.83×10^5. This product was also analyzed by Praznik and Eberman using a Sepharose column, water as eluant, and synthetic amylose or pullulan calibration (68) and by the author using a PLgel Mixed column, a DMSO and 0.03 M $NaNO_3$ mobile phase, and dextrancalibration. Both groups obtained the same weight-average molecular weight of 3.2×10^5.

Figure 9 is the universal calibration curve of a SEC system equipped with a differential viscometric detector (Viscotek Model 100). The calibration standards are narrowly distributed pullulans. Two PLgel mixed-bed columns are used. The calibration curve is not a straight line. It concaves slightly upward at the high end. Table 3 shows the preliminary results of the molecular weights of some dextran and starch samples calculated from Figure 9. The starch molecular weights, which are determined by static light scattering, are not all in agreement with those from SEC-viscometry, but the overall results are encouraging.

Dimethylacetamide as the Mobile Phase

Dimethylacetamide (DMAc) with lithium bromide was used by Wasserman and Timpa to study the effect of extrusion on the molecular weight of corn starch (39). The instrument has an on-line viscometric detector and is run at 80°C.

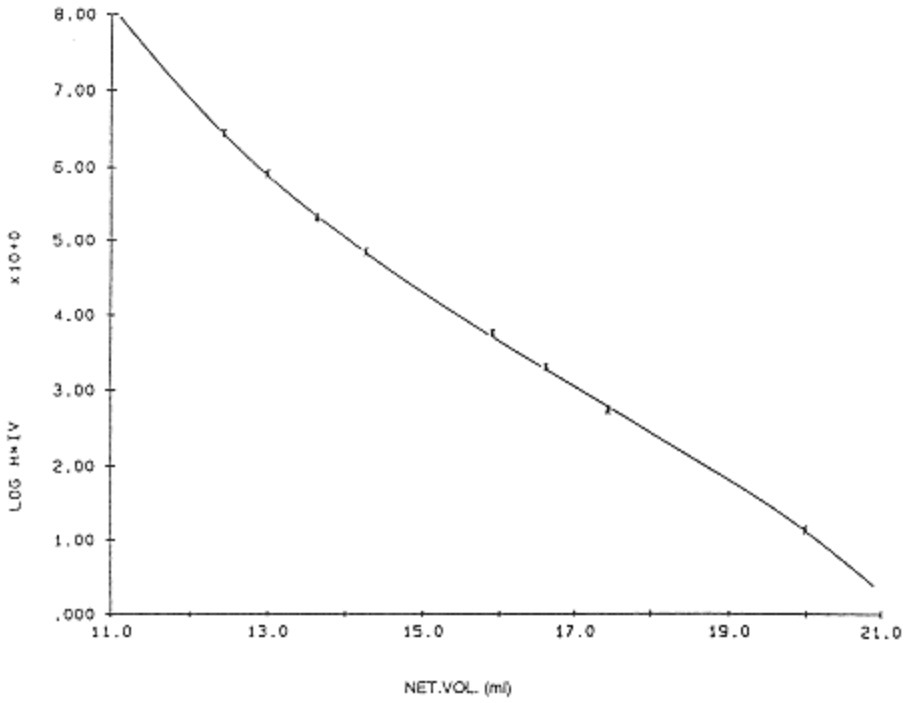

Figure 9
Universal calibration curve established with a Viscotek Model 100 differential viscometer detector. Calibration standards are narrowly distributed pullulans at 0.12% concentration. All other conditions as in Figure 8.

Table 3 Comparison of the Molecular Weights Determined by SEC-Viscometry and Suppliers' Data[a]

	SEC-viscometry		Supplier[b]	
Sample	M_w	M_n	M_w	M_n
Dextran				
T-500	5.56×10^5	1.89×10^5	5.11×10^5	1.92×10^5
T-40	3.64×10^4	2.40×10^4	3.95×10^4	2.31×10^4
T-20	1.93×10^4	1.45×10^4	2.23×10^4	1.50×10^4
Starch[c]				
Waxy corn 1	2.8×10^5	—	2.8×10^5	
Waxy corn 2	4.5×10^5	—	4.2×10^5	
Corn 1	9.7×10^5	—	9.4×10^5	
Waxy corn 3	3.8×10^5	—	5.6×10^5	
Corn 2	6.8×10^5	—	4.9×10^5	
Corn 3	1.5×10^6	—	2.8×10^6	

[a]Dextran concentration ≃ 1.20 mg/ml; starch concentration ≃ 2.50 mg/ml. Other conditions as in Figure 8.

[b]Dextran: Pharmacia, Piscataway, NJ. Starch: Natural Polymer Research Group, National Starch and Chemical Company, Bridgewater, NJ.

[c]Molecular weights of samples were determined by a low-angle laser light-scattering device in pure DMSO.

Samples were heated and stirred at 150°C for 2 h and cooled to 100°C, LiBr was added, and the mixture shaken for 1–2 h, diluted, and analyzed.

Comparison of Aqueous SEC, DMSO SEC, and DMAc SEC for Starch Characterization

Most SEC papers published in scientific journals for starch characterization use an aqueous mobile phase. Because of the instability of the starch in aqueous solution, the sample is usually analyzed within 1 h after it is prepared. It is difficult to use an autosampler in an aqueous SEC system.

Starch DMSO solutions are very stable. Except native starches, most samples dissolve in DMSO within 3 days or less at 80°C. Sample preparation is minimal. Repeat injections are possible. With an

autosampler, samples can be run automatically.

DMAc is a new solvent for starch SEC analysis. It has not yet been used widely. Polystyrene is soluble in DMAc. This solvent may have the advantage of using polystyrene to construct the universal calibration curve. Polystyrene standards are cheaper, and their molecular weight can be as high as 21 million,

which is much higher than that of commercially available polysaccharide standards.

DMSO and DMAc are readily absorbed by skin. Precaution should be taken when using these solvents.

Application of SEC Starch Analysis

As shown in Table 1, many investigators use SEC to study the structure of native or modified starches. In industry, most starch products have been treated with acids, enzymes, chemicals, or physical means to obtain the desired properties. It is important to know the molecular structure, the molecular weights, and the molecular weight distribution of the samples after treatment. Viscosity, gel formation, and film formation are some of important factors for starch applications. With modern SEC instruments, we may be able to find how these factors are affected by the molecular structure, the molecular weight, and the molecular weight distribution of samples.

Starch molecules are very interesting polymers. They are either highly branched amylopectin with an extremely high molecular weight, or they are lightly branched amylose with a moderate molecular weight. Both molecules can be degraded by enzymes. Some enzymes attack only branch points, and some enzymes attack only from the end of the branches. After the debranching reaction, the degree of polymerization of the product can be precisely determined by modern HPLC or SEC techniques. Starch molecules can be model polymers to study how the branch density and the branch length affect SEC separation. Because the molecular weight of amylopectin is well over 10 million, it can be an ideal polymer to determine the void volume of SEC columns.

Conclusion

For degraded starches, it is possible to determine relative molecular weights routinely by using the SEC systems discussed in this chapter. By coupling the SEC with light scattering and viscometric detectors, it is possible to determine the absolute molecular weight, molecular size, and the branch density of samples. For native starches, the problem of preparing the sample solution must be overcome. Another problem for the SEC characterization of native starch is that the molecular weight of native starch may be simply too high to be handled by any SEC column.

Acknowledgments

The author acknowledges Dr. C.W. Chiu for many helpful comments and discussion; the assistance of Mr. R.R. Ciccihino in the preparation of the draft; and the permission of the National Starch and Chemical Company to publish this review article.

References

1. W. Banks, R. Geddes, C.T. Greenwood, and I.G. Jones, Starke, 8, 245 (1972).

2. A.H. Young, in Starch: Chemistry and Technology (R.L. Whistler, J.N. Bemiller, and E.F. Paschall, eds.), Academic Press, New York, 1984, p. 252.

3. S.C. Churms, Advances in Carbohydrate Chemistry, 25, 13 (1970).

4. R.L. Whitler and A.K.M. Anisuzzaman, In Methods in Carbohydrate Chemistry, Vol. VIII (R.L. Whistler and J.N. BeMiller, eds.), Academic Press, New York, 1980, p. 45.

5. W. Parznik, Starch/Starke, 38, 292 (1986).

6. A. Corona and J.E. Rollings, Separation Science and Technology, 23, 855 (1988).

7. M. Rinaudo and B. Tinland, Journal of Applied Polymer Science, 48, 19 (1991).

8. J. Kruger and B.A. Marchylo, Cereal Chemistry, 59, 488 (1982).

9. S. Hizukuri and T. Takagi, Carbohydrate Research, 134, 1 (1984).

10. D.S. Jackson, M.H. Gomez, R.D. Waniska, and L.W. Rooney, Cereal Chemistry, 67, 529 (1990).

11. D.S. Jackson, C. Choto-Owen, R.D. Waniska, and L.W. Rooney, Cereal Chemistry, 65, 493 (1988).

12. C. Takeda, Y. Takeda, and S. Hizukuri, Cereal Chemistry, 66, 22 (1989).

13. A. Huber, Journal of Applied Polymer Science, 48, 95 (1991).

14. J.F. Kennedy, Z.S. Rivera, L.L. Lloyd, and F.P. Warner, Starch/Starke, 44, 53 (1992).

15. S. Endo, K. Okada, and S. Nagao, Nippon Shokuhin Kogyo Gakkaishi, 38, 7 (1991).

16. D.S. Jackson, Starch/Starke, 43, 422 (1991).

17. F.P. Dintzis and R. Tobin, Journal of Chromatography, 88, 77 (1974).

18. J.A.P.P. Van Dijk, W.C.M. Henkens, and J.A.M. Smit, Journal of Polymer Science, 14, 1485 (1976).

19. M. Papantonakis, Tappi, 63, 65 (1980).

20. R.G. Stone and J.A. Krasowski, Analytical Chemistry, 53, 736 (1981).

21. P. Colonna, A. Buleon, M. Lemaguer, and C. Mercier, Carbohydrate Polymers, 2, 43 (1982).

22. P. Colonna and C. Mercier, Carbohydrate Research, 126, 233 (1984).

23. A.H. Young, In Starch: Chemistry and Technology (R.L. Whistler, J.N. Bemiller, and E.F. Paschall, eds.), Academic Press, New York, 1984, p. 257.

24. P. Salemis and M. Rinaudo, Polymer Bulletin, 11, 397 (1984).

25. S. Kobayashi, S.J. Schwartz, and D.R. Lineback, J. Chromatography, 319, 205 (1985).

26. S. Kobayashi, S.J. Schwartz, and D.R. Lineback, Cereal Chemistry, 643, 71 (1986).

27. P. Reinikainen, T. Suortti, J. Olkku, Y. Malkki, and P. Linko, Starch/Starke, 38, 20 (1986).

28. J. Chuang and R.J. Sydor, Journal of Applied Polymer Science, 34, 1739 (1987).

29. J. Chuang, Journal of Applied Polymer Science, 45, 227 (1990).

30. Y. Takeda, T. Shitaozono, and S. Hizukuri, Starch/Starke, 40, 51 (1988).

31. Y. Takeda, S. Hizukuri, and B.O. Juliano, Carbohydrate Research, 186, 163 (1989).

32. S. Hizukuri, Carbohydrate Research, 147, 342 (1986).

33. Y. Takeda, S. Hizukuri, and B.O. Juliano, Carbohydrate Research, 148, 299 (1986).

34. S. Hizukuri, Carbohydrate Research, 141, 295 (1985).

35. (a) L. Yu and J.E. Rollings, Journal of Applied Polymer Science, 33, 1909 (1987); (b) 35, 1085 (1988).

36. G. Callec, A.W. Anderson, G.T. Tsao, and J.E. Rollings, Journal of Polymer Science, 22, 287 (1983).

37. J. Lesec and G. Volet, Journal of Liquid Chromatography, 13, 831 (1990).

38. D.J. Nagy, Journal of Liquid Chromatography, 13, 677 (1990).

39. B.P. Wasserman and J.D. Timpa, Starch/Starke, 43, 389 (1991).

40. A. Heyraud and M. Rinaudo, Journal of Chromatography, 166, 149 (1978).

41. J.F. Kennedy, J.E. Fox, and J.C. Skirrow, Starch/Starke, 32, 309 (1980).

42. J.F. Kennedy, D.L. Stevenson, and C.A. White, Starch/Starke, 40, 396 (1988).

43. J.F. Kennedy, D.L. Stevenson, and C.A. White, Starch/Starke, 41, 72 (1989).

44. H. Sloan, B. Kerzner, and C. Serckel, Preparative Biochemistry, 14, 245 (1984).

45. W. Praznik, R.H.F. Beck, and E. Berghofer, Starch/Starke, 39, 397 (1987).

46. (a) S. Hizukuri, S. Tabata, and Z. Nikuni, Starke, 22, 338 (1970); (b) S. Tabata and S. Hizukuri, Starke, 23, 267 (1971).

47. Y. Takeda and S. Hizukuri, Carbohydrate Research, 89, 174 (1981).

48. A. Suzuki, S. Hizukuri, and Y. Takeda, Cereal Chemistry, 58, 286 (1981).

49. Y. Takeda and S. Hizukuri, Carbohydrate Research, 102, 321 (1982).

50. Y. Takeda, K. Shirasaka, and S. Hizukuri, Carbohydrate Research, 132, 83 (1984).

51. Y. Takeda, S. Hizukuri, and B.O. Juliano, Carbohydrate Research, 168, 79 (1987).

52. Y. Takeda, N. Tokunaga, C. Takeda, and S. Hizukuri, Starch/Starke, 38, 345 (1986).

53. C. Takeda, Y. Takeda, and S. Hizukuri, Cereal Chemistry, 60, 212 (1983).

54. J.A.P.P. Van Dijk, F.A. Varkevisser, and J.A.M. Smit, Journal of Polymer Science, 25, 149 (1987).

55. C.J. Kim, A.E. Hamielec, and A. Benedek, Journal of Liquid Chromatography, 5, 425 (1982).

56. A.L. Spatorico and G.L. Beyer, Journal of Applied Polymer Science, 19, 2933 (1975).

57. Unpublished data.

58. W.A. Atwell, R.C. Hoseney, and D.R. Lineback, Cereal Chemistry, 57, 12 (1980).

59. Y. Ikawa, D.V. Glover, Y. Sugimoto, and H. Fuwa, Starch/Starke, 33, 9 (1981).

60. J.F. Kennedy, R.J. Noy, J.A. Stead, and C.A. White, Starch/Starke, 37, 343 (1985).

61. M. John, G. Trenel, and H. Dellweg, Journal of Chromatography, 42, 476 (1969).

62. J.G. Sargeant, Starch/Starke, 34, 89 (1982).

63. T. Suortti and E. Pessa, Journal of Chromatography, 536, 251 (1991).

64. Y. Takeda, N. Maruta, and S. Hizukuri, Carbohydrate Research, 226, 279 (1992).

65. A. Suzuki, M. Kaneyama, K. Shibanuma, Y. Takeda, J. Abe, and S. Hizukuri, Cereal Chemistry, 69, 309 (1992).

66. K. Sommermeyer, F. Cech, and E. Pfitzer, Chromatographia, 25, 167 (1988).

67. H.W. Leach and T.J. Schoch, Cereal Chemistry, 39, 318 (1962).

68. V.W. Praznik and R. Ebermann, Starch/Starke, 31, 288 (1979).

69. S. Hizukuri and Y. Maehara, Carbohydrate Research, 206, 145 (1990).

16
Size Exclusion Chromatography of Proteins

Michael E. Himmel and John O. Baker National Renewable Energy Laboratory, Golden, Colorado

David J. Mitchell Somatogen, Inc., Boulder, Colorado

Introduction

Historically, workers in the biophysical sciences have been concerned with the rapid and gentle isolation of macromolecules of all sizes and types. Although the exact dates of early thoughts on the subject are difficult to place, records from *Discussions of the Faraday Society* in 1949 (1) reflect both speculation and evidence that porous media may be useful in separating biomolecules by size. The chronology of the subsequent discovery of the particle-sieving effects of starch and cross-linked dextran gels in the 1950s at the Institute of Biochemistry, University of Uppsala, Sweden, was well reviewed in a recent article by Hagel and Janson (2). The separation and collection of many water-soluble biopolymers has since been possible using the principle first called gel filtration. Sephadex was the first commercial separation medium made from water-insoluble cross-linked polydextran gel and was originally described by Porath and Flodin in 1959 (3). Soon after this initial breakthrough, Granath and Flodin clearly demonstrated the relationship between the elution of fractionated dextrans and proteins and some function of the molecular size of the solute (4). In fact, the early work showed a tendency for elution in reverse order of molecular weight. This observation then stimulated interest in finding a simple relationship between the absolute molecular weights of macromolecules and their elution volumes in the hope that such a relationship might be useful as a predictive analytical tool for unknown systems. The early uses of Sephadex were broadly

reviewed by Porath (5) in 1967; however, the popularity of these packing materials diminished with the availability of stronger, more efficient preparations.

The success of size exclusion chromatography (SEC) for protein separation is undeniable and has been well chronicled. Milestone reviews of protein SEC present treatments of applications and theory and, in chronological order, include the works of Bly (6), Yau et al. (7), Barth (8), Giddings (9), Regnier (10), Dubin and Principi (11), and Gooding and Regnier (12). Column and/or packing material selection guidelines have also been well described by Montelaro (13), Unger and Kinkel (14), Makino and Hatano (15), and Gooding and Freiser (16). Protein SEC in detergents was recently reviewed (13,17). In the present review, we explore fundamental partition parameters appropriate to protein SEC and SEC theory and then focus on several important aspects of protein SEC that are not well and widely treated. These topics are column and elution calibrations, non-SEC partitioning, and industrial-scale protein SEC.

Column Compartmentalization

The volume elements found in the chromatography column filled with porous media are usually defined in a manner that follows the first suggestions by Porath (18) and later modified by Andrews (19). Here, the total geometrical volume of the SEC column V_g is defined as the sum of the total mobile-phase volume V_t and the volume of the packing material of stationary phase V_s. The mobile-phase volume is further defined as the sum of the volume external to the pores in the packing material or void volume V_0 and the volume occupied by the "stagnant" mobile phase found in the internal pore structural elements V_i. V_0 was recently shown to be near $0.2595 \times V_g$ for columns of rigid SEC packing materials (20) by approximating the gel bed as an assembly of hexagonal closest-packed spheres. It is thought that the differential solute distribution between the volumes internal and external to the pores results in the separation of the solutes. The volume of elution of these solutes is known as V_e.

Protein Partitioning in SEC

General Retention Mechanisms

Retention mechanisms for SEC are generally given on hydrodynamic (actually hydraulic) or thermodynamic grounds. The validity of interpreting SEC behavior in terms of thermodynamic generalities was well expressed and defended by Yau et al. (21–23) and is not stressed here. The hydrodynamic description of the SEC process, especially when describing well-behaved protein systems, has

been reasonably rewarding in its ability to converge theory and predictive elution.

Fundamentally, V_e is the sum of the void volume occupied by all solutes, a portion of the internal pore volume defined by the size exclusion differential equilibrium constant K_{SEC}, and a portion of the surface of the column packing defined by the distribution coefficient describing interactions between the column and solute K_{LC}. This condition leads to the general equation

$$V_e = V_0 + K_{SEC}V_i + K_{LC}V_s \quad (1)$$

In the execution of SEC procedures it is usual and desirable, however, to reduce adsorptive effects as much as possible using appropriate packing materials, buffers, or detergents so that the last term in Equation (1) is reduced to insignificance.

Solute partitioning in other forms of liquid chromatography involves primarily the solute-stationary phase interactions, but solute partitioning in SEC can be described loosely as an entrapping effect, in which solute molecules lose configurational freedom upon entering the gel pores, a process that results in entropic changes with the occupation of different column volumes (24). This explanation represents the basis for thermodynamic characterization of K_{SEC}. K_{SEC} may also be explained in terms of column compartmentalization and geometry, however.

Protein Elution Calibration

It became clear that two parameters must be understood before such a tool could be usable: the correct description of the solute (protein) exposed to the SEC process and the physical description of the internal pore spaces seen by the eluting species, usually as some function of V_e. The correct physical or hydrodynamic description of the protein solute and the column packing material exists as a challenge today.

Column Partitioning Effects: Pore Geometries

The early work of Andrews (19) is typical of the approach first used to study the elution of proteins from SEC columns. Here the volume passing through the column before the protein emerges in maximum concentration V was plotted as a function of the logarithm of protein molecular weight. The agreement was considered, at the time, to be surprisingly good. Also in the early 1960s, Whitaker (25) reported good correlations between the ratio of the elution volume to the void volume V/V_0 and the logarithm of the molecular weight. A new elution volume parameter K_{av}, based on comparisons with the void and total column

volumes, was soon derived (7,26,27):

$$K_{av} = \frac{V_e - V_0}{V_t - V_0} \quad (2)$$

The relationship described as K_{av} was recommended by Pharmacia as the method of choice for column calibration from the earliest days of Sephadex use. These results, and others like them, set the stage for a unique analytical tool at the time, one capable of predicting the molecular weights of unknown proteins. The elution of 37 purified proteins and two small solutes was plotted by this method and is shown in Figure 1.

Modern theoretical models used to describe SEC elution behavior must allow for possible variations in both the solute and bead pore size and shape while remaining consistent with current concepts regarding SEC as an equilibrium-controlled process. The shape of the "pore" in SEC is important in the prediction of elution behavior. Gel pores were originally described in terms of the penetrability of "hard sphere" solutes, and extensions of this model are still employed today. Early theories of hard sphere solute models, in chronological order of appearance in the literature, are the random spheres pore model of Ogston (28), the randomly occurring cones, cylinders, and crevices pore model of Squire (29), and the random rod pore model of Laurent and Killander (30). The model proposed by Squire for the description of pores in Sephadex for a solute eluting at V_e was given as

$$V_e = V_0 + kV_0\left(1 - \frac{r}{R}\right)^3 \text{(cones)} + k'V_0\left(1 - \frac{r}{R}\right)^2 \text{(cylinders)} + k''V_0\left(1 - \frac{r}{R}\right)\text{(crevices)} \quad (3)$$

Where r = the protein radius. The cones and cylinders are of radius R, and the crevices of width $2R$. An arbitrary assignment of the distribution of these pores, $k'' = 9g$, $K' = 9g^2$, and $k = 3g^3$, leads to the simplified equation describing the contribution of all pore types to elution volume:

$$\frac{V_e}{V_0} = \left[1 + g\left(1 - \frac{r}{R}\right)\right]^3 \quad (4)$$

It is generally agreed today that the random sphere models (resulting in uniform pore geometry systems), based on the close packing of spherical gel beads, are best suited to describing SEC using porous silica microspheres or controlled pore glass beads. The random pore models and the models based on statistical distributions of shapes may indeed by more accurate for the majority of the rigid SEC packings used today, however.

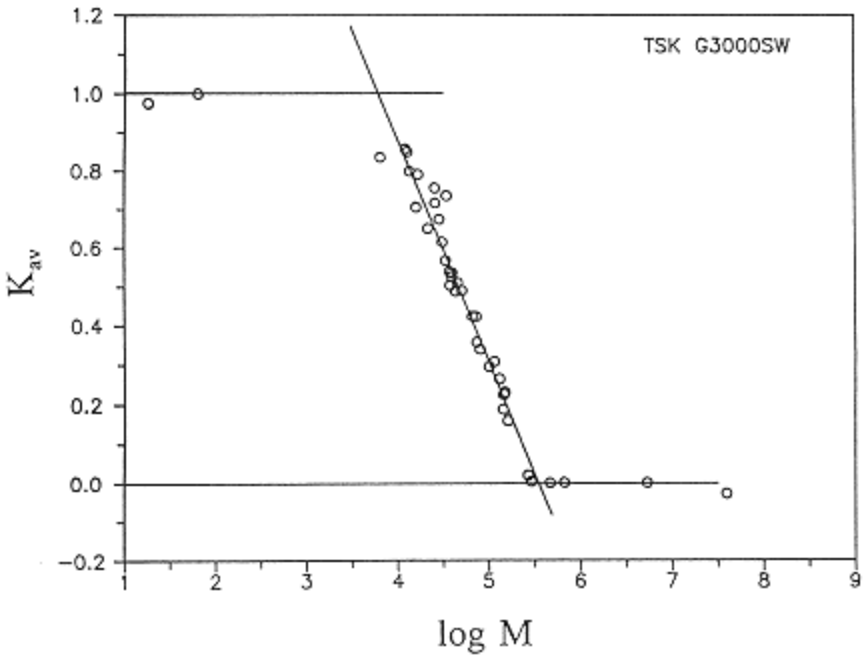

Figure 1.
Plot of K_{av} versus log M for 37 purified proteins and two V_t markers. Solutes, from low to high M, are D_2O, NaN_3, trypsin inhibitor, cytochrome c, elastase (subunit), ribonuclease A, myoglobin, chymotrypsinogen A, carboxypeptidase, hemoglobin (subunit), elastase, carbonic anhydrase, myokinase, deoxyribonuclease, malate dehydrogenase, superoxide dismutase, peroxidase, alcohol dehydrogenase (subunit), α-galactosidase II, ovalbumin, α-amylase, 3-phosphoglycerate kinase, lactate dehydrogenase (subunit), bovine serum albumin, malate dehydrogenase, aldolase (subunit), catalase (subunit), glucose 6-phosphate dehydrogenase (subunit), bovine serum albumin (dimer), glucose oxidase, lactate dehydrogenase, β-glucouronidase (subunit), aldolase, fructosidase, β-glucouronidase, apoferritin, thyroglobulin, turnip yellow mosaic virus, and tobacco mosaic virus. The chromatography was performed at 1.0 ml/minute with two 7.8 mm × 30 cm TSK G3000 SW columns. The mobile phase was 10 mM phosphate buffer, pH 7, in 100 mM NaCl. Each injection included D_2O as an internal standard for V_t. The correlation coefficient for the linear portion of the data is 0.989.

The first of such statistical pore models was proposed by Giddings et al. (31) in 1968. In this landmark study, general expressions were formulated that described the partitioning of hard sphere solutes in a random pore system, described as a “porous network.” Also unique to this study was an attempt to express SEC partitioning as a function of both complex pore and solute contri-

butions. Furthermore, the authors treated the distribution of solutes of various shapes (spherical, thin rod, dumbbell, and capsular shaped) in pores described as cylinders, slabs, spheres, and rectangular pockets. Giddings concluded that SEC partitioning may best be defined as

$$K = e^{-s\bar{L}/2} \quad (5)$$

Where K is the SEC equilibrium constant for a random plane pore model and $s\bar{L}$ is the product of the mean external molecular length $\bar{L}$ and the "effective pore radius" s. The equilibrium partitioning of rigid solutes in a random fiber pore model was also proposed by Giddings et al. (31). Here the SEC equilibrium constant was defined as

$$K = e^{-\bar{A}h} \quad (6)$$

where $\bar{A}$ is the projection of the molecular dimension A_x averaged over all directions in space and h is the fiber length per unit volume. The fiber diameter is assumed similar to the size of the solute molecule.

Further contributions to SEC theory were made by Glandt (32) for the description of the spatial density distribution for "crowded pores." This work contrasts with earlier studies based solely on dilute solutions of solutes, in which solute-wall effects were primarily considered.

Proteins as SEC Solutes

It is noteworthy that the field of SEC elution theory turned largely to the description of partitioning of random coil polymers during the late 1960s and throughout the following decade. Contributions from Cassassa and Tagami (33), based on Flory theory (34), served to further the understanding of high-polymer SEC. This work focused on new descriptions of flexible solutes. When considering the elution of proteins as SEC solutes, the treatment of solution conformation becomes somewhat simplified when viewed from the perspective of the statistical mechanical arguments needed to describe high polymers. The hard shell or rigid sphere solute models are probably adequate for proteins. This approach was used by Squire (29) to extend Equation (4) to

$$\frac{V_e}{V_0} = \left[1 + g\left(\frac{M^{1/3}}{C^{1/3}}\right)\right]^3 \quad (7)$$

by considering the protein solutes to be spherical. The term r is proportional to the cube root of the molecular weight. Equation (7) may then be rearranged in the manner described by Himmel and Squire (35), yielding two forms, one relating elution to the void volume of the column and the other to the total

volume accessible to the mobile phase:

$$F'_v = \frac{V_e^{1/3} - V_0^{1/3}}{V_t^{1/3} - V_0^{1/3}} = \frac{C^{1/3} - M^{1/3}}{C^{1/3} - A^{1/3}} \quad (8)$$

$$F_v = \frac{V_e^{1/3} - V_t^{1/3}}{V_0^{1/3} - V_t^{1/3}} = \frac{M^{1/3} - A^{1/3}}{C^{1/3} - A^{1/3}} \quad (9)$$

Where C and A correspond to the molecular weights of solutes just large enough to be rejected from the column pores and solutes small enough to be included in all volumes of the column, respectively. Note that the right-hand quantity in Equations (8) and (9) predicts a linear relationship between F_v and $M^{1/3}$. The set of 37 proteins shown in Figure 1 is replotted according to the equation for F'_v and shown in Figure 2.

To use Equations (8) and (9) effectively, one must decide if, in the context of a given experiment, V_0 or V_t may be determined less ambiguously. Himmel and Squire assumed that in most cases V_t may be less accurately determined than the void volume because of adsorptive effects experienced with most small

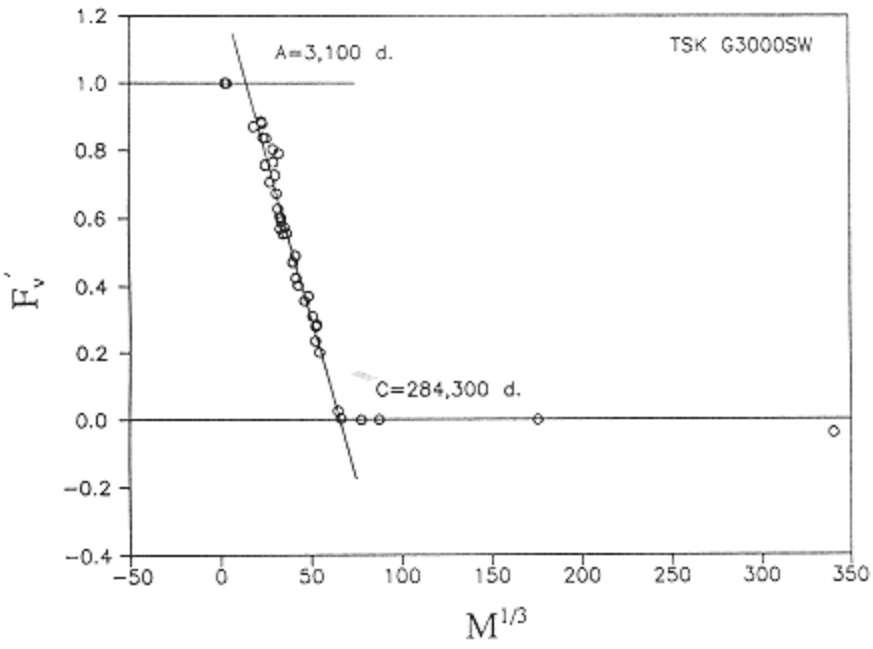

Figure 2.
Plot of K'_v versus $M^{1/3}$ for the same data given in Figure 1. The correlation coefficient for the linear portion of the data is 0.992.

solutes and, hence, recommended the use of F'_v. However, Noll et al. recently showed (36) that the elution of deuterium oxide can be used as a reliable marker for V_t and reevaluation of the use of Equation (9) may be in order. A further benefit of Equations (8) and (9) is that the values C and A can be accurately calculated from the limiting chromatographic conditions; that is, at $F'_v = 1$, $M^{1/3} = A^{1/3}$, and at $F'_v = 0$, $M^{1/3} = C^{1/3}$. The calculation of the column parameters C and A for a series of similar columns, in different laboratories, is shown in Table 1. The method of Himmel and Squire has been applied to a wide range of native protein SEC conditions, including TSK columns (38) and Waters I125 columns (39), as well as denatured protein SEC using Sephadex (40). An important extension to the method based on equation (8) was proposed by Bindels and Hoenders (41), in which F_v was plotted against $(M\bar{v})^{1/3}$. These workers found that his approach gave better results than plots of $M^{1/3}$ or log M.

Assuming that the left side of Equations (8) and (9) provides an adequate description of the column pores in SEC, then the predictive power of this method may be improved by enhancing the picture of the solute during SEC beyond molecular weight. Although proteins are indeed roughly spherical, they can usually be more accurately described as ellipsoids of revolution, either prolate or oblate, with axial ratios normally ranging from 1.0 to 6 (34). Also, as found by Bindels and Hoenders, the correct SEC molecular radius must consider other factors. A thorough treatment of proteins and nonflexible-chain polymers as SEC solutes has been contributed by Potschka (42). In this study, the parameters considered included the equivalent (or effective) hydrodynamic radius R_e, the Stokes' radius R_s, the root-mean-square radius of gyration R_g, and the root-mean-square end-to-end distance r_{rms}. In an important recent contribution by Dubin and Principi (43), globular proteins and selected flexible-chain polymers were found to elute predictably when the "viscosity radius" R_η (equal to $[\eta]M$) was used as the solute parameter. These authors found that rod-like molecules did not obey this elution rule, however, and concluded that the universal "SEC

Table 1 Calibration Constants for Toyo Soda TSK SW Series SEC Columns

Column type	A (daltons)	C (daltons)
G2000 SW	940	91,000
G3000 SW	2460	340,000
G3000 SW	3900	330,000
G3000 SW[a]	3100	284,000
G4000 SW	550	3.4×10^6

[a]This study.

Source: Adapted from Himmel and Squire (37).

radius" had not been found. This may indeed by true for the broad-based SEC of biomacromolecules; however, the R_{SEC} (Dubin's term) must be similar, if not equal, to the effective hydrodynamic radius proposed by Cassassa and Tagami (33), and must occupy the effective hydrodynamic volume V_h. For many proteins, R_e may be equivalent to R_η. Yet, R_e may also be calculated from known parameters, such as the molecular weight (from sedimentation equilibrium or gene sequence), molecular dimensions (from x-ray crystallography), surface hydration (from titration or modeling), and partial specific volume (from composition or actual measurement). Following Oncley's approach (44), based on an extension of the Stokes relationship for a perfectly spherical protein $f_0 = 6\pi\eta R_0$, globular proteins may be described more accurately than as simple spherical, hydrated structures (34). This frictional coefficient f is defined as

$$f = 6\pi\eta \frac{f}{f_0}\left(\frac{3M\,(\bar{v}_2 + \delta_1 v_1^0)}{4\pi N}\right)^{1/3} = 6\pi\eta \frac{f}{f_0} R_e \qquad (10)$$

where f/f_0 is the frictional ratio, $\bar{v}_2$ is the protein partial specific volume, v_1^0 is the pure solvent specific volume, δ_1 is the protein hydration, and N is Avogadro's number. The bracketed quantity in Equation (10) is the highly protein-specific radius R_e. If needed, the frictional ratios may be found from experimental data (s, M, and $\bar{v}_2$ where s is the sedimentation coefficient) or from protein dimensional information, assuming best fit for x-ray structural data to either prolate or oblate spheroids of revolution. This estimation may be accomplished using the relationships developed long ago by Perrin (45) and modified by Herzog et al. (46). For prolate ellipsoids (semiaxes a, b, and b),

$$\frac{f}{f_0} = \frac{(1 - b^2/a^2)^{1/2}}{(b/a)^{2/3} \ln\left[1 + (1 - b^2/a^2)^{1/2}\right]/(b/a)} \qquad (11)$$

and for oblate ellipsoids (semiaxes a, a, and b),

$$\frac{f}{f_0} = \frac{(a^2/b^2 - 1)^{1/2}}{(a/b)^{2/3} \tan^{-1}(a^2/b^2 - 1)^{1/2}} \qquad (12)$$

where R_0 is the radius of a sphere of equal volume to the ellipsoid; that is, $^4/_3\pi R_0^3 = {}^4/_3\pi ab^2$ (prolate ellipsoid) or $4/3\pi a^2 b$ (oblate ellipsoid).

Unfortunately, these parameters are known accurately for only a relatively small group of globular proteins, the 21 globular proteins reported by Squire and Himmel in 1979 (47). The test of fit for globular protein elution from SEC based on the estimation of R_e from such a database is promising but has not yet been examined.

Non-SEC Partitioning

In connection with the SEC of proteins, the term "nonsize effects" refers, inclusively, to all phenomena affecting the retention of proteins on size exclusion

columns, other than the classic partitioning of solutes between pore volume and interstitial volume based on the ratio of solute dimensions to pore dimensions. These nonsize effects may include attractive interactions, such as ion exchange and hydrophobic (43) binding, which tend to increase the elution volumes of solutes, thus causing them to appear smaller than they actually are, and forces of electrostatic repulsion (ion exclusion), that have the effect of denying otherwise accessible volumes to the solutes, thereby causing them to appear larger than they are.

In some applications, such as development of purification protocols, these additional effects may not be regarded as problems but may instead be exploited in the "fine-tuning" of procedures for separating proteins that would coelute if separated purely on the basis of size (48). It is when investigators attempt to use SEC data to draw quantitative conclusions concerning absolute or relative sizes of proteins that these non-size effects pose a major problem. The most obvious example is, of course, the use of SEC to estimate the molecular weight of proteins, but distortions resulting from non-SEC effects can potentially be even more severe when SEC is used to measure changes in the shape of a given protein (i.e., experiments measuring conformational changes and/or subunit dissociation and recombination phenomena, which may expose new and different protein surfaces for potential contact with packing materials) (49,50).

A variety of modifications of stationary and mobile phases have been made to eliminate, or at least reduce, nonsize effects. The results of these measures are complicated, however, because at least three general categories of phenomena can be affected (often differently) by these measures: packing material-solute interactions, geometrical changes in the column packing material itself, and changes in the physicochemical state of the proteins being studied.

Packing Material-Solute Interactions

Electrostatic Interactions

The surfaces of most packing materials used for aqueous SEC tend to have slight negative charges under the conditions most often used for the chromatography of proteins. Silica-based packings are negatively charged because of weakly acid silanol groups (51–53); even capped silica materials tend to exhibit some of this property, inasmuch as the "capping" process usually leaves some unmodified silanols (50,51) and more silanols may be produced by erosion of capping groups during use of the column (51). Some polymeric packing materials tend to be negatively charged because of the presence of small numbers of carboxyl groups (54). Proteins with net positive charges therefore tend to be adsorbed on the matrix, retained longer on the column, and assigned erroneously small molecular sizes. Negatively charged proteins (to a first approximation; see

later) tend to be repelled from the surface of the packing material, which results in their being denied access to some of the pore volume and eluted earlier than expected on the basis of size alone.

For a given packing material, the most generally useful means of suppressing electrostatic interactions with proteins is to increase the ionic strength of the mobile phase until a region of ionic strength is encountered in which elution volume is essentially independent of ionic strength (55,56). It should be kept in mind that high ionic strengths tend to promote hydrophobic interactions; if a simple minimum in elution volume is observed in the dependence of elution volume on ionic strength, instead of a "flat" plateau of significant width, the results may not mean that "ideal" SEC is taking place at the ionic strength producing the minimum elution volume. Both electrostatic and hydrophobic binding to the packing may influence the elution significantly, the minimum elution volume simply marking the ionic strength at which the sum of the two interactions is at its minimum (57).

Another approach to suppressing electrostatic interactions is to adjust the charges on the protein or the packing material, or both, by adjusting the pH of the mobile phase (48,54,55,56). In (oversimplified) theory, if the positive and negative charges on the protein can be equalized, so that the *net* result is an electrically neutral molecule, there should be no electrostatic attraction or repulsion between protein and packing material. In practice, however, one rather extensive evaluation of this strategy found that the most nearly ideal SEC occurred when the mobile-phase pH was slightly *above* the isoelectric point of the protein (48).

Strategies based on protein pI values appear to work well in a number of instances (54,55), although pH adjustment is not an appropriate response to non-SEC effects in the not unlikely event that a given pH value is an integral part of the experiment being conducted, not a variable that can be varied for purely analytical reasons, or, as discussed later, in the event that protein stability becomes a problem at the pH that would be chosen for chromatographic reasons. Deviations from predictions based solely on net charges of proteins and packing materials may also arise from chromatographic implications of the macromolecular nature of proteins. In most cases, charged proteins cannot be represented adequately as point charges equal to their net charges; the charged groups on the exterior of proteins have definite distributions about quite appreciable diameters, and these distributions are by no means always symmetrical. Chromatographic behavior may reflect attraction between charged packing materials and local patches of opposite charges on the protein, even when the net charge on the protein as a whole has the same sign as the charge on the packing material (58). Small-molecule examples of such local interactions are found in the binding of polyelectrolytes to proteins even at pH values such that the net charges on the polyelectrolytes and proteins are the same sign (59).

Hydrophobic Interactions

Significant hydrophobic interactions between proteins and packing material may be inferred from increases in elution volume as ionic strength is increased to fairly high values (generally 0.5 or higher, for ionic strength supported by NaCl). A strong "salting-out" salt, such as ammonium sulfate, is especially useful in assessing the potential for such interactions in a particular protein-matrix pair (50). The hydrophobic adsorption of proteins may be reduced by decreasing the ionic strength of the mobile phase (which may concurrently *increase* electrostatic interactions, however) or by adding organic solvents (60).

Geometrical Changes in the Packing Material

Gels, such as Sephadex and the BioGel P series, depend upon swelling of the gel material in a solvent for the formation of pores; the pores collapse completely upon removal of the solvent (61). This critical dependence of the gel structure on solvation of the polymeric material raises the possibility of changes in effective pore size when the chemical nature of the mobile phase is changed significantly in an attempt to suppress adsorptive effects, as in the addition of detergents or organic solvents (60) for the chromatography of hydrophobic proteins. Such considerations may also apply to hybrid gels (61) in which a hydration-dependent material has been bonded inside the large pores of a macroreticular supporting framework. A second type of pore size change may affect rigid, permanent-pore packing materials as well as the solvent-swollen materials, in that detergents added to the mobile phase to solubilize or denature proteins or to suppress hydrophobic interactions between proteins and packing may bind to the surfaces inside the pores to such an extent that the effective pore size is significantly decreased (62). The straightforward, though laborious, countermeasure to both these effects is the calibration of the SEC column under each and every set of conditions employed experimentally.

Changes in the Physicochemical State of the Proteins

When changing the pH of the mobile phase to eliminate electrostatic interactions between protein and packing material, one should keep in mind the tendency of most proteins to be maximally stable at a certain pH value or range of values and to display diminishing stability as the pH is varied in either direction from this optimal value (or range). As pointed out in recent reviews (63,64), considerable evidence exists that some proteins (those that can be described as deformable, or "soft," in that they have relatively low structural stability) are bound to surfaces in a two-step process (65). First, the native protein forms a fairly weak interaction with the surface (this interaction may be either hydrophobic or electrostatic, depending on the nature of the surface and of the exterior

of the protein). A subsequent conformational change in the loosely bound protein allows a substantial increase in the extent of contact between the protein and the surface and therefore in the number of binding interactions (64,65). If the second step (the conformational change in the bound protein molecule) proceeds to a sufficient extent, this may result in an overall tight binding of such a soft protein to the packing material, even under conditions such that the equilibrium in the first step (the original association of the protein with the packing material) is in favor of the protein remaining in the mobile phase. In contrast to this behavior, a more structurally stable, relatively "hard," or nondeformable protein, even though it has the same surface chemistry as the "soft" protein, exhibits only the first, weak step of binding and remains principally in the mobile phase.

The relevance of the foregoing to the question of adsorptive interactions in SEC is that as the pH of the mobile phase is moved away from the pH of maximum protein stability, the protein is progressively "softened," becoming much less resistant to structural changes induced upon contact with packing material. It is important to note that this softening of the structure can proceed to a significant extent, long before the pH change reaches the point of causing denaturation of the protein in solution.

The result of all these concurrent and often opposing effects is that an experimenter who wishes to use protein SEC data to support specific, quantitative conclusions concerning protein sizes and shapes is required to test multidimensional arrays of sets of conditions, rather than a one-dimensional array in which only the variable of specific interest is changed.

Preparative Protein SEC

The inherent effectiveness of SEC for large-scale protein purification is based on the equilibrium nature of the method, which results in high yields because little solute is denatured, and in the predictability of elution once column parameters are known.

Applications

The first industrial application of SEC for protein solutions were for desalting dairy products (66). Large columns (2500 liters) were used to separate proteins in whey or skim milk from low-molecular-weight sugars and salts. SEC is also used in the "deethanolization" of human serum albumin (HSA) (67) produced by the Cohn cold ethanol procedure. The purification of insulin was the first successful industrial application of SEC for protein fractionation (68), followed by the fractionation of HSA proteins (69).

The term “preparative SEC” encompasses all forms and scales of SEC depending on requirements for product. Preparative protein SEC has been categorized by the scale of the separation (70), which includes the following:

1. Preparative-analytical: analytical columns (diameter < 1 cm), single injection, microgram to milligram quantities prepared

2. Semipreparative: analytical columns (diameter 0.7–2 cm), multiple injections, milligram quantities prepared

3. Standard preparative: preparative columns (diameter 2–20 cm), single or multiple injections, milligram to gram quantities prepared

4. Large-scale preparative: large preparative column (diameter ≥ 20 cm), automated injections, gram to kilogram quantities prepared

The complexities of large-scale applications arise from the absolute requirements for optimal productivity (gram product/cm^2/hour), cost effectiveness, and product purity. Many technical factors affect these issues. Evaluating these factors for a given application is paramount to successfully utilizing SEC at the industrial scale.

Column diameter and length are primary factors affecting the scale of preparative SEC. For preparative separations, it is most cost effective to operate at the highest sample loading and flow rate possible without loss of adequate resolution. In general, both the sample size and the flow rate can be increased proportionally to the column's cross-sectional area (Pharmacia). With soft gels, however, bed compression is a major factor for large-diameter columns, even at moderate flow rates (>50 cm/h). This compression imposes an additional physical limitation, beyond that of resolution, on the throughput that can be attained in scaling up from analytical columns using soft resins. Column length is also a major factor affecting productivity. The chromatographic resolution R_{SC} is weakly affected by the length $(R_{sc} \propto \sqrt{L})$, so doubling the bed length increases the R_{SC} by only 40%. However, doubling the bed length doubles the overall backpressure at a given flow rate. Moreover, R_{SC} is a weak inverse function of linear velocity, and in some preparative applications it may even be advantageous to the overall productivity actually to shorten the bed length and run at higher flow rates (71). This approach may be taken to a point of diminishing returns or to the physical flow limitations described earlier. In general, this optimum must be determined empirically for each resin and protein sample.

Sample loading is also important to the overall productivity of SEC. Different loadings are recommended for desalting ($\simeq$ 30% bed volume) and protein fractionation ($\leq$5% bed volume). These loadings are low compared with other forms of chromatography and tend to limit the use of SEC to the final (more concentrated) steps of protein purification schemes. In fact, recent advances in ultrafiltration membrane technology have further limited the large-scale use of SEC for protein desalting. In many cases, SEC has been replaced by ultrafiltra-

tion as the more cost effective method for buffer exchange for all but the most shear sensitive proteins.

Resin particle size has a pronounced effect on chromatographic resolution and column backpressure. However, large-scale applications usually dictate that the only cost-effective choice of resin particles are those with a diameter ≥ 30 μm. It is important to realize this limitation before scaling up based on information gained from analytical resins ($d_p \leq 20$ μm).

One issue of SEC unique to processes involving the production of parenteral drugs, and of many proteins, is that of validated resin regeneration. This is especially important for large-scale, cost-challenged processes, in which resins must be reused hundreds of times. Resins used to purify proteins from bacterial sources must be depyrogenated (to remove cell wall fractions); resins used to purify proteins from other sources must be disinfected (e.g., destruction of viruses). This can be done effectively by exposure to sodium hydroxide (72). Sodium hydroxide solutions have many advantages over organic solutions, including low cost, ease of disposal, and minimal risk of product contamination.

Selection of Resins

In all chromatographic work, the most critical choice before scale-up is that of resin selection. The separation can never be better than the selectivity of a given packing material allows. Therefore, time spent on identifying the required selectivity for the separation and subsequent choice of the appropriate resin is invaluable. Once several resins have been identified as possibilities, empirical data, technical parameters, and cost must be considered in the final selection. Selected performance parameters are presented for modern preparative SEC resins in Table 2.

All the resins described in Table 2, except Superdex, have been utilized extensively for protein purifications. Superdex preparative resins are an agarosedextran composite (73) and became commercially available in late 1991. Superdex resins are reported to have higher productivities than earlier gels because of the increased physical stability of agarose coupled with the steep selectivity of dextran. Note in Table 2 that the resins normally used for analytical-scale protein purifications display maximum linear flow rates much lower than those of the preparative resins. The new generation of preparative resins are smaller in size and more rigid than earlier materials, making rapid high-efficiency separations possible.

Selection of Hardware

Once the most productive resin has been identified, an appropriately configured column must be selected. Information about the required throughput, sample volume, chemical resistance, and cycle time must be included in choice of col-

Table 2 Characteristics of Resins Currently Available for Preparative Protein SEC

Support	d_p (μm)	V_{max_a}	Selectivity[b] (kD)	Manufacturer
Analytical				
Sephadex G-25F	20-80	5	1-5	Pharmacia[c]
Sephadex G-50F	20-80	5	1.5-30	Pharmacia
BioGel P-60 med	90-180	6	3-60	Bio-Rad[d]
BioGel P-100 med	90-180	6	5-100	Bio-Rad
Preparative				
Sepharose CL-2B	60-200	15	$70\text{-}40 \times 10^3$	Pharmacia
Sepharose CL-4B	45-165	26	$60\text{-}20 \times 10^3$	Pharmacia
Sepharose CL-6B	45-165	30	$10\text{-}4 \times 10^3$	Pharmacia
Superdex 75 prep	24-44	30	3-70	Pharmacia
Superdex 200 prep	24-44	30	10-600	Pharmacia
Superose 12 prep	20-40	30	1-300	Pharmacia
Superose 6 prep	20-40	0	$5\text{-}5 \times 10^3$	Pharmacia
Sephacryl S-100HR	25-75	39	1-100	Pharmacia
Sephacryl S-200HR	25-75	39	5-250	Pharmacia
Sephacryl S-300HR	25-75	48	$10\text{-}1.5 \times 10^3$	Pharmacia
Sephacryl S-400HR	25-75	63	$20\text{-}8 \times 10^3$	Pharmacia
Matrex Cellufine GC700	45-105	100	10-400	Amicon[e]
Toyopearl HW-40C	50-100	200	0.1-10	TosoHaas[f]
Toyopearl HW-55F	30-60	90	1-700	TosoHaas
BioGel A-0.5M med	80-150	20	10-500	Bio-Rad
BioGel A-1.5M med	80-150	20	$10\text{-}1.5 \times 10^3$	Bio-Rad
BioGel A-5M med	80-150	0	$10\text{-}5 \times 10^3$	Bio-Rad
BioGel A-15M med	80-150	20	$40\text{-}15 \times 10^3$	Bio-Rad
BioGel A-50M fine	80-150	15	$100\text{-}50 \times 10^3$	Bio-Rad

[a]Maximal linear velocity (cm/hr) for columns in 1-6 cm diameter range.

[b]Fractionation range (kilodaltons) for peptides and globular proteins.

[c]Adapted from *Gel Filtration: Principles and Methods,* 5th ed., Pharmacia, Lund, Sweden, 1991.

[d]Adapted from *Life Sciences Research Products,* Bio-Rad Laboratories, Richmond, CA, 1992.

[e]Adapted from *Matrex Silica Media,* Publication No. 514, Amicon, Danvers, MA.

[f]Adapted from TosoHaas Technical Report, Philadelphia, PA, 1990.

umn(s). Conventional preparative and process SEC columns (packed or empty) are available from Amicon/Wright (Danvers, MA), Pharmacia Biotechnology (Lund, Sweden), TosoHaas (Philadelphia, PA), and Millipore/Waters (Milford, MA). The Pharmacia Process Stack Column PS 370 is the most noteworthy because of the configuration and versatility of the stack (74). The stack may contain up to six individual columns (37 × 15 cm) connected in series. This translates into a 90 cm bed height or a 96 liter total bled column. The separation

of the total bed into a series of discrete 16 liter beds allows high throughput and resolution by supporting the gel and alleviating the bed compression associated with large bed volumes while introducing minimal band spreading.

Finally, process automation is also essential for efficient, reproducible, preparative SEC of proteins. Several companies produce automated chromatography systems equipped for preparative sanitary protein SEC. The Dorr-Oliver Protein LC, Pharmacia BioProcess and BioPilot, TosoHaas Protein Prep LC, Separations Technologies (Wakefield, RI) Pilot/Production Preparative HPLC, Millipore Kiloprep LC, and Waters KiloPrep systems are all fully automated liquid chromatography systems designed to support “turnkey” preparative SEC. The capabilities of these systems range from low-throughput, high-resolution preparative high-performance liquid chromatography systems to low-pressure, high-throughput, skid-mounted systems. These systems can be custom designed to a limited extent, however.

Acknowledgements

The authors dedicate this work to the memory of Phil G. Squire. His passion for gel filtration began with a visit to Uppsala in 1960, before widespread interest in the field of column chromatography ignited. His passing in 1989 diminished our collective potential to fully explore this important technology. This work was funded by the Ethanol from Biomass Program of the Biofuels Systems Division of the U.S. Department of Energy.

References

1. *Disc. Faraday Soc., 7:* 114 (1949).

2. L. Hagel and J.-C. Janson, in *Chromatography, Part A: Fundamentals and Techniques* (E. Heftmann, ed.), Vol. 51A, Elsevier, Amsterdam, 1992, pp. A267–A307.

3. J. Porath and P. Flodin, *Nature, 183:* 1647 (1959).

4. K. A. Granath and P. Flodin, *Macromol. Chem., 48:* 160 (1961).

5. J. Porath, *Lab. Pract., 16:* 838 (1967).

6. D. D. Bly, in *Gel Permeation Chromatography in Polymer Chemistry, Physical Methods in Macromolecular Chemistry* (B. Carroll, ed.), Vol. 2, Dekker, New York, 1972.

7. W. W. Yau, J. J. Kirkland, and D. D. Bly, *Modern Size Exclusion Chromatography,* Wiley, New York, 1979.

8. H. G. Barth, *J. Chromatogr. Sci., 18:* 409 (1980).

9. J. C. Giddings, in *Advances in Chromatography* (J. C. Giddings, E. Grushka, J. Cazes, and P. R. Brown, eds.), Vol. 20, Dekker, New York, 1982, p. 217.

10. F. E. Regnier, *Adv. Enzymol., 91:* 137 (1983).

11. P. L. Dubin and J. M. Principi, *Macromolecules, 22:* 1891 (1989).

12. K. M. Gooding and F. E. Regnier, in *HPLC of Biomolecules*, Dekker, New York, 1990.

13. R. C. Montelaro, in *Aqueous Size Exclusion Chromatography* (P. L. Dubin, ed.), Elsevier, Amsterdam, 1988, p. 269.

14. K. K. Unger and J. N. Kinkel, in *Aqueous Size Exclusion Chromatography* (P. L. Dubin, ed.), Elsevier, Amsterdam, 1988, p. 193.

15. K. Makino and H. Hatano, in *Aqueous Size Exclusion Chromatography* (P. L. Dubin, ed.), Elsevier, Amsterdam, 1988, p. 235.

16. K. M. Gooding and H. H. Freiser, in *High Performance Liquid Chromatography of Peptides and Proteins* (C. T. Mant and R. S. Hodges, eds.), CRC Press, Boca Raton, FL, 1991, p. 135.

17. G. W. Welling and S. Welling-Wester, in *High Performance Liquid Chromatography of Peptides and Proteins* (C. T. Mant and R. S. Hodges, eds.), CRC Press, Boca Raton, FL, 1991, p. 155.

18. J. Porath, *Biochim. Biophys. Acta, 39:* 193 (1960).

19. P. Andrews, *Nature, 196:* 36 (1962).

20. P. G. Squire, A. Magnus, and M. E. Himmel, *J. Chromatogr., 242:* 255 (1982).

21. W. W. Yau, C. P. Malone, and S. W. Fleming, *J. Polym. Sci., 6:* 803 (1968).

22. W. W. Yau, H. L. Suchan, and C. P. Malone, *J. Polym. Sci., 6:* 1349 (1968).

23. W. W. Yau, C. P. Malone, and H. L. Suchan, *Sep. Sci., 5:* 259 (1970).

24. J. V. Dawkins, *J. Polym. Sci., 14:* 569 (1976).

25. J. R. Whitaker, *Anal. Chem., 35:* 1950 (1963).

26. Pharmacia Fine Chemicals, *Sephadex Filtration in Theory and Practice*, Uppsala, Sweden, 1979.

27. P. Andrews, *Biochem. J., 96:* 595 (1965).

28. A. G. Ogston, *Trans. Faraday Soc., 54:* 1754 (1958).

29. P. G. Squire, *Arch. Biochem. Biophys., 107:* 471 (1964).

30. T. C. Laurent and J. Killander, *J. Chromatogr., 14:* 317 (1964).

31. J. C. Giddings, E. Kucra, C. P. Russell, and M. N. Meyers, *J. Phys. Chem., 72:* 4397 (1968).

32. E. D. Glandt, *J. Colloid Interface Sci., 77:* 512 (1980).

33. E. F. Cassassa and Y. Tagami, *Macromolecules, 2:* 14 (1969).

34. C. Tanford, *Physical Chemistry of Macromolecules,* Wiley, New York, 1961.

35. M. E. Himmel and P. G. Squire, *Int. J. Peptide Protein Res, 17:* 365 (1981).

36. G. R. Noll, N. Nagle, J. O. Baker, D. J. Mitchell, K. Grohmann, and M. E. Himmel, *J. Liq. Chromatogr., 13:* 703 (1990).

37. M. E. Himmel and P. G. Squire, in *Aqueous Size Exclusion Chromatography* (P. L. Dubin, ed.), Elsevier, Amsterdam, 1988, p. 3.

38. T. S. Burcham, D. T. Osuga, H. Chino, and R. E. Feeney, *Anal. Biochem., 139:* 197 (1984).

39. M. Dennis, C. Lazure, N. G. Seidah, and M. Chretien, *J. Chromatogr., 266:* 163 (1983).

40. C. Lazure, M. Dennis, J. Rochemont, N. G. Seidah, and M. Chretien, *Anal. Biochem., 125:* 406 (1982).

41. J. G. Bindels and H. J. Hoenders, *J. Chromatogr., 261:* 381 (1983).

42. M. Potschka, *Anal. Biochem., 162:* 47 (1987).

43. P. L. Dubin and J. M. Principi, *Macromolecules, 22:* 1891 (1989).

44. J. L. Oncley, in *Proteins, Amino Acids, and Peptides* (E. J. Cohn and J. T. Edsall, ed.), Reinhold, New York, 1943, Chapter 22.

45. F. Perrin, *J. Phys. Radium, 7:* 1 (1936).

46. R. O. Herzog, R. Illig, and H. Kudar, *Z. Phys. Chem.,* A167, 329 (1934).

47. P. G. Squire and M. E. Himmel, *Arch. Biochem. Biophys., 196:* 165 (1979).

48. W. Kopaciewicz and F. E. Regnier, in *High-Performance Liquid Chromatography of Proteins and Peptides* (M. T. W. Hearn, F. E. Regnier, and C. T. Wehr, eds.), 1982, p. 151.

49. J. E. Dyr and J. Suttnar, *J. Chromatogr., 408:* 303 (1987).

50. R. Majuri, *J. Chromatogr., 387:* 281 (1987).

51. W. Flapper, A. G. M. Theeuwes, J. T. G. Kierkels, J. Steenbergen, and H. J. Hoenders, *J. Chromatogr., 533:* 47 (1990).

52. L. G. Daignault, D. C. Jackman, and D. P. Rillema, *J. Chromatogr., 462:* 71 (1989).

53. Y.-B. Yang and F. E. Regnier, *J. Chromatogr., 544:* 233 (1991).

54. B.-L. Johansson and J. Gustavsson, *J. Chromatogr., 457:* 205 (1988).

55. I. Drevin, L. Larsson, I. Eriksson, and B.-L. Johansson, *J. Chromatogr., 514:* 137 (1990).

56. K. M. Gooding and H. H. Freiser, in *High-Performance Chromatography of Peptides and Proteins:* Separation, Analysis, and Conformation (C. T. Mant and R. S. Hodges, eds.), CRC Press, Boca Raton, FL, 1991, p. 135.

57. P. L. Dubin, in *Aqueous Size-Exclusion Chromatography* (P. L. Dubin, ed.), Elsevier, New York, 1988, p. 55.

58. W. Kopaciewicz, M. A. Rounds, J. Fausnaugh, and F. E. Regnier, *J. Chromatogr., 266:* 3 (1983).

59. J. M. Park, B. B. Muhoberac, P. L. Dubin, and J. Xia, *Macromolecules, 25:* 290 (1992).

60. K. Inouye, *Agr. Biol. Chem., 55:* 2129 (1991).

61. L. Kagedal, B. Engstrom, H. Ellegren, A.-K. Lieber, H. Lundstrom, A. Skold, and M. Schenning, *J. Chromatogr., 537:* 17 (1991).

62. R. M. Chicz and F. E. Regnier, *Methods Enzymol., 182:* 392 (1990).

63. M. A. Cohen Stuart, G. J. Fleer, J. Lyklema, W. Norde, and J. M. H. M. Schleutjens, *Adv. Colloid Interface Sci., 34:* 477 (1991).

64. A. Sadana and R. R. Raju, *Bioseparation, 1:* 119 (1990).

65. K. Benedek, S. Dong, and B. L. Karger, *J. Chromatogr., 317:* 227 (1984).

66. L. O. Lindquist and K. W. Williams, *Dairy Ind. Int., 38:* 459 (1973).

67. H. Friedli and P. Kistler, *Chimia, 26:* 25 (1972).

68. J.-C. Janson *Agr. Food Chem., 19:* 581 (1971).

69. J. M. Curling, in *Methods of Plasma Protein Fractionation* (J. M. Curling, ed.), Academic Press, London, 1980, p. 77.

70. G. L. Hagnauer, in *Preparative Liquid Chromatography* (B. A. Bidlingermeyer, ed.), Elsevier, New York, 1987, p. 289.

71. Pharmacia Fine Chemicals, *Gel Filtration: Theory and Practice*, Rahms i Lund, Sweden, 1984, p. 45.

72. G. K. Sofer and L.-E. Nystrom (eds.), *Process Chromatography: A Practical Guide*, Academic Press, New York, 1989, p. 93.

73. Pharmacia LKB Biotechnologies, *Downstream*, Piscataway, NJ, No. 7 (1990).

74. Pharmacia LKB Biotechnology, *Process Stack Column*, Data File No. 5040, Piscataway, NJ, 1990.

17
Size Exclusion Chromatography of Nucleic Acids

Yoshio Kato TOSOH Corporation, Yamaguchi, Japan

Introduction

Conventional size exclusion chromatography (SEC) has been employed for a long time for the separation and purification of nucleic acids, but it has not been very successful. On the other hand, high-performance SEC was applied to the separation of nucleic acids in 1979 (1), and the performance in SEC of nucleic acids was greatly improved.. As a result, SEC became one of the effective methods to separate various types of nucleic acids according to molecular size. Since then, successful separations of RNAs (1–8), DNA fragments (7–17), plasmids (17–20), and oligonucleotides (21) have been reported. In this chapter, separations of these types of nucleic acids by high-performance SEC and guidelines to optimize chromatographic conditions are described.

RNA

SEC has been applied to various types of RNA, such as transfer RNA (tRNA), ribosomal RNA (rRNA), and messenger RNA (mRNA).

Although there are a variety of species in tRNA, their molecular weights are in a narrow range, approximately 25,000–30,000. Therefore, it is rather difficult to separate different species of tRNA by SEC. Single peaks are usually observed in SEC of tRNA samples even if they contain many species. Only one example of the separation of tRNA species has been reported. Two species,

tyrosine-specific and *N*-formylmethionyl-specific tRNAs, were separated on a MicroPak TSK 3000SW column (30 cm × 7.5 mm inner diameter, ID), although only partially (1). However, it is easy to separate tRNA from other types of RNA such as rRNA, as exemplified in Figure 1. tRNA was separated from rRNA on a TSKgel G3000SW two-column system (each column 60 cm × 7.5 mm ID).

Separation of different species of rRNA is also easy. Figure 2 shows an example of the separation: 5*S*, 16*S*, and 23*S* rRNAs, whose molecular weights are approximately 39,000, 560,000, and 1,100,000, were separated well on a TSKgel G4000SW two-column system (each column 60 cm × 7.5 mm ID) in about 40 minutes. Although the separation between 16*S* and 23*S* rRNAs seems insufficient, it is caused by other components that eluted at the same position as they did. A pure mixture of 16*S* and 23*S* rRNAs was separated almost completely. The 5*S* and 5.8*S* rRNAs with approximate chain lengths of 120 and 158

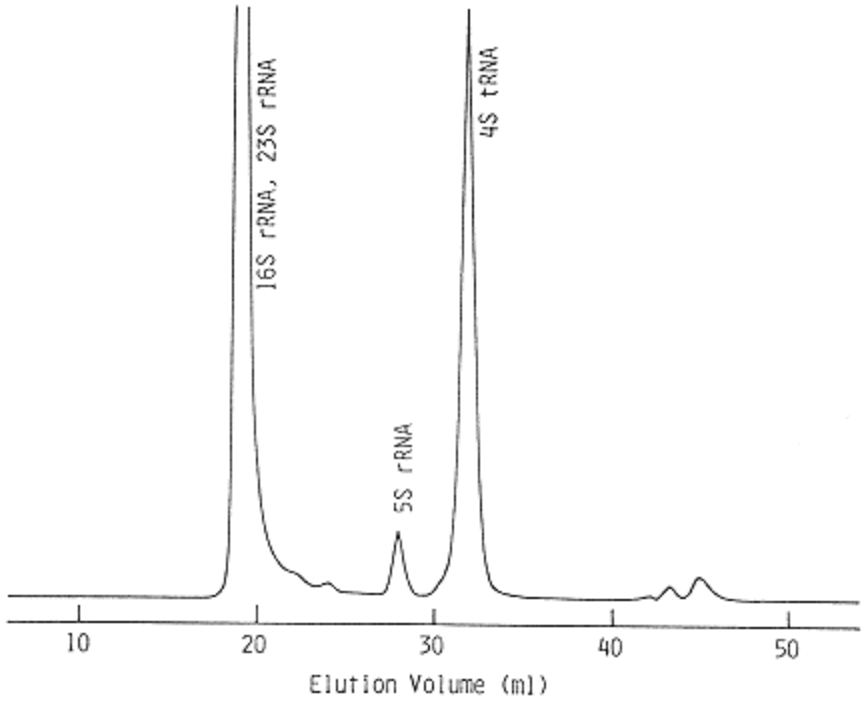

Figure 1.
Separation of total E. coli RNA containing 4S tRNA and 5S, 16S, and 23S rRNAs obtained on a TSKgel G3000SW two-column system (each column 60 cm × 7.5 mm ID) in 0.1 M phosphate buffer (pH 7.0) containing 0.1 M sodium chloride and 1 mM EDTA at a flow rate of 1 ml/minute. (Data from Reference 8.)

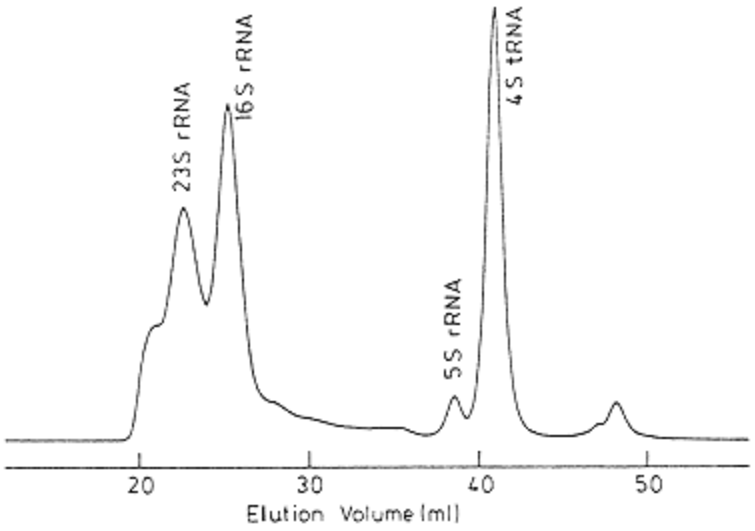

Figure 2.
Separation of total E. coli RNA containing 4S tRNA and 5S, 16S, and 23S rRNAs obtained on a TSKgel G4000SW two-column system (each column 60 cm × 7.5 mm ID) in 0.1 M phosphate buffer (pH 7.0) containing 0.1 M sodium chloride and 1 mM EDTA at a flow rate of 1 ml/minute. (From Reference 7.)

were also separated well on a TSKgel G3000SW column (60 cm × 7.5 mm ID) in about 20 minutes (2).

Samples of mRNA usually contain many components whose molecular weights differ continuously in a rather wide range. Consequently, single broad peaks are usually obtained in the SEC of mRNA mixtures. However, it has been confirmed by in vitro translation test of the fractionated mRNA samples that the separation of mRNA is roughly based on molecular size (3,6). mRNA easily aggregates in nondenaturing buffers, which results in inferior resolution. Therefore, it is recommended to separate mRNA under denaturing conditions in the presence of 6 M urea. Under denaturing conditions, aggregation formation is avoided and the resolution is considerably improved (3,6). SEC under denaturing conditions has a resolution equivalent to or even better than that of sucrose gradient centrifugation, which has been the most common method to separate mRNA.

Satisfactory separation has also been obtained for small nuclear RNAs on UltroPac TSK SW type columns (4).

According to the test for loading capacity in SEC on columns of 7.5 mm ID, RNA samples could be applied without a decrease in resolution up to a few milligrams (5).

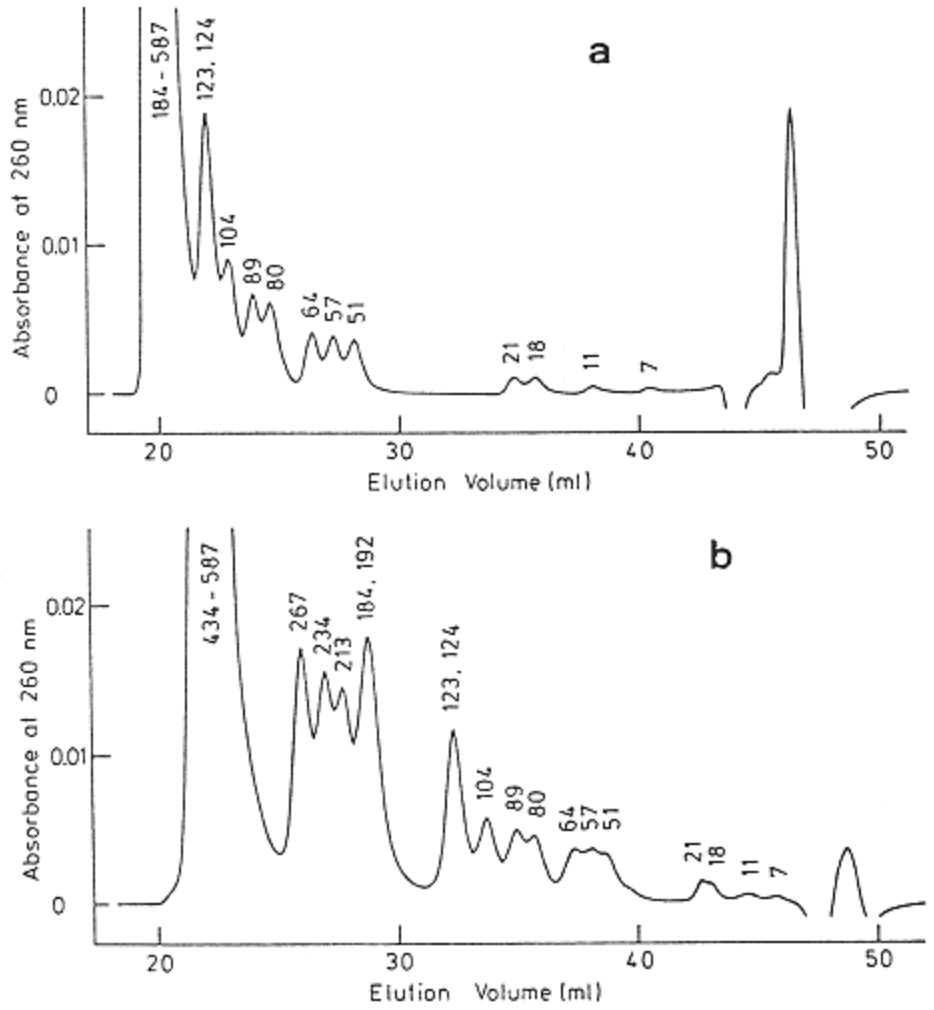

Figure 3.
Separation of HaeIII-cleaved plasmid pBR322 obtained on a TSKgel G3000SW two-column system at a flow rate of 1 ml/minute (a) or on a TSKgel G4000SW two-column system at a flow rate of 0.33 ml/minute (b) (each column 60 cm × 7.5 mm ID) in 0.05 M Tris-HCl buffer (pH 7.5) containing 0.2 M sodium chloride and 1 mM EDTA. (From Reference 10.)

DNA Fragments

DNA fragments of up to approximately 7000 base pairs have successfully been separated by SEC. Figure 3 shows chromatograms of HaeIII-cleaved plasmid pBR322 obtained on column systems consisting of two TSKgel G3000SW columns or two G4000SW columns (each column 60 cm × 7.5 mm ID). The numerals above the peaks represent the base pairs of DNA fragments contained in the peaks. On G3000SW, DNA fragments of less then 124 base pairs were well separated, whereas larger DNA fragments were eluted together in the void volume of the column system (approximately 20 ml). On G4000SW, DNA fragments up to 267 base pairs were separated. According to these results, it can be said that relatively small DNA fragments can be separated by SEC if they differ by more than 10% in chain length. The chain length of DNA fragments is plotted against elution volume in Figure 4. The average chain lengths were used for peaks containing more than one DNA fragment. The results demonstrate that DNA fragments were separated according to their chain length. Therefore, it is

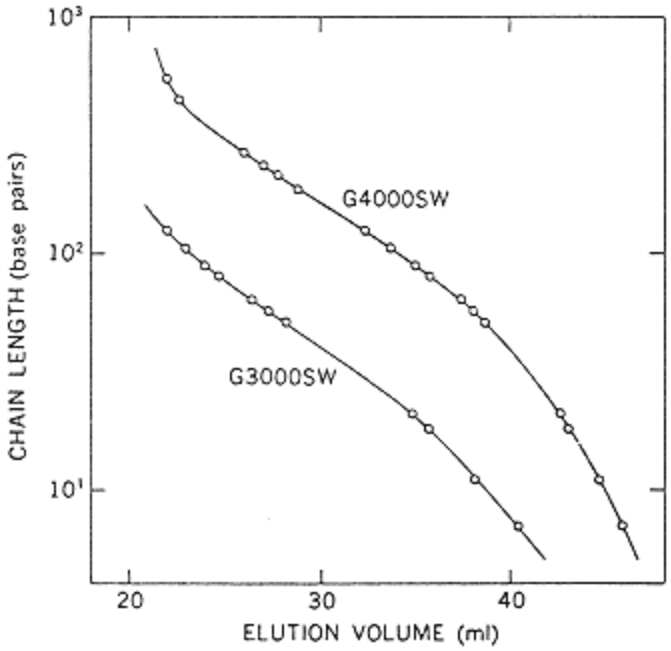

Figure 4.
Plots of chain length against elution volume for double-stranded DNA fragments obtained in SEC on TSKgel G3000SW and G4000SW in Figure 3. (From Reference 10.)

possible not only to purify fragments but also to estimate the chain length of unknown DNA fragments. Figure 5 shows the separation of larger DNA fragments. A mixture of EcoRI-cleaved plasmid pBR322 and BstNI-cleaved plasmid pBR322 was separated on a TSKgel DNA-PW four-column system (each column 30 cm × 7.8 mm ID). The sample contains seven fragments of 13, 121, 383, 928, 1060, 1857, and 4362 base pairs. Peaks a-f contained fragments of 4362 (a), 1857 (b), 1060 and 928 (c), 383 (d), 121 (e), and 13 (f) according to polyacrylamide gel electrophoresis of collected eluates corresponding to the peaks. Although two fragments of 928 and 1060 base pairs were eluted together as one peak, all the other fragments were well separated from each other. The separations of 1060 and 1857 base pair fragments and of 1857 and 4362 base pair fragments were also almost complete. This means that even fragments of greater than 1000 base pairs can be separated with little cross-contamination, provided that the chain length of one is more than twice that of the other. The void volume of the column system was determined with λ-DNA. The exclusion limit of TSKgel DNA-PW estimated by utilizing the value of void volume was approximately 7000 base pairs. Therefore, SEC should be very useful in the field of genetic engineering, in which the separation of large DNA fragments in the range of 1000–5000 is important. However, it seems that DNA fragments larger than 7000 base pairs cannot be separated at present because no commer-

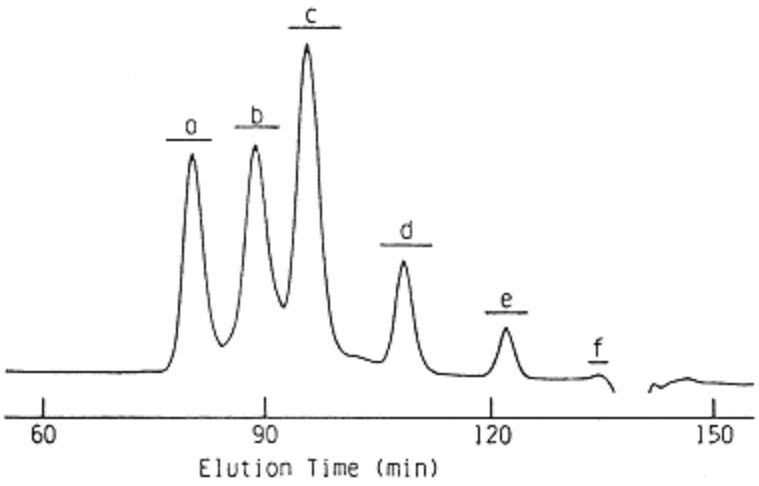

Figure 5.
Separation of a mixture of EcoRI-cleaved plasmid pBR322 and BstNI-cleaved plasmid pBR322 obtained on a TSKgel DNA-PW four-column system (each column 30 cm × 7.8 mm ID) in 0.1 M Tris-HCl buffer (pH 7.5) containing 0.3 M sodium chloride and 1 mM EDTA at a flow rate of 0.3 ml/minute. (From Reference 11.)

cially available aqueous SEC columns have higher exclusion limits than TSKgel DNA-PW.

The recovery of DNA fragments has been reported to be almost quantitative (9,10).

Plasmids

SEC has been applied to the purification of various forms of plasmids. It is possible to obtain plasmid free of proteins, RNA, and chromosomal DNA from cleared lysate of *Escherichia coli* cells. Figure 6 shows an example of the purification of plasmid. Cleared lysate of *E. coli* cells containing amplified plasmid pBR322 and its phenol extract were separated on a TSKgel G6000PW two-column system (each column 60 cm × 7.5 mm ID). Plasmid pBR322 was eluted between 27 and 31 minutes and was perfectly separated from RNA and proteins, which were eluted after 36 minutes. Chromosomal DNA was also removed fairly well, but not completely, because it was eluted continuously after 22 minutes. The purities of plasmid fractions collected from cleared lysate and phenol extract were almost equivalent. The phenol extract sample was treated with ATP-dependent deoxyribonuclease to digest linear double-stranded DNA-like chromosomal DNA and was subjected to SEC on a TSKgel G6000PW column

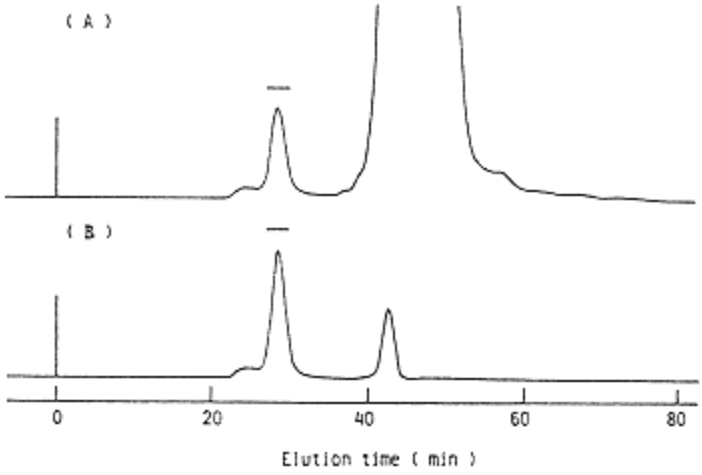

Figure 6.
Separation of cleared lysate of E. coli cells (A) and its phenol extract (B) obtained on a TSKgel G6000PW two-column system (each column 60 cm × 7.5 mm ID) in 0.1 M Tris-HCl buffer (pH 7.5) containing 0.3 M sodium chloride and 1 mM EDTA at a flow rate of 1 ml/minute. (From Reference 20.)

(30 cm × 7.5 mm ID). The result is shown in Figure 7. The chromatogram suggests that chromosomal DNA was almost completely eliminated from the plasmid fraction. According to a purity test by agarose gel electrophoresis, the collected plasmid fraction was free of RNA, proteins, and chromosomal DNA. The separation between plasmid and other components was sufficient even when a 0.5 ml solution of the enzyme-treated phenol extract was applied to a column of 30 cm × 7.5 mm ID and the separation was completed in about 15 minutes. It is also possible to eliminate proteins and chromosomal DNA from cleared lysate by precipitating them at high concentrations of potassium acetate (3 M, pH 4.8) (19).

Oligonucleotides

SEC has also been applied to oligonucleotides. However, there have not been many applications of SEC to oligonucleotide separation because SEC generally has a considerably lower resolution than other modes of high-performance liquid chromatography such as reversed-phase and ion-exchange chromatography. One example of the separation of oligonucleotide is shown in Figure 8. A mixture of oligodeoxyadenylic acids was separated on a TSKgel G2000SW two-column system (each column 60 cm × 7.5 mm ID). It is also possible to separate other

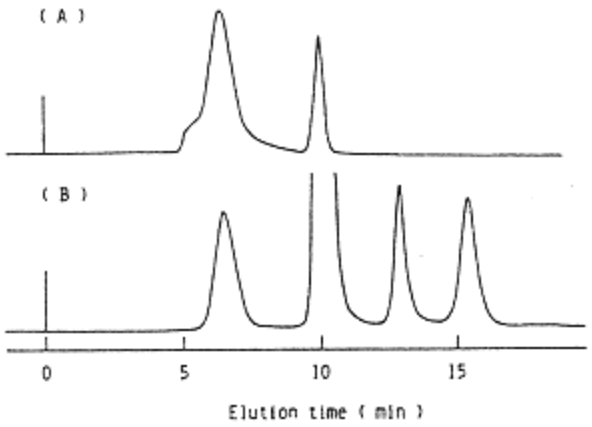

Figure 7.
Separation of phenol extract of cleared lysate of E. coli cells before (A) and after (B) treatment with ATP-dependent deoxyribonuclease on a TSKgel G6000PW column (30 cm × 7.5 mm ID) in 0.1 M Tris-HCl buffer (pH 7.5) containing 0.3 M sodium chloride and 1 mM EDTA at a flow rate of 1 ml/minute. (From Reference 20.)

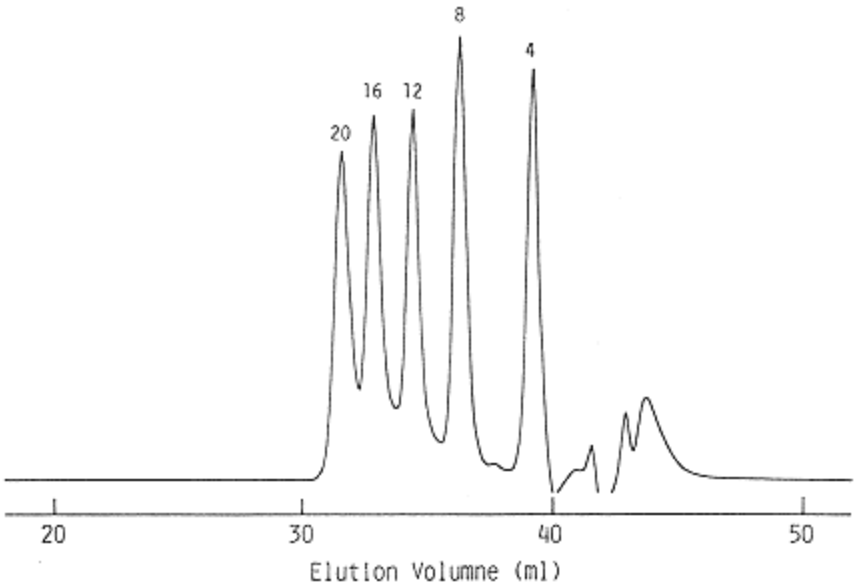

Figure 8.
Separation of a mixture of oligodeoxyadenylic acids with chain lengths of 4, 8, 12, 16, and 20 nucleotides on a TSKgel G2000SW two-column system (each column 60 cm × 7.5 mm ID) in 0.1 M phosphate buffer (pH 7.0) containing 0.1 M sodium chloride and 1 mM EDTA at a flow rate of 1 ml/minute. (From Reference 22.)

types of homogeneous oligonucleotides, such as oligodeoxythymidylic acid, and heterogeneous oligonucleotides by SEC.

Columns

Two types of columns have been employed in the SEC of nucleic acids, chemically bonded porous silica columns and hydrophilic resin columns. Among them, TSKgel SW and PW columns have been well accepted. They are available in different pore sizes, and each has a different separation range. The exclusion limits for RNA and double-stranded DNA fragment are listed in Table 1. A sample of a certain molecular weight can be in general separated on different columns. However, the resolution depends on the column employed. For example, in the separation of HaeIII-cleaved plasmid pBR322, the best separation is obtained for base pairs of 7–21, 51–104, 123–267, and 434–587 on G2000SW, G3000SW, G4000SW, and G5000PW, respectively, Therefore, it is

Table 1 Exclusion Limits of TSKgel SW and PW Columns for RNA and Double-Stranded DNA Fragments[a]

	Exclusion limit (molecular weight)	
Column	RNA	Double-stranded DNA fragment
G2000SW	70,000	50,000 (70)[b]
G3000SW	150,000	100,000 (150)
G4000SW	1,500,000	300,000 (500)
G5000PW	>5,000,000	1,000,000 (1500)
G6000PW	—[c]	5,000,000 (7000)
DNA-PW	—[c]	5,000,000 (7000)

[a]In 0.1 M phosphate buffer (pH 7.0) containing 0.1 M sodium chloride and 1 mM EDTA.

[b]Values in parentheses are the exclusion limits in base pairs.

[c]Not determined.

Source: Data from References 7 and 11.

very important to select the best column depending on the molecular weights of the samples to be separated. Table 2 and 3 summarize the best columns in relation to molecular weight range.

Eluant

Eluant ionic strength affects the elution volume and resolution in the SEC of nucleic acids, and therefore it must be properly adjusted to obtain good results. Figure 9 shows the effect of eluant ionic strength on the elution volumes obtained on TSKgel G3000SW, G4000SW, and G5000PW columns. Elution of both RNA and DNA fragments is delayed by increasing the eluant ionic strength. Elution volumes vary greatly in the low ionic strength region, but at high ionic strength the elution volumes seem to become constant. Furthermore, the elution volumes of small molecules are more markedly affected than those of large

Table 2 Best Columns for the Separation of RNA

Molecular weight range	Best column
<60,000	G2000SW or G3000SW
60,000–120,000	G3000SW
120,000–1,200,000	G4000SW
1,200,000–10,000,000	G5000PW

Source: Data from Reference 7.

Table 3 Best Columns for the Separation of Double-Stranded DNA Fragments

Molecular weight range	Best column
<40,000 (<60)[a]	G2000SW or G3000SW
40,000–80,000 (60–120)	G3000SW
80,000–250,000 (120–400)	G4000SW
250,000–800,000 (400–1200)	G5000PW
800,000–5,000,000 (1200–7000)	G6000PW or DNA-PW

[a]Values in parentheses are ranges in base pairs.

Source: Data from Reference 7.

molecules. The peak widths broaden with increasing eluant ionic strength, although slightly. Accordingly, in general, an eluant ionic strength of 0.3–0.5 may be optimum. When an eluant of low ionic strength is used, the exclusion limits of the columns are considerable lowered. The main source of variation in elution volume with eluant ionic strength is probably the repulsive ionic interaction between samples and column packing materials, because both nucleic acids and TSKgel SW and PW are negatively charged. TSKgel SW is based on silica and contain some residual silanol groups on its surface, whereas TSKgel PW is based on hydrophilic synthetic resin and contains some carboxyl groups. Most other commercially available columns for aqueous SEC are also negatively charged, and the phenomenon of increasing elution volume with increasing eluant ionic strength has been observed on them, too. Other sources may also be responsible in some cases. For example, elution volumes increase regularly with eluant ionic strength, even in the high ionic strength region, where ionic interactions should diminish, in the case of 16*S* and 23*S* rRNAs (see 16*S* rRNA in Figure 9b). The retardation of elution in the high ionic strength region may be attributed to the adsorption of samples on column packing materials by hydrophobic interaction.

Flow Rate

Figure 10 shows the dependence of height equivalent to a theoretical plate (HETP) on flow rate observed in the SEC of RNA and DNA fragment on 7.5 mm ID columns. The HETP decreased with decreasing flow rate. Especially with high-molecular-weight samples, such as 16*S* rRNA and a DNA fragment of 383 base pairs, the HETP was significantly dependent on flow rate and reached a minimum at flow rates lower than 0.1 ml/minute. Flow rates of 0.3–0.5 ml/minute seem to be a good compromise when separation time and resolution are taken into consideration.

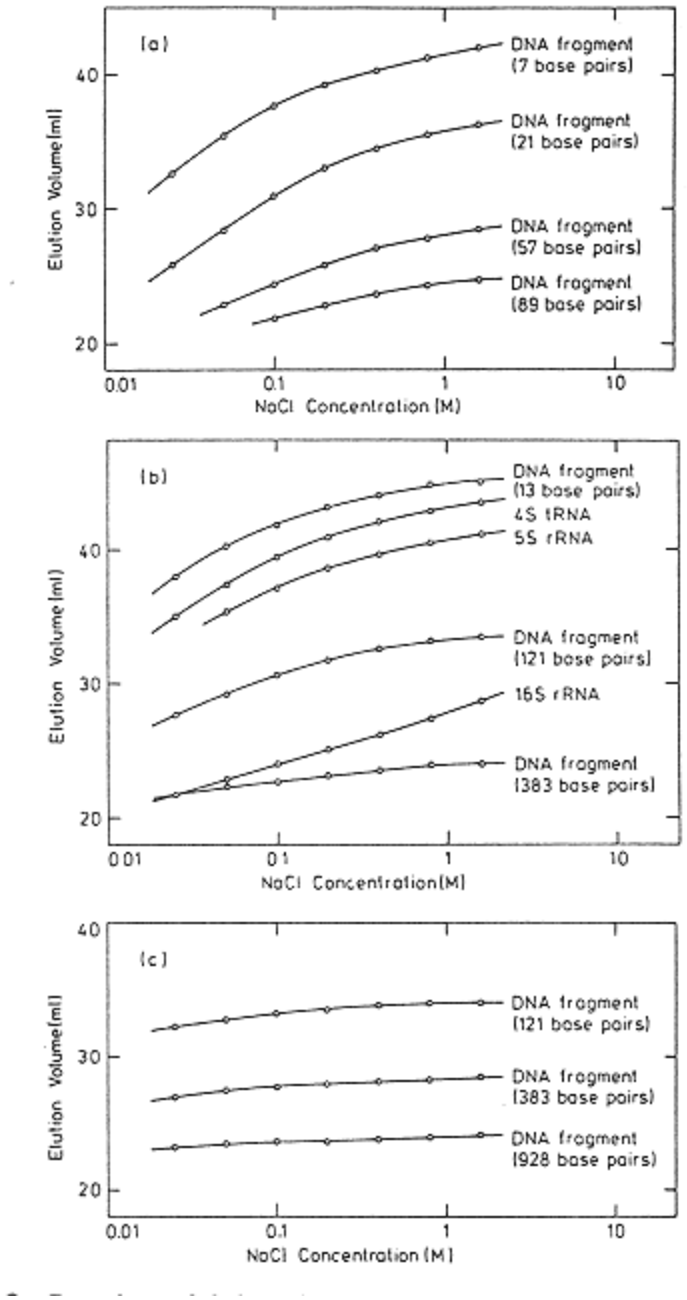

Figure 9.
Dependence of elution volume on eluant ionic strength obtained on TSKgel G3000SW (a), G4000SW (b), and G5000PW (c) two-column systems (each column 60 cm × 7.5 mm ID) in 0.01 M Tris-HCl buffer (pH 7.5) containing 0.025–1.6 M sodium chloride and 1 mM EDTA at a flow rate of 1 ml/minute. (From Reference 7.)

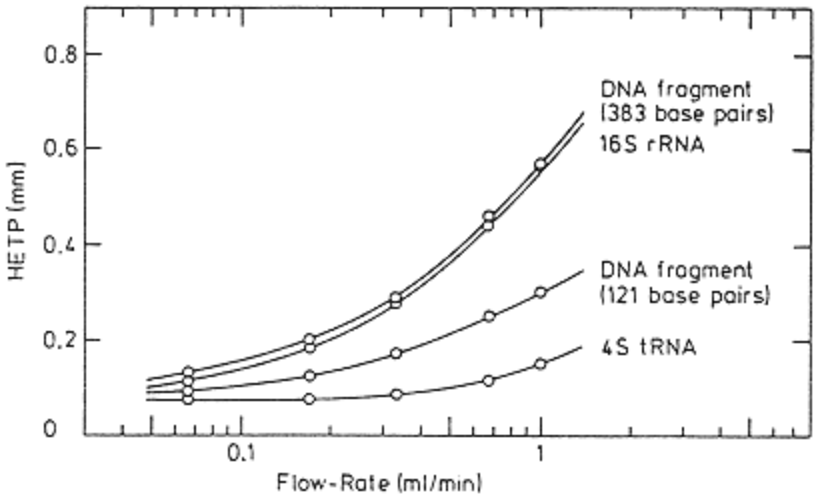

Figure 10.
Dependence of HETP on the flow rate for RNAs on a TSKgel G4000SW two-column system and for DNA fragments on a TSKgel G5000PW two-column system (each column 60 cm × 7.5 mm ID). (From Reference 7.)

Conclusion

A wide range of nucleic acids including RNAs, DNA fragments, plasmids, and oligonucleotides can be separated effectively by SEC on the basis of molecular size. Accordingly, it is possible to adopt SEC as an alternative to gel electrophoresis for analytical purposes. Furthermore, because the separated components in samples can be recovered easily and yet almost quantitatively by collection of column effluent, SEC should be superior to gel electrophoresis for preparative purposes. Consequently, SEC seems to be a useful technique for the separation and purification of nucleic acids.

Appendix

Polymer	Columns	Mobile phase	Comments	Reference
RNA	MicroPak TSK 2000SW and 3000SW (Varian)	67 mM potassium phosphate buffer (pH 6.8) containing 0.1 M potassium chloride and 0.6 mM sodium azide		1
RNA	TSKgel G3000SW (Tosoh)	0.2 M sodium phosphate buffer (pH 7.0) containing 0.1% sodium dodecyl sulfate (SDS)		2
RNA	UltroPac TSK G4000SW (LKB)	A. 50 mM Tris -HCl buffer (pH 7.5) containing 25 mM potassium chloride and 5 mM magnesium chloride B. 75 mM Tris-HCl buffer (pH 7.5) containing 6 M urea, 0.1% SDS, and 1 mM EDTA		3
RNA	UltroPac TSK G2000SW, G3000SW and G4000SW (LKB)	A. 0.1 M acetate buffer (pH 7.0) containing 0.75 M sodium chloride, 0.1% velcorin, and 1% methanol B. 10 mM acetate buffer (pH 5.5) containing 0.2 M sodium chloride, 5 mM magnesium chloride, and 0.2% SDS C. 75 mM Tris-HCl buffer (pH 7.5) containing 6 M urea, 1 mM EDTA, and 0.1% SDS		4
RNA	TSKgel G4000SW (Tosoh)	50 mM Tris-HCl buffer (pH 7.5) containing 0.2 M sodium chloride and 1 mM EDTA		5
RNA	TSKgel G4000SW and G5000PW (Tosoh)	A. 0.25 M acetate buffer (pH 5.4) containing 1 mM EDTA B. 10 mM phosphate buffer (pH 7.0) containing 0.1 M potassium chloride		6

(table continued on next page)

(table continued from previous page)

Polymer	Columns	Mobile phase	Comments	Reference
RNA and DNA fragment	TSKgel G2000SW, G3000SW, G4000SW, and G5000PW (Tosoh)	A. 0.1 M phosphate buffer (pH 7.0) containing 0.1 M sodium chloride and 1 mM EDTA B. 10 mM Tris-HCl buffer (pH 7.5) containing 0.025–1.6 M sodium chloride and 1 mM EDTA		7
RNA and DNA fragment	TSKgel G2000SW, G3000SW, and G4000SW (Tosoh)	0.1 M phosphate buffer (pH 7.0) containing 0.1 M sodium chloride and 1 mM EDTA		8
DNA fragment	UltroPac TSK G3000SW and G4000SW (LKB)	50 mM triethylammonium acetate (pH 7.0)		9
DNA fragment	TSKgel G3000SW and G4000SW (Tosoh)	50 mM Tris-HCl buffer (pH 7.5) containing 0.2 M sodium chloride and 1 mM EDTA (and 7 M urea)		10
DNA fragment	TSKgel DNA-PW (Tosoh)	0.1 M Tris-HCl buffer (pH 7.5) containing 0.3 M sodium chloride and 1 mM EDTA		11
DNA fragment	Spherogel TSK 6000PW (Beckman)	50 mM Tris-HCl buffer (pH 7.6) containing 0.3 M sodium chloride and 1 mM EDTA		12
DNA fragment	TSKgel G4000PW, G5000PW, and G6000PW (Tosoh)	0.1 M sodium nitrate		13
DNA fragment	UltroPac TSK G4000SW, G5000PW, and G6000PW (LKB)	0.25 M ammonium acetate (pH 6.0) containing 0.1 mM EDTA		14
DNA fragment	Bioseries GF-250 (DuPont)	Tris-acetic acid buffer (pH 7.5) containing 0.5 mM EDTA		15

(table continued on next page)

(table continued from previous page)

Polymer	Columns	Mobile phase	Comments	Refere
DNA fagment	Superose 6 (Pharmacia LKB)	20 mM Tris-HCl buffer (pH 7.6) containing 0.15 M sodium chloride		16
Plasmid and DNA fragment	TSKgel G5000PW (Tosoh)	50 mM Tris-HCl buffer (pH 7.4) (containing 15 mM EDTA)		17
Plasmid	Bioseries GF-250 (Dupont)	0.2 M phosphate buffer (pH 9.0)		18
Plasmid	Fractogel TSK HW75S (Merck)	10 mM Tris-HCl buffer (pH 8.0) containing 0.2 M sodium chloride and 1 mM EDTA		19
Plasmid	TSKgel G6000PW (Tosoh)	0.1 M Tris-HCl buffer (pH 7.5) containing 0.3 M sodium chloride and 1 mM EDTA		20
Oligonucleotide	I-125 Protein Column (Waters)	0.1 M triethylammonium acetate (pH 6.4–7.0)		21

References

1. C. T. Wehr and S. R. Abbott, *J. Chromatogr., 185:* 453 (1979).

2. S. Uchiyama, T. Imamura, S. Nagai, and K. Konishi, *J. Biochem. (Tokyo), 90:* 643 (1981).

3. L. Graeve, W. Goemann, P. Földi, and J. Kruppa, *Biochem. Biophys. Res. Commun., 107:* 1559 (1982

4. L. Graeve, J. Kruppa, and P. Földi, *J. Chromatogr., 268:* 506 (1983).

5. Y. Kato, T. Hashimoto, T. Murotsu, S. Fukushige, and K. Matsubara, *HRC & CC, 1:* 626 (1983).

6. T. Ogishima, Y. Okada, and T. Omura, *Anal. Biochem., 138:* 309 (1984).

7. Y. Kato, M. Sasaki, T. Hashimoto, T. Murotsu, S. Fukushige, and K. Matsubara, *J. Chromatogr., 266.* 341 (1983).

8. Y. Kato, H. Parvez, and S. Parvez, in *Gel Permeation and Ion-Exchange Chromatography of Proteins and Peptides* (H. Parvez, Y. Kato, and S. Parvez, eds.), VNU Science Press, Utrecht, 1985, p. 1.

9. J. Kruppa, L. Graeve, A. Bauche, and P. Földi, *LC Magazine, 2:* 848 (1984).

10. Y. Kato, M. Sasaki, T. Hashimoto, T. Murotsu, S. Fukushige, and K. Matsubara, *J. Biochem. (Tokyo) 95:* 83 (1984).

11. Y. Kato, Y. Yamasaki, T. Hashimoto, T. Murotsu, S. Fukushige, and K. Matsubara, *J. Chromatogr., 320:* 440 (1985).

12. J.-M. Schmitter, Y. Mechulam, and G. Fayat, *J. Chromatogr., 378:* 462 (1986).

13. T. Nicolai, L. V. Dijk, J. A. P. P. V. Dijk, and J. A. M. Smit, *J. Chromatogr., 389:* 286 (1987).

14. R. Dornburg, *LC/GC, 6:* 254 (1988).

15. B. E. Boyes, D. G. Walker, and P. L. McGeer, *Anal. Biochem., 170:* 127 (1988).

16. H. Ellegren and T. Laas *, *J. Chromatogr., 467:* 217 (1989).

17. M. E. Himmel, P. J. Perna, and M. W. McDonnell, *J. Chromatogr., 240:* 155 (1982).

18. P. A. D. Edwardson, T. Atkinson, C. R. Lowe, and D. A. P. Small, *Anal. Biochem., 152:* 215 (1986).

19. N. Mareau, X. Tabary, and F. L. Goffic, *Anal. Biochem., 166:* 188 (1987).

20. Y. Yamasaki, Y. Kato, T. Murotsu, S. Fukushige, and K. Matsubara, *HRC & CC, 10:* 45 (1987).

21. D. Molko, R. Derbyshire, A. Guy, A. Roget, R. Teoule, and A. Boucherle, *J. Chromatogr., 206:* 493 (1981).

22. Y. Kato, unpublished data.

Index

A

D

E

F

G

H

M

R

S

T

Z